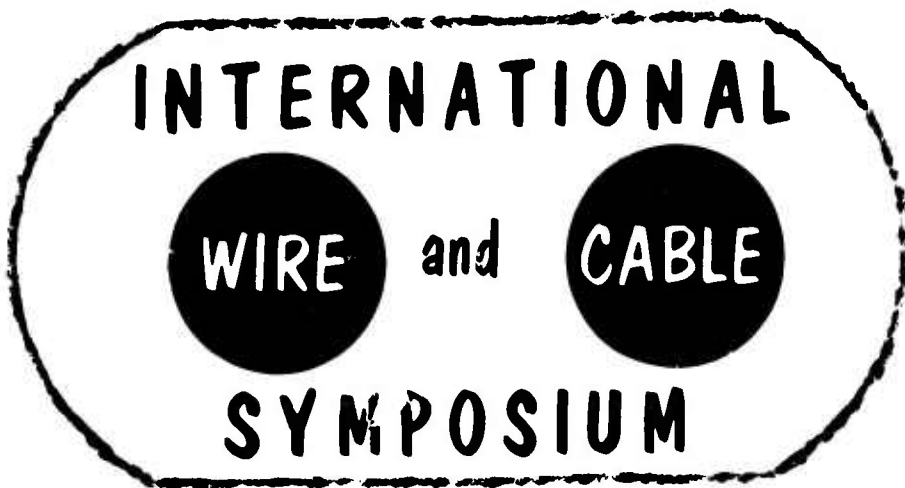


24th INTERNATIONAL WIRE AND CABLE SYMPOSIUM PROCEEDINGS 1975

ADA01787

**PROCEEDINGS**  
**of the 24th**

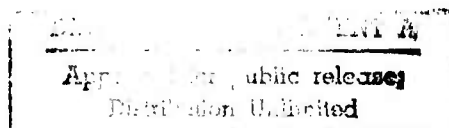
12



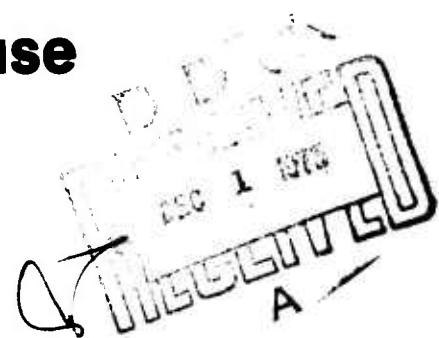
**18th, 19th, 20th November 1975**

**Cherry Hill Hyatt House**

**Cherry Hill, N.J.**



**SPONSORED BY THE U.S. ARMY ELECTRONICS COMMAND**



✓

NAME	
NO.	
DATE	
BY	
INITIALS	
A	



11 Nov 75  
12  
42-1

**PROCEEDINGS OF  
24th INTERNATIONAL  
WIRE AND CABLE  
SYMPOSIUM (42-1)**

**Sponsored by  
U.S. Army Electronics Command**

14-1  
**Cherry Hill, New Jersey,  
November 18, 19 and 20, 1975,**

**APPROVED FOR PUBLIC RELEASE; DISTRIBUTION  
UNLIMITED**

# 24th INTERNATIONAL WIRE AND CABLE SYMPOSIUM

## SYMPOSIUM COMMITTEE

Elmer F. Godwin, Co-Chairman, USAECOM (201-544-2770)  
Milton Tenzer, Co-Chairman, USAECOM (201-544-4834)  
Marta Farago, Northern Electric  
F. M. Farrell, BM Company  
Joseph M. Flanigan, Rural Electrification Administration (REA)  
Jerome Hager, Northern Petrochemical Co.  
George Heller, Tensolite Co.  
Irving Kolodny, General Cable Corp.  
Joe Neigh, AMP Inc.  
James Kanely, Superior Continental Corp.  
Ronald Soloman, McDonnell Aircraft Co.  
George H. Webster, Bell Laboratories

## TECHNICAL SESSIONS

### Tuesday, 18 November 1975

9:30 a.m. Session I: Tutorial on Wire and Cable Considerations in Fires  
2:15 p.m. Session II: Flammability Consideration in Cables  
2:15 p.m. Session III: Manufacturing & Processing

### Wednesday, 19 November 1975

9:15 a.m. Session IV: Cable Applications I  
9:15 a.m. Session V: Cable Design  
2:15 p.m. Session VI: Testing & Evaluation  
2:15 p.m. Session VII: Cable Materials I

### Thursday, 20 November 1975

9:15 a.m. Session VIII: Cable Applications II  
9:15 a.m. Session IX: Cable Materials II  
2:15 p.m. Session X: Waterproof Cable

## PROCEEDINGS

Responsibility for the contents rests upon the authors and not the Symposium Committee or its members. After the symposium all the publication rights of each paper are reserved by their authors, and requests for republication of a paper should be addressed to the appropriate author. Abstracting is permitted, and it would be appreciated if the symposium is credited when abstracts or papers are republished. Requests for individual copies of papers should be addressed to the authors. Extra copies of the Proceedings may be obtained from the Symposium Co-Chairman (Requests should include a check for \$10.00 per copy, in US currency, made payable to the International Wire & Cable Symposium). Copies may also be obtained for a nominal fee from the National Technical Information Service (NTIS), Operations Division, Springfield, Virginia 22151.

Copies of papers presented in previous years may also be obtained from the National Technical Information Service. Papers from the first 20 years, with their AD numbers are catalogued in the "KWIC Index of Technical Papers, Wire and Cable Symposia (1952-1971)," December 1971.




### MESSAGE FROM THE CO-CHAIRMEN

Your co-chairmen heartily welcome you to the 24th International Wire and Cable Symposium. Last year's successful symposium (the 23rd) evoked many favorable comments on the high caliber and timely relevance of the presentations. Participation by countries other than the United States was maintained at the high level achieved in the past two years. Eighteen (18) papers from seven of these countries were presented, 35% of all papers given. We are indeed gratified that this symposium continues to attract such a sizeable representation from the world-wide wire and cable community.

The emphasis this year is being placed on the flammability characteristics of potential cable material. Such considerations are assuming increasing importance in the interest of safety, performance reliability, and economy. The tutorial session and one following session is devoted to this topic. The tutorial session is the only offering in its time slot and we strongly recommend your attendance.

Two of our hard working committee members, Jerome Hager of Northern Petrochemical Company and George Heller of Tensolite Company are retiring from the committee after three years of service. Jerry and George by their efforts and specialized knowledge both contributed materially to the success of the committee's mission. On behalf of the rest of the committee, your co-chairmen wish to thank them both and wish them well in their future activities.

The committee is looking forward to the symposium's first year at its new location, the Cherry Hill Hyatt House. Attractive surroundings, adequate convention facilities, local and nearby urban recreational activities and easily accessible transportation should combine to make this year's symposium a stimulating and pleasant experience. We hope you enjoy it!

  
M. TENZER, Co-Chairman

  
E. F. GODWIN, Co-Chairman



(Left) Major General Hugh F. Foster, Jr.; Commanding General of Fort Monmouth, making his keynote address at the banquet.



(Right) Mrs. Helene Spergel and daughter Ilene receiving bound volume of technical papers authored by the late Jack Spergel.

## HIGHLIGHTS OF THE 23rd INTERNATIONAL WIRE AND CABLE SYMPOSIUM

December 3, 4 and 5, 1974  
Shelburne Hotel, Atlantic City, N. J.



Awards were presented by the symposium co-chairman to Dr. H. Martin, Kabelmetal (left), for Outstanding Technical Paper, and to R. J. Oakley, Northern Electric Co., Ltd. (2nd left), for Best Presentation of a Technical Paper. Certificates of Appreciation were presented to W. R. Smith, Hercules Inc. (2nd right) and L. Dunlop, GTE Service Corporation (right), for serving three years on the Symposium Committee.



Dr. W. Wells, IIT Research Institute, discussing "Testing and Hardening Techniques for Cables and Connectors," during tutorial session on Effects of EMP on Cable Systems. Mr. I. Kolodny, General Cable, was Chairman of the session.

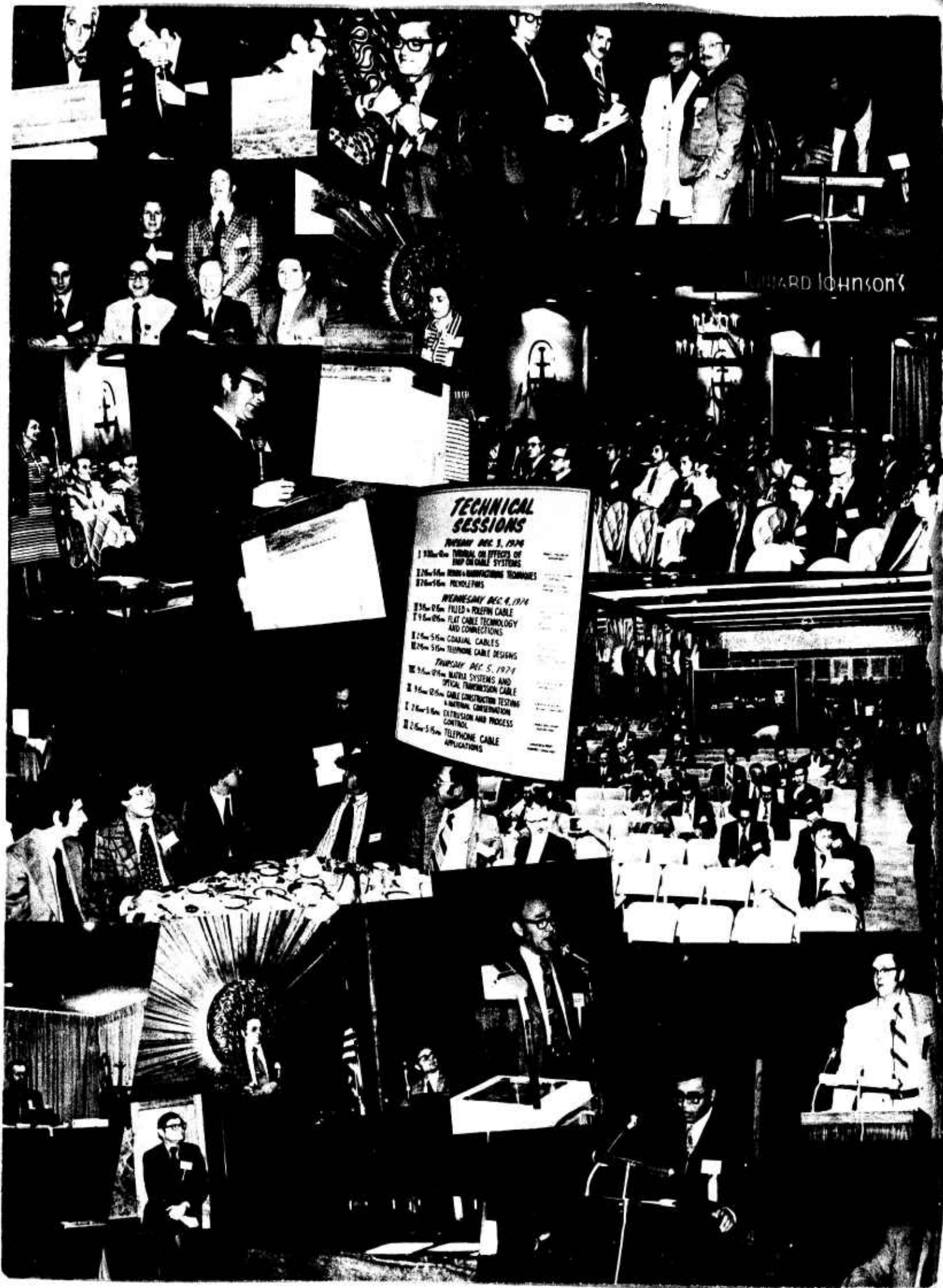


Breakfast for speakers and co-authors of Session II.

## CANDID SCENES AT THE 23rd IWCS







Richard Johnson's

**TECHNICAL SESSIONS**

**TUESDAY, DEC. 3, 1974**

- 1:00-2:00 PM TUTORIAL ON EFFECTS OF IMP ON CABLE SYSTEMS
- 2:15-3:15 PM RING-BUILDING TECHNIQUES
- 3:20-4:15 PM FIBER OPTICS

**WEDNESDAY, DEC. 4, 1974**

- 8:30-9:15 AM FIELD & FIBER CABLE
- 9:15-10:15 AM FLAT CABLE TECHNOLOGY AND CONNECTIONS
- 10:15-11:15 AM COAXIAL CABLES
- 11:20-12:15 PM TELEPHONE CABLE DESIGNS

**THURSDAY, DEC. 5, 1974**

- 10:15-11:15 AM NARROW BAND SYSTEMS AND OPTICAL TRANSMISSION CABLE
- 11:15-12:15 PM CABLE CONSTRUCTION TESTING: A METHOD, CONSTRUCTION, EXTENSION AND PROCESS CONTROL
- 12:15-1:15 PM TELEPHONE CABLE APPLICATIONS



23<sup>rd</sup> INTERNATIONAL  
WIRE & CABLE SYMPOSIUM  
*Reception & Banquet*  
LEFT MIGNON DINNER & ENTERTAINMENT  
GRAND BALLROOM  
THURSDAY DEC 5, 1974 7:30 PM  
See  
TICKETS  
12.  
RESERVATIONS  
ALL PRICES

## AWARDS

### *Outstanding Technical Paper*

### *Best Presentation*

H. Lubars and J. A. Olszewski, General Cable Corp.—"Analysis of Structural Return Loss in CATV Coaxial Cable"	1968	N. Dean, B.I.C.C.—"The Development of Fully Filled Cables for the Distribution Network"
J. B. McCann, R. Sabia and B. Wargotz, Bell Laboratories—"Characterization of Filler and Insulation in Waterproof Cable"	1969	J. D. Kirk, Alberta Government Telephones—"Progress and Pitfalls of Rural Buried Cable"
D. E. Setzer and A. S. Windeler, Bell Laboratories—"A Low Capacitance Cable for the T2 Digital Transmission Line"	1970	Dr. O. Leuchs, Kabel und Metalwerke—"A New Self-Extinguishing Hydrogen Chloride Binding PVC Jacketing Compound for Cables"
R. Iyengar, R. McClean and T. McManus, Bell Northern Research—"An Advanced Multi-Unit Coaxial Cable for Tool PCM Systems"	1971	S. Nordblad, Telefonaktiebolaget LM Ericsson—"Multi-Paired Cable of Nonlayer Design for Low Capacitance Unbalance Telecommunication Network"
		N. Kojima, Nippon Telegraph and Telephone—"New Type Paired Cable for High Speed PCM Transmission"
J. B. Howard, Bell Laboratories—"Stabilization Problems with Low Density Polyethylene Insulations"	1972	S. Kaufman, Bell Laboratories—"Reclamation of Water-Logged Buried PIC Telephone Cable"
Dr. H. Martin, Kabelmetal—"High Power Radio Frequency Coaxial Cables, Their Design and Rating."	1973	R. J. Oakley, Northern Electric Co., Ltd.—"A Study into Paired Cable Crosstalk"
D. Doty, AMP Inc.—"Mass Wire Insulation Displacing Termination of Flat Cable"	1974	G. H. Webster, Bell Laboratories—"Material Savings by Design in Exchange and Trunk Telephone Cable"



## CONTRIBUTORS

**AEG-Telefunken Kabelwerke AG, Rheydt**  
Mülheim/Ruhr-Saarn, West Germany

**3M Company—TelCom Department**  
Washington, D.C.

**Abbott Industries**  
**Chemical Division**  
Leominster, Massachusetts

**Albert H. Surprenant Inc.**  
Jaffrey, New Hampshire

**American Hoechst Corporation**  
Somerville, New Jersey

**Amoco Chemicals Corp.**  
Chicago, Illinois

**The Anaconda Company**  
**Aluminum Division**  
Louisville, Kentucky

**ARCO/Polymers, Inc.**  
Philadelphia, Pennsylvania

**Arnold Field Associates**  
Hackensack, New Jersey

**Arvey Corporation**  
Jersey City, New Jersey

**Austral Standard Cables Pty. Ltd.**  
Melbourne, Victoria, Australia

**Australian Telecommunication Comm.**  
**Central Administration**  
Australia

**Autometrix**  
Dayton, Ohio

**Baker Industries, Inc.**  
Hartselle, Alabama

**Belden Corporation**  
Geneva, Illinois

**Berk-Tek, Inc.**  
Reading, Pennsylvania

**BICC Limited**  
**Telephone Cables Division**  
Prescot, Merseyside, England

**Blane/Cooke Division**  
**Reichhold Chemicals, Inc.**  
White Plains, New York

**Boston Insulated Wire and Cable Company Limited**  
Hamilton, Ontario, Canada

**Brand-Rex Company**  
Willimantic, Connecticut

**Brand-Rex Limited**  
Glenrothes, Scotland

**Buchanan Crimp Tool Products**

**Amerace Corporation**  
Union, New Jersey

**Burgess Pigment Company**  
Sandersville, Georgia

**Burndy Corporation**  
Norwalk, Connecticut

**Cable Concepts Corp.**  
Levittown, Pennsylvania

**Cable Consultants Corp.**  
Larchmont, New York

**Cables de Comunicaciones S.A.**  
Zaragoza, Spain

**Camden Wire Co., Inc.**  
Camden, New York

**Campbell Technical Waxes Limited**  
Crayford, Kent, England

**Canada Wire and Cable Limited**  
Winnipeg, Manitoba, Canada

**Canadian Industries Limited**  
Brampton, Ontario, Canada

**Carlew Chemicals Ltd.**  
Montreal, Quebec, Canada

**R. E. Carroll, Inc.**  
Trenton, New Jersey

**Cerro Communication Products**  
Freehold, New Jersey

**Cerro Wire and Cable Company**  
New Haven, Connecticut

**Chase & Sons, Inc.**  
Randolph, Massachusetts

**Chemplast Inc.**  
Wayne, New Jersey

**Cimco Wire & Cable, Inc.**  
Allendale, New Jersey

**Cities Service Company**  
**Chester Cable Operations**  
Chester, New York

**Columbia Cable & Electric Corp.**  
Brooklyn, New York

**Communications Technology Corporation**  
Los Angeles, California

**Copperweld Corporation**  
Glassport, Pennsylvania

**Dart Industries**  
Paramus, New Jersey

**Davis Standard**  
Pawcatuck, Connecticut

**Delco Wire & Cable Inc.**  
Bristol, Pennsylvania

**Devcon Corporation**  
**Telephone & Power Products Div.**  
Danvers, Massachusetts

**Diamond Shamrock Corp.**  
Cleveland, Ohio

**The Dow Chemical Company**  
Midland, Michigan

**E. I. du Pont de Nemours & Co., Inc.**  
Wilmington, Delaware

**Economy Cable Grip Co., Inc.**  
So. Norwalk, Connecticut

**Edmands Company**  
**Division Wanskuck Company**  
Providence, Rhode Island

**Elco Corporation**  
Willow Grove, Pennsylvania

**Electrical Cable Div.**

**U. S. Steel Corp.**  
Worcester, Massachusetts

**Electroconductores C.A.**  
Caracas, Venezuela

**Electron Machine Corp.**  
Umatilla, Florida

**The Entwistle Company**  
Hudson, Massachusetts

**Essex International, Inc.**  
Decatur, Illinois

**Exxon Chemical Company, U.S.A.**  
Houston, Texas

**Fabiricon Manufacturing Limited**  
Trenton, Ontario, Canada

**Felten & Guillaume Carlswerk Aktiengesellschaft**  
5 Köln-Mülheim (Germany)

**Firestone Plastics Company**  
Pottstown, Pennsylvania

**Formulabs Industrial Inks Inc.**  
Escondido, California

**Foster Grant Co., Inc.**  
Leominster, Massachusetts

**The Fujikura Cable Works, Ltd.**  
Tokyo, Japan

**The Furukawa Electric Co., Ltd.**  
Tokyo, Japan

**Gavitt Wire & Cable Division**  
**RSC Industries, Inc.**  
Brookfield, Massachusetts

**General Cable Corporation**  
Colonia, New Jersey

**General Electric Company**  
**Chemical and Metallurgical Div.**  
Waterford, New York

**Glenair/Air Borne Controls, Inc.**  
Glendale, California

**B.F. Goodrich Chemical Company**  
Cleveland, Ohio

**W. R. Grace & Co.**  
**Hatco Plastics Div.**  
Brooklyn, New York

**Great American Chemical Corporation**  
Fitchburg, Massachusetts

**NKF Groep B.V.**  
Rijswijk, Holland

**GTE Service Corporation**  
Stamford, Connecticut

**Hardman Incorporated**  
Belleville, New Jersey

**Hepco Wire & Cable Industries**  
Garnerville, New York

**Hercules Incorporated**  
**Scott Wise Industries**  
Crowley, Louisiana

**Hercules Incorporated**  
Wilmington, Delaware

**Hewlett-Packard Company**  
**Manufacturing Division**  
Palo Alto, California

**High Voltage Eng. Corp.**  
Burlington, Massachusetts

**Hitachi Cable, Ltd.**  
Tokyo, Japan

**J. M. Huber Corporation**  
Edison, New Jersey

**Hudson Wire Company**  
Ossining, New York

**Ibaraki Electrical Communication Laboratory**  
**Nippon Telegraph & Telephone Public Corporation**  
Tokai, Ibaraki, Japan

**ICI United States Inc.**  
Wilmington, Delaware

**Icore International**  
Sunnyvale, California

**Independent Cable**  
Hudson, Massachusetts

**International Wire Products Co.**  
Wyckoff, New Jersey

**The J P M Company**  
Lewisburg, Pennsylvania

**Judd Wire Division**  
Turners Falls, Massachusetts

**Kenrich Petrochemicals, Inc.**  
Bayonne, New Jersey

**The Kerite Company**  
Seymour, Connecticut

**Lamart Corporation**  
Clifton, New Jersey

**S.A. Lignes Telegraphiques et Telephoniques**  
Conflans Sainte Honorine, France

**J. J. Lowe Associates, Inc.**  
Bedford Hills, New York

**Mobay Chemical Corporation**  
Pittsburgh, Pennsylvania

**Monsanto Industrial Chemicals Co.**  
St. Louis, Missouri

**The Montgomery Company**  
Windsor Locks, Connecticut

**S. R. Morrow Co.**  
Chatham, New Jersey

**Nesor Alloy Corporation**  
West Caldwell, New Jersey

**New England Printed Tape Co.**  
Pawtucket, Rhode Island

**NKF Groep B.V.**  
Rijswijk, Holland

**NKF Kabel B.V.**  
Delft, Holland

**NL Industries**  
**Industrial Chemicals Division**  
Philadelphia, Pennsylvania

**Nonotuck Manufacturing Company**  
South Hadley, Massachusetts

**Northeast Wire Company, Inc.**  
Holyoke, Massachusetts

**Northern Electric Co. Ltd.**  
Montreal, Quebec, Canada

**Northern Petrochemical Company**  
Des Plaines, Illinois

**The Okonite Company**  
Providence (Rumford), Rhode Island

**Olex Cables Ltd.**  
Cottenham, Victoria, Australia

**OY NOKIA AB**  
Helsinki, Finland

**The Pantasote Company of N.Y., Inc.**  
Passaic, New Jersey

**Pennwalt Corporation**  
Philadelphia, Pennsylvania

**Penreco**  
Butler, Pennsylvania

**Petro-Tex Chemical Company**  
Warminster, Pennsylvania

**PFD/Penn Color, Inc.**  
Doylestown, Pennsylvania

**Phelps Dodge Communications Co.**  
Yonkers, New York

**Phelps Dodge Copper Products Company**  
**Division of Phelps Dodge Industries, Inc.**  
Elizabeth, New Jersey

**Phelps Dodge Corporation**  
Puerto Rico

**Phillips Cables Limited**  
Brockville, Canada

**Phillips Petroleum Company**  
Bartlesville, Oklahoma

**Plastoid Corporation**  
Long Island City, New York

**Plymouth Rubber Co. Inc.**  
Canton, Massachusetts

**Polymer Services, Inc.**  
East Brunswick, New Jersey

**Radiation Dynamics, Inc.**  
Westbury, New York

**Radix Wire Company**  
Euclid, Ohio

**Raychem Corporation**  
Menlo Park, California

**Ray Proof Corp.**  
Norwalk, Connecticut

**Rexene Polymers Co.**  
Paramus, New Jersey

**Roanwell Corp.**  
New York, New York

**The Rochester Corporation**  
Culpeper, Virginia

**John Royle and Sons**  
Paterson, New Jersey

**Santech Incorporated**  
Toronto, Ontario, Canada

**Shell Chemical Company**  
Houston, Texas

**Soltex Polymer Corporation**  
Deer Park, Texas

**Southwest Chemical & Plastics Company**  
Seabrook, Texas

**Southwire Company**  
Carrollton, Georgia

**Sterling Davis Electric div.**  
**Sterling Extruder Corp.**  
Wallingford, Connecticut

**Storm Products Co.**  
Inglewood, California

**Sumitomo Electric U.S.A., Inc.**  
New York, New York

**Sun Chemical Corporation**  
Paterson, New Jersey

**Superior Continental Corporation**  
**Superior Cable Division**  
Hickory, North Carolina

**Syncro Machine Company**  
Perth Amboy, New Jersey

**Tamaqua Cable Products Corporation**  
Schuylkill Haven, Pennsylvania

**Technical Coatings Co.**  
Nutley, New Jersey

**Technion S.P.A.**  
Novara, Italy

**Teknor Apex Company**  
Pawtucket, Rhode Island

**Teledyne Thermatics**  
Elm City, North Carolina

**Teledyne Western Wire & Cable**  
Los Angeles, California

**Tenneco Chemicals, Inc.**  
**Organics & Polymers**  
Piscataway, New Jersey

**Tensolite Company**  
**Division of Carlisle Corp.**  
Tarrytown, New York

**Thermax Wire Corporation**  
Flushing, New York

**Times Wire & Cable**  
Wallingford, Connecticut

**Tracor, Inc.**  
East Orange, New Jersey

**Trea Industries, Inc.**  
East Greenwich, Rhode Island

**UBE Industries, Ltd.**  
Tokyo, Japan

**Uniroyal, Chemical Division**  
Naugatuck, Connecticut

**Union Carbide Corporation**  
**Chemicals & Plastics**  
Hackensack, New Jersey

**Videx Equipment Corp.**  
Paterson, New Jersey

**Western Electric Company, Inc.**  
Kearny, New Jersey

**G. Whittfield Richards Co.**  
Philadelphia, Pennsylvania

**Whitmor Wire & Cable Corp.**  
North Hollywood, California

**Wilson Products Company**  
Neshanic, New Jersey

**Wire & Textile Machinery Corp.**  
Pawtucket, Rhode Island

**Witco Chemical Corp.**  
**Sonneborn Division**  
New York, New York

**Wyre Wynd, Inc.**  
Jewett City, Connecticut

**Wyrrough and Loser, Inc.**  
Trenton, New Jersey

# TABLE OF CONTENTS

## TECHNICAL PROGRAM

**Tuesday, November 18, 1975 — 9:30 AM**  
**Hunterdon and Cumberland Rooms**

SESSION I: *Tutorial* — Wire and Cable Considerations in Fires

*Chairman* — I. Kolodny, General Cable Corp.

Panel Members

V. Sielert — General Telephone and Electronics Corp.  
 E. J. Coffey — Underwriters Laboratories, Inc.  
 G. Landis — Allendale Insurance

**Tuesday, November 18, 1975 — 2:15 PM**  
**Gloucester Room**

SESSION II: Flammability Consideration in Cables

*Chairman* — Marta Farago, Northern Electric

SOME DIFFERENCES NOTED IN THE FLAMMABILITY OF WIRE CONSTRUCTIONS BETWEEN TESTING AT ROOM TEMPERATURE AND AT ELEVATED CONDUCTOR TEMPERATURE, <i>E. C. Lupton, Jr., D. C. Tahlmore, J. Obsasnick, Allied Chemical Corp.</i>	1
HEAT RESISTANT CABLES FOR FIRE-PREVENTION SYSTEM, <i>T. Maezawa, Y. Murayama, and A. Yoshizawa, Furukawa Electric Co., Ltd.</i>	4
DEVELOPMENT OF IMPROVED FLAME RETARDANT INTERIOR WIRING CABLES, <i>S. Kaufman and C. A. Landreth, Bell Laboratories.</i>	9
THE DEVELOPMENT OF NEW FIREPROOF WIRE AND CABLE, <i>H. Matsubara, C. Matsunaga, A. Inoue and N. Yasuda, Sumitomo Electric Industries, Ltd.</i>	15
FIRE HAZARD EVALUATION OF CABLE AND MATERIALS, <i>E. J. Gouldson, G. R. Woollerton and J. A. Checkland, Northern Electric Co. Ltd.</i>	26

**Tuesday, November 18, 1975 — 2:15 PM**  
**Hunterdon Room**

SESSION III: Manufacturing and Processing

*Chairman* — J. M. Flanigan, Rural Electrification Administration

THE EXTRUSION OF HIGH DENSITY POLYETHYLENE INSULATED WIRE FOR FILLED TELEPHONE CABLES, <i>B. M. Brokke and J. C. Remley, Western Electric Co.</i>	37
PLASTIC INSULATING OF TELEPHONE WIRES IN ULTRA HIGH SPEEDS, <i>A. Riekkinen, Oy Nokia Ab, Finnish Cable Works</i>	43
ULTRA-HIGH SPEED EXTRUSION OF FOAMED POLYETHYLENE INSULATION FOR USE IN MULTI-PAIR TELEPHONE CABLES, <i>M. Okada and M. Rokunohe, Dainichi-Nippon Cables, Ltd.; Y. Ueno and J. Konishi, Mitsui Petrochemical Industries, Ltd.</i>	53
A NEW INSTRUMENT FOR NON-CONTACT TEMPERATURE MEASUREMENT OF MOVING WIRE, <i>D. L. Rall, Trans-Met Engineering, Inc. and S. M. Beach, Phillips Cable, Ltd.</i>	62
TELECOMMUNICATION OPTICAL FIBERS MANUFACTURING METHODS, <i>Dr. G. Manfre, Technion SPA</i>	67
FACTORS AFFECTING THE GRIP OF DIELECTRIC CORE WITHIN SUBMARINE COAXIAL CABLE, <i>J. H. Daane and S. Matsuoka, Bell Laboratories</i>	75

**Wednesday, November 19, 1975 — 9:15 AM**  
**Gloucester Room**

SESSION IV: Cable Applications I

*Chairman* — J. Neigh, AMP Inc.

SUBMARINE COAXIAL CABLE FOR CS-36M SYSTEM, <i>Y. Negishi, T. Yashiro and K. Aida, Nippon Telegraph and Telephone Public Corporation</i>	83
---	----

RF SHIELDING OF CABLES USING A PROTECTIVE AND CONDUCTIVE POLYMER, C. H. Clatterbuck and J. J. Park, NASA, Goddard Space Flight Center .....	92
WELDED POLYETHYLENE SPLICE CLOSURES — A RELIABLE ALTERNATIVE, D. Gill, Siemens Corp. ....	99
DESIGN CONSIDERATIONS, CHEMISTRY AND PERFORMANCE OF A REENTERABLE POLYURETHANE ENCAPSULANT, M. Brauer, N. L. Industries, Inc. and R. Sabia, Bell Laboratories .....	104
A "UNIVERSAL" COMMUNICATION COMPOUND?, J. E. Billigmeier, M. Filreis and J. D. Groves, 3M Co. ....	112

**Wednesday, November 19, 1975 — 9:15 AM**  
**Hunterdon Room**

SESSION V: Cable Design

*Chairman* — G. H. Webster, Bell Laboratories

OPTIMUM SHIELDED TWISTED PAIR CABLE DESIGN FOR DIGITAL DATA TRANSMISSION, J. Kincaid, Belden Corp. ....	126
GLASSFIBRE ARMoured PIC-TRUNK CABLES ASSEMBLED WITH CONNECTING PLUGS, Dr. G. Thonnessen, H. G. Dageforde and P. Gregor, AEG-Telefunken Kabelwerke AG Rheydt .....	136
MECHANICAL CHARACTERIZATION OF CABLES CONTAINING HELICALLY WRAPPED REINFORCING ELEMENTS, T. C. Cannon, Jr., and M. R. Santana, Bell Laboratories ....	143
RELATING THE TWIST DETECTION MEASUREMENTS OF TWISTED PAIRS TO THEIR CROSS-TALK PERFORMANCE, H. W. Friesen, Bell Laboratories .....	150
ECONOMIC ANALYSIS OF PROTOTYPE CABLE DESIGNS, J. Fairfield, General Cable Corp. ....	158

**Wednesday, November 19, 1975 — 2:15 PM**  
**Gloucester Room**

SESSION VI: Testing and Evaluation

*Chairman* — M. Tenzer, US Army Electronics Command

A CRITIQUE OF MILITARY WIRE MAXIMUM TEMPERATURE RATINGS, R. P. Fialcowitz, Douglas Aircraft Co. ....	164
A NEW FAULT LOCATOR FOR COAXIAL CABLES, T. Naruse, H. Yasuhara and M. Oguchi, The Fujikura Cable Works, Ltd., K. Asada, Nippon Telegraph & Telephone Public Corp. ....	168
PRECISION INSERTION LOSS MEASUREMENTS AND DATA ANALYSIS ON MULTIPAIR CABLE, J. Kreutzberg and T. D. Nantz, Bell Laboratories .....	175
DESIGN AND OPERATIONAL CHARACTERISTICS OF CABLE PRESSURE TELEMETRY SYSTEM, Y. Goto and M. Kusunoki, Nippon Telegraph & Telephone Public Corp. ....	180
CORROSION STUDIES ON SHIELDING MATERIALS FOR UNDERGROUND TELEPHONE CABLES, T. S. Choo, The Dow Chemical Co. ....	190

**Wednesday, November 19, 1975 — 2:15 PM**  
**Hunterdon Room**

SESSION VII: Cable Materials I

*Chairman* — J. E. Hager, Northern Petrochemical

OXIDATIVE STABILITY OF HIGH DENSITY POLYETHYLENE CABLES, Dr. P. N. Lee and B. S. Bernstein, Phelps Dodge .....	202
LOW TEMPERATURE BRITTLINESS OF LOW DENSITY POLYETHYLENE FOR CABLE JACKETING, H. Takashima, K. Yamaguchi, H. Kishi and S. Otomo, UBE Industries, Ltd. ....	213
COMPARISON OF TEST METHODS FOR DETERMINATION OF STABILITY OF WIRE AND CABLE INSULATION, Ms. E. T. Kotta, Bell Laboratories .....	220
IMPROVED TELEPHONE JACKET COMPOUNDS, S. Kottle and R. B. McAda, Dow Chemical U.S.A. ....	225
OXIDATIVE STABILITY STUDIES ON CELLULAR HIGH DENSITY POLYETHYLENE INSULATION FOR COMMUNICATIONS WIRE, D. D. O'Rell and A. Patel, Ciba-Geigy Corp. ....	231

**Thursday, November 20, 1975 — 9:15 AM**  
**Gloucester Room**

SESSION VIII: Cable Applications II

*Chairman — F. Farrell, 3M Corp.*

THE BARE BASE ELECTRICAL SYSTEM, <i>J. E. Wimsey, US Air Force</i>	237
MASS WIRE INSULATION DISPLACING HARNESS CONNECTOR SYSTEM, <i>D. Doty, AMP Inc.</i>	255
ENGINEERING FOR CABLE INSTALLATION, <i>V. W. Pehrson, General Cable Corp.</i>	260
UNDER-CARPET POWER AND COMMUNICATION WIRE SYSTEM, <i>J. Fleischhacker, AMP, Inc.</i>	270
INSERTION FORCES AND MECHANICAL STRENGTH OF 700-SERIES CONNECTOR INSTALLATIONS, <i>A. T. D'Annessa, J. J. Blee and D. T. Smith, Bell Laboratories</i>	276
ADVANTAGES OF OPTICAL T-CARRIER SYSTEMS ON GLASS FIBER CABLE, <i>Dr. J. E. Fulenwider and G. B. Killinger, GTE Laboratories</i>	282

**Thursday, November 20, 1975 — 9:15 AM**  
**Hunterdon Room**

SESSION IX: Cable Materials II

*Chairman — G. Heller, Tensolite*

THERMOPLASTIC POLYESTER COPOLYMERS AND THEIR BLENDS WITH VINYLs FOR MOLDED AND EXTRUDED ELECTRICAL APPLICATIONS, <i>Dr. M. Brown, E. I. du Pont de Nemours Co.</i>	292
ORGANO TITANATE COUPLING AGENTS FOR FILLED POLYMERS, <i>P. D. Sharpe, S. J. Monte and Dr. G. Sugerman, Kenrich Petrochemicals, Inc.</i>	300
TYPE 66 NYLON FOR WIRE AND CABLE APPLICATIONS, <i>A. Chen, Celanese Plastics Co.</i>	325
BLOCK POLYMER RUBBERS FOR WIRE AND CABLE APPLICATIONS, <i>J. L. Snyder and W. R. Hendricks, Shell Development Co.</i>	329
POLYMER ALLOYS FOR FLEXIBLE CABLE JACKETING, <i>F. Roesler and J. W. McBroom, Tenneco Chemicals</i>	335
RHEOLOGICAL AND MECHANICAL PROPERTIES OF A NEW POLYVINYLIDENE FLUORIDE RESIN SUITABLE FOR HIGH SPEED WIRE COATING, <i>J. E. Dohany, K. N. Davis and H. Stefanou, Pennwalt Corp.</i>	340

**Thursday, November 20, 1975 — 2:15 PM**  
**Hunterdon Room**

SESSION X: Waterproof Cable

*Chairman — J. Kanely, Superior Continental*

FULLY-FILLED CABLE WITH CELLULAR POLYETHYLENE INSULATION AFTER 10 YEARS SERVICE, <i>J. Pritchett, British Post Office; E. I. Mather, BICC Telecommunications Ltd., and S. Verne, BICC Research and Engineering Ltd.</i>	347
A NEW TYPE OF LONGITUDINALLY WATERPROOF TELEPHONE CABLE, <i>Dr. F. H. Kreuger, H. L. Gorissen, J. F. Kooy and J. P. I. van Kesteren, N. K. F. Kabel B. V.</i>	361
CHANGE OF CROSS-TALK PROPERTIES IN CORRELATION WITH THE INTERACTION OF POLYETHYLENE/PETROLEUM-JELLY, <i>H. A. Mayer, H. J. Anderka and H. G. Dageforde, AEG-Telefunken Kabelwerke AG Rheydt</i>	365
EVALUATION OF ADHESIVE AND COHESIVE CHARACTERISTICS OF PETROLATUM BASED FLOODING COMPOUNDS, <i>T. E. Luisi and J. J. Kaufman, Witco Chemical Corp.</i>	374
THE PROPERTIES OF CELLULAR POLYETHYLENE INSULATED FILLED COMMUNICATION CABLE AND ITS INCREASING USE, <i>D. F. Cretney, S. M. Beach and K. R. Bullock, Phillips Cables Ltd.</i>	379
CAPACITANCE RELATIONSHIPS IN FILLED TELEPHONE CABLES AND EQUILIBRIUM PREDICTION FROM WATER IMMERSION TESTS, <i>J. A. Olszewski, General Cable Corp.</i>	399



SOME DIFFERENCES NOTED IN THE FLAMMABILITY OF WIRE  
CONSTRUCTIONS BETWEEN TESTING AT ROOM TEMPERATURE  
AND AT ELEVATED CONDUCTOR TEMPERATURE

E. C. Lupton, Jr., C. D. Tahlmore and J. Obsasnik  
Allied Chemical Company  
Morristown, NJ 07960

#### SUMMARY

Theoretical and experimental work has indicated that the flammability of a material increases as its temperature at the moment of flame exposure is increased. We have noted that when flammability tests are conducted on various wire types with their conductor at the rating temperature, results are sometimes observed which are substantially different from results at room temperature. These data are discussed.

#### I. INTRODUCTION

Flammability of wire and cable is becoming an increasingly important consideration for selection of the styles to use for particular applications. In several recent fires, including the telephone switching center fire in New York City, and the Brown's Ferry Nuclear Power Plant fire<sup>1</sup>, it is believed that the wiring system was either partially or totally responsible for allowing a small fire to propagate, spread and do extremely extensive damage. Many tests are now in use or proposed to help an engineer evaluate the flammability and fire retardance of constructions but we have recently become aware of a possible use condition which none of these tests, to our knowledge, take into account.

In a survey of wire and cable engineers, Watkins<sup>2</sup> found that the temperature rating of a construction is considered the second most important single factor in deciding whether its use is appropriate for a particular application. Constructions are now commonly considered which range in continuous high temperature limit from +60°C or below to +260°C or above. The advantages of high temperature, high performance, small diameter constructions are becoming well understood in terms of space saving, weight saving, conductor diameter reduction, ease of installation, and long service life and these constructions take advantage of higher possible use temperatures. Energy saving consideration, and long service life and these conductor diameter reduction, ease of installations and optimum efficiency of industrial operations can also necessitate higher temperatures. It therefore seems realistic to expect that wire and cable constructions will be in common use in the future at increasingly higher temperatures. There is data in the literature indicating that when the temperature of a material is increased, before it is exposed to flame, the flammability increases

also. Johnson<sup>3</sup> has shown that, for a variety of materials, the limiting oxygen index decreases in a predictable way as the temperature of the material increases. (The limiting oxygen index measures the percentage of oxygen required in the atmosphere for an equilibrium downward burning flame to be sustained.) Johnson<sup>3</sup> shows that for several different materials, the limiting oxygen index can be approximately predicted by the use of Table I.

Table I. Effect of Material Temperature upon Oxygen Index

Temperature (°C)	Fraction of 25°C Oxygen Index Retained
25	1.00
100	.92
200	.78
300	.55

While limiting oxygen index does not correlate directly with any flammability properties of wire and cable, these data suggested to us that flame testing on wire and cable constructions which are at their intended use temperature might yield results which are significantly different from room temperature results.

#### II. SCOPE

The results reported here will involve measurements of several different types on several different constructions. Examples are chosen to illustrate differences between room temperature and elevated temperature results.

It is beyond the scope of this work to delineate exhaustively the safe limits of any construction. It is specifically not our intent to single out constructions as "good" or "bad" but rather to suggest that the observed phenomena are so ubiquitous that they should generally be considered by engineers. For this reason, individual wire styles will not be identified by insulation or conductor type but only as styles A through E. In selecting examples, we chose conditions such as the following which would indicate degradation in the fire retardant properties of wire:

- a) Dripping flaming insulation
- b) Propagating flame more rapidly

- c) Propagating flame for a longer period of time or a greater length

### III. RESULTS

All measurements were conducted in a flame hood which was made as draft free as possible. This hood did not have the capability of being raised to elevated temperature, so for the elevated temperature testing a current was passed through the test wire or wires to raise it to its recommended rating temperature. The temperature of the wire was measured by thermocouples placed next to the conductor and on the outside of the insulation and these measurements were confirmed by optical pyrometer. The currents required are higher than would normally be used with these constructions but in the absence of an oven equipped for safe flame testing, this seemed the most appropriate way to attain the required temperatures. The current was measured by a clamp-on ammeter.

Example A - A sample of wire insulated by material A was placed in the draft free hood at an angle canted 30° away from the vertical. A piece of Johnson and Johnson surgical cotton, with no pretreatment or drying, was placed at the base of the wire. A bunsen burner with a flame height of 3 inches was applied to the test wire four inches from its base. The barrel of the burner was parallel to the base of the chamber and pointed as in Figure I. The following results were obtained at room and at rating temperature. The insulation was colorless.

	Affected Length	Afterburn Time	Drips
Room Temp.	3 in.	2 sec.	Yes
Rating Temp.	4 in.	14 sec.	Yes (25% lit the cotton)

Example B - Wire insulated with material B, which is similar in rating temperature and chemical structure, to material A, was tested in a manner similar to material A. The insulation was colorless. The results were:

	Affected Length	Afterburn Time	Drips
Room Temp.	2 in.	0 Sec.	None
Rating Temp.	2.5 in.	0 Sec.	None

Example C - Four wires insulated with material C were twisted together to form a bundle. The bundle was placed in a vertical position. The flame holder was a piece of pipe 4 inches long and 1/16 in inside diameter. It used no premixing of gas with air, so that there was a cold (yellow) flame, which was approximately 3 inches long.

When the flame was applied perpendicular to the wire continuously, the following results are obtained. The times listed are the

time to set on fire a marker flag a particular distance above the place of fire introduction.

	6"	12"	18"
Room Temp.	120 Sec.	Never	Never
Rating Temp.	20 Sec.	75 Sec.	180 Sec.

The wires tested at room temperature burned approximately 7 inches above the point of flame exposure. After 200 seconds, the wires tested at rating temperature had to be extinguished for safety reasons, but had propagated upward for approximately 22 inches and were continuing to propagate vigorously.

In another test of the 4 cable bundle of material C the flame was applied for 30 seconds and the afterburn time was determined.

	Afterburn Time
Room Temperature	1-5 Seconds
Rating Temperature	25-55 Seconds

Example D - Wire insulated with material D was tested in a vertical position. When a bunsen burner is exposed to the wire with the flame perpendicular to the wire, the following afterburn times are noted:

	5 Sec.	10 Sec.	15 Sec.
	Exposure	Exposure	Exposure
Room Temp.	0 Sec.	3 Sec.	7 Sec.
Rating Temp.	3 Sec.	7 Sec.	11 Sec.

If the small cold flame described in Example C is exposed to the wire for a long duration, the observed results are

	Length of the bare wire, charred or melted insulation
Room Temp.	1 1/2 inches
Rating Temp.	4 inches

Example E - Wire insulated with material E, which is identical in rating temperature to Material D, was tested in a vertical flame test with the flame canted 10° to the test wire. The results are the following:

	Bare, Charred or Melted Insulation	Afterburn
Room Temp.	2 inches	0 Sec.
Rating Temp.	1.5 inches	0 Sec.

### CONCLUSIONS

In several different examples it is shown that for some insulation materials under some conditions the following differences are noted between flammability testing at room temperature and at the materials rating temperature:

- The test wire is charred for a greater portion of its length
- The wire continues to burn for a longer period of time after the test flame is removed
- The flame propagates upward more rapidly

For at least one material, the following differences were noted:

- A construction which would not propagate flame upward at room temperature



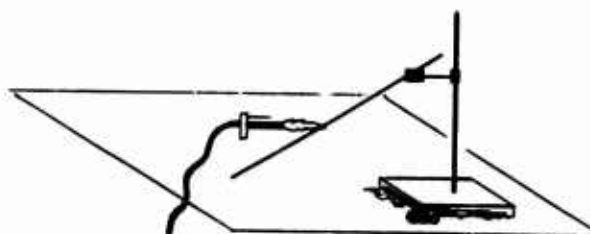
- would at the rating temperature
- e) A construction dripped flaming insulation at the rating temperature which would not at room temperature

These results suggest that room temperature flammability testing is not always adequate to determine the fire retardance of a wire construction. For those constructions which are intended for use at temperatures significantly above 25°C and which require fire retardance, testing at use temperature would seem to be required in order to assure fire safety.

#### References

1. L. King, Chemical Tech. 348 (June 1975)
2. W. D. Watkins, U.S. Naval Avionics Facility, Personal Communications
3. P. R. Johnson, Journal of Applied Polymer Science, 18, 491-504 (1974)

Figure I. Testing Arrangement for Examples A & B



Dr. Elmer C. Lupton, Jr. directs fluoropolymer Applications Research for the Specialty Chemicals Division of the Allied Chemical Corporation. He is engaged in development of wire and cable products in several areas including transit, utility, military and computers. Dr. Lupton is a member of the Society of Plastics Engineers, the American Chemical Society, Phi Lambda Upsilon and Sigma Xi and is technical consultant to the NEMA high temperature wire committee and the A2H committee of the SAE. He holds an S. B. degree from MIT and a PhD from Yale University.

Mr. C. David Tahlmore is a research engineer with the Specialty Chemicals Division of the Allied Chemical Corporation. Presently he is responsible for characterizing the electrical properties of a broad line of both thermoplastics and thermosets, with emphasis on line and cable products. Previously his efforts were devoted to thermoset compound development for electrical applications.

Mr. Tahlmore is a member of ASTM Committee D-09 on electrical insulation.

Mr. John Obsasnik is a Process Engineer with the Specialty Chemical Division of the Allied Chemical Co. Currently he is developing several improved processes for monomer and polymer synthesis. He has a BS degree from Newark College of Engineering and is a member of the American Institute of Chemical Engineers.

# HEAT-RESISTANT CABLES FOR FIRE-PREVENTION SYSTEMS

T. MAEZAWA, Y. MURAYAMA and A. YOSHIKAWA

The Furukawa Electric Co., Ltd, Tokyo, JAPAN

## ABSTRACT

It is necessary to effectively connect sensors and indicators to prevent fires in subways, hotels, etc.

The present report describes the details of the designs and the evaluation of the cables for this purpose. This report discusses the following.

1. The cores of the cable are separated by means of the S-shaped heat-resistant tape. (Type 1)
2. The cable is designed simply using cross-linked polyethylene. (Type 2)
3. The cable is designed so as to resist higher temperatures by using silicon rubber. (Type 3)
4. The cable is designed so as to be used also in the frequency ranges beyond the voice frequency. (Type 1, 2 and 3)

## 1. INTRODUCTION

When a fire breaks out where many people are gathered, for example in subways, hotels, offices, and department stores, there is a possibility that peoples movements by the mob spirit may result in an unexpected disaster. In order to prevent such disaster, it is necessary to systematically and effectively arrange sensors and indicators, and to monitor and control them at required places.

For example, when a sensor, which reacts to the rise in temperature or to the generation of smoke, and a liaison interphone is installed in each room of a hotel, they should be monitored somewhere and adequate instructions should be given through the interphone. If the cable connecting such equipment is damaged and put out of commission by a fire, these many sensors and interphones would become meaningless. Therefore, the construction, materials, and testing methods for the cables that are fit for such purpose are discussed. The materials for such cables are required to be heat-resistant and have good electrical properties when they should be easy. Consequently, glass mica tape, cross-linked polyethylene and silicon rubber have been chiefly examined. Basing on the actual circumstances of Japan, the cables were tested by burning them under two conditions: at 380°C for 15 mins. (Grade B), and at 840°C for 30 mins. (Grade A). A large number of designs for cable construction have been discussed with many materials. As the result, three types of the cables, Type 1, Type 2 and Type 3, have been developed, of which details are described in the present report.

## 2. REQUIREMENTS

Since the most important property necessary for the cables of a fire-prevention system is to fulfill their functions when a fire breaks out, satisfactory properties at high tem-

peratures are required. And the method of use of the cables, which decides the temperature, should also be duly considered.

The temperature when a fire breaks out depends upon the structure of the building, amount of combustibles, amount of air that flows in, and so on. But in Japan, the standard curve of heating temperature shown in Fig. 1 is generally received. Basing on it, some wiring methods have been developed, such as the wiring by burying a cable in a main fire-retardant construction and the wiring with an adequate heat protection (see Fig. 2 and Fig. 3). These wiring methods can chiefly be adopted when ordinary cables are used for a fire-prevention system, but they can not be adopted where the buildings are not newly-built or the equipment is to be enlarged. Thus, we have developed a new open wiring method, that is wiring cable of the same properties as those used in the above-mentioned methods without burying the cable in the structure.

This method requires the following cable properties.

Table 1 Requirements

	Grade A	Grade B
Tensile Strength		
Conductor:	> 28.0 Kg/mm <sup>2</sup>	> 28.0 Kg/mm <sup>2</sup>
Insulator:	> 1.0 Kg/mm <sup>2</sup>	> 1.0 Kg/mm <sup>2</sup>
Sheath:	> 1.0 Kg/mm <sup>2</sup>	> 1.0 Kg/mm <sup>2</sup>
Heat-Resistant Properties (see Fig. 1)		
Insulation Resistance:		
	0.2MΩ or over (840°C, 30mins)	0.1MΩ or over (380°C, 15mins)
Dielectric Strength:		
	AC 250 V/min (840°C, 30mins)	AC 250 V/min (380°C, 15mins)

The heat resistant properties of Grade A are the most severe requirements, which seem hard to be satisfied by usual methods. Of course, the same properties as those of ordinary communication cables are required.

## 3. HEAT-RESISTANCE TEST

The testing methods for the heat-resistant properties are as shown in Fig. 4, Fig. 5 and Fig. 6. A cable sample is fixed to the heat-resistant board and the insulation resistance is measured after being heated in accordance with the curve of heating temperature shown in Fig. 1. And while the sample is heated, the insulation resistance and dielectric strength are measured.

## 4. DESIGN AND MANUFACTURE

After the requirements of the heat-resistant cables had been fixed, the cables were designed and manufactured.

For designing the cables, materials and construction of the cables was investigated. The following materials shown in Table 2 were investigated.

Table 2 Heat-Resistant Materials

Material	Application
Heat-resistant polyvinyl chloride (PVC)	Extruding
Cross-linked polyethylene (PE)	Extruding
TFE	Extruding
Polyimide	Coating
Mica polyester tape	Lapping
Silicon glass tape	Lapping
Glass mica tape	Lapping
Silicon rubber	Extruding

Heat-resistant polyvinyl chloride was not considered because it was inferior to polyethylene in its insulation resistance under normal conditions. TFE was also not considered because its extruding was difficult and it was costly. Polyimide was also not considered because it was difficult to remove polyimide, which was used as an insulator, when connecting cables. But this material seems to be useful as an effective heat-resistant material for cables of large-sized conductors. The S-shaped construction as shown in Fig. 8 was adopted for lapping cores with tape in order to make it easy to manufacture cables. It was desirable to insert the tape during twisting of the cores, because the same properties as those of ordinary communication cables were required of the cable. Silicon rubber was employed as an insulating material because the use of special silicon rubber appeared to make it possible to manufacture the cables that satisfy Grade A.

Then, three types of cables shown in Fig. 7, Fig. 8, and Fig. 9 were manufactured and the evaluation tests were made on them. Several kinds of shields and sheaths of the cable were selected and combined. The results of the evaluation tests are shown in Table 3.

As for the cables of Type 1, both the silicon glass tape (glass tape on which silicon rubber is coated) and the mica polyester tape (polyester tape on which mica tape is stuck) short-circuited after the heat-resistance test, which, therefore, was judged to be unsatisfactory. But the glass mica tape (glass tape on which mica tape is stuck) appeared to satisfy the requirements having no reference to the presence of the shield. Therefore, the final design was made using such construction.

Since the cables of Type 2 were affected by the sheath materials, heat-resistant polyvinyl chloride was adopted for the sheath for the final design.

As for the cables of Type 3, the heating temperature reaches as high as 840°C which burns or melts all the materials except copper, and it is very difficult to keep the form of the cable. Therefore, it was desired to keep the cable form to satisfy Grade A, and the construction shown in Fig. 10 was adopted for the final design.

## 5. EVALUATION

Three kinds of cables of Type 1 of different outside diameters were manufactured and the heat-resistance tests were made on them. These results are shown in Fig. 11. These results considerably exceed the goal values and it is confirmed that this design satisfies Grade B. The results of the measurements of the electrical characteristics are shown in Fig. 12. These results conclude that the cables

of Type 1 can be used for Grade B in a similar way as ordinary communication cables.

The cables of Type 2 of three different outside diameters were manufactured, and their heat-resistances and electrical characteristics were measured. The insulation resistances of the heat-resistance tests were lower than those of the cables of Type 1, but they satisfy Grade B. Consequently we estimate that, if great importance is attached to the electrical characteristics under normal conditions, the use of the cables of Type 2 may be more advantageous. The results of the tests are shown in Fig. 13 and Fig. 14.

The cables of Type 3 were manufactured in accordance with the final design and the tests were made on them. The test results, shown in Fig. 15, shows that the cables satisfy Grade A. Only the cables of small outside diameters were manufactured because it is well known, by the former tests when a weight (W in Fig. 4, 5, and 6) of two times cable's own weight is loaded on the cable, that the smaller cables are more readily deformed.

## 6. CONCLUSION

The open wiring of the heat-resistant cables is possible and the cables of the same degree as those of ordinary communication cables can be manufactured. We made it possible to choose various combinations of the cables depending, especially, on the temperature and time. (For example, if the cable for 380°C, 30mins. is required, it may be obtained by combining the cables of Type 1 and 2.) And the cables that will resist the temperature as high as 840°C are also obtainable.

We believe that these cables are absolutely necessary for the development of fire-prevention systems.

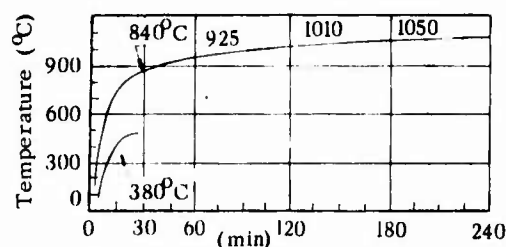


Fig. 1 Standard curve of heating temperature

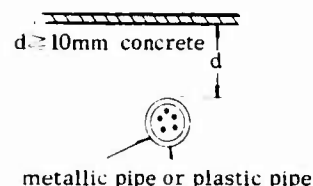


Fig. 2 Wiring in fire retardant main construction

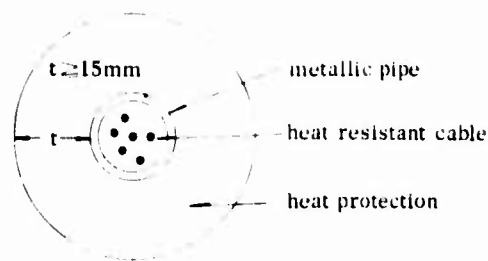


Fig. 3 Heat protection of unburied wiring

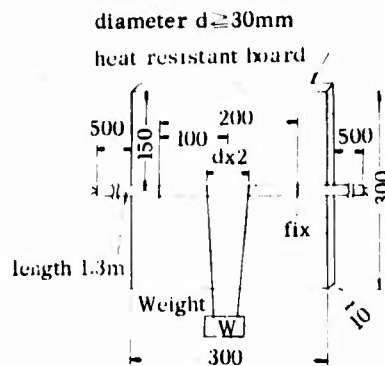


Fig. 4 Sketch of cable sample fixed for heat resistance test

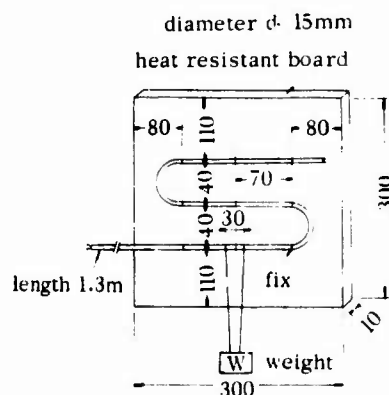


Fig. 5 Sketch of cable sample fixed for heat resistance test

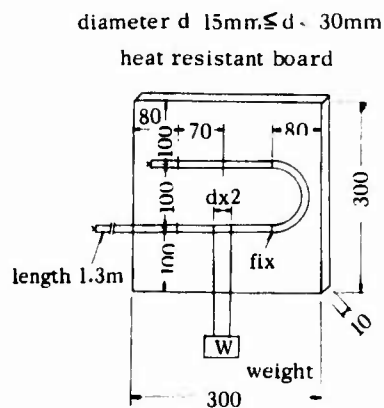


Fig. 6 Sketch of cable sample fixed for heat resistance test

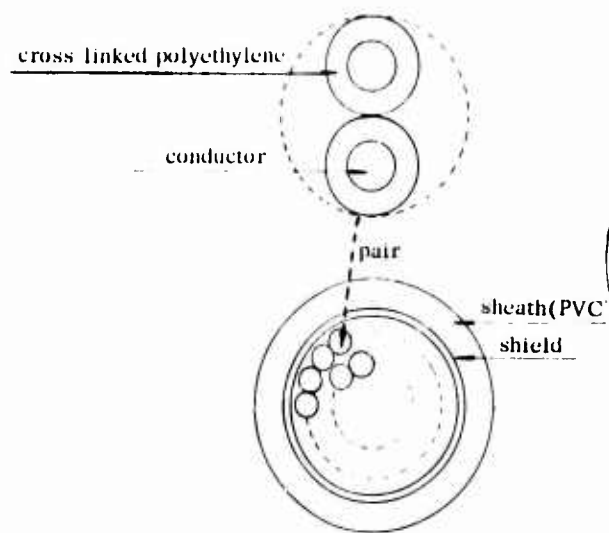


Fig. 7 Construction of cable (Type 2)

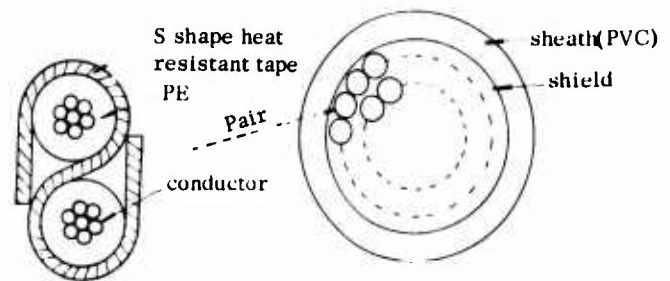


Fig. 8 Construction of Cable (Type 1)

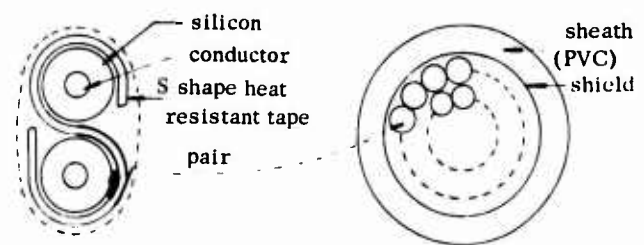


Fig. 9 Construction of cable (Type 3)

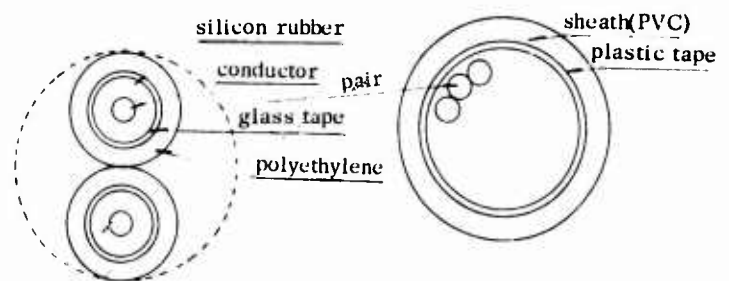


Fig. 10 Construction of cable (Type 3)

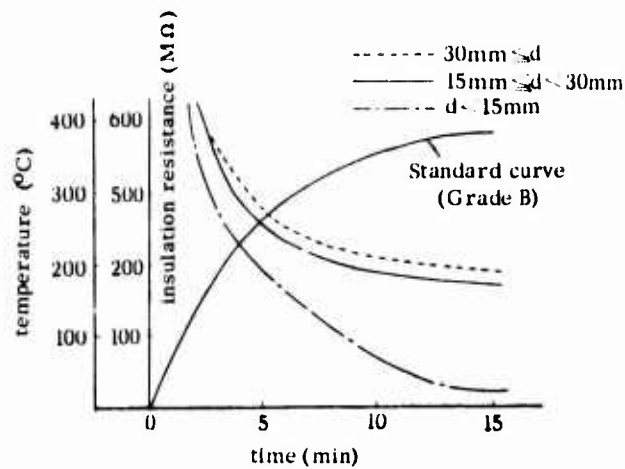


Fig. 11 Heat resistance test

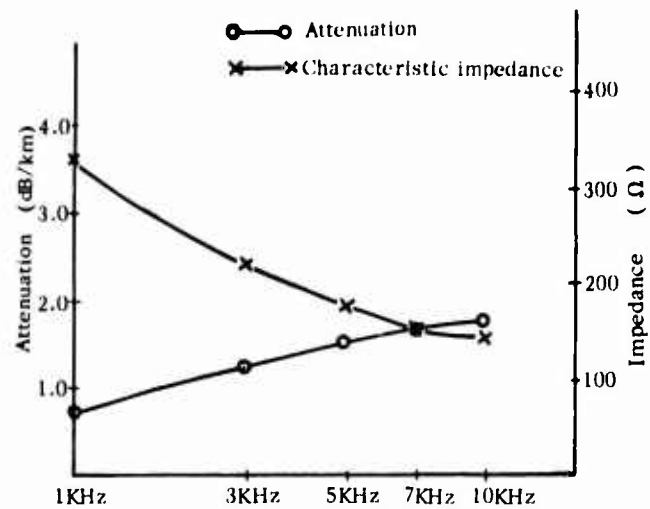


Fig. 14 Frequency characteristic of heat resistant cable

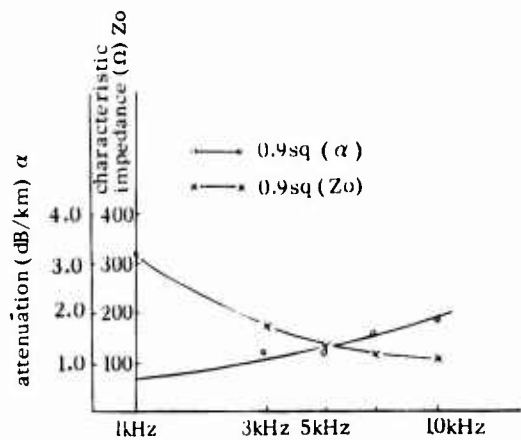


Fig. 12 Frequency characteristic of heat resistant cable

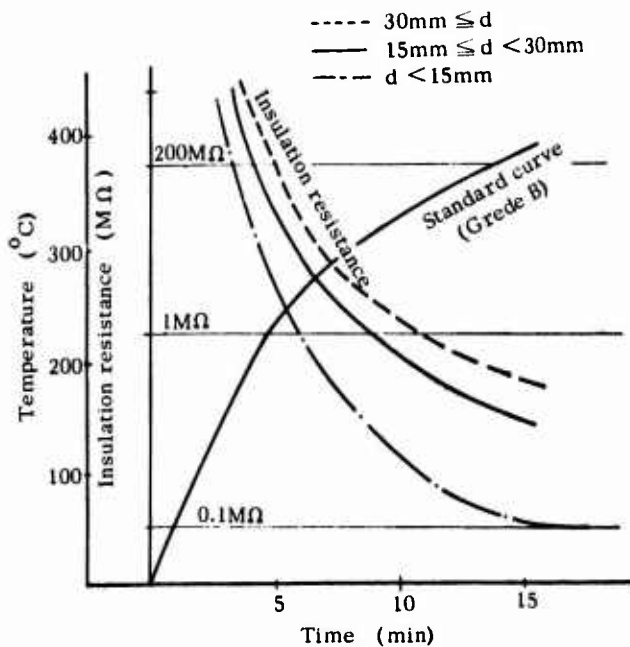


Fig. 13 Heat resistance test

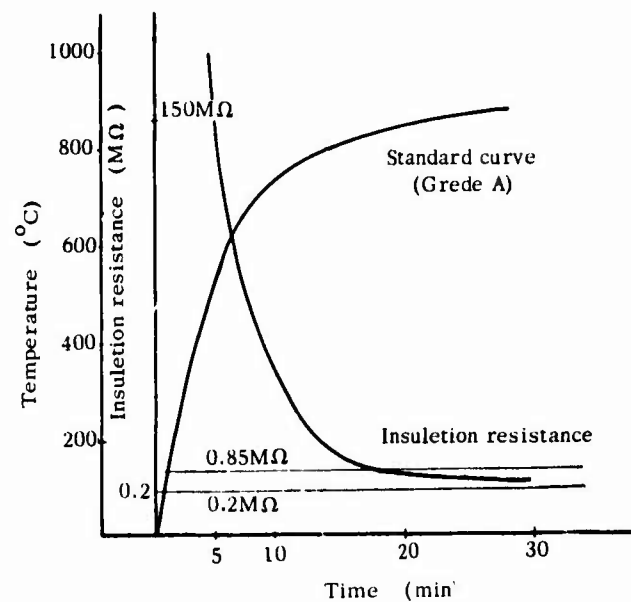


Fig. 15 Heat resistance test

## 7. REFERENCE

- 1) T. Maezawa, A. Yoshizawa: Heat resistant cable for fire-preventive system [1]  
The Furukawa Electric Review No. 57
- 2) T. Maezawa, I. Nakajima: Fireproof leaky coaxial cable  
The Furukawa Electric Review No. 57

### TAKAYOSHI MAEZAWA

Furukawa Electric Co., Ltd.  
6-1 Marunouchi 2-chome  
Chiyoda-ku, Tokyo 100, Japan



TAKAYOSHI MAEZAWA is Assistant Manager, Engineering Section Telecommunication Division, The Furukawa Electric Co., Ltd. and is mainly engaged in the designing of the telecommunication cable.

He received his B. E. degree in electrical engineering Keio University in 1963.

### YOSHIAKI MURAYAMA

Furukawa Industrial S.A. Produtos Eletricos  
Avenida Sao Joao, 473-15.º Andar.  
Caixa Postal 176,  
Sao Paulo, Brazil



YOSHIAKI MURAYAMA joined the Furukawa Electric Co., Ltd. in Japan in 1954 and had been associated with the development, the design and the manufacture of telephone cables since that time.

In 1975 he transferred to Furukawa Industrial S.A. in Brazil and is now the Manager of the Telephone Cable Engineering Department. He received his B. E. degree in Telecommunication Engineering from Waseda University in 1954.

### AKIO YOSHIZAWA

Furukawa Electric Co., Ltd.  
6-1 Marunouchi 2-chome  
Chiyodaku, Tokyo 100, Japan



Graduating from NIHON University Mr. AKIO YOSHI-ZAWA joined The Furukawa Electric Co., Ltd. in Japan in 1970 and had been associated with the development, the design of telephone cables since that time.

At present he is Engineering section, telecommunication Division of the Company.



# DEVELOPMENT OF IMPROVED FLAME RESISTANT INTERIOR WIRING CABLES

by

S. Kaufman and C. A. Landreth  
Bell Laboratories  
Norcross, Georgia 30071

## ABSTRACT

A PVC flexible jacket compound with an oxygen index of 32% has been developed without sacrificing good low temperature brittleness properties. The high oxygen index was achieved by minimizing the plasticizer level and substituting fine particle size hydrated alumina as a filler/flame-retardant for the inert filler, calcium carbonate. Preliminary data on inside wiring cable jacketed with the new material satisfied the goal of a flame spread classification of 25. A vertical corner test also shows the progress made in improving the cable's resistance to flame spread.

## INTRODUCTION

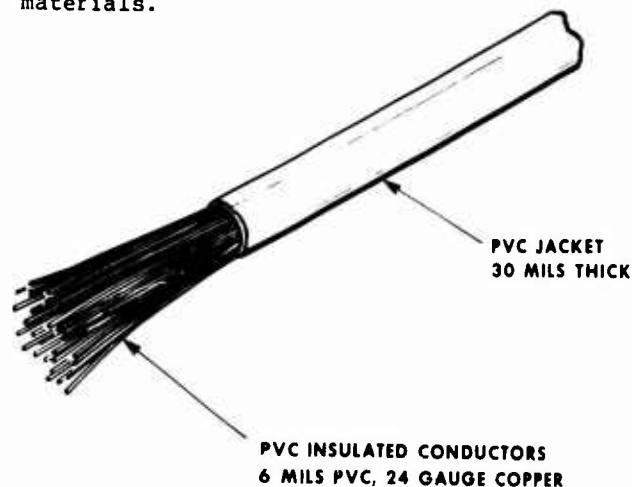
Since flame retardancy is a prime requirement for the Bell System's inside wiring cables, these cables are insulated and jacketed with poly(vinyl chloride) (PVC) compounds. Rigid (unplasticized) PVC is a highly flame retardant polymer (oxygen index 45%), but it is unsuitable for wire insulation and cable jackets. Compounding with 30 phr (parts per hundred of resin) of plasticizer yields a semirigid compound suitable for wire insulation, but the combustible plasticizer causes the oxygen index of the compound to be lowered to approximately 28%. A typical flexible jacket compound containing 45 phr plasticizer and 3 phr of a flame retardant also has an oxygen index of approximately 28%.

In recent years there has been an evolution toward increasingly stringent flame spread standards in building codes, fire codes, and in the Bell System's design standards. At the present time a flame spread classification (FSC) of 25 or less, when the cables are tested in the twenty-five foot tunnel test (ASTM E-84)\* is being sought. Bell Laboratories has undertaken a flame resistant PVC project with the objective of developing improved PVC compounds which permit the design of cables that satis-

fy the FSC of 25. This paper describes the development and testing of an inside wiring cable that has a flame spread classification of 25 as determined in a twenty-five foot tunnel test. Also, the results of a vertical corner fire test are presented. This type of test could be more indicative of the flame spread of vertical cable installations.

## CABLE CONSTRUCTION

Inside wiring cable (Figure 1) is primarily used for wiring to key telephone sets. The core is made up of twisted pairs of 24 gauge copper conductors insulated with 6 mils of semirigid PVC compound. Unlike outside plant cables, inside wiring cables do not have a core wrap or shield. The jacket is a 30-35 mil thick (depending on cable size), flexible, light olive grey, PVC compound. Central office cable is of similar construction and uses identical materials.



25 PAIR INSIDE WIRING CABLE

FIGURE 1

The formulation of the current insulation and jacket compounds are shown in Table I. Alternate formulations incorporating other phthalate plasticizers are used, but for convenience only those with a C<sub>7</sub>, C<sub>9</sub>, C<sub>11</sub> (711) phthalate are shown. The key properties of the jacket compound are a brittleness temperature of -28°C and an oxygen index of 28%. The wire insulation has the same oxygen index.

\* Strictly speaking ASTM-E84 is a building materials test and does not apply to cable. However, appropriate modifications have been made in order to test cable.

TABLE I

Component	Current Flexible Jacket		Semirigid Wire Insulation	
	phr	wt.-%	phr	wt.-%
Resin PVC	100	52.9	100	71.2
Plasticizer 711 Phthalate	45	23.8	24	17.6
Processing Aid Diphenyl Phthalate	-	-	5	3.7
Flame Retardant Antimony Trioxide	3	1.6	-	-
Stabilizer Dibasic Lead Phthalate	-	-	7	5.1
Tribasic Lead Sulphate	5	2.5	-	-
Filler Calcium Carbonate	35	18.5	-	-
Lubricant Petroleum Wax	0.5	0.3	-	-
Dibasic Lead Stearate	0.5	0.3	0.3	0.2
Amide Wax	-	-	0.3	0.2

### MATERIALS DEVELOPMENT

The objective of the materials development was to design a PVC compound which maximized flame retardancy while at the same time maintaining the flexibility and low temperature impact resistance of the flexible jacket compound in Table I, i.e., maintain a brittleness temperature of  $-28^{\circ}\text{C}$  while maximizing oxygen index. A more extensive discussion of the problems involved in balancing flame retardancy and low temperature properties in the design of PVC compounds is given in Reference 1.

In order to investigate the effect of plasticizer concentration and filler levels on brittleness temperature and other properties, a series of compounds were prepared. A 711 phthalate plasticizer was used at three concentrations, 35, 40, and 45 phr. At each plasticizer concentration, the effect of varying the level of hydrated alumina filler was determined. A fine particle size (1 micron) alumina was used since it has been shown that larger particle size fillers severely degrade low temperature properties<sup>1</sup>. Standard sample preparation and test methods were used (See Appendix A).

Figure 2 shows the variation of brittleness temperature with plasticizer concentration and filler level. Filler level is expressed as volume fraction and not phr since volume fraction is a more fundamental parameter. For convenience, the filler level in phr is also shown. The brittleness temperature objective can be met with 40 phr plasticizer, and up to 30 phr of fine particle size filler. Use of 45 phr plasticizer (the level in the flexible jacket compound) results in compounds that meet the brittleness temperature objective if the filler level is below 50 to 55 phr.

The effects of plasticizer concentration and flame retardant filler level on oxygen index are shown in Figure 3. Antimony trioxide ( $\text{Sb}_2\text{O}_3$ ), at 3 phr, is included in all the compounds. The predominant influence of plasticizer level in determining oxygen index is evident. The compound con-

taining 40 phr plasticizer and no filler has an oxygen index of 31%. In order to attain this oxygen index with a compound containing 45 phr plasticizer, approximately 50 phr of hydrated alumina must be added. Based on brittleness temperature and oxygen index, the optimum compound is one with 40 phr plasticizer and 30 phr hydrated alumina. It has an oxygen index of 32%.

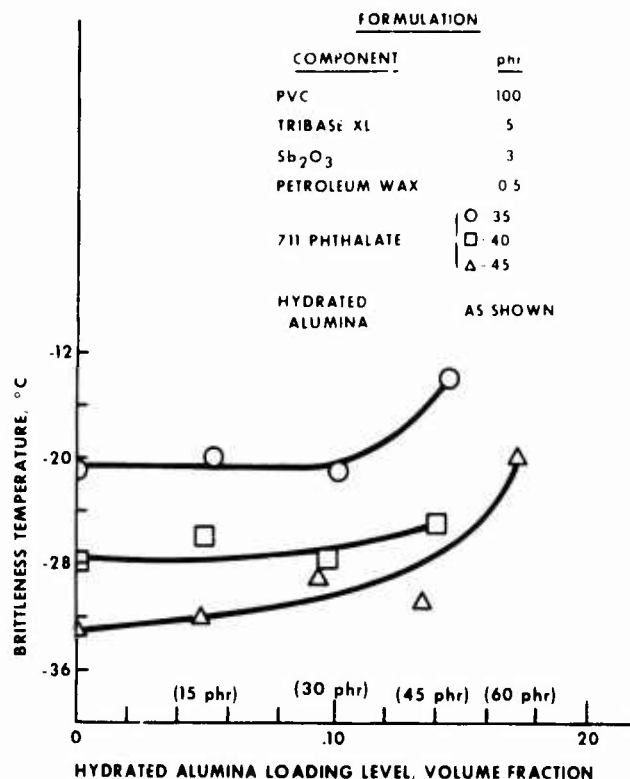


FIGURE 2

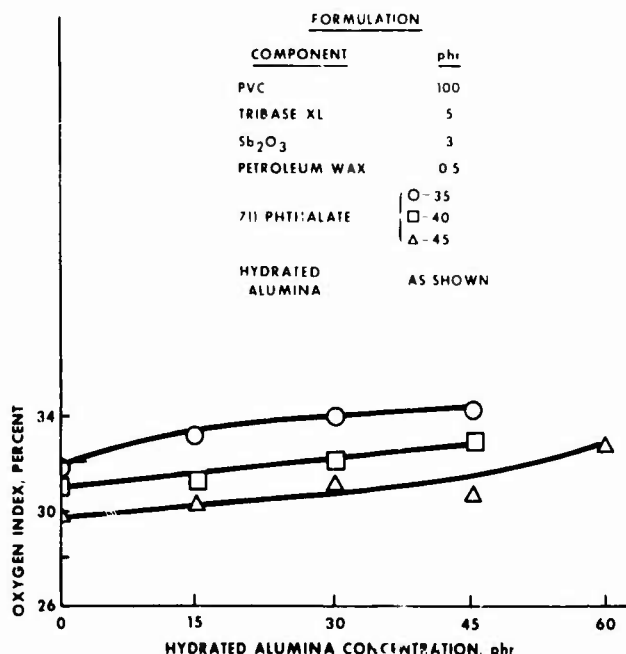


FIGURE 3



Figures 4, 5, and 6 show the variations of shear, tear and tensile strengths, respectively. In order to provide a frame of reference, the typical properties of the flexible jacket are also shown. The addition of the fine particle size hydrated alumina has its greatest effect on shear strength, Figure 4. The decrease in shear strength that occurs with increasing filler loading is most pronounced in the compounds containing 35 phr of plasticizer. The shear strengths of the 40 phr plasticized compounds are close to the typical value for the flexible jacket compound. The tear strength of the 40 and 45 phr plasticized compounds are close to the typical value for flexible jacket compound, Figure 5. Tensile strength decreases gradually with increasing filler loading, Figure 6. The compounds have tensile strengths close to the typical value for the flexible jacket compound.

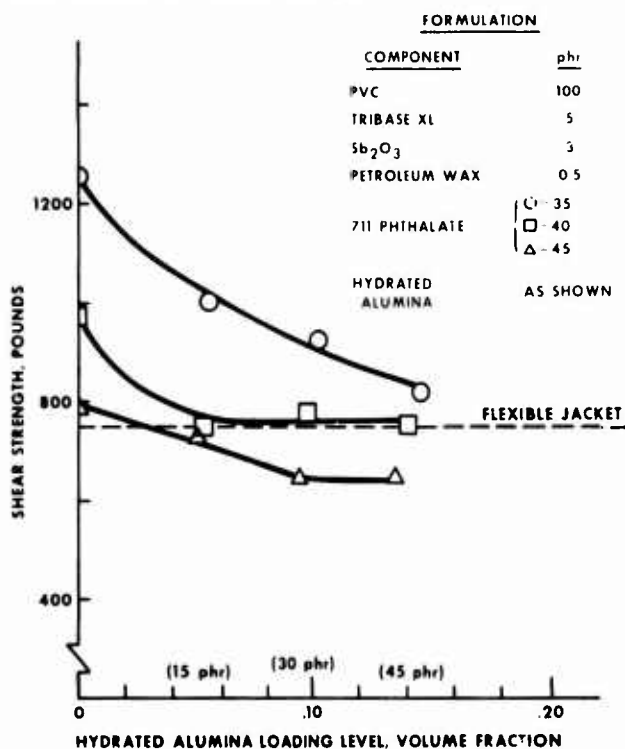


FIGURE 4

Table II compares the properties of the flexible jacket compound with those of the experimental jacket compound containing 40 phr plasticizer and 30 phr hydrated alumina.

TABLE II  
COMPARISON OF PHYSICAL PROPERTIES OF JACKET COMPOUNDS

	Flexible Jacket	Experimental Jacket
Oxygen Index, Percent	28	32
Brittleness Temperature, °C	-28	-27
Shear Strength, pounds	750	780
Tear Strength, pounds/inch Die C	550	560
Tensile Strength, psi	2700	2900
Elongation at Break, percent	250	225
Coefficient of Friction		
Static	.6	.6
Sliding		.5

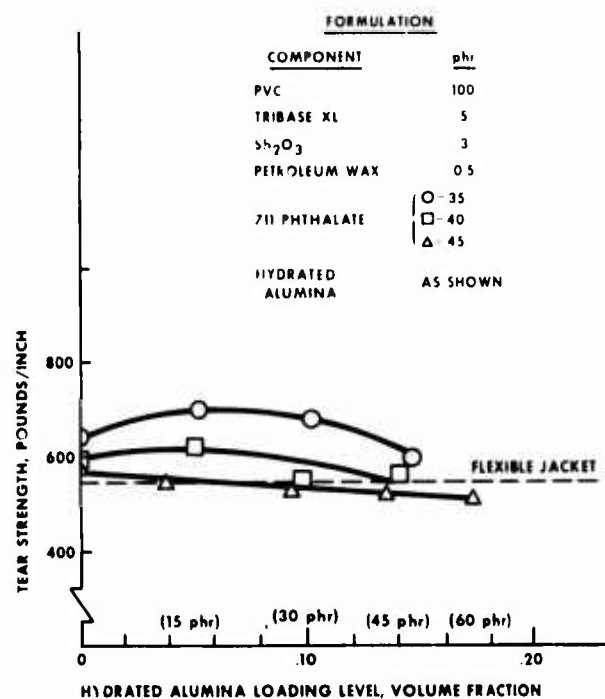


FIGURE 5

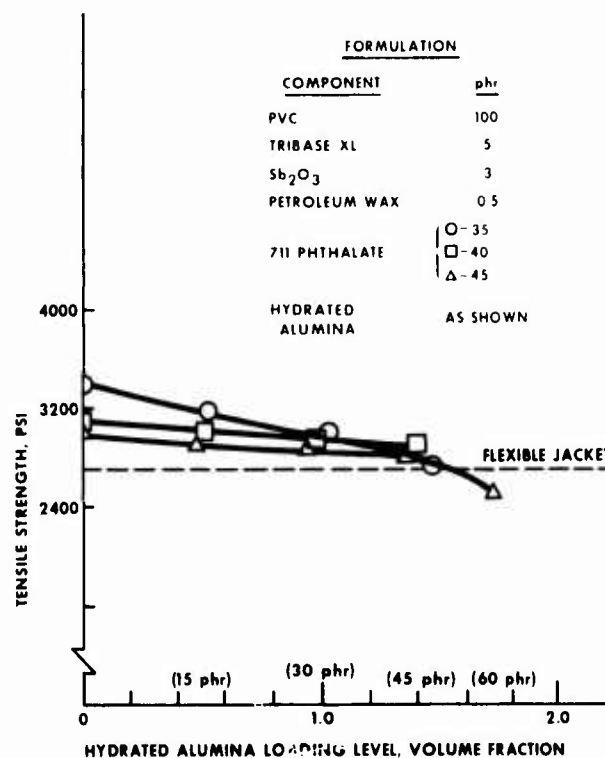


FIGURE 6

#### FIRE TESTING

##### Cable Samples

Standard and experimental designs of 25 pair inside wiring cables were fire tested. The constructions of all the cable were identical, only the materials were varied. The three cables tested are described in Table III.

TABLE III  
CABLE CONSTRUCTIONS

	PVC Insulation	O.I.	PVC Jacket	O.I.
Cable A	Std. Semirigid	28%	Std. Flexible	28%
Cable B	Std. Semirigid	28%	Experimental	32%
Cable C	Std. Semirigid + 2 phr Sb <sub>2</sub> O <sub>3</sub>	32%	Experimental	32%

### Test Procedures

#### 25 Foot Tunnel (Modified ASTM E-84)

All samples were mounted in the top section of the tunnel (see Figures 7,8,9) over a support system consisting of 2 inch hexagonal poultry netting, and 1/4 inch rods at 2 foot intervals. Forty cables, each 24 feet in length, were placed to fill the 20 inch tunnel width.

Standard conditions for the duration of the test are a 300,000 BTU/hr. gas fueled ignition fire at one end of the tunnel and an induced draft with a velocity of 240 feet/minute. The test runs for 10 minutes. The ignition flame engulfs 4-1/2 feet of the test samples. Flame spread is measured from this point. As the flame spread down the tunnel, its advance is observed by the test engineer through small glass windows spaced one foot apart. Using red oak, the conditions spread the flame to the end of the tunnel in 5.5 minutes (a flame spread classification, FSC, of 100). Asbestos-cement board has an FSC of 0.

#### Vertical Corner Flame Test (BTL Facilities)

Twenty cables, 27 feet in length, were loosely bundled in the corner of a two story fire test building. The cables were ignited by a propane fueled ribbon burner which yielded a 215,000 BTU/hr. flame. The flame is four feet high and is kept on for the duration of the test.

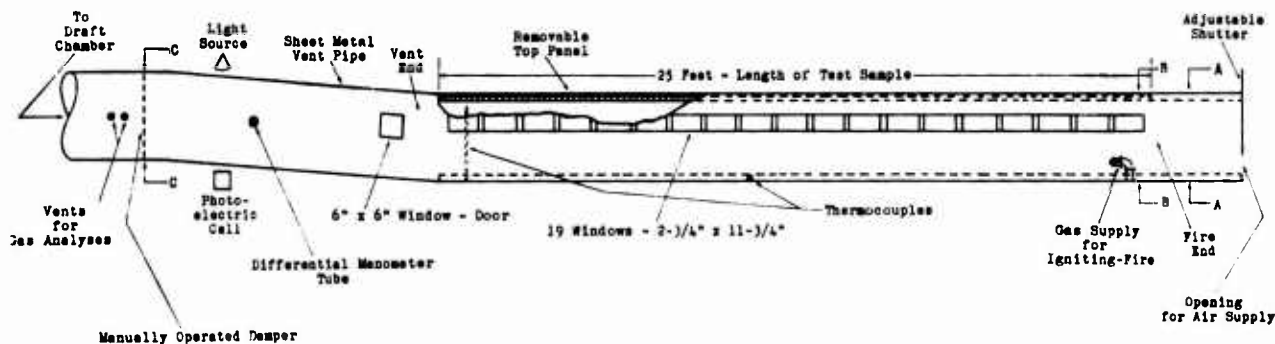


FIGURE 7  
Details of Test Furnace

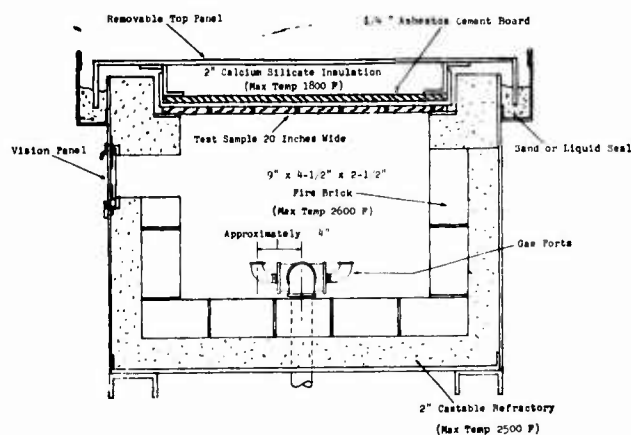


FIGURE 8  
Cross Section of Furnace at Fire End



FIGURE 9  
Cable Samples Mounted  
in the Top of the Tunnel

## Test Results

Figure 10 shows flame spread versus time for the standard cable (Cable A) in the 25 foot tunnel. The flame reached a maximum spread of 7 feet in 3 to 4-1/2 minutes and then receded. The fire self-extinguished immediately after the ignition flame was turned off. A flame spread classification of 36 was obtained. This is higher than the goal of 25. This cable does have improved fire resistant properties compared to earlier designs (pre-1972). The experimental cable has good low temperature handling characteristics that are similar to those of the standard cable.

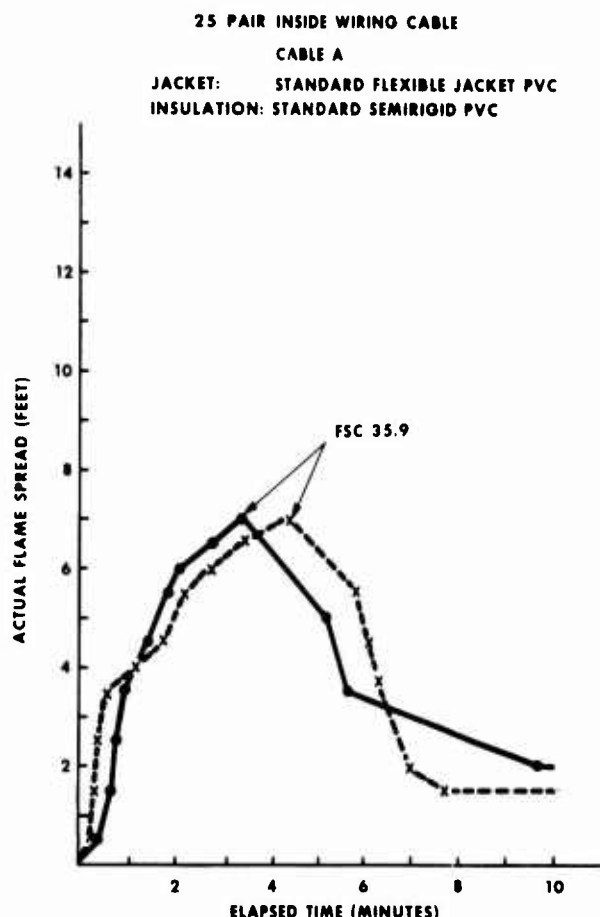


FIGURE 10

Figure 11 shows the flame spread results for the experimental inside wiring cables. As was the case for the standard cable, the flame propagated to a maximum point and then receded and self-extinguished immediately after the ignition flame was turned off. The cable with the experimental jacket (Cable B) had a flame spread classification of 27\*. Improving both the jacket and the insulation (Cable C) results in a flame spread classification of 23.

\* Flame spread classifications between 22.5 and 27.49 are rounded off to 25 when the test is run for official classifications. Thus a value of 27 meets our design objective of obtaining a 25 classification.

## EXPERIMENTAL 25 PAIR 24 GAUGE INSIDE WIRING CABLES

### CABLES B & C

JACKET: EXPERIMENTAL JACKET

INSULATION: { CABLE B - STANDARD SEMIRIGID PVC  
CABLE C - MODIFIED SEMIRIGID PVC

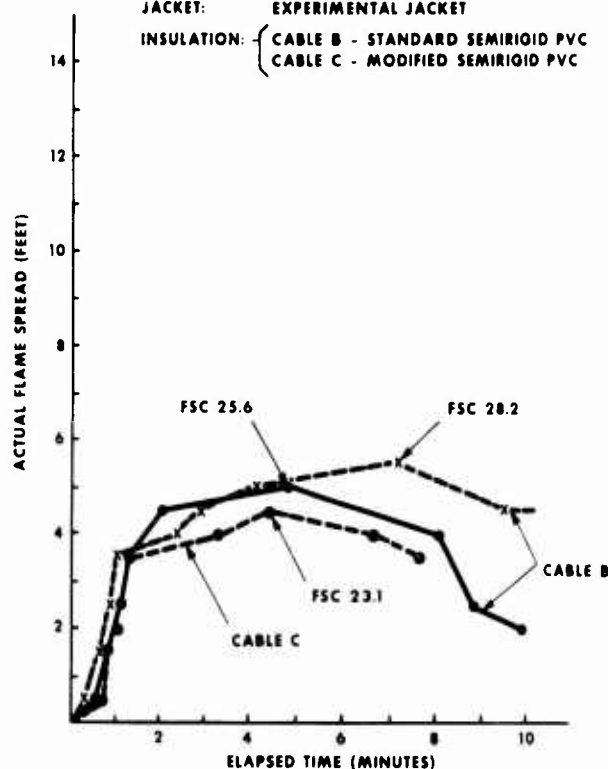


FIGURE 11

Vertical tests yielded results consistent with those obtained with the 25 foot tunnel. The standard cable (Cable A) propagated flame 9 feet above the four foot ignition flame while the cable with the improved jacket (Cable B) propagated flame 5 feet. The cable with improved jacket and improved insulation (Cable C) spread the flame 4 feet.

## CABLE HANDLING TESTS

An improvement in the fire resistance of this cable is the primary objective. The secondary objective is to accomplish this without sacrificing the handling characteristics of the inside wiring cable. This cable undergoes installation in a wide range of temperatures. Operations include pulls through conduit and sharp bends to position the cable to provide service.

A room temperature conduit pull test was made to evaluate the new cable versus the existing design. The procedure is to pull 50 foot lengths through a 1 inch diameter steel conduit (three 90° bends) until no additional lengths can be pulled through. The number of lengths pulled in and the pulling forces are recorded. The cable jacketed with the experimental compound was equivalent to standard cable.

Low temperature properties were checked by recording the rate at which cracks occur in the cable jacket of samples subjected to an impact test (a 4 pound weight dropped from 10 inches above the sample). Samples are tested at 20, 14, 7 and 0°F. The experimental jacket is similar to the standard material in this temperature range.

## CONCLUSIONS

The development of a flexible jacket compound with an oxygen index of 32% has resulted in the design of an inside wiring cable that meets the objective of a flame spread classification of 25. Additional tests are planned. Vertical corner tests of the experimental and standard cables verify that progress has been made in reducing the flame spread of the inside wiring cable. All other properties of the new cable are nearly identical to those of the cable it is designed to replace.

## REFERENCES

1. S. Kaufman and M. M. Yocum, "Balancing Flame Retardancy and Low Temperature Properties in PVC", paper presented at the International Symposium on Flammability and Fire Retardants, May 23, 1975, Montreal, Canada. To be published in Advances in Fire Retardants, late 1975.

## APPENDIX

### MATERIALS PREPARATION AND TEST METHODS

All samples were prepared by mixing the ingredients (approximately 1500 grams) in mixer followed by fluxing in a Banbury mixer for four minutes at 350°F and sheeting out on a two roll mill. Test plaques, 75 mils thick, were compression molded. The test methods used are shown below.

### TEST METHODS

Property	Method of Test
Tensile Strength and Ultimate Elongation	ASTM D412 using Specimen and a speed of 20 inches/minute.
Tear Strength	ASTM D624 using Specimen Die C and a speed of 20 inches/minute.
Shear Strength	Bell Labs Test. Shear strength is the force required to drive a one inch 45° wedge with a 30 mil flat edge through a 75 mil thick test plaque.
Low Temperature Brittleness	ASTM D746. Only complete breaks were considered failures.

## ACKNOWLEDGEMENTS

The authors gratefully acknowledge the contributions of Ms. M. M. Yocum, Mr. G. J. Hessler, and Mr. C. J. Arroyo.



Stanley Kaufman

Stanley Kaufman is a Member of Technical Staff at Bell Telephone Laboratories. He received a B.S. in Physics from the City College of the City University of the City of New York, and a Ph.D. in Chemistry from Brown University. Before joining Bell Laboratories in 1970, he was a research scientist at the Uniroyal Research Center.



C. A. Landreth

C. A. Landreth is an Associate Member of the Technical Staff at Bell Laboratories. All of his 16 years Bell System experience has been in the area of wire and cable development. His most recent responsibilities center on the design of fire resistant building cables. Mr. Landreth received his B.S.M.E. from Fairleigh Dickinson University in 1966.

## DEVELOPMENT OF NEW FIRE-PROOF WIRE AND CABLE

H. MATSUBARA, C. MATSUNAGA, A. INOUE, N. YASUDA  
SUMITOMO ELECTRIC INDUSTRIES, LTD.  
OSAKA, JAPAN

### Summary

Recently the Japan Fire Defence Board made a regulation whereby owner of most buildings must provide emergency circuits for fire equipments such as indoor fire plugs, smoke blowers, emergency elevators and emergency exit indicator lamps. These fire equipments must be able to operate as long as people can be evacuated when a fire breaks out. Therefore, when these circuits are exposed, "Fire Proof Wires" which meet the specifications of Japan Fire Defence Board can be used.

It is desirable, though not regulated by law, that trains are provided with power and control circuits which have sufficient fire proof properties.

We have developed the following two types of new fire-proof cables which satisfy the above requirements.

- 1) Low voltage wire (600 V class) which has a proof layer between conductor and polyethylene insulation. The special fire-proof layer is designed to prevent the high conductive flame from contacting the conductor. This wire is covered by polyvinylchloride jacket. This wire withstands A.C. 600 V for 30 minutes and has insulation resistance of over 0.4 Megohm.
- 2) High voltage Fire-Proof cable (6.6 KV class) which is comprised of conventional 6.6 KV class XLPE insulation, PVC jacket and outer heat resistance layer. This heat resistance layer consists of an asbestos layer and a cotton mesh tape coated with intumescent paint. This cable withstands A.C. 6.6 KV in a flame at 840 °C for more than 1 hour.

### 1. Introduction

In Japan, cities have continued to grow. Many tall buildings have been built and many shopping malls, subways etc. have been built underground in order to utilize the limited space more efficiently. But once a fire breaks out in such places, the damage to buildings and the danger to people can be severe. Because of this it is most important to improve the fire-proof efficiency of building materials.

There are two important ways to improve the fire-proof efficiency of wire and cable.

- (1) A fire does not transfer to another place along wire and cable.
- (2) Wire and cable continue to function for a certain time in a fire.

Item (1) has been studied for years, and many studies have been established and published by improving the "fire retardance" of wire and cable materials. These fire-retardant materials can only prevent fire propagation for certain kinds of fire<sup>1)</sup>. In an actual fire there are few cases where only wire and cable are inflammable, but they are heated by other burning materials. In this case most organic materials burn. Even the oxygen index (O.I.) of polytetrafluoroethylene (O.I.=98) becomes 21 as shown in Table 1 at 500 °C and easily burns<sup>2)</sup>.

Table 1. Dependence on temperature of Oxygen Index (O.I.)

Materials	O.I. at 25°C	Temperature at which O.I. becomes 21
Nylon	24	130 °C
Neoprene	41	325 °C
Rigid PVC	47.6	375 °C
PTFE	98	500 °C

It has been reported that many people suffocate in a fire because they are unable to get out of the building as the electric current for lights, escape equipment etc. is cut off<sup>3)</sup>. We consider that item (2) is more important. In this paper we will explain the development of fire-proofing wire and cable from this point of view.

### 2. Development of Low Voltage Fire-proof Cable

#### 2.1. Present Status of National Regulations

In Japan, the owners of buildings are obliged by the Fire Service Law to install fire-prevention and alarm systems. The kinds of systems and buildings are shown in Tables 2 and 3.

Table 2. Fire fighting and alarm equipment prescribed by the Fire Service Law

#### 1. Fire fighting equipment

- (1) fire extinguisher, water tank etc.
- (2) sprinkler, water-fog extinguisher
- (3) bubbling extinguisher
- (4) CO<sub>2</sub> extinguisher
- (5) halogenation extinguisher
- (6) indoor hydrant
- (7) outdoor hydrant
- (8) dry chemical extinguisher etc.

#### 2. Fire alarm equipment

- (1) automatic fire alarm equipment
- (2) electric leak detector
- (3) fire alarm system transmitting an alarm to a fire department
- (4) a. emergency bell  
b. automatic siren  
c. emergency announce equipment, etc.

#### 3. Evacuation equipment

- (1) fire escape, sliding way, etc.
- (2) emergency light, guiding light etc.

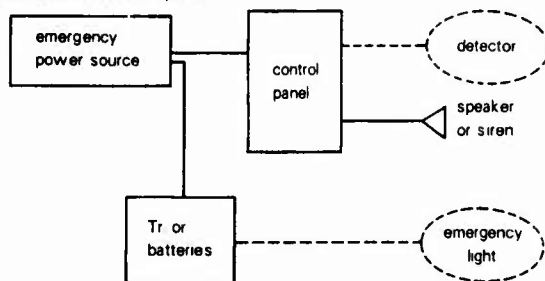
Table 3. The buildings and other structures prescribed by the fire Service Law

1. a. theater, movie theater, entertainment hall  
b. public hall, assembly hall,
  2. a. cafe, bar, cabaret, night club, similar  
b. recreation hall, dance hall,
  3. restaurant, similar facilities
  4. department store and other markets
  5. hotel, inn, hostel, dormitory, apartment
  6. a. hospital, clinic, maternity hospital  
b. sanatorium for old or disabled people  
c. kindergarden, school for disabled people and children
  7. school, university
  8. library, museum, art museum
  9. public bath house
  10. waiting room at railway station and airport
  11. temple, shrine, chapel
  12. a. factory, work shop,  
b. movie and TV studio
  13. warehouse
  14. a. car garage, parking place  
b. aircraft or helicopter hanger
  15. general buildings not prescribed in the above items
  16. multi-purpose buildings or facilities subject to the Fire Service Law
  17. underground market,
  18. buildings or structures designated as important cultural properties by Cultural Preservation Laws
  19. shopping arcade extending over 50 m,
- etc.

The systems depend on the use and structure of the building. Most fire-prevention systems must have their own emergency electric source (batteries or independent power plant) and the wiring methods in these systems are also specified. These are shown in Table 4. Exposed wiring must be fire-proof cable (Table 5).

Fig. 1 Example of systems and their wiring

a Automatic fire alarm system



b Indoor hydrant system

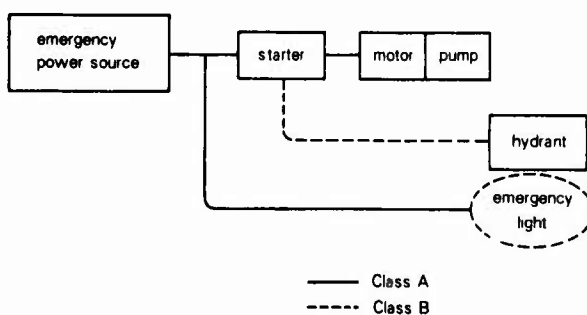
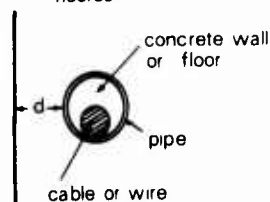


Table 4  
Wires and cables for fire prevention systems

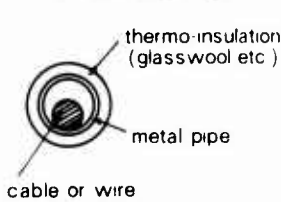
- 1 Aluminum sheathed cable
- 2 Lead sheathed cable
- 3 Steel tape armoured cable
- 4 Chloroprene sheathed cable
- 5 Corrugated metal sheathed cable
- 6 Combined duct cable
- 7 Heat resistant PVC insulated wire
- 8 Chlorosulfanated polyethylene insulated wire
- 9 Ethylene fluoride insulated wire
- 10 Varnished glass tape insulated wire
- 11 Asbestos sheathed cable
- 12 Silicone rubber insulated wire
- 13 \* MI cable
- 14 \* Fire resistant cables specified in the Fire Service Law

#### Wiring method

- (1) in case of wiring in fire resistant walls and floors



- (2) in case that the wire can not be installed in walls and floors



$d < 20\text{mm}$  — PVC pipe  
 $d \geq 10\text{mm}$  — metal pipe etc.

- (3) exposed wiring

\* These cables may be used without any protection, i.e. exposed wiring.

Table 5

	Special fire-proof cable	Fire-proof cable
Voltage	600 V (power)	60 V (control)
Test Condition	class A	class B

There are two kinds of fire-proof cable as shown in Table 5 which are tested under the class A or B methods. Fig. 1 shows the places where class A and class B cables can be installed as exposed wiring, in emergency circuits of automatic fire alarm systems and indoor hydrant systems prescribed by the Fire Service Law.

**Fire test of fire-proof cable** The test intends to examine whether a cable functions satisfactorily in fire for a certain length of time. After applying the flame at a specified temperature for a specified time, the cable is examined to see whether it can withstand the insulation resistance and insulation withstand voltage tests. The following two methods are



used for the special fire-proof cable (class A) and fire-proof cable (class B).  
 (a) Special fire-proof cable (for 600V circuit)  
 The test consists of a heating test and a withstand voltage test.  
 Heating test  
 Fix a 1.3 m long wire sample with copper wire to a 10 mm thick perlite plate as illustrated in Fig. 2.

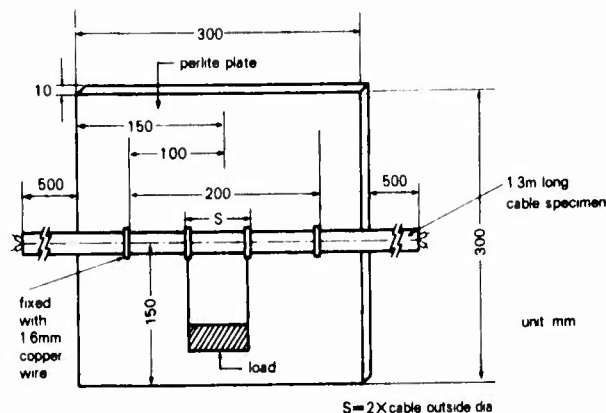


Fig. 2

Put the sample into the furnace, with a load 2 times the sample weight and apply AC 600 Volts. Apply heat for 30 minutes raising the temperature according to the indoor fire heat curve specified in JIS C 1304 "Method of Fire-resistance Test for Structural Parts of Buildings" as illustrated in Fig. 3 (curve 1).

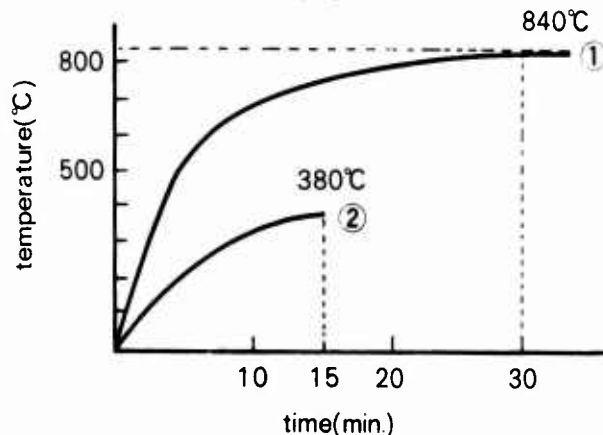


Fig. 3

After heating, measure the insulation resistance with a DC 500V megger. The value should be greater than 0.4 megohms.

Withstand voltage test

Immediately after the heating test, apply AC 1,500 volts.

The sample will withstand the above voltage for 1 minute.

(b) Fire-proof cable (for circuit upto 60V)

Fix the 1.3 m long wire sample with copper wire to a 10 mm thick perlite plate as illustrated in Fig. 4.

Put the sample into the furnace with a load 2 times the sample weight and at the same time apply AC 250 Volts. Then heat the sample at temperatures which are half of those in the indoor fire heat curve in JIS A 1304 (380 °C)

for 15 minutes as illustrated in Fig. 3 (curve 2).

After the test, measure the insulation resistance with a DC 500V megger. The value will be not less than 0.1 Megohms.

These two kinds of fire-proof cables were first authorized by the Fire Defence Board but now a Committee authorizes them.

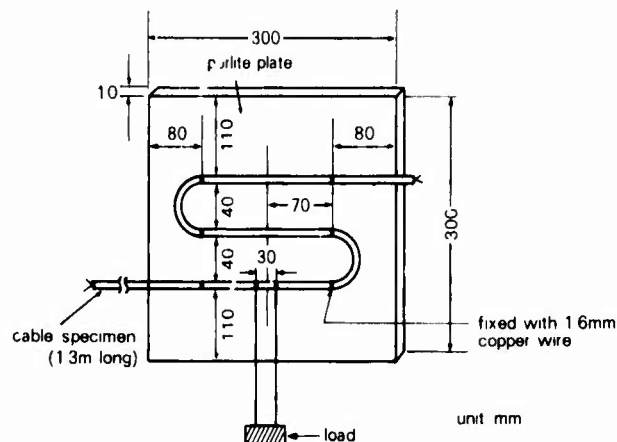


Fig. 4

**Other Specifications** The general performance specifications (except fire test) are also specified. The specifications for the special fire-proof cable (class A) are listed in JIS C 3342 "Standard for 600V PVC Insulated and PVC Sheathed Cable (VV)", and in JIS C 3307 "Standard for 600V PVC Insulated Wire (IV)" for the fire proof cable (class B). It is specified that the sheath shall not burn over 15 cm in length from the inside wall of the test chamber.

## 2.2. Direction of Development

The purpose of this development is to make a cable which has the same performance, is easier to handle and is cheaper, than M.I. cable. In accordance with the requirements of the Fire Defence Board the wire shall be exposed at 840 °C. At such high temperature, however, most organic materials will burn completely. For the purpose of assuring cable performance in such a high temperature environment the following two methods can be considered.

- (1) Preventing temperature rise of cable components by using heat-resistant layer
  - (2) Maintenance of the wire performance using both inorganic and organic materials
- Method (1) is not practical. These kinds of cables are low voltage class cables and it is desirable to handle them as they are at present, since the workers who install them work for small companies and they are not familiar with special handling techniques.  
 Method (2) (combination of organic and inorganic materials) is useful; i.e. the cable performance can be maintained with only the inorganic materials which are good insulation, after the organic materials are burnt out in a fire.

## 2.3. Electrical Characteristics of Flame

It is useful to know the electrical characteristics of a flame before beginning development of a cable that functions in a fire.

Many studies concerning flame conductivity have been done. Practical measurements of flame conductivity have been performed recently, since many buildings have been built near high voltage lines, making fire fighting very dangerous when a fire breaks out in such buildings. An example is shown in Fig. 5, which shows that the flames are rather conductive<sup>4</sup>). These problems were investigated as being due to ionization of combustibles in a high temperature flame.

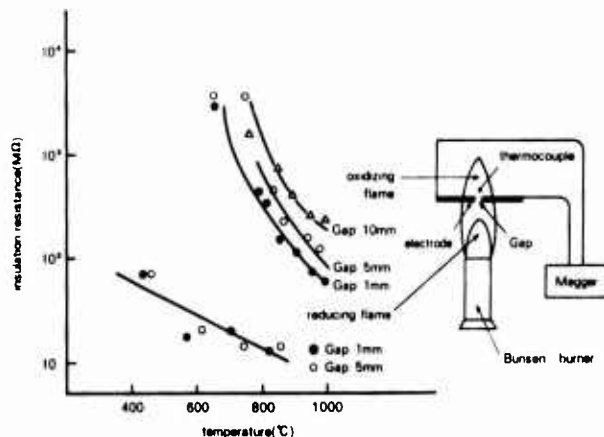


Fig.5 Conductivity of a fire

Saha proposed an expression as follows<sup>5</sup>).

$$\log K = \frac{E_1}{1.982 \times 10^{-4} T} + \frac{5}{2} \log T - 6.49 + \log \left( \frac{g_a^+ \cdot g_e^-}{g_a} \right)$$

$K$  : equilibrium constant for ionization  
 $E_1$  : ionization potential

$g_a^+$ ,  $g_e^-$ ,  $g_a$  : statistical weight of ion, electron and atom

A high temperature flame ionizes atoms which are contained in fuel and as a result the flame become more conductive. Of course since the ionization potentials are determined by the ion source, the conductivity of a flame is influenced by the burning material. Many fuel gases and radicals, such as  $O_2$ ,  $N_2$ ,  $H_2$ ,  $H_2O$ ,  $CO_2$ ,  $CO$ ,  $OH$ ,  $H$ ,  $CH_4$  have less influence on the rate of ionization of the flame because of their high ionization potentials (over 12 eV). For example,  $CO$  can supply only  $10^0$  ions per cc to the flame at  $3000^\circ K$ . The most popular ion source which has a low ionization potential in a flame is  $NO$  (9.5 eV) and this 1% nitrogen monoxide produces  $10^{11}$  ions per cc. The flame conductivity can be changed remarkably by the metal impurities (for example  $K$ : 4.3 eV,  $Ca$ : 6.1 eV,  $Cu$  : 7.7 eV etc.).  $10^{-6}\%$  potassium atom ( $K$ ) in the flame produces more ions than nitrogen monoxide.

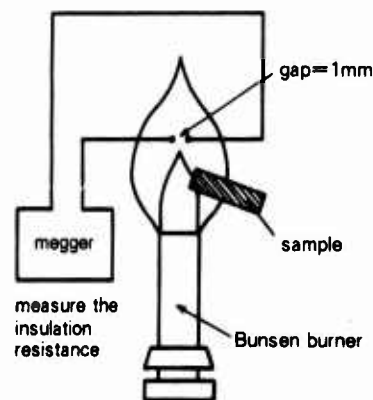
**Experiment-1.** The high conductivity of flame when wood is burning is caused by these  $K$  and  $Ca$  atoms. Taking the above into account we conducted experiments (experiment-1) and the results are shown in Table 6.

The data shows that the insulation resistance of a flame varies according to the fuel. When soft PVC, the most popular material for cable jackets, burns, the flame becomes highly conductive. When the flame is highly conductive, it is difficult to insulate the cable, by applying inorganic fiber separators which a flame

can easily pass through.

Table 6 Insulation resistance of flame

Sample	insulation resistance ( $M\Omega$ )
none	70
PE	50
PVC	5
wood	10



experimental method-1

**Experiment-2.** Table 7 and Fig. 6 show the results of a fire test in which the wires were wrapped with glass tapes etc. The experiment was carried out in the following way. Wires wrapped with an inorganic separator are twisted. Then these wires are burnt with four Bunsen burners. At the same time combustibles are burnt under them and the insulation resistance between the two conductors is measured. The results lead to two conclusions.

- (1) The insulation resistance does not rise with an inorganic fiber separator which a flame can pass through.
- (2) The insulation resistance decreases when some inorganic fibers such as glass tape with organic binder which is easy to ionize and carbonize are used.

A heat-resistant separator should be made of materials which (1) a flame cannot pass through; (2) does not include contaminations which carbonize and (3) can maintain good insulation resistance at high temperature.

Table 7 Minimum insulation resistance ( $M\Omega$ )

Inorganic separator Combustibles	Glass tape (1) (non heat-cleaned)	Glass tape (2) (well heat-cleaned)
Burner only	3	50
PE	2	10
PVC	0.05	0.05
wood	2	7





Fig 6 The experimental method 2

Fig. 7 Glass tape+clay powder

#### 2.4. The Development of a Heat-resistant Separator and Improvement of Materials

We began to develop a heat-resistant inorganic fiber separator which prevents a conductive flame from reaching the conductor. At first, a glass tape which had a good insulation resistance at high temperature was chosen as a base separator and the meshes of the tape were filled with inorganic powder.

**Experiment-3.** The method is the same as experiment-2. In this experiment PVC was burnt for the purpose of making the flame conductive. Table 8 shows the separator structures and their minimum insulation resistance. These experimental results show that the mineral powder rubbed in the tape meshes prevents a conductive flame from reaching the conductor.

Table 8 The results of experiment-3

Structure of separator*	Minimum insulation resistance (KΩ)
1. glass tape wrapped 2 times thickness = 0.25 mm	10
2. glass tape + aluminum oxide powder thickness = 0.3 mm	800
3. glass tape + clay (Whitetex) powder thickness = 0.3 mm	400
4. glass tape + Hi-sil powder thickness = 0.3 mm	200
5. glass tape + mica powder thickness = 0.3 mm	100

\* The powder was made into a paste with toluen and was rubbed in the glass tape and covered with another glass tape.

In order to prevent the powder from coming off the tape, a layer of glass tape is added. In this case the separator cracks in the fire. Figs 7 and 8 show the samples after experiment-3. It is assumed that the inorganic powder cannot provide enough insulation resistance for the wire because it is coming off and the separator cracks. A good binder is necessary to prevent the powder from coming off and the separator from cracking

Fig. 8 Glass tape+Hi-sil powder

**Experiment-4.** The method is the same as experiment-3. As a result of these experiments, it was found that a material such as silicon which burns and becomes an inorganic powder, is a more effective binder than polyvinylacetate which burns completely and does not come off and the separator does not crack if a silicon rubber is used as the binder. The results of experiment-4 are shown in Fig. 9 and Table 9. As described above the development of an effective heat-resistant separator was accomplished.

Table 9 The results of experiment-4

Structure of separator	Minimum insulation resistance (MΩ)
1. glass tape + a compound of Hi-sil and poly-acetate (5:50) glass tape thickness = 0.3 mm	0.3-0.4
2. glass tape + a compound of Hi-sil and silicon oil (5:50) glass tape thickness = 0.3 mm	8-15
3. glass tape + a compound of mica powder and silicon oil (5:50) thickness = 0.3 mm	8-15
4. glass tape + a compound of Hi-sil and silicon rubber (5:50) glass thickness = 0.3 mm	8-10
5. glass tape + silicon oil glass tape thickness = 0.3 mm	0.5

\* This rubber is a liquid type which can be crosslinked at room temperature to a solid.



Fig. 9 Glass tape with Hi-sil and silicon rubber

Improvement of cable materials Many important facts which improve the other cable components were discovered during the investigations. The two most important are:

- (1) The insulation resistance is greatly improved when the cable components are burnt as completely as possible without emitting smoke or soot, and
- (2) using the endothermic reaction of the hydrate water and the like is an effective way to prevent the cable component temperature from rising.

Considering the above points, smokeless PVC compound (PVC which does not emit a lot of smoke) was used as the jacket material and atactic polypropylene compound which was highly loaded with aluminum hydroxide as a cable filler instead of jute and polypropylene was also used.

Table 10 shows the construction and Fig. 10 shows the result of a fire test on these fire-proof wires using these new materials, which was conducted in accordance with the method specified by the Fire Defense Board of Japan.

Table 10 The structure of new fire-proof wire

Conductor	Copper 5C x 30 mm <sup>2</sup>
Heat-resistant	A glass tape applied with a silicon rubber compound or a glass tape applied mica
Insulation	Polyethylene
Filler	An atactic polypropylene compound with a great amount of aluminum hydroxide
Jacket	smokeless PVC

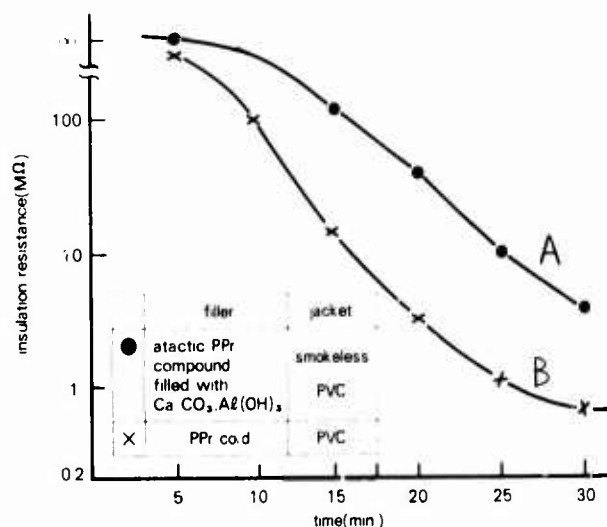
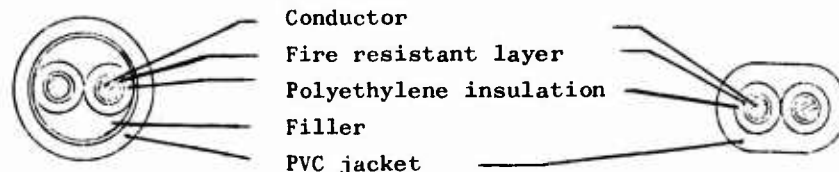


Fig. 10 Relation between IR and time in a fire

(B.D. voltage after fire test A: >3000V  
B: 2300V)

Table 10 (2) The structure of fire-proof cable (extracts)  
(class A)

Core No. x size (mm <sup>2</sup> )	Conductor		Heat resistant layer (mm)	Insulation thickness (mm)	Jacket thickness (mm)	Overall diameter (mm)	Cable weight (kg/km)
	Structure (No./mm)	Outside diameter					
1 x 38	7/2.6	7.8	0.8	1.2	1.5	17	540
1 x 100	19/2.6	13.0	0.8	1.5	1.5	22	1190
1 x 400	61/2.9	26.1	0.8	2.5	2.1	37	4280
1 x 1000	127/3.2	41.6	0.8	3.5	2.8	56	5400
3 x 38	7/2.6	7.8	0.8	1.2	1.8	30	1570
3 x 100	19/2.6	13.0	0.8	1.5	2.4	46	3980
3 x 400	61/2.9	26.1	0.8	2.5	3.6	79	14070



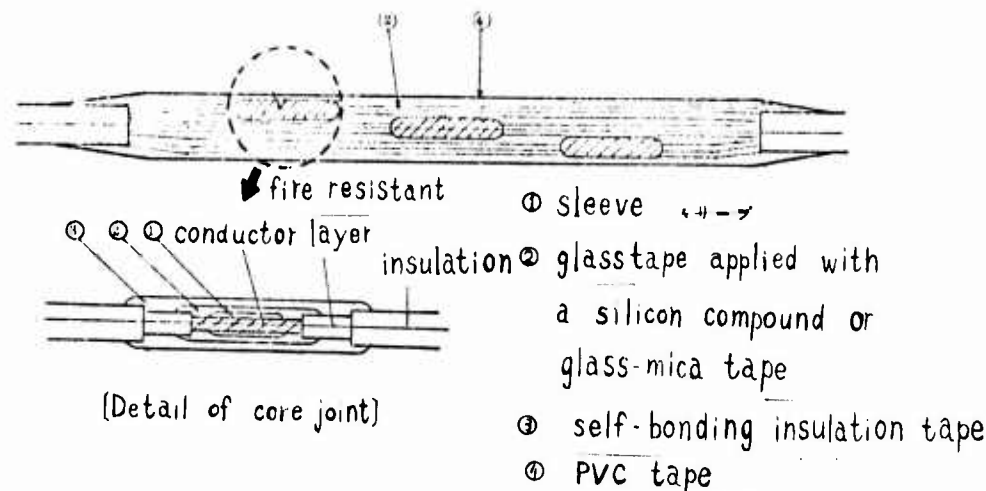


Fig. 10 (2) Straight joint of fire-proof cable

In this way, we made a better fire-proof wire and cable by improving the cable materials and producing them which are up to 1000mm<sup>2</sup> of conductor size and the maximum core number is 30. Table 10 (2) shows the extracts of them. At the wiring of fire-proof cable, the terminal is equal to that of common wiring because it is assembled in a fire resistant box. But the straight joint and the branch of the cable need to meet the same test as the cable. Fig. 10 (2) shows the construction of straight joint for them.

### 3. Development of the high-voltage fire-proof cable

#### 3.1. The speciality of high voltage cable

The structure of high-voltage cable over 3 KV has been fixed and the cable consists of (1) an inner semiconductive layer, (2) insulation, (3) outer semiconductive layer. Concerning the guarantee of the cable life in general (excluding fire), it is not favorable to obtain the fire-proof efficiency by changing the structure. It is necessary to develop methods other than those used for the low voltage fire-proof wire and cable.

#### 3.2. The possibility of the effective heat-resistance method

The most effective fire-proof method for inherently combustible organic materials is to use a heat resistant method so that the heat resistant layer prevents the temperature of the cables materials from rising to their thermal decomposition temperature. Table 11 shows the thermal conductivity of various kinds of materials. It is natural that the thermal conductivity of gases are very low. The effective heat resistance is supposedly possible if it intumesced materials can be used.

However, when these intumesced materials are actually applied to the wire and cable components the following problems are encountered:

- (1) The heat from the cable cannot diffuse and the cable becomes hot
- (2) the intumesced material does not keep its shape at high temperatures in a fire.

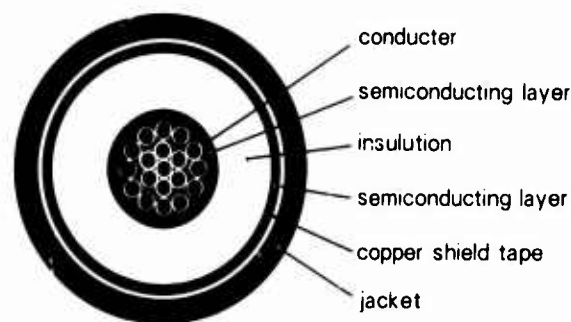


Fig. 11 Structure of power cable for over 3KV

Table 11 Thermal conductivity of various kinds of materials (K cal/m·hr·°C)<sup>6)</sup>

materials	thermal conductivity	materials	thermal conductivity
Al	150	prastics	0.0 - 0.2
Fe	50	water	0.5 - 0.1
glass	1.3 - 0.6	air	0.02
concrete	0.5 - 0.4	steam	0.010
asbesto	0.2 - 0.1	CO <sub>2</sub>	0.011

An intumescent fire-proof paint has been developed in order to solve the above problems. It begins to foam at a high temperature and makes a layer which is 20 times thicker than usual. The intumesced foam can maintain its shape at over 800 °C. These special characteristics solve the above two problems. An example of the paint is shown in Table 12<sup>7)</sup>. The observed thermal conductivity of this intumescent fire-proof paint is shown in Table 13.

The conversion heat resistance is the ratio of total heat resistance due to the increase of thickness which is increased over 20 times in a fire. This paint only provides effective heat resistance in a fire because the layer of paint is very thin.

Table 12 An example of formulation<sup>(7)</sup>

water	31.0
wetting agent	0.5
TiO <sub>2</sub>	8.0
ammonium polyphosphate	24.0
urea-formaldehyde resin	2.0
Dicyanidiamide	8.0
Dipentaerythritol	4.0
Chlorinated paraffine	5.0

Table 13 Thermal conductivity of this intumescent fire-proof paint

	heat-resistant C·cm/w	conversion heat resistance
PVC	600	-
fire-proof paint (in usual use)	709	1
" (in a fire)	1620	740

We calculated the heat resistant efficiency in a fire by actually using this paint. An intumescent layer of cable is considered to be an infinite cylinder because the intumescent paint becomes a thicker intumescent layer in a fire, and it is assumed that the temperature difference exists only in the radial direction. The rate of increase of temperature of this cylinder in a non-stationary state is formula-  
rized as follows.

$$\frac{T}{t} = K \left( \frac{1}{r} \cdot \frac{\partial T}{\partial r} + \frac{\partial^2 T}{\partial r^2} \right) \dots \dots \dots (1)$$

$k = \lambda / C \rho$   $\lambda$  : thermal conductivity  
 $T$  : temperature  
 $C$  : specific heat  
 $t$  : time  
 $\rho$  : specific gravity  
 $R$  : outer radius

Under the boundary conditions  $t = 0$ ,  $T = T_1$  and  $t = 0$ ,  $r = R$  and  $T = T_0 = \text{constant}$ , Jaeger et al. solved this equation (1) and interpreted it for  $k$  and  $r/R$  graphically<sup>8)</sup>. The result of this calculation is shown in Table 14<sup>9)</sup>. The time it takes the temperature of the cable core surface to reach 500 °C and 700 °C from 20 °C when the cable sample is in a fire at 850 °C is calculated. The constants used in this calculation are shown in Table 15.

### 3.3. The experimental result and solution of problems using a proto-type cable

We would like to explain the test results of several prototype cables, with various kinds of heat resistant layers, which were carried out on the basis of the results of Section 3.2.

Table 14 Calculations<sup>(9)</sup>

sample	radius in a fire (mm)	time un- til the surface temp. become 500 °C (min.)	time un- til the surface temp. become 700 °C (min.)
cable	heat resistant layer		
6KV-22mm <sup>2</sup> CV cable	none	9.25	3.4
"	intumescent paint (2mm thick)	49.25	38
"	asbestos tape (5mm thick) + intumescent paint (2mm thick)	54.25	48
"	asbestos tape (5mm thick) + intumescent paint (4mm thick)	94.25	144

Table 15 Constant

	$\lambda$ (cal/cm·sec·°C)	$\rho$ (g/cm <sup>3</sup> )	$C$ (cal/g·°C)
intumescent layer	0.00015	0.2	0.2
PVC Jacket	0.0004	1.3	0.5

The prototype cable was fixed in the test chamber for fire-proof wire and cable. Then the temperature of the gas burner flame was set at 850 °C and the time until the cable broke down (this time is called the life time hereafter) under 6 KV was measure. The result is shown in Table 16.

The intumescent fire-proof paint can greatly lengthen the cable life. A high voltage cable used for a main power line should be able to function for one hour in a fire. The data in Table 16 is compared with the result of calculations in order to investigate how to lengthen this lifetime.

Table 16 Improvement of fire-proof performance with the improvement of heat resistance

method of heat resistance	time until the cable breaks down under AC 6.6KV
none (1)*	3'45"
none (2)**	4'
asbestos tape wrapping (3mm thick)	10'30"
corrugated pipe	12'5"
intumescent fire-proof paint (2mm thick)	17'0"
asbestos tape (5mm thick) + intumescent fire-proof paint (2mm thick) asbestos tape (5mm thick) + intumescent fire-proof paint (5mm thick)	29'30"
	38'0"

\*cable: 6.6KV 1 x 22 mm<sup>2</sup> PV cable

\*\*cable: 6.6KV 3 x 22 mm<sup>2</sup> CV cable

The time until the core surface temperature reaches 500 °C is close to the life time. But there is a great difference between these two times when the fire-proof layer is rather thick. When the samples were observed after the test it was found that the intumescent paint layer fell away from the cable as shown in Fig. 12. The life time can be prolonged if this paint layer does not come out.

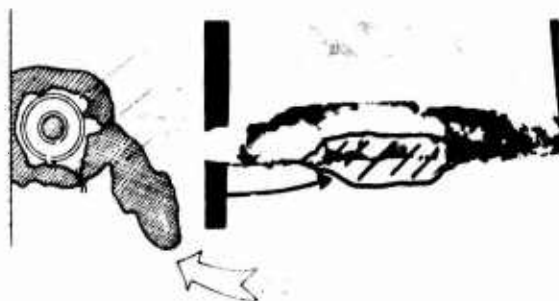


Fig. 12 Result after fire test

When cable breakdown does not occur until the cable core surface temperature reaches 700 °C as calculated before in Table 14, the life time can be prolonged. Fig. 13 shows the sample after the fire test.

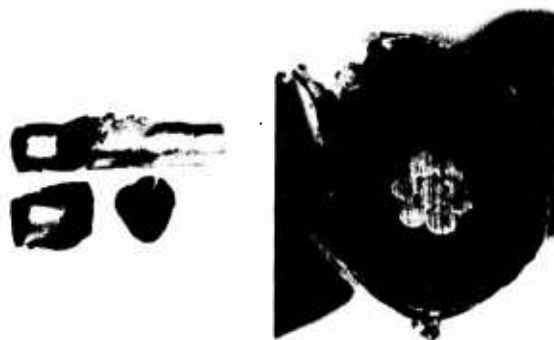


Fig. 13

As the temperature of the core rises the cross-linked polyethylene expands to make the copper wrapping tape like a pipe, which stops oxygen from reaching the insulation. It is supposed that in this state the insulation does not catch fire but when the temperature rises more the copper tape breaks because of the expansion pressure or the insulation and then the components of the core, the inner semiconductive layer, insulation and outer semiconductive layer, burst out, catch fire and cause the cable to breakdown.

It is difficult to solve the problem of insulation burst. Using copper pipe instead of copper tape can stop oxygen from reaching the insulation but the flexibility is lost and in case of copper corrugated pipe the space of the corrugated fold creates other oxygen and electrical problems. Double layers of copper tape were applied to obtain mechanical strength and a semiconducting spacer was provided between the copper tape layer and the outer semiconducting layer to cancel the heat expansion.

Table 1 The time until the insulation burst out and catch a fire

Structure of shield	Time
Copper tape one layer over the core	300 / 300
" two "	300 / 300
" " "	300 / 300
with a spacer between tape and core	300 / 300
Temperature of flame	300 / 300

Table 17 shows the time it takes these various kinds of core samples wrapped with only copper tape to catch fire.

In order to prevent the intumescent carbonized layer from dropping down and to maintain uniform thickness when the layer was intumescent, a cotton mesh tape, previously coated with the intumescent paint, was wrapped around the cable. The tape prevented the paint from running and it became a supporter of the intumescent layer after carbonization.

As a result the cable has an intumescent heat resistant layer which is thick enough, as shown in Fig. 14. Table 18 shows the fire-proof performance of the prototype cable with these countermeasures. Fig. 15 shows the typical construction of the cables.

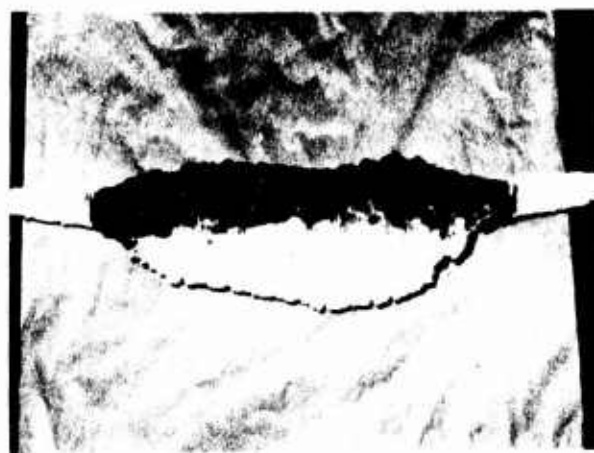


Fig. 14 Result after fire test

Table 18 The fire-proof performance of the prototype cables

No.	Cable	Fire-proof structure	Life time	time (calculated) <sup>+</sup>
1	6KV-22mm <sup>2</sup>	none	4*	3*24"
2	"	asbestos (5mm thick) + intumescent layer (2mm thick)	43*30*	38*
3	"	asbestos (5mm thick) + intumescent layer (4mm thick)	61*25"	48*
4	"	asbestos (5mm thick) + intumescent layer (6mm thick)	72*20"	144*

<sup>+</sup>time until the temperature of the core surface comes to 700°C.

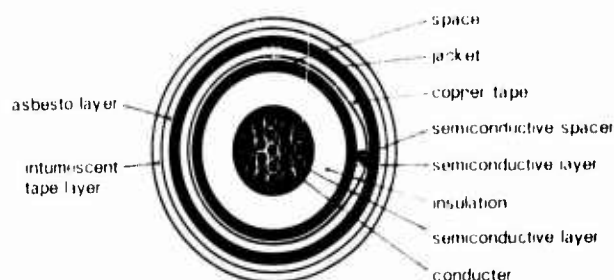


Fig 15 Structure of High Voltage fire proof cable

Mean while, many high voltage circuits are also used in the building and it is planned by the Board to ought to use fire-proof high voltage cable for emergency high voltage circuits. The cable mentioned above will meet this regulation.

In this case, the cable termination is set in a fire resistant box. Normal joint and branch will be unnecessary because of the short distance of the circuit, but we are going to study about them to apply to the high voltage power and control circuit of railroad and highway in tunnel.

#### 4. Conclusion

We reported two examples of our development of "Fire-proof wire and cable." We tried to improve the fire-resistance of cable from the stand point of the "maintenance of cable func-

tion in a fire", and not from the usual study on flame retardant material. Many problems, such as preventing the cable from generating gas like HCl and smoke, remain, but they are not thought to be important because many other materials are used together with wires and cables which give off a lot of gas and smoke in a fire.

The high voltage fire-proof cable which could operate for from 30 minutes to an hour in a fire was obtained as a result of this study.

#### 5. Acknowledgement

We wish to express our sincere appreciation to Mr. Yasui, Mr. Shiga, Mr. Inagaki and other many people of our company.

#### References

- 1) T. Hagihara, H. Matsubara, Reports of Study Meeting on Insulating Materials, IEEJ IM-74-16 (1974)
- 2) P. R. Johnson et. al. ACS 106th Rubber Meeting preprint No.10 (1974)
- 3) J. H. Petajan, ibid., No.14 (1974)
- 4) M. Yoshida et. al., unpublished data (1973)
- 5) J. N. Bradley, "Flame and combustion phenomena" Methuen & Co. Ltd., (1969)
- 6) "Handbook of Chemical Engineering", Maruzen (1958)
- 7) K. Okada et. al., Hyomen 13 231 (1974)
- 8) H. S. Carslaw, J. C. Jaeger, "Conduction of Heat in Solids" 2nd edition Oxford University Press (1959)
- 9) K. Ishise, unpublished data (1974)

#### Authors



Hironaga Matsubara

Hironaga Matsubara was born on October 12, 1942 in Shiga Prefecture.

He received the B.S. and the M.S. Degrees in Applied Chemical Engineering from Kyoto University in 1965 and 1967 respectively. He joined the Research & Development Laboratories of Sumitomo Electric Industries, Ltd. in 1967. He has been working on research of high polymeric material insulation and jackets ever since. Mr. Matsubara is a member of the Society of Polymer Science of Japan, the society of Rubber Industries of Japan and the IEEE of Japan.



Chiaki Matsunaga

Chiaki Matsunaga was born on August 30, 1937 in Osaka.

He received the B.S. Degree in Mechanical Engineering from Osaka University in 1961 and joined Sumitomo Electric Industries, Ltd. in April, 1961. He is now the manager of insulated wire & cable production engineering section.





Akihiko Inoue

Akihiko Inoue was born on April 13, 1938 in Manchuria.

He received the B.S. Degree in Electrical Engineering from Kyushu University in 1961 and joined Sumitomo Electric Industries, Ltd. in April, 1961. He is now the manager of rubber and plastic wire and cable engineering section. He is a member of the IEEE of Japan.



Norihiko Yasuda

Norihiko Yasuda was born on March 6, 1946 in Osaka.

He received the B.S. Degree in applied Chemistry and M.S. degree in petroleum chemistry from Osaka University in 1969 and 1971, respectively.

In 1971, he joined R & D group of Sumitomo Electric Industries, Ltd. He has been working on the research of high polymeric material insulation and jackets ever since. Mr. Yasuda is a member of the Chemical Society of Japan.

Mailing address

Sumitomo Electric Industries, Ltd.  
1-3, Shimaya 1-chome, Konohana-ku, Osaka, 554  
Japan.

## FIRE HAZARD EVALUATION OF CABLES & MATERIALS

by

E.J. Gouldson, G.R. Woollerton & J.A. Checkland  
NORTHERN ELECTRIC CO. LTD.  
Montreal, Quebec

### ABSTRACT

Test methods currently used for testing cables and cable materials are discussed and improved techniques are proposed. The virtues of the proposed techniques are illustrated by means of a typical fire retardant cable compound development. Finally the concept of a fire hazard rating system is introduced as a rationalization of the interpretation of cable and materials flammability testing.

### INTRODUCTION

The wire and cable approach to flammability has been changing over the last few years. Originally cables were constructed of materials designed to minimise the possibility of ignition and propagation of fire from short circuits, arcing, etc. The standard test for these constructions has been the vertical flame test as described in standards issued by such bodies as ASTM, U.L., CSA and IEC.

More recently a drive for improved performance has been felt where interest centres on the contribution of wire and cable to an existing fire rather than as a source of combustion. In some areas cable volume is small compared with other flammable materials and can be ignored, but in such locations as telephone exchanges, power stations, subways etc. the amount of cable can be substantial. Recent fires in the New York telephone exchange and Montreal Metro have shown that the cables contributed significantly once the fire had started.

With this changing emphasis in the interpretation of the role of cable materials in a fire situation in mind, this paper presents a critique of some of the test methods currently used for fire evaluation of cables and materials, and leads to proposals for new test methods. Inside cable is used as an example of how these methods may be used to follow improvements in the insulating and jacketing materials, and provide evaluation of modified cable constructions. Finally the concept of a fire hazard rating is introduced as a realistic assessment of the total test data.

### FLAMMABILITY OF PLASTICS

While one of the objects for wire and cable is to improve their response to fire, very few of their electrical or physical characteristics can be sacrificed. Thus it is unlikely that a unique solution can be found, but rather that different approaches will be used in different applications. However a basic understanding of what occurs during the combustion of a polymer is useful.

In the early stages of a fire, heat from an external source reaches the polymer and low temperature vaporization takes place followed by degradation of the polymer beginning with the breaking of the weakest bonds. As decomposition continues, the volatile flammable products diffuse to the surface and mix with the air. Continued heating causes the temperature to reach a critical value and ignition takes place. If pyrolysis products and oxygen continue to reach the combustion zone, and if the energy liberated by the combustion is sufficiently in excess of the heat losses to maintain the temperature above the ignition temperature, the process becomes self perpetuating.

Heat dissipating beyond the area of the actual fires is considered the primary hazard in well ventilated fires where there is a good supply of oxygen. Plastic compounds have a high calorific value and their combustion results in the liberation of large quantities of heat. In poorly ventilated fires, the oxygen is depleted, combustion is incomplete and large volumes of carbon monoxide are given off. Adding to this highly toxic gas are the toxic and corrosive gases from the burning materials such as hydrogen chloride from PVC and chlorinated polyethylene; and other halides from flame retardant non-chlorinated plastics.

Finally during the fire, smoke, which is the airborne mixture of heated gases, liquid droplets and solid particles, can be given off in large volumes. This is a hazard in itself, causing panic and obscuring exits.

### FLAMMABILITY TEST METHODS

Having defined the factors which must be considered, namely heat, fire spread, toxic and corrosive gases and smoke, the tests presently available for the evaluation of materials and products can be critically reviewed.

#### Horizontal and Vertical Flame Tests - Materials

This is a standard test and variations of the method are found within specifications issued by ASTM, Underwriters Laboratories as well as other National and International standards writers.

The test consists of exposing a bar of the material to the flame from a bunsen burner for a specified period of time or number of times. For these tests pass/fail criteria are based on the time for the flame to extinguish after the removal of the burner together with the distance the flame travels. Although suitable for most materials, there are some, e.g. nylon which move away from the flame during testing and cannot be properly assessed.

### Vertical Flame Test - Cables

For a typical vertical flame test on a cable, the cable is mounted vertically and exposed to the flame from a bunsen burner inclined at 20° to the horizontal. An indicator of gummed paper is wrapped around the wire 10" above the point of application of the flame. The flame is applied to the wire for fifteen seconds five times, with fifteen seconds between applications and the wire is considered to fail if the indicator is burnt when the flame extinguishes.

It is accepted that this test is not representative of behaviour in a fire but does give a good indication of behaviour under short circuit conditions. To try to better simulate the fire conditions various tests have been devised using more than one burner or larger burners. As an example of how these changes in burner size or number affect the end result, a polyethylene jacketed cable which passed the standard vertical test was tested with two burners. The cable burst into flame and burned quite ferociously. Another example is quoted in Ref.<sup>7</sup> where PVC jacketed cables which had previously been considered flame retardant spread fire badly when a larger burner was used.

### Oxygen Index Test - Materials

The limiting oxygen index of a material is defined as the minimum percentage of oxygen, expressed as volume percent which will just support combustion of the material. The method gives results which are highly reproducible from sample to sample and from laboratory to laboratory and is now an ASTM and International standard. It gives an indication of the flammability of a material under limited conditions and is a good tool in the areas of research, quality control and material classification but because of its artificiality its usefulness in fire research is questionable.

### Smoke Measurement - Materials

Most smoke chambers are similar in that they use the attenuation of a light beam as a measure of the smoke density when a material is pyrolysed using either radiant heat (non-burning) or a flame (burning). There are presently two standard methods within ASTM for the measurement of smoke, the N.B.S. chamber and the Rohm and Haas equipment - Refs.<sup>15,16</sup>. A chamber has been developed in the Northern Electric laboratories and is referred to as the N.E. Smoke Chamber. It has the advantages of being inexpensive to build and gives reproducibility acceptable for plastic materials.

The N.E. Smoke Chamber is a totally enclosed box made as leakproof as practical in order to contain all smoke produced during a combustion test (background of Fig. 1). The smoke is measured by attenuation of two light beams, one vertical and the other horizontal. Voltage output from the detectors is recorded on a two pen chart recorder and from this can be calculated:

- 1) The total maximum smoke concentration produced
- 2) The time required to generate the maximum smoke concentration.

More details of this chamber are given in Appendix 1.

### Tunnel Test - Materials and Cables

The preceding test methods are suitable for evaluation in the laboratory, but the tunnel test, because of its size and the expense of operating it, is not considered a laboratory test. Testing to qualify for building code acceptance is usually done by independent testing laboratories.

The test equipment consists of a horizontal tunnel 25 feet in length and of rectangular cross-section 18 inches wide and 12 inches deep. The roof is removable and the material to be tested is attached to the underside of it. At one end of the tunnel are two fixed burners, set so that their flames impinge on the test specimen and the flame is forced down the tunnel by a draught of air of 245 feet/minute. One wall of the tunnel has a series of observation windows along its length. The exhaust end has a photoelectric detector system to measure smoke emissions. Thermocouples are mounted in the floor of the tunnel to give an indication of the fuel contributed by the combustion.

The equipment is calibrated using asbestos cement board for the zero level and red oak flooring to give the 100 level for smoke and flame spread. Ratings quoted for building materials are therefore a comparison with red oak, and numbers less than 100 mean the flame spread and/or the smoke of the test material is less than red oak and for numbers greater than 100, they are more than red oak.

Applied to building materials, the test has now become accepted as the standard, but there are still no approved methods for mounting wires and cables and if the insulation itself is tested it tends to melt and drop and needs special support. Therefore, although numbers are quoted in building codes for the flame spread and smoke ratings allowable for cables, there is no standard method available for their measurement. It does seem probable, however, that all wires and cables with non-metallic coverings which are now used would fail the requirements if a mounting method was developed.

Recent investigations have indicated that for foamable plastics at least, there is not a true correlation between the tunnel test and the real fire environment. To quote from a recent paper Ref.<sup>19</sup> the tunnel test "is simply a tool and one of many tools available for the protection of the community. It may provide a good comparison between wood ceiling products which have low ignition temperatures, but a poor comparison of other building materials like foamed plastics which have higher ignition temperatures. Continued use of this method alone to predict actual building fire behaviour of foamed plastic

building materials is improper". This type of criticism could well start a move away from the tunnel test as the standard method of evaluating the fire hazard of many building materials and methods of mounting wire and cables might never be developed.



FIG. 1 FLAMMABILITY LABORATORY

The Ohio State University Release Rate Apparatus (OSU RRA) - Materials

The disadvantage of developing compounds for flame retardancy using the previously described methods is that data has to be collected from different tests on the compounds and from this data, the best formulation must be chosen to make cables which are then further evaluated. The ideal would be a test method which would give all of the required data from one test and which could be used for testing compounds, cable models and finished cable.

The Ohio State University Release Rate Apparatus with modifications, some of which are described and others which are still being developed, is capable of supplying all the information required for fire research on wire and cable.

The Apparatus is shown in the foreground of Fig. 1 with an outline sketch in Fig. 2. Detailed descriptions of its operation are given in Refs. <sup>10</sup> and <sup>11</sup> and for our purposes a brief description will suffice.

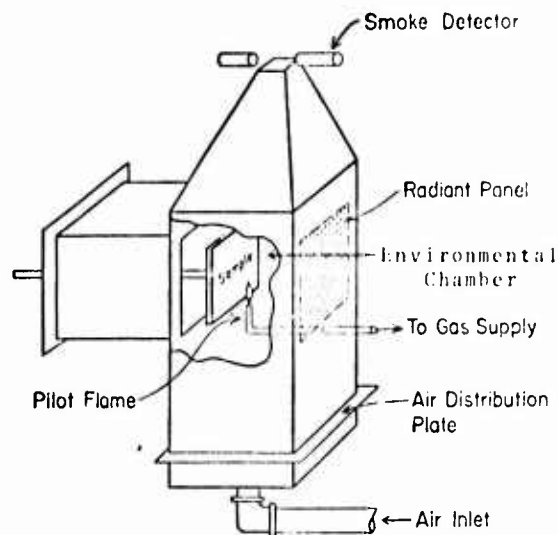
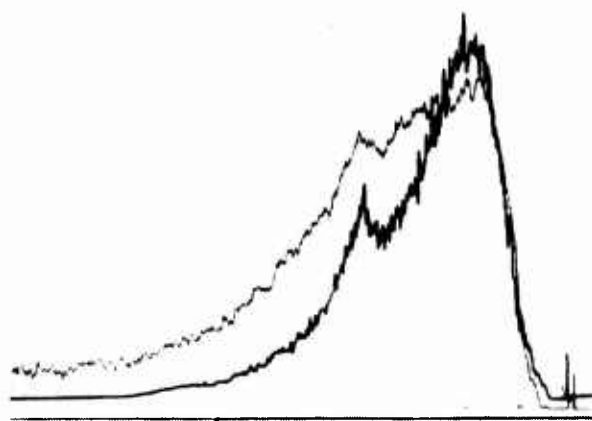


FIG. 2 OHIO STATE UNIVERSITY RELEASE RATE APPARATUS

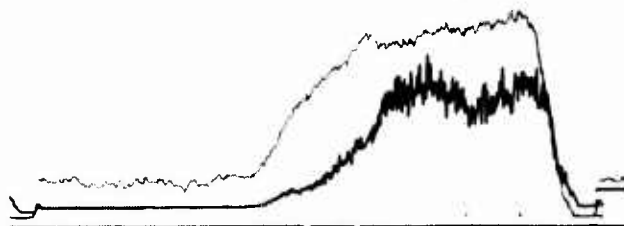
The apparatus consists of the environmental chamber through which a constant flow of air passes. The specimen's exposure is determined by a radiant heating panel adjusted to produce the desired radiant heat flux to the specimen. The specimen is mounted in the sample holder - Fig. 3 and positioned so that a small pilot flame impinges on its surface when a piloted ignition is wanted. The change in temperature and optical density (light absorbance) of the gas leaving the chamber are monitored, from which the rates of heat and smoke release are calculated. Typical outputs from the apparatus are shown in Fig. 4 for a standard formulation and an improved compound respectively. The darker line in each case represents smoke and the lighter line temperature change.



FIG. 3 SAMPLE HOLDER



a) Standard Compound



b) Improved Compound

FIG. 4 TYPICAL RELEASE RATE OUTPUTS

The environmental chamber can be used to hold assemblies or pieces of material with a surface area of 10" x 10" and with a maximum thickness of 4". Air flow rate can be varied but for normal operation a standard flow is recommended. The system is designed to permit easy mixing or substitution of flow gases other than air so that burning studies in enrichment or depletion of oxygen are possible.

The present chamber is equipped with an electrically heated radiant panel which is capable of an output of up to 35 kW/m<sup>2</sup> radiant heat flux at a sample position of 4" from the specimen surface. This corresponds to a panel surface temperature of approx. 700°C, although a maximum condition of 600°C is recommended (approximately 30 kW/m<sup>2</sup>). Investigations are underway within the ASTM Task Group on a gas-fired radiant panel to raise this upper limit to approximately 1000°C (approximately 50 kW/m<sup>2</sup>).

The range of heat conditions required to establish an appraisal of the combustion characteristics of a material, appears at the moment to be a subject of controversy, or of at least a divergence of opinions. Based on observations with cable insulation and jacketing materials it would appear that for all

intents and purposes, nearly total decomposition takes place quickly at heat flux conditions of 30 kW/m<sup>2</sup> (600°C). It is probable that any flame retardant mechanism which could be devised for a polymeric material would be of little effect, if any, at heat flux conditions greater than 30 kW/m<sup>2</sup> (600°C). Higher heat flux conditions may be useful in the evaluation of extremely high heat-resistant materials but their use for normally encountered insulating and jacketing materials would appear to be quite limited. This could be confirmed by further experimentation such as the use of Thermal Gravimetric Analysis.

Flame travel across the exposed surface of the sample is observed visually - Fig. 5, and the average rate of flame propagation over the samples width is noted. Sampling of exhaust stack gases is being carried out by Ohio State University and other members of the ASTM task group including our own laboratory working on standardizing the equipment.

The test method is designed to provide a description of the behaviour of materials and products under a specified exposure in terms of ease of ignition, flame travel rate, and release rate of heat and smoke, and toxic and corrosive gases. By changing the radiant heat flux exposure for subsequent tests, the change in behaviour of materials and products with different heat conditions can be estimated.

Data generated from the Release Rate Apparatus includes:-

Heat Release Rate. Reported in terms of Watts output per square meter of specimen surface area.

Smoke Release Rate. Reported in terms of SMOKE Units per minute per square meter of specimen surface area. By definition one SMOKE (Standard Metric Optical Kinetic Emission) unit is a concentration of smoke in one cubic meter of air which reduces the percentage transmittance of light through one meter of this air to 10%, i.e. Optical Density (Absorbance) - 1.0

Ease of Ignition or Time to Ignition. Reported in seconds and is the time elapsed from exposure of a specimen to the heat flux to the time of a significant release rate of heat, i.e. when more heat is being evolved from the specimen than is being absorbed from the heating panel.

Flame Travel Rate. Reported in mm/s and is calculated using the time for flame to travel from the centre to the side edge of the specimen.

Total Heat and Smoke Release, is the area under the respective release rate curves between the start of a run to some suitable time when release rates are diminished to insignificant levels.



FIG. 5 SAMPLE UNDER TEST VIEWED THROUGH OBSERVATION PORT

#### Toxic and Corrosive Gas Emission

At the present time research into the area is only in its initial stages. The ultimate objective is to make the apparatus capable of measuring not only fuel, flame spread and smoke but also corrosive and toxic gases. It is proposed that the corrosive gases will be determined by the effect on copper strip from the exhaust gases but an actual quantitative method has yet to be fully developed. Toxic gas evaluation is presently being attempted by the use of specific ion electrodes and infra-red analysis from samples of gases taken from the exhaust gases. Even when the analysis method is considered satisfactory it will still be difficult to relate this to people safety until research currently under way in the U.S. to determine safe exposure levels is complete.

#### Fire Retardant Inside Cable Compounds

The first use of the OSU RRA was to measure changes in fire behaviour of cable compounds developed to improve inside cables, which are PVC insulated and jacketed multi-pair cables. Since PVC is inexpensive and had until recently been considered a fire retardant material, effort was expended to analyse the performance of plasticised PVC in fire situations to generate improved confidence in the material.

The first phase of the work focused on a characterization of the PVC compounds presently used, followed by formulation modification designed to provide improvements in fire retardant performance while retaining those properties necessary for a good cable compound. Tables 1 and 3 show those properties which were considered essential for acceptable jacketing and insulating compounds.

TABLE 1  
INSIDE CABLES - PVC JACKETING - PHYSICAL PROPERTIES

PROPERTY	REQUIREMENT	FORMULATION		
		STANDARD - 1	A	B
TENSILE STRENGTH - PSI	2400 MIN	3120	2430	2037
ELONGATION - %	200 MIN	535	240	280
RETENTION AFTER AGING 7 DAYS AT 100C				
Tensile - %	80 MIN	90	80	101
Elongation - %	75 MIN	85	80	85
BRITTLE POINT - $P_{20}C$	-40 MAX	-51	-39	-48
HARDNESS - DUROMETER $A_2$	85 MAX	94	88	87
VOLATILE LOSS - %	5 MAX	3.6	2.4	3.7
HEAT DISTORTION - %	20 MAX	16	10	16
COLD FLEX TEMPERATURE - C	-20 MAX	-33	-27	-40
SURFACE FRICTION - LB	1.0 MAX	0.7	0.66	0.74

#### Jacketing Materials

Three compounds, Standard -1, A and B are shown in Table 1 from amongst those evaluated in this study. Apart from the marginal failure of the brittle point for Compound A, all are considered acceptable for use on cable.

These compounds were evaluated for their response to fire with the results shown in Table 2. From the results normally quoted, the new formulations have higher oxygen indices and better retention of HCl when pyrolysed at 600C. However, the data from the Release Rate Apparatus shows that we have also reduced smoke for the flaming condition but not for the non-flaming condition; have reduced the heat output at the lower temperature flaming conditions but not for other conditions; and had no appreciable affect on the flame spread.

TABLE 2  
INSIDE CABLES - PVC JACKETING FLAMMABILITY PROPERTIES

PROPERTY	FORMULATION		
	STANDARD - 1	A	B
LOI %	22.8	25.6	23.8
HCl EMISSION			
Theoretical % W/W	37.6	29.9	27.1
Measured at 600C % W/W	34.5	14.6	10.5
Efficiency %	8.2	51.3	61.2
AREA UNDER SMOKE CURVE - SMOKE UNITS			
Flaming Conditions - 550C	642	422	410
- 450C	505	222	248
- 350C	276	178	133
Non-Flaming Conditions - 550C	648	624	480
- 450C	489	467	507
- 350C	130	130	157
AREA UNDER HEAT CURVE - ARBITRARY UNITS			
Flaming Conditions - 550C	252	232	257
- 450C	236	145	199
- 350C	217	96	159
Non-Flaming Conditions - 550C	176	202	201
- 450C	46	50	61
- 350C	42	63	59
FLAME SPREAD - SEC.			
Flaming Conditions - 550C	18	10	14
- 450C	49	62	59
- 350C	131	135	103
Non-Flaming Conditions - 550C	103	77	62
- 450C	6	6	6
- 350C	6	6	6

\* No Ignition

This is a good example of the difficulties in fire research for cables. To date no way of making cable compounds completely fire-proof has been found and trade-offs have to be made of some physical and electrical properties to gain improvements in the materials response to fire. There are also trade-offs to be made in some of the fire properties. The dream of a compound which will do everything is not yet possible and the manufacturing industry must rely on the customer to help determine which trade-off can be accepted.



TABLE 3  
INSIDE CABLES - PVC INSULATION PHYSICAL PROPERTIES

PROPERTY	REQUIREMENT	FORMULATION		
		STANDARD - 2	C	D
ON MOULDED PLATES				
TENSILE STRENGTH - PSI	2600 MIN	3500	3500	3050
TENSILE AT 100% ELONGATION - PSI	2300 MIN	2400	2700	2550
ELONGATION RETENTION AFTER AGING 7 DAYS AT 100C %	200 MIN	320	220	210
Tensile %	90 MIN	100	95	94
Elongation %	70 MIN	94	100	94
BRITTLE POINT $F_{70}^C$	-13 MAX	-21	-13	-11
HARDNESS - DUROMETER $A_2$	95	97	95	95
COLD FLEX TEMPERATURE - C	+5 MAX	-3.5	+3	+1
SIC AT 1 SHS	-	4.24	4.48	4.84
POWER FAILURE AT 1 SHS	-	0.10	0.06	0.06
VOLUME RESISTIVITY - $\Omega\text{CM}$	-	$1 \times 10^{14}$	$4 \times 10^{14}$	$4 \times 10^{14}$
ON 24 AWG WIRE				
ELONGATION %	175 MIN	205	200	200
ADHESION - LB	5 MAX	1.4	0.8	1.0
COMPRESSION - LB	600 MIN	920	880	750
AGING - 48 HOURS AT 121C	NO CRACKS	PASS	PASS	PASS
WAVE LENGTH AT 1/4" AROUND A 1/4"	NO CRACKS	PASS	PASS	PASS
SHRINKAGE - IN	16/64" MAX	NONE	NONE	NONE

A similar exercise was then made for the insulating compound. The physical parameters were set from the needs for a good insulating compound and insulated wire (Table 3). Although for this application the electrical properties were not considered as important requirements the data are shown for comparative purposes. As for the jacketing compound the property which was difficult to meet was the brittle point and both compounds C and D are marginal but would be acceptable.

The evaluation of these compounds for flammability properties (Table 4) showed the improvement in the oxygen index and HCl emission. Less smoke was generated for the improved formulation for flaming conditions, and non-flaming showed some improvement. One definite improvement to be noted is that the new formulations did not ignite at any temperature tested under the non-flaming conditions.

TABLE 4  
INSIDE CABLES - PVC INSULATION FLAMMABILITY PROPERTIES

PROPERTY	FORMULATION		
	STANDARD - 2	C	D
L.O.I.			
	24.2	50	28.4
HCl EMISSION			
Theoretical	29.2	34.4	32.4
Measured at 400C % W/W	26.0	25.3	18.6
Efficiency	8.2	26.4	42.4
AREA UNDER SMOKE CURVE - SMOKE UNITS			
Flaming Conditions - 550C	858	448	445
- 450C	729	322	252
- 350C	494	262	195
Non-Flaming Conditions - 550C	858	664*	534*
- 450C	525*	640*	470*
- 350C	227*	195*	38*
AREA UNDER HEAT CURVE - ARBITRARY UNITS			
Flaming Conditions - 550C	224	185	196
- 450C	203	220	158
- 350C	239	51	92
Non-Flaming Conditions - 550C	217	55*	71*
- 450C	82*	69*	49*
- 350C	60*	53*	104*
FLAME SPREAD - SEC.			
Flaming Conditions - 550C	17	16	14
- 450C	43	65	48
- 350C	124	222	198
Non-Flaming Conditions - 550C	62	*	*
- 450C	*	*	*
- 350C	*	*	*

\* No Ignition

### Cable Testing in the Release Rate Apparatus

Up to this point all of the evaluations have been made using moulded plates of material to compare the materials properties. As mentioned earlier, one of the problems with fire research on cables is that apart from the bunsen burner test no laboratory tests are available which will give data on the behaviour of the product when exposed to fire. As it is our opinion that the Ohio State Apparatus is capable of doing all that is needed, the equipment was modified so that wires and cables could be evaluated under the same condition.

### Testing Insulated Wires

A thin stainless steel picture frame holder was made with projections at each corner to ensure that the wire remained in place (Fig. 6). The frame was designed to fit inside the standard slab sample holder -

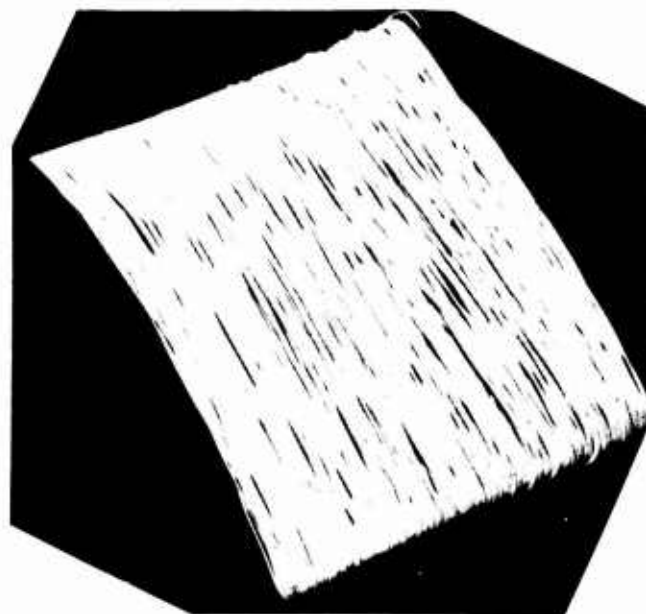


FIG. 6 INSULATED CONDUCTORS ON FRAME

Fig. 7 so that the test results could be compared between the compound and the insulated wires. To make the comparison simpler the length of wire chosen for the testing was that which had the same compound weight as the 6" x 6" x 75 mil moulded plate.

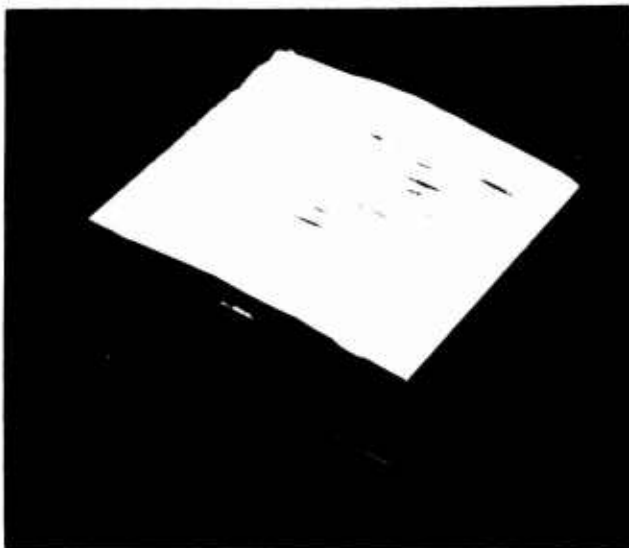


FIG. 7 FRAME IN SAMPLE HOLDER

Results of the comparison on the formulation Standard C and D are shown in Table 5 and it is obvious that testing insulated wires gives different results from testing plates. Although the same pattern follows of less smoke and more heat when moving to the special formulations, generally all of the levels are higher for the insulated wire. The most probable explanation of this is that the surface area exposed to the heat is greater for the wire configuration and gains made by char formation will be less marked on wires. It also serves as a warning that for defining the product, data collected from flat plates will not give absolute data, even though they can be used for comparisons where improvements are sought.

TABLE 5  
COMPARISON OF RESULTS ON MOULDED PLATES AND TWISTED PAIRS  
TESTED AT 550C

PROPERTY		FORMULATION					
		STANDARD - 2		C		D	
		PLATES	WIRES	PLATES	WIRES	PLATES	WIRES
AREA UNDER SMOKE CURVE							
Flaming Conditions	Smoke Units	858	722	448	608	445	524
Non-Flaming Conditions		858	983*	664*	835*	534*	697*
AREA UNDER HEAT CURVE							
Flaming Conditions	Arbitrary Units	229	327	185	294	196	302
Non-Flaming Conditions		217	82*	55*	89*	71*	74*

\* No Ignition

#### TESTING CABLES

Having found the difference between insulated conductors and plates, testing cables was considered. These are a much more complex structure consisting of insulated conductors, perhaps metallic shields and jackets. It was felt that by having such a tool available it would be possible to modify insulations, shield and jacket materials to see what advantages could be derived from material and construction change on the final properties of the cable.

To enable the different constructions and cable materials to be evaluated in a multiple cable situation a frame was built with removable pins, which were spaced at the approximate diameter of the finished cable.

Where a cable was available for testing lengths of 6" were placed side by side on the pins and held in place by a light corrosion-resistant wire. However, if a new formulation of jacket and/or construction was required to be evaluated, insulated wire core bundles were covered by weaving over the cores and under the pins with a thin pressed sheet of jacketing material. A single pressed slab 12" square, cut in two, provided the correct length of sheet to completely cover the wire cores - Fig. 8. The face presented to the radiant heat source in the chamber closely resembled cables placed side by side, both visually and configuratively.

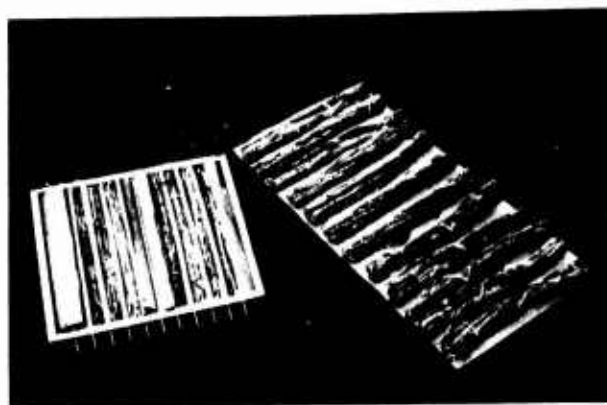


FIG. 8 CABLES MODELS BEING PREPARED

Thus, by a simple pressing, a new cable design could be evaluated for flammability characteristics without the expense of shop extrusion and attendant waste of time and materials.

The method can be used with the cable holder oriented horizontally or vertically, simulating the actual use condition.

Information using the frame with a simulated cable configuration indicated excellent agreement in smoke and heat figures compared to a similar burn test of standard production cable, showing that the method is a valid method for evaluation of cable constructions and materials. A slight difficulty encountered in not being able to pack the core as tight as a production core did not seem to affect results to any significant detectable level.



FIG. 9 CABLES MODELS AFTER TESTING

To evaluate the use of this method to detect flammability changes with change of design, cable models were compared using the standard jacketing compound and the improved compounds. Other models were constructed using an aluminum shield over the insulated conductors. The results from these tests are shown in Table 6.

TABLE 6  
COMPARISON OF RELEASE RATE APPARATUS RESULTS  
FOR INSIDE CABLE WITH MODIFIED DESIGNS  
CORE 50 PAIRS 24 AWG OF STANDARD 2  
TESTED AT 550C FLAMING CONDITIONS

PROPERTY	JACKET FORMULATION			
	STANDARD 1	A	B	WITH ALUMINUM SHIELD
AREA UNDER SMOKE CURVE - SMOKE UNITS	1910	1590	1790	1250
AREA UNDER HEAT CURVE - ARBITRARY UNITS	1004	996	965	926
FLAME SPREAD - SEC	17	18	60	49

It is clear from this data that the improvements detected during the compound development have followed through into the cable models; and that this cable construction can be improved, albeit only a little in some instances. It can also be seen that the introduction of an aluminum screen over the conductors further reduces the smoke and heat output.

#### A PROPOSED FIRE HAZARD RATING FOR CABLES

In this paper, five factors have been identified which are most important in a fire, namely: fuel contribution, flame spread, smoke, toxicity and corrosivity. Methods have been shown whereby some of these parameters can be measured and varied in specific formulations. It has also been shown that it is impossible to make insulating materials such that they are completely fire proof. One possible solution is to make all wires and cables with a metallic sheath or place them in metallic conduit. This would overcome the fire problem but is not practical for many applications nor would it stop smoke being conveyed to other areas during a fire.

Unfortunately there is no consensus as to which is the most important factor. Ask any group of code officials, safety personnel and users and they will all give different answers. Some want to protect the equipment; some to protect the building; and some are interested in evacuation of people and fighting the fire. This means that the best the manufacturing industry can do is show for each product what the relative ranking of each factor is and allow the user to choose his product from the rankings. From this will develop a Fire Hazard Rating for the product and although it is appreciated that it will be subject to discussion and modification we believe that the basic concept is correct and is the direction to be taken.

To develop the rating a one foot sample of cable should be considered to have burned in one cubic foot of space. In this way the user can determine from his own knowledge of placing methods the total cable in any given space and by simple ratios can calculate the particular hazard and decide on the limits he must set himself in his own particular application. To assist him the industry should make available the data on the five factors under varying conditions, and for these we are proposing radiant panel temperature of 300 and 600C with and without flaming conditions.

So as not to move too far away from the classical approach of the Wire and Cable industry to flammability, a test should also be included at ambient conditions under flaming condition to relate to the presently used vertical flame test.

The evaluation should be based on the following:

Fuel Contribution: Compared to a standard sample of red oak flooring. This may seem strange, but firemen can relate to this comparison and because of this it is used for other evaluations such as the tunnel test. The red oak sample should be given number 100 and cables should have numbers greater than 100 for more heat than red oak and smaller than 100 for less heat.

Flame Spread: Should be based on red oak with the flame spread of red oak considered to be 100.

Smoke: Could be based again on red oak but most meaningful if SMOKE units are used directly.

Corrosive Gases: Should be based on the corrosion of copper by exhaust gases

Toxic Gases: The limits set on this factor cannot be finalized until more data is available on the effects of short time exposure to the types of toxic gas of interest.

If a Fire Hazard Rating such as this was introduced for wire and cables, a system would be in use to identify all of the necessary factors important in a fire. They can be collected from one piece of test equipment and based not on testing of materials but on the actual cable construction. Real improvements which can be gained by changes of construction or materials become readily apparent and the user will be able to choose a product for any particular application. Further, code officials will be able to write meaningful specifications for cables to which the manufacturing industry can relate.

#### USE OF THE FIRE HAZARD RATING

An example of the use of the rating system is some recent work on comparison of two types of wire. Although the numbers were not experimentally derived as described in the text but based on an earlier method they are sufficient to show the advantages of such a system.

Table 7 shows the rating derived for wires E and F under a certain set of conditions.

HAZARD	RATING	
	WIRE E	WIRE F
Fuel	120	200
Flame Spread	200	120
Smoke	20	200
Corrosive Gas	4	200
Toxic Gas	100	120

TABLE 7 FIRE HAZARD RATING

Normal evaluation of these wires by the vertical flame test showed that Wire F was better and based on this alone would have been more acceptable. However from the fire hazard evaluation the only property where it was best, was flame spread, and on all other properties Wire E was superior. Given this data we ask the reader to decide which wire he would choose.

#### Acknowledgements

The authors are grateful to J.F.W. Bentham now with Canada Wire and Cable for his work on the initial development of the NE Smoke Chamber, together with the members of Northern Electric Wire and Cable Division R&D Departments who contributed to the data presented in this paper.

Thanks are also due to Professor E.E. Smith, Professor Chemical Engineering at Ohio State University for his help and guidance.

#### References

- (1) ASTM D2633 Standard Methods of Testing: Thermoplastic Insulated and Jacketed Wire and Cable. Para. 30, Vertical Flame Test
- (2) "New Considerations in Flammability Testing of Lead and Hook-up Wires" - R.L. R.L. Spade Belden Corporation. Proceedings of the 11th Electrical Insulation Conference Oct. 1974 IEEE Publication 73CHO 777-3E1-33.
- (3) Underwriters' Laboratories Inc. Standard for Safety UL94 Tests for Flammability of Plastic Materials for Parts in Devices and Appliances.
- (4) Canadian Standards Association Standard C22.2 No. 0.3 Test Methods for Electrical Wires and Cables Para. 4.11 Flame Retardance
- (5) British Standards Institutions Specification B.S. 4066: 1966 (IEC Specification 332 is similar) Specification for Flame-Retardant Characteristics of Electric Cables, Para. 7(e) - Two Burners for Cables Larger than 50 mm (2 in) diameter
- (6) IEEE Standard 383 Para. 2.5 Flame Tests - Specification on Electric Cables, Field Splices and Connections.
- (7) Ontario Hydro Designation Bruce Generating Station Specification L-744-74 Fire Retardant Control Cable - 300 Volts
- (8) D.J. Stonkus, Ontario Hydro Research Division "Flammability Tests on Grouped PVC Jacketed Control and Power Cables" Canadian Electrical Association Meeting March 72  
D.J. Stonkus and S.J. Oda: "Fire Protection of Grouped Control Cable Installations" CEA 1973 Fall Meeting.
- (9) Draft-Control Specification CSA Certification Requirements for Type Fire Retardant Control Cable (FR 75-600).
- (10) Draft of a Proposed ASTM Test Method: Edwin E. Smith Ohio State University "Test for Heat and Smoke Release Rates"
- (11) E.E. Smith: "Heat Release Rate of Building Materials" ASTM Publication STP502 pp 119-134 E.E. Smith: "An Experimental Method for Evaluating Fire Hazard" presented at 11th International Fire Protection Seminar, Zurich, Switzerland October 1973.
- (12) J.F.W. Bentham: "A Method for the Determination of Optical Density of Emissions from Decomposing Polymers in a Simulated Fire Environment" Summer Meeting of ASTM Committee E05 Philadelphia, Pennsylvania June 1973.

- (13) S. Kaufman: Bell Laboratories, Norcross Georgia.  
R.S. Dedier: Emery Industries, Cincinnati, Ohio 23rd International Wire and Cable Symposium Atlantic City 1974. "A PVC Jacket Compound with Improved Flame Retardancy and Superior Physical Properties".
- (14) ASTM Copper Mirror Test D2671 Standard Methods of Testing Heat-Shrinkable Tubing for Electrical Use; Corrosion Testing Paras. 79-83 - Method A.
- (15) Rhom & Haas Smoke Chamber XP2 F.J. Rarig and A.J. Bartosic: "A Method of Measuring Smoke Density". Quarterly of the NFPA, Vol. 57 No. 3 January 1964 pages 276-287 (NFPA Publication Q57-9)
- (16) NBS Smoke Chamber (A method for Measuring Smoke from Burning Materials" Symposium on Fire Test Methods - Restraint and Smoke 1966 ASTM Special Technical Publication STP 422, 1967.
- (17) ASTM E84 Standard Method of Test for Surface Burning Characteristics of Building Materials.
- (18) ASTM D2863 Standard Method of Test for Flammability of Plastics Using the Oxygen Index Method
- (19) "SLRP Analysis of Recommended Protection for Foamed Plastic Wall Ceiling Building Insulations" - W.F. Maroni, Factory Mutual Research Corporation. Presented at the National Fire Protection Association Annual Meeting, Miami, Florida, May 1974.

## APPENDIX I

### THE N.E. SMOKE CHAMBER

Reproducibility is possible with the smoke chamber because controls are provided:

- 1) To regulate the temperature of the radiant tube furnace to simulate different combustion heat flux conditions.
- 2) To control the temperature of the chamber to simulate different ambient air temperature environments in fire conditions.
- 3) To adjust the detector sensitivities to critical optimum levels.
- 4) To initiate a spark source for ignition of emerging combustible gases to simulate flaming combustion conditions.

Standard samples used in the apparatus are discs 12 mm in diameter with a thickness of 1.9 mm. These weigh a nominal 300 mg. They are placed in a small combustion boat leaned at approximately 45° and inserted into the hot furnace (Fig. 10). The cooling effect



FIG. 10 SAMPLE INSERTION

of the sample triggers the controller to provide heat to the furnace immediately, resulting in a reproducible heating condition. Insulation sample lengths are chosen to provide an appropriate weight of combustible sample. Several 1" lengths are used and results are expressed in terms of sample length.

Reasons for Close Control of the Chamber Temperature. Walls of the chamber must be heated and insulated, and photometer windows must be in intimate contact with the walls to avoid condensation which will affect the result in an unpredictable way. Up to ten or more runs without detectable window fogging with this instrument is normal performance.

However, too high an ambient temperature of the chamber will cause premature coagulation or agglomeration of the smoke. Too low an ambient temperature creates a very slow clearing smoke but allows condensation on the chamber walls and windows. A temperature range of approximately 64C to 84C is a suitable compromise. The wall heaters are turned on when a sample run is started. This creates convective currents in the chamber which effectively homogenize the smoke.

Smoke units are expressed in terms of Smoke Units/gram if a weighed sample is used or Smoke Units/metre if a length of wire or cable sample is used. These are abbreviated forms of Absorbance/m<sup>3</sup> Volume/m light path length/(gram of sample or m sample length). Average deviation of values has been found to be approximately  $\pm 10\%$  for both light paths. These are standard units which should be comparable to results from any other smoke chamber if its results can be expressed in the same units.



Eric Gouldson graduated from London England with an Engineering Degree in 1960. Until he emigrated to Canada in 1967 he was employed by AEI Ltd. working on EHV cables. Since 1967 he has been at Northern Electric Co. Ltd where he is now Manager of Cable Development in the R&D laboratories of the Wire and Cable Division.



Greydon R. Woollerton, was born in Sherbrooke, Quebec in 1934, obtained a B.Sc degree at Bishop's University and has been active in wire and cable research at Northern Electric Co. Ltd. - Lachine, since 1956. With a background in spectroscopy, his present field is flammability research. He is a member of the Order of Chemists of Quebec, the Chemical Institute of Canada, the Spectroscopy Society of Canada, and an associate member of the Canadian Society of Chemical Engineering.



John Checkland was born in England and received his M.Eng. degree in Chemical Engineering from McGill University Montreal. He has been with Northern Electric since 1971 where he is now a member of R&D Staff of the Wire & Cable Division, Lachine, specializing in compound development and fundamental studies.



# THE EXTRUSION OF HIGH DENSITY POLYETHYLENE INSULATED WIRE FOR FILLED TELEPHONE CABLES

J. C. REMLEY  
B. M. BROKKE

WESTERN ELECTRIC COMPANY, INC.  
PHOENIX, ARIZONA

## ABSTRACT

THE EXTRUSION CHARACTERISTICS OF HIGH DENSITY POLYETHYLENE FOR FILLED TELEPHONE CABLES ARE EXAMINED IN DETAIL. CRITICAL CONTROL OF MELT TEMPERATURES, WATER TROUGH TEMPERATURES, AND PREHEAT TEMPERATURES IS REQUIRED TO PRODUCE HIGH QUALITY WIRE. HIGH DENSITY POLYETHYLENE IS AN ACCEPTABLE SUBSTITUTE FOR POLYPROPYLENE FOR FILLED CABLE APPLICATIONS.

## INTRODUCTION

IN APRIL, 1974, THE SUPPLY OF POLYPROPYLENE INSULATION COMPOUND FOR USE IN FILLED TELEPHONE CABLES WAS NOT ADEQUATE FOR THE REQUIREMENTS OF THE BELL SYSTEM. AT THAT TIME, THE PHOENIX WORKS CONVERTED FROM POLYPROPYLENE TO HIGH DENSITY POLYETHYLENE INSULATION. SINCE THIS PRODUCT HAD NOT BEEN MANUFACTURED ON A PRODUCTION BASIS, IT WAS NOT KNOWN WHAT PROBLEMS WOULD EXIST. AFTER THE CONVERSION HAD BEEN COMPLETED, A SIGNIFICANT INCREASE IN CAPACITANCE UNBALANCE IN FINISHED CABLES INDICATED AN INTENSIVE STUDY WOULD HAVE TO BE UNDERTAKEN TO PRODUCE HIGH QUALITY CABLES USING HIGH DENSITY POLYETHYLENE. IT WAS DETERMINED THAT THE INSULATED WIRE HAD TO BE MANUFACTURED USING VERY TIGHT TOLERANCES IN ORDER TO ACCOMPLISH THE OBJECTIVES OF THE TELEPHONE SYSTEM IN CONTROLLING NOISE IN THE CIRCUITS. THIS REPORT DETAILS THE EFFORTS EXPENDED TO PRODUCE HIGH QUALITY CABLES FOR THE TELEPHONE SYSTEM.

SINCE THE DIELECTRIC CONSTANT OF HIGH DENSITY POLYETHYLENE IS HIGHER THAN POLYPROPYLENE, FOR A GIVEN MUTUAL CAPACITANCE (0.085 UF/MILE), SLIGHTLY HEAVIER WALL THICKNESSES ARE NEEDED FOR THE POLYETHYLENE INSULATION. USING THE RELATIONSHIP:

$$C_c = \frac{7.36 E_r}{\log_{10} \frac{D_D}{D}} \quad (1)$$

$C_c$  = COAXIAL CAPACITANCE (MICROMICROFARAD/FOOT)

$E_r$  = RELATIVE DIELECTRIC CONSTANT

$D_D$  = DIAMETER OVER DIELECTRIC (INCHES)

$D$  = WIRE DIAMETER, CONDUCTOR (INCHES)

THE NOMINAL INSULATION DIAMETERS FOR POLYPROPYLENE AND HIGH DENSITY POLYETHYLENE ARE SHOWN IN TABLE I.

TABLE I: INSULATION DIAMETERS FOR POLYPROPYLENE AND HIGH DENSITY POLYETHYLENE

GAUGE	POLYPROPYLENE, DIAMETER OVER INSULATION	POLYETHYLENE DIAMETER OVER INSULATION
19	.0735	.075
22	.052	.054
24	.042	.043
26	.033	.0345

ALTHOUGH HEAVIER WALL THICKNESSES ARE REQUIRED FOR POLYETHYLENE, THERE WAS NOT A SIGNIFICANT INCREASE IN THE FINAL SIZE OF A POLYETHYLENE FILLED CABLE AS COMPARED TO AN IDENTICAL POLYPROPYLENE FILLED CABLE. THIS IS DUE TO A TIGHTER PACKING OF THE POLYETHYLENE WIRES.

THE HIGH DENSITY ETHYLENE PLASTIC IS AN ASTM D 1248, TYPE III, CLASS A, BASE POLYMER TO WHICH AN APPROVED ANTIOXIDANT SYSTEM HAS BEEN ADDED. AN ANTIOXIDANT AND A COPPER INHIBITOR ARE BOTH INCLUDED IN THE BASE POLYMER AND PROVIDE EFFECTIVE STABILIZATION.

## EXTRUSION EQUIPMENT

THE TANDEM INSULATING LINES AT PHOENIX ARE USED TO MANUFACTURE 19, 22, 24 AND 26 GAUGE WIRE INSULATION FOR FILLED CABLE APPLICATIONS.

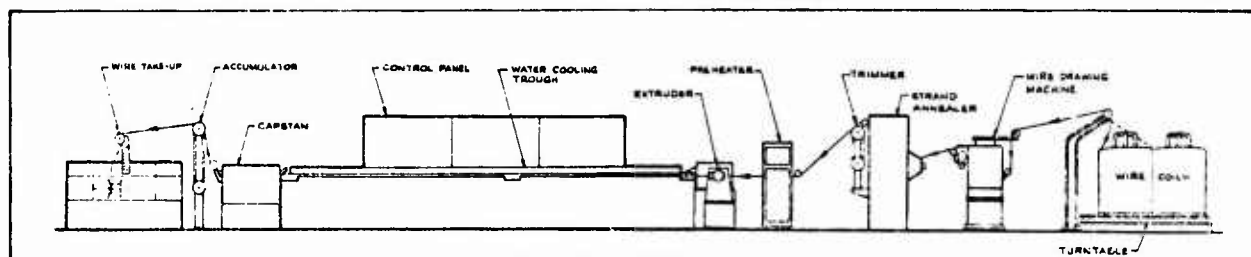


FIGURE 1: SCHEMATIC REPRESENTATION OF A TANDEM INSULATING LINE - PHOENIX WORKS

TWELVE GAUGE COPPER WIRE IS DRAWN TO THE APPROPRIATE GAUGE, STRAND ANNEALED, PREHEATED, EXTRUSION COATED, COOLED, AND WOUND ON A REEL. A SCHEMATIC REPRESENTATION OF THE TANDEM INSULATING LINES IS SHOWN IN FIGURE 1. EXTRUDERS USED FOR 19 AND 22 GAUGE WIRE MANUFACTURE ARE 3 1/2" DIAMETER, 24:1 L:D, AND EXTRUDERS USED FOR 24 AND 26 GAUGE WIRE MANUFACTURE ARE 2 1/2" DIAMETER, 24:1 L:D.

### TOOLING

POLYPROPYLENE TOOLING CONSISTS OF A CAPSULE TOOL HOLDER, EXIT DIE, CORE TUBE, ADAPTER, AND A LOCKING DEVICE TO CENTER THE CORE TUBE IN POSITION. A VERY SIMPLE THREE-COMPONENT TOOL CONSISTING OF A SMALLER CAPSULE TOOL HOLDER, CORE TUBE, AND EXIT DIE IS USED FOR THE HIGH DENSITY POLYETHYLENE. A SCHEMATIC REPRESENTATION OF THE TOOLING IS SHOWN IN FIGURE 2.

CHANGES IN THE INTERIOR ANGLES OF THE EXIT DIE, GUM SPACE, DRAW-DOWN RATIOS, AND EXTERIOR CORE TUBE TIP ANGLES ALL AFFECT THE ROUGHNESS OF THE EXTRUDATE. THE EFFECTS OF ALL THESE VARIABLES ARE CURRENTLY UNDER INVESTIGATION. WHEN PROCESSING POLYPROPYLENE INSULATING COMPOUND, THE EXTRUSION TOOLING WAS CHANGED APPROXIMATELY EVERY TWELVE HOURS, POLYETHYLENE TOOL CHANGES ARE AVERAGING APPROXIMATELY EVERY 60 HOURS.

### EXTRUDABILITY

POLYPROPYLENE CAN UNDERGO VERY SEVERE DRAW DOWNS DURING LINE START-UP AND STILL MAINTAIN A VERY UNIFORM AND CONTINUOUS EXTRUSION COATING OF THE WIRE. UNFORTUNATELY, SEVERE DRAW DOWNS WITH POLYETHYLENE RESULT IN SEGMENTED GLOBULES WHICH ARE NOT UNIFORM. THIS NON-UNIFORM FLOW RESULTS IN A POLY JAM OR LINE STOP. SMOOTHNESS OF THE POLYETHYLENE EXTRUDATE,

ESPECIALLY WITH 19 GAUGE WIRE, INCREASES WITH DRAW-DOWN, BUT A HAPPY MEDIUM SOMEWHERE BETWEEN FEW POLY JAMS AND ROUGH WIRE HAS TO BE ESTABLISHED.

PREHEAT TEMPERATURE, MELT TEMPERATURE, WATER TROUGH TEMPERATURE, LENGTH OF WATER TROUGH, AND FOOTAGE ON THE WET CAPSTAN ALL HAVE A VERY SIGNIFICANT EFFECT ON THE COAXIAL CAPACITANCE OF HIGH DENSITY POLYETHYLENE WIRE. THESE VARIABLES DID NOT HAVE A SIGNIFICANT EFFECT ON THE COAXIAL CAPACITANCE OF POLYPROPYLENE WIRE.

MICROSCOPIC EXAMINATION OF HIGH DENSITY POLYETHYLENE WIRE SAMPLES WITH ERRATIC CAPACITANCE REVEALED NUMEROUS CONTRACTION VOIDS, OVAL WIRE, AND VERY ECCENTRIC WIRE OR COMBINATIONS OF THESE. SMALL CHANGES IN ANY OF THE TEMPERATURE ADJUSTMENTS ON THE TANDEM INSULATING LINES PRODUCED A SIGNIFICANT CHANGE IN THE COAXIAL CAPACITANCE OF THE POLYETHYLENE WIRE DUE TO THE PRESENCE OR ABSENCE OF CONTRACTION VOIDS, OVALITY, OR ECCENTRICITY.

THE FORMATION OF CONTRACTION VOIDS IS THE RESULT OF TOO RAPID COOLING FOLLOWING THE EXTRUSION PROCESS.<sup>2</sup> CONTRACTION VOIDS ARE MORE PREVALENT WITH HIGH DENSITY POLYETHYLENE, AND THIS IS PROBABLY DUE TO THE HIGHER THERMAL EXPANSION OF HIGH DENSITY POLYETHYLENE DURING SOLIDIFICATION.<sup>3</sup> THE CONTRACTION VOIDS ARE VERY PREVALENT IN 19 AND 22 GAUGE POLYETHYLENE WIRE. A TYPICAL PHOTOMICROGRAPH OF A LARGE CONTRACTION VOID IN 19 GAUGE POLYETHYLENE WIRE INSULATION IS SHOWN IN FIGURE 3.

CONTRACTION VOIDS USUALLY ASSUME THIS HALF MOON SHAPE AND APPEAR ADJACENT TO THE COPPER CONDUCTOR. WHEN THE CONTRACTION VOIDS ARE NUMEROUS, THEY ARE USUALLY CONNECTED AND PROVIDE A CONNECTED PASSAGEWAY ALONG THE

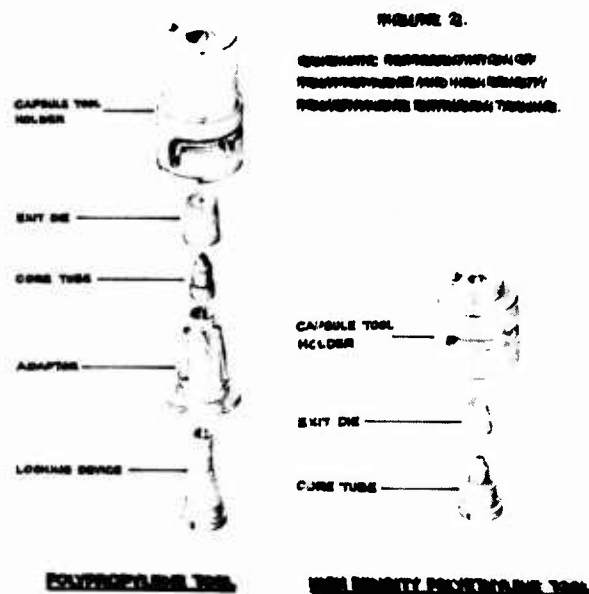




FIGURE 3. Photomicrograph Of A 19 Gauge Polyethylene Wire With Contraction Void. 45X

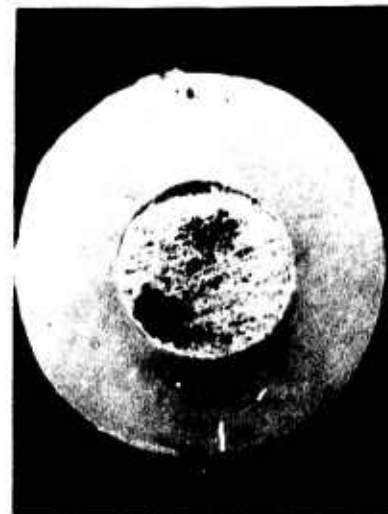


FIGURE 4. Photomicrograph Of A Properly Cooled 19 Gauge Polyethylene Wire. 45X

ENTIRE CONDUCTOR LENGTH. THE CAPACITANCE UNBALANCE OF WIRES WITH NUMEROUS CONTRACTION VOIDS BECOMES VERY HIGH AND RESULTS IN REJECTED CABLES.

THE VOLUME CHANGES ASSOCIATED WITH THE SOLIDIFICATION OF HIGH DENSITY POLYETHYLENE IS CONSIDERABLY GREATER THAN WITH POLYPROPYLENE, AND MINIMIZATION OF THESE VOIDS IS ACCOMPLISHED BY ADJUSTING THE AMOUNT AND TEMPERATURE OF THE WATER IN THE COOLING TROUGH AND USING A VERY NARROW PREHEAT RANGE.

HOT WATER IN THE COOLING TROUGH IS ESSENTIAL, AND THERE MUST BE A SUFFICIENT QUANTITY OF WATER TO COMPLETELY COVER THE WIRE IN THE ENTIRE TROUGH LENGTH. A PHOTOMICROGRAPH OF A 19 GAUGE POLYETHYLENE WIRE SAMPLE THAT WAS PROPERLY COOLED IS SHOWN IN FIGURE 4.

IF THE TROUGH WATER IS TOO HOT, THE PLASTIC WILL NOT BE SUFFICIENTLY COOLED WHEN IT ENTERS THE WET CAPSTAN TO MAINTAIN ITS ROUND SHAPE, AND IT WILL BECOME DEFORMED. OVAL WIRE ALSO PRODUCES VERY HIGH CAPACITANCE UNBALANCE IN FINISHED CABLE AND CAN CAUSE REJECTED CABLES. A CRITICAL WATER TROUGH TEMPERATURE IN COMBINATION WITH A CRITICAL PREHEAT RANGE ARE REQUIRED TO PRODUCE SATISFACTORY WIRE INSULATION.

#### PROCESS CONTROLS

TO OBTAIN A FINISHED CABLE WHICH MEETS THE CAPACITANCE REQUIREMENTS, THE TANDEM INSULATING LINES ARE CONTROLLED BY A CAPACITANCE MONITOR. THIS MONITOR CONTINUALLY MEASURES THE COAXIAL CAPACITANCE OF THE WIRE BEING

INSULATED AGAINST A PRESET VALUE. THE CAPACITANCE VALUE CAN BE ADJUSTED TO COMPENSATE FOR TEMPERATURE VARIATIONS AND PROCESSING DEVIATIONS. THE MONITOR CORRECTS FOR DEVIATIONS IN CAPACITANCE BY EITHER INCREASING OR DECREASING THE LINE SPEED OF THE INSULATING LINE.

IN ORDER TO OBTAIN FINISHED WIRE FROM SEVERAL INSULATING LINES WHICH MEETS A NOMINAL CAPACITANCE OF 51.5 PF PER FOOT, THE WIRE FROM EACH LINE IS CHECKED ON A CAPACITANCE UMPIRE TO ARRIVE AT A TRUE COAXIAL CAPACITANCE AT AN AVERAGE TEMPERATURE. IF ANY WIRE FAILS TO MEET THIS CAPACITANCE VALUE, THE PRESET VALUE ON THAT INSULATING LINE IS ADJUSTED TO BRING THE CAPACITANCE BACK TO THE NOMINAL VALUE.

DURING THE NORMAL INSULATING PROCESS, THE CAPACITANCE VALUE IS CONTINUALLY FLUCTUATING AROUND A GIVEN VALUE. THIS IS DUE TO CHANGES IN EXTRUDER HEAT, COOLING EFFICIENCY, AND PRESSURE FLUCTUATIONS. IN ORDER TO ASSURE THAT THE AVERAGE COAXIAL CAPACITANCE OF ALL THE WIRE INSULATED IS 51.5 PF PER FOOT, A STRIP CHART RECORDER WAS INSTALLED ON EACH INSULATING LINE. THIS RECORDER CONTINUALLY PLOTS THE MEASURED CAPACITANCE FROM THE MONITOR PROBE. A LINE REPRESENTING THE NOMINAL CAPACITANCE VALUE IS ESTABLISHED ON THE CHART AND A COMPLETE HISTORY OF THE CAPACITANCE VARIATION IS RECORDED. FIGURE 5 ILLUSTRATES A CAPACITANCE TRACE FOR 19 GAUGE WATERPROOF WIRE PRIOR TO THE MAJOR LINE MODIFICATIONS. THIS FIGURE ILLUSTRATES THE VERY WIDE FLUCTUATIONS EXPERIENCED AT THIS TIME. FIGURE 6 ILLUSTRATES A CAPACITANCE TRACE FOR 19 GAUGE WATERPROOF WIRE AFTER THE

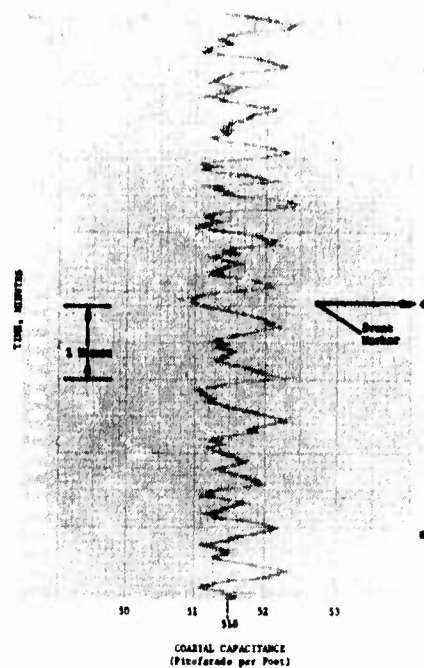


FIGURE 5. Capacitance Chart Of 19 Gauge Polyethylene Wire Prior To Major Line Modifications.

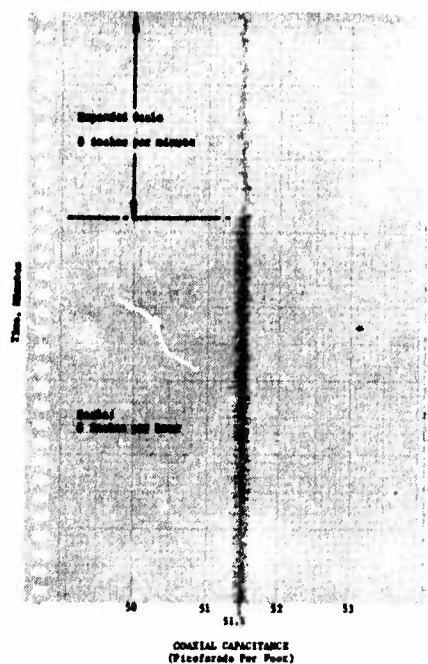


FIGURE 6. Capacitance Chart Of 19 Gauge Polyethylene Wire After Major Line Modifications.

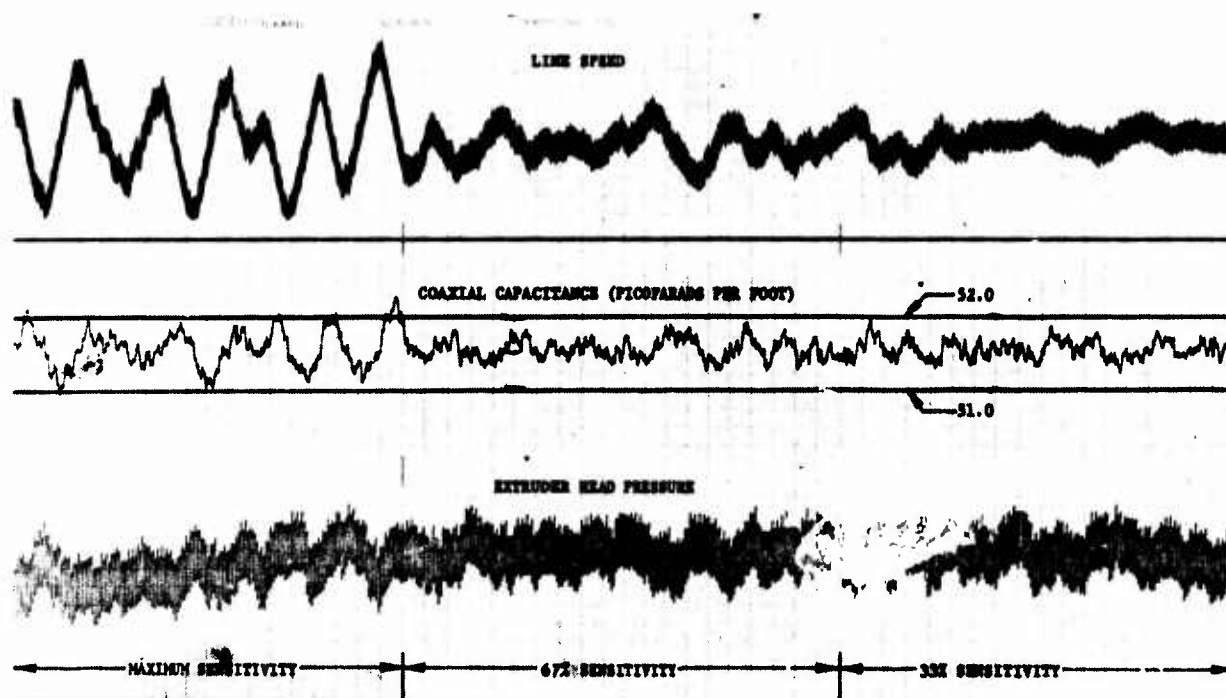


FIGURE 7. Four Channel Chart Recorder Trace Of Sensitivity Study.  
Chart Speed: 50% Per Minute

## INSTALLATION OF THE MAJOR MODIFICATIONS TO THE INSULATING LINES.

WHenever a sample of wire is to be compared to the capacitance umpire the true capacitance of that wire is determined as follows:

(1) THE SAMPLE OF WIRE IS REMOVED AND CHECKED ON THE UMPIRE BY TAKING FIVE READINGS AND AVERAGING THESE READINGS; (2) THIS READING IS COMPARED AGAINST THE STRIP CHART RECORDER, WHICH HAS A HISTORY OF THE CAPACITANCE, TO DETERMINE WHAT THE EXPECTED CAPACITANCE SHOULD BE FOR THAT GIVEN SAMPLE; (3) THE RECORDER PLACES AN IDENTIFICATION MARK ON THE CHART TO INDICATE THE ACTUAL POINT ON THE TRACE WHERE THE SAMPLE WAS TAKEN; (4) IF THE MEASURED CAPACITANCE FROM THE UMPIRE COMPARES WITH THE EXPECTED READING FROM THE CHART, THE TRUE AVERAGE CAPACITANCE WILL BE NOMINAL, AND (5) ADJUSTMENTS ARE MADE ON THE INSULATING LINE MONITOR IF THE DEVIATION EXCEEDS A GIVEN VALUE.

IF ANOTHER STUDY CONDUCTED ON 19 GAUGE WIRE, THE SENSITIVITY OF THE CAPACITANCE MONITOR WAS ANALYZED. A FOUR-CHANNEL CHART RECORDER WAS USED TO MEASURE CAPSTAN LINE SPEED, COAXIAL CAPACITANCE, AND EXTRUDER HEAD PRESSURE. THE SENSITIVITY OF THE CAPACITANCE MONITOR WAS VARIED BETWEEN 10 PERCENT AND 100 PERCENT. FIGURE 7 ILLUSTRATES A TRACE OF THESE VARIABLES STARTING WITH 100 PERCENT SENSITIVITY ON THE LEFT OF THE CHART. THE CENTER OF THE CHART WAS RECORDED AT 67 PERCENT SENSITIVITY AND THE RIGHT-HAND PORTION OF THE CHART WAS RECORDED AT A SENSITIVITY OF 33 PERCENT. IT CAN BE SEEN THAT THE COAXIAL CAPACITANCE FLUCTUATION WAS REDUCED ALONG WITH THE REDUCTION IN THE CAPACITANCE MONITOR SENSITIVITY. IT WAS DETERMINED THAT A SENSITIVITY OF 33 PERCENT RESULTED IN A CAPACITANCE TRACE WITH THE LEAST AMOUNT OF FLUCTUATION. FROM THE EXPERIMENTS CONDUCTED ON THE CAPACITANCE MONITORS, IT WAS DETERMINED THAT THE MONITOR WOULD ONLY BE USED TO CORRECT FOR LONG TERM DRIFTS IN THE CAPACITANCE OF THE WIRE.

THE STRIP CHART RECORDER PERFORMS ANOTHER USEFUL FUNCTION IN ADDITION TO RECORDING THE CAPACITANCE OF THE WIRE. SINCE NORMAL PROCESSING TECHNIQUES RESULT IN A GOOD CAPACITANCE TRACE, ANY ABNORMAL CONDITIONS RESULT IN A WIDER TRACE. THIS TRACE, THEREFORE, SERVES AS A MEANS FOR TROUBLESHOOTING PROCESSING IRREGULARITIES ON EACH INSULATING LINE.

### PROBLEMS UNDER INVESTIGATION

A MAJOR PROCESSING FUNCTION WHICH CONTRIBUTES TO THE MANUFACTURING OF HIGH QUALITY INSULATED WIRE IS THE COOLING PROCESS. IN ORDER TO CONTROL AND MAINTAIN THE COAXIAL CAPACITANCE WITHIN THE VERY TIGHT LIMITS, IT IS NECESSARY TO HAVE ADEQUATE AND CONSISTENT COOLING. CURRENTLY, DIFFERENT EXPERIMENTS ARE BEING CONDUCTED TO DETERMINE THE METHODS WHICH ARE NECESSARY IN ORDER TO COOL ALL GAUGES OF WIRE TO ONE SINGLE, CONSISTENT TEMPERATURE. WHEN ALL LINES HAVE THE CAPABILITY TO ACCOMPLISH THIS COOLING, THE INSULATING LINE MONITORS COULD BE USED TO MEASURE TRUE COAXIAL CAPACI-

TANCE. THESE MEASUREMENTS SHOULD THEN COMPARE DIRECTLY WITH THE CAPACITANCE UMPIRE READING WHEN QUALITY CHECKS ARE PERFORMED. ADDITIONAL STUDIES SHOULD ALSO BE CONDUCTED TO DETERMINE THE PROPER RATE OF COOLING ON THE VARIOUS GAUGES OF WIRE.

AT THE PRESENT TIME, THE PROCESSING CHARACTERISTICS OF HIGH DENSITY POLYETHYLENE DIFFER SIGNIFICANTLY AMONG SUPPLIERS. THE VARIOUS SUPPLIERS OF THIS MATERIAL USE DIFFERENT METHODS OF MANUFACTURING, AND THIS RESULTS IN DIFFERENT PROCESSING CHARACTERISTICS WHEN INSULATING WIRE. VARIATIONS WHICH HAVE BEEN EXPERIENCED AND WHICH AFFECT THE INSULATED WIRE ARE LISTED BELOW:

1. HEAD PRESSURE CHANGES - UP TO 5,000 PSI CHANGE.
2. CAPACITANCE FLUCTUATIONS - CHANGES BY A FACTOR OF FOUR.
3. EXTRUDER WIRE DRAG - A CHANGE IN DRAG AFFECTS THE ELONGATION AND RESISTANCE OF THE COPPER CONDUCTOR.
4. SURFACE ROUGHNESS - A CONSIDERABLE DIFFERENCE EXPERIENCED IN THE SURFACE ROUGHNESS WHEN A CHANGE IN PLASTIC IS MADE. IT HAS NOT BEEN DETERMINED IF THIS HAS ANY DETRIMENTAL EFFECT ON THE ELECTRICAL CHARACTERISTICS OF THE WIRE.

THESE VARIATIONS WHICH PRESENTLY EXIST IN THE PROCESSING OF THE DIFFERENT TYPES OF PLASTIC MAKE IT NECESSARY TO SEGREGATE ONE TYPE OF MATERIAL FOR USE IN MANUFACTURING WIRE FOR WATERPROOF CABLE.

ANOTHER AREA WHICH IS STILL UNDER INVESTIGATION IS THE TOOLING USED IN MANUFACTURING. THE PHYSICAL DIMENSIONS AND ANGLES OF THE EXIT DIE AND CORE TUBE HAVE AN EFFECT ON THE PROCESSING CHARACTERISTICS OF THE PLASTIC. WHEN RUNNING PLASTIC WHICH PRODUCED A VERY ROUGH OUTER SURFACE ON THE WIRE, A CHANGE TO A DIFFERENT EXIT DIE RESULTED IN A SIGNIFICANTLY SMOOTHER SURFACE ON THE WIRE. A DETAILED STUDY MUST BE UNDERTAKEN TO DETERMINE THE PROPER DIMENSIONS OF THE TOOLING WHICH WORKS SATISFACTORILY FOR ALL TYPES OF HDPE.

### CONCLUSION

EVEN THOUGH PROBLEMS STILL EXIST IN THE AREAS JUST DESCRIBED, IT IS NOW POSSIBLE TO MANUFACTURE HIGH QUALITY INSULATED WIRE FOR FILLED CABLE USING HIGH DENSITY POLYETHYLENE PLASTIC. THE MAJOR PROBLEMS ENCOUNTERED WHEN THE CHANGE FROM POLYPROPYLENE TO HDPE TOOK PLACE HAVE BEEN SOLVED. EFFICIENT MANUFACTURING OF INSULATED WIRE TO MEET THE VERY TIGHT CAPACITANCE UNBALANCE REQUIREMENTS HAS BEEN ATTAINED, AND THE OVERALL QUALITY OF THE CABLES IS VERY GOOD.

THE COMPREHENSIVE EFFORT TO BRING THE CAPACITANCE UNBALANCE TO GROUND INTO BETTER CONTROL BEGAN IN LATE 1974. THE STATISTICAL DATA COLLECTED DURING 1975 REFLECTS A REDUCTION OF AT LEAST 50 PERCENT IN THESE READINGS FOR ALL FOUR GAUGES OF CABLE MANUFACTURED.

SOLUTIONS TO THE PROBLEMS STILL UNDER INVESTIGATION WILL RESULT IN THE ABILITY TO

USE MATERIAL INTERCHANGEABLY IN THE MANUFACTURING PROCESS WITH NO SIGNIFICANT VARIATIONS IN THE FINISHED PRODUCT. WHILE THIS WOULD NOT RESULT IN A HIGHER QUALITY PRODUCT, IT WOULD RESULT IN A MORE FLEXIBLE MANUFACTURING OPERATION IF ANY MATERIAL WAS IN SHORT SUPPLY.

#### REFERENCES

1. REFERENCE DATA FOR RADIO ENGINEERS, INTERNATIONAL TELEPHONE AND TELEGRAPH CORPORATION, NEW YORK, FOURTH EDITION, P. 134.
2. W. M. FLEGAL, "PREDICTING CONTRACTION VOID FORMATION IN HIGH DENSITY POLY-ETHYLENE," WESTERN ELECTRIC TECHNICAL REPORT, JANUARY 1975.
3. MODERN PLASTICS ENCYCLOPEDIA, Vol. 51, No. 10A, OCTOBER, 1974, PP. 558 AND 560.



JAMES C. REMLEY, A SENIOR ENGINEER WITH WESTERN ELECTRIC COMPANY AT THE PHOENIX WORKS, GRADUATED FROM THE UNIVERSITY OF ILLINOIS IN 1965 WITH A BACHELOR OF SCIENCE DEGREE IN METALLURGICAL ENGINEERING. IN 1965 HE JOINED WESTERN ELECTRIC AT THE HAWTHORNE WORKS, AND TRANSFERRED TO THE ENGINEERING RESEARCH CENTER IN PRINCETON, NEW JERSEY IN 1966. HE RECEIVED A MASTER OF SCIENCE IN MATERIALS SCIENCE FROM LEHIGH UNIVERSITY IN 1968. IN 1968 HE TRANSFERRED TO PHOENIX, AND WORKED IN MATERIALS ENGINEERING. CURRENT RESPONSIBILITIES INCLUDE PRODUCT ENGINEERING FOR ALL PLASTIC INSULATED WIRE MANUFACTURED AT PHOENIX.



BRUCE M. BROKKE IS A PLANNING ENGINEER WITH WESTERN ELECTRIC COMPANY AT THE PHOENIX WORKS. HE RECEIVED A BACHELOR OF SCIENCE DEGREE IN INDUSTRIAL ENGINEERING FROM NORTH DAKOTA STATE UNIVERSITY IN 1961. HE JOINED WESTERN ELECTRIC IN 1969 AFTER 8 YEARS OF WORK IN THE AEROSPACE INDUSTRY. CURRENT RESPONSIBILITIES INCLUDE PRODUCT ENGINEERING FOR ALL TYPES OF PLASTIC INSULATED WIRE MANUFACTURED AT THE PHOENIX WORKS.



# PLASTIC INSULATING OF TELEPHONE WIRES AT ULTRA HIGH SPEEDS

by

A. Riekkinen and R. Ekholm

Oy Nokia Ab  
Finnish Cable Works  
Helsinki, Finland

## 1 General

Recently the maximum speed of extrusion lines for telephone wire has risen remarkably. As late as 5 - 10 years ago the speeds of 1000 - 1200 m/min were quite common, while now we speak in general of speeds from 2000 to 2500 m/min. However, actual production speeds have remained remarkably lower for several reasons. Higher speeds cause difficulties with wire tension, extrusion, cooling and spooling, and accordingly reduce the reliability of the lines.

In order to raise actual production speed it is important to study these factors and try to eliminate them as far as possible.

## 2 Problems

The problems occurring in extrusion lines can be divided into two groups (fig. 1):

- problems coming from equipment or technology, which can be eliminated by different technical approaches
- problems arising from physical laws and limitations which cannot be overcome.

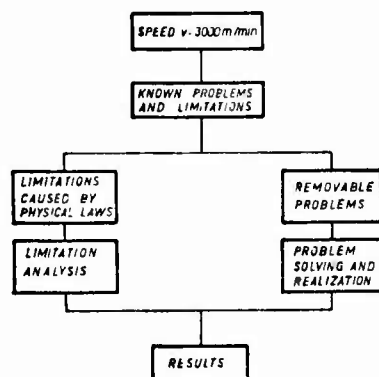


Figure 1 Problem analysis

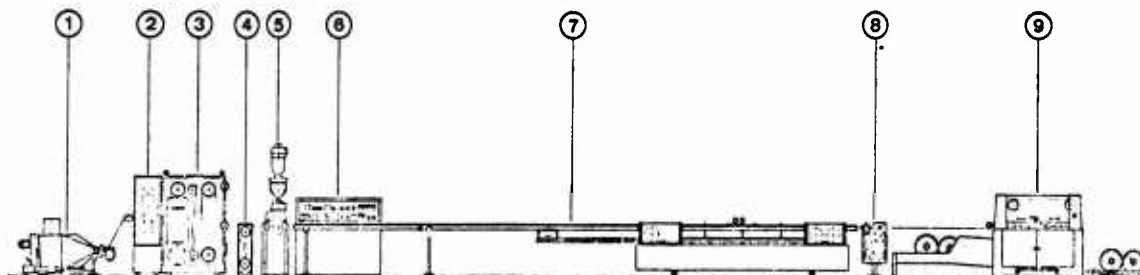


Figure 2 Extrusion line composition MEL 2321

In the Machine Department of NOKIA we decided to research these problems. We set up a test line for operation at a speed of at least 3000 m/min. At the same time theoretical studies of physical limitations were conducted.

## 3 Line introduction (fig. 2)

The test line consists of:

Dual Pay-Off KS 652 E  
designed for continuous paying-off of wire from 0.4 to 1.4 mm

Mini Drawing Machine VK 9  
designed and developed especially for plastic extrusion lines. The machine is provided with nine drawing dies max.

Annealer HL 350  
with DC resistance annealing

Accumulator V 20 (fig. 3)  
to control the drive of the drawing-annealing unit to follow the line speed.

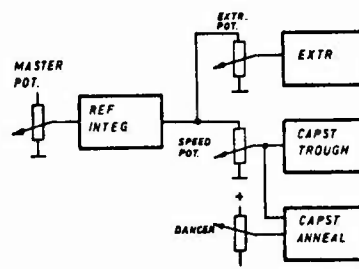


Figure 3 Speed reference circuit of high speed line

Extruder R 3 1/2" (L/D 24)  
heavy duty extra high pressure extruder with standard thyristor temperature controls and DC-drive, plus standard granulate conveyor and color-o-meter.

Line Control Cabinet OPM 2000  
Standard control cabinet of a tandem line, provided with necessary equipment for line control and temperature controls for the extruder.

Cooling Trough JR 33-15-4 E  
a standard construction provided with some special features. The straight cooling length is  $20 + 1.4$  m (total length and telescope).

Instrument Cabinet  
All the instruments used are of standard type. Diameter gauge and capacitance monitor with controls are used. These influence the line speed and the telescope position correspondingly.

Dual Take-Up EKP 5010  
A new fully automatic spooler, which is designed for operation at the speed of 3000 m/min max.

#### 4 The different phases of the process and problems encountered

##### 4.1 Drawing

There are always some difficulties with wire drawing. Defects in the material cause wire breakages, stopping the whole process. The frequency of wire breakages depending on the copper, is in the range of 0.2 - 3 breakages/ton and on an average about one breakage/ton, which means that when running 0.5 mm (24 AWG) at 2000 m/min the operation of the line is interrupted because of the drawing machine, every 2 - 24 h and on an average 5 h. Down time caused by breakage is relatively long due to rethreading of the drawing machine, and diminishes the production efficiency of the line. Additionally the start-up scrap increases at higher speeds, which, again, reduces the advantage of high speeds.

On the other hand we cannot completely eliminate the drawing machine, because the alternate method being continuous paying-off of ready drawn and annealed wire from dual flyers, is even less reliable at high speeds, especially at the moment of change-over in pay-off.

For these reasons we chose a third alternative, the so-called Mini-Drawing. In the mini drawing machine only a few drawing dies are used, having the following advantages:

- the worst raw material defects have already been eliminated in the previous drawing processes

- threading of wire is easier and quicker and the production efficiency of the line increases

- paying-off of thicker wire,  $\varnothing$  0.8 - 1.3 mm (20-16 AWG), at fairly low speeds 500 - 1000 m/min does not create problems.

Since nowadays it is possible in one operation to draw down 8 mm rod directly to 1.0 - 1.3 mm, the solution is also economical.

One rod drawing machine is able to feed four mini-tandem extrusion lines.

Wire drawing process alone does not limit the line speed. In the future we ought to concentrate on the selection of good copper qualities, in order to minimize wire breakages.

##### 4.2 Annealing

Annealing is always a critical process. We can say that there is no annealer in the world that would be satisfactory for everyone. This is not necessarily due to the annealer as it is, but it is due to the difficult process. Wire is charged momentarily with a lot of electric power, which causes great currents at the contact surfaces and therefore trouble with the contact. Defects in the conductor, slag defects, etc., cause local overheating, sometimes wire breakages. Additionally, the wire is subjected to centrifugal force (fig. 4). This centrifugal force is also transmitted to the annealing zone, where the wire is vulnerable. Wire tension caused by centrifugal force is only a function of speed and not e.g. of the radius of the pulley.

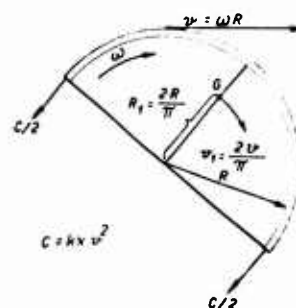


Figure 4 Centrifugal force acting on the wire on a pulley

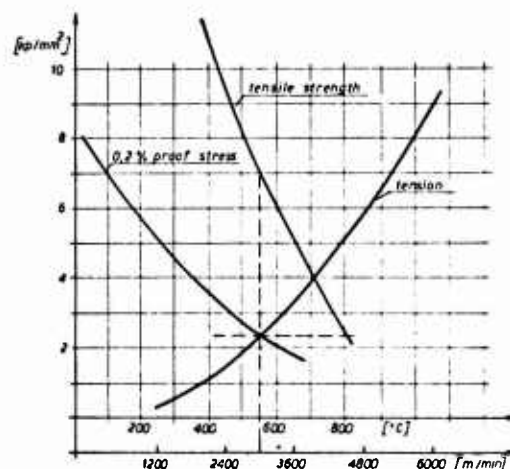


Figure 5 Mechanical strength of copper at various temperatures and wire tension due to centrifugal force at various speeds

The fig. 5 shows the wire tension as a function of speed and also the durability of copper as a function of temperature. We can conclude from these calculations that the highest possible annealing speed with annealers of today is about 60 - 70 m/s or 3500 - 4000 m/min. Accordingly annealing at 3000 m/min is not yet an unsurmountable problem, although we are now approaching the limit.

#### 4.3 Extrusion

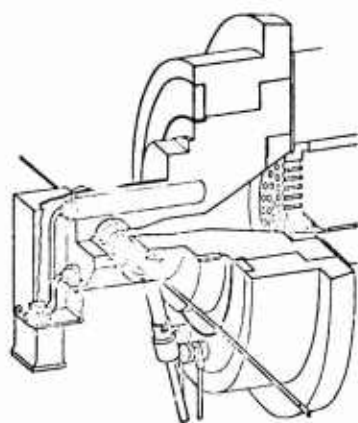


Figure 6 Cross-head NH 50

At higher speeds the wire tension increases in the crosshead. Without special actions the wire tension easily grows so much that the wire is stretched.

Nokia has analyzed the use of high pressures in order to decrease wire tension. The idea is to use a slightly smaller die diameter than the final insulation diameter and to extrude plastic at a somewhat higher rate than that of the wire.

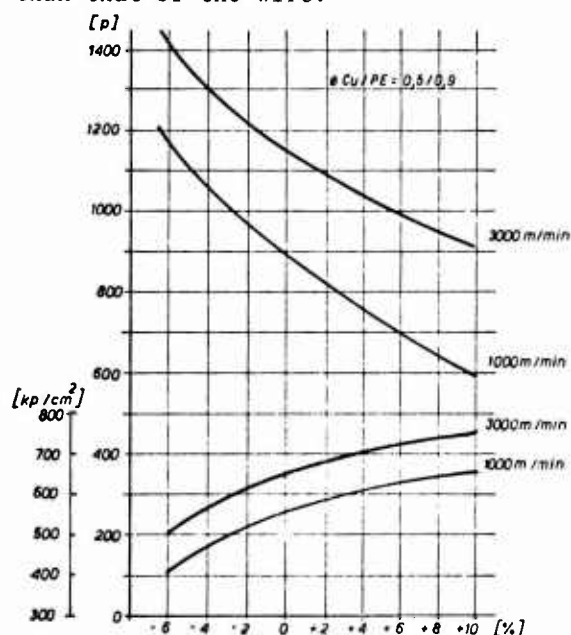


Figure 7 Increase of wire tension in cross-head and corresponding pressure versus die swell

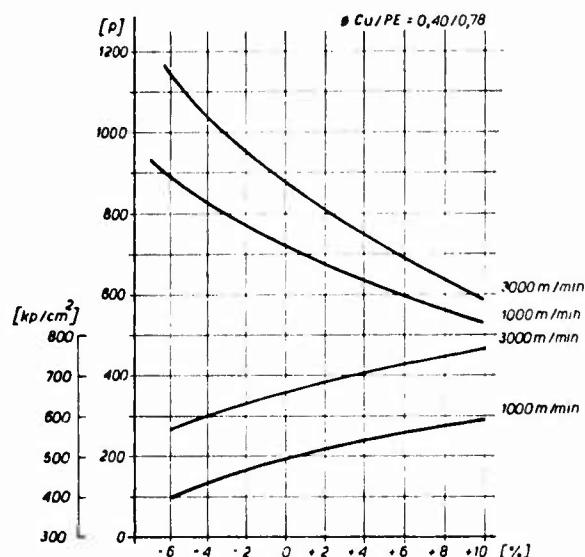


Figure 8 Increase of wire tension in cross-head and corresponding pressure versus die swell

Figures 7 and 8 show results of test measurements. We can see, how dependent the wire tension is on swelling. Compared with the nominal diameter (swelling = 0), the tension is reduced by 30 % at 10 %'s swelling. The wires insulated in this way have met with the test specifications and we have found no disadvantages in the use of high pressures. (Table 1)

Table 1

Test results for polyethylene-insulated telephone wire		
Wire size	0.5 mm (24 AWG)	
Insulation dia.	1.0 mm	
Insulation material	DFDS 6032	MDPE UNION CARBIDE
Wire speed	3000 m/min	
Tensile strength unaged	276 kp/cm <sup>2</sup>	VDE 0472c/9.71
aged	219 kp/cm <sup>2</sup>	and 0209/3.69
Elongation unaged	530 %	"
aged	500 %	"
Shrinkback	1 %	"
Compatibility-test	no fracture	DB FTZ 72 TV 1
Stress-cracking	no cracks	BPO CW 128 Q

#### 4.4 Cooling

The problems in cooling induced from the fact that the cooling requirements

- efficient cooling
- low wire tension
- space saving

are difficult to fulfill simultaneously.

Cooling has become a more problematic process with increasing speeds, and this has motivated the development of more advanced techniques.

Previously a simple V-shaped trough and compact water cooling was generally used, which was quite a simple and cheap solution. However, as speeds increase, longer cooling distances are required and since friction between wire and water increase with the speed, we come up against a contradictory situation: wire tension simply increases to an unacceptable level. Actually we should try to eliminate all wire tension in cooling, because the wire in this process is subjected to the friction created in the cross-head plus the required, preset tension before cross-head.

$$F = F_1 + F_2 + F_3$$

$F$  = wire tension after cooling

$F_1$  = wire tension before cross-head

$F_2$  = wire tension caused in cross-head

$F_3$  = wire tension caused in cooling

$F_1$  and  $F_2$  have to be minimized, but together they are still of considerable influence.

Therefore a new technique was employed. Nokia developed the spray cooling method (fig. 9). The principle of spray cooling is to cool the wire with high velocity water sprays, directed in a parallel direction with the wire run. In this way the friction which would otherwise arise between wire and water, can be avoided.

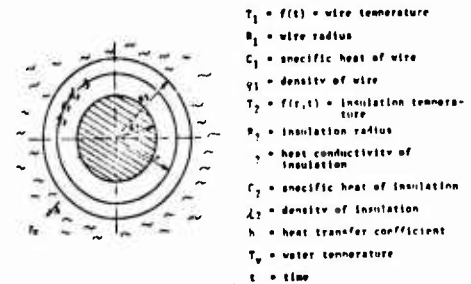
The spray system enables the wire to cool without an increase in wire tension.

When studying the cooling process, we can note the following (fig. 10).

At the beginning of cooling process the outermost plastic surface is cooled first.

As a consequence of the created temperature difference between the inside and outside insulation surfaces, heat transfer occurs.

Since plastic is a fairly good heat insulating material, the rate of heat transfer is very low. Therefore the amount of heat, transferred to the outside surface per unit of time, is very small.



$$\begin{aligned}
 (T_2)_{1,1,t} &= \frac{\lambda_2}{C_2 \rho_2} \left\{ \frac{(\lambda_2)_{1,t}}{(\Delta r)^2} - \left[ \frac{(\lambda_2)_{1,t}}{r_1} + \frac{(\lambda_2)_{1,t} \cdot (\lambda_2)_{1,t}}{2 \Delta r} \right] \frac{1}{2 \Delta r} \right\} (T_2)_{1,1,t} \\
 &\cdot \left( 1 - \frac{\Delta r}{C_2 \rho_2} \frac{1}{\Delta r^2} \right) (T_2)_{1,1,t} \\
 &\cdot \frac{\Delta r}{C_2 \rho_2} \left\{ \frac{(\lambda_2)_{1,t}}{(\Delta r)^2} - \left[ \frac{(\lambda_2)_{1,t}}{r_1} + \frac{(\lambda_2)_{1,t} \cdot (\lambda_2)_{1,t}}{2 \Delta r} \right] \frac{1}{2 \Delta r} \right\} (T_2)_{1,1,t}
 \end{aligned}$$

Figure 10 Heat transfer equation

This rate of heat transfer is dependent only on the temperature difference and it cannot be accelerated much as long as water is used as a cooling media.

Also lowering the temperature of the water does not appreciably effect the rate of cooling in its first stage, because the possibility to change the temperature difference is relatively limited, e.g.  $280^\circ\text{C} - 20^\circ\text{C} = 260^\circ\text{C}$  or  $280^\circ\text{C} - 5^\circ\text{C} = 275^\circ\text{C}$ , the difference is only 6 %.

On the other hand the temperature of the water is very important in the after-cooling zone, where the temperature differences between the water and the wire are smaller, e.g.  $40^\circ\text{C} - 20^\circ\text{C} = 20^\circ\text{C}$  or  $40^\circ\text{C} - 5^\circ\text{C} = 35^\circ\text{C}$ , the difference 75 %.

We can now draw the following conclusions:

- a) From the point of view of cooling efficiency it is important to cool down the surface of the insulation as quickly as possible, in order to initiate heat transfer immediately.

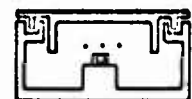
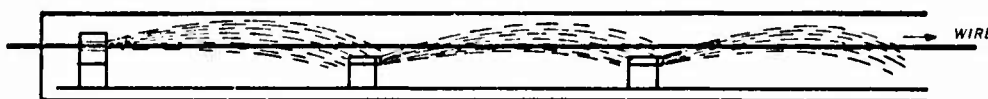


Figure 9 Spray cooling method

- b) When the cooling process has begun, it is sufficient only to maintain a low temperature on the insulation surface. Since the rate of heat transfer is low, the required volume of water is small, but it must be constantly circulated.
- c) The cooling phenomenon requires a specific constant time, regardless of the speed.

The cooling trough was designed according to these principles. In the front trough we placed a short compact water bath, where the wire was completely immersed. The rest of the cooling was accomplished by using water sprays, which only washed the wire. However, the cooling in the front trough was not quite satisfactory. A layer of air and steam formed around the wire, preventing water contact with the insulation. The front trough section was improved by water sprays directed perpendicularly towards the wire. In this way the cooling efficiency was remarkably improved.

Because of the required constant cooling time, the length of the trough increases in direct proportion to the wire speed. Simply a straight trough would easily become too long and spacious, especially when trying to achieve low final temperatures. The rate of cooling at the end of the process is very slow, as shown in fig. 11.

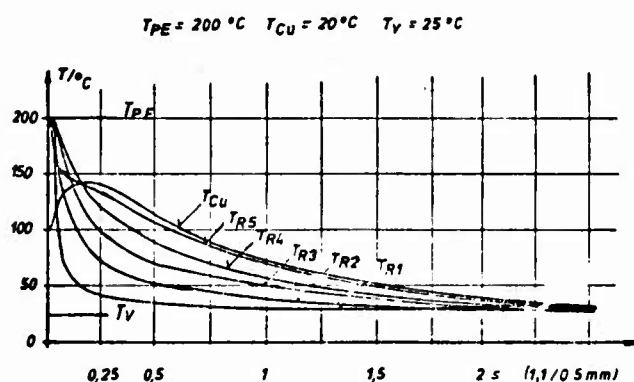


Figure 11 Insulation cooling curves

It is now of great interest to examine, at which stage the wire can be turned over a turn pulley without being deformed. It was discovered that this is possible at relatively high wire temperatures, (average  $100^\circ\text{C}$ ). This is explained by the fact that the wire is subjected to side forces for only a very short period of time, 10 - 15 ms, during which no measurable deformations can occur, owing to the high viscosity of the plastic material.

On the other hand the wire must be well-cooled before it is spooled on a reel, because there the wire is subjected to side forces for a long time. Also as the insulation slowly cools down, it shrinks and this causes difficulties when the wire is payed off the reel. (Fig. 12.)

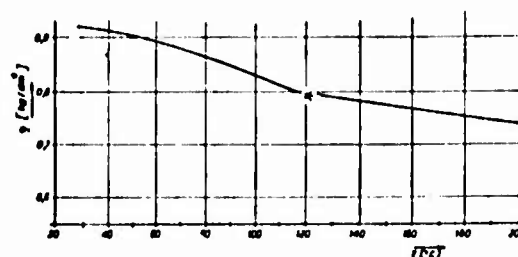


Figure 12.1 Density of PE

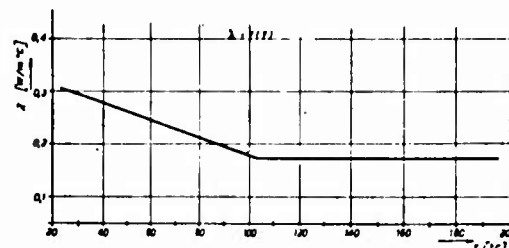


Figure 12.2 Heat transmission of PE

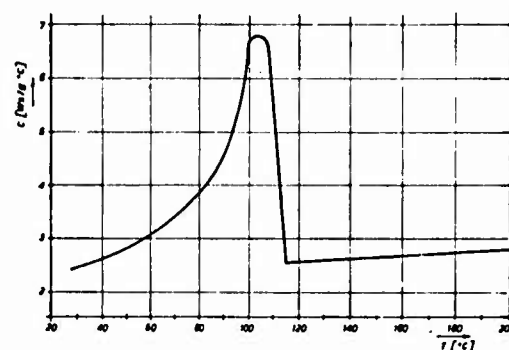


Figure 12.3 Specific heat of PE

In order to attain sufficient cooling within a reasonable space, we have to employ in high-speed lines a so-called multi-loop trough (fig. 13). The advantage of a multi-loop trough is that it is easy to obtain sufficient after-cooling without using too much space. On the other hand the multi-loop solution does not mean that the overall length of the trough would not increase as speeds increase.

Additionally the multi-loop trough creates another problem, the turn pulleys tend to increase wire tension and to stretch the wire. Therefore we had to try to minimize the number of pulleys as well as eliminate the friction of the necessary pulleys. (Fig. 14 and 15.)

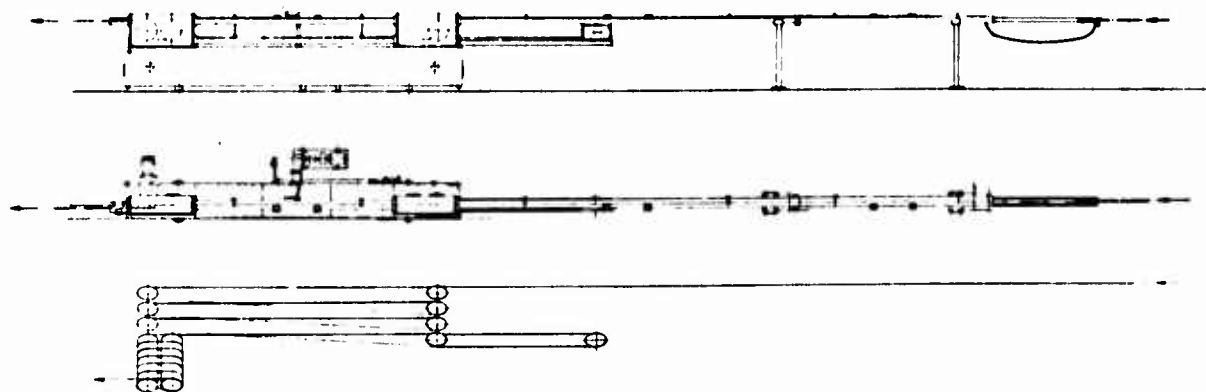


Figure 13 Multi-loop trough JR 33-15-4 E

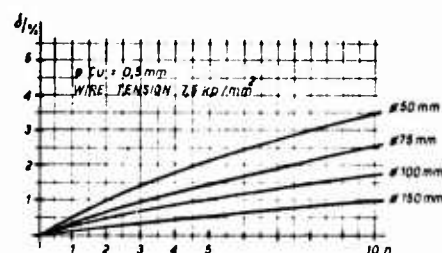


Figure 14 Percentage of stretch of annealed copper wire versus number of pulleys of various wire tensions

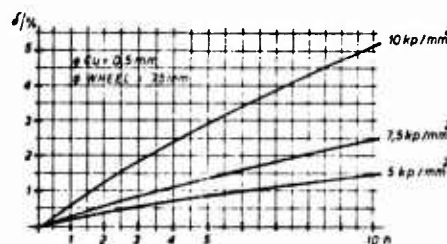


Figure 15 Percentage of stretch of annealed copper wire versus number of pulleys at various wire tensions

Partially because of the above, the line capstan was incorporated in the cooling trough with the following advantages:

- The capstan operates in a water spray and the wire is cooled also while on the capstan. Therefore less loops are required.
- A smaller number of turn pulleys is used, since the wire does not have to be guided to a separate capstan.
- Since the distance between the extruder and the first turn pulley is decisive we can save the space required by a separate capstan in the total length of the line.

- The driven capstan shaft can be used to eliminate the bearing friction of the turn pulleys (fig. 16). Because of the natural order of the wire loops the turn pulleys are mounted on the capstan shaft, which is driven at a constant speed by DC-motor.

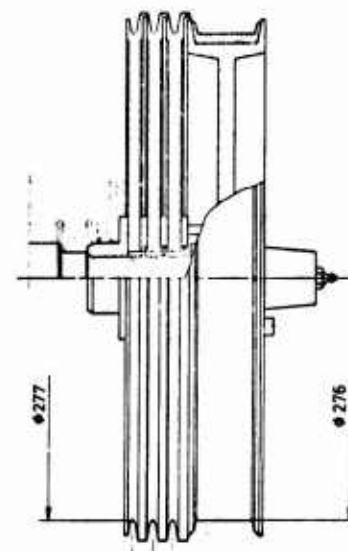


Figure 16 Capstan pulley assembly

By selecting the diameters of the turn pulleys slightly larger than the diameter of the capstan pulley we create a situation where the turn pulleys are rotated at a slightly less speed than the capstan shaft. In this way we create a negative friction which means that this friction tends to drive the wire. This assisting torque can also be increased e.g. by an additional axial friction on the turn pulleys.

Another source of additional tension is a second pulley assembly in the trough. These bearing frictions were eliminated by a separate torque drive.



Accordingly we can see that cooling is not a problem that cannot be solved, and it does not limit increased production speeds. We meet the physical limit only at the stage, where wire tension caused by centrifugal force is too high, i.e. at speeds from 4000 to 5000 m/min.

#### 4.5 Spooling

The continuously operating dual take-up has always been more or less a critical component in extrusion lines. Some ten years ago the take-up actually limited the line speeds to range of 700 - 1000 m/min. The parallel shaft principle in take-ups gave them a much better speed performance, over 2000 m/min. Then, however, the other components and the extrusion process turned out to be speed limiting factors. Today, when these components and the process itself have been further developed, and the speed has increased over 2500 m/min, the dual take-up has again become a critical unit. This is due to both imperfect technology as well as to the fact that we are approaching limitations caused by physical laws.

The spooling process can be divided into two operations

- a) spooling
- b) change-over

The problems of spooling relate to centrifugal forces. In order to spool successfully, the spooling tension must be higher than that supplied by the centrifugal force. The highest theoretical take-up speed for insulated copper wire is approximately 4500 - 5000 m/min with a wire tension of 7 to 8 kp/mm<sup>2</sup> (appr. 10000 psi). (Fig. 17.)

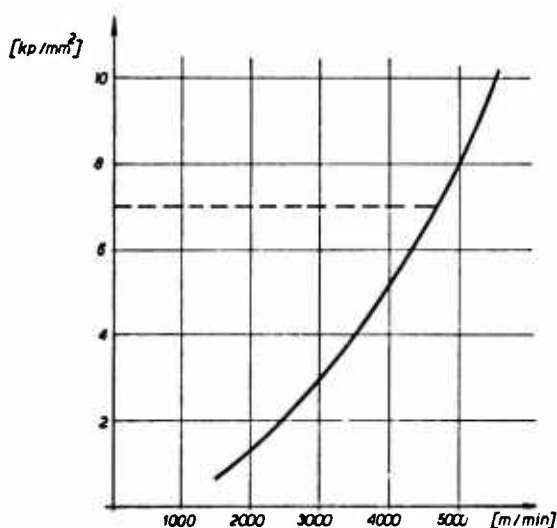


Figure 17 Wire tension of insulated wire due to centrifugal force at various speeds

In ordinary equipment, however, there are several characteristics that set speed limitations. Gradual increase of wire tension is caused by e.g. the turn pulleys in the dancer. In other words, in order not to exceed the wire tension value 7 - 8 kp/mm<sup>2</sup> in spooling we shall have to use a lower wire tension before the dancer and correspondingly accept a lower maximum speed. This problem could be eliminated by using a torque drive in the turn pulleys, which compensates for their friction. However, because of the above mentioned problems and the necessity of maintaining a certain safety margin, it is hardly justified to aim at speeds over 4000 m/min.

Greater demands are made on speed control as speeds increase. Uniform traverse is of great importance because every little hill and valley mean fast speed fluctuations. These difficulties, however, can be overcome by the application of modern electronic control technics.

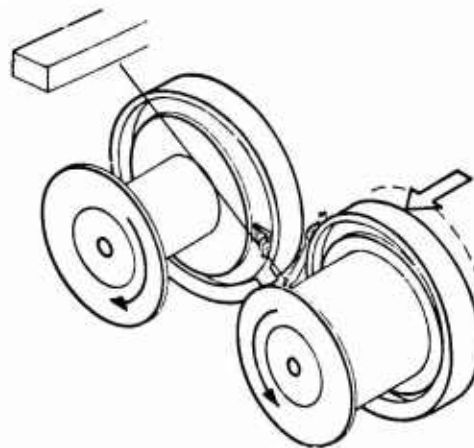


Figure 18.1 Wire change-over in parallel shaft take-up

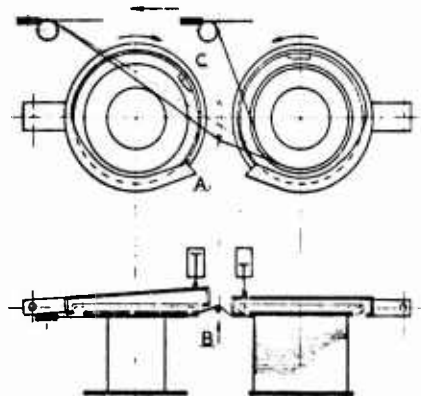


Figure 18.2 Wire change-over in parallel shaft take-up

It is interesting to observe the wire change-over in a parallel-shaft take-up. Fig. 18 illustrates the change-over moment where the traverse has moved to the side of the empty reel. The speed of the empty reel is synchronized with the wire speed.

At the moment of change-over the wire is cut between the snagger and the full reel and the winding is continued on the empty reel. The speed diagram (fig. 19) indicates that the speed of the snagger in the direction of the wire run is equal to the wire speed, which therefore remains constant at the moment of change-over. The change-over is so accomplished without jerks in the wire direction. E.g. the dancer does not move. On the other hand, the wire is accelerated very rapidly in a perpendicular direction. The wire length  $A$  has to be conveyed instantly from a lateral to a rotational motion. E.g. when spooling at 2500 m/min the speed of the snagger is already about 6000 m/min, equal to 100 m/s. It is obvious that if the speed of the snagger is high enough, the wire will not follow the snagger, but it will break.

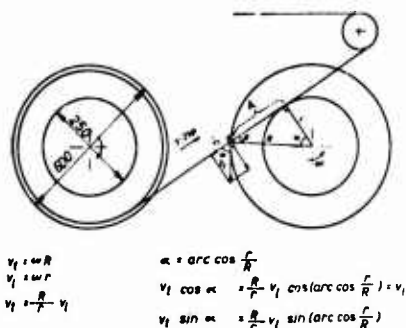


Figure 19 Speed diagram

It is of great interest to try to examine the theoretical maximum speed at change-over. At first we observe that the greatest stress occurs at a point on the wire adjacent to the snagger.

Mathematically we can define that even at low speeds the yield point is exceeded and the change-over causes local strain. Fortunately copper has a high yield capacity which diminishes accelerations and thus provides for a smooth change-over. Besides the tensile and ultimate strength of copper is greater when it is subjected to high velocity deformations. According to our studies the change-over becomes critical at speeds in the range of 3000 - 3500 m/min. However, a speed of 2500 m/min can be considered quite reliable.

One noteworthy reason for change-over failure is the risk that the snagger tip cuts the wire. The probability that the snagger tip hits the wire at the moment when the wire is being guided towards the snagger flange, increases with the wire speed. Let us assume that the snagger rotates at 3800 r.p.m. equal to 63 r.p.s. which corresponds to the wire speed of 3000 m/min in our example. In addition let us assume a condition where the finger speed is e.g. 0.5 m/s, the insulated wire diameter 1 mm and the width of the snagger tip is 0.25 mm. Let us also

assume, that the contact area, where the snagger tip has to hit the wire in order to cut it, is 0.25 mm. The probability that the snagger tip hits this area is

$$100 \frac{0.25 \text{ mm}}{1/63 \text{ s} \times 500 \text{ mm/s}} \% = 3 \%$$

which is rather high. This probability is directly proportional to the line speed and, at speeds of 1500 - 2500 m/min it is still high, 1 - 2 %. This disadvantage, however, is relatively easy to overcome by synchronizing the finger motion with that of the snagger.



Figure 20 Collision between snagger and wire

Other possibilities of failure in spooling are unreliability of the snagger e.g. caused by a piece of loose wire in the snagger, wire vibrations, wire disengagement from pulleys and inaccurate speed control. All these problems can be overcome at least to some extent by improved technics. However, we still have inevitable limits with the tension caused by centrifugal force, limiting us to 4000 m/min as well as the perpendicular acceleration phenomenon at the moment of change-over, which limits us upto appr. 3500 m/min. These were dealt with before.

##### 5 Conducted test runs

The test runs were made with wire sizes of 0.4/0.78 mm and 0.5/0.90 mm dia. with PE-insulation.

The runs were carried out in the speed range of 1000 - 3000 m/min. Measurements were made of the wire tension in the line (fig. 21) and of elongations of the insulated wires (fig. 22). Quality analysis (table 1) indicated that it is technically possible to produce high quality wire at 3000 m/min and probably also at higher speeds.

The test results were very encouraging. During the test run we observed several possibilities for technical improvements, which when developed and adapted will further improve these results.

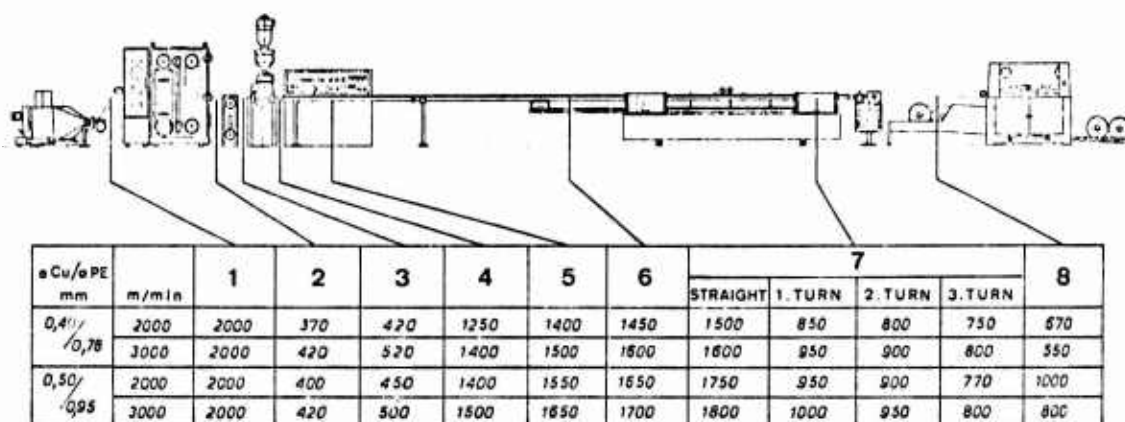


Figure 21 Wire tension levels (p) in Extrusion Line MEL 2321

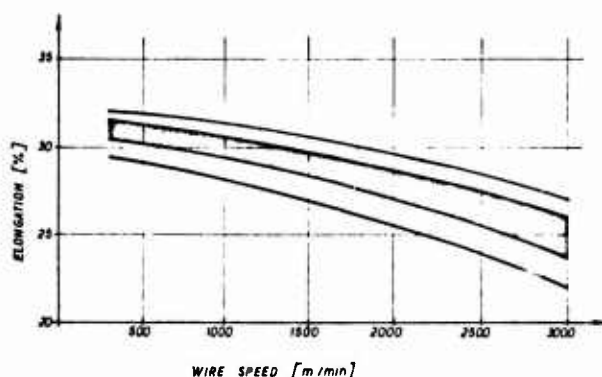


Figure 22 Wire speed (m/min)

## 6 Summary

The purpose of our research was to analyze problems and physical limitations, which prevent further increase of present production speeds. In brief, an increase of actual production speeds to the level of 2000 - 2500 m/min is quite possible. Even 3000 m/min is achievable, but it may be advantageous to lower the line speed during change-over e.g. to 2500 m/min, so that the change-over does not take place too close to the critical speed range.

Essential conditions for ultra high production speeds are low wire tension level throughout the process, excellent speed control and last but not least high quality copper.

Higher speeds than 3500 m/min seem hardly achievable. The physical limitations in annealing, spooling and wire tension in general soon become unsurmountable. Therefore it is more important to concentrate on improving the overall reliability of the line in the speed range of 2000 - 2500 m/min.

The benefits of the analyses of ultra high speed extrusion are that they reveal more clearly the critical factors and thus assist in improving reliability at normal production speeds.

The motivation of line operators and their desire to achieve good results are also decisive factors which should be assisted by eliminating manual reel handling with e.g. automatic reel transport. Also computer control would be a progressive step towards better motivations of production people.

## References

- 1 Mechanical Properties at High Rates of Strain, Proceedings of the Conference on Mechanical Properties of Materials at High Rates of Strain held in Oxford, 2-4 April 1974, Conference Series Number 21, The Institute of Physics, London Bristol
- 2 J Karppo: "Analyzing the cooling of plastic insulation using an electrical analog", Wire Technology 3/4:74
- 3 E Kertscher: "Recent developments in the high speed insulation of quality telephone wires", 22nd International Wire and Cable Symposium 1973
- 4 J Lammervuo: "Calculating of temperatures in plastic insulation by computer", Helsinki University of Technology, Graduate Work 1974, in Finnish (unpublished)
- 5 E Pennala: "Stress Analysis of a wire in a certain dual take-up by using modified large deflection theory", Helsinki University of Technology, 1975.



A Riekkinen  
Oy Nokia Ab  
Finnish Cable Works  
Helsinki, Finland

Asko Riekkinen born in 1937, graduated in 1963 from Helsinki University of Technology with a degree of Master of Science in Mechanical Engineering. In 1960 he joined The Finnish Cable Works and was engaged with research and development of cable machinery. From 1967 he worked as Manager of Product Development in the Machine Department. At present he is Manager of The Cable Machinery Department of Nokia, Finnish Cable Works.



R Ekholm  
Oy Nokia Ab  
Finnish Cable Works  
Helsinki, Finland

Ralf Ekholm born in 1943, graduated from Helsinki Institute of Technology with a degree in Electronic Engineering. In 1970 he joined the Machine Department of Nokia, Finnish Cable Works, as an electronic design engineer, engaged in electronic control technology. He is currently chief of Electronic Development where he is responsible for research and development of automatic high speed extrusion lines.

ULTRA-HIGH SPEED EXTRUSION OF FOAMED POLYETHYLENE INSULATION  
FOR USE IN MULTI-PAIR TELEPHONE CABLES

Mitsuru Rokunohe

Dainichi-Nippon Cables, Ltd.

Osaka, Japan

Masaaki Okada

Yuzo Ueno

Mitsui Petrochemical Industries Ltd.

Yamaguchi, Japan

Jun Konishi

Summary

A composite technique was established for ultra-high speed extrusion at 3000 m/min of foamed high density polyethylene insulation for use in multi-pair telephone cables.

Until now extrusion of polyethylene insulated conductors have been carried out at a speed of at most at 1000 ~ 1700 m/min for foamed insulation.

As previously reported in the past IWCS, in Japan the conventional paper insulated Stalpeth sheathed city junction cable was replaced by the new foamed polyethylene insulated bonded metal sheathed cable. To meet the expected growing demand for the new type of cable, a developmental research work was started for the ultra-high speed extrusion of insulated conductor as one of the efforts for the improvement of cable productivity as a whole.

Major problems in the development of a 3000 m/min extrusion of foamed high density polyethylene insulation were the wire draw down, the wire preheat, and the crosshead pressure. Capacity control was also difficult at this level of extrusion speed. All these were solved by the optimization and rearrangement of each equipment of the extrusion line.

Development of a new high density polyethylene was also a key to the success. A series of test produced polymers along with conventional ones was subjected to the ultra-high speed extrusion and examined to develop a final one for the 3000 m/min extrusion.

Quality of the insulation and of the finished cable obtained from a test production run of the ultra-high speed extrusion proved to meet all the requirements of the specification of Nippon Telegraph and Telephone Public Corporation.

1. Introduction

The program of Nippon Telegraph and Telephone Public Corporation (NTT) to replace conventional paper insulated Stalpeth sheath cable by foamed high density polyethylene insulated bonded aluminum sheathed cable for the city junction lines in Japan was already reported in the past International Wire and Cable Symposia.<sup>1,2</sup>

As Jitsukawa et al<sup>3</sup> reported in 1970, thin walled insulation of foamed polyethylene had distin-

guished advantages over conventional paper insulation because of the excellent properties of polyethylene itself over natural paper. Polyethylene is non-hygroscopic and has excellent dielectric properties. Because of its uniform thickness, extruded polyethylene insulation has superior crosstalk characteristics even in the form of star quad which is necessary for reducing the overall diameter and therefore the cost of the finished cable. But a slightly higher cost of the polyethylene foam insulated cable retarded the replacement of paper insulated cable by it.

However, as reported by Ogawa<sup>1</sup>, it was found that the foamed polyethylene insulation could replace paper best when it was used in city junction cable. Because with paper cables test splices are necessary each time to compensate for the capacitance unbalance. The slightly increased cost of the foamed polyethylene cable is compensated for sufficiently enough if the new cable eliminates the test splicing which costs not so little as a whole.

Starting from the year of 1974, all of the newly installed city junction cable in Japan was replaced by foamed polyethylene insulation from the conventional paper. Annual demand for this line of cable is about 25 b.c.f. in Japan.

Dainichi-Nippon Cables, Ltd. is an important supplier of this type of cable and in preparation for the expected growing demand of the cable started a systematic developmental research for the improvement of the cable productivity in which an ultra-high speed extrusion of polyethylene foam insulation came first.

High speed extrusion of polyethylene foam insulation was reported by several authors. For example, Kawazoe et al<sup>4</sup>, Jitsukawa et al<sup>3</sup>, Normanton<sup>5</sup>, and Ogawa et al<sup>1</sup> reported a polyethylene foam extrusion of 1000 m/min, 1250 m/min, 1650 m/min, and over 1000 m/min, respectively with the use of a chemical blowing agent. In a gas injection process, Verne et al<sup>6</sup> reported an extrusion at a speed of 5000 ft/min, and Orimo et al<sup>2</sup> a speed of 1700 m/min. With solid insulation which is relatively easier to extrude as compared with foamed insulation, Kertscher<sup>7</sup> reported installations which are capable of production speeds up to 8000 ft/min (2500 m/min).

Our developmental work was aimed at the extrusion of chemically blown foamed high density polyethylene insulation at a speed of 3000 m/min (10,000 ft/min).



Before the start of the work it was expected that the development of a new polyethylene which fulfilled all of the requirements for the new ultra-high speed process was a "must" in order to lead the work to a success. Mitsui Petrochemical Industries Ltd. took part in the joint work, who has the longest career in the production of high density polyethylene in Japan since 1958.

## 2. Equipment and Materials

### 2.1 Extrusion Line

An extrusion line to which were attached a wire drawing machine, an annealer, and a preheater was used throughout this developmental work (Figure 1). Previous to the present joint work, using another but the same design of equipment, a separate developmental work was carried out in Dainichi-Nippon successfully to achieve a 3000 m/min extrusion of solid low density polyethylene. Accordingly many details of design and manufacturing know-how come from the previous work.

On the other hand, because the extrusion line was originally designed for solid insulation, in order to make it compatible with foamed insulation it was necessary to modify and improve the line at many points.

### 2.2 Materials

Mitsui Petrochemical Industries Ltd. is a major supplier of the electrical wire grade high density polyethylene including the world first solution coating grade for more than 10 years in Japan. The accumulated research for the extrusion wire coating grade and the superior technique on high density polyethylene production using Ziegler type catalyst made Mitsui highly qualified to develop the ultra-high speed extrusion foam grade.

In general, besides the excellent mechanical properties such as stress crack resistance and abrasion resistance, and electrical properties, the wire coating grade is required to have excellent processability.

At the beginning, resin A, shown in Table 1, was used for the extrusion of foamed insulation wire coating. Resin A is a unique grade with excellent mechanical and electrical properties compared to general high density polyethylene, but when it is used for thin walled insulation extrusion the extrusion speed is limited at most to 1000 m/min.

To meet the requirement of a higher speed extrusion, based on resin A, was developed a next polyethylene resin B which can be processed at a speed of 2000 m/min or higher. This improvement of the processability was attained by slightly lowering the average molecular weight (in other words, raising the melt index) and by broadening the molecular weight distribution as much as possible. It maintains mechanical and other properties at the same high level as resin A. The production of resin B is now on a commercial base and the resin is one of the grades with the broadest molecular weight distribution among high density polyethylenes.

The present joint developmental work aimed at the extrusion at 3000 m/min requested Mitsui a further improvement of the processability of resin B. After many trials and tests, was finally developed resin C which could afford the extrusion of foamed insulation at the wire speed of 3000 m/min. The key point of the final improvement was that the molecular weight distribution of the resin was changed in its pattern, while the distribution was kept as broad as possible, to meet the processing in the range of extremely high rate of shear.

A selected commercial grade of anti-plating type of chemical blowing agent was used in which azodicarbonamide was the main component. The blowing agent was mixed and dispersed in melt polyethylene to produce ready for use expandable compound.

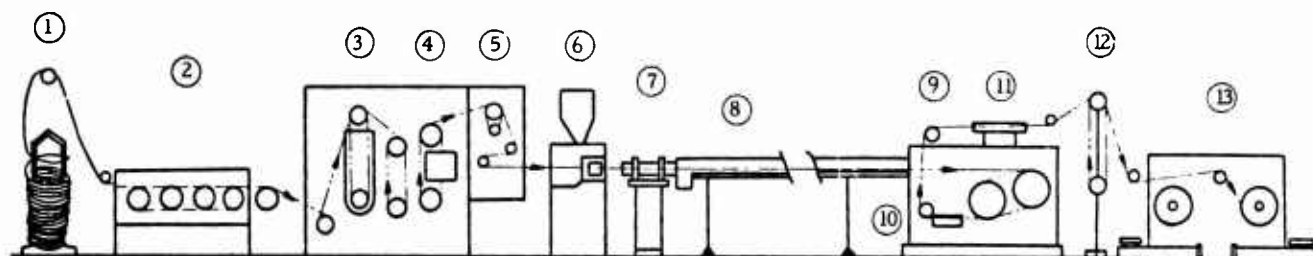


Figure 1.

Ultra-High Speed Extrusion Line for Foamed HDPE Insulation.

- |                         |                          |
|-------------------------|--------------------------|
| 1. Pay-Off              | 8. Water Spray Trough    |
| 2. Wire Drawing Machine | 9. Capstan               |
| 3. Annealer             | 10. Water Electrode      |
| 4. Preheater            | 11. Spark Tester         |
| 5. Tension Helper       | 12. Dancer Roll Assembly |
| 6. 65mm Extruder        | 13. Take-Up              |
| 7. Quenching Trough     |                          |



Table 1. Properties of Wire Coating Grades

Materials Items	Original wire coating grade Resin A (commercial)	High speed wire coating grade Resin B (commercial)	Ultra high speed wire coating grade Resin C	Remarks
Density (g/cm <sup>3</sup> )	0.945	0.948	0.948	ASTM D-1505
Melt Index (MI <sub>2</sub> ) (g/10 min)	0.22	0.40	0.40	ASTM D-1238 Condition E
MI <sub>10</sub> /MI <sub>2</sub>	22	25	25	
Tensile Strength (kg/mm <sup>2</sup> )	2.30	2.20	2.20	ASTM D-638
Tensile Elongation ( % )	800	800	800	ASTM D-638
Environmental Stress Cracking Resistance F <sub>50</sub> (hrs.)	over 500	over 500	over 500	ASTM D-1693 10% Igepal CO 630 at 50°C
Thermal Stress Cracking Resistance F <sub>50</sub> (hrs.)	over 1000	over 1000	over 1000	100°C oven based on REA 6.01 (A)
Brittleness at -60°C	No Failure	No Failure	No Failure	ASTM D-746
Dielectric Constant (1 MHz)	2.3	2.3	2.3	ASTM D-150
Dissipation Factor (1 MHz)	$2.1 \times 10^{-4}$	$2.0 \times 10^{-4}$	$2.0 \times 10^{-4}$	ASTM D-150
Volume Resistivity ( $\Omega$ -cm)	$4.4 \times 10^{16}$	$2.5 \times 10^{16}$	$2.6 \times 10^{16}$	ASTM D-257

### 3. Extrusion of Foamed High Density Polyethylene

There were many problems to be solved in order to make the whole system adequate for the extrusion of foamed high density polyethylene insulation at an ultra-high speed. Generally speaking, there are various different aspects in the extrusion of foamed insulation from that of the solid insulation. On the other hand, there are also many common aspects in both types of insulation extrusion.

Common aspects of an ultra-high speed extrusion are as follows:

- 1) The wire tension must be kept uniform and minimum to keep wire draw down minimum.
- 2) The crosshead pressure should be kept minimum to assure an safety operation.
- 3) The design of die should be made optimum to make the extrudate surface smooth, to keep the wire tension minimum, and to leave the least residual stress in the insulation layer.

In addition, the automatic dual take-up should work at a least failure rate especially at an ultra-high speed in order to keep the wire scrap minimum.

Different aspects in the extrusion of foamed insulation from that of solid insulation could be

listed as follows:

- 1) Wire tension has to be more rigorously controlled and reduced because of the unavoidable tension increasing elements such as quenching trough, water electrode of capacitance monitor.
- 2) Wire preheat is more critical because of the balance between the tensile elongation of the foamed insulation, cell structure of the foam, and the wire draw down.
- 3) Crosshead pressure is higher due to the smaller clearance between the conductor and the die.
- 4) The whole haul off and take up system has to be carefully designed so as to keep the surface damage of the extrudate minimum.

Essentially, the most serious problems in the extrusion of foamed insulation of high density polyethylene as compared with that of solid insulation of low density polyethylene were the severer wire draw down, higher sensitivity of various properties to the wire preheat, and the increased crosshead pressure. In addition, capacity control is more difficult at an ultra-high speed. All of these problems had to be solved while keeping the extrudate surface smooth and keeping the insulated conductor capacity uniform within a narrow range.

### 3.1 Capacity Control

An ultra-high speed extrusion causes to the capacity control a difficulty peculiar to the level of the wire speed. Capacity control in the extrusion of foamed insulation is usually made by the use of a capacitance monitor which is coupled with a movable water trough in order to quench the expanding insulation after it emerges out of the die at a point that allows a sufficient expansion while suppresses an excess.

In the early stage of the present work, it was noticed that capacity fluctuated very much as the extrusion speed increased while at lower speeds it was sufficiently stable. Soon it was found that the fluctuation was caused by the air drawn into the quenching and electrode troughs accompanied by the running wire. Drawn in air unstabilizes the quenching point and the effective length of water electrode. Both effects lead to the fluctuation of the capacitance.

In order to overcome this problem, the use of a pressurized quenching trough was found to be the right answer. Electrode trough of the capacitance monitor should also be water pressurized to prevent air coming in accompanied by the fast running wire. In Figure 2, it is seen how the capacity is stabilized when the troughs are sufficiently pressurized by water.

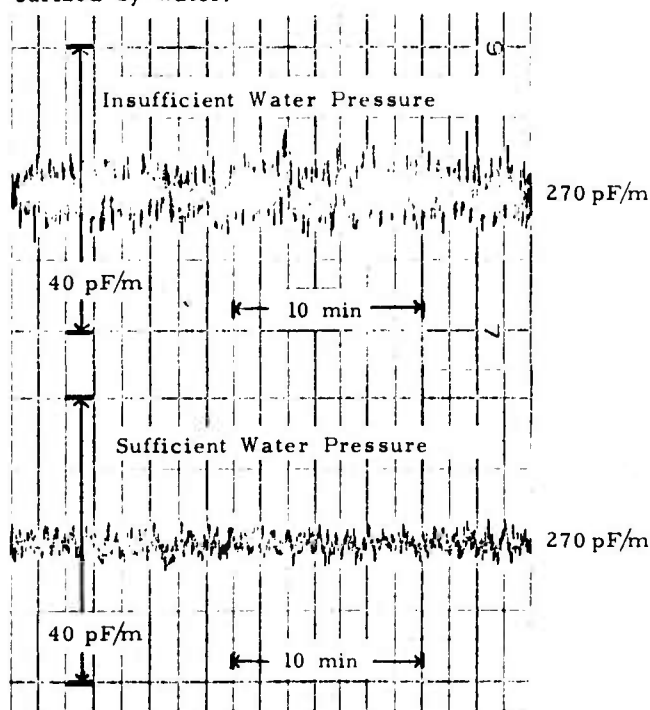


Figure 2.

Effect of Water Pressurization of the Quenching and Electrode Troughs on Capacitance Stability.

### 3.2 Wire Draw Down

As already mentioned, more wire draw down is expected in the extrusion of foamed polyethylene insulation than in the case of solid poly-

ethylene insulation, because in the former a quenching water trough and a water electrode for the capacitance monitor must be equipped in the line, in addition to water spray cooling trough which contributes to the wire tension very little. Both water filled troughs are expected to contribute appreciably to the increase of the wire tension, especially at an ultra-high speed.

Figure 3 shows that is true. In the Figure, diameter of the copper conductor after taken up which was fed into the extruder crosshead at a diameter of 0.510 mm, is plotted against the extrusion line speed at a total length of troughs of 1700 mm. As the wire speed increases, the conductor diameter is seen to decrease with a drastic change when the speed exceeds 2000 m/min. This shows that only limited length of water troughs is allowed to be used in the extrusion at 3000 m/min.

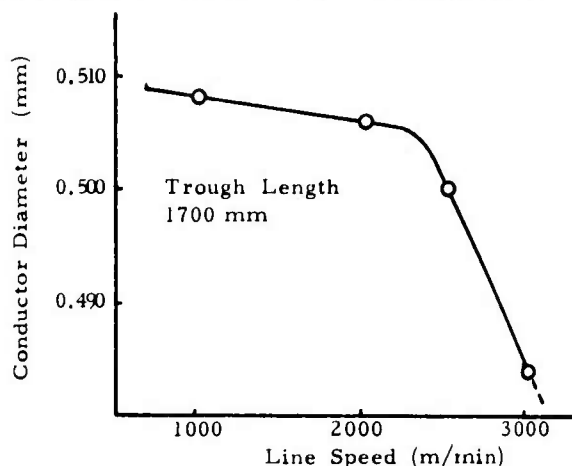


Figure 3.

Effect of Line Speed on Wire Draw Down.

It is obvious that the shorter the length of the water troughs the less the wire draw down. On the other hand, complete and stable quenching of the foamed extruded insulation is necessary which requires sufficient length of water troughs.

It was found that the best solution to this contradiction was to move away the capacitance monitor out of the high tension area of the extrusion line, and to set the monitor between the capstan and the take up, thus the problem of the wire draw down by the electrode water was essentially eliminated. Only the length of the quenching trough was left for the optimization between draw down and cooling.

Wire draw down was also found to be affected by the temperature of anneal and preheat. Anneal temperature had to be optimized so that the copper wire was annealed soft enough but not in excess not to be drawn down in the course of insulation extrusion. Preheat temperature should be selected to give the best balance between the various factors, including draw down, which are described in the following section.

In Figure 4, the effect of wire preheat temperature on the conductor draw down is illustrated. Also in this case a drastic effect is observed in the area of ultra-high speed, more drastic at a higher preheat temperature.

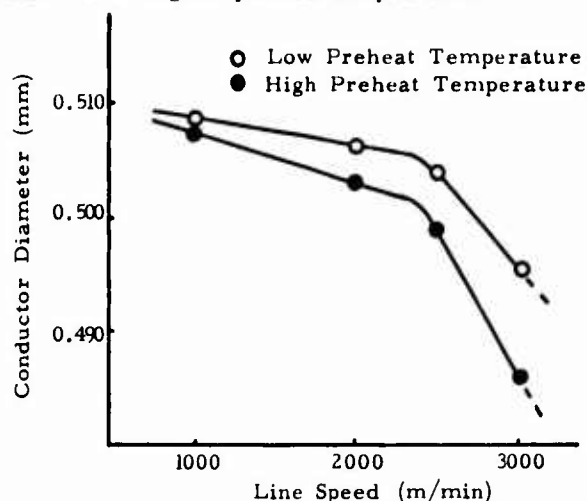


Figure 4.

Effect of Preheat Temperature on Wire Draw Down.

### 3.3 Wire Preheat

The tensile elongation of the foamed insulation is critically affected by the wire preheat temperature. (See Figure 7) As mentioned earlier the present equipment was originally designed for the extrusion of solid insulation, not for the foamed one. In the case of the foamed insulation tensile properties of the insulation is much more sensitive to the wire preheat. It did not take much time before we recognized that the capacity of the preheater in the original design was completely insufficient to be used for the foam extrusion. The capacity was trippled to make the whole line capable for the extrusion of the whole intended range of conductor size and wire speed.

Wire preheat also affects the cell structure

of the foamed insulation. In Figure 5 a set of examples is shown photographically, which was prepared under control so that each insulation had a same level of capacity. At a low preheat temperature fine cells are seen to be dispersed throughout the whole insulation. On the other hand, at a higher temperature coarse cells are found especially in the inner half layer of the insulation. At the highest temperature in this set of experiment, some of the cells are observed to have burst inside at the interface between the conductor and the insulation.

The preheat temperature should be low enough to maintain a good cell structure as well as to avoid unnecessary wire draw down, while it should be high enough to assure a good tensile elongation of the insulation foam.

### 4. Development of a New Polyethylene

As already described in the chapter 2.2 in this paper, the extrusion grade for foamed insulation of Mitsui Petrochemical high density polyethylene started with resin A which had a reputation of many years. Resin B, a new easy processing version of Mitsui high density polyethylene was developed recently before resin A was made obsolete.

In the present work both resins A and B were difficult to be used for the present purpose. In Figure 6, the crosshead pressure of the extruder is plotted against the wire speed for the three types of polyethylene, A, B, and C which was newly developed in the course of the present joint work. It is apparent from the Figure that resin A can be used only at a limited speed range when the insulation is thin and foamed as in the present case. Resin B is seen to be capable for use at an appreciably higher speed, but the extrusion at 3000 m/min should be avoided because of a too high pressure in the crosshead. In the development of a new polyethylene which would fulfill the requirements of the present work, the first criterion of the selection was the crosshead pressure.

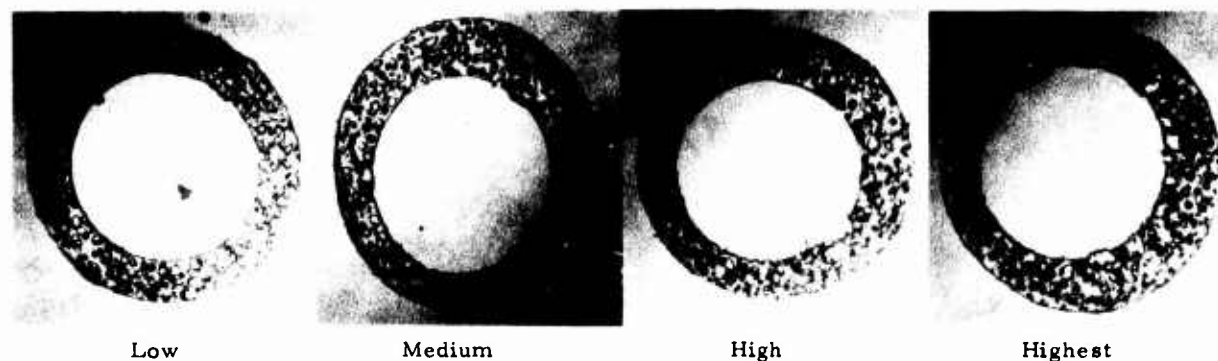


Figure 5.

Effect of Preheat Temperature on Cell Structure.  
(conductor diameter : 0.5mm, capacity : 270 pF/m)

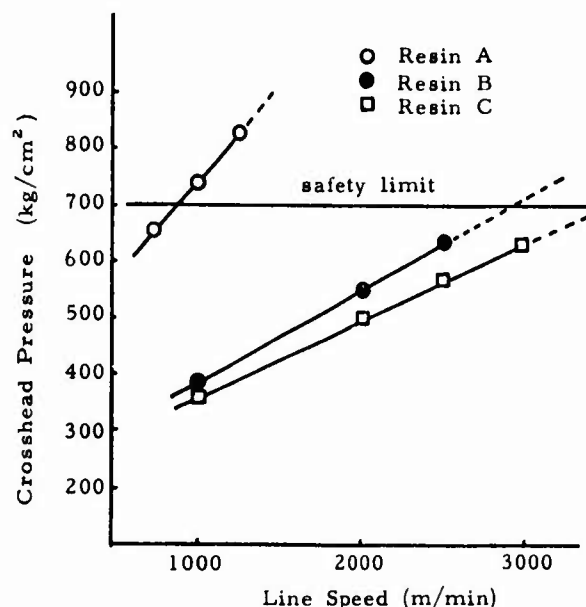


Figure 6.  
Effect of Line Speed on Crosshead Pressure.  
(conductor diameter : 0.5mm)

Physical properties of the insulation foam were also important. In Figure 7, are plotted typical data of tensile elongation of the insulation foam of a few base resins as affected by the degree of the wire preheat. It is seen in the Figure that resin P has low tensile elongation even at a highest wire preheat while resins B and C have a level of tensile elongation high enough at a reasonable preheat temperature range.

Resin P was made to have a molecular weight distribution as broad as that of resins B and C, but have a different pattern of the distribution from that of either resin B or C. It is generally

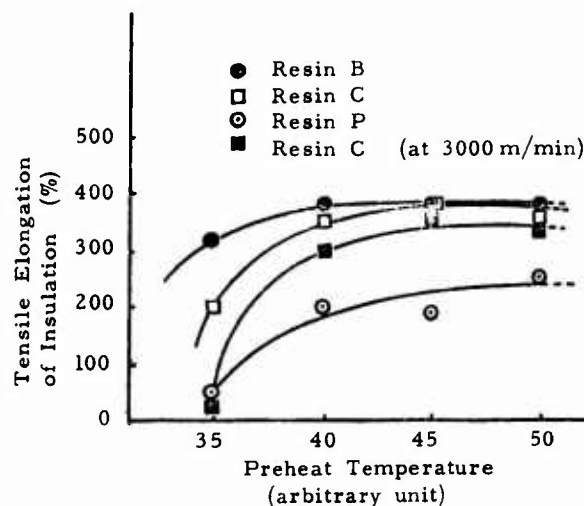


Figure 7.  
Effect of Preheat Temperature on Tensile Elongation of Insulation. (conductor diameter : 0.5mm, line speed : 2500 m/min)

known that the processability of a polyethylene would be improved by broadening the molecular weight distribution, but to improve the processability as reflected in the physical properties of the extruded product, in the range of extremely high shear rate as in the present work, it is learnt that not only the broadening of the molecular weight distribution but the pattern of molecular weight distribution is a very important factor.

Flow curves of resins A, B, and C are shown in Figure 8 in the range of high rate of shear which is close to the actual rate of shear in the wire insulation extrusion.

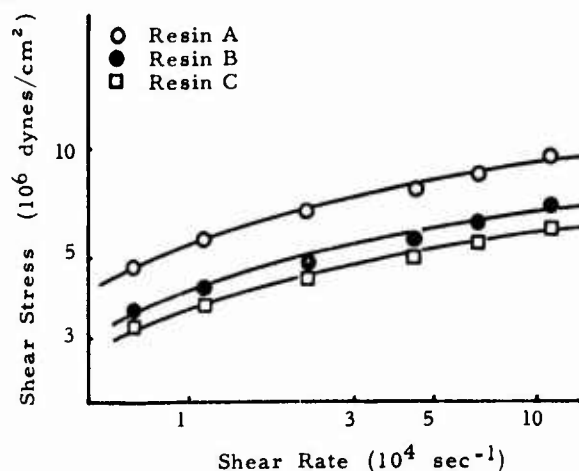


Figure 8.

Melt Flow Curve. (Capillary Rheometer Temp. 190°C, Die 0.49mm diameter, L/D = 30)

##### 5. Test Production Run and a Finished Cable

A test production run at the speed of 3000 m/min was carried out to make a finished cable for a test.

Tensile properties of the test produced foamed insulation of different colors and conductor sizes are shown in Table 2. In the Table are also listed the test results of thermal stress cracking, heat shrinkage, abrasion resistance, and surface roughness. Abrasion resistance of the foamed high density polyethylene insulation as extruded at 3000 m/min is compared in Figure 9 with that of solid low density polyethylene insulation.

All these data show that foamed high density polyethylene insulation obtained by an ultra-high speed extrusion has a satisfactory balance of properties in respect to the effect of the ultra-high speed processing. Most of the long term properties especially those associated with the chemical phenomena are reflections of the chemical composition of the compound. These also seem satisfactory with resin C as is supported by the results of thermal stress cracking in Table 2.

Table 2. Properties of Foamed Insulation Conductor.

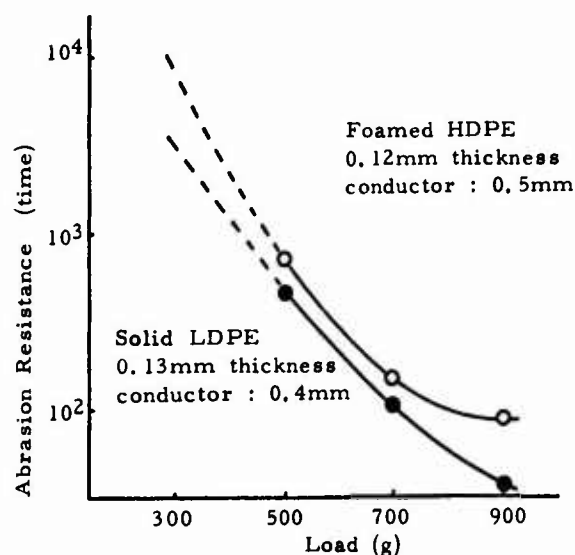
Items	Conductor Dia. (mm) (Color)	0.5		0.4	0.65	0.9	Remarks
		(Red)	(White)	(Natural)	(Natural)	(Natural)	
Line Speed	(m/min)	3000	3000	3000	2500	1200	
Wall Thickness	(mm)	0.12	0.12	0.10	0.15	0.21	
Percentage Expansion (%)		25	25	20	26	28	Specific Gravity Method
Tensile Strength	(kg/mm <sup>2</sup> )	2.34	2.24	2.57	2.28	2.21	JIS K 6760
Tensile Elongation (%)		352	314	408	393	344	JIS K 6760
Abrasion Resistance	(time)	743	809	521	over 10 <sup>4</sup>	over 10 <sup>4</sup>	*1
Thermal Stress Cracking Resistance	(hrs)	over 1000	over 1000	over 1000	over 1000	over 1000	*2
Heat Shrinkage	(%)	0.0	0.0	0.0	0.0	0.0	*3
Surface Roughness	(μm)	1.8	2.2	2.0	1.3	1.2	*4

\*1 A rotating cage machine provided with 36 steel rods of 8 mm diameter was used. A load of 500g was applied to each insulated conductor specimen.

\*2 The insulated conductor specimens were wrapped 25 times around their own diameter, and tested at 100°C in an air oven.

\*3 The insulated conductor specimens were maintained at 100°C for 24 hours in a talc bath.

\*4 Root mean square according to JIS B 0601-1970.



An optical micrograph of a typical cross-section of the foam insulation made in this work is shown in Figure 10.



Figure 10. Micrograph of Cross Section of Foamed HDPE Insulation. (conductor : 0.5 mm)

Using the insulated conductor obtained from the test run, a 1800 pair city junction cable with bonded aluminum sheath was made in accordance with the specification of NTT. The construction of the test produced cable is shown in Table 3.

The electrical properties of the cable are shown in Table 4 and Figures 11 and 12.

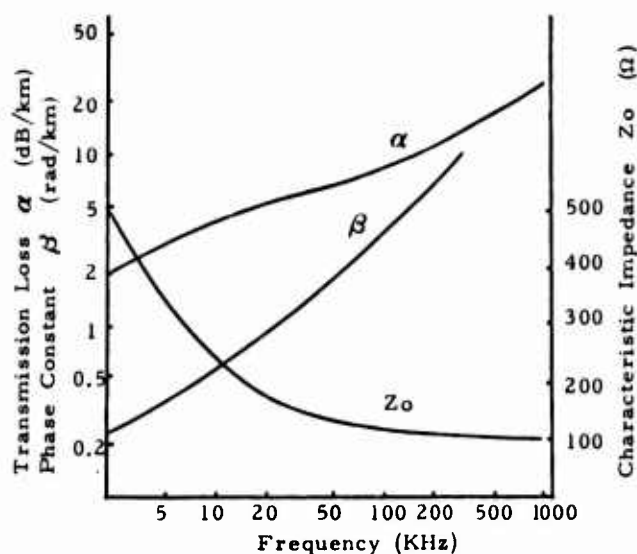


Figure 11.

Propagation Constants of the Cable.

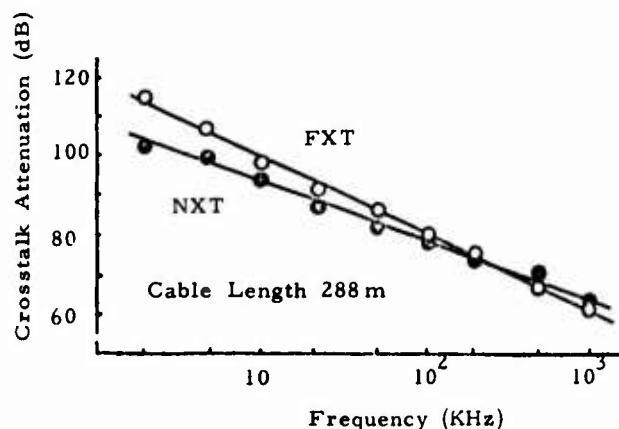


Figure 12.

Crosstalk between Pairs within Quad.

Table 3. Structural Outline of the Trial-Produced Cable.

Number of Pairs	1800 pairs
Conductors	0.5mm copper wires
Insulation	cellular high density polyethylene, wall thickness 0.12mm
Twisting	star-quad formation
Unit Stranding	50 quad (100 prs.) units, concentric layer type
Cabling	center : 1 unit 1st layer : 6 units 2nd layer : 11 units
Core Wrap	polyester and insulating paper tapes
Jacket	laminated jacket of 0.2mm aluminum/weather resistant polyethylene, overall diameter : 67.6mm

## 6. Conclusions

A developmental work was undertaken for the extrusion at 3000 m/min of thin walled foamed high density polyethylene insulation with a joint effort of a cable manufacturer and a polyethylene supplier. In the course of the research it was elucidated that the ultra-high speed extrusion at a speed of 3000 m/min, especially in combination with thin walled foam insulation, was not a simple extrapolation of what was experienced in the conventional lower speed extrusion but it was a different and difficult technical problem. However, after analyzing the difficulties, by modification, optimization, and rearrangement of the equipment it was made

Table 4. Electrical Characteristics of Finished Cable.

Items	Specification for 0.5mm Conductor Junction Cables	0.5mm-1800prs. Cable made-up with insulated conductors by this process
Conductor Resistance ( $\Omega/\text{km}$ )	nominal 88.7 maximum 93.5	maximum 87.4
Insulation Resistance ( $\text{M}\Omega\text{-km}$ )	minimum 2,000	260,000
Dielectric Strength	AC 350V or DC 500V 1 minute	withstood
Average Mutual Capacitance ( $\text{nF}/\text{km}$ )	$50 \pm 5$	48.0
Capacitance Unbalance, Pair to Pair within Quad ( $\text{pF}/150\text{m}$ )	Individual, max. 300 Average, max. 50	Individual, max. 83 Average, 18.6



possible to establish the ultra-high speed extrusion as initially aimed at, with the help of the development of a new polyethylene. The extruded foamed insulation and a test produced finished cable proved satisfactory in quality in accordance with the specification of NTT.

It is expected that the experimental line will be scaled up to a production plant in a near future.

#### Acknowledgments

The authors would like to express their thanks to Mr. Akihisa Matsushita, Mr. Yasuaki Fujiwara, and Mr. Katsutoshi Ohkita, all of Dainichi-Nippon Cables, Ltd., and to Mr. Hiroaki Matsubara, Mr. Yoshinori Akana, and Mr. Shun-ichi Hamada, all of Mitsui Petrochemical Industries Ltd., for their devotion to the present work.



Figure 13.

Test-Produced 0.5mm-1800 pairs PEF Insulated Bonded Aluminum Polyethylene Sheathed Junction Cable.

#### References

1. K. Ogawa, S. Tanaka, A. Tsujikawa, and H. Ishihara, "A new foamed polyethylene insulated junction cable for telecommunication", 20th IWCS Proceedings, pp.183-193, Dec. 1971.
2. K. Orimo, T. Shimano, S. Yamamoto, and M. Azuma, "A new technique for foaming plastics insulation and its application to junction cable", 22nd IWCS Proceedings, pp.302-314, Dec. 1973.
3. M. Jitsukawa, Y. Fujiwara, A. Utsumi, A. Asai, "A method for manufacturing polyolefin insulated communication cable by solvent injection foaming process", 19th IWCS Proceedings, pp.259-269, Dec. 1970.
4. C. Kawazoe, T. Ichiba, H. Shimba, and K. Kadoya, "New extrusion technique for foamed high density polyethylene insulation", 17th IWCS, Dec. 1968.
5. J. K. Normanton, "Extrusion of telephone cable insulation using expandable medium density polyethylene compounds", 21st IWCS Proceedings, pp.182-187, Dec. 1972.
6. S. Verne, B.G. Howell, G.A.L. Ward, "A new process for manufacture of telephone cores with cellular insulation", 18th IWCS, Dec. 1969.
7. E. Kertscher, "Recent developments in the high speed insulation of quality telephone wires", 22nd IWCS Proceedings, pp.315-335, Dec. 1973.



Mitsuru Rokunohe  
Dainichi-Nippon Cables, Ltd.  
3-4-1, Marunouchi,  
Chiyoda-ku, Tokyo,  
Japan

Mitsuru Rokunohe joined Dainichi in 1973 with a 25 year career in Nippon Telegraph and Telephone Public Corp. where he had been mainly engaged in the development of new telephone cables among which the solution coating process for city cable was also the subject of the thesis of Doctorate awarded by Tohoku University, his Alma Mater, in 1962. In the present company he is Deputy General Manager of Telecommunication Headquarters.



Masaaki Okada  
Dainichi-Nippon Cables, Ltd.  
Higashimukaijima,  
Amagasaki,  
Japan

Masaaki Okada, born in 1935, graduated from Kyoto University majoring industrial chemistry in 1957 and immediately joined Dainichi where he has been engaged in the research and development of plastic materials and related products.

He is now a Senior Research Engineer in Material Laboratory of his company. He is also a member of the Society of the Plastics Engineers.



Yuzo Ueno  
Mitsui Petrochemical  
Industries, Ltd.  
Waki-cho, Kuga-gun,  
Yamaguchi, Japan

Yuzo Ueno graduated from Kyushu University in 1953 with a B. Sc. in Applied Chemistry. He joined the Mitsui Petrochemical Industries Ltd. in 1963 and has been engaged in research and development of plastic materials. Mr. Ueno is now a manager of 2nd Polymer Physics Laboratory, Research Center.



Jun Konishi  
Mitsui Petrochemical  
Industries, Ltd.  
Waki-cho, Kuga-gun  
Yamaguchi, Japan

Jun Konishi graduated from Hokkaido University in 1956 with a B. Sc. in Applied Chemistry. He joined the Mitsui Petrochemical Industries Ltd. in 1961 and has been engaged in research and development of plastic materials. Mr. Konishi is now a manager of Plastics Application Division, Research Center.

A NEW INSTRUMENT FOR  
NON-CONTACT TEMPERATURE MEASUREMENT OF  
MOVING WIRE

by

D. L. Rall, Trans-Met Engineering, Inc., La Habra, California

S. M. Beach, Phillips Cable, Ltd., Vancouver, British Columbia

ABSTRACT

A new instrument for non-contact temperature measurement of moving wire during wire coating is described. The instrument employs the calibrated convective heat flow concept of comparing the wire temperature to the known and controlled temperature of a sensing head placed in close proximity to the wire. The temperature comparison is made by employing a heat flow sensor at the bottom of a slot in the head through which the wire passes.

Specific applications to preheat control on cellular and solid polyethylene and polypropylene insulated telecommunications wire is discussed. Close preheat temperature control of the wire assures reliable bonding of the plastic to the wire as well as proper foaming of the insulation thus assuring the desired insulation characteristics and hence high quality wire.

The method of measurement is applicable for wire sizes ranging from 0.010 inch to several inches in diameter by use of various sensing head sizes and configurations. Temperatures which can be measured range from ambient to 400°C for speeds up to several thousand feet per minute. Use of the convective heat flow measurement, rather than a radiant measurement, make the instrument insensitive to changes in finish and emissivity of the wire surface.

INTRODUCTION

The manufacture of paired telephone cable has, over the past twenty years, seen many significant refinements in both materials and design. The processes for the manufacture of these cables have necessarily required coincidental refinements.

The adoption of solid thermoplastic polyethylene for the primary insulation of conductors for telephone cables occurred about 1950. In the mid 1960's a cellular thermoplastic insulation was introduced. This type of insulation has been employed in increasing quantities and today replaces a considerable quantity of both the solid thermoplastic insulation and the paper insulation used on older telephone cable conductor assemblies.

The use of the cellular insulation has required the development of equipment not previously available. In the case of certain existing equipment, significant refinements in measurement capability and techniques were found to be necessary.

The application of the cellular insulation to the

metallic conductor is, of course, accomplished by basically standard extrusion equipment. Elevating the surface temperature of the metallic conductor above room temperature is critical to the proper extrusion coating of both the solid thermoplastic and the cellular thermoplastic insulation. The critical wire temperatures required for both types of insulation become apparent when the product from automated extrusion lines is checked for uniformity of the principal parameters needed for paired telephone cable conductors. These parameters are discussed in detail in reference (1).

The critical wire temperature will vary with the specific polymer employed. The selection of the critical temperature must be initially determined by empirical observation. Once determined, automatic temperature control becomes essential. In the past a rotating contacting copper constantan thermocouple located immediately upstream of the extrusion head was employed. This device was coupled to a bridge followed by a high gain amplifier and servo control unit.

The maintenance frequency required by this type of temperature sensor was high and varied proportionately to the lineal throughput speed. The maintenance involved principally:

- (a) Surface condition of the rotating elements.
- (b) Lubrication of the bearings involved.
- (c) Voltage pick-up contacts on each rotating element.

It became apparent that a non-contact device for measuring and controlling the critical surface temperature of the metallic conductor would be desirable.

As a consequence of this need a technique originally developed for use in the synthetic fiber industry for measuring moving fiber line temperatures was adopted for use on wire coating machines to measure and control wire temperature. This measuring technique has the advantage of being non-contacting at the point of measurement and non-optical, since it utilizes a convective heat transfer measurement. The measurement is thus insensitive to surface finish of the wire, can operate in a relatively contaminated environment and does not create frictional heating or heat sink cooling of a moving wire by the presence of the sensing device at the point of measurement.

PRINCIPAL OF OPERATION

The instrument operates on the patented principle of comparing the temperature of the wire to a sensing

head at a known controlled temperature. The comparison is made by positioning a heat flow sensor, mounted at the bottom of a slot in the sensing head, in close proximity to the wire but not touching it (typical spacing from the wire is 0.030 to 0.040 inches). As the wire passes the heat flow sensor there will be an exchange of heat across the small air gap. If the wire is colder than the sensor, a very small amount of heat will flow from the sensor to the wire and if the wire is hotter, the reverse will occur. If the wire and sensor are at the same temperature there will be zero heat flow. The heat flow sensor acts, in essence, as a thermal galvanometer. Since the rate of heat transfer ( $\dot{q}$ ) is essentially by conduction across the small air gap it is directly proportional to the temperature difference ( $\Delta T$ ) and the thermal conductance of the gap ( $K$ ) and inversely proportional to the dimension of the gap ( $\Delta x$ ). This relationship is defined by the simple heat conduction equation,

$$\dot{q} = K \frac{\Delta T}{\Delta x} \quad (1)$$

By the use of ceramic coated sheaves or standard ceramic guides at the entry and exit of the slot, the physical spacing between the wire and the sensor can be fixed. For limited ranges of temperature, for example  $\pm 50^\circ\text{C}$  difference between the sensing head and wire temperature, the thermal conductance also remains constant and thus all variables of equation (1) are fixed and

$$\dot{q} \propto \Delta T \propto E_h \quad (2)$$

where  $E_h$  is the voltage signal from the heat flow sensor.

If one amplifies the signal from the heat flow sensor so that it has the same sensitivity, in terms of volts per degree, as a temperature sensor in the sensing head and electronically takes the algebraic sum of the two signals, one obtains a voltage signal proportional to head temperature + the temperature difference between the head and the wire and hence the absolute temperature of the wire. This wire temperature is then displayed digitally thru a readout on the front of the instrument for observation by the operator.

In addition to displaying true wire temperature the instrument produces an output signal which can be used to complete feed-back control of the wire preheater to automatically control wire temperature. This is best accomplished by setting the sensing head temperature to the desired control point temperature and utilizing the output from the heat flow sensor to cause the wire heating system to heat the wire until the heat flow signal goes to zero at which time the wire is at null-heat-balance with sensing head and is thus at the desired control point temperature.

A picture of a typical temperature measuring instrument is shown in Figure 1. A more complete discussion of the principle of measurement for these instruments is available in Reference (3).

#### CALIBRATION

When using the instrument to monitor wire temperature it is necessary to calibrate the signal from the heat

flow sensor so that its output will present the same number of volts per degree as the reference temperature sensor in the head. This is accomplished by a simple on-line procedure in which three readings are taken at three different head set-point temperatures while operating on a constant temperature wire line. The three uncalibrated readings are plotted as a function of head temperature as shown in Figure 2 (both coordinates of the graph must be identical). The true wire temperature is obtained by drawing a straight line thru the three points. The temperature where this line crosses the  $45^\circ$  line (point where wire temperature and head temperature are equal and hence deviation signal zero) is the true wire temperature. With the head temperature at least  $10$  to  $20^\circ$  different than the true wire temperature, a potentiometer on the instrument is adjusted so that the digital reading on the instrument displays true wire temperature as determined from the graph. The instrument is now calibrated and can be used to monitor moving wire temperatures. Greatest accuracy is obtained by setting the head at the average wire temperature and monitoring the temperature variations about that average. A more complete discussion of calibration procedures can be found in reference (3).

#### CHARACTERISTICS OF INSTRUMENT

Wire size:	Minimum dia. = 0.010 inch Maximum dia. = no limit (for large variations in wire size different head designs are used)
Temperature range:	Monitoring mode: ambient to $400^\circ\text{C}$ Control mode: ambient to $350^\circ\text{C}$
Wire velocity:	3,000 ft./min. with guide sheaves 10,000 ft./min. with ceramic guides
Accuracy:	$\pm 1\%$ of full scale
Repeatability:	$\pm 1^\circ\text{C}$
Resolution:	$\pm 1^\circ\text{C}$
Response:	Less than one second time constant

#### RESULTS OF WIRE TEMPERATURE CONTROL TESTS ON INSULATION QUALITY

Using non-contact temperature measurement and preheat control for the wire, tests were conducted to determine the relationship between critical insulation parameters and wire preheat temperature on the following combinations of wire sizes and coatings.

##### (A) A fully annealed copper conductor insulated with a cellular medium density polyethylene:

The gaseous portion of this type of insulation is present in the form of many small discrete non-communicating cells. These cells are uniformly dispersed through the insulation cross-section. At the same time they must not occur close enough to either the inner or outer surface of insulation so as to produce a microscopic rupture. In effect a solid skin must be present on both surfaces. In this way the optimum physical and electrical properties are assured. The foregoing is applicable to both methods of closed cell production i.e. chemical decomposition or injected gas.

The skin on the outer surface is obtained through a combination of die configuration, polymer selection, blowing agent masterbatch technique, temperature

control and quench arrangement in which the air gap between die and quench bath is automatically varied by use of a coaxial capacitance monitoring and control device.

The skin on the inner surface is directly related to conductor surface temperature and cleanliness.

A condensation of the original study for one size of conductor is shown below:

Size	#19 AWG Copper wire Insulated to Diameter 0.062 Inches			
% Blow	30%	30%	30%	30%
Conductor Surface Temperature	R.T.(70°F)	150°F	200°F	230°F
% Elongation (2 inches/min)	45/50%	160%	425%	490%
D.C. Voltage Breakdown	4500	6000	9500	5000
Capacitance (pf/ft.)	53	53	53	53

The investigation also covered sizes #22, #24, #26, and #28 AWG. Essentially the same results were obtained.

(B) A fully annealed copper conductor insulated with a solid low density polyethylene:

This type of insulation is produced in such a way that the best physical and electrical properties present in the base compound are retained in the insulated wire. The tandem lines producing this class of insulated wire are identical to those producing cellular insulated wire. Coaxial capacitance measuring and controlling devices are used to automatically trim the line speed.

A condensation of the original study for one size of conductor is shown below:

Size	#19 AWG Copper wire Insulated to Diameter 0.062 Inches			
Conductor Surface Temperature	R.T.(70°F)	150°F	200°F	250°F
% Elongation (10 inches/min.)	240%	350%	500%	560%
D.C. Voltage Breakdown	18000	20000	20000	20000
Capacitance (pf/ft.)	72	72	72	72

The study also covered sizes #22, #24, and #26 AWG and essentially the same pattern emerged.

Additionally the studies were repeated with

- (a) Gas injected polyethylene and polypropylene.
- (b) Solid insulation of medium and high density polyethylene.
- (c) Solid insulation of homo and co-polymer polypropylene.

In all cases the lines were controlled using capacitance techniques, i.e., on solid coatings the capstan speed was varied while on foamed coatings the air gap between die and quench bath was varied both being based on the coaxial capacitance measurement technique.

## CONCLUSIONS

A new instrument for non-contact temperature measurement of wire has been described. Application of the instrument to study the relationship between wire preheat temperature and the critical parameters effecting insulation quality of both foamed and solid plastic coated wire was conducted.

The tests substantiate the direct relationship that wire preheat temperature has on the quality of the resulting insulation.

On the basis of the results it can be concluded that the use of this non-contact measuring technique can assure proper preheat temperature monitoring and control which is essential to the production of high quality foamed and solid insulated wire.

## REFERENCES

- (1) Beach, S. M., D. Cretney, and J. Ruskin, "Cellular Polyethylene Insulated Fully Filled Cable With High Dielectric Strength," 22nd International Wire and Cable Symposium, Dec. 1973.
- (2) Hornbaker, D. R., and D. L. Rall, "Non-contact Temperature Measurement of Fibers, Sheets, etc. by the Convective Null-Heat-Balance Method," TEXTILE INSTITUTE AND INDUSTRY, January, 1974.
- (3) Hornbaker, D. R., and D. L. Rall, "The Convective Null-Heat-Balance Concept for Non-contact Temperature Measurement of Sheets, Rolls, Fibers and Wire," presented at the 5th Symposium on Temperature, Its Measurement and Control in Science and Industry, Washington, D. C., June 21-24, 1971



WIRE TEMPERATURE  
MEASURING SYSTEM  
FIGURE 1

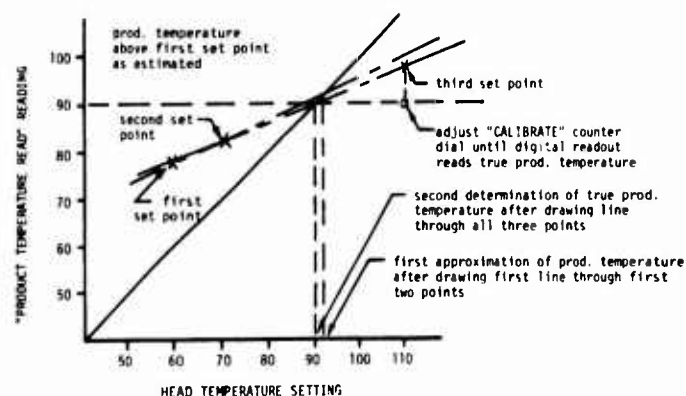
# AUTHOR'S BIOGRAPHY INFORMATION



DIETER RALL is General Manager of Trans-Met Engineering, a company which specializes in the manufacture of instruments for temperature measurement and control of industrial processes. He is a graduate of the University of California, at Berkeley, with a B.S. and M.S. in Mechanical Engineering. He has authored numerous articles and papers in the field of temperature measurement and heat transfer, and holds several patents on various thermal measuring and control devices.



SHIRLEY (MIKE) BEACH was educated in Brockville, Ontario and has been employed by Phillips Cables Limited principally since 1936. He has been employed in both administrative and technical capacity relating to rubber and plastics technology and processing. During this period he has attended a number of courses provided by the industry related to the rubber and plastics industry.



TYPICAL WIRETEMP™ CALIBRATION PLOT  
FIGURE 2



## TELECOMMUNICATION OPTICAL FIBERS MANUFACTURING METHODS

G. Manfré - R & D Division - Technion SpA - Novara - Italy

**Summary:** The advent of optical fibers with a remarkably low transmission loss (less than 10 dB/km) has oriented the glass fiber manufacturers to find new technologies in order to produce suitable fibers. The main aim of world wide research of the 3 last years has been to reduce the optical fiber attenuation with a surprising results of 2 dB/km obtained with very special purified and/or doped silica fibers. Further we know now that features of the fiber depend on impurities absorption, bulk scattering, interface scattering, fundamental absorption. A part the impurities present on the bulk glass other fibers features seem mainly to depend on drawing method from melt. Thus, as any drawing optical fiber technology is basically a spinning method from a molten material, our research and experience on the drawing zone of the glass spinning process, let us to describe the present approach which intends to compare the main methods today in use at laboratory stage:

- rod-tube simultaneous molten attenuation;
- double crucible;
- ion exchange (Selfoc);
- rod molten attenuation of glass obtained by chemical vapour deposition;
- glass plastic cladbed fibers.

Each method will be shown on both process parameters and fibers features and so the involved engineering is emphasized in order to give practical indication to choice a method with better chances to industrial scale up. This to adapt a fiber drawing method to a continuous process with attendant economical gains.

### Introduction

Optical glass fibers has attracted a particular interest for its possibility as a communication cable in the optical region and the major effort has been directed toward reduction of light propagation loss. Although optical fiber cable are expected to start carrying telecommunication signals within four or five years, at least over short distances, since now we think that the selection of the fibers for specific installation will require physical, engineering and economical factors which will play a great influence to decide their exploitation. The paper intends to give comprehensive review on the actual fiber forming methods for manufacture optical fibers to try and compare their particular characteristics in function of fiber properties and engineering factors to predict the future industrial possibilities. This also to give the reader a picture of the basic fiber features in function of the present fiber forming technology. Finally to inform that there will be not only one technology on one suitable fiber but a variety of technology for a selection of suitable fibers in conformity of different type of applications.

In any way our paper has to be considered only a simple approach because it is impossible to be very definitive at this time.

### Optical attenuation

A part the modulation, amplification, equalization and other equipment which must be tailored to fit the optical fiber, the strong recent research has been devoted towards reduction of light propagation loss [1], [2], [3], [4], [5].

In its simplest form, an optical fiber wave guide consists of a "core" of optically transparent material of given refractive index, surrounded by a "cladding" of optically transparent material having a slightly lower refractive index. Light launched into the core of such a waveguide is confined there and guided along the length of the waveguide by total internal reflection at the interface between the core and cladding. Optical attenuation or loss, in such a structure, mainly arises from four sources:

- a) Impurities: In fact any impurity ion present in the glass performs an electronic transitions, with energies corresponding to the wavelength of light being transmitted and thus this ion gives rise to absorption. The main absorber ions are the transition metals [6], iron, cobalt, nickel, copper, chromium, manganese, vanadium, platinum and rhodium. In addition, the presence of traces of water [7] in the glass (as hydroxyl ions) causes absorption bands in the near infrared [8].
- b) Bulk optical scattering: Any part of material within the core, performing a refractive index different from the core, will cause the transmitting light to be scattered. Gas bubbles, inclusions, chemical inhomogeneities will generate scattering. The lower limit of scattering should be the Rayleigh contribution which results from density and microphase fluctuation in the glass structure.
- c) Interface scattering: As the light is confined to the core by total internal reflection at the core-cladding interface, any irregularities at that interface will also generate scattering losses.
- d) Fundamental optical absorption: Due to exciton processes in the glass matrix itself any given compound glass system shows absorption in dependence of the spectral region. For instance silicate glasses show an extremely intense absorption in the ultraviolet range which can not be reduced. On the other hand recent work [9] suggests that the fundamental absorption in the infrared region can be reduced by impurity control. The remaining fundamental absorption, when extrapolated to the near infrared region, becomes so low as to be insignificant when compared to residual impurity absorption and scattering loss, even in the case of ultra-low

loss fibers.

From above the optical loss arising from the four sources can be simply divided in four parts:

- 1 - losses caused by impurities present in raw materials;
- 2 - losses due to impurities or inhomogeneities generated during the glass melting or the fiber forming process;
- 3 - losses due to the structure of the selected glass system;
- 4 - losses strictly dependent on the fiber forming technology.

More precisely losses 1 and 3 can be reduced as by preparing glasses from special ultra-high purity raw materials as by selecting a given compound glass system performing a low fundamental absorption for the given light to be launched through the core. But this matter is not treated in the present analysis which particularly involves only losses 2 and 4 directly dependent on both melting glass and fiber forming processes, as follows:

- impurities can be minimized carrying out both processes in an environment which does not contribute any additional contaminants. Our experience indicated that the main contaminating sources can be: the crucible materials for both batch and molten glass; the crucible wall material can diffuse into the glass either ion or particles. Further the atmosphere surrounding the drawing zone of the forming fiber, chemical surface reaction and ion or gas diffusion, can contaminate the surface or create bubbles at the interface [10];
- crystallisation and phase separation may be avoided during both glass melting and fiber drawing procedures;
- interface irregularities depend on fiber drawing technology. For this the best procedure seems that in which two molten glass surfaces flow together to form the interface of the forming optical fiber, as for instance in a double crucible technique;
- stability of drawing process to assure the dimensional stability of the fiber.

The aim of the present paper is to make a comparison of the fiber forming technique in function of the optical attenuation and other fiber features included the dimensional uniformity.

#### Fiber Drawing Methods

First of all the selected glasses for waveguides must be suitable for drawing into fibers. Properties such as viscosity, its variation with temperature, surface tension, thermal expansion coefficient, devitrification and crystallisation curve versus temperature and relaxation time in addition, of course, to refractive index, have to be known as described by the author [11], [12]. The present main optical fiber drawing methods are the following five:

- rod and tube;
- double crucible containing two glasses which flow simultaneously through two concentric nozzles;
- special double crucible containing two glasses; one glass flows through a second glass while ion exchange occurs at interface (SELFOC);
- composite rod;
- single rod for obtaining glass-plastic clad fibers.

#### Rod and Tube

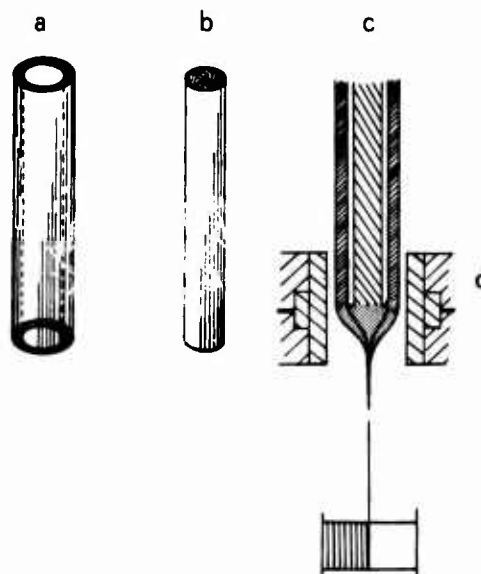


Fig. 1 - Rod and tube method;

- a = tube;
- b = rod;
- c = rod and tube simultaneous drawing
- d = heating furnace: flame, resistor, radiofrequency, laser.

A rod of selected glass (Fig.1b) possessing the desired core characteristics is inserted into a tube (Fig. 1 a) possessing the desired cladding characteristics. The temperature of this combination is then raised (Fig. 1 a) until the viscosity of both materials is in the range of  $7 \cdot 10^2 \div 10^3$  poises, that is a viscosity low enough for drawing the glass from molten state. During the drawing process, the rod and tube are normally fed at different speeds to produce a fiber with the desired core to cladding diameter ratio. This method shows good results to produce glass optical fibers having a large core and thin outside cladding. From the manufacturing view, the selected materials, rod and tube, must have the main following characteristics:

- 1 - the glass purity requested as mentioned above;
- 2 - the desired refractive index difference;

- 3 - a viscosity temperature curve nearly overlapped at least in the viscosity range  $10^4 \div 10^5$  poises;
- 4 - a thermal expansion coefficient-temperature variation nearly close;
- 5 - both inside wall of the tube and the surface of the rod especially treated and cleaned;
- 6 - the rod and tube sizes with a very low tolerance.

Thus it is evident that the selection is strongly difficult and rarely available on the market, this limits the industrial development of the rod and tube method which leaves the best chances to a very specialized manufactures.

In addition to the mentioned 6 points which strongly restrict this method, furtherly the final fiber characteristics depend on the process variables which, on the base of the mass continuity equation, are related as follows:

$$(1) \quad \frac{(R_t^2 - R_i^2) V_t}{R_b^2 V_b} = \frac{R_f^2 - R_c^2}{R_c^2}$$

$$(2) \quad V_f = \frac{R_b^2}{R_c^2} V_b$$

with  $R_t, R_i, R_b$ , radius of tube, inside of tube and of rod;  $R_f, R_c$ , radius of total fiber and core;  $V_t, V_b, V_f$ , speed of tube, rod and fiber.

Our experience on fiber forming of soda-lime, borosilicate and high silica glasses [12] let us to conclude that formula (1) and (2) can be positively applied only when the following conditions are taken into account:

- 3, 4, 6 above conditions are satisfied;
- both drawing ratio  $R_b/R_c, R_t/R_f$ , to be  $< 100$ ;
- the ratio  $K = R_i/R_b$  tend to 1; infact the best rod-tube combination is prepared by raising the temperature until the tube collapses around and fuses to the inside rod.

The  $K$  ratio has carefully been analysed through a lot of experiments: its value affects the stability of the process which is usually satisfactory when the following condition:

$$(3) \quad (R_t^2 - K^2 R_b^2) V_t = R_b^2 V_b$$

is verified, that means the glass volume of the tube and the glass volume of rod are nearly equal on the drawing process. As a consequence, simple calculations by formula (1) and (3) show that the process can produce good optical fibers having a large core and a thin outside cladding, which ratio is in the range of  $1 \div 10$ .

It is in fact extremely difficult to maintain the core and cladding dimensions in manufacturing fibres with a very small core and very thick cladding. On the other hand the irregularities affect the transmission characteristics of the waveguide.

An additional problem is often caused by numerous tiny air bubbles and foreign particles being trapped at the core and cladding interface.

Size and quantity of the bubbles depend on both  $K$  ratio and room atmosphere surrounding the drawing zone of the forming fiber. A reduction of air pressure decreases the number of bubbles as well as  $K$  nears 1.

The above limitations furtherly reduce the exploitation of this drawing method which, on the contrary, remains very attractive as for a very simple feeding part as for the possibilities of drawing a large quantity of available glasses, included the high silica ones, without the contaminating problems of containers. The speed of drawing fibers of  $R_f = 100 \mu m$  can achieve the range of  $100 \div 500$  m/minute.

The heating source can be an induction furnace, a resistor furnace, gas combustion burner, radio frequency, induction heater or a laser.

#### Double Crucible

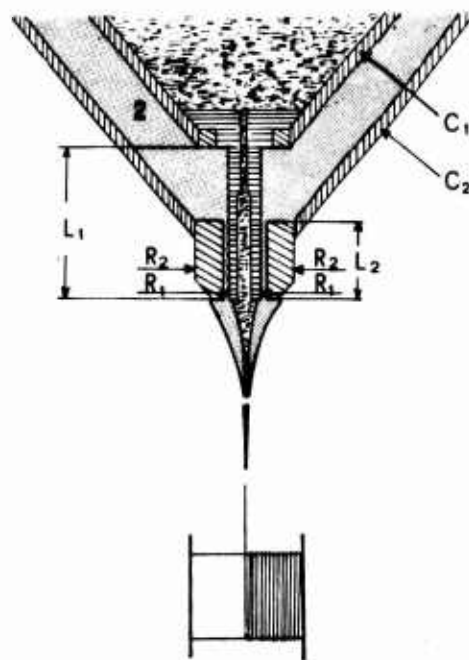


Fig. 2 - Double Crucible:  $C_2$  = external crucible;  $C_1$  = internal crucible; 1 = glass with density  $\rho_1$ , viscosity  $\eta_1$  and  $n_1$  refraction index; 2 = glass with density  $\rho_2$ , viscosity  $\eta_2$  and  $n_2$  = refractive index

In this method, two cylindrical platinum (or platinum alloy) crucibles, each with an orifice in its bottom, are fitted together concentrically (Fig. 2).

The inner crucible contains the core glass and the outer the cladding glass.

The whole arrangement is heated in the furnace of a fiber drawing machine or simpler the crucible can be electrically heated as a resistor.

This method may be used for both soda-lime and borosilicate glasses, but not for high silica glasses.

In fact the upper temperature obtainable with this method is not higher than 1500°C. The selected glasses must have the main characteristics mentioned above except points 5 and 6 which directly refer to rod and tube method. On the other hand, the contamination of the glass by impurities from the platinum crucible (mainly iron and copper) seems one of the limits to overcome in order to reduce the absorption loss. The tendency is also to reduce the temperature in the drawing crucible (~900°C for the sodium borosilicate glasses).

The raw materials for a core, as silica sodium carbonate, calcium carbonate, boric acid and others, in powder form, have to be prepared of ultra-high purity; in most cases individual transition metal ion concentrations of parts per billion or less is requested.

To prepare a core glass, to introduce afterwards in a crucible for drawing, a batch is melted in a special crucible with a very controlled atmosphere (dry and redox) and the obtained glass is to be fined and stirred by a very experimented procedure [13] in order to achieve chemical homogeneity. Thus from above the exploitation of this method seems to be limited by the purity of raw materials and the contaminations from the crucible on both batch melting furnace and drawing crucible. Anyhow fibers of 25-30 dB/km attenuation loss over the spectral range 700-800 nm have been obtained [14] with sodium borosilicate glasses. In fact the interface contaminations, foreign particles and bubbles can be completely avoided. From the manufacturing view the process variables can be related as following:

$$(4) \quad \frac{R_t^2 - R_c^2}{R_c^2} = \frac{R_2^4 h_2 \eta_1 L_1}{R_1^4 h_1 \eta_2 L_2} \left[ (1 - K^4) - \frac{(1 - K^2)^2}{\ln 1/K} \right]$$

$$(5) \quad \frac{R_1^4 \rho_1 g h_1}{8 \eta_1 L_1} = R_c^2 V_f$$

with  $R_t, R_c$  radius of total and core fiber;  $R_2, R_1, L_1, L_2$ , radius and length of external and internal orifices of the two concentric crucibles;  $g$  = gravity constant;  $h_2, h_1$  head of gravity inside the external and internal crucible;  $\rho_1, \eta_1, \eta_2$ , density and viscosity of the two glasses.  $K = R_1/R_2$  the orifice ratio;  $V_f$  = speed of drawing fiber at the drum winding machine.

Formula (4) and (5) has been obtained combining the mass continuity equation and the law of flow through a cylindric capillary for a viscous liquid; the two glasses are assumed with the same density, at least at high temperature. Further the value of  $L_1, L_2$ , have to consider also the end effects involved as the capillary are very short [29].

With the further actually possible assumption  $h_1 = h_2$  and  $\eta_1 = \eta_2$  formula (4) becomes:

$$(6) \quad R^2 - 1 = \frac{L_1}{L_2} \frac{1}{K^4} \left[ (1 - K^4) - \frac{(1 - K^2)^2}{\ln 1/K} \right]$$

with  $R = R_t/R_c$ .

Formula (6) has been used in our experiments to obtain fibers with several  $R$  and has been essential for designing the double crucible orifices in function of the predicted final fiber dimensions (Fig. 2). It is possible to obtain fibers of  $R_t = 100, 50, 10 \mu m$  at drawing speed respectively 10, 30, 50 m/min. with  $R$  up to 10 or more in some case. The uniformity of fiber dimensions and characteristics depend both on the stability of the drawing zone [15].

Generally good results are obtainable with drawing ratio  $R_2/R_1, R_t/R_c < 100$ .

A part the limitations, concerning the raw material purity, temperature upper limit (high silica glasses cannot be used because a suitable material crucible are not available for temperatures higher than 1600°C) and the contamination from crucible (which might be furtherly minimized through future experience), this method can be considered very attractive and versatile to be industrially developed at least for medium loss fibers and for glasses with not very high melting zone.

#### Special Double Crucible

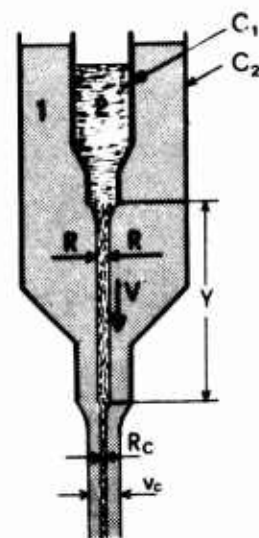


Fig. 3 - Special double crucible (Selfoc);  $C_1$  = internal crucible;  $C_2$  = external crucible; 1 = sodium borosilicate glass; 2 = Tallium borosilicate glass;  $Y$  = length of ion exchange zone;  $V, R$  = average speed and radius of ion exchange zone;  $R_c, v_c$  = core and fiber drawing speed

This process, produces the so called "SELFOC" fibers (self-focusing light) showing a relatively step change of refractive index in the core region.

The SELFOC process has been developed in Japan since 1968, firstly by drawing a fiber from rod pretreated with an ion exchange procedure, more recently by a

double crucible process (Fig. 3). The inner crucible contains a glass (usually a sodium borosilicate) with ions to form the core, the outer crucible contains a second glass (also sodium borosilicate) with different ions to form the cladding. The core ions are selected as thermally diffusing ions which contribute to the "graded index" profile in the fiber [16].

Among all monovalent ions, Tl ion has been selected for core glass for its largest electronic polarizability with a considerably small ionic radius. The ion in cladding glass is usually Na due to its high diffusion thermal coefficient. The fiber is normally drawn at speed of about 20 m/minute, while (see Fig. 3) the ion exchange of Tl and Na ions quickly takes place in the vicinity of the nozzles as a result of the high temperature (900 ÷ 1000°C).

A part the ion-exchange part, this process can be considered as the double crucible method above described: raw materials high purity, contamination from material crucible are less as drawing temperature is low and surrounding atmosphere is controlled. Further the process parameters controlled by formula (6) for double crucible.

For this special attention has to be drawn to know the actual value of the length  $L$ , by which the ion exchange length  $Y$  has to be taken into account as an end effect through a capillary tube so reducing the rate of flow of the core glass through the inner orifice. On the other hand, the condition  $\eta_1 = \eta_2$  to apply formula (6) is well satisfied as the two glasses can be considered very similar for viscosity - temperature behaviour. This lets the crucible designer to consider the correct nozzle geometry. In addition to relation (6) a further relation, involving the ion diffusion process variables, has to be established in order to know the possible drawing speed and its relation with the fiber features.

In fact (Fig. 3) the flow rate  $Q_1$  of the core glass is given:

$$(7) \quad Q_1 = R^2 V = R_c^2 V_c$$

with  $R$  an average value of the radius of the core glass flowing downward in the outer crucible,  $V$  its average speed,  $R_c$ ,  $V_c$  radius and speed of the core of the forming fiber.

The exchange ion parameter [17] can be defined:

$$(8) \quad S = D t / R^2$$

Where  $D$  is the diffusion constant of the diffusive ions and  $t$  the ion exchange time along the  $Y$  length (10 ÷ 15 mm) at which the core glass contacts the cladding glass. Thus through (7), (8), (9) and  $Y = V_c$  we obtain:

$$(9) \quad S = Y D / R_c^2 V_c$$

The concentration profile of Tl seems to determine the parabolic-like refractive index distribution in the core region which can be obtained by selecting a proper value of  $S$ , that is,  $Y$ ,  $D$ ,  $R_c$ ,  $V_c$ . The main controllable parameter to achieve the desired  $S$  value is surely  $Y$ . The value of  $S$  is at present time about 0.04 [18].

The inventors [18] of this method claimed very recently to obtain optical fibers with transmission loss down to about 10 dB/km at wavelengths 0.81 ÷ 0.85  $\mu\text{m}$

The fibers can be manufactured with outer diameters 150 ÷ 250 with the core region showing a parabolic like refractive index distribution of 30 ÷ 50.

This method has the same attributes of the double crucible process with the main characteristic to produce core with graded index. On the other hand, the diffusion process needs more sophisticated drawing process which surely will limit the final drawing speed of the forming fiber. In fact the diffusion constant  $D$  can increase arising the temperature with the effect of contamination from crucible as well as dimensional instability.

An additional limitation may be the difficulty to obtain core region with very small cross-section. On the other hand better eccentricity and dimensional stability can be achieved by this method in comparison as with double crucible technique producing step index fibers as with the following composite fiber technology.

#### Composite fibers

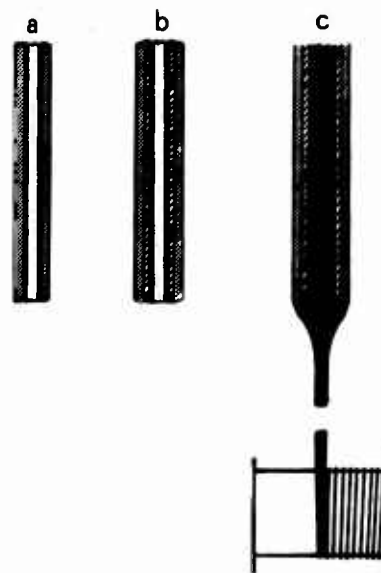


Fig. 4 - Composite fibers:

- a = tube with an inside doped layer;
- b = tube with multiple doped layer;
- c = composite preform drawing after the tube collapsing

For composite fibers we intend those, step or graded index, obtained by pulling a glass composite rod prepared as a preform.

The preform (Fig. 4 a and 4 b) to draw subsequently into fibers is composed with two or three concentric layers of different compounded glasses.



The glasses are usually silica based glasses doped by the addition of another oxide to form a simple compound glass containing a high proportion of silica. The oxides can be titanium oxide, germanium oxide, tantalum oxide, tin oxide, niobium oxide, zirconium oxide, aluminium oxide and phosphorus pentoxide or others. The composite preform rod is usually prepared by forming inside the wall of a silica tube, one or multiple films of the desired materials (Fig. 4a, 4b).

The films are formed by applying a layer of the desired glass or a layer of doping material or doped glass that will diffuse into the inside surface of the tube. The layer is deposited by several methods as flame hydrolysis, vapour deposition, radio frequency sputtering, bathing the inside wall in a fluid that will make an ion exchange.

So far very low loss, less than 3 dB/km, fibers have been obtained by:

- flame hydrolysis of  $\text{SiCl}_4$  and  $\text{TiCl}_4$  vapours to obtain a layer of fused silica doped with titanium. The composite preform has been subsequently heated for sintering the layer as well as for collapsing the tube to obtain the rod. The two steps index fiber [19] obtained, show total loss less than 3 dB/km at 780 and 1080 nm wavelength;
- chemical vapour deposition (CVD) has been successfully used to obtain graded index fiber having a silica cladding and a core of  $\text{GeO}_2 / \text{SiO}_2$  [20] or  $\text{B}_2\text{O}_3 / \text{SiO}_2$  [21] or  $\text{P}_2\text{O}_5 / \text{SiO}_2$  [22] or  $\text{B}_2\text{O}_3 - \text{GeO}_2 / \text{SiO}_2$  [23]; or more recently fluorine /  $\text{SiO}_2$  (Suprasil W) [24].

The main characteristic of the composite preform method is that very pure core material can be obtained and so far the very low loss optical fiber produced have only been obtained by this process.

However the composite preform is obtainable by a very long and sophisticated process. Unless CVD, sintering and collapsing could be obtainable by a continuous and in line controlled process, we think that the cost of the fiber will be a limit.

In addition the dimensional stability, the concentricity and circularity of the core in the final fiber are up to day limitations to overcome.

These depend mainly on the composition, dimension and homogeneity of the preform as well as the stability of the drawing process likely what we have pointed out for the tube and rod technique. On the other hand so far it is the only method to obtain fiber with very small core diameter for singlemode light propagation [19].

## Glass Plastic Cladded Fibers

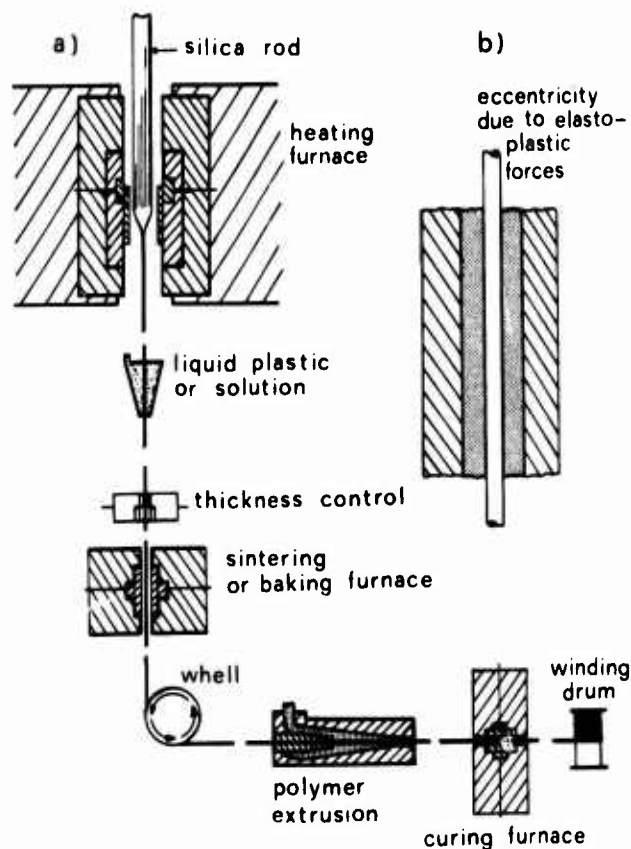


Fig. 5 - Sketch of method to produce glass-polymer clad optical fibers.

Usually an optical glass fiber needs to be plastic coated for handling performances and mechanical properties to obtain practical cables.

Recently among various kind of polymers, special ones, as perfluorinated - ethylene - propylene (Teflon - FEP 100) [25], fluorocarbon resin [26]; and more recently silicon resin [27], have been utilized as a cladding material. The core is normally fused quartz fibers with very low loss [28].

The mentioned resins show usually a lower refractive index than normal glasses and relatively high losses ( $10^3$  dB/km). Optical plastic clad fibers have been obtained with losses less than 20 dB/km with numerical aperture of  $0.05 \div 0.2$  at wavelength corresponding to the minimum loss for the silica core.

A possible manufacturing process is shown in Fig. 5 where a silica fiber is drawn from rod, then the unclad forming fiber is dipped into a resin dispersion and passes through a furnace for sintering, finally the clad fiber is dipped in a molten polymer and



passes through a furnace for curing before the winding drum. The drawing and cladding operations can be in line with production speed up to 100 m/minute. A part the fiber characteristics which can be gained, our opinion is that from industrial view this technology could be scaled up very speedily. In fact our experience on metallic enamelled wire and plastic coating wire for the present telephone cables as well as on ordinary glass fiber spinning [29] let us to consider these fibers the most convenient. In fact rate of production, dimensional stability, handling performances and mechanical properties could be achieved by a technology with several operations in line. Our investigation on elastoplastic forces (See fig. 5b) in wire plastic coating for preventing eccentricity is part of our research [30]. Further the availability of silica rods from the silica manufacturers as a raw material [28], [31] is an important facility in favour of this method.

### Conclusion

Table 1 - Comparison of main feature of the drawing methods to obtain optical fiber for telecommunication and communication

	rod-tube	double crucible		Selfoc	CVD	glass/plastic clad
		a	b			
Attenuation	+	+	-	-	-	+
Temperature Control	-	+	-	-	-	+
Versatility	+	+	-	-	-	+
Interface Contaminants	-	+	+	+	+	-
Dimensional Control in line	-	+	+	+	-	-
Reproducibility	-	+	+	+	-	+
Cost	-	+	-	+	-	+
Dimensional Stability	-	+	+	-	-	+
Optical properties	+	-	?	+	+	?

⊕ = Advantages

⊖ = Limits and disadvantages

a = Glasses drawn at temperature below 1400°C

, = Glasses (high silica contents) drawn at very high temperature above 1600°C.

The conclusions of our comparison among the present drawing technology to obtain optical waveguide for telecommunication systems, are summarized in table 1. Although at present time the composite rod method, better known as CVD method, seems the only one able to produce the today available very low loss fibers for telecommunication systems, our opinion is that double crucible, included the SELFOC, and the glass

plastic clad fiber will show better chances when the cost of the fiber will play an important role to decide the convenience to use glass fiber waveguide as a telecommunication transmission medium. For this the large quantity of experiments to obtain a soda-lime and borosilicate glasses with higher purity are justified as well as for doped silica as an available rod.

On the other hand as the practical design requirements for optical transmission cable and systems is still in development, various technologies to manufacture optical fibers certainly assure a range of different fiber characteristics, including the mechanical and the cost, which certainly leaves space to select in the near future different as telecommunication systems as well as communication systems. In fact in addition to telecommunication application there will exist other applications as digital optical systems, military communications and others for which fiber with losses less than 100 dB/km will be exploited.

For this, among other laboratories, we are trying to improve the double crucible and polymer cladding technologies.

### References

- [1] Maurer, R.D., Proc IEE, 61 (1973), 452
- [2] French, W.G.; Pearson, A.D., Appl. Phys. Letters, 23, (1973), 338
- [3] a) U.S. Patent 3,659,915, Maurer, R.D., Schultz, P.C.  
b) " 3,737,293 "  
c) " 3,711,262 Keck, D.B., Schultz, P.C.  
d) " 3,737,292 " "
- [4] French, W.G.; Tenth Intern. Congr. on Glass (Kyoto 1974) 6, 46
- [5] Ikeda, Y., Yoshiyagawa, M.; Ibid. 6, 82
- [6] Kawashima, T. Takahashi, S. and others; Ibid. 6, 9
- [7] a) Hetherington, G., Jack, K.H.; Phys. and Chem. of Glasses 3, 4(1962) Part 1, 129  
b) Bell, T.; Ibid. 3, 5 Part 2, 141
- [8] Kerk, D.B., Tynes, A.R.; Appl. Opt., 11, (1972) 1502
- [9] Bagley, B.C., French, W.G.; Bull. Am. Ceram. Soc. 52 (1973), 701
- [10] Pearson, A.D., French, W.G.; Bell Lab. Record, 50, (1972), 103
- [11] Manfré, G. Verre et Refractaire, 26, 2 (1972), 57
- [12] Manfré, G.; Rheol. Acta; 12, (1973), 346
- [13] Pearson, A.D.; Tenth Inter. Congress on Glass, (Kyoto 1974) 6, 31
- [14] Day, C.R., Beales, K.J. and others; IEE(Pub. 132) First Europ. Conf. on optical fiber Comm. (London. 1975), p. 33
- [15] Manfré, G. VII Congress Intern. du Verre (Bruxelles

1965), 78

- /16/ Uchida, T., and others, Appl. Opt. 13, 2 (1974) 255
- /17/ Koizumi, K., and others; Appl. Opt. 13, 2 (1974) 255
- /18/ Koizumi, K., Ikeda, Y., IEE Pub. 132, First Europ. Conf. on Optical Fiber Comm. (London 1975) p. 24
- /19/ Maurer, W.G.; Proc. IEE, 61 (1973), 452
- /20/ French, W.G., Macchesney, J.P., and others; Bell Syst. Tech. J. (1974), 951
- /21/ French, W.G. and others; Appl. Phys. Letters 17, (1970), 423
- /22/ Payne, D.N., Gainbling, W.A.; Electron Letter 10, (1974), 289
- /23/ Di Marcello, F.V., Williams, J.C.; IEE Pub. 132, First Europ. Conf. on Optical Fiber Comm. (London 1975), 36
- /24/ Muhlich, A., Rau, K. and others; "Post dead Line session" " A new doped synthetic fused silica as bulk material for low-loss optical fibers"; Ibid (London 1975)
- /25/ Kaiser, P. Hart, A.C. Jr.; Appl. Optics 14, 1 (1975), 156
- /26/ Yoshimura, K., Nakahara, T., and others; Sumitomo Electric Ind. Ltd. - Technical Report.
- /27/ Inada, K.; Akimoto, T. and others, IEE Pub. 132, First Europ. Conf. on opt. Fiber Comm (London 1975) 57
- /28/ Kaiser, P., Tynes, A.R. and others; J. Opt. Soc. Am. 63, 9 (1973), 1141
- /29/ Manfré G.; Limit of the spinning process in manufacturing synthetic fibers. - Udine 1975 - Ed. Springer - Verlag
- /30/ Tadmor, Z., Bird, R.B.; Polym Eng. Sci. 14, 2 (1974), 124
- /31/ Miyashita, T., Edahiro, T; Tenth Inter. Cong. on glass (Kyoto 1974) 6, 52

Name : Mr. Giovanni Manfré

Address: R & D Division Director  
TECHNION SPA  
Via A. M. Ampère n. 28/A  
20131 MILANO - ITALY  
Telex 32512 TECHMIL



Biographical Sketch :

Mr. G. Manfré, degree in Physics Mathematics on 1959 at Padova University, Italy

M. Sc. in Rheology on 1965 at Surrey University, England, has been working on glass, plastics, metal fibers rheology in several research industrial laboratories.

Many publications on glass spinning show his contribution to the spinning art of organic and inorganic fibers included the metal microwires and optical fiber. Now he is the Director of R & D Division of TECHNION SpA working on metal drawing, including the lubricants, plastic insulation for cables, inorganic fibers for materials composites, optical fibers.

# FACTORS AFFECTING THE GRIP OF DIELECTRIC CORE WITHIN SUBMARINE COAXIAL CABLE

by

J. H. Daane  
Bell Laboratories  
Murray Hill, New Jersey 07974

## ABSTRACT

The factors likely to affect the grip of dielectric core upon the inner copper conductor of submarine coaxial cable are assessed. Manufacturing data, as well as laboratory simulation runs and materials properties, are used to determine that the frictional gripping force developed during the cooling of newly manufactured cable core is perhaps more important than the conventional bonding adhesion in preventing slippage between dielectric and center conductor.

Expressions are developed for calculation of gripping force utilizing the temperature dependence of specific volume and tensile modulus. The effect of other material properties such as die swell and melt elasticity which affect orientation and thereby gripping force are discussed, as well as means to measure these properties. Projections are made which should allow the cable manufacturer to select materials and processing parameters to enhance grip.

## INTRODUCTION

A typical submarine coaxial cable contains a center strand of steel wires as the load carrying member, around which copper is wrapped to function as an electrical conductor. The dielectric insulation which is extruded over this conductor must grip it strongly enough to prevent slip when the cable is grabbed by the jacket during laying. The force required to slide the insulation off the center conductor of a length of the cut cable is called the force of adhesion. Although this terminology is perhaps inaccurate, we will follow this customary use of the word to mean any form of resistance against slippage between the center conductor and dielectric. A sufficiently strong adhesion is also necessary in the cable splicing operation for preventing excessive shrink-back from the heated region.

Large variations have been observed in the adhesion values obtained from manufactured cable even when using identical processing conditions on two materials reputed to be identical. These variations may arise from any of several sources such as actual material differences, processing, i.e. extrusion or cooling conditions and the adhesion testing itself. These kinds of effects are of long standing interest to Bell Laboratories and have been the subjects of study since the 1950's.

## NATURE OF ADHESION

There are two obvious ways in which the adhesive force may arise. The first is a conventional interfacial adhesion such as exists between bonded surfaces. It is difficult to determine how important this is, but a microscopic examination of the center conductor after stripping off the dielectric shows a trace of polyethylene left on the copper surface (Figure 1), as would be expected in a good bonded surface. On the other hand, the current grade of polyethylene used is very pure and free of polar impurities, and the copper surface is required to be very clean so that minimal variation in this type of adhesive strength may be expected among the same type cables.

Adhesion may also arise from the grip afforded by the radial compressive force developed as the dielectric shrinks onto the center conductor. This gripping force will depend on how the polymer was extruded and cooled. Test results show that adhesion in submarine cable depends on the temperature during test and that it decreases during the first several days after the extrusion but then increases after longer storage. This type of behavior indicates to us that this frictional gripping force, and not the conventional adhesive strength, is perhaps the most important factor to consider.

## ANALYSIS OF THE GRIPPING FORCE

One of the primary reasons for variation in the gripping force arises from variation in the cooling of the dielectric immediately after extrusion. The gripping force is weaker if the outer region of the dielectric crystallizes to form a hard shell before the inner region begins to crystallize, because in such a case the polymer will tend to contract away from the center conductor. A large temperature gradient in the polyethylene will encourage this type of behavior and result in poor adhesion in the finished cable. In an extreme case voids might form near the center conductor. Fast cooling and high line speeds will obviously lead to such a situation. It must also be realized that crystallization of the dielectric through evolution of latent heat of fusion retards the radial heat flow so that the extrusion of a large diameter core of high-density polyethylene with a good adhesion characteristic is particularly difficult. This was demonstrated during

recent extrusion experiments in one of our cable development programs<sup>1</sup>. More recently, Lemainque and Terramorsi<sup>2</sup> have reported a successful extrusion of a large diameter core of high-density polyethylene by air cooling the cable for the first hour. Air is hundreds of times less efficient in removing heat than water<sup>3</sup>, and these authors have shown that the temperature gradient stayed small, ca 1.6°C/mm, in spite of the large heat of crystallization of the polymer.

We have devised a similar experiment to examine heat transfer in a one inch diameter cable with low-density polyethylene insulation. Three-inch long samples were cut from the insulation, and three thermocouples were imbedded in each - (1) near the outer surface (2) halfway between the outer and inner surfaces, and (3) near the inner surface which faced the center conductor. The first sample was heated to 185°C and subsequently transferred to water baths at the temperatures of the cooling troughs to simulate the cooling cycle in a plant. In Figure 2 we have shown the temperatures measured by the three thermocouples. For this polyethylene, primary crystallization is over in a minute at 100°C, but at 90°C it is over in several seconds. The outer surface temperature traced by Curve 1 follows the cooling water temperature closely, whereas the two inner regions cool much more slowly; and a substantial temperature gradient of 25°C/mm develops between them, as shown by Curves 2 and 3. This is a large gradient even for low-density polyethylene, so that the grip in the finished cable may be expected to be substantially lower than when crystallization is more uniform throughout. In Figure 3 are shown the results when a similar sample was air cooled. Since air is a poorer heat removing medium, as mentioned before, crystallization is much slower; and the gradient between the two inner regions is considerably smaller than in the previous case. Crystallization, detected by the temporary leveling of the curve (because of the exothermic process), is observed to occur simultaneously in the two inner regions. Adhesion was found to be markedly improved.

Now let us estimate what sort of variation in the gripping force one may expect with various heat transfer conditions. We do this by estimating first the final size of the hole in the dielectric without the center conductor and next the stress arising when the center conductor is left in place. The cross section is depicted schematically in Figure 4. If the center conductor were absent, the radius of the center hole,  $a$ , after uniformly cooling from 190°C to 20°C, would be

$$a = a_0 \left[ 1 - \frac{1}{n} \left( \frac{\Delta V}{V} \right) \frac{190}{20} \right] \quad (1)$$

where  $a_0$  is the radius of the center conductor,  $\frac{\Delta V}{V}$  is the fractional volume change

between the two temperatures, and  $n$  is the ratio of the bulk to radial linear expansion. If the contraction of the core is isotropic,  $n$  is 3. If there is no lateral contraction,  $n$  is 2. During the cooling of extruded cable core, no lateral contraction is allowed, so we will use  $n = 2$ .

Now, when there is a large enough temperature gradient radially, the outer region solidifies while the inner region still remains molten. Such a shell becomes sufficiently stiff at 80°C to interfere with subsequent contraction of the inner region. At this time the temperature of the molten region, which is about to crystallize, should be about 100°C. If we designate the radius of the boundary between the outer solid shell and the inner molten core as  $S$ , we obtain for the radius of the center hole

$$a = a_0 \left[ 1 - \frac{1}{2} \left( \frac{\Delta V}{V} \right) \frac{190}{20} \right] + S \cdot \frac{1}{2} \left( \frac{\Delta V}{V} \right) \frac{100}{80}. \quad (2)$$

Our object is to estimate the stress around the conductor. The incremental tangential stress,  $\delta\sigma_\theta$ , arising from stretching a back to  $a_0$  is

$$\delta\sigma_\theta = E \frac{\delta(2\pi a)}{2\pi a} \quad (3)$$

and

$$\frac{\delta a}{a} = \frac{1}{2} \left( \frac{\delta V}{V} \right) \quad (4)$$

where  $E$  is the tensile modulus of the polymer, which varies widely with temperature. Thus

$$\sigma_\theta = [\sigma_\theta]_0 + \int_{V(20)}^{V(190)} E \cdot \frac{1}{2} \left( \frac{dV}{V} \right) - \frac{S}{a_0} \int_{V(80)}^{V(100)} E \cdot \frac{1}{2} \left( \frac{dV}{V} \right). \quad (5)$$

We obtained dynamic modulus and specific volume of this polyethylene as a function of temperature, as shown in Table I. From the data we evaluate  $\sigma_\theta$  shown in Equation 5 as

$$\sigma_\theta = [509 - \frac{S}{0.105} \times 93.6] \text{ psi}. \quad (6)$$

For a one-inch cable,  $S$  cannot exceed 0.5 inch. In the worst case, therefore, where the gradient is high and the shell is largest, the minimum of the tangential stress of 255 psi is calculated from Equation 6, whereas in the best case where crystallization occurred uniformly the stress can be as great as 509 psi. The radial pressure,  $p$ , exerted on the conductor is given by the formula<sup>5</sup>

$$p = \sigma_\theta \frac{b^2 - a^2}{b^2 + a^2}. \quad (7)$$

An inch-long conductor has an area of  $2\pi a_0$

square inches and the total normal force of 0.8310<sub>9</sub> pounds per inch of the cable. The friction coefficient of polyethylene can vary from 0.3 to 0.6. In the case such as when the plastic is pushed from one end, as in the adhesion test, the force ought to be just as great as if it is being slipped off with a uniformly applied force. If we take the maximum value of 0.6, we obtain the maximum force required for stripping the insulation off to be 254 pounds per inch when the cooling steps were ideal, and 128 pounds per inch under the adverse condition. If the friction coefficient is 0.3, the grip can be as poor as 60 pounds per inch.

#### TESTING EFFECTS

One way of evaluating the force required to slide the dielectric off center conductor is to use a fixture which pulls the inner conductor composite member through a hole in a steel plate which restrains the dielectric. Test data indicates that such a procedure gives a gripping force per inch which is dependent on the sample length. For instance, a three-inch sample exhibited a total resistive force of 450 pounds or 150 pounds per inch, whereas a six-inch sample exhibited about the same total force or 75 pounds per inch. It is evident that the load is not uniformly distributed along the length of the cable at the time of stripping, but the first short length must bear a large portion of the load. This is probably because of the greater compressive load at the tip of the sample as illustrated in Figure 5. This underscores the need for squarely cut ends on test specimens. In a test such as this, the first inch or less would probably take the entire load and the corresponding gripping pressure will be greater than the intrinsic pressure derived in Equation 6 because of the additional compressive load.

Other data such as that in Figure 6 indicates that the adhesion diminishes with increasing temperature. This underscores that the adhesion in question is indeed derived from the gripping by friction such as discussed earlier. Since polyethylene expands with temperature much more than the center conductor, its grip diminishes accordingly.

Thus, the interval from time of manufacture to testing, temperature of testing and preparation of specimens must be carefully controlled to minimize variations introduced in the evaluation procedure itself.

#### COOLING EFFECTS

We have seen that the formation of the hard outer shell is critical and what is desired is as uniform cooling as is possible to minimize large temperature gradients in the dielectric. Slow line speeds with long cooling troughs and small temperature differences from trough to trough are indicated. The use of air cooling appears desirable but is impractical from a manufacturing viewpoint because cooling line lengths become excessive.

#### EXTRUSION EFFECTS

The gripping force which arises as the polymer shrinks onto the center conductor is also influenced by the extrusion conditions. The effect of line speed on the cooling rate has already been mentioned. The amount of orientation induced by throughput, melt temperature and line speed will also influence adhesion. This is shown schematically in Figure 7.

The top illustration shows the case where the drawing is severe or the case where the polymer melt with long relaxation time is extruded, and a large amount of molecular orientation resulted in the longitudinal direction. This orientation can be examined by the amount of shrinkage the dielectric will undergo when heated well above the melting temperature. Shortly after it is extruded, the residual longitudinal stress corresponding to this orientation relaxes and diminishes. This will tend to make the diameter larger, so that the grip on the center conductor will also diminish. After that, however, polyethylene will continue slow secondary crystallization long after primary crystallization has taken place, so that the grip will begin to rise again. Data has been gathered which shows that the adhesion initially falls but will rise again, as shown in Figure 8. If the core can be extruded with minimal orientation, due to either a high melt temperature, a low viscosity due to narrow molecular weight distribution, or slow line speed, the grip should not diminish as much after extrusion. This is illustrated by the pictures at the bottom of Figure 7. Here the initially less oriented cable will have less to relax, but the stress is not likely to increase sharply with secondary crystallization.

The effect of orientation on adhesion can look at times very confusing. Since the gripping force varies with time from manufacture by as much as 100 percent, if the adhesion is plotted against orientation (shrinkback) without being carefully measured simultaneously, a shotgun plot results. We have not seen data in which care was taken about this point.

#### MATERIALS EFFECTS

We have already mentioned the heat of crystallization of the polymer as the single most important property on overall heat transfer, which in turn affects the magnitude of adhesion. Since the cooling steps in most manufacturing plants are compromises and thus not ideal so far as temperature gradients are concerned, a subtle variation in other material properties may magnify an already unpredictable feature of the core, such as the adhesion. Rheological characterization of polymers by standard techniques may then need to be supplemented by non-standard ones



when manipulation of normal material properties and processing parameters fail to resolve product property problems.

In the case where improvement of adhesion by processing changes was not effective, a study of the polymer's melt elasticity may be in order in light of the effect of too much orientation on adhesion. A striking illustration of this approach is J. Meissner's work in which three branched polyethylenes with equal density, melt flow index and shear viscosity over seven decades of shear rate were shown to have different melt strengths and processing properties.<sup>6</sup> One may note that the first properties cited would normally go a long way in the specifying of a material.

In our work, two materials produced by the same manufacturer and intended to be identical gave vastly different adhesion values. Subsequent examination of melt flow rate, density, swelling ratio (at low shear rate), viscosity over several decades of shear rate (Figure 9) and stress relaxation after steady shearing at different (low) shear rates in a Weissenberg Rheogoniometer (Figure 10) failed to denote any differences in the materials. However, when the swelling ratio or die swell on relaxed extrudates was measured at higher rates of shear, a noticeable difference was seen (Figure 11). In line with the reasoning set forth earlier in this report, the lower die swell material exhibited superior adhesion, i.e. assuming the same throughput, the less the extrudate swells, the less strain to relax after extrusion and the less the diameter of the core will increase and cause the grip on the center conductor to lessen.

Die swell measurements, however, are tedious, dependent on careful measurement of extrudate diameters and require a rheometer capable of variable output. Hence, an apparatus was constructed using a small, motor-generator driven, piston extruder with interchangeable dies to give an extrudate which is then drawn over a set of pulleys, one of which is attached to a balance arm monitored by a force transducer. The draw rate is variable by a set of takeup wheels driven by a precision motor-generator set. The total apparatus is shown in Figure 12. An example of the data obtainable is shown in Figure 13 for resin A at four different temperatures. Force increases with rising viscosity as the temperature is decreased. Comparison of the drawing force of resins A and B at the same temperature is shown in Figure 14. Here one can see that the higher die swell resin A exhibits a higher melt tension for a given draw rate. Thus more elastic strain energy would be imparted to the resin at a given extruder throughput, thereby leading to greater relaxation and retraction from the center conductor.

Thus we have shown what others have inferred, namely that melt tension increases with

increased die swell<sup>7</sup> and further that this can be related to product properties such as adhesion. We are attempting to confirm, as has been shown in some cases, that at a given melt index, long chain branching significantly increases melt strength.<sup>8</sup>

Unfortunately the ability to measure properties hitherto not monitored has not allowed us to consistently obtain materials meeting our highest desires. As has been mentioned, the melt strength is believed to be related to the nature of the branching of the polymer, which is a molecular property not easily determined or precisely controlled by polymer manufacturers since the long branches in polyethylene molecules are thought to be produced by intermolecular chain transfer between polymer molecules and growing polymer radicals.<sup>9</sup> Given the above techniques of die swell and extensional stress measurement, they may now have tools to monitor changes in production product, which may then be related to the polymerization process parameters which ought to result in tailor-made materials for our applications.

#### SUMMARY

Care should be taken in the preparation, temperature and timing of the adhesion test specimens. The following will then be useful in enhancing adhesion:

1. Processing-air cooling, slower cooling down to 100°C, and smaller diameters to minimize the temperature gradient within the core. Higher temperature cooling water, preheating the center conductor, keeping down the line speed and increasing the polymer temperature should also help.
2. Materials properties-lower density polymers have lower heats of crystallization and smaller volume change during crystallization, which will help greatly. Also of help would be lower die swell materials, narrower molecular weight distributions, lower viscosity and a strong tendency for secondary crystallization.

#### REFERENCES

1. S. Matsuoka, private communication.
2. H. Lemainque and G. Terramorsi, Conférence Internationale des Grands Réseaux Électriques, 1972, Paper 21-07.
3. H. S. Carslaw and J. C. Jaeger, "Conduction of Heat in Solids," Second Edition, Page 20, Clarendon Press, Oxford, 1959.
4. H. E. Bair, private communication.
5. S. Timoshenko and J. N. Goodier, "Theory of Elasticity," McGraw-Hill Book Company, Incorporated, New York, 1950, Page 60.
6. J. Meissner, Trans. Soc. Rheol. 16, 405 (1972).



7. A. Bergorizoni and A. J. DiCresce, Polym. Engr. Sci., 6, 50(1966).
8. W. F. Busse, J. Polym. Sci., A-2, 5, 1249(1967).
9. R. A. V. Raff and K. W. Doak, "Crystalline Olefin Polymers," Interscience, New York, 1965, Part I, Page 349.



John H. Daane

Temperature °C	Modulus 10 <sup>4</sup> psi	Volume cm <sup>3</sup> /g	Maximum $\sigma_{\theta}$ psi
110	0		0
100	0.10	1.180	0
90	0.28	1.160	45
80	0.55	1.140	93
70	0.67	1.127	132
60	1.17	1.116	191
50	1.38	1.107	252
40	2.07	1.097	338
30	2.76	1.091	413
20	3.45	1.085	509

Mr. Daane received a B.S. in Science from Adelphi University in 1962 and a M.S. in Chemistry from Union College, Schenectady, New York, in 1966. He has been a member of the Plastics Research and Development Department at Bell Laboratories, Murray Hill, New Jersey, since 1966. Prior to that time he was employed by the General Electric Co. at their Research Center in Schenectady and their Silicone Products Department, Waterford, New York. For the past six years, he has been engaged in the study of polymers for use in submarine cable systems.



Figure 1 Photograph of polyethylene left on copper inner conductor after stripping away the dielectric ( $\sim 100\times$  magnification).

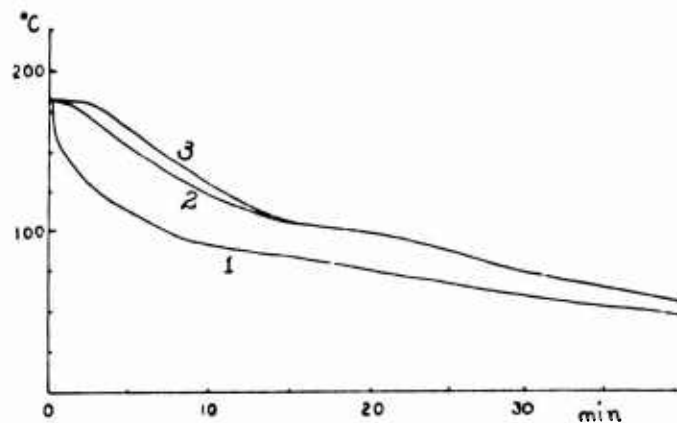


Figure 3 Temperature curves at three points within one inch O.D. dielectric core undergoing ambient air cooling.

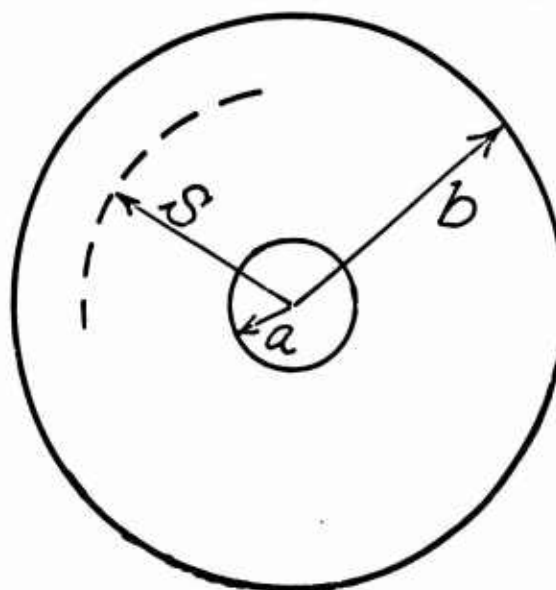


Figure 4 Schematic cross section of dielectric core.

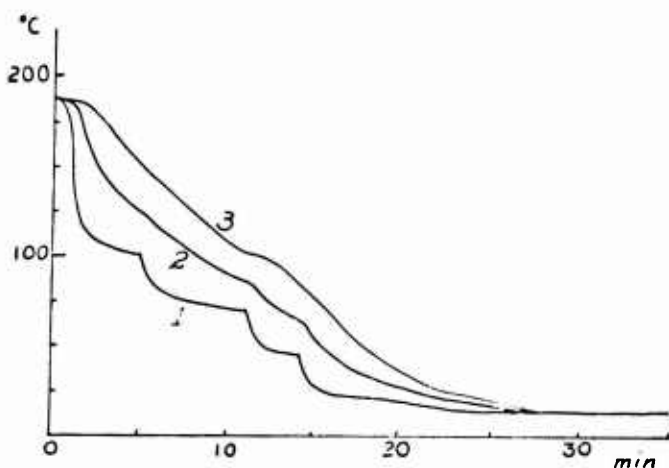
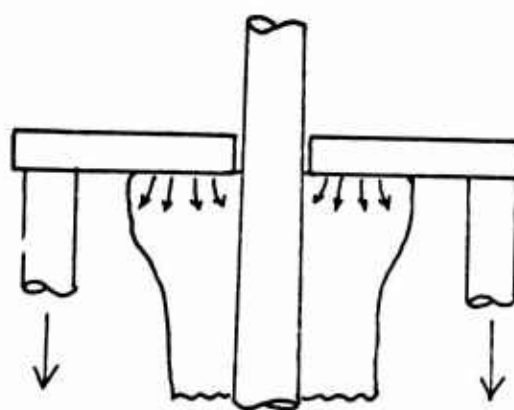


Figure 2 Temperature curves at three points within one inch O.D. dielectric core undergoing cooling through simulation treatment.



## EXAGGERATED VIEW OF ADHESION TEST

Figure 5 Schematic of compressive action at tip of adhesion specimen.

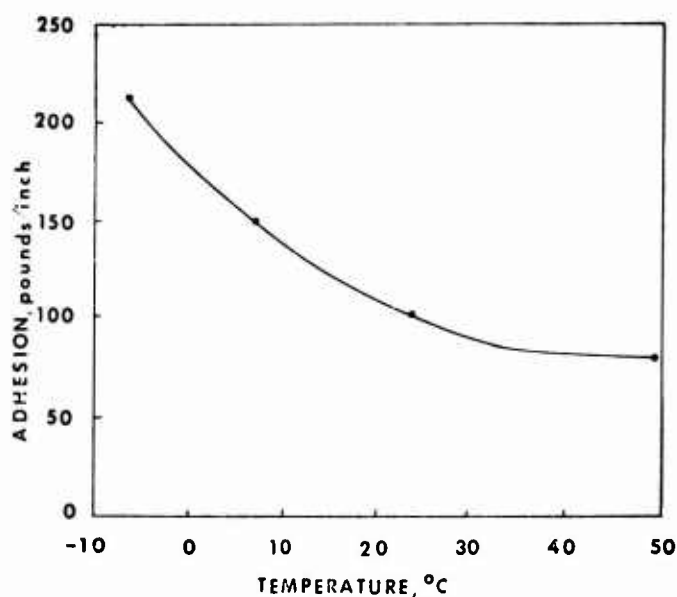


Figure 6 Adhesion versus temperature of testing.

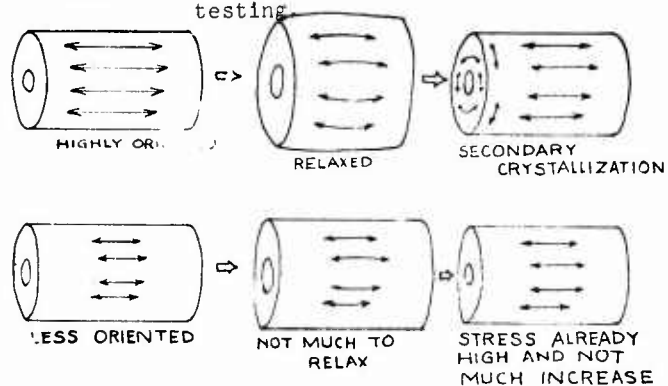


Figure 7 Schematic view of effect of orientation upon adhesion.

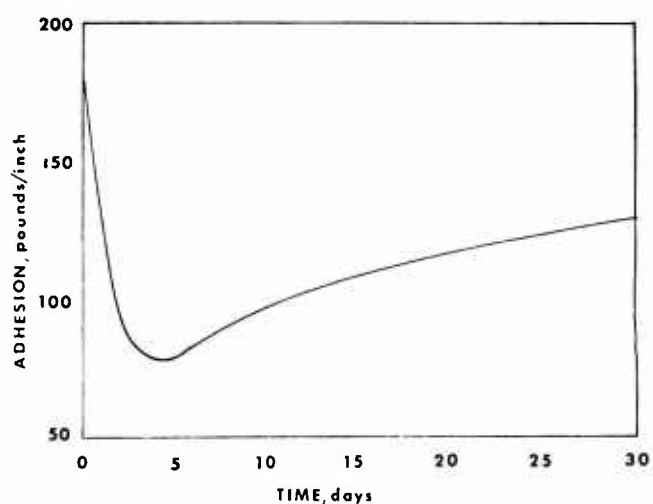


Figure 8 Adhesion versus time of storage.

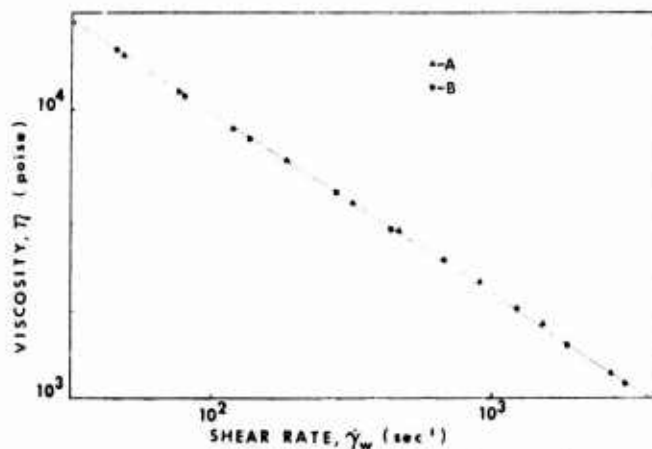


Figure 9 Viscosity versus shear rate.

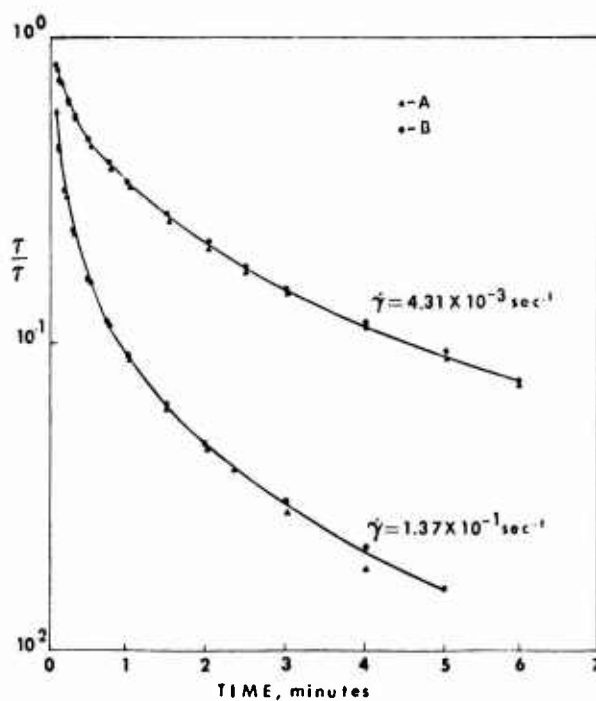


Figure 10 Normalized shear relaxation stress versus time at two shear rates.

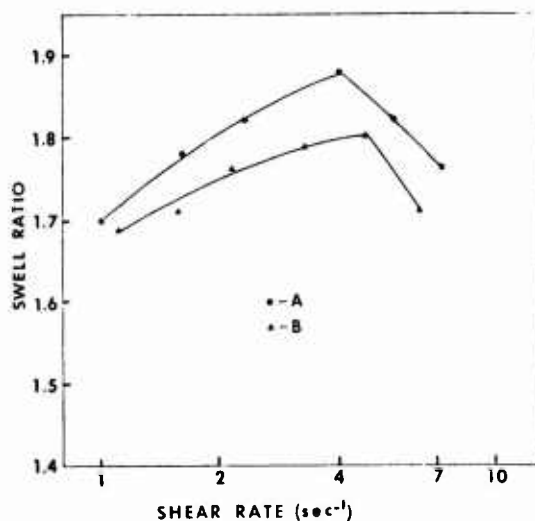


Figure 11 Die swell versus shear rate.



Figure 12 Photograph of melt tension apparatus.

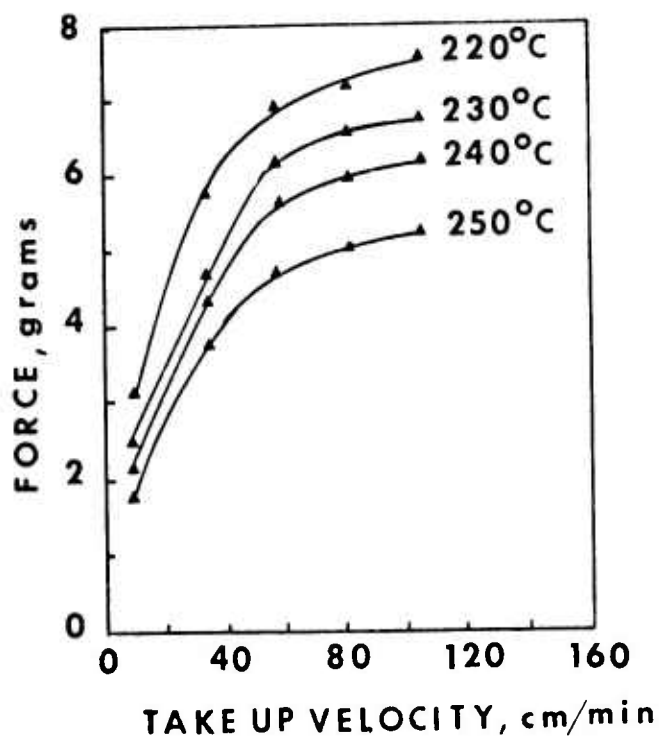


Figure 13 Drawing force at four temperatures versus take-up rate.

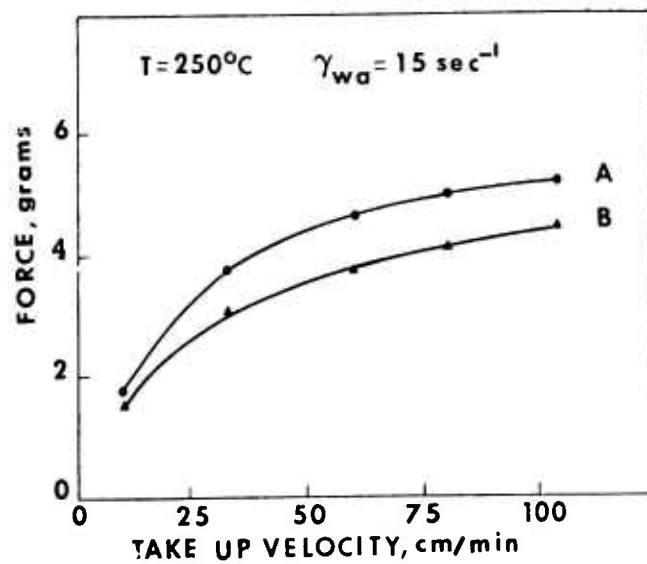


Figure 14 Drawing force of two resins versus take-up rate.

# SUBMARINE COAXIAL CABLE FOR CS-36M SYSTEM

Y.Negishi, T.Yashiro and K.Aida

Ibaraki Electrical Communication Laboratory,  
Nippon Telegraph and Telephone Public Corp.  
Tokai, Ibaraki, Japan

## Summary

This paper describes the study of problems which were caused in regard to a submarine cable while the CS-36M submarine coaxial cable system was being developed. The serious problems were the investigation of high frequency transmission characteristics of the cable in the ocean bottom environment and the assurance of the high frequency transmission characteristics uniformity of the cables. The study results of those problems such as temperature and pressure dependences of the transmission properties, handling, aging effects on cable loss and so on are described. The results of a sea trial are also reported.

## 1. Introduction

In Japan, CS-36M system development was started in 1968. Transmission in one direction is carried in the frequency band of 4.3 MHz to 17.0 MHz and in the other direction by the band of 22.8 MHz to 35.5 MHz, and 2,700 telephone channels or 900 telephone channels and 1 color TV channel can be provided in each direction.

Application of this system began with the domestic inter-island system, which was about 1,000 km long.

Submarine coaxial cable, whose diameter is 38.1 mm, is selected for use as the transmission medium for the system. This cable structure is the same as that of SF cable. However, it was necessary to investigate some problems in order to widen the frequency band up to 35.5 MHz. Misalignments between the repeater and the cable characteristics must be minimized because of the difficulty in re-setting the equalizer after the cable is laid.

Though computer aided adjustable equalizers were adopted for reducing accumulated transmission deviation, the following problems had to be investigated for the equalization plan.

- (1) Determine high frequency transmission characteristics and assure cable loss homogeneity.
- (2) Determine cable high frequency characteristics in the ocean bottom environment.
- (3) Predict laying effect on the cable loss.
- (4) Predict aging effect on the cable loss.

This paper describes the study of the above problems and the equalization characteristics at a sea trial.

## 2. Cable Structure and Design Objective

The 38 mm (1.5 inch) submarine coaxial cable consists of five components. They are, (1) a steel strand strength member to provide high strength cable, (2) a copper inner conductor which surrounds the steel strand, (3)

a low density solid polyethylene dielectric, (4) copper outer conductor overlapped in the longitudinal seam and (5) a high density polyethylene outer jacket. A cable loss deviation of  $\pm 0.5$  percent was included to minimize system misalignment. Change in cable loss resulting from variations in inner and outer conductor diameter, eccentricity of inner conductor, copper conductivity or dielectric constant can be within  $\pm 0.1$  percent with present industrial engineering. A dissipation factor, however, should be controlled because of the increased effect on the cable loss at higher frequencies. The relation of the cable loss deviation to the dissipation factor at 50 MHz is shown in Fig.1, obtained from experimental cables. The effect of  $15 \times 10^{-6}$  change causes  $\pm 0.37$  percent change in the cable loss. A tolerance of  $17 \times 10^{-6}$  on the dissipation factor at 50 MHz was included for the cable loss objective.

## 3. Ocean Bottom Environment Effect on Cable Electrical Properties

### 3.1 Measurement Facility

It is necessary to estimate, as accurately as possible, cable attenuation on the sea bottom in order to construct a long distance submarine cable system with little misalignment. An artificial ocean, therefore, which can simulate deep sea conditions ( $3^{\circ}\text{C}$ , 500  $\text{kg}/\text{cm}^2$ ), and a precise attenuation measuring set, which can have a measuring accuracy of  $\pm 0.1$  percent, were constructed.

The artificial ocean consists of two high pressure steel tubes 100 meter in length, settled in a temperature controlled water bath. Hydrostatic pressure in the steel tubes is controlled by an oil powered pump. A cross section view of the artificial ocean is shown in Fig.2. There are two high pressure steel tubes and a platinum string used as a thermometer between the two steel tubes. Thirty-four tubes in which cold or hot water flows to control the temperature in the water bath are mounted inside the inner concrete wall surrounding the water. The thermal insulator and the outer concrete wall cover the inner concrete water bath. This artificial ocean can simulate any sea condition wherein the temperature range is between  $3^{\circ}\text{C}$  to  $20^{\circ}\text{C}$  ( $\pm 0.01^{\circ}\text{C}$ ) and the pressure range is between 0  $\text{kg}/\text{cm}^2$  to 500  $\text{kg}/\text{cm}^2$  ( $\pm 0.5 \text{ kg}/\text{cm}^2$ ).

As small an attenuation change as 0.0002 dB (5 MHz), 0.0008 dB (60 MHz) has to be measured, in order to investigate the attenuation pressure dependence of 38 mm coaxial cable using a 100 m test piece. The attenuation is obtained by a Q factor of a cavity constructed from the cable to be tested. (Fig.3). Transmission power of the cavity is measured to obtain the Q factor.

A distinctive feature of the present measurement circuit is that precision variable resistance attenuator exists at the two pole cavity constructed from both ends of the cable shunted with a small coupling loop at both ends through a coaxial switch. This arrangement eliminates not only the problems of correcting the signal generator's level and detector's gain during the Q measurement, but also obviates problems concerning frequency characteristics of signal generator and detector. The attenuation of the cable is determined from unloaded  $Q_0$  factor and phase constant, as follows:

$$\alpha l = \beta l / 2Q_0. \quad (1)$$

At the coupling loss of the present measurement is sufficiently small (below 0.1%), it is possible to use loaded Q instead of unloaded  $Q_0$  to calculate the attenuation from Eq.(1).

### 3.2 Transmission Characteristics Temperature Dependence

3.2.1 Attenuation Temperature Coefficient Attenuation temperature coefficient at  $T_1^\circ\text{C}$  is defined by the following equation:

$$a_T = \left[ \frac{\partial \alpha(T)}{\partial T} \right]_{T=T_1} / \alpha(T_1). \quad (2)$$

Figure 4 presents the  $a_T$  which was obtained by measuring attenuation values at temperatures of  $5^\circ\text{C}$ ,  $10^\circ\text{C}$  and  $15^\circ\text{C}$ . The temperature coefficient decreases as the frequency increases, and then becomes zero at approximately 100 MHz. The frequency dependence of  $a_T$  is mostly due to the dissipation factor versus temperature characteristics. ( $-4 \times 10^{-3}/^\circ\text{C}$  at 10 MHz,  $-7 \times 10^{-3}/^\circ\text{C}$  at 50 MHz)

3.2.2 Phase Constant and Characteristic Impedance Temperature Coefficients Phase constant and characteristic impedance are known to be given at high frequency by the following equations, respectively.

$$\beta = \beta_\infty + \beta_p \sqrt{f}. \quad (3)$$

$$Z_0 = Z_\infty + Z_p / \sqrt{f}. \quad (4)$$

As measuring results, all of those coefficients vary linearly with temperature from  $5^\circ\text{C}$  to  $15^\circ\text{C}$ . Their temperature coefficients are given in Table 1.

3.2.3 Cable Diameter Temperature Characteristics Cable diameter variation due to temperature change can be derived from dielectric constant temperature dependence and cable capacitance, as follows:

$$\frac{1}{d_2} \frac{\partial d_2}{\partial T} = \left( \frac{1}{\epsilon} \frac{\partial \epsilon}{\partial T} - \frac{1}{C} \frac{\partial C}{\partial T} \right) \cdot \ln \left( \frac{d_2}{d_1} \right) \quad (5)$$

where  $d_1$ ; inner conductor diameter,  $d_2$ ; dielectric diameter,  $\epsilon$ ; dielectric constant. Diameter temperature coefficient becomes  $0.021\%/^\circ\text{C}$ , by using the measured values  $1/\epsilon \cdot \partial \epsilon / \partial T = -0.031\%/^\circ\text{C}$  and  $1/C \cdot \partial C / \partial T = -0.046\%/^\circ\text{C}$ .

$$\frac{1}{d_2} \frac{\partial d_2}{\partial T} = 0.021 (\%/^\circ\text{C}) \quad (6)$$

### 3.3 Transmission Characteristics Pressure Dependence

3.3.1 Pressure Response Characteristics The capacitance of 38 mm submarine coaxial cable, under a rapidly applied hydrostatic pressure in a pressurized steel pipe, is

measured as a function of time. After about one hour, the rate of capacitance change becomes very small, but does not become zero. The experimental result of capacitance change, observed over a long period, is shown in Fig.5. After about an hour, its change is proportional to  $\log t$ . The inclination of capacitance with  $\log t$  is not a function of applied pressure. The inclination is obtained from Fig.5, in the following formula:

$$\frac{\partial(\Delta C/C)}{\partial \log_{10} t} = (9+1) \times 10^{-5}. \quad (7)$$

This phenomenon can be explained as Maxwell's viscoelastic model applied to the polyethylene cable insulator. On this model, the relation between stress P and strain e is given by

$$\frac{de}{dt} = \frac{1}{\gamma} \frac{dP}{dt} + \frac{1}{\eta} P \quad (8)$$

where  $\gamma$  is elastic modulus and  $\eta$  is given by Eq.(9) as a function of specific volume V.

$$\eta = A \exp \{ BV / (V - V_0) \} \quad (9)$$

where A and B are constants and  $V_0$  is volume occupied by polymer molecules. In the case of small strain e, Eq.(9) becomes

$$\eta = A' \exp (B'e). \quad (10)$$

In the case of applied stepped pressure, the time dependence of strain e is given by Eq.(11). Using Eqs.(10) and (8),

$$e = \frac{1}{\gamma} P_0 + \frac{1}{B'} \log \left\{ P_0 \frac{B'}{A'} \exp(-B' \frac{P_0}{\gamma}) + \frac{1}{B'} \log \left\{ t + \frac{1}{B'} \frac{A'}{P_0} \exp(B' \frac{P_0}{\gamma}) \right\} \right\}. \quad (11)$$

Capacitance change  $\Delta C$  with pressure is proportional to the cable outer diameter change, so

$$\Delta C = k \cdot e. \quad (12)$$

Therefore, capacitance change  $\Delta C$  becomes as given by Eq. (13) in the case of long time t, from Eqs. (11) and (12).

$$\Delta C \approx k \left[ \frac{1}{\gamma} P_0 + \frac{1}{B'} \log \left\{ P_0 \frac{B'}{A'} \exp(-B' \frac{P_0}{\gamma}) \right\} + \frac{1}{B'} \log(t) \right] \quad (13)$$

$\Delta C$  changes linearly with  $\log t$  and its inclination is constant, not depending on applied pressure within this experiment.

Cable attenuation variation due to pressure is chiefly determined by changes of cable diameter and dielectric constant. It is experimentally determined that these parameters are linear functions of capacitance. Therefore, attenuation variation can be deduced from the measured capacity change  $\Delta C$  value.

$$\frac{\Delta \alpha}{\alpha} \approx \frac{1}{2} \frac{\Delta \epsilon}{\epsilon} - \left\{ \frac{1}{\ln(d_2/d_1)} + \frac{1}{1 + d_2/d_1} \right\} \frac{\Delta d_2}{d_2} = k \frac{\Delta C}{C} \quad (14)$$

During time period  $t_1$ , cable loss change and capacitance change are expressed as  $\Delta \alpha(t_1)$  and  $\Delta C(t_1)$ , respectively. Therefore, the following equation results.

$$\frac{\Delta \alpha(t_1)}{\Delta \alpha(t_2)} = \frac{\Delta C(t_1)}{\Delta C(t_2)} \quad (15)$$

For example, it can be estimated from Eq.(15) and Fig.5 that cable loss variation during one hour just after laying the cable amounts to 97 percent of that during the twenty year period after laying the cable.



3.3.2 Phase Constant and Characteristic Impedance Pressure Characteristics Capacitance, phase constant and characteristic impedance of 38 mm diameter, 100 m long submarine cable were measured from 5°C to 20°C and under pressures of 0 kg/cm<sup>2</sup> to 500 kg/cm<sup>2</sup>. The resonance method was used with a measurement accuracy of  $1 \times 10^{-5}$ .

Observed phase constant pressure characteristics are shown in Fig.6. When pressure is applied to the cable, phase constant increases linearly with increasing pressure. The phase constant pressure coefficient is given in

$$\frac{1}{\beta} \frac{\partial \beta}{\partial P} = \frac{1}{\beta_{\infty}} \frac{\partial \beta_{\infty}}{\partial P} = 1.1 \times 10^{-5} \text{ (1/kg/cm}^2\text{)} \quad (16)$$

The characteristic impedance pressure coefficient is given by Eq.(17) under the same conditions.

$$\frac{1}{Z_0} \frac{\partial Z_0}{\partial P} = \frac{1}{Z_{0\infty}} \frac{\partial Z_{0\infty}}{\partial P} = -1.9 \times 10^{-5} \text{ (1/kg/cm}^2\text{)} \quad (17)$$

3.3.3 Polyethylene Dielectric Constant Pressure Characteristics Polyethylene dielectric constant characteristics under hydrostatic pressure have not been clarified because of difficult measurement techniques involved. From phase constant pressure characteristics, it can be deduced as follows. Coaxial cable phase constant is generally expressed in Eq.(3).  $\beta_{\infty}$  is expressed in Eq.(18), where  $\epsilon$  is a relative dielectric constant of cable insulator.

$$\beta_{\infty} = 2\pi \sqrt{\mu \epsilon_0 \epsilon} \text{ (rad/Hz/m)} \quad (18)$$

$$\text{(where } \mu = 4\pi \times 10^{-7}, \epsilon_0 = 8.854 \times 10^{-12} \text{)}$$

$$\epsilon = 2.2766 \times \beta_{\infty}^2 \times 10^{15} \quad (19)$$

The low density polyethylene dielectric constant pressure characteristics, obtained from observed phase constant and Eq.(19), are shown in Fig.7. Dielectric constant  $\epsilon$  is found to increase linearly with increasing pressure. The pressure coefficient of  $\epsilon$  becomes,

$$\frac{1}{\epsilon} \frac{\partial \epsilon}{\partial P} = 2.0 \times 10^{-5} \text{ (1/kg/cm}^2\text{)} \quad (20)$$

The nonpolar molecule dielectric constant is generally given by

$$\frac{\epsilon - 1}{\gamma \epsilon + (3 - \gamma)} = \frac{N \alpha p}{3 \epsilon_0 M} \quad (21)$$

$\gamma$  : local electric field constant  
 $\rho$  : density  
 $N$  : Avogadro's constant  
 $M$  : molecular weight  
 $\alpha$  : electric polarity of molecule  
 $\epsilon$  : relative dielectric constant  
 $\epsilon_0$  : dielectric constant in vacuum.

If  $\gamma$  is unity in Eq.(21), Eq.(21) becomes Clausius Mosotti's equation. It is known that polarity  $\alpha$  does not depend on temperature. The polyethylene density change with pressure within 500 kg/cm<sup>2</sup> is very small, so  $\gamma$  and  $\alpha$  are thought to be constant, not depending on temperature and pressure. Thus,  $\epsilon$  and  $\rho$  in Eq.(21) are the only two parameters which vary with variation of temperature and/or pressure. For that reason, temperature and pressure characteristics of  $\epsilon$  may be expected to combine with those of  $\rho$ . The relation between  $\epsilon$ , calculated from Eq.(19), and  $\rho$ ,

observed by using an autoclave, is shown in Fig.8, as parameters of temperature and pressure. It is clarified that the supposition,  $\epsilon$  is a function of only parameter  $\rho$ , can be applied to the polyethylene.

Then, experimental results are compared with Clausius Mosotti's equation. Equation (21) becomes the following equations, where  $\rho_s$  is unity.

$$\epsilon = \frac{2k\rho + 1}{1 - k\rho} \quad (22)$$

$$k = \frac{1}{\rho_s} \frac{\epsilon_s - 1}{\epsilon_s + 2} \quad (23)$$

where  $\rho_s$  is standard density.

As  $\epsilon_s$  is 2.2887 where  $\rho_s$  is 0.92235 at 20°C and sea level atmospheric pressure, so constant  $K$  in Eq.(22) becomes 0.32578. Using these values, the relation between  $\epsilon$  and  $\rho$  results in the dotted line in Fig.8. Inclinations of  $\epsilon$  with density  $\rho$  are given by the following equations:

$$\text{Clausius Mosotti} \quad \frac{1}{\epsilon} \frac{\partial \epsilon}{\partial \rho} = 0.88 \quad (24)$$

$$\text{Measured} \quad \frac{1}{\epsilon} \frac{\partial \epsilon}{\partial \rho} = 0.73 \quad (25)$$

The inclination obtained from Clausius Mosotti's equation is 20% larger than that of observed values. It is considered that this is due to  $\gamma=1$  in Eq.(21). Polyethylene density is larger than that of all gases, so electric charges are overlapped with each other. It is considered that  $\gamma$  may be smaller than unity. Then, Eq.(21) leads to Eq.(22) and Eq.(23) where  $\gamma$  is not unity. Calculated  $\gamma$  and  $K$  values are, respectively, 0.4538 and 0.3897.  $\gamma$  is found to be much smaller than unity. From this, the relation between  $\epsilon$  and  $\rho$  becomes,

$$\epsilon = \frac{1 + 0.99237 \rho}{1 - 0.17686 \rho} \quad (26)$$

Equation(26) expresses the standard relation between  $\epsilon$  and temperature and pressure characteristics of low density polyethylene as a parameter of density  $\rho$ . According to these discussions,  $\epsilon$  of polyethylene is only a function of density  $\rho$ . However, the quantitative expression of  $\epsilon$  as temperature and/or pressure characteristics is more correctly given by Eq.(25), where  $\gamma$  is less than unity, rather than by Clausius Mosotti's equation.

3.3.4 Cable Diameter Pressure Dependence The relation between capacitance and insulator permittivity is as follows:

$$\frac{\Delta d_2}{d_2} = \left( \frac{\Delta \epsilon}{\epsilon} - \frac{\Delta C}{C} \right) \cdot \ln \left( \frac{d_2}{d_1} \right) \quad (27)$$

where it is assumed that inner diameter change  $\Delta d_2$  of outer conductor follows outer diameter change of insulator, but outer diameter of inner conductor is independent of pressure. Therefore, a change of  $d_2$  can be obtained by measurement of capacitance and permittivity change. Figure 9 shows the result. The result, obtained by using another method, is also shown, in which the diameter change is directly measured with a differential transformer. This result agrees with that obtained by using Eq.(27). According to these results, pressure coefficient of the inner diameter of the outer conductor is as follows:

$$\frac{1}{d_2} \frac{\partial d_2}{\partial P} = -1.6 \times 10^{-5} \quad (1/\text{kg/cm}^2) \quad (28)$$

In case cable length is much longer than cable diameter, it can be estimated that insulator changes only in the direction of radius, because inner conductor elastic modulus is a hundred times larger than that of insulator. As polyethylene is considered as a fluid and  $V$  is the volume of cable insulator per unit length, outer conductor diameter change  $\Delta d_2/d_2$  is as follows:

$$\frac{\Delta d_2}{d_2} = \frac{1}{2} \frac{\Delta V}{V} \{1 - (\frac{d_1}{d_2})^2\} \quad (29)$$

The dotted line in Fig.9 shows the calculated value by using eq.(29), which agrees with the measured value. The dash dot line in Fig.9 also shows calculated value with material dynamics. It is reasonable that polyethylene is considered as a fluid in investigating the deformation of PE due to hydrostatic pressure.

**3.3.5 Attenuation Pressure Characteristics** Attenuation characteristics of 38 mm coaxial cable 100 meters in length were measured at 5°C-10°C and 0 kg/cm<sup>2</sup>-500 kg/cm<sup>2</sup>. High precision measurement techniques are needed to obtain attenuation pressures dependence, because test piece attenuation is very low (0.2 dB at 5 MHz, 0.56 dB at 36 MHz). Figure 3 shows the measurement circuit.

Figure 10 shows attenuation pressure coefficient at 5°C and 10°C. Attenuation pressure coefficient up to 36 MHz, which is little dependent on frequency, is

$$\frac{1}{\alpha} \frac{\partial \alpha}{\partial P} = (2.5 \pm 0.2) \times 10^{-5} \quad (1/\text{kg/cm}^2) \quad (30)$$

Attenuation deviation due to pressure is as follows:

$$\begin{aligned} \frac{\Delta \alpha}{\alpha} = & \left\{ \frac{1}{2} \frac{\Delta \epsilon}{\epsilon} + \frac{1}{2} \frac{\Delta \rho}{\rho} - \left( \frac{1}{\ln(d_2/d_1)} + \frac{d_1}{d_1 + d_2} \right) \frac{\Delta d_2}{d_2} \right. \\ & - \left( -\frac{1}{\ln(d_2/d_1)} + \frac{d_2}{d_1 + d_2} \right) \frac{\Delta d_1}{d_1} \left. \right\} \frac{\alpha_r}{\alpha_r + \alpha_g} \\ & + \left( \frac{1}{2} \frac{\Delta \epsilon}{\epsilon} + \frac{\Delta \tan \delta}{\tan \delta} \right) \frac{\alpha_g}{\alpha_r + \alpha_g} \quad (31) \end{aligned}$$

If  $\Delta \tan \delta / \tan \delta$  is assumed to be zero, Eq.(32) and the dotted line in Fig.10 are obtained from Eq.(31), using the pressure characteristics of other parameters.

$$\frac{1}{\alpha} \frac{\partial \alpha}{\partial P} = (2.23 \cdot \frac{\alpha_r}{\alpha_r + \alpha_g} + 1.04 \cdot \frac{\alpha_g}{\alpha_r + \alpha_g}) \times 10^{-5} \quad (1/\text{kg/cm}^2) \quad (32)$$

This calculated value is a little smaller than the observed value. The attenuation change difference between calculated and observed values seems to be caused by the pressure characteristics of  $\tan \delta$ . The pressure coefficient of  $\tan \delta$  is as follows:

$$\frac{1}{\tan \delta} \frac{\partial \tan \delta}{\partial P} = 3.6 \times 10^{-5} \quad (1/\text{kg/cm}^2) \quad (33)$$

### 3.4 Aging Effect on Attenuation Constant under Hydrostatic Pressure

The cable (100 m long) were maintained at 5000-meter depth sea bottom temperature and pressure. Temperature and pressure were measured as  $\pm 0.01^\circ\text{C}$  and  $\pm 0.5 \text{ kg/cm}^2$ , respective-

ly. Attenuation measuring set accuracy was 0.1%. Overall measurement facility accuracy made it possible to detect a changes of 0.1% in a frequency range covering from 5 MHz to 80 MHz. Measurements have been taken for over 6 months and no change has been observed.

On the other hand, an attenuation change can be estimated from the changes of the dielectric constant and the dielectric diameter, derived from the phase constant change. Figure 11 presents the dielectric constant aging change calculated with measured  $\beta_\infty$  and Eq.(18). The dielectric constant change increases linearly with  $\log t$ . The inclination is expressed by:

$$\frac{\partial(\Delta \epsilon / \epsilon)}{\partial \log t} = 0.093 \times 10^{-2} \quad (34)$$

The dielectric constant changes 0.040% under a pressure of 500 kg/cm<sup>2</sup> over a period of twenty years. ( $\epsilon$  at a time after ten hours' compression is used as a basis.) Density change is given by the following, with  $\Delta \epsilon / \epsilon$  and Eq.(25).

$$\Delta \rho = 0.054 \times 10^{-2} \quad (35)$$

As the outer conductor diameter ( $d_2$ ) may follow that of the dielectric, the  $d_2$  change is expressed as follows:

$$\frac{\Delta d_2}{d_2} = - \frac{1 - (d_1/d_2)^2 \Delta \rho}{2 \rho} \quad (36)$$

The attenuation constant change is obtained by putting  $\Delta \epsilon / \epsilon$  and  $\Delta \rho / \rho$  into the first term and the second term in Eq.(31).

$$\frac{\Delta \alpha}{\alpha} = 0.043 \times 10^{-2} \quad (\text{for 20 years, at } 500 \text{ kg/cm}^2) \quad (37)$$

Further, dissipation factor change should be studied at high frequency.

### 3.5 Handling Effect on Attenuation

Attenuation change due to mechanical stress in cable laying is called laying effect. It is generally determined by actual cable laying. This method, however, cannot always be successful because of the inherent uncertainties of the laying route data.

The handling effect, which may be a portion of the laying effect, can be easily estimated. It seems that the smaller the handling effect on the cable characteristics, the smaller the laying effect becomes. Three pieces of cable (6 km long), were transferred from factory tanks to other tanks. Measurements of attenuation constant, capacitance, delay and pulse echo were performed before and after the transfer (i.e. turnover).

Table 2 presents capacitance and delay changes. No change were observed with regard to cables #2 and #3, considering the experimental error.

As the results of the pulse echo test, seventeen echos, whose value lay between 50 dB to 60 dB, were observed in cable #1 before turnover, and only six echos were observed after turnover. Echos in cables #2 and #3, all of which were above 70 dB, were not observed to change.

The change in #1 cable attenuation is shown in Fig.12. A change of about 0.07% can be seen in the measured frequency range.

The change can be caused by an elimination of air gap between the outer conductor and the insulator, because the cable is

slightly tented during turnover and impedance irregularities are improved after turnover. Therefore, the change in the outer conductor diameter of cable #1 becomes -0.026 % (i.e. -0.010 mm for 38 mm cable) calculated with changes in  $C$  and  $\tau_{\infty}$ .

Changes in equivalent dielectric constant and equivalent dissipation factor caused by air gap elimination are +0.05% and +0.04%, respectively. As a result, the change in attenuation can be estimated to be +0.05% (1 MHz-80 MHz). Considering the uncertainties of measured values ( $\alpha$ ,  $C$  and  $\tau_{\infty}$ ), the calculated attenuation changes agree well with the measured ones. The result can conclude that the elimination of air gap mainly causes the attenuation change.

#### 4. Standard Cable Attenuation Characteristics

The standard attenuation characteristics of 38 mm submarine coaxial cable at sea bottom is given as the following equation from the results described above for the CS-36M system design.

$$\alpha = \alpha_0 [ 1 + a_T \times (T-10) + a_p \times \frac{D}{1.0} + a_l ] \quad (38)$$

where  $\alpha$ : sea bottom cable attenuation at temperature  $T$  ( $^{\circ}\text{C}$ ) and depth  $D$  (meter)

$\alpha_0$ : measured cable attenuation at 10  $^{\circ}\text{C}$  and zero pressure

$T$ : temperature at sea bottom ( $^{\circ}\text{C}$ )

$a_T$ : attenuation temperature coefficient (1/ $^{\circ}\text{C}$ )

$D$ : sea depth (meter)

$a_p$ : attenuation pressure coefficient (1/kg/cm $^2$ )

$a_l$ : laying effect on attenuation.

The  $\alpha_0$  is given as Eq.(39) by considering the results of measurements of 70 pieces of cable (6 km long).

$$\alpha_0 = 0.8529\sqrt{f} + (0.01013 + 0.0010\sqrt{f})f \quad (\text{dB/km}) \quad (39)$$

where  $f$ : frequency in MHz.

Coefficients,  $a_T$  and  $a_p$ , are given as Eqs.(40) and (41), respectively.

$$a_T = \{0.15 - 0.083(\log \frac{f}{4})^2\} \times 0.01 \quad (40)$$

$$a_p = 2.5 \times 10^{-5} \quad (41)$$

where  $f$ : frequency in MHz (4MHz-36MHz).

Though no sufficient data have been obtained,  $a_l$  is temporarily determined as 0.2 %, which is about three times of that of handling effect, for designing an ocean block equalizer.

#### 5. Sea Trial

A sea trial was made in October 1973, on an approximately 450 km long link with 82 repeaters involved to confirm a new equalization technique. The CS-36M system layout is shown in Table 3.

Ocean block equalizers (OBE) were designed to be inserted after every 20'th repeater in the CS-36M system to reduce misalignment to a tolerable limit.

Misalignments to be equalized by OBE are as follow :

- (1) Sum of repeater designed deviation and manufactured deviation.
- (2) Sum of cable designed deviation and manufactured deviation.
- (3) Difference between standard temperature at the sea bottom and the temperature of individual cable sections.
- (4) Difference between standard pressure and the pressure of individual cable sections.
- (5) Error in measuring cable length.
- (6) Error in estimating the temperature and pressure of individual cable sections.
- (7) Cable laying effect.

Misalignments based on items from (1) to (4) are equalized by the fixed equalizer. Total misalignment to be equalized, due to items from (1) to (4), is  $\pm 3.6$  dB for one ocean block section (120 km) at 36 MHz.

Misalignments based on items from (5) to (7) are equalized by the variable equalizer. Those deviations consist of a combination of terms  $\sqrt{f}$  and  $f$ . Table 4 summarizes misalignments to be equalized by the variable equalizer for one ocean block section at 36 MHz. Figure 13 presents misalignment reduction by the ocean block equalizer. The misalignment could be reduced to within  $\pm 2$  dB.

#### 6. Conclusion

The effect of the ocean bottom environment on submarine coaxial transmission characteristics was investigated for the CS-36M system. Cable loss temperature coefficient decreases at high frequency and then becomes a negative value over about 100 MHz. Cable loss pressure coefficient is approximately constant,  $2.5 \times 10^{-5}$  /kg/cm $^2$ , in a frequency range of 4 MHz to 36 MHz. Aging effect and handling effect were also investigated. All of the results investigated can provide cable transmission characteristics at a typical sea bottom environment.

#### Acknowledgements

The authors would like to thank Dr.D.Kumagai and Mr.H.Tabata, who conducted the project. The authors also wish to express sincere thanks to Dr.G.Marubayashi and Mr.N.Kojima for providing the facilities on the researches, and to the personnel of Ocean Cable Co., Ltd. for their co-operation in cable manufacturing.

#### Reference

- (1) A.W.Lebert and G.J.Schaible: Ocean Cable and Coupling, B.S.T.J., 49, 5, 1970.

Table 1.  $\beta$  and  $Z_0$  Temperature Coefficients

	Temperature Coefficient (%/°C)
$\beta_o$	-0.015
$\beta_p$	-0.16
$Z_{oo}$	+0.032
$Z_p$	+0.22

Table 2. Change in Capacitance and Delay after Handling

Cable	$\Delta C/C$	$\Delta \tau_o/\tau_o$
#1	+0.039%	+0.0109%
#2	-0.004	-0.0005
#3	-0.006	-0.0016

Table 3. The CS-36M System Layout

System Length	Maximum 6,700 km
Transmission Band	Low 4.332 ~ 17.004 MHz High 22.796 ~ 35.468 MHz
Capacity	2,700 CH (telephone) or 900 CH (telephone) + 1 Color TV CH
Total Noise	$\leq 1$ PW/km (relative level: 0 dB)
Cable	38.1 mm (1.5") submarine coaxial cable
Repeater Spacing	5.84 km
Power Feeding	156 mA DC Constant Current $\pm 5,800$ V Normal Voltage
Water Depth	Maximum 8,000 m
Repeater Gain	35 dB at 36 MHz
Equalization	An Ocean Block Equalizer after Every 20'th Repeater
Fault Locating	Supervisory Tone Method (for Power Feeding) Cable Capacitance Measuring Method (for Non Power Feeding)

Table 4. Misalignment to be adjusted by an Ocean-block Equalizer (at 36 MHz, 20 sections)

Factor	Cable Loss Deviation (dB)		Note
	$\sqrt{f}$ part	f part	
Error in cable length	$\pm 1.0$	$\pm 0.09$	$\pm 0.2$ km
Uncertainty in ocean bottom temperature	$\pm 1.28$	$\pm 0.69$	$\pm 1.0$ °C
Uncertainty in ocean bottom depth	$\pm 0.02$	0	$\pm 20$ m
Laying effect	$\pm 1.21$	$\pm 0.11$	$\pm 0.2$ %

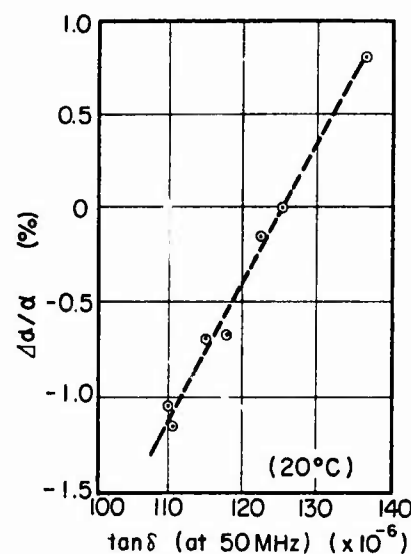
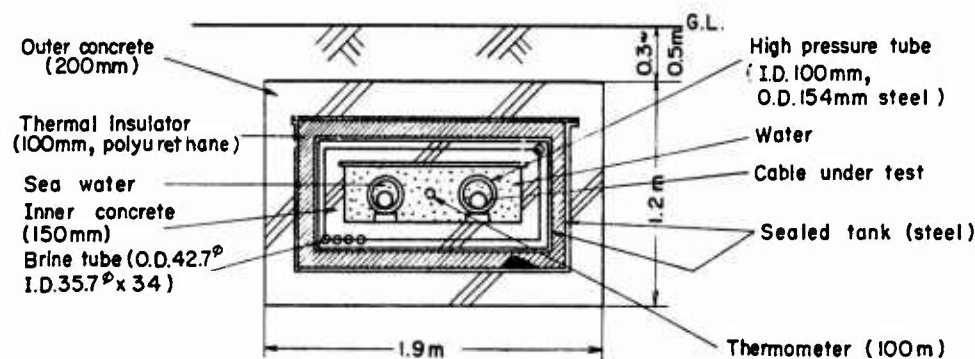
Fig.1 Effect of Change in  $\tan \delta$  on Cable Attenuation

Fig.2-Cross section of artificial ocean (length 100m)

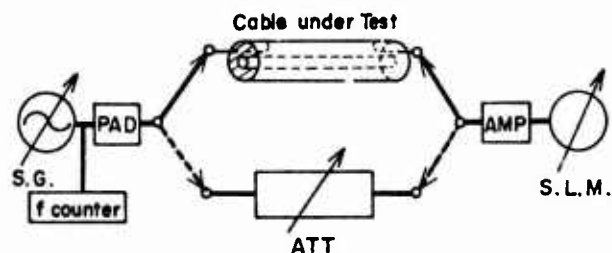


Fig.3 Attenuation measurement arrangement with Q method

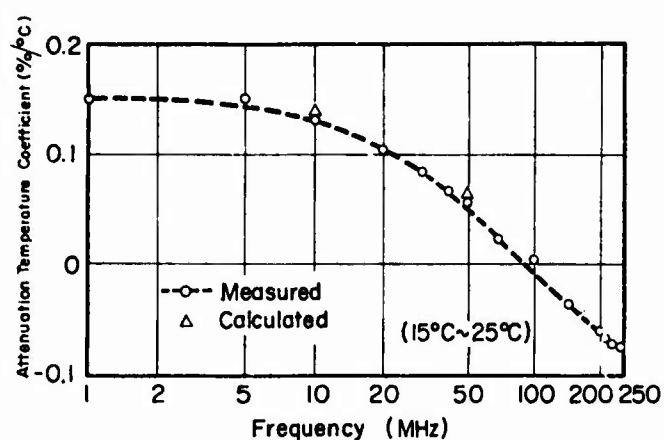


Fig.4 Attenuation Temperature Coefficient

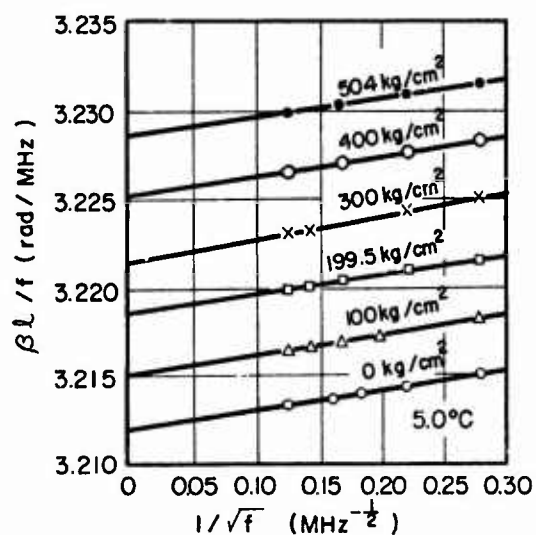


Fig.6 Phase Constant Pressure Characteristics

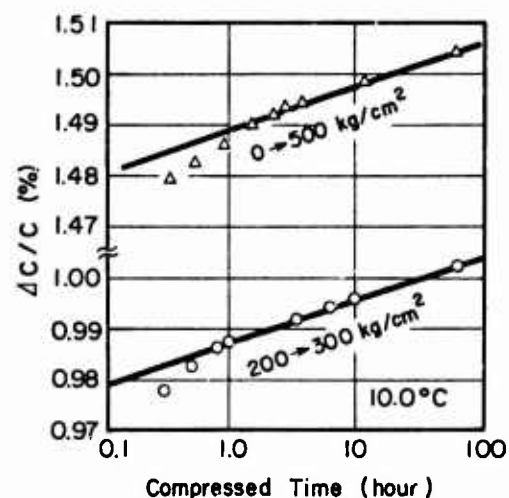


Fig.5 Capacitance Variation with Time under Pressure

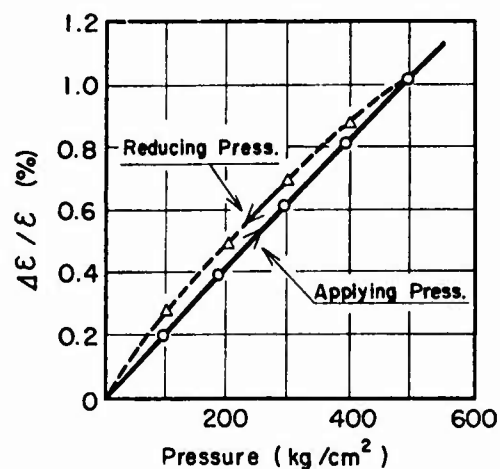


Fig.7 Polyethylene Dielectric Constant as a Function of Pressure

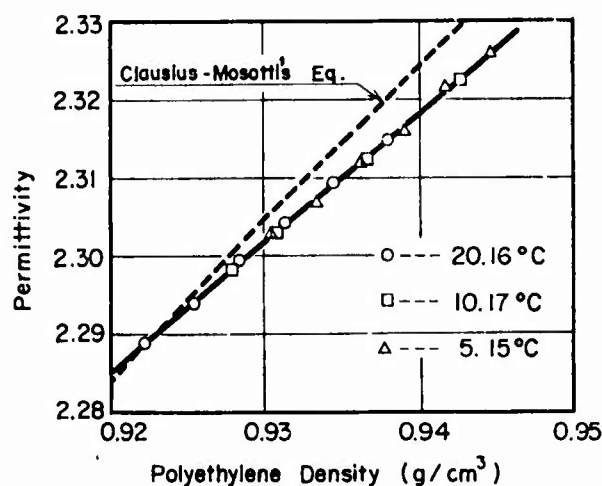


Fig.8 Polyethylene Dielectric Constant as a Function of Density

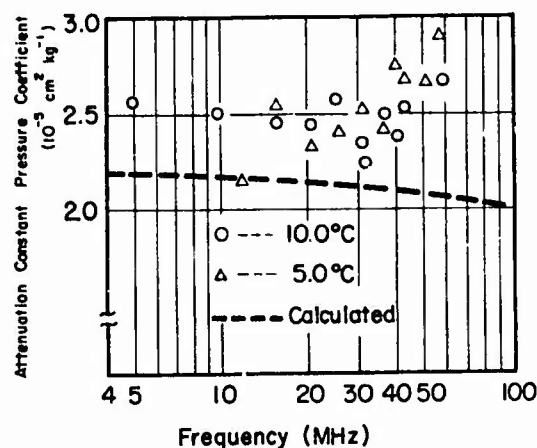


Fig.10 Attenuation Constant Pressure Coefficient

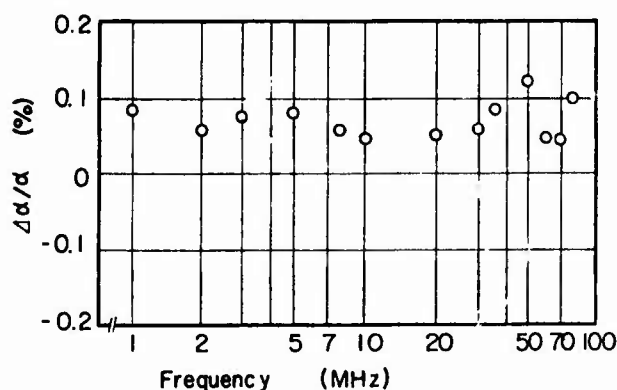


Fig.12 Attenuation Constant Change due to Handling

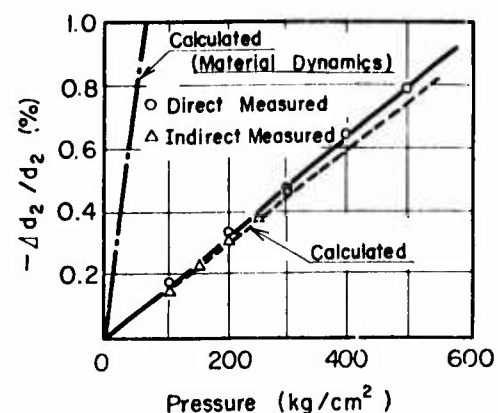


Fig.9 Cable Diameter as a Function of Pressure

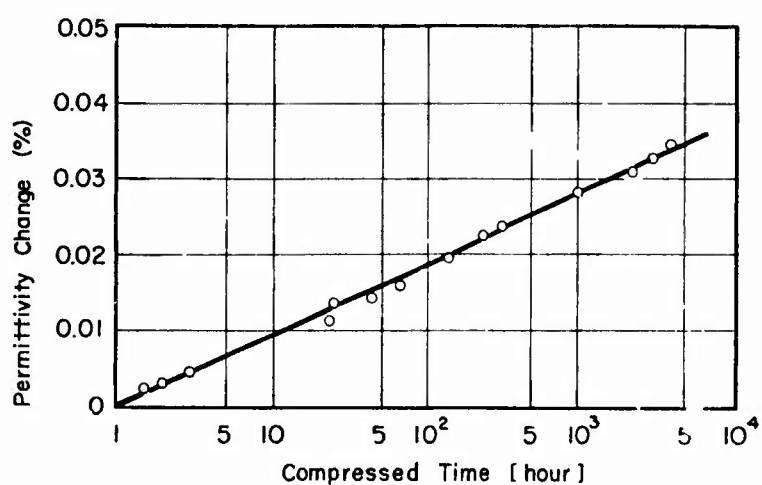


Fig.11 Permittivity Change under Hydrostatic Pressure for Low Density Polyethylene

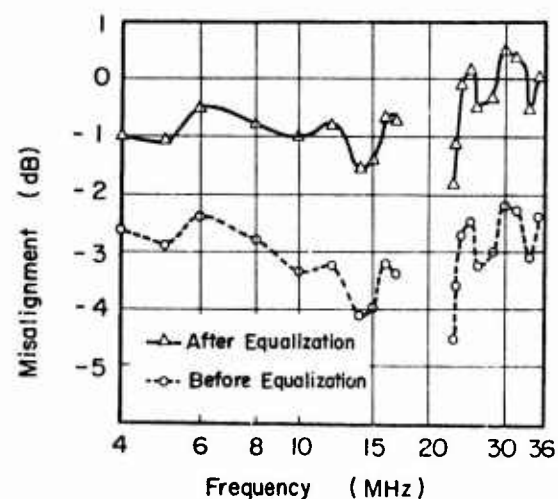


Fig.13 Misalignment reduction by OBE





Y. Negishi  
Electrical Communica-  
tion Laboratory, NTT  
Tokai, Ibaraki, 319-11  
Japan

Mr. Negishi joined the Electrical Communica-  
tion Laboratory, NTT after his graduation  
from Tohoku University in 1964. He is present-  
ly engaged in research on coaxial cables and  
submarine cable. He has worked on study of  
high frequency transmission characteristics  
of cables and development of submarine co-  
axial cable for the CS-36M system.



T. Yashiro  
Electrical Communica-  
tion Laboratory, NTT  
Tokai, Ibaraki, 319-11  
Japan

Mr. Yashiro joined the Electrical Communica-  
tion Laboratory, NTT after his graduation  
from Keio University in 1968. He is present-  
ly engaged in research on low loss dielectric  
material. He has been engaged in research of  
insulation material for submarine coaxial  
cables.



K. Aida  
Electrical Communica-  
tion Laboratory, NTT  
Yokosuka, Kanagawa, 238-03  
Japan

Mr. Aida joined the Electrical Communication  
Laboratory, NTT after his graduation from  
Waseda University in 1970. He is presently  
engaged in developmental research on sub-  
marine coaxial cable for the CS-36M system.  
He has done research on submarine coaxial  
cable.

# RADIO FREQUENCY SHIELDING OF CABLES USING A PROTECTIVE AND CONDUCTIVE POLYMER

Carroll H. Clatterbuck and John J. Park

Goddard Space Flight Center, Greenbelt, Maryland

Electronic systems operating in the radio frequency (r.f.) environments normally require shielded cables, wherein a number of signal carrying internal wires are electrically shielded by an outer braided conductive covering. The wires in the shielded cable interconnect with the posterior terminals of a multi-pinned connector and the shielding of the cable is connected in various ways to the metallic housing of the cable connector. By this process, the internal, electronic signal-carrying wires are protected from extraneous electromagnetic and r.f. signals. However, with this arrangement, there is a problem of providing total shielding in the area where the braided shield joins with the connector housing, since the metallic cable braid must be terminated above the connector to allow for the stripping of the wires, and the soldering of the wires to the connector pins. If this unprotected junction is not shielded by a conductive path, extraneous electromagnetic and radio frequency signals are picked up by the internal wires which will accentuate or neutralize the flow of normal electronic intelligence through the wires, resulting in deterioration of signals or even malfunctions of electronic systems. To eliminate this effect, the shielding system of a cable harness must be continuous from the connector metal housing at one end to the connector metal housing at its other end.

This shielding process being described provides total electrical protection at the junction between the cable shield and the connector housing, replacing the wire insulation which had previously been removed. It also provides the electrical continuity through an applied conductive coating between the connector metal housing and the metal shielding braid covering the wires, thus completing the grounding circuit. Finally, a protective coating is cast around all of the conductive coating, as well as the metallic braid end and connector housing to protect the system. This technique allows frequent connecting and disconnecting of the cable to be made safely without flexure breakdown.

The particular need for such a system surfaced when the experimenter asked for assistance. His original insulating technique used a low viscosity epoxy resin which was applied to one side of the row of wires going into a connector and then permitted to cure overnight; the next day this epoxy was coated on the other side and permitted to cure overnight. This procedure was not the best for a number of reasons: using a low viscosity resin resulted in little control of where the resin went, possibly coating the surfaces of the electrical contacts or possibly freezing the desired floating characteristics of the pins. The epoxy was covered with a metallic shield to complete the conductive path.

The procedure took too much time, it was too bulky, it became too cumbersome, and it also required especially careful techniques.

Most of the above problems could be alleviated by the selection of a thixotropic resin, one which was spreadable and non-sagging. The curing speed could be adjusted by the addition of certain accelerators. Also, a luminescent material could be added to permit observation of the resin for uncoated areas, and to help locate bubbles.

The particular technique presented here was used in numerous instances for the eighth Interplanetary Monitoring Platform launched, the IMP-I(EYE). Tables I and II list those spacecraft components on which r.f. shielded cables were treated.

TABLE I

## IMP-I-Scientific and Engineering Experiment

Contributing Organization	Experiment Title	Discipline	No. of Cables Shielded
GSFC	Cosmic Ray	Energetic Particles	10
Univ. of Iowa	Low Energy Particles	Plasma	2
Univ. of California	Medium Energy Particles	Plasma	2
GSFC	Plasma	Plasma	1
GSFC	Magnetic Fields	Fields	2
Univ. of Iowa	AC Electric & Magnetic Fields	Fields	6

TABLE II

## Spacecraft Instrumentation

	No. of Cables Shielded
Telemetry and Command	1
Attitude Control System	6
Electrical Power System	5

## Application Procedure

The shielding process consists of four separate stages of application, namely:

1. Cleaning
2. Insulating
3. Shielding
4. Protecting

These various stages will be briefly described and the complete details are in the attached

appendix.

### 1. Preinsulating Cleaning Procedure

An important first step is a thorough cleaning of the cable connector system, connector housing, metallic braid and the wire elements, and this step will improve total adhesion of the resin to all surfaces contacted. A light abrasion of the upper radius section of the connector metallic housing is recommended for adhesion improvement. Completion of the abrasion is followed by an effective solvent cleaning.

### 2. Connector Insulation Procedure

The insulating material used is a modified, thixotropic prepolymer composition which is filled with a thickening agent, making it highly viscous when prepared and applied by use of a trigger-action pressurized gun. The viscous resin will exhibit very little flow, regardless of the angle of the connector cable harness or the application angle. The insulation prepolymer resin contains the following ingredients: Polyester diisocyanate prepolymer<sup>2</sup>, Polyol curing agent<sup>3</sup>, Thixotropic agent<sup>4</sup>, Accelerator<sup>5</sup>, and fluorescent dye<sup>6</sup>.

The above insulating material is first prepared by the addition of the curing agent to the base resin and well blended. The thixotropic agent, accelerator, and fluorescent dye are then blended into the total mixture.

The thixotropic agent is a finely subdivided fused silica, which will increase the resin viscosity to prevent flow. The accelerator increases cure speed for the prepolymer and it will shorten the curing time. In addition, the insulation includes an aromatic heterocyclic fluorescent dye to allow for the insulation material to be examined with a small hand operated ultraviolet light<sup>7</sup>. After completion of the application of the insulating material, the ultraviolet lamp is used to determine whether or not pin holes, voids, air bubbles, or uncoated areas are present in the insulation. Any defects observed at this time should be removed or filled as necessary before the insulation material cures.

To remove the entrapped air from the mixing, the blended mixture is put into a high capacity vacuum chamber system, one capable of pulling a vacuum to about 1 Pascal ( $10^{-2}$  torr) or lower. The formulated and degassed mixture is carefully transferred into the dispensing gun cartridge. The resin mixture is then dispensed through the pressurized gun having a nozzle size of about 1.5 millimeter diameter (1/16 in) and 50 mm (2 in) long; these dimensions are preferred but not limited. The easily controlled trigger action pressurized gun is activated with approximately 4.9 k gms/cm<sup>2</sup> (60 psi) of pure dry nitrogen (or any pure dry inert gas) to deliver the insulation material to the posterior end of the connector cable assembly. The viscous thixotropic resin

is applied in and around the connector pins and cable wires as shown in figure 1. Additional



Figure 1. The insulation layer around the connector pins and wires may be applied for a short distance (left) or for the total distance (right).

material is directed such that it overlaps the cable metallic braid by approximately six millimeters (1/4 in), thus tying down the braid and stabilizing the braid's frayed ends.

The non-sagging nature of this resin mixture causes it to remain and cure in the region where it is applied with very little subsequent flow, regardless of the angle of its application. The foregoing ingredients, formulated, and cured as described, will achieve a tack-free touch within thirty hours and will provide a tough, semi-flexible solid polyurethane material when cured. An overnight cure at ambient temperature is sufficient for the next step of the conductive coating application. This insulating material, as shown in figure 1, will provide excellent protection to the exposed connector pins and cable wires, as well as supporting and rigidizing the connector cable system.

### 3. Connector R.F. Shielding Procedure

The next step is to apply a conductive coating between the metallic outer shielding braid and the metal connector housing, as well as entirely enclosing the insulating material.

The coating resin is filled with a fine silver powder that will exhibit a low resistance between the connector housing and metallic shielding braid when cured, i.e., 0.1 ohms or less. The conductive coating formulation contains the following ingredients: polyester diisocyanate prepolymer, polyol curing agent, and accelerator. This formulation is prepared and blended well to serve as a base resin, to which is added: silver powder<sup>8</sup> and C.P. Hydrocarbon solvent<sup>9</sup>. This particular formulation requires much blending and may take several minutes to prepare, based on small quantities. The hydrocarbon solvent is used to fluidize the mixture, thus making the silver powder easier to mix.

When mixing is completed, the conductive coating is evenly brushed onto the entire surface area of the insulation resin by using

\*Numerals indicate materials which will be identified in the appendix.

a small stiff nylon brush. Those areas of most importance for good adhesion are the upper and radius portion of the connector housing as well as the metallic shielding braid, as shown in Figure 2.



Figure 2. The conductive coating is applied between the braid and the metal connector.

It is important that the conductive coating overlap the insulation resin onto the metallic braid by about 6 millimeters (1/4 in). The total thickness of the conductive coating should be about 0.8 millimeter (1/32 in). If the conductive coating consistency decreases during the application because of evaporation of solvent, additional small amounts of solvent must be added. Finally, the conductive coating surface is uniformly smoothed out by the brushing and necessary small amounts of hydrocarbon solvent. Electrical resistance at this time between connector and metallic braid will be high, approximately 0.5 to 1.0 ohm but will improve to 0.1 ohm or less with resin cure.

Complete cure of the under layers is not necessary before the second and third layers are applied.

#### 4. Protective Outer Coating

After the conductive coating has partially cured and the resistance of 0.1 ohms or less has been achieved, the final step of the process is performed. This comprises the formation of an outer protective coating that encompasses a part of the connector housing and the newly applied conductive r.f. shielding. It should overlap the metallic braid at least 1.5 millimeters (about 1/16 in). The preferred method of forming the protective coating requires a mold to be made. This requires forming a jacket pattern from a wax<sup>10</sup> block, shaping it into a form that has the external general dimensions of the connector with insulation and the conductive coating. The wall thickness of the final coating will vary; however, approximately 1 millimeter (0.04 in) additional on each side works well.

The shaped wax block will next be encapsulated with a molding silicone resin<sup>11</sup> which cures around the wax pattern so that the configuration formed has the base and top of the

wax block exposed. An overnight cure at ambient temperature for the silicone is sufficient, and the wax block is removed the following day. The mold is then gently fitting onto the connector and adjusted to be substantially uniformly spaced around the cable; Teflon tape is used circumferentially to provide both slit sealing of the mold and lateral pressure, thus preventing leakage at the connector base during the resin casting.

The same base resin as used in the second and third application is also used for the final coating. The titanium dioxide is used as a white coloring agent for the final coating. The ingredients are: polyester diisocyanate prepolymer, polyol curing agent, filler (TiO<sub>2</sub>-Rutile)<sup>13</sup>, and accelerator. It is recommended that a high speed blender<sup>14</sup> be used for mixing because the filler material does not spread readily into the resin with normal spatula mixing. A vacuum degassing of the mixture is necessary to remove entrapped air.

The resin formulation is then placed into a gun dispensing cartridge and injected into the mold cavity from the top side into the bottom of the lowest part of the slightly tilted mold. The mold must remain around the outer cavity until the resin has permanently set. Usually an over-night cure is sufficient, then gentle removal of the mold and handling of the connector is permissible on a limited scale. Full cure of these resins and the underneath composite layers will develop within five to seven days. The four steps of forming the various layers are shown in Figure 3.

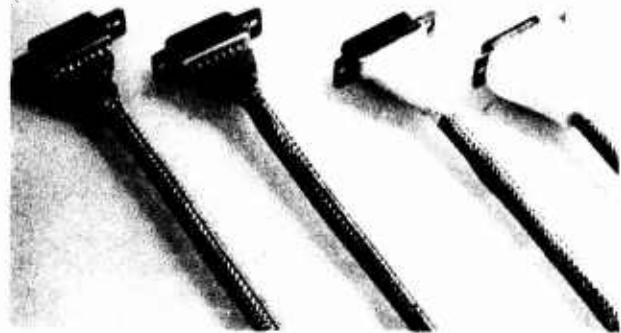


Figure 3. Steps in r.f. shielding: from left, uninsulated; with insulating layer; with conductive layer; with protective layer.

The protective coating just described, as having been molded within a cavity, has another mean of being covered, i.e., by not using the silicone mold. By adding a second filler, such as Cab-O-Sil, to the formulation to thicken the mixture, it can be applied by spatula or brushing. If this method is used, there would be less likelihood of obtaining a uniform symmetrical shape, nor having smooth surfaces, nor the aesthetic appearance of the above. This material also cures tack-free and produces an opaque whitish poly-

urethane polymer coating. To illustrate the various layers, a cross sectional drawing is shown in Figure 4.

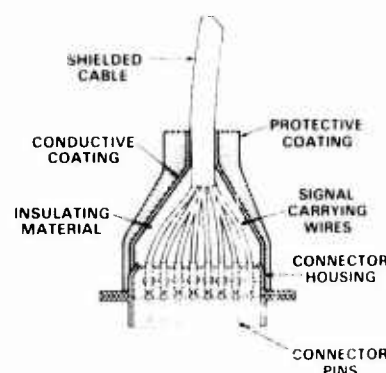


Figure 4. Cross-section drawing of the completed r.f. shielded cable.

### Results

The IMP-I spacecraft was launched March 1971 into high apogee orbit to perform detailed, and essentially continuous, studies of the interplanetary environment. The specific objectives were to assist in providing capability to predict solar flares; to expand the total knowledge of the relationships between sun, earth, and moon, by observation of the cis-lunar environment concurrent with studies of the magnetic field characteristics; and to explore the magnetosphere near the earth and into near interplanetary space.

Prior to launch and in the test phases, radio frequency radiated susceptibility tests were performed on the components and on the spacecraft in accordance with Marshall Space Flight Center Specification - 279. Specification 279 required that the vehicle subsystem be tested individually, and while operating on full power. Finally, the assembled vehicle was tested with each subsystem being energized one at a time until all subsystems were operating. The response of each subsystem as determined by the susceptibility data review, should not be affected by r.f. radiated interference. Any indications of degradation or malfunction caused by energization or by operation of another subsystem required shielding protection and had to be fixed.

The signal source output levels, antennae and frequency ranges used during the testing are presented in Table III

Table III

Frequency Range	Antenna	Output Level
0.15 to 25 MHz	41 in. rod	5 watts
25 to 35 MHz	35 megacycle dipole	+30DBM
35 to 1000 MHz	Tuned dipole	+30DBM

The final series of tests were performed

on flight units after all cables had been treated and installed in the experiments.

In addition to the successful operation of the IMP-I, the contractor for the following IMP (H&J) has also utilized this procedure successfully and has treated approximately as many cables as for IMP-I on each. Both the IMP H&J have also had successful flights and are still operating, a further indication of the versatility and reliability of the process.

A more recent use of this procedure has been with the ATS-6 spacecraft. In addition, the IUE and the ISEE spacecraft are presently using this technique in a number of instances.

### Summary

This customized process which readily lends itself for r.f. shielding of cables, has been discussed, consisting of four distinct stages in its application. The processing time will invariably decrease significantly with experience and familiarity with each step in the operation of this shielding method. A most important advantage of this process is that it is less costly to implement than fabricating expensive metallic molds.

The r.f. shielded connector process does provide a supportive semi-flexible connector structure, while complete shielding is thereby obtained to ground unwanted r.f. signals. In addition, the angles of approach of the cable to the connector becomes of little importance since the process permits shielding connectors with cables approaching the connector at even 90° angles.

In the critical area of the exposed connector pins and wires, one can thoroughly examine this crucial area where large entrapped air bubbles could cause serious corona problems, when used in an extreme environment such as the vacuum of space. We have never experienced any problem with this process since most of our work has been used in low voltage systems. This procedure is not recommended for any high voltage applications. One important feature of this r.f. shielding procedure is that the work can be performed on the laboratory bench or *in situ* in cases where the hardware is not available for the laboratory or is too large to be moved.

Another important asset of this procedure is that the initial insulating resin cannot flow into the connector and thereby reduce connector designed tolerances, such that the cured resin allows the pins of the female connector structure to remain free floating and mating of the connectors is not inhibited. It should also be noted that all process stages of this r.f. shielding use the same prepolymer resin and curing agent and are therefore compatible, thus providing the maximum of adhesion between each composite layer formed. In the specialized area of space flight use, this particular method is especially useful in that the unusual characteristic of low outgassing in vacuum is achieved with this system.



## APPENDIX

### Detailed Procedure for Cleaning, Insulating, Shielding, and Final Coating of Exposed Wires in Cable Connectors.

This process applies to connector-cable assemblies and specifically to that area or gap between the shielded cable and the metallic connector housing, wherein the wire terminals fan out from the cable to where they are soldered to the connector pins, and in which region no provision is normally made for r.f. protection. The total technique for each process involves four major separate operations which are indicated below. Some of these operations are common to all connector application.

#### 1. Cleaning

The first step involves thorough cleaning of the cable connector system, connector housing, metallic braid and the wire elements. These procedures are very important and will improve total adhesion of the resin to all surfaces contacted. It is recommended that the cable connector metallic housing be lightly abraded on its upper and radius section with a 320 grit aluminum oxide paper. The shielding braid should be similarly treated. Completion of the abrasion is followed by an effective solvent cleaning to remove impurities from the braid and connector housing. In addition, the insulated wires, exposed metallic wires, and connector pins are also solvent cleaned. The use of cotton fabric, lightly dampened with C.P. Ethyl Alcohol, works well as a cleaning technique; however, the cotton fabric should be thoroughly cleansed of residual oils by alcohol/chloroform soxhlet extraction before use. Operators should use nylon or cotton gloves for handling cable connectors during this entire r.f. shielding procedure.

#### 2. Insulation

The second step consists of building up, rigidizing and insulating the individual wires as they emerge from the metal braid sleeving and fan out to connect to the individual terminals on the connector. The material used is a Cab-O-Sil modified, thixotropic prepolymer resin system, i.e., grease-like in consistency, and highly viscous when prepared. The resin is applied via pressurized gun with very little subsequent resin flow, no matter what the angle of application or base support. The formulation, after cure, becomes a flexible, fluorescent, solid polyurethane, having very low outgassing in a vacuum environment at 125°C for 24 hours and a vacuum of 10<sup>-4</sup> Pascal. It will be called Insulation Material.

##### Insulating Material Formulation

Solithane S-113	30.0 gms
Solithane C-113-300	21.9 gms
Cab-O-Sil MS-5	4.0 gms
Dibutyl Tin Dilaurate	0.05 gms
Vyac Luminescer 174	0.05 gms

A. The above formulation is based on quantities of resin needed for several connectors and may be increased proportionately as necessary if many connectors are being prepared.  
B. Weigh out 30.0 gms of fresh (from an unopened can and less than three months old) Solithane S-113, and 21.9 gms of solithane catalyst C-113-300 into a 250 cc glass beaker. Blend thoroughly with a stainless steel spatula or stirrer.

C. Weigh out, and add to the above the remaining ingredients, 4.0 gms of dried Cab-O-Sil (the Cab-O-Sil must have been previously preheated at 150°C for 48 hours in a clean shallow pan to remove moisture) - 0.05 gms of Vyac Luminescer 174, - 0.05 gms of dibutyl tin dilaurate, and blend thoroughly.

D. Place the prepared blend in a vacuum chamber at 1 Pascal or lower for 10 minutes to remove occluded air. During this period, the chamber pressure should be cycled from 1 Pascal to atmospheric several times ('bumped') to facilitate air elimination.

E. Remove the blend from the chamber and gently transfer via spatula to the pressure gun dispenser cartridge, being extremely careful not to entrap air bubbles. The loaded cartridge is then placed back into the chamber and again deaerated for 10 minutes.

F. The gun dispenser is then locked and pressurized to 4.9k gms/cm<sup>2</sup> of nitrogen. The viscous thixotropic resin is applied in and around the insulated cable wires and connector pins by the easily controlled trigger action application gun. Additional material is directed so that it overlaps the braided r.f. shielding, by approximately 6 millimeters, thus stabilizing the braid's frayed edges.  
G. Upon completion of Step F, it is important that the resin be inspected for air bubbles, uncoated areas, and pin holes. These defects are easily observed with an ultraviolet lamp and should be corrected at this time by removing or adding resin as needed. The dye fluoresces a light blue-green color when activated by a 365 nanometers excitation source.

H. The resin is then allowed to cure at room temperature overnight and the surface should be almost tack free, before applying the later described conductive coating.

#### 3. Conductive Coating

The third application or conductive coating is applied to completely cover the insulating material and make an adhering conductive contact with the metal braid and metal connector housing. This coating is a silver filled polyurethane resin type exhibiting approximately 0.1 ohm or better resistance between the connector housing and the metallic braid covering when fully cured.

##### Resin Formulation for Conductive Coating

Solithane S-113	30.0 gms
Solithane C-113-300	21.9 gms
Dibutyl Tin Dilaurate	0.05 gms



### Conductive Coating

#### Resin Formulation

as prepared above	3.0 gms
Hexane	1.5 gms
Silflake 135	16.0 gms

- A. Prepare the bulk resin formulation, in a glass beaker and blend well with a stainless steel spatula or stirrer.
- B. Add Silflake 135 slowly to the required small amount of resin formulation in a glass beaker, with intermittent Hexane addition. Blend well by hand stirring until all the Silflake has been added. This conductive coating mixture requires a lot of blending and may take three to five minutes to prepare using the above amounts.

Hexane is used to fluidize the mix and is both volatile and inflammable. Work should be done under a hood preferably.

- C. Do not vacuum evacuate this blend as it will remove all of the volatile solvent, causing the conductive coating to become too dry for brushing onto the insulation base coat. If brushing consistency decreases during the application, due to loss of solvent by evaporation, a few drops of additional Hexane should be added.

D. The conductive resin system is brushed onto the entire surface of the insulating material. It is also most important to coat the upper and radius portion of the metal connector housing as well as the metallic braid end. The conductive resin should overlap the insulating material onto the metallic braid by approximately 6 millimeters. The total resistance of the conductor coating should be approximately 0.5 to 1.0 ohm or less and will improve with resin cure. If higher resistance exists after several hours, rebrush the surface with additional well blended conductive coating, working the resin into the metal parts, yet applying the least amount necessary for obtaining a lower resistance. The brush should be a small nylon type of excellent quality, and trimmed down to 3 millimeters; this modification will allow the application of a fairly smooth coating and no loss of brush hair. The surface can be uniformly smoothed out by quickly dipping the brush in hexane, flicking off the excess, and gently going over the surface. Upon completing the application of the conductive coating, a 6-hour ambient temperature cure is sufficient for handling and the addition of the final protective coating.

#### 4. Protective Outer Coating

The outermost protective coating resin is cast in a mold encompassing the connector, the newly applied conductive r.f. shielding, and the metallic braid. Upon cure, the mold is removed, leaving a tough encapsulated permanent r.f. shielded system which can be handled and flexed without fear of protection loss. The material cures tack free depending on time, temperature, and formula to an opaque, flexible, whitish polyurethane polymer. Tack-free cure

time for the protective coating is overnight at ambient temperature. Five to seven days are required for complete cure at room temperature.

#### Resin Formulation

Solithane S-113	30.0 gms
Solithane C-113-300	21.9 gms
Titanium Dioxide	0.26 gms
Dibutyl Tin Dilaurate	0.025 gms

- A. A connector pattern is made by smoothly shaping a wax block to the contours desired. The cavity is so designed at its base that it provides a fitted circumferential counter-sunk recess into which the rectangular connector mounting tabs and side walls of the connector mounting plate can be later tightly accommodated. This prevents leakage during the jacket casting operation. An RTV silicone resin, Dow Corning 589 with 10%-589 catalyst, is then cast and cured around the wax pattern so that the above configuration is formed at the pattern base. The mold wall should be about 12 millimeters thick. The mold is then allowed to cure at ambient temperature overnight.

B. Carefully slit the mold vertically on one side of its longest rectangular surface so that it can be later gently opened, fitted around the cable and lowered around the connector to be protected. If elevated temperature cure is desired, it is recommended that, prior to fitting the mold onto the connector, an acrylic barrier coating be applied to the mold cavity. This is easily done by spraying the inner cavity surface. Allow the spray coating to air dry for 15 minutes followed by an elevated temperature cure at 75 to 100°C for 15 minutes. Teflon tape is then applied circumferentially to the mold to provide both slit sealing and the lateral pressurization which prevents leakage of the casting resin.

C. Using the same dispensing gun, the above prepared resin, previously outgassed for 6-8 minutes at 1 Pascal or lower, is injected into the silicone mold cavity until it is filled. This level is normally 2 millimeters above the conductive coating on the metallic braid. To avoid entrapped air during the process the mold is tilted a few degrees and the resin injected at the bottom of the lowest part of the cavity. The mold is then leveled when the resin reaches the cable braid region.

D. The mold must remain around the outer coating until partially cured, usually overnight at ambient temperature. The mold can then be gently removed and handling of the cable connector is permissible. Full cure will develop in five to seven days. If a faster total cure is desired, the entire connector cable assembly may be heated to 70°C for 24 hours.

A patent has been granted to Mr. Aaron Fisher and Mr. Carroll Clatterbuck of NASA for r.f. shielding cable-connectors (Patent No. 3,744,128). Mr. Fisher, now retired, was very deeply involved with the original work.

# MATERIALS SOURCE LIST

- |   |   |
|---|---|
| 1. Resin Dispenser Gun<br>Model 102, 20cc capacity<br>cartridge | Kenics Corp.<br>Wakefield, Mass.                                |
| 2. Solithane S-113  | Thiokol Chem.<br>Co. Trenton,<br>New Jersey                     |
| 3. Solithane C-113-300<br>catalyst                              | Thiokol Chem.<br>Co. Trenton,<br>New Jersey                     |
| 4. Cab-o-Sil, MS-5  | Cabot Corp.<br>Boston, Mass.                                    |
| 5. Dibutyl Tin Dilaurate<br>(T-12)                              | General Elec.<br>Co. Waterford,<br>New York                     |
| 6. Vyac luminescer 174  | American<br>Cyanamide, Bound<br>Brook, New<br>Jersey            |
| 7. Ultra-Violet lamp<br>UVSL-25                                 | Ultra Violet<br>Products<br>San Gabriel,<br>California          |
| 8. Silflake 135   | Handy and Harman<br>New York, New<br>York                       |
| 9. Hexane (Fisher<br>Certified)                                 | Fisher Scien.<br>Co. Pittsburg,<br>Penna.                       |
| 10. Paraffin  | Local   |
| 11. RTV Silicone 589  | Dow Corning<br>Corp. Midland,<br>Michigan                       |
| 12. Acrylic Barrier Coat,<br>Aerosol spray, type II             | Cosden Chem. Co.<br>Beverly, N.J.                               |
| 13. Titanium Dioxide<br>Rutile R-960                            | Dupont<br>Wilmington,<br>Delaware                               |
| 14. Brookfield Mixer<br>Model L-2789                            | Brookfield<br>Engineering<br>Laboratory,<br>Stoughton,<br>Mass. |



Carroll H. Clatterbuck has been with the Goddard Space Flight Center's Materials Engineering Branch for twelve years, where his work has been directed toward polymeric development and application. Prior to his government career he spent eight years in private industry, working with materials research and development in ceramics and coatings.



John J. Park, born in Atchison, Kansas, earned a B.S. in chemistry at St. Benedict's College, an M.S. in chemistry at Catholic University, and a Ph.D. in chemical Engineering at the University of Maryland. After 11 years at the National Bureau of Standards, he transferred to the Goddard Space Flight Center in 1963, where he is now Head of the Chemistry and Physics Section of the Materials Engineering Branch.

# WELDED POLYETHYLENE SPLICE CLOSURES

## A RELIABLE ALTERNATIVE

By

Daniel F. Gill  
Siemens Corporation

### Introduction

In recent years, polyethylene sheathed communications cables have become the industry standard for rapidly growing communications networks. Although such cables are outstanding for their transmission characteristics, their installation can present problems. These problems occur when it becomes necessary to join polyethylene sheathed cables to plastic or metal accessories at the installation site. Similar problems can occur when joining two polyethylene cables to each other and trying to maintain water and air tight integrity. The reliable joining of these materials is made difficult because of the unwetability of polyethylene, a basically non-polar substance. Thus a new method had to be developed which would not only satisfy the above requirements but would also meet the following objectives.

### Requirements

The jointing method and sleeve technique that we chose for polyethylene sheathed cables meets a number of specific requirements. Fig. 1

Economic. Decrease substantially existing material costs.

Decrease inventory costs.  
Increase productivity.

Application. Buried, underground and aerial plant.

Reliability. Maintain watertightness under extreme physical and climatic conditions. Pressurized and non-pressurized applications.

Flexibility. Easy adaption to existing and expanding polyethylene and metal plant.

Installation. Produce extremely reliable closures with shorter installation times. Maintain ability to reopen and retrofit to existing uncut cables.

In addition to the above requirements, the objective of a new sleeve technique was to considerably reduce the number of defects which occur when conventional

lead, fiberglass, metal and plastic sleeves are used. Since in many applications, both inside and outside plant, the surface of the sleeves are not accessible from all sides, this design was chosen to allow convenient handling.

To fulfill these tasks, a new sleeve was developed which used the sheath material, i.e. polyethylene, welded together to form a homogeneous installation for cable distribution networks.

### Constructional Design

The individual parts of the sleeve are shown in Fig. 2.



Fig. 2.

The cables to be joined are connected to the sleeve heads and these are linked to the sleeve tube. In the majority of cases, the sleeve tube is provided with a longitudinal slit to offer the possibility of reopening the sleeve later on. The supporting shell is used for taking up the pressure during the welding process.

The method we employ for welding the polyethylene sleeves together using Joule's heat is depicted in Fig. 3.

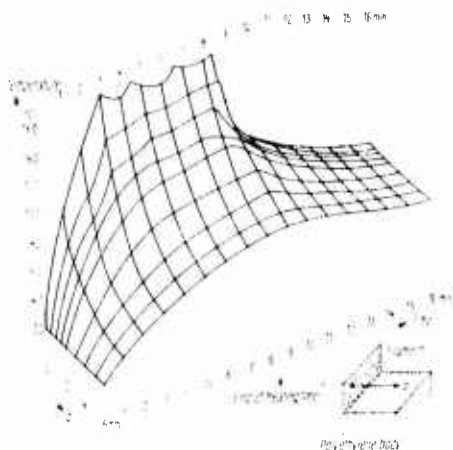


Fig. 3 Temperature as a function of position and time in welding polyethylene with a program device

Various manufactures have investigated the possibility of welding PE with the heat source lying at the external surface of the sleeve. Since the temperature cannot be controlled reliably enough with this arrangement, it is impossible to avoid faulty welding spots. We chose to place the heat source between the parts to be joined.

The low density polyethylene used for our sleeves with admixtures of carbon black to protect against aging by light and polyisobutylene to prevent environmental stress cracking has a softening temperature of about 212°F (95°C) and an optimum welding temperature of about 356°F (180°C). Fig 3 shows the temperature in the welding seam as a function of time and material density.

It can be seen that the optimum welding temperature is reached directly at the jointing areas. Moreover, from the behavior of the temperature in the welding zone, it can be seen that the softening temperature is only slightly exceeded 2mm away from the heating element. This means that polyethylene parts can be welded beginning with a minimum wall thickness of 2mm and extremely favorable results.

The heating source for welding is a heating tape of meander shaped, polyethylene coated, enameled copper wire embedded between polyethylene foils (Fig. 4A). The distance between two windings has been chosen in such a manner that the entire zone is homogeneously fused around the current carrying conductor during the heating process. The fusing zone, the so called welding ellipse can be clearly recognized in Fig. 4B. The width of the heating tape has been fixed so that the strength of the welded seam is greater than that of the PE itself. The resistance of the filament has been adapted to the constructional design of the heating tape and the heating energy re-

quired in the welding zone. The energy required is essentially dependant on the ambient temperature. For instance, if a given constant current is used, the welding time must be adapted to the ambient temperature. The welding time required for ambient temperatures between 32°F and 122°F (0°C and + 50°C) lie between 10 and 4 minutes. A 12v storage battery with an 84oh charge would be sufficient for welding 5 sleeves.



Fig. 4A Heating Tape



Fig. 4B Micrograph of a section through a welding seam coupling three polyethylene bodies

The welding control device, shown in Fig. 5 is circuited between the energy source and the heating tape. The lid of the PE welding control device holds the time switch and the supervisory circuits, while the current regulating circuits are within the box. The device meets the shake and impact tests in accordance with the Spec. IEC-50 used for equipment of the German Federal Post and Railroads.

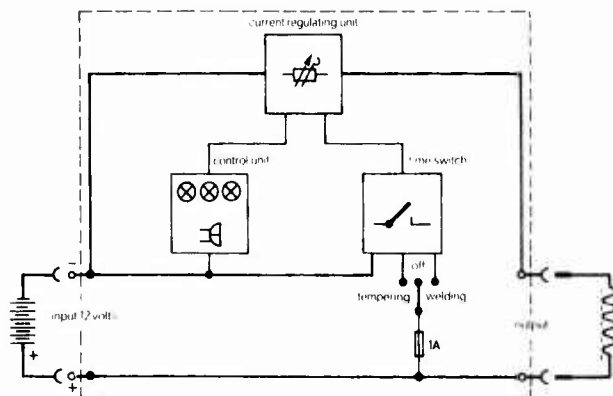


Fig. 5. Schematic of welding device

The welding control device switches the current in definite stages so that the temperature in the welding zone remains constant during the welding time. Depending on the ambient temperature, the duration of these current phases are switched automatically. The device also contains alarms for open or short circuit operation and also over current or under current supply.

In addition to the correct temperature, the welding operation also requires the correct pressure. A pressure of 14 lbs/sq. in. guarantees perfect fusion of the welding zones. This is done with the tools depicted in Fig. 6.

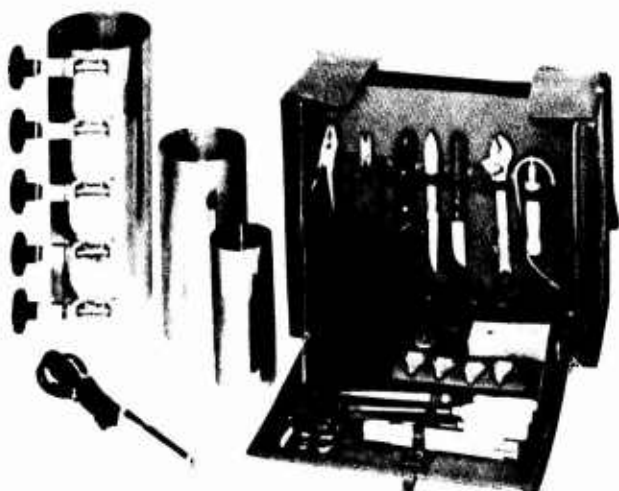


Fig. 6.

Reinforced rubber tapes are used for supplying the required pressure at the transition points between the cable and the sleeve head. The welding pressure between the sleeve cylinder and the sleeve heads, as well as at the longitudinal seam of the sleeve cylinder, is supplied by a tension plate and clamps. These simple tools have been designed to produce the required pressure without the use of elaborate measurements.

The combined spreading and tempering mandrel is used for adapting the sleeve head to the cable diameter and inserting the heating tape into the sleeve head cone. The installation of the heating tape is accomplished by applying current to the wires of the tape for  $1/3$  the welding time. (position "tempering" on welding controller). This operation insures the heating tape remains in a fixed position when the sleeve head is slipped over the cable head.

#### Sleeve Installation.

Fig. 7 shows the installation process.

The heating tapes on the circular seams of the sleeves are already tempered on during manufacture. The heating tapes for the circular seams of the cable are installed in the cones of the sleeve heads, as described above, and the sleeve heads then slipped over the cable.

Next, perform the wire splicing and sheath bonding operations and wrap with joint insulation per local requirements. The welding process may then be carried out by fastening the cable in the manhole. Before welding, the sleeve heads are positioned by snapping the central support shell in place; then placing the sleeve cylinder between the stops on the sleeve heads and installing the pressure tools. Welding is then carried out in the following sequence: circular seams of the sleeves, circular seams of the cable, longitudinal seam of sleeve. In each case, the heating tape is left in the seam after welding should it become necessary to reopen the sleeve. If a sleeve must be reopened for repair or to add a new cable, it is only necessary to connect the welding controller to the ends of the heating tape and select the tempering mode. After the seams of the sleeve have become soft, the cylinder can be removed without being destroyed. After the necessary work has been accomplished, the sleeve can be closed again by inserting new heating tapes in the guides provided and repeating the welding process.



Fig. 7 Polyethylene distribution sleeve with attached welding control unit

#### Sleeve Tests

Before this new sleeve technique was released for general use, it was tested with several methods.

a. Longitudinal Stress. The testing of the welded seams as to tensile and shearing strength revealed that the values measured on the welded seam were equal or greater than those of the virgin polyethylene. Typical values of tensile strength exceed 1,000 lbs.

b. Internal Pressure Test. Completed sleeves with a diameter of 7.7/8" or 3-1/8" (200mm or 80mm) will burst when subjected to internal pressures between 85 and 145 lbs/sq. in. (6 to 10 atm). In every case, the bursting point occurred far off the welded seam. The bursting pressure is a function of the longitudinal cross section of the sleeve. In the case of bending tests with connected cables and impact tests on sleeves which were pressurized with 71 lbs/sq. in. (5 atm) the sleeves remained tight.

c. Temperature Aging. Under a pressure of 10 lbs/sq. in. (7 atm) the sleeves have been put through over 100 temperature cycles from -40F (-40C) to +140F (+60C) without leakage.

d. Environmental Stress Cracking (ESC) Test. Samples were taken from welded and non-welded parts of the sleeve and subjected to an ESC test. In addition, the entire sleeves were laid in a test fluid. The test method was the same as that carried out on cable sheaths and has indicated faultless performance.

e. Branching-off Distribution. Fig. 7A shows an example of the "Dedicated Outside Plant System" which is the preferred local network in the United States. The main feeder cables run from the central office to control points. At these points, the lines are branched off as "branch feeder cables" which, at access points, branch off again in "distribution cables". In these cables-at points marked "D"-distribution sleeves must be provided where subscriber cables are to be branched off. Here only the pairs for these subscribers must be cut, while the others remain intact. The PE welding sleeve method can be used for this purpose also.

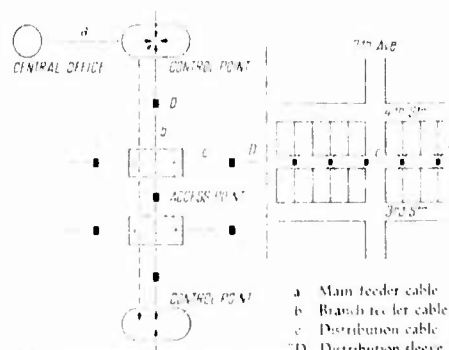


Fig. 7A Structure of an American local network according to the "dedicated plant" system.

The sleeve heads are cut to the correct diameter, slit and slipped over the cable. Then the usual splicing work is carried out. In order to close the longitudinal slip, a heating tape, prepared for this purpose, is inserted into the slit and welded in the previous manner. The only difference being the pressure clamping device. Once this operation is completed, the sleeve is closed as previously described.

f. Jointing of Metal Sheaths to PE Sheaths. Adapters shown in Fig. 8 have been developed for jointing metal sheaths to PE sheaths. They consist of a combination of copper cylinders and bonded PE cones. Metal sleeves can be jointed to the copper tube by means of wiped joints; PE sheaths are welded into the PE cones with heating tapes as shown before.

The jointing problem between PE cone and metal cylinder was solved as follows: The surface of the PE is oxidized with inorganic acid so that bonding is possible. In this way the PE cone can be jointed to the metal cylinder with the aid of a two-component adhesive on an epoxy resin base. When tensile tests were carried out in the temperature range between -4 and +122°F (-20 and +50°C) this joint proved to be so excellent that cracks only occurred in the polyethylene but never between metal and PE in spite of the different expansion coefficients of both.

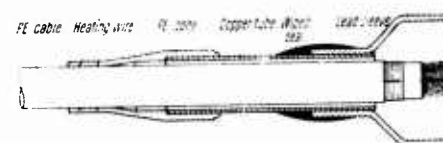


Fig. 8 Adapter for inserting a polyethylene-sheathed cable into a lead sleeve

g. Constructional Design of Sleeves and Adapters. In conclusion a summary shall be given showing how the requirements for a universal application of the PE welding sleeves were met, using as small a type spectrum as possible. Fig. 9 shows the sleeve spectrum used in the method described.

The combined jointing and branch-off sleeves have sleeve heads each of them with 2 connecting cones. They encompass the following ranges if a 26 AWG (0.4mm) cable is used:

Diameter Sleeve (in.)	(mm)	Sleeve Capacity (number of pairs)
3-1/8	80	5... 200
4-3/4	120	50... 500
5-7/8	150	100...1000
7-7/8	200	200...2000



PE sleeve 80, 120, 150, 200



PE sleeve 150E, 200E



PE sleeve 80 T



PE sleeve 50

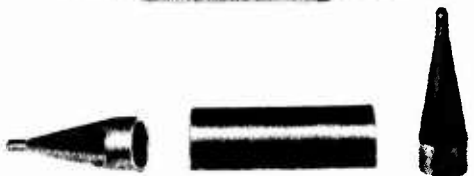
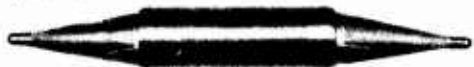


Fig. 9

The sleeve heads can at option be provided with valves so that compressed air tests or feeding of compressed air can be accomplished. Furthermore, a jointing sleeve with a diameter of 2" (50mm) is available for jointing cables with 5 to 100 pairs of the same 26 AWG standard.

A special sleeve type which is particularly suitable for installation in places which are inconvenient to reach and for thin flexible cables, is the pot sleeve. Only one sleeve head with 4 connecting cones is used in this method. The seal is made by welding the hood to the head.

The various sleeve heads may also

be combined, e.g. a head of the sleeve type 80 or of the type 80 T (80 T = pot sleeve) may be connected to the cone of a sleeve type 150 or 200. In this way a very large number of branching-off possibilities are given.

A 5-stage spectrum of the adapters described above is available (Fig. 8). The external diameter of the copper tube varies from 1-1/8" to 3-1/2" (30 to 90 mm) so that all diameters of cables with metallic sheath are covered.

Summary. It has been shown how the development of a sleeve joint for cables with PE sheaths using the sheath material for jointing was carried out using the electro-welding process. The new technique promises to meet in every case the rough requirements of practical operation. All variations necessary for universal application of these sleeves for conduit cables as well as buried and aerial cables have been taken into account in the constructional design.

By exact observation of the working process prescribed for this new technique the splicer is able to work without previous special training. Over the last few years more than 200,000 sleeves have been installed, in all applications, under the most extreme climatic conditions with results never achieved before utilizing previous methods.

#### References.

1. E.D. Latimer, H.E. Robinson: Sheath Jointing of Plastik-Sheathed Cables. POEEJ 59 (1966) Part 3, Pages 206 to 210
2. H. Ishikawa, K. Nagata: Method of Jointing Plastic-Sheathed Cables with Electric Heating Wire. Fourteenth Annual Symposium on Wire and Cable, Dec. 1965, Atlantic City, New Jersey.
3. W. Buchholz: Welding and Bonding of Polyethylene Materials for Communications Cables. Siemens Review, Vol. XXXIII (1966) No. 1 Pages 25 to 28.
4. W. Kuhfus, W. Muller: Sleeves for Polyethylene-Sheathed Communications Cables. Siemens Review, Vol. XXXIII (1966) No. 5 Pages 289 to 291.
5. Horst-Edgar Martin: Sleeve Joints for Polyethylene Sheathed Communications Cables. Sixteenth Annual Wire and Cable Symposium Dec. 1, 1967, Atlantic City, N. J.

DESIGN CONSIDERATIONS, CHEMISTRY AND  
PERFORMANCE OF A REENTERABLE POLYURETHANE  
ENCAPSULANT

by

Melvin Brauer - N L Industries  
R. Sabia - Bell Telephone Laboratories

ABSTRACT

Encapsulants are used in the nonpressurized distribution plant to maintain the electrical properties of cable splices in the presence of water. Polyurethanes and grease-like materials are both used widely as splice encapsulants and both have shortcomings. A reenterable, non TDI based, two component polyurethane encapsulant has been developed which combines the best features of polyurethanes and greases. The rapidly gelling encapsulant is readily mixed and penetrates all splice voids at temperatures as low as 0°F. The encapsulant can be easily reentered without tools even at temperatures below 0°F without crumbling, and has low water absorption and high volume resistivity. Laboratory and performance test data illustrate these end use characteristics and indicate that the encapsulant can be used in buried, underground and aerial plant applications.

I. INTRODUCTION

The multipair telephone cable plant consists of pulp and PIC air core and waterproof cables which are spliced together to provide service. The splice may be in an above ground pedestal or in a closure. Closures are designed to restore the cable's integrity by acting as an extension of the cable sheath. The splice is the weak link in the buried or underground plant, because it is highly vulnerable to water degradation.

Pressurization is a method to keep out moisture in air core cables. For the non-pressurized plant, use of moisture resistant connectors has increased system reliability but possible failure modes have remained. To further increase the reliability of the non-pressurized plant, waterproof cable was introduced. However, total encapsulation of the splice with greases (waterproof cable) or hard polyurethane encapsulants (non-pressurized air core cable) is believed to provide the greatest reliability of a non-pressurized cable splice.

Polyurethanes and grease-like materials both have shortcomings. Grease encapsulated splices are easily reentered by hand, but the greases are limited to waterproof cables and small splices in the underground or buried distribution plant. The use of hard polyurethane encapsulants for air core cable

splices and at the waterproof cable interface with air core cable does not permit reentry for possible rearrangement (for example, to change the loading) or for trouble shooting.

This paper will discuss the development of a two component polyurethane encapsulant which combines the best features of polyurethanes and greases.

II. DESIGN CONSIDERATIONS

Design considerations in the development of a reenterable encapsulant involved the environment (buried and underground), cable types (waterproof and air core), and cable size (25 to 900 + pairs), which were fixed, as well as the hardware used to splice cables and the characteristics of the encapsulant itself, which would have to be defined.

A. Hardware

In order to simplify installation, it was decided that the closure would not be hermetically sealed. Therefore, the encapsulant would be the primary moisture barrier. Moisture resistant connectors were designated for use with the new encapsulant to minimize craft sensitivity. The splice was centered in the closure by wrapping it with a porous tape thereby pulling the splice together. The porous tape can be easily located and can be used to rip apart the encapsulant without tool damage to the splice (see Figure 1). This method eliminated the need for bonding the encapsulant to the closure, and ensured complete encapsulation of the wires. Bonding of the encapsulant directly to closure was rejected as an alternative to the use of porous tape, since reentry would have been more difficult in this design. Thus, polypropylene was chosen as the closure material since other materials do not readily bond to it. Sealing tapes and vinyl tapes can be used to keep the splice case properly oriented while the encapsulant cures.

B. Encapsulant Design Characteristics

The design of the encapsulant was governed by a multiplicity of goals. Firstly, the encapsulant would have to meet OSHA



Figure 1 - Branch Splice in 16 Type Closure

requirements and be free of hazardous materials under a wide variety of field conditions. Secondly, it was desirable to develop a product which exhibited good shelf stability and reproducibility, mixed and poured easily, was insensitive to errors in the mix ratio and to moisture, and was fast gelling. Finally, a high degree of hydrophobicity and a high volume resistivity, coupled with low weight losses and high degree of oxidative and hydrolytic stability under field use conditions was required.

The desire to combine the reenterability of greases with the superior mechanical properties of polyurethanes required that the encapsulant have unique mechanical properties. An easily reenterable, high impact strength elastomeric polyurethane, which would maintain its properties between 0°F and 140°F was sought. New pours of the encapsulant would have to bond to the old, under these conditions. Since the encapsulant would come in contact with a variety of cable and splice components, compatibility of the material with the insulation, connectors, splice case, etc., had to be considered.

### III. THE CHEMISTRY AND PHYSICAL PROPERTIES OF THE REENTERABLE ENCAPSULANT

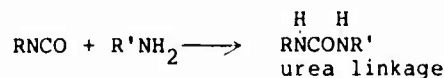
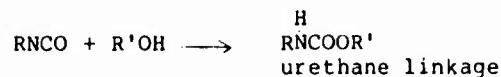
#### A. Chemistry

The chemistry of the encapsulant was governed by the design consideration discussed in Section II. The factors which particularly influenced the chemistry were:

1. mechanical properties
2. waterproofing and insulation requirements
3. environmental conditions
4. cost

The requirement for ease of reenterability was translated into a consideration of urethane chemistry with respect to tear strength. It will be recalled that isocyanates react with compounds containing labile hydrogen. The most common sources of labile hydrogen are the hydroxyl group (OH) and

the amine group (NH<sub>2</sub>). The reactions which occur readily at room temperature without the formation of a gas are shown below.

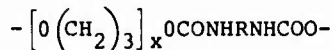


It is known that the urea linkage yields much higher tear strengths than the urethane linkage. For instance, Axelrood et al. studied a polyurethane series employing toluene diisocyanate (TDI), polypropylene glycol (PPG) of 2000 molecular weight and an aromatic amine (MOCA). It was found that when the NH<sub>2</sub>/OH ratio was changed from 50/50 to 56/44, the tear strength increased by almost 20 percent. Since the urea linkage is approximately two times more polar than the urethane linkage, these data and other literature have led to the conclusion that the tear strength of polyurethane elastomers is directly related to the ability of the urethane to form hydrogen bonds. Since a low tear strength was desired, the urethane rather than the urea linkage would have to be employed in the polymer. In addition, aromatic amines are toxic and unsuitable for use under field conditions.

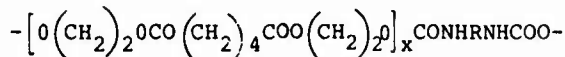
Avenues other than the elimination of urea linkage could be employed to reduce hydrogen bonding. Thus, reduction in the concentration of urethane linkages has also been shown to dramatically reduce tear strength. Axelrood and Frisch reduced the tear strength of a TDI-PPG polyurethane by a factor of 4 by doubling the molecular weight of the polyol.

In addition, the backbone of the OH-bearing constituent has a large effect on tear strength. The polymer structures obtained from the principal polyol types are shown below.

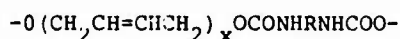
Polyether based urethane



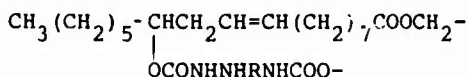
Polyester based urethane



Polybutadiene (PBD) based polyurethane



Castor oil based polyurethane



It will be noted that polyether and polyester urethane backbones are dominated by carbon-oxygen linkages, while the castor oil and PBD based urethane backbones are made up primarily of hydrocarbon linkages. These structures would lead one to expect that the PBD and castor oil polyurethanes would have lower tear strength than the polyether and polyester urethanes.

Moreover, the castor oil backbone has a large hydrocarbon sidechain which tends to force polymer chains apart, thereby reduces hydrogen bonding. Typical tear strength values obtained for the various types of urethanes are shown in Table I and confirm the expectations that the tear strengths of the polymer could be reduced by use of castor oil, PBD and/or combinations of both materials.

TABLE I  
EFFECTS OF POLYMER  
BACKBONE ON TEAR STRENGTH  
OF POLYURETHANES

Polymer Type	Functionality	Equivalent Weight	Source of Isocyanate	Tear Strength* (lbs. in)
Polyester	2.6	140	TDI	72
Polyether	1	140	TDI	4
Polybutadiene	2.3	1100	TDI	14
Castor oil	2.7	140	TDI	11

\* determined per ASTM D-624 at 77 F., cross head speed of 20 in. min. with B tie specimen.

Having chosen castor oil and PBD as the hydroxyl constituents, a choice of isocyanate source also had to be made. The most practical possibilities from availability and cost/performance basis are two aromatic isocyanates, TDI and MDI (4,4'-diphenylmethane diisocyanate) and various aliphatic isocyanates such as IPDI (3-isocyanatomethyl-3, 5, 5-trimethylcyclohexyl isocyanate), HMDI (hexamethylene diisocyanate) and H<sub>12</sub>MDI (methylene bis cyclohexyl isocyanate). TDI was eliminated from consideration because of the TDI vapor hazard in spite of the attractive cost and the known ability of TDI to produce low viscosity prepolymers. The aliphatic isocyanates are the costliest source of isocyanate and are known to produce dermatitis in many individuals. Therefore, in spite of the fact that use of MDI normally leads to higher tear strengths than the other isocyanates considered (due to symmetry and the contribution of two rigid phenyl groups in the polymer backbone), MDI was chosen as the source of the NCO group.

Using polybutadiene, castor oil and polymeric MDI several low tear strength polymers were developed, and the final choice of polymer structure was made on the basis of cost, hydrophobicity, electrical characteristics, field applicability, as well as mechanical properties. The choice of polymer raw materials from the standpoint of tear strength was not in conflict with waterproofing and volume resistivity requirements. In fact, it was found

that the molecular features which lead to low tear strength also produced the greatest degree of waterproofing and the best electrical properties. Therefore, the final choice between polymers of essentially the same tear strength could be made on the basis of ease of use in the field.

The design goal of encapsulation and reenterability was considered from the standpoint of field temperatures. Normally the outside plant environment is considered to be -40°F to 140°F. However in designing the encapsulant a minimum temperature of 0°F was adopted as being more realistic.

Use at 0°F required a very low viscosity urethane system in order to ensure ease of mixing, pouring, and complete penetration of the encapsulant into the void spaces of the splice. Furthermore, it was found that the need for reenterability at 0°F required a lower tear strength than was available from the best polymer produced during the elastomer investigation. The need for a low tear strength and mix viscosity and the desire for the lowest possible cost all appeared to be satisfied by the same solution--the use of an extender.

To satisfy all the design goals of the buried splice, the extender would have to have the following properties:

1. compatibility with the polyol, prepolymer and polyurethane
2. low viscosity
3. low pour point
4. negligible effect upon electrical properties and hydrolytic stability
5. splice component compatibility and
6. low volatility under field use conditions.

A program was carried out to develop an extender which had these characteristics,

The compatibility of the insulation with a gelled oil system, petrolatum, is well established in filled cables.

In general, high density polyethylene or polypropylene insulation in contact with gelled oils exhibit a minor loss in oxidative stability and mechanical properties which is considered acceptable. It was expected that compatibility of the insulation with an oil extended polyurethane would not present any problems.

The compatibility of the connector housing with oils was more complex. An aromatic oil is used as an extender in B Reclamation compound. This compound stress cracks and dissolves polycarbonate, commonly used for connector housings. Also, aromatic oils of low volatility exhibit high pour points.

Similarly, chlorinated paraffins crack polycarbonate and, at low volatility, exhibit high pour points. Ester based oils are commonly used in commercial greases and may exhibit low pour points as well as low volatility. However, esters are known stress cracking agents for polycarbonates. Paraffinic and naphthenic oils do not stress crack polycarbonate and may exhibit low volatility. Oils which are high in naphthenic content exhibit low pour points.

Based on these considerations and performance tests to be discussed in section IV, an extender was developed consisting of a paraffinic oil in combination with an ester. The effect upon the cost/performance characteristics of the encapsulant as a function of extender concentration was studied. It was found that the optimum encapsulant consisted of 35 percent low tear strength polymer and 65 percent extender.

#### Mechanical and Handling Properties

As expected, the effects of extending the basic polyurethane structures were dramatic. As shown in Table II, the tear strength was reduced from 24 lbs/in to 4.8 lbs/in by utilizing 65 percent extender. Moreover, it was found that there is only a 1.8 lbs/in increase in tear strength, when the encapsulant is cooled from room temperature to 0°F (see Table III). Another important aspect of the mechanical properties of the encapsulant is that, in spite of very low tear strength which leads to an ease of reenterability approaching that of a grease, the product still maintains elastomeric qualities. Thus, the product at room temperature has an average tensile strength of 31 psi and an average elongation of 132 percent. Consequently, as will be shown in Section IV, the encapsulant is strong enough to hold back a significant water head and will not shatter under impact forces even at 0°F.

Use of 65 percent extender also resulted in very low component pour points and viscosities, and low mix viscosities. The effect of temperature on the viscosity of the product is shown in Table IV. It will be noted that the mix viscosity of the encapsulant at room temperature is only 250 cps, 621 cps at 40°F and 1800 cps at 0°F. Because of these low viscosities complete encapsulation could be accomplished at 0°F. However, the effect of low temperatures on gel time had to be considered. The upper temperature limit for encapsulation is governed solely by the gel time-viscosity profile of the encapsulant. To establish the upper temperature limit on encapsulation, gel time as a function of temperature was determined, Table V. It was found that the gel time at 100°F was 15 minutes. At a temperature of 100°F the mix viscosity is 150 cps. This low mix viscosity permits complete encapsulation of splices in spite of the fast gel time. At higher temperatures, storage in the shade and other precautions should be taken to keep the gel

TABLE II  
EFFECT OF POLYMER CONTENT  
ON THE REENTERABLE ENCAPSULANT

Polymer Content	Tear Strength (lbs/in)
100	24.0
78	16.4
50	6.8
35	4.8
30	3.7

TABLE III  
EFFECT OF TEMPERATURE  
ON MECHANICAL PROPERTIES OF  
THE REENTERABLE ENCAPSULANT

Temperature (°F)	Tensile* Strength (PSI)	Elongation* (%)	Tear Strength* (lbs/in)
73	31	132	4.8
50	31	137	5.5
25	38	179	5.8
0	49	207	6.6

\*Determined per ASTM D412 at 20" min., 1" dia.

time as long as possible for ease of handling. The gel times of 103 and 260 minutes at 40 and 0°F were not considered to be excessive. However, it is unlikely that the encapsulant components would ever be conditioned to 0°F prior to use, as was the case in these experiments.

TABLE IV  
EFFECT OF TEMPERATURE ON  
HANDLING PROPERTIES OF THE REENTERABLE ENCAPSULANT

Temperature (°F)	Viscosity of Polyol (cps)	Viscosity of Prepolymer (cps)	Mix Viscosity (cps)
0			1800
40	700	235	621
50	550	195	490
60	360	155	340
70	250	120	250
80	180	90	200
90	125	65	165
100	125	50	150

#### Pour Point

Polyol	Prepolymer
-10°F	-10°F

#### Effects of NCO/OH Ratio

The new product was designed to be dispensed accurately and precisely into cans by means of mechanical metering devices. Such devices occasionally experience a drift of about  $\pm 3$  percent of the nominal weight. Knowledgeable packagers check and reset dispensers so that a full drift rarely occurs. Under field conditions, it is possible that extra material may be left in one of the cans. Thus, it was desirable to determine



TABLE V

EFFECT OF TEMPERATURE ON THE GEL TIME  
OF THE REENTERABLE ENCAPSULANT

Temperature (°F)	Gel Time* (Minutes)
0	260
40	103
58	50
73	29
88	19
106	11

\*Gel time is defined as the time to reach a viscosity of  $10^5$  cps.

just how much deviation in the mix ratio could be tolerated in the reenterable encapsulant.

It has been found that the product has a high degree of tolerance for mix ratio errors. As shown in Table VI, when the mix ratio was disturbed by an excess or deficiency of 12 percent isocyanate the gel time changed by only 1 minute and the tear strength only varied by  $\pm 0.5$  lbs/in. The rest of the mechanical properties, as well as the electrical properties and water-proofing quality of the encapsulant also exhibited relatively small and acceptable deviations from the mean. Even when gross and extremely unrealistic changes in the mix ratio of +29 and -24 percent NCO were made, the encapsulant gel time only varied by +5 and +14 minutes, respectively. Moreover, the mechanical properties, as well as the electrical and water absorption data indicate that these grossly off-ratio encapsulants would perform satisfactorily in the field. These data also indicated that a high degree of reproducibility should be demonstrated by the encapsulant. Quality control data from the first 25 production lots of the encapsulant and field experience show that the encapsulant is indeed highly reproducible.

TABLE VI  
EFFECT OF MIX RATIO ON  
THE REENTERABLE ENCAPSULANT

Mix Ratio (NCO/PU)	% Change in Mix Ratio	Gel Time (min)	Tear Strength (lbs/in)	Tensile Strength (psi)	Elongation (%)	Dielectric Constant at 1 MHz 25°C	Volume Resistivity (ohm-cm)	Water Absorbed After 4 Weeks Immersed at 25°C
22.78	+28	31	7.2	40	158	3.3	$4 \times 10^{11}$	0.071
19.01	+12	27	7.4	40	135	3.2	$4 \times 10^{11}$	0.058
17.81	-	26	4.4	36	128	3.5	$8 \times 10^{11}$	0.228
15.85	-12	25	4.3	36	172	3.3	$2 \times 10^{12}$	0.070
11.07	-24	40	1.5	24	133	4.0	$1 \times 10^{12}$	0.088

## Volatility

The maximum design service temperature in the buried environment is 90°F. Extensive weight loss tests, were run in closed environments which were analogous to those found in splice designs. These data repeatedly indicated that the weight loss after 500 hours at 140°F was only 0.2 percent. Performance tests were run to determine the effect of accelerated weight loss and are discussed in Section IV.

Feedback from various telephone companies indicated applications for the reenterable encapsulant in above ground pedestals and in some aerial closures. The design temperature in these environments is 140°F, and it was necessary to reduce the volatility of the encapsulant by developing a less volatile extender.

It was possible to reduce the volatility of the encapsulant by an order of magnitude by modifying the extender without significantly changing other characteristics of the encapsulant. Volatility data after 600 hrs at various temperatures are given in Table VII for the improved encapsulant. The temperature-mechanical property profile of the encapsulant and its modification are the same, within experimental error. As shown in Table VIII the modified encapsulant exhibits low mix viscosities over the field temperature range of 40 -100°F, although these viscosities are somewhat higher than those obtained with the original encapsulant, Figure 2. The improved encapsulant was also found to have a more favorable time-temperature curve than the original encapsulant. As shown in Figure 3, shorter gel times at low temperatures and longer gel times at high temperatures are obtained.

TABLE VII

WEIGHT LOSSES\* OF IMPROVED ENCAPSULANT

Temperature °C	Sample Weight	Weight Loss after 600 hrs.
98	88	4.0
71	86	0.6
61	91	0.4
53	87	0.2
RT	90	0.0

\* Encapsulant cured in disposable beaker, removed and exposed to environment.



TABLE VIII  
EFFECT OF TEMPERATURE ON HANDLING PROPERTIES  
OF IMPROVED REENTERABLE ENCAPSULANT

TEMPERATURE (°F)	100% RECLAIMED	92% RECLAIMED	80% RECLAIMED
40	800	600	400
50	600	400	300
60	400	300	200
70	300	200	150
80	200	150	100
90	150	100	75
100	100	75	50

The improved encapsulant was subjected to the same test program as previously described and it was found to meet all acceptance criteria. Therefore the encapsulant is being made available to the telephone companies for use in buried and underground plant. Specific applications in the aerial plant are under consideration.

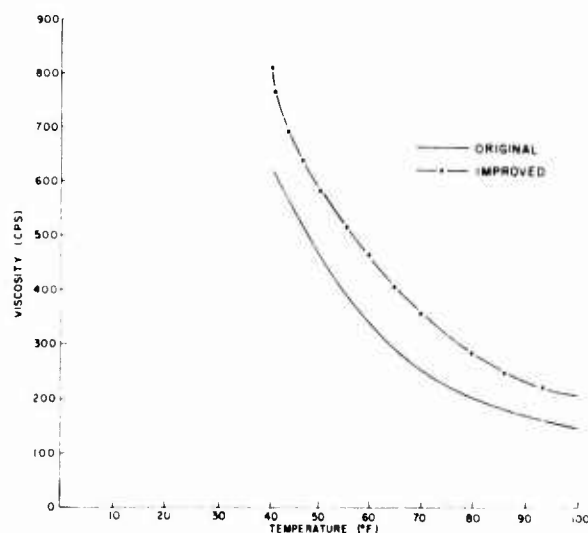


FIGURE 2  
COMPARISON OF REENTERABLE ENCAPSULANT MIX VISCOSITY-TEMPERATURE PROFILES

#### IV. PERFORMANCE TESTS

Performance of the reenterable encapsulant was examined as a function of the various components in a closure as well as in the filled closure system.

##### A. The Cable Sheath and Insulation

The current cable jacket materials are highly stress crack resistant and have been approved for use in waterproof cables where they age in contact with gelled oils (petrolatum)<sup>6,7</sup>. Some cable jackets installed prior to 1963 are more susceptible to stress cracking. However, the incidence of failure involving cables of the Alpeth and PAP construction (typical air core cable sheaths) is unknown and probably negligible.

No cable sheath failures have been reported with use of B Reclamation Compound<sup>5</sup>, an 92 percent oil extended polyurethane used to reclaim waterlogged cables. In tests to be described in Section IV stress cracking of the polyethylene jackets by the reenterable encapsulant was not observed. Thus, the engineering judgment was made that the encapsulant could be used on all air core and waterproof cables jackets in the outside plant.

The mechanical and oxidative properties of the insulation exposed to the oil extended polyurethane were considered. The presence of an oxidation stabilizer in the polyurethane insured good oxidative performance of the insulation at the air interface, if present. High density polyethylene and polypropylene insulation aged at 70°C for 30 days in pigtail configurations did not exhibit any mechanical degradation. Low density polyethylene insulation in cables reclaimed with B Reclamation Compound has been successfully reentered and spliced although softened by the reclamation compound. In the case of PVC insulation as in load coil stubs some plasticizer extraction could occur but no gross deterioration of properties is possible.

Thus, the engineering judgment was made that the oil extended encapsulant could be used on all plastic insulation in the outside plant.

##### B. Hardware

Sealing tapes may be softened by the encapsulant during curing. Since the performance of the filled closure is not dependent on its presenting a hermetic seal, the softening is not a problem. This was confirmed by performance tests on the filled closure system. The above arguments on polypropylene insulation also hold for the polypropylene closure.

Polycarbonate is highly sensitive to stress. A properly designed part should not be strained above 0.6%. Many common liquids will crack, craze or dissolve polycarbonate at lower strains. Annealing increases the stress cracking susceptibility. A test was designed in which an annealed flexural bar was strained to 0.75% and exposed to the encapsulant at room temperature for 30 days. The requirement was that the bar should not craze or crack during or after curing. The encapsulant passed this test. It should be noted that the susceptibility of polycarbonate to cracking increases as the temperature increases. Thus, at 50 C test bars crazed in air as well as in the encapsulant.

Polycarbonate connector housings (Bell System 700 and 710 series) were also tested. These connectors were known to exhibit low molding stresses based on tests using known stress cracking agents, (e.g., hexane will craze polycarbonate strained at 0.8% but does not affect the 700-710 series connector). The reenterable encapsulant did not craze these connectors

after 30 days below 60°C. At 70°C crazing occurred. However, the encapsulant around the crazed connectors could be ripped off without destroying the connector housing. Thus, the engineering judgment was made that if some field conditions not duplicated in the laboratory resulted in crazing of the polycarbonate connectors, the integrity of the splice was not degraded. However, the connector housing must be molded with low residual strain levels because of the susceptibility of polycarbonate to cracking. Poorly designed polycarbonate connector housings can crack in an ambient air environment.

Other materials which may be used with other closure systems would have to be examined individually to ensure long term performance.

### C. The Encapsulant

Encapsulation of new construction at 0°F is unusual. However, reentry is not. Thus, craft sensitivity was tested at low temperatures. A highly viscous encapsulant would be difficult to mix and pour at 0°F. With the new encapsulant, the prepolymer is poured into the polyol. It must exhibit a low viscosity for ease of pour. Although an allowance is made in the packaging for prepolymer remaining in the original can, this amount varies under field conditions. The gelling characteristics of the encapsulant were found to be insensitive to possible mix ratio violations, as expected from the discussion in Section III. Thorough mixing at 0°F is accomplished in 2-3 minutes since the viscosity is low and there is no precipitate to disperse. Pouring is equally easy. The gel time for the improved encapsulant of about 80 minutes at 40°F is acceptable. However, conditioning of the encapsulant at higher temperatures accelerates the gel time and is effective in cold weather.

Addition of water to Part II of the mix followed by thorough mixing did not result in any foaming. Water, which is heavier than the encapsulant, settled to the bottom or was encapsulated. This is in marked contrast to many older encapsulant materials.

Reenterability of an encapsulated splice without tools was accomplished at temperatures well below 0°F. Bonding of new pours on existing encapsulant was verified, that is, failure on tearing was cohesive and not at the interface. However, the reenterable encapsulant will not bond to some commercial encapsulants.

### D. The Closure System

The reenterable encapsulant was intended for use in the buried and underground plant using PIC air core and filled cable with moisture resistant connectors. As previously indicated, feedback from the telephone companies also indicated desired applications in pedestals and aerial closures.

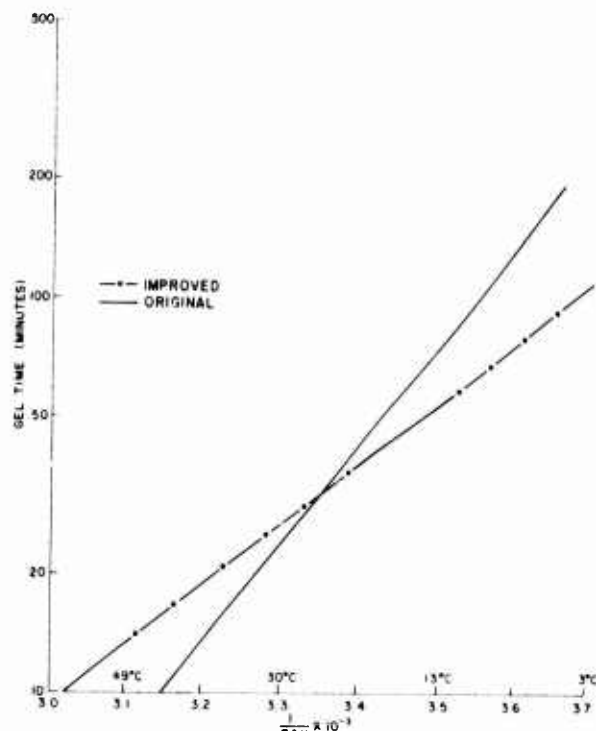


FIGURE 3  
COMPARISON OF GEL TIME-TEMPERATURE CURVES FOR REENTERABLE ENCAPSULANT

For the buried and underground exposures performance tests were directed to determining the ability of the splice to resist water migration. Since there are field conditions which may not be reproducible in laboratory performance tests, the procedure was biased to failure by using connectors which were not moisture resistant. Eight splices were constructed using air core and filled cable of 50 and 400 pair 22 gauge copper. These were encapsulated at 32 and 77 F. Some splices were placed in one foot of water saturated sand and cycled from 0 to 100 F every 12 hours for 50 days. Other splices were placed under 3 feet of water for 50 days at room temperature. To aggravate the latter tests, all splices were also exposed to a 5 foot head of water through the cable sheaths during the tests. Insulation resistance tip to ring, tip to ground and ring to ground was monitored. The requirement was a minimum insulation resistance of  $10^9$  ohms at completion of the tests. At completion of the tests, splices were reentered at various temperatures. Some were reencapsulated and retested for 25 days. The insulation resistance remained in excess of  $10^9$  ohms. The cycle tests are still in progress.

For exposure above ground, the number of tests was reduced. Encapsulated splices with the closure removed were exposed to 140°F for various periods of time. Using the encapsulant with the higher volatility discussed in Section III, an encapsulant weight loss of about 5% was allowed. At this point the closure was immersed in the wet sand for 100 cycles from 30-140°F. The insulation resistance remained in excess of  $10^9$  ohms. Then, this splice was again

aged at 140°F for a total weight loss of 15% and reimmersed in wet sand. After 100 cycles from 0 to 100°F, all insulation resistance readings remained high. An encapsulated splice using the improved encapsulant is being aged at 140°F for subsequent immersion in wet sand.

#### V. CONCLUSION

An encapsulant material which combines the best features of polyurethanes and greases has been developed. It is a non-TDI based, two component, rapid gelling, extended polyurethane. Because of low component viscosity and mix viscosities, even at 0°F, the polyurethane encapsulant is easily mixed and penetrates all void spaces of the splice. It does not foam in presence of water. End use characteristics are: high volume resistivity, low water absorption, splice component compatibility and very low tear strength, coupled with high elongation and adequate tensile strength. The material is not tacky and does not present cleanup problems and is quite insensitive to NCO/OH ratio. The encapsulant bonds to old pours to restore splice integrity. Laboratory data and performance tests under simulated adverse field conditions show that the encapsulant can be used in buried, underground and aerial plants. The encapsulant is easily reentered without use of tools at temperatures below 0°F.

#### REFERENCE

1. Axelrood, S. L., C. W. Hamilton, K. C. Frisch, Ind. Eng. Chem., 53, 889 (1961).
2. Quant, A. T., Soc. Plast. Eng. J. 15, 298 (1959).
3. Axelrood, S. L. and K. C. Frisch, Rubber Age (N.Y.) 88, 465 (1960).
4. Turbett, R. J., Proceedings of the 21st International Wire and Cable Symposium, 1972.
5. Kaufman, S. and R. Sabia, Proceedings of the 21st International Wire and Cable Symposium, 1972.
6. McCann, J. P., R. Sabia and B. Wargotz, 18th International Wire and Cable Symposium, 1971.
7. Bostwick, R., Proceedings of the 23rd International Wire and Cable Symposium, 1974.
8. Sabia, R. and B. Wargotz, unpublished data.



Raffaele Sabia

Raffaele Sabia, a graduate of St. Francis College of Brooklyn (B.S.) and Polytechnic Institute of Brooklyn, (Ph.D.), was employed by the Polymer Chemical Division of W. R. Grace prior to joining Bell Telephone Laboratories in 1963. Since 1963 he has been active in the research and development of materials for application in the wire and cable area and in the preparation of the text in the series "Physical Design of Electronic Systems" published by Prentice Hall. Since 1967 he has been supervisor of the Chemical Engineering Group in the Transmission Media Laboratory.



Melvin Brauer

Melvin Brauer received his B.A. degree from Hunter College and did graduate work at this college. Prior to joining NL Industries in 1972 he was employed by Hercules Incorporated as a propellant development chemist. Since 1973 he has been exclusively involved in the development of potting, encapsulation and cable reclamation compounds. He has two patents pending in connection with this work.

# A "Universal" Communication Compound

## ABSTRACT

A candidate, universal splice encapsulating and damming compound for both plastic and pulp insulated cable has been formulated. A polydiene-type polyurethane resin was optimized with regard to gel time and mixed viscosity as a function of temperature and mixed viscosity as a function of time.

Utilizing the new compound and a direct sheath injection method, pressure dams in both PIC and pulp cable were prepared and thermally cycled. The performance test results confirm the "universality" of the compound and its method of use.

## INTRODUCTION

Historically, in order to satisfy its rapidly evolving construction practices, the telecommunications industry has presented numerous, demanding material development challenges to the engineer and chemist. Working together toward the common, ultimate goal of an efficient, trouble-free plant, they have made many outstanding, coordinated contributions: the transistor, the laser, optical fibers, compositions for waterproofing buried cable, compounds for reclaiming wet cables, esthetic and improved telephone pole preservatives, and improved polyolefin conductor insulation.

In spite of these advances, the everyday task of protecting splices and plugging air core cables, offers yet another material development challenge. In recent years, the diversified nature of cable construction and conductor insulation has unfortunately led to a proliferation of encapsulating compounds (primarily polyurethane resins) and their application practices in an attempt to satisfy a particular application requirement.

For the ultimate user, this has led in some instances to confusion, hence the occasional misuse of these compounds. For many of these demanding applications, the resin selected may have been chemically and/or physically incapable of satisfactory performance. Unfortunately, the

all too frequent result has been cables with leaky plugs and/or wet encapsulated splices. The obvious solution — a more "universal compound" with simplified application practices should be sought. This paper describes our efforts to achieve these goals.

## PREVIOUS WORK — AN UPDATE

In our previous paper<sup>1</sup>, a modified open-sheath method using a polyurethane compound was described, which successfully and reliably plugged PIC and pulp cables. Our attempts at that time to utilize the popular "sheath injection method" gave nonreproducible results, particularly at lower temperatures (20°F). As a result, this method was not recommended. During the latter course of this work it became evident that the major deficiency of the total system was the polyurethane compound. Obviously, one or more of the compound's interdependent variables were not optimized in order to reliably perform. We shall discuss in detail the deficiencies of this compound and of other typical polyurethane compounds in the body of the paper.

As a result, a program was initiated to formulate a more universal splice encapsulating and blocking compound by attempting to optimize several important variables. In our experience, the successful damming of air core cable has been more difficult to achieve than that of reliably encapsulating a cable splice. In fact, with very few exceptions a resin which will plug air core cable will also serve to encapsulate its splices. Thus, most of our efforts were directed toward reproducibly damming PIC and pulp cables by a sheath injection method.

## PREFERRED RESIN SYSTEM

For one or more reasons the following two-part, ambient temperature curing resin systems were considered and rejected: polyester-styrene, bisacrylates-styrene, polyacrylates in their monomer and/or plasticizer, polyisocyanurates and liquid elastomers. The obvious advantages and disadvantages of the remaining candidates, epoxy and polyurethane resins are reviewed in Table I.

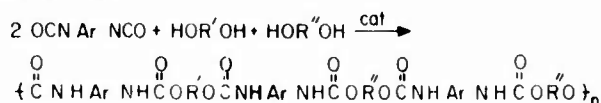
TABLE I

<u>EPOXY RESINS</u>	VS.	<u>"TDI-FREE" POLYURETHANES</u>
— High Tensile Strength		— Moderate to Low Tensile Strength
— High Exotherm		— Relatively Low Exotherm
— Poor Thermal and Mechanical Shock Properties		— Good Shock Properties
— Fair Electrical Properties		— Fair to Good Electrical Properties
— Amine Toxicity		— Low Toxicity
— Good Adhesion		— Adequate Adhesion
— High Cost		— Moderate Cost
— Resin Cure: Moisture Insensitive		— Resin Cure: Moisture Sensitive
— Gel Time: Requires a Formulation Change		— Gel Time: Function of Catalyst Concentration
— Good to Fair Hydrolytic Stability		— Good Hydrolytic Stability
— Viscosity: Moderate to High (Variable)		— Viscosity: Moderate to Low (Variable)

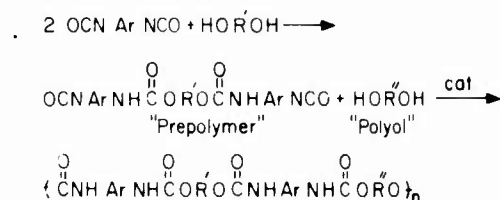
Polyurethanes are still considered to possess the greatest potential to "universally" satisfy both the requirements of pressure damming and splice encapsulating.

## THE BASIC TYPES AND CHEMISTRY OF POLYURETHANES

Most polyurethane resins, presently utilized in splicing and damming applications are two-part, reactive, ambient temperature curing, low viscosity systems. One part contains a polyfunctional aromatic isocyanate\* and the other, one or more polyfunctional alcohols. Reaction can be accomplished most simply in a one-step process, in which all reactants are initially mixed together to give a random copolymer.



On the other hand, the reaction may be conducted in two distinct stages. The first would involve, for example, the reaction of 2 moles of diisocyanate with 1 mole of diol to form a prepolymer (Part A). When this reaction is completed, a second mole of diol (Part B) would be added and the polymerization continued to give an alternating (block-type) copolymer.

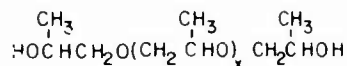


We prefer the prepolymer method for several reasons:

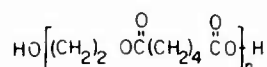
- 1) The desired weight ratio, A/B = 1 can be more easily attained.
- 2) Incompatible polyols can often, after prepolymer formation, be incorporated into the polymer backbone to give a more compatible resin.
- 3) Partial prereaction of the isocyanate decreases further the total toxicity of the system, even though polyisocyanates of low volatility may be utilized.
- 4) The resin formulator has more control over crosslinking sites and/or the ratio of high and low molecular weight segments, which he may want to incorporate into the polymer.

Polyurethanes are often described according to the type of polymeric polyol utilized in their preparation; polyether, polyester, ricinoleate (castor oil and its derivatives), hydroxy terminated polydienes or mixtures of these polyols.

### 1) Polyethers — poly(oxypropylene) polyols

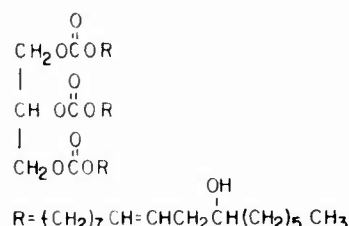


### 2) Polyesters — polyethylene adipate

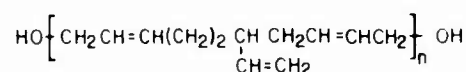


\*The most common aromatic diisocyanate, 2,4-toluene diisocyanate (TDI), was not utilized in these studies because of its toxicity. In addition, no reactive aromatic or aliphatic amines were considered in our formulations because of their potential carcinogenic and/or toxicological properties.<sup>2</sup>

### 3) Ricinoleates — castor oil and derivatives



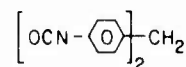
### 4) Polydienes — hydroxy terminated polybutadiene



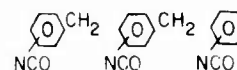
Each type possesses chemical and economical advantages and disadvantages. In our work we utilize all except the polyesters in an effort to combine the attributes of each class while attempting to minimize their specific, inherent disadvantages. In addition, lower molecular weight diols and triols (reinforcing polyols) such as 1,4-butanediol, dipropylene glycol, trimethylolpropane, etc. are often used to strengthen the polymer by crosslinking and/or by increasing the intermolecular hydrogen bonding (cohesive energy of urethane group = 8.7 kcal/mole).

In the majority of polyurethanes being specifically formulated for the communications industry, two types of polyfunctional aromatic isocyanates are most commonly used:

#### 1) Diphenylmethane diisocyanate (MDI)



#### 2) Polyaromatic Polyisocyanate (PAPI or MR)



## FOAMING VS. NON-FOAMING RESINS

Polyurethanes which exhibit limited foaming during cure have been formulated and tried, but not widely accepted for encapsulating cable splices. In fact, both the manufacturer and user take care to avoid excessive foaming within a cable splice.

However, foaming resins have been widely utilized in cable pressure damming.<sup>3</sup> It was reasoned that foaming counteracts the normal resin shrinkage to form a compressive seal within the cable. Masterson<sup>4</sup> in 1969 found that a number of commercially available, foaming polyurethanes successfully blocked 100 pr., 22 gauge Alpeh cable with uncoated shields by a sheath injection method.



In spite of this, we chose to optimize a "non-foaming" formulation for the following reasons:

- 1) The degree of foaming, hence resin density is very sensitive to and inversely proportional to the ambient temperature. It was felt that a prime requisite of a universal compound should be reproducible resin density.
- 2) Convenient packaging systems for polyurethane foams are presently relatively expensive, thus little or no economic advantage could be realized by their utility.
- 3) When moisture is either internally or externally present, all polyurethanes exhibit varying degrees of foaming. In spite of the precautions taken during their manufacture or use, most resins will at some time be exposed to moisture. Thus, in practical applications, their final volume shrinkage will be minimal, usually less than 2%.

#### TARGET REQUIREMENTS — UNIVERSAL SYSTEM

Obviously, both compound and practice of use should be conceived, developed and made available with "economically reliable performance" as the main objective. In order to achieve this, there are a number of requirements which the total system should meet.

##### A. Application Requirements

1. Compound
  - a. Storage stability
  - b. Convenient to mix and dispense
  - c. Free of objectionable odor
  - d. Non-toxic, non-carcinogenic and non-hazardous
  - e. Low volume shrinkage
  - f. Possess an optimized gel time and mixed viscosity to reliably splice encapsulate or block both PIC and pulp cable over a wide temperature range (20° to 95° F) within a reasonable length of time (2 hours).
2. Method of Use
  - a. Simple as practically possible
  - b. Well defined (Require a minimum of judgment)
  - c. Time saving
  - d. Reliable

##### B. Post Application Requirements

The service lifetime of a cable splice or block in an adverse environment is all important. In order to predict these lifetimes, accelerated and extreme screening tests are first performed on the compound. These are followed by application tests on the cable splice or block, again under accelerated conditions.

##### 1. Compound

- a. Non-corrosive to metals (Cu, Al, Fe, etc.)
- b. Chemically inert with regard to all types of conductor insulation, splicing connectors, mastics and tapes.
- c. Resistant to chemicals (oils, solvents, greases, acids, bases, etc.)
- d. Hydrolytically and thermally stable over a wide, but practical temperature range.

- e. Possess adequate electrical and physical properties to satisfy application requirements.

##### 2. Total System

###### Cable Splice Protection

- REA Specification
- Cable Manufacturers' Specification
- Connector Manufacturers' Specification
- Users' Specifications (Continental, General Telephone, Bell System, etc.)

###### Cable Plugs

- J Plug Compound

With few exceptions, the majority of the polyurethane resins and their accompanying methods of use, which are available to the industry, satisfy to varying degrees most but not all of these broad requirements, and as a result are not universal. This in no way implies that these compounds and practices do not perform well for the specific application or applications for which they were intended.

#### INITIAL WORK — AN ASSESSMENT OF SEVERAL CANDIDATE COMPOUNDS

Recall that our previous attempts to reproducibly dam PIC and pulp cables over a wide temperature range (20° to 95° F) were unsuccessful because of compound deficiencies. Since this compound (A) was a polyether-type urethane, it was of interest to compare it with two other commercially available encapsulating and damming compounds (B and C), representing castor oil and polydiene-types respectively.

(Note: A, B and C were all catalyzed with the same catalyst.)

In other words, which chemical type of polyurethane would best serve as a building block to "tailor-make" a universal resin? The "typical properties" of each compound are given in Table II.

It was evident that the question could not be answered by comparing the data in Table II. All possess adequate properties to apparently satisfy the requirements of the application or applications for which they were formulated. The excellent hydrolytic stability, the electrical properties and the extremely low glass transition temperature (T<sub>g</sub>, the temperature at which a compound goes from a rubbery to glassy state) of the polydiene compound (C) are worthy of particular attention. It is important that the compound possess a low T<sub>g</sub>, in order for it to internally absorb the extreme thermal and mechanical shocks to which a cable splice or dam may be subjected throughout its service lifetime.

#### IMPORTANT TEMPERATURE DEPENDENT VARIABLES

It was obvious that initial compound performance would be the most difficult to achieve at the high and low application temperature limits.

At low temperatures (20° F), the compound must possess a mixed viscosity sufficiently low to penetrate the tight conductor bundle (also conductor insulation in pulp cables) and between the sheath layers. After penetration, it must cure at a reasonably rapid rate (< 2 hours) in order to avoid a prohibitively long wait until application of pressure.



**TABLE II**  
**PROPERTIES OF COMPOUNDS A, B AND C**

I. Uncured Properties	Method	A	B	C
— Viscosity (cps, 25°C)	Brookfield Viscometer			
Prepolymer		4,000-4,500	3,500-4,000	5,500-7,000
Polyol		800-1,000	700-900	2,000-3,000
Mixed (1 minute)		1,750	1,200	3,200
— Gel Time (min., 25°C)	Sunshine Gel Meter			
	100 g. Mass	20-25	14-17	9-12
— Maximum Exotherm (°C)	100 g. Mass	85-88	80-82	61-64
II. Cured Properties				
— Tensile Strength (psi)	ASTM D-412-68	1500-2000	600-700	500-600
— Elongation (%)	ASTM D-412-68	150-200	100-120	180-200
— Hardness (Shore A)		85-90	67-70	68-70
— Density (gm/cc)	3M*	1.10	1.07	1.05
— Volume Shrinkage	3M*	1.53	1.57	1.52
— Copper Corrosion	3M*	None	None	None
— Fungus Resistance	ASTM G-21-70	"O" Growth	"O" Growth	"O" Growth
— Hydrolytic Stability (7 days, H <sub>2</sub> O, 100°C)	3M*			
a. Weight Increase (%)		2.5-3.5	.95-1.0	.57
b. Shore A Loss		10-15	9-10	8
— Heat Stability (21 days, 135°C)	3M*			
a. Weight Loss (%)		3.0-3.5	4.0-4.5	2.75-3.0
b. Shore A Increase		10-15	10-12	15
— Thermal Shock	3M* (10 cycles, 1/4" Insert, -55°C to 130°C)	No Cracking	No Cracking	No Cracking
— Glass Transition Temperature (°C)	3M*(DTA)	-39 to 9	-12 to 20	-76 to -65
III. Electrical Properties				
— Dielectric Strength (volts/mil) (125 mil Sample)	ASTM D-149-64	450-500	550	475-500
— Dielectric Constant (10 <sup>3</sup> Hz, 25°C, 50% RH)	ASTM D-150-70	5.3	3.9	3.7
— Dissipation Factor (10 <sup>3</sup> Hz, 25°C, 50% RH)	ASTM D-150-70	0.065	0.094	0.022
— Insulation Resistance (ohms) (28 days, 40°C, 96% RH)	3M*	1.0 x 10 <sup>10</sup>	4.0 x 10 <sup>13</sup>	2.0 x 10 <sup>12</sup>

\*Internal 3M Test Method

At high temperatures (95°F), the compound's mixed viscosity should still be sufficiently high to prevent excessive flow down the cable. This is partially compensated for by the compound's increased rate of reaction and viscosity build-up at higher temperatures. The latter must be carefully controlled in order to allow sufficient time for the compound to thoroughly penetrate all of the conductor interstices and sheath layers.

In other words, to insure reliable, initial performance, the mixed viscosity and the gel time of the compound must be carefully optimized at both ends of the temperature spectrum.

With this background, we shall now examine these variables of Compounds A, B and C as a function of temperature. In addition, the compounds' mixed viscosities as a function of time at various temperatures will also be evaluated. Hopefully, this will answer the question, "Which chemical-type of polyurethane would possess the most potential for a universal resin?"

#### AVERAGE MIXED VISCOSITY — TEMPERATURE PROFILES

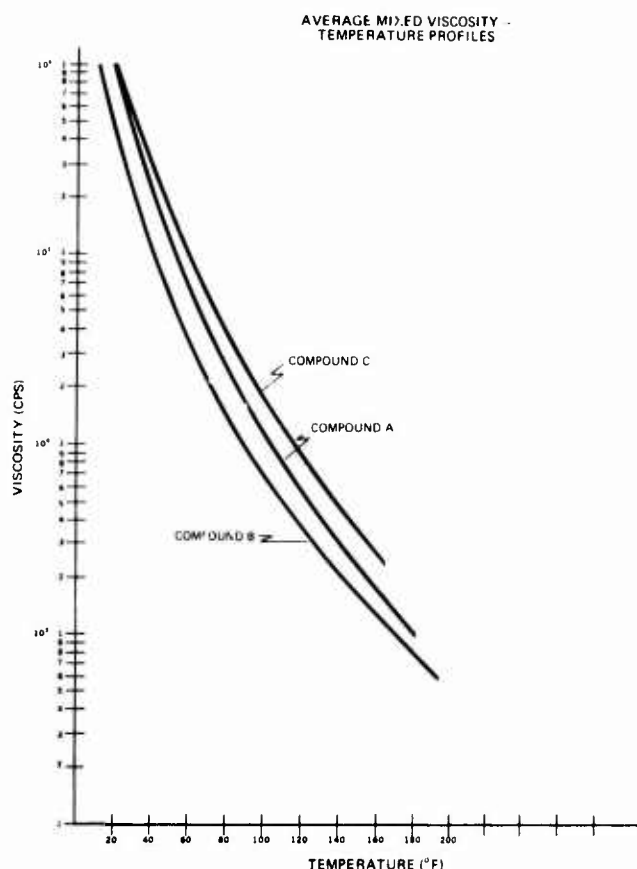
The measurement of the absolute mixed viscosity of a polyurethane over a broad temperature range was imprac-

tical. However, in order to compare the potential, initial performance capabilities of Compounds A, B and C with regard to viscosity and then correlate this with chemical structure, it was important that we have some idea of these profiles.

To accomplish this, the viscosity of the polyol and prepolymer of each resin was independently measured, then arithmetically averaged at the same temperature to give an "average mixed viscosity." This method of normalization, of course, neglected the effects of the catalyst, reaction exotherm and the heat generated by mixing. Agreement of these average mixed viscosities and actual mixed viscosities was surprisingly good at 75° and 98°F. However, at 20°F, a large discrepancy (70,000 cps) was noted in the case of Compound C, apparently due to the heat of mixing.

The actual procedure involved heating the polyol or prepolymer to 200°F or cooling them to 10°F in a foam insulated cup, then both the temperature and viscosity were continuously recorded until room temperature was reached. These profiles are shown in Figure I.

FIGURE I



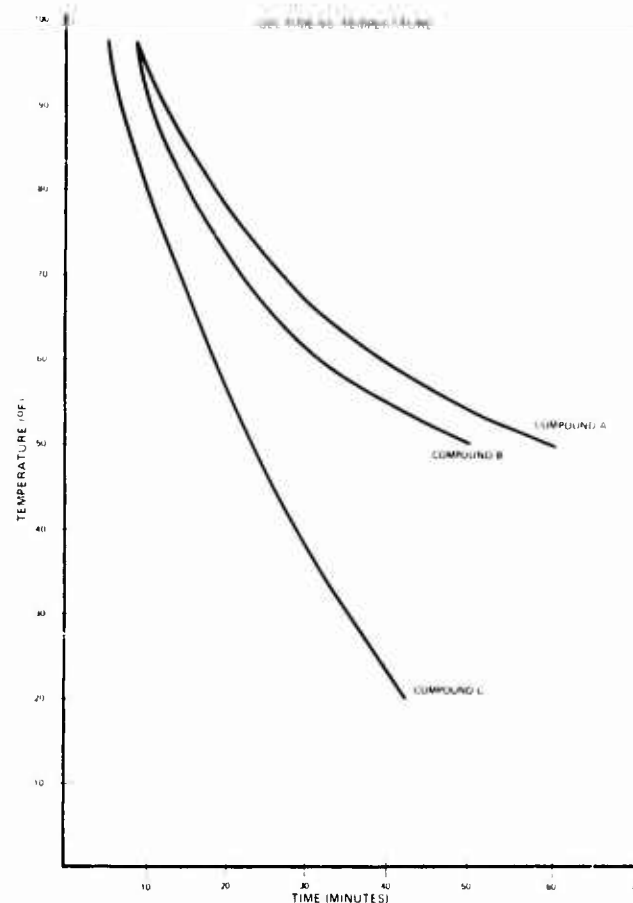
Although Figure I depicts the worst case for each of the compounds at 20°F, it was apparent that all possessed mixed viscosities of greater than 10<sup>4</sup> cps, which is considered too high to effect the penetration required to successfully block or splice encapsulate PIC or pulp cable. Of the three, the castor oil compound (B) appeared to be the best candidate. However, it is important to note that the curve of Compound C actually intercepted the curve of

Compound A, at about 25°F even though its viscosity was significantly higher at room temperature.

#### GEL TIME VS. TEMPERATURE

The rate at which the compound will cure over the entire temperature range is of primary importance for initial performance within the cable. The gel times of the compounds were determined on a 100 gram mass of resin with a Sunshine Gel Meter in a chamber, stabilized at the desired temperature. All samples were equilibrated for 12 hours in the chamber at the testing temperature prior to mixing and testing. The results are shown in Figure II.

FIGURE II



Only the polydiene compound (C) possessed measurable gel times over the entire temperature range. Both the polyether (A) and castor oil (B) compounds appeared to gel within 60-80 minutes at 20°F; however, on warming they became thermoplastic and decreased in viscosity. In addition, it was found that neither A or B cured at 40°F. Both of these compounds appeared to assume a glassy state at these temperatures, thus losing a degree of freedom of molecular motion required for reaction. This again in no way implies that properly formulated and catalyzed polyurethanes based on polyether polyols and/or castor oil and/or its derivatives would not cure at 20°F or below. However, in these studies the polydiene compound (C) was clearly superior in this regard. Its state of cure was by no means optimum since all polyurethanes achieve this only after an extended time at high temperature; it was, however, sufficiently cross-

linked to be non-thermoplastic after warming to room temperature. This was attributed to: (1) the unsaturated nature of the polydiene polyol's backbone resulting in a lower glassing temperature and (2) the increased reactivity of the allylic hydroxyl groups present in the polyol.

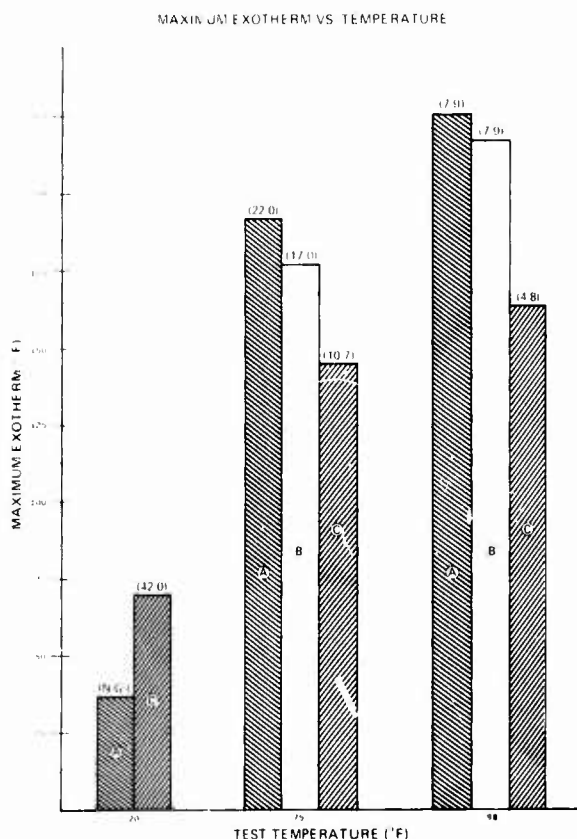
#### MAXIMUM EXOTHERM OF COMPOUNDS A, B AND C

The amount of heat generated by a curing polyurethane within a cable splice cannot be excessive (200°F) since damage to the insulation and/or cable sheath could result. The maximum temperature reached will depend upon:

- Cross Sectional Area of Curing Resins
- Ambient Temperature
- Gel Time
- Conductor Density (Heat Sink)
- Type of Catalyst
- Polymer Concentration
- Chemical Type

Recall that the Compounds A, B and C were all catalyzed with the same catalyst, but with varying concentrations to effect different gel times. In spite of this, it was hoped that some comparison of the three chemical types could be made by measuring the maximum exotherm of a 100 gram mass of curing compound at 20°, 75° and 98°F. This data is presented in Figure III. For reference, the gel times (min.) are given in parentheses.

FIGURE III



From Figure III, it can be seen that the polydiene compound (C) exhibited lower exotherms at all ambient temperatures studied except at 20°F, where neither Compound A or B cured. This was somewhat surprising since Compound C had a significantly shorter gel time than Compound A or B at all ambient temperatures. The castor oil compound (B) was slightly superior to the polyether compound (A); however, both are considered to exhibit reaction temperatures at 98°F which could potentially deform or damage conductor insulation. However, it should be pointed out that in actual application these temperatures are rarely achieved within the cable because of heat transfer by the metallic conductors.

#### VISCOSITY VS. TIME

It is important to have an understanding of how the viscosity of the compound increases in the cable during cure as a function of time at various temperatures. This relationship is commonly called the compound's induction curve, and the time from initial mixing to the time at which a sharp viscosity increase is noted — the induction period. Again, these curves could be obtained for Compounds A and B at only 75° and 98°F.

FIGURE IVA

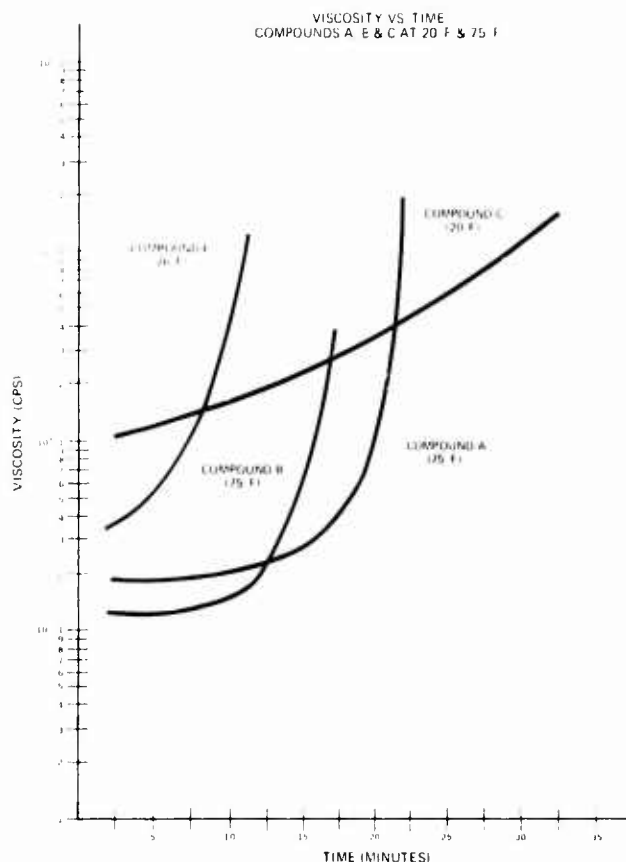
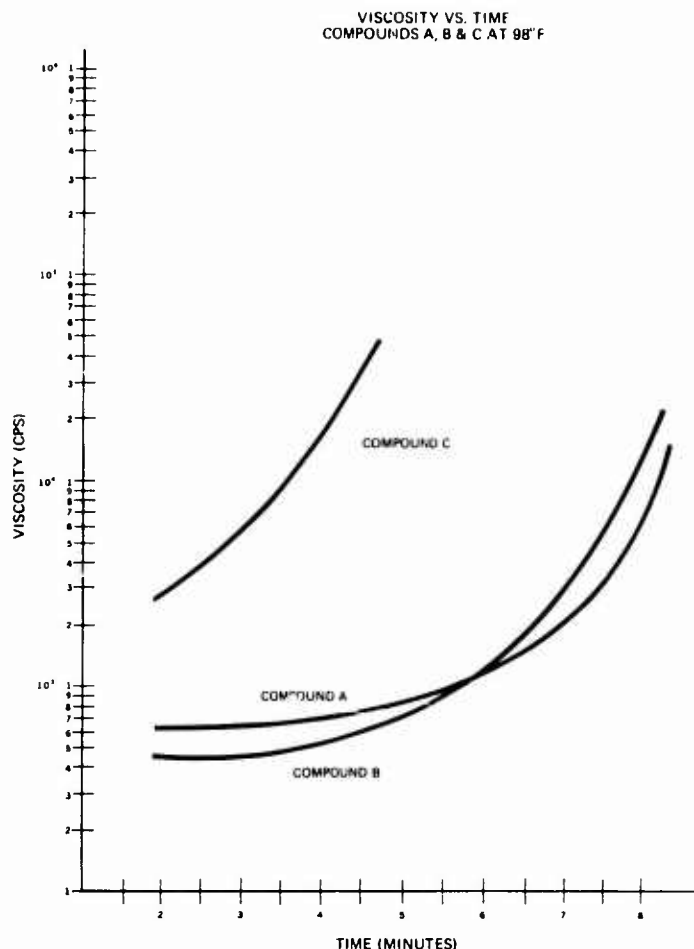


FIGURE IVB



The shape of these induction curves depends primarily upon the following compound variables:

- Type and concentration of catalyst
- Chemical type of urethane
- Polymer concentration
- Average molecular weight of reacting species
- Reaction exotherm

In a given polyurethane system, the catalyst has the greatest influence on the shape of the compound's induction curve. In Compounds A, B and C this variable was constant and allowed us to study the effect of other variables on the curves.

The effect of the average molecular weight of reacting species and reaction exotherm can be seen by comparing the curves of Compounds A, B and C at 75°F. At this temperature, the castor oil compound (B) actually decreases in viscosity for a period, due to the reaction exotherm and a relatively high concentration of low molecular weight reacting species. The rate of reaction rapidly overcomes this viscosity decrease (due to the reaction exotherm) — the viscosity then increases rapidly to gel. The polyether compound (A) does not decrease in viscosity after mixing, remaining relatively constant for 10-15 minutes. Within this

time interval, the reaction of the higher molecular weight polyether polyols balances the viscosity decrease due to the reaction exotherm. In contrast, the polydiene compound (C), with its relatively low reaction exotherm and high molecular weight species, increases in viscosity quite rapidly exhibiting little or no induction period.

It can be seen that temperature does not appreciably alter the general shape of the curves. At higher temperatures, the curves are displaced downward toward lower viscosities and are compressed because of the faster gel time. The reverse being the case at the lower temperatures.

The optimum shape of the induction curve to best satisfy the requirements of a universal compound can be debated. It has generally been accepted that a curve comparable to Compounds A and B would be optimum for damming pulp cable. Presumably, the compound has time to penetrate into the conductor bundle, sheathing and insulation before rapidly increasing in viscosity. On the other hand, only compound penetration between the sheathing and into the conductor bundle is required in PIC cables. Compounds with induction curves comparable to A and B may flow too far down the cable, resulting in an excessively long block or splice. Some manufacturers have recommended mixing their compounds and waiting for a specified time until the viscosity of the compound has increased in order to overcome this. In this case, an induction curve comparable to that of Compound C probably would be optimum. It is our opinion that a compound possessing an induction curve between the two extremes might be optimum.

#### SUMMARY OF INITIAL WORK

From the results of these studies the reasons for our non-reproducible attempts to block PIC and pulp cable by a sheath injection method with Compound A were apparent.

- 1) The mixed viscosity of the resin was extremely temperature sensitive and too high to thoroughly penetrate the conductor bundle of the pulp cable, particularly at low temperature. Similarly, it could not progress far enough between the inner and outer sheath to reliably effect a block in PIC.
- 2) Its gel time was too long to prevent compound flow down paths of least resistance in PIC, although this was partially compensated for by its relatively high viscosity.
- 3) It did not cure at temperatures of 40°F or below.
- 4) Its induction curve was suitable for blocking pulp but not optimum for PIC cable.

These deficiencies were further exemplified by studying leak paths with dye solutions and plotting compound flow profiles from 2" cross sections of failed cable samples. The results showed that the majority of the PIC failures occurred between the inner and outer sheath interface, while the pulp specimens leaked near the center or bottom of the conductor bundle. In addition, the frequency of failure was proportional to the pair count. This can only be generalized because of differences in cable design and uniformity.

Also apparent was the fact that neither Compound B or C, as formulated, would satisfy the requirements of a universal resin. However, it was concluded that Compound C possessed more potential than either A or B, particularly with regard to its low temperature curing capability, and lower reaction exotherm. Thus, we initiated our formulation studies utilizing the basic starting materials of a hydroxy-terminated polybutadiene of about 2500 molecular weight and a polyaromatic polyisocyanate.

### A UNIVERSAL CANDIDATE — COMPOUND U

From our previous studies on Compounds A, B and C with regard to gel time and viscosity as a function of temperature, we were able to establish what we felt were specific, yet realistic target requirements to insure that Compound U would initially perform in both cable splices and dams over a broad temperature range. In addition, we hoped that reformulation would not alter Compound C's excellent cured properties of low temperature flexibility and hydrolytic stability. These requirements are outlined in Table III.

TABLE III  
TARGET REQUIREMENTS — COMPOUND U

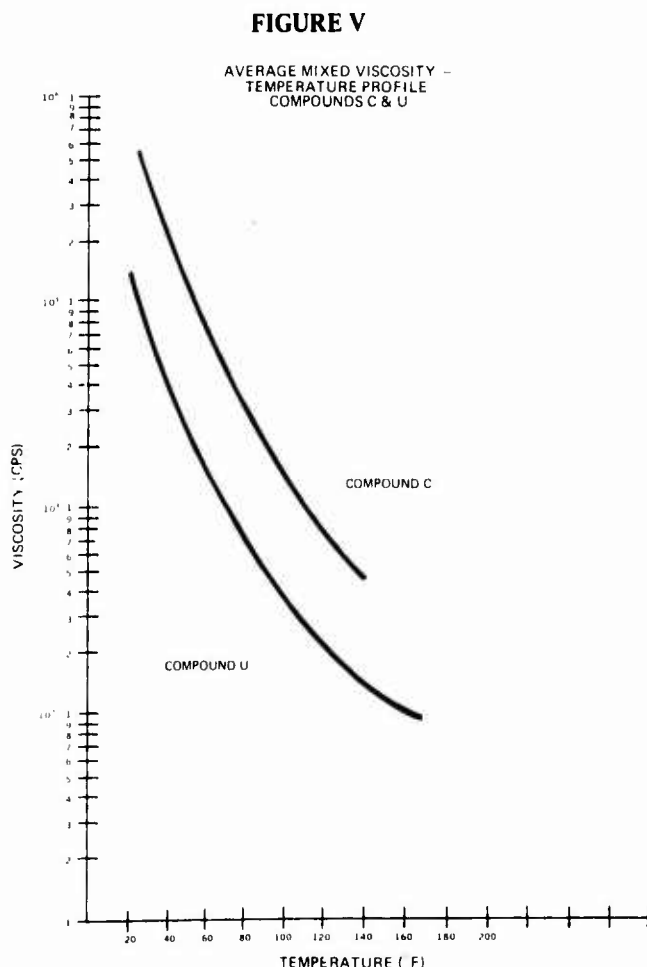
	20°F	75°F	98°F
VISCOSITY MIXED (cps)	< 10,000	1,000-1,500	> 500
GEL TIME (Min.)	120	15-20	> 10
EXOTHERM (°F)	—	—	< 175

Recall that the primary deficiencies of Compound C were a short gel time, a high mixed viscosity and possibly its steep induction curve.

Let us now compare Compound U and C in the manner of our earlier studies.

### MIXED VISCOSITY VS. TEMPERATURE

The average mixed viscosity-temperature profiles for Compounds C and U are shown in Figure V.

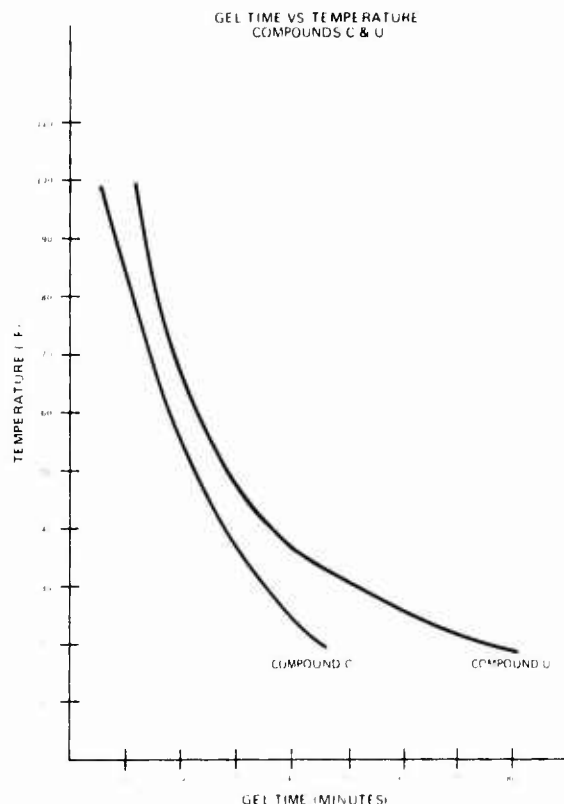


From Figure V it was apparent that the mixed viscosity of Compound U was significantly lower than that of Compound C and very close to the target requirements. In general, the viscosity of Compound C was lowered by blending the viscous polydiene polyol with less viscous, compatible polyols and by the addition of a plasticizer of very low volatility.

### GEL TIME VS. TEMPERATURE

It was hoped that the excellent low temperature curing capabilities of Compound C would not be sacrificed by the modifications required to formulate Compound U.

FIGURE VI



From Figure VI it was apparent that the gel times of Compound U, over the entire temperature range, fall within the target requirements. From this data, it was felt that the following conservatively stated times to cable pressurization could be established for Compound U.

TABLE IV

TIME TO PRESSURIZATION

Temperature (°F)	Time (Min.)
20	120
40	60
75	30
95	30

These times are considerably shorter than any we have previously recommended.

## REACTION EXOTHERM

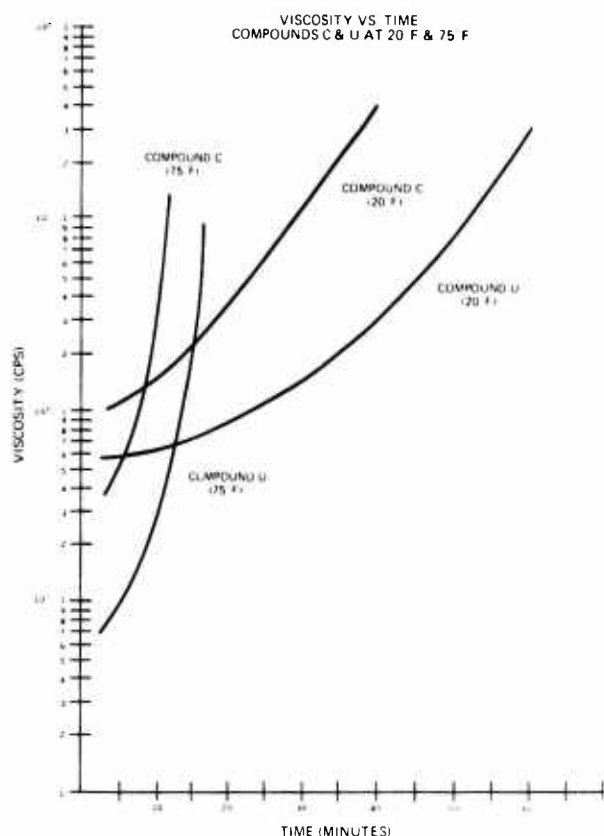
Compound U, during cure, fortunately exhibited moderate reaction exotherms comparable to Compound C. At 20°, 75° and 98°F the measured exotherms of a 100 gram mass were 55°, 145° and 166°F respectively.

## VISCOSITY VS. TIME

The induction curves of Compound U, Figures VIIA and VIIB closely paralleled those of Compound C, except that they were displaced due to the longer gel time of Compound U. Although Compound U shows little induction period at 75° and 98°F, it is significant to note that its viscosity remained below 10,000 cps for about 80% of the time required to gel at both temperatures.

It was felt that this should allow sufficient time to penetrate the conductor bundle (and the insulation in the case of pulp) and between the sheaths of the cable.

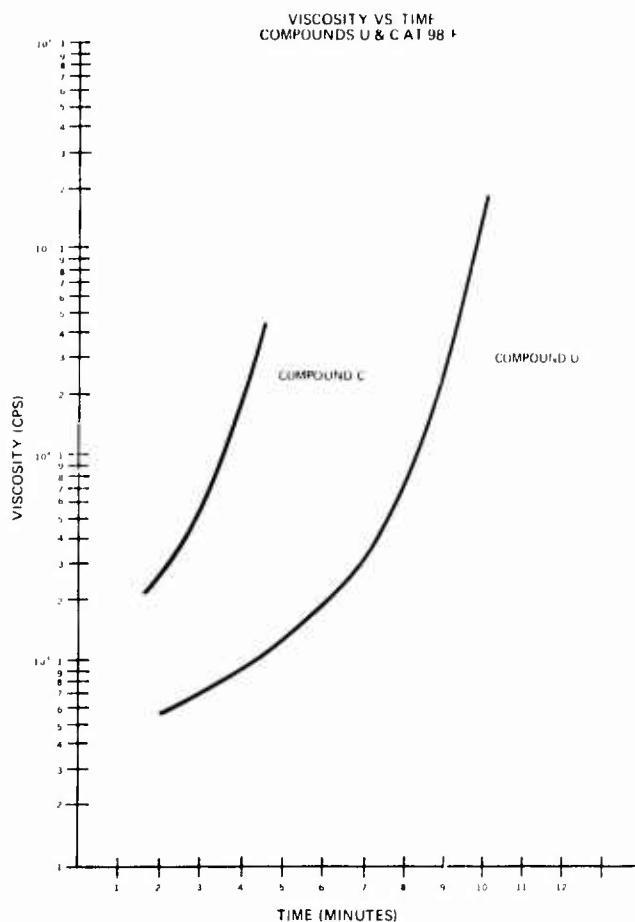
FIGURE VIIA



## SURFACE TENSION STUDIES

In a brief study, the addition of various surfactants to Compound U was investigated in order to lower its surface tension. It was theorized that this would increase the penetration of the resin through the pulp insulation as well as increase resin wetting of the polyolefin insulation in PIC cable. Despite the fact that we could significantly lower the surface tension of the mixed resin from about 35 dynes/cm to 29 dynes/cm, it did not appear to influence either the rate or the amount of resin penetration through the pulp insulation.

FIGURE VIIB



Apparently, the critical surface tension of wetting of a polar substrate such as pulp is so high that it is easily wet by most liquids, thus viscosity is the most important parameter influencing penetration. On the other hand, the critical surface tension of wetting of a polyolefin is so low that no known liquid effectively wets it without surface pretreatment. Thus, there would be no advantage in adding surfactants to the resin in either case.

## SUMMARY — COMPOUND U

It would appear then that we have, at least in theory, optimized the important variables of gel time and viscosity as a function of temperature and of mixed viscosity as a function of time.

In addition from the tabulated properties of Compound U in Table V it can also be seen that neither the excellent low temperature flexibility nor the hydrolytic stability of Compound C were compromised during reformulations.



**TABLE V**  
**PROPERTIES OF COMPOUND U**

I. <u>Uncured Properties</u>	<u>Method</u>	<u>Value</u>
• Viscosity (cps, 25°C) Prepolymer Polyol Mixed (1 minute)	Brookfield Viscometer	900-1200 550-800 700-800
• Gel Time (Min., 25°C)	Sunshine Gel Meter, 100g mass	14-17
• Maximum Exotherm (°C)	100g mass	63
II. <u>Cured Properties</u>		
• Tensile Strength	ASTM D-412-68	500-600
• Elongation (%)	ASTM D-412-68	150-200
• Hardness (Shore A)		70-73
• Density (gm/cc)	3M*	1.08
• Volume Shrinkage (%)	3M*	1.50
• Copper Corrosion	3M*	None
• Fungus Resistance	ASTM C 21-70	"0" Growth
• Hydrolytic Stability (7 days, H <sub>2</sub> O, 100°C)	3M*	
a) Weight Increase (%)		1.5
b) Shore A (Loss)		10
• Heat Stability (21 days, 135°C)	3M*	
a) Weight Loss (%)		2.5-3.5
b) Shore A Increase		15
• Thermal Shock	3M* (10 Cycles, 1/4" Insert, -55°C to 130°C)	No Cracking
• Glass Transition Temperature (°C)	DTA	-80 to -60
III. <u>Electrical Properties</u>		
• Dielectric Strength (volts/mil) (125 mil sample)	ASTM D-149-64	450-500
• Dielectric Constant (10 <sup>3</sup> Hz, 25°C, 50% RH)	ASTM D-150-70	4.2
• Dissipation Factor	ASTM D-150-70	.038
• Insulation Resistance (ohms) (28 days, 40°C, 96% RH)	3M*	7 x 10 <sup>11</sup>

\*3M Internal Test

#### APPLICATION TESTING

It now remained to be proven in the laboratory whether the theoretical properties which we designed into the compound would function in a cable to give a reliable dam with a long service life.

#### SAMPLE PREPARATION

To accomplish this, sample plugs were prepared using the direct sheath injection (4" window) method and injecting the compound from tubes with an injection gun.

Small PIC and pulp and large PIC and pulp samples were injected at three different temperature conditions, 20°, 70° and 95°F. They were conditioned at these temperatures for 2 hours prior to being injected. The test included 24 samples each of PIC and pulp cables.

#### TEST PROCEDURE

The PIC samples were placed in a temperature cycling chamber and cycled from -40° to 140°F (3 cycles per 24 hours) for 50 cycles with 10 psig nitrogen pressure maintained on the samples. The pulp samples were cycled from 0° to 100°F (3 cycles per 24 hours) also with 10 psig nitrogen pressure. At the end of the 50 cycles, the leakage rate was measured using a Mass Flow Meter as per Figure VIII. A maximum leak rate of 1cc/min. was permitted for PIC samples and 10cc/min. for pulp samples. These measurements were taken with the samples stabilized at 0°, 40° and 95°F. Tables VI and VII give these leak rates for samples plugged using the direct sheath injection method. Table VIII tabulates the data for plugs using a method of completely opening up the cable, removing sheaths and shields, placing a sleeve over the opened cable, pouring in approximately 3/4 of the compound and injecting the balance.

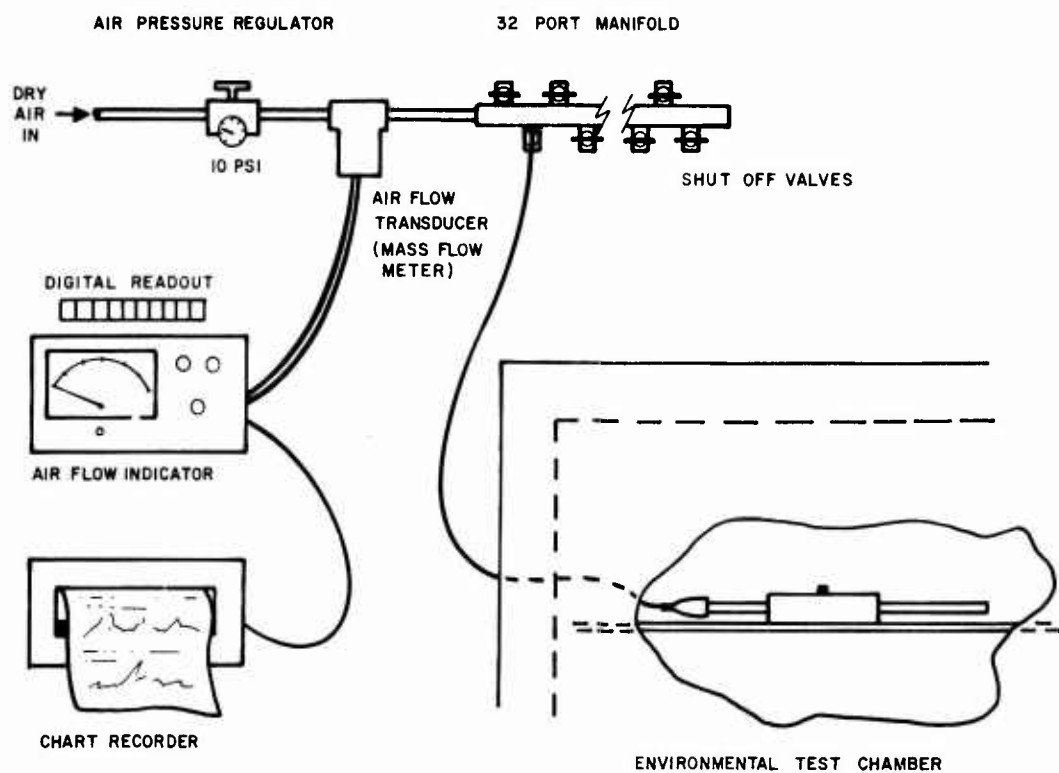


FIGURE VIII. CABLE PLUG TEST FACILITY

TABLE VI  
PERFORMANCE TEST DATA FOR DIRECT SHEATH INJECTION

PIC CABLE			LEAKAGE RATE cc/min.			
SAMPLE NO.	°F PREP. TEMP.	CABLE SIZE	0°F	40°F	95°F	EXPLANATION
1	20	100/26	0	0	0	Semkit Break Short Resin
2	20	100/26	41	6	1	
3	20	100/26	0	0	0	
4	20	100/26	0	0	0	
5	20	900/26	0	0	0	
6	20	900/26	0	0	0	
7	20	900/26	0	0	0	
8	20	900/26	0	0	0	
9	95	100/26	0	0	0	
10	95	100/26	0	0	0	
11	95	100/26	0	0	0	
12	95	100/26	0	0	0	
13	95	900/26	0	0	0	
14	95	900/26	0	0	0	
15	95	900/26	0	0	0	
16	95	900/26	0	0	0	
17	70	100/26	0	0	0	
18	70	100/26	0	0	0	
19	70	100/26	0	0	0	
20	70	100/26	0	0	0	
21	70	900/26	0	0	0	
22	70	900/26	0	0	0	
23	70	900/26	0	0	0	
24	70	900/26	0	0	0	

**TABLE VII**  
**PERFORMANCE TEST DATA**

STALPETH CABLE			LEAKAGE RATE cc/min.			
SAMPLE NO.	°F PREP. TEMP.	CABLE SIZE	0°F	40°F	95°F	EXPLANATION
1	20	300/26	0	0	0	Compound leak around flange during resin injection
2	20	300/26	3.1	0	0	
3	20	300/26	0	0	0	
4	20	300/26	0	0	0	
5	20	2400/26	7.5	0	0	
6	20	2400/26	0	0	0	
7	20	2400/26	0	0	0	
8	20	2400/26	0	0	0	
9	95	300/26	0	0	0	
10	95	300/26	0	0	0	
11	95	300/26	0	0	0	
12	95	300/26	0	0	0	
13	95	2400/26	0	0	0	
14	95	2400/26	0	0	0	
15	95	2400/26	0	0	0	
16	95	2400/26	7.0	3.6	0	
17	70	300/26	0	0	0	
18	70	300/26	0	0	0	
19	70	300/26	0	0	0	
20	70	300/26	0	0	0	
21	70	2400/26	2.0	0	0	
22	70	2400/26	0	0	0	
23	70	2400/26	0	0	0	
24	70	2400/26	11.5	0.4	0	Injection Problem Semkit Breakage

**TABLE VIII**  
**PERFORMANCE TEST DATA OPEN SHEATH METHOD**

PIC CABLE			LEAKAGE RATE cc/min.		
SAMPLE NO.	°F PREP. TEMP.	CABLE SIZE	0°F	40°F	95°F
1	20	600/24	0	0	0
2	70	600/24	1	0	0
STALPETH CABLE			LEAKAGE RATE cc/min.		
3	20	2400/26	2	0	0
4	70	2400/26	2	0	0

After the above testing, PIC samples 6, 13 and 24 from Table VI and pulp samples 6, 13 and 22 from Table VII were then thermally aged for 140 days at 140°F (60°C) together with sample sheets of the cured Compound U.

Table IX gives the weight loss of Compound U and Table X gives the leakage rates of the sample blocks.

**TABLE IX**  
**THERMAL AGING OF COMPOUND U, 140°F (60°C)**

SAMPLE NO.	DAYS	% WEIGHT LOSS	HARDNESS ALL SAMPLES - AVG.	
			INITIAL	FINAL
1	90	- 0.12	65	73
2	90	- 0.125		
3	90	- 0.13		

**TABLE X**  
**BLOCKED SAMPLES**  
**THERMAL AGED AT 140°F (60°C)**

SAMPLE NO.		
PIC	DAYS	LEAKAGE cc/min.
6	30	0
13	30	0
24	30	0
6	60	0
13	60	0
24	60	0
6	140	5
13	140	15
24	140	2
STALPETH		
6	30	0
13	30	0
22	30	0
6	60	0
13	60	0
22	60	0
6	140	0
13	140	0
22	140	0

#### JAMES E. BILLIGMEIER

James Billigmeier received a B.S. in Chemistry from North Dakota State University, an M.S. from the University of Washington and a Ph.D. in Organic Chemistry from Oregon State University in 1972. After two years of work in polymer chemistry at the Aerojet Chemical Company he joined 3M Company as a Senior Research Chemist in the TelComm Products Department, Materials Research Group.



#### SUMMARY

In summary, Compound U was developed based on theoretical considerations. The compound's final test was its ability to provide a reliable dam in both PIC and pulp cable of different cable sizes and over a wide temperature range. As shown by performance data in Tables VI and VII, this goal was realized. Thus, it appears that a significant step has been taken towards the development of a universal plugging and splice encapsulating compound.

#### BIBLIOGRAPHY

1. Farrell, F.M., Filreis, M., Groves, J.D. and Kapell, H.K. "Economics and Performance Considerations of Telephone Cable Plugging." Proceedings of the International Wire and Cable Symposium, December, 1974.
2. Saunders, J.H. and Frisch, K.C. "Polyurethanes Chemistry and Technology," Parts I and II, Interscience, New York, 1962 and 1964.
3. "Final OSHA Standards on Carcinogens," Federal Register, January 29, 1974.
4. Hervig, H., U.S. 3,639,567 (to 3M Co.)
5. Masterson, J.B. "Pressure Dams in Communication Cables." Proceedings of the International Wire and Cable Symposium, October, 1969.

#### MANUEL FILREIS

Manuel Filreis holds a B.S. Degree from North Carolina State University in Textile Engineering in 1949. Since then he worked for Burlington Industries, Incorporated, and B.F. Goodrich Chemical Company prior to joining 3M Company in 1960 as a Product Development Engineer. Currently, he is employed as a Product Development Specialist in the TelComm Department, Cable Accessories Group.



JAMES D. GROVES

James Groves received a B.S. in Chemistry from Washington State University, an M.S. from the University of Minnesota and a Ph.D. in Physical Organic Chemistry from the University of Colorado in 1958. He joined the 3M Company in 1959 as an Organic Research Chemist. Since 1967 he has worked exclusively in the area of Materials Research and Development for the power and communications industries. Currently, he is Senior Research Specialist in the TelComm Department Laboratory.



OPTIMUM SHIELDED TWISTED PAIR CABLE  
DESIGN FOR DIGITAL DATA TRANSMISSION

By

J. W. Kincaid, Jr.  
Belden Corporation  
Richmond, Indiana

ABSTRACT

Shielded, twisted pair cable design in relation to application in balanced digital data transmission links is discussed. Measured attenuation, 10% - 90% rise time and 20% peak-to-peak time jitter as a function of bit rate and transmission distance are presented for a selection of prototype test cables. Theoretical results for attenuation are discussed. The basic balanced (differential) digital data transmission link is reviewed. Selection of an optimal cable to meet specific bit rate and distance of transmission requirements is discussed.

INTRODUCTION

This paper presents answers to some of the questions asked by users and manufacturers of digital computer based systems regarding selection of shielded, twisted pair cable for digital data transmission. Coaxial cable has been treated extensively in the literature and there seems to be adequate technical data available for the successful application of this type cable for computer based applications.<sup>1</sup> With respect to shielded twisted pair cable the attention received has been much less and certain aspects of shielded twisted pair design which are critical for optimum performance in balanced digital data transmission links have not been readily available.

Questions relating to cable size, capacitance, impedance, shielding, etc., are routinely answered for many applications. However, special efforts have been required to determine the attenuation and bit rate versus transmission distance characteristics of shielded, twisted pair cable.

Optimal cable design, in the most general sense, must take many factors into consideration. The final cable design must meet all physical and electrical characteristics the user may impose, as well as conform to applicable industry or government standards.

This paper concentrates on presenting the attenuation and bit rate versus transmission distance characteristics which are requisite for optimal digital data transmission.

Attenuation of shielded twisted pair cable has been treated theoretically.<sup>2</sup> However, the rise time characteristics, upon which bit rate versus transmission distance capability is dependent, are not known to be accurately described by theory. To overcome this lack of theory concerning rise time response, and to provide experimental attenuation data for correlation with theoretical results, a selection of prototype cables was manufactured and tested.

PROTOTYPE CABLE DESIGN

The prototype designs were selected to allow a study of measured attenuation, 10% - 90% rise time and percent peak-to-peak time jitter under the following three design conditions:

- I. Variable conductor diameter, (d), with constant cable diameter under the shield, (D).
- II. Variable cable diameter under the shield, (D), with constant ratio of conductor diameter to insulation wall thickness, (d/w).
- III. Variable cable diameter under the shield, (D), with constant conductor diameter, (d).

A cross-section of the typical prototype cable is given in figure 1.

The essential features of the prototype cable construction are summarized in table 1.

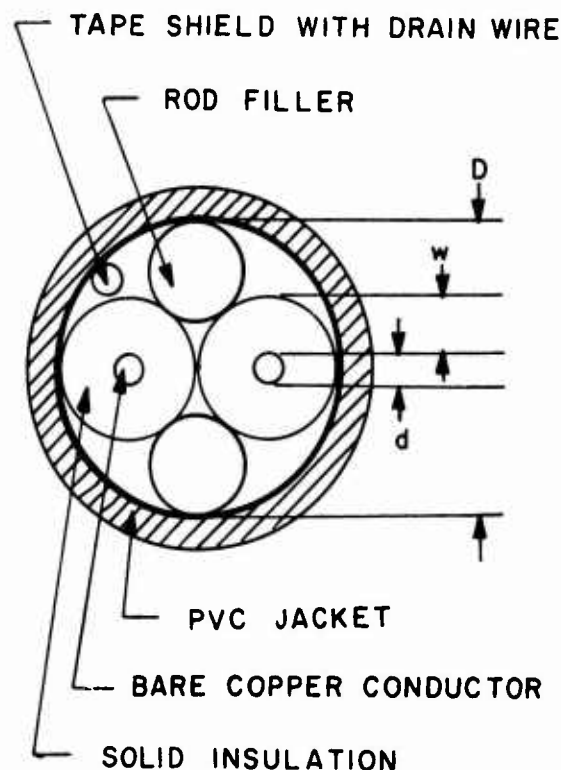


FIGURE 1- TYPICAL CROSS-SECTION.



Table 1

Construction Summary for Prototype Cables

Jacket:	Polyvinylchloride.
Shield:	100% coverage mylar/foil tape with drain wire.
Fillers:	2 solid polyethylene rods.
Insulation:	Solid polyethylene (see figure 2 for thickness).
Conductor:	Bare copper (see figure 2 for diameter).
Pair Lay:	Ten times cable diameter under shield.
Unbalance:	Capacitance, less than 5%. Resistance, less than 5%.

Design points for the prototype cables are given in figure 2 which is a plot of uninsulated conductor diameter, (d), versus thickness of insulation wall, (w). The straight lines with constant positive slope correspond to combinations of conductor diameter, (d), and insulation wall thickness, (w), which result in constant characteristic impedance, (Z), and cable capacitance, (C). The curves with negative slope are for constant cable diameter under the shield, (D). The theoretical impedance and capacitance data is applicable to solid polyethylene insulated shielded pairs and is in close agreement with measured capacitance and impedance determined for the prototype cables. Each prototype cable is identified in Figure 2 with a number. Table 2 associates groups of prototype

numbers with the appropriate design condition under study. Thus design condition I was studied with groups IA and IB; design condition II was studied with groups IIA and IIB, and design condition III was studied with groups IIIA, IIIB, and IIIC. Test data presented later in the paper references this notation system. See the appendix for a definition of capacitance unbalance, resistance unbalance, cable capacitance and impedance.

Table 2

Design Condition Versus Prototype Design Number

Design Condition	Prototype Design Number									
	1	2	3	4	5	6	7	8	9	10
I, Variable (w,d) constant (D)	A	A	A	A	A	A			B	B
II, Variable (D) constant (d/w)		B					A	A	B	A
III, Variable (W,D) constant (d)	B		A	C			E	A	A	C

ATTENUATION OF PROTOTYPE CABLESExperimental Procedure

Attenuation of each of the prototype cables was measured with the test set-up diagrammed in figure 3.

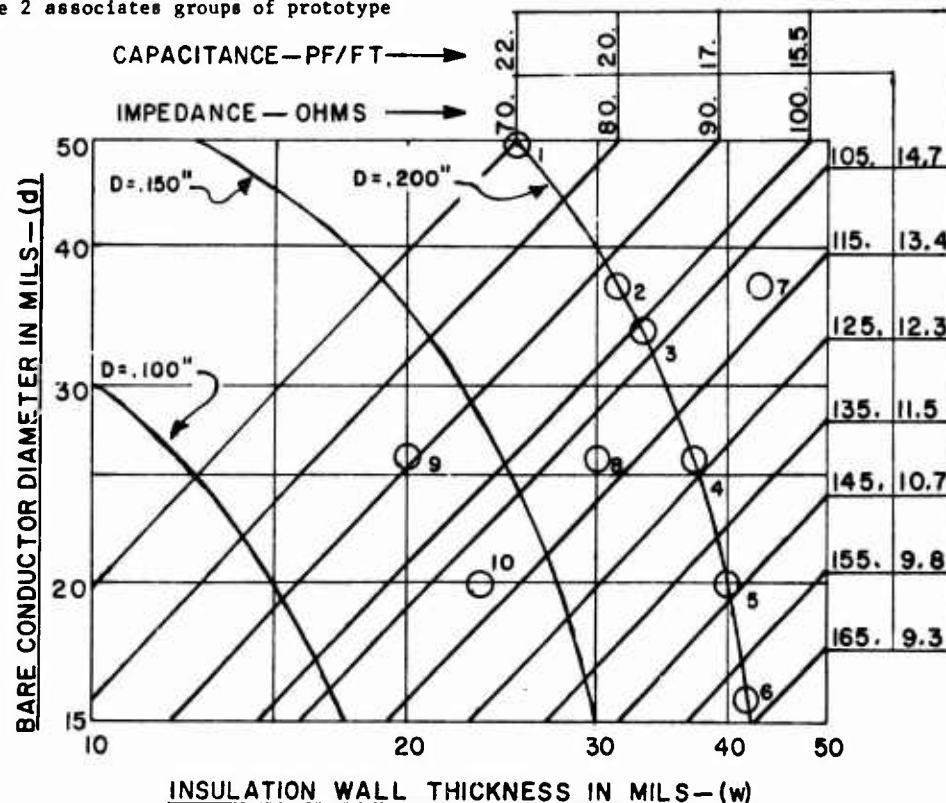


FIGURE 2- CAPACITANCE AND IMPEDANCE CHART.

Attenuation of the shielded twisted pair is found from the following expression:

$$\alpha_f = \alpha_{if} - \alpha_{2f} \quad \text{DECIBELS/UNIT LENGTH} \quad (1)$$

$$\alpha_{if} = 20 \cdot \log_{10} \frac{|V_{21}|}{|V_{11}|} \quad (2)$$

$$\alpha_{2f} = 20 \cdot \log_{10} \frac{|V_{22}|}{|V_{12}|} \quad (3)$$

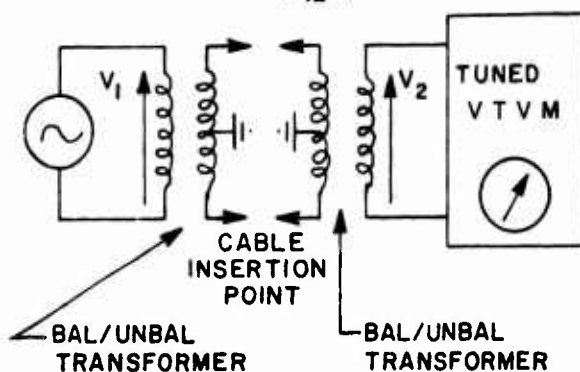


FIGURE 3—BALANCED INSERTION LOSS TEST SET-UP.

$\alpha_{2f}$  is the reference level determined with a 1 foot length of the prototype cable under test. When the full length sample is inserted as indicated in figure 3 the loss level changes to  $\alpha_{if}$ .

$|V_2|$  and  $|V_1|$  are the amplitude in volts of sinusoidal signal of frequency,  $f$ , in hertz, at the output and input of the cable test circuit, respectively.

The balanced to unbalanced transformers provide an impedance mismatch no greater than 10% of the characteristic impedance of the prototype cable under test.

#### Test Results

Test data for design conditions IA, IIA, and IIIA are presented in figures 4, 5, and 6 respectively. Test data for the remaining conditions are in agreement with the trends established by the reported data. When plotted on log-log paper, the measured attenuation versus frequency data does not yield straight line curves of constant slope. For engineering purposes, however, the curves in figures 4, 5, and 6 have been made straight line approximations of the measured data.

Design condition IA results: Variable (w,d), constant (D). Data plotted in figure 4 indicates too large a conductor (Prototype #1,2) or too small a conductor (Prototype #6) will result in excessive attenuation. The data indicates there is a conductor to insulation wall thickness ratio which gives minimum attenuation, but is inconclusive in establishing the optimal value. In terms of impedance the data means there is an optimal impedance which gives minimum attenuation.

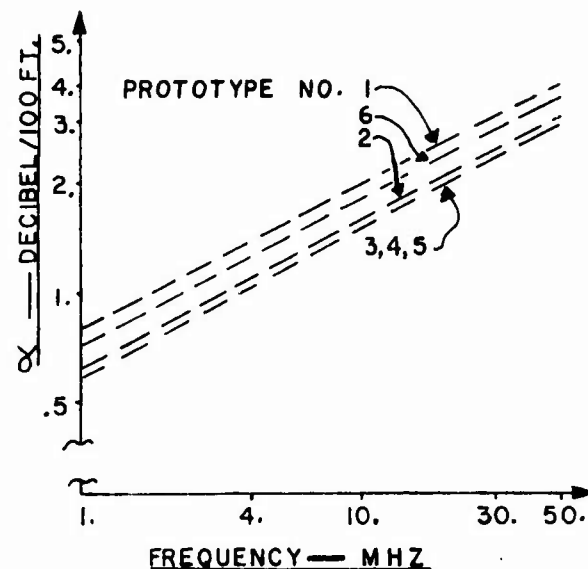


FIGURE 4 —  $\alpha$  VERSUS FREQUENCY.

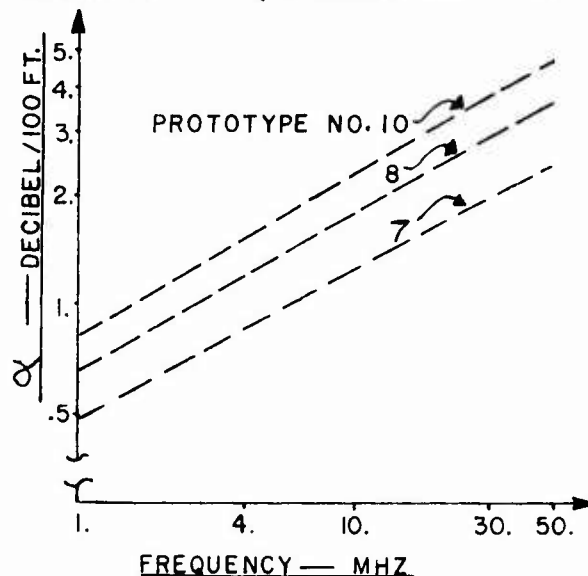


FIGURE 5 —  $\alpha$  VERSUS FREQUENCY.

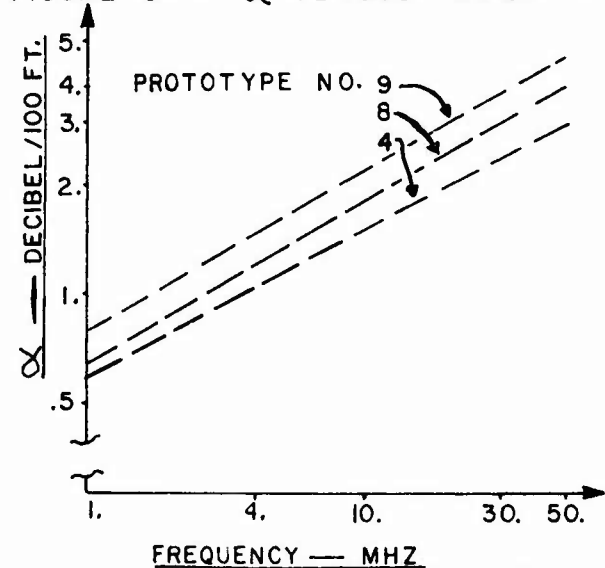


FIGURE 6 —  $\alpha$  VERSUS FREQUENCY.

Design condition IIA results: Variable (D), constant (d/w). Data plotted in figure 5 indicates that for fixed impedance, or constant (d/w) ratio, the larger the conductor diameter, (d), the less the attenuation.

Design condition IIIA results: Variable (w,D), constant (d). Data plotted in figure 6 indicates that for constant conductor diameter, the attenuation decreases as insulation wall thickness is increased. This implies that to obtain minimum attenuation the characteristic impedance should be as high as possible. However, design condition IA results indicate that for a given cable diameter under the shield the impedance or (d/w) ratio may be adjusted for minimum attenuation.

The results obtained are analogous to the well known impedance versus attenuation theory of coaxial cable.<sup>3</sup> The results are in general agreement with the theory of "Shielded Cable System" developed by S. P. Mead.<sup>4</sup>

#### Mead's Theoretical Results

S. P. Mead has derived the equations from which proportioning ratios for minimum attenuation in twisted pair cables at high frequencies may be determined.<sup>5</sup> At high frequencies, where  $(2\pi fL)^2$  is large compared with  $R^2$ , and the leakage,  $G$ , is zero, the attenuation per unit length is given by:

$$\alpha = \frac{R}{2} \sqrt{\frac{C}{L}} \text{ NEPERS/UNIT LENGTH} \quad (4)$$

Where  $R$ ,  $L$ , and  $C$  are the distributed resistance, inductance, and capacitance for the element of a transmission line given in figure 7.<sup>6</sup>

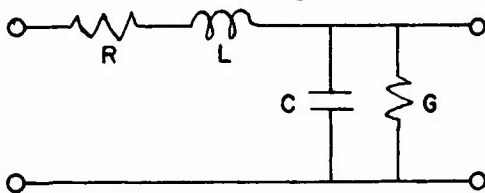


FIGURE 7—DISTRIBUTED MODEL FOR TRANSMISSION LINE.

Under these conditions, Mead has shown  $\alpha$  is given by:

$$\alpha = \frac{R}{V \cdot L} \sqrt{\epsilon} \cdot F \quad (5)$$

Where  $\epsilon$  is the relative dielectric constant of the insulation,  $V$  is the velocity of light,  $R$  is the high frequency resistance of the conductor,  $L$  is the inductance of the cable, and  $F$  is a function of cable dimensions which may be minimized. It follows that the cable dimensions which make  $F$  a minimum also make  $\alpha$  a minimum. Mead's work should be referenced for detail on the assumptions made and the various formulae which were derived. The formulae, which are too involved to reproduce here, were implemented in Fortran IV and solved on the company operating system. Certain results, which were not made explicit in the patent, and have not been located otherwise in the literature are given in figures 8, 9, and 10.

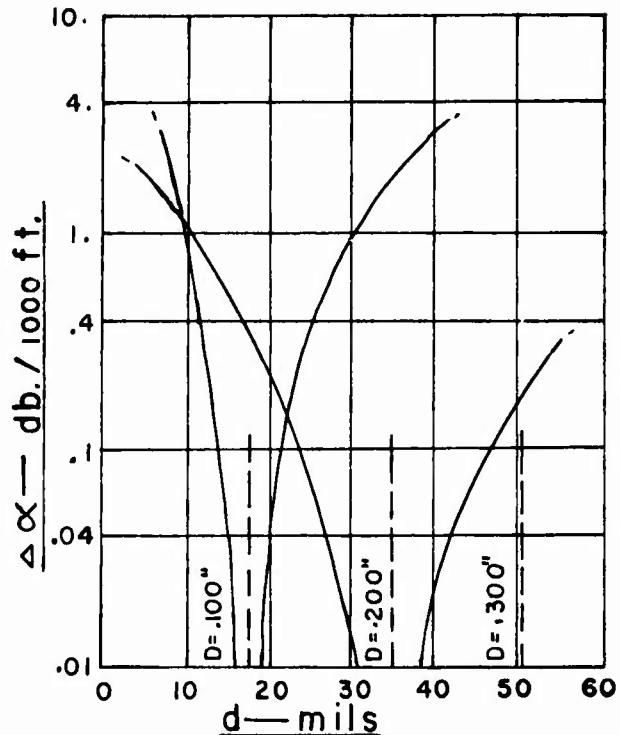


FIGURE 8—INCREASE IN  $\alpha$  DUE TO NONOPTIMAL  $d$ .

Figure 8 presents the theoretical increase in attenuation over the theoretical minimum for cable diameter under the shield equal to .100", .200", and .300". The curves are valid at 50 MHz and would shift up at higher frequencies and down at lower frequencies. Due to Mead's proportioning ratio for minimum attenuation, the conductor diameter must increase as the cable diameter under the shield increases.

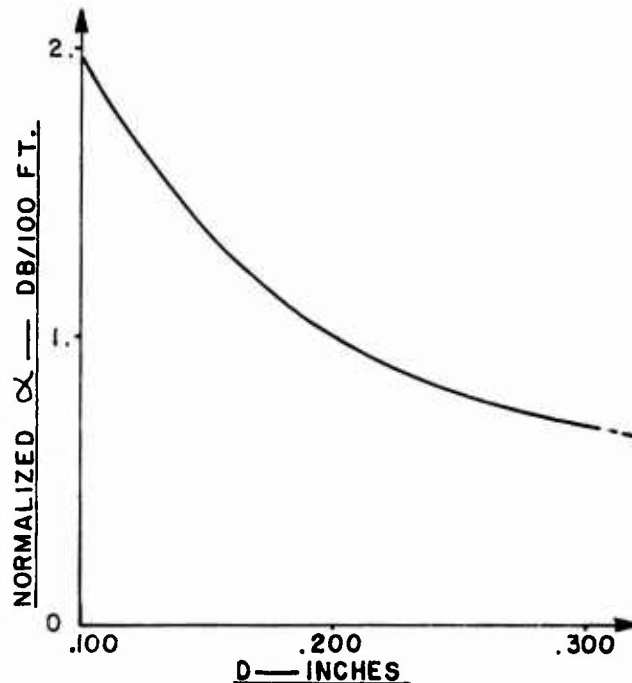


FIGURE 9— $\alpha$  VERSUS  $D$ .

Figure 9 plots change in theoretical minimum attenuation for changing cable diameter under the shield. The plot is normalized based on minimum theoretical attenuation obtained for .200" cable diameter under the shield.

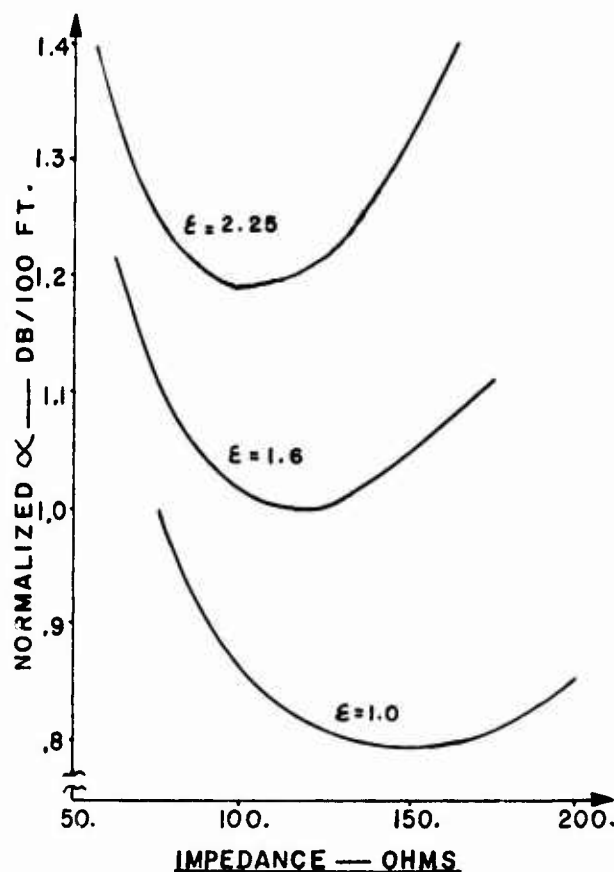


FIGURE 10— $\alpha$  VERSUS  $Z$ .

Figure 10 gives normalized curves for impedance versus attenuation. The curves are normalized based on the minimum attenuation obtained for dielectric constant equal to 1.6.

It is clear that shielded twisted pair cable may be designed for minimum attenuation. If for a particular application there are overriding factors which specify certain design features such as conductor diameter, or insulation material, it is still feasible to analyze the effect of these features on attenuation and adjust the unspecified parameters to achieve low attenuation.

#### DATA TRANSMISSION ON THE BALANCED LINE

A brief review of certain basic aspects of digital data transmission is in order prior to describing the bit rate versus transmission distance capabilities of shielded twisted pair cable.

Balanced data links are used to transmit digital data between system components in a wide variety of computer based applications. Balanced transmission is advantageous over unbalanced transmission when system ground shifts or electrical disturbances between system components could make unbalanced links unacceptably error prone. One disadvantage of unbalanced coaxial links is that electrical disturbances may be coupled into the link by the shield which may be part of the signal carrying path. With shielded pair cable, however, the shield is not directly a signal carrying member. Additionally, electrical disturbances which

do traverse the shield may be neutralized by the twist of the conductors or the common mode rejection capability of the line receiver. The common mode noise rejection ratio and noise margin of balanced links are dependent on line driver - receiver design and ultimately determine the bit rate versus transmission distance characteristics of the balanced transmission link.<sup>8</sup>

A simplified diagram of a typical balanced digital data link is shown in figure 11. The twisted pair cable is an important part of the data link and for a given line driver - receiver combination the cable design will determine the bit rate and transmission distance capabilities of the link.

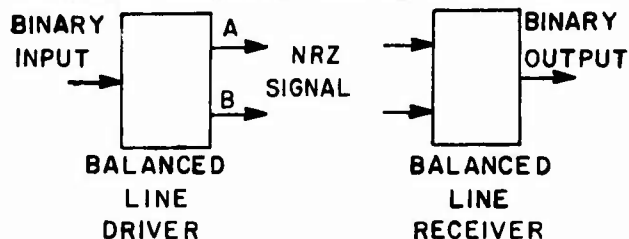


FIGURE 11—BALANCED DATA LINK.

#### NRZ BASICS

Digital signals which may typically occur at driver input, driver output, and receiver output of figure 11 are shown in figure 12a, 12b, and 12c respectively.

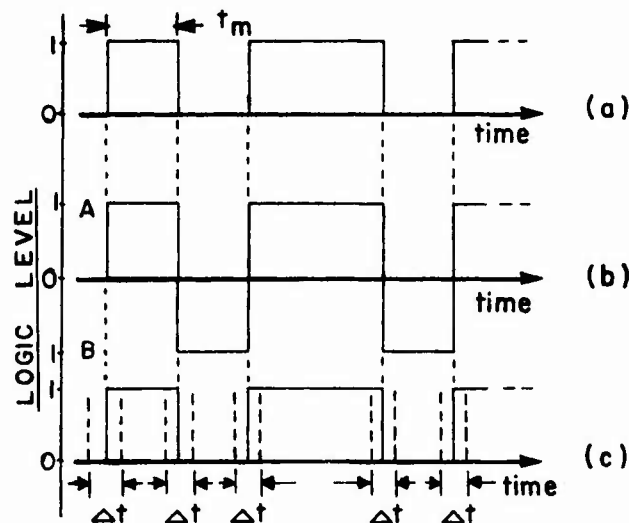


FIGURE 12—DIGITAL SIGNALS.

The particular line driver output configuration of figure 12b is referred to as NON-RETURN-TO-ZERO (NRZ) code. Here, the uncomplemented output, A, is applied to one conductor of the twisted pair cable and the complemented output, B, is applied to the remaining conductor.

Bit rate for the NRZ code is defined to be the reciprocal of " $T_m$ ". As shown in figure 12a, " $T_m$ " is the minimum signal time duration at the logic "one" or "zero" level.<sup>9</sup>

Peak-to-peak time jitter,  $\Delta t$ , is shown in figure 12c to be twice the maximum time difference between the switching instants of the binary input signal to the driver and the binary output signal

from the receiver. If the time jitter is large enough, it is possible for the binary output signal bits to overlap, thus causing error or change in the original bit pattern.<sup>10</sup>

Percent peak-to-peak time jitter is given by the following expression.

$$\% \Delta t_{pp} = 100 \cdot \Delta t / t_m \quad (6)$$

The amount of peak-to-peak time jitter which can be tolerated is dependent on the line driver - receiver design. However, for any given line driver - receiver design the amount of peak-to-peak time jitter for a given bit rate and transmission distance is determined by the cable design.<sup>11</sup>

#### RISE TIME AND TIME JITTER RESULTS

##### Experimental Procedure

The equipment set-up diagrammed in Figure 13 was used to measure peak-to-peak time jitter, and 10% - 90% rise time of the prototype cables. The set-up simulated the differential data link of figure 11. The receiving end of the cable was parallel terminated in its characteristic impedance across the differential probe terminals. This arrangement obviated the line receiver. The pseudo random binary sequence (PRBS) generator with complementary outputs provided binary sequences up to  $2^{15}-1$  bits long. The PRBS generator simulated the line driver and essentially provided to the cable the combinations of bits, or voltages corresponding to "0" or "1" logic levels, which could be contained in binary code to be transmitted by the line driver.<sup>12</sup>

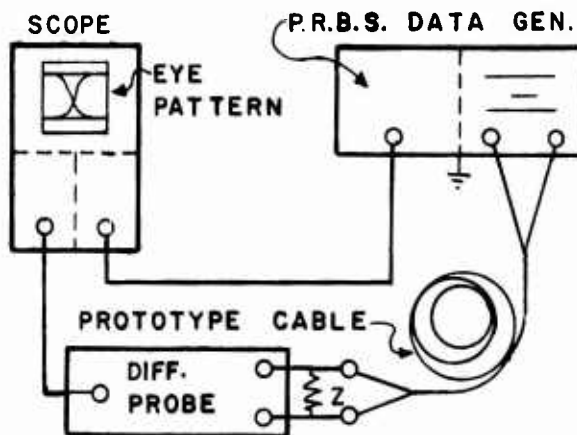


FIGURE 13—EYE PATTERN TEST.

The oscilloscope was used to monitor the cable output. Triggering was provided by the PRBS clock. The oscilloscope display for any given cable length and clock frequency is referred to as an eye pattern. As shown in figures 14 and 15, both rise time and peak-to-peak time jitter may be read from the eye pattern.

Measured 10% - 90% rise time results. Test data for design conditions IA, IIA, and IIIA are presented in figures 16, 17, and 18 respectively. Test data for design conditions IIB and IIIB, C is in agreement with the trends reported for design conditions IA, IIA, and IIIA.

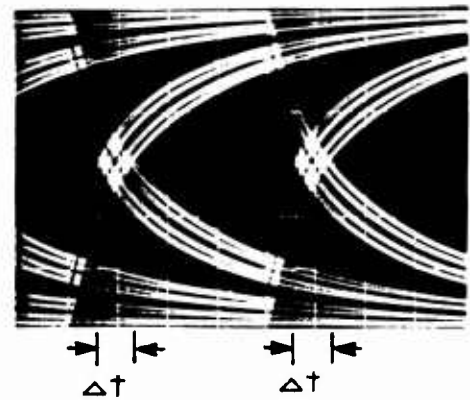


FIGURE 14—EYE PATTERN.

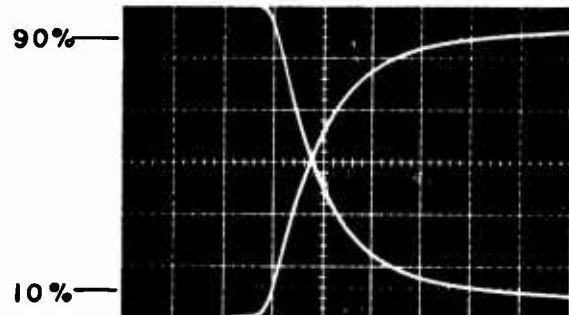


FIGURE 15—RISE TIME.

Design condition IA results: Variable (w,d), constant (D). Data plotted in figure 16 indicates the rise time decreases with increasing cable impedance (for constant diameter under the shield) for prototype cable lengths between 400 feet and 2000 feet. For the 100 feet and 200 feet prototype cable lengths, the precise relationship could not be resolved. However, the measured values were within the limits indicated in figure 16. The data does not indicate the existence of an optimum insulation thickness to conductor diameter ratio for which rise time is minimum.

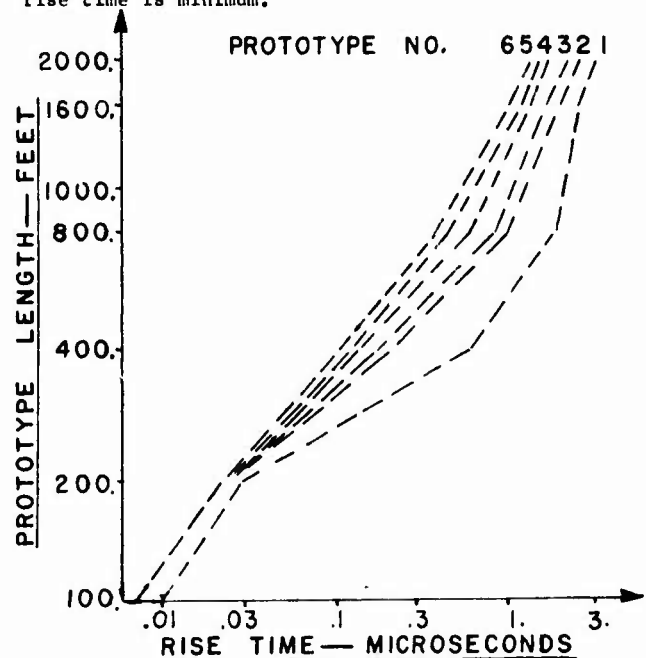


FIGURE 16—LENGTH VERSUS TIME.

Design condition IIIA results: Variable (w,D), constant (d). Data plotted in figure 17 indicates that as insulation wall thickness is increased with constant conductor diameter the rise time decreases. In terms of impedance this implies the higher the impedance, the shorter the rise time. The data indicates the increase in impedance from 95 Ohms to 110 Ohms reduces rise time disproportionately more than the increase from 110 Ohms to 120 Ohms.

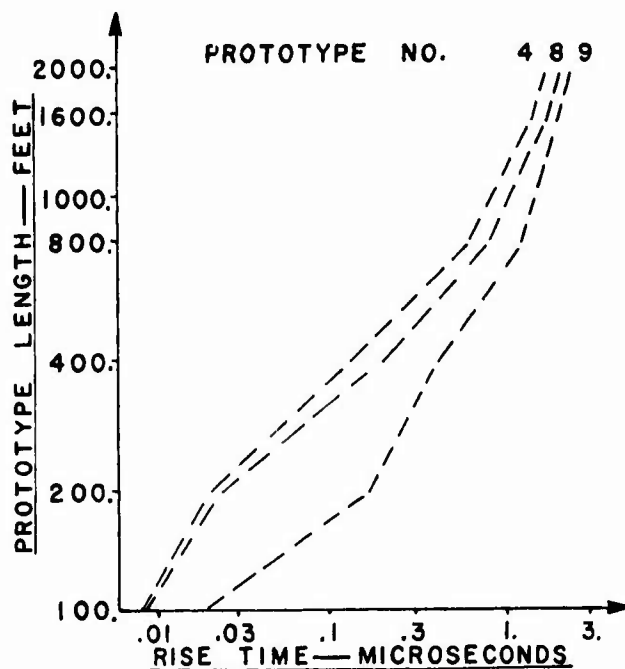


FIGURE 17—LENGTH VERSUS TIME.

Design condition IIA results: Variable (D), constant (d/w). Data plotted in figure 18 indicates that for the 1600 feet and 2000 feet transmission distances, the prototype cable with the smallest conductor provides marginally greater rise times than the cable with the largest conductor. However, for prototype sample lengths less than 800 feet, the larger conductor provides much shorter rise times than the small conductor. This implies that for equal impedance cables, the cable with the greater cable diameter under the shield will display much shorter rise times up to a certain point, beyond which, the smaller cable could be used with only slight loss of rise time.

Measured 20% peak-to-peak time jitter. Figures 19, 20, and 21 present bit rate versus transmission distance operating limits for prototype cables of design conditions IA, IIA and IIIA.

Operation limits for a bit rate corresponding to four times the 10% - 90% rise time, which is a realistic limit for 0% peak-to-peak time jitter, are also plotted in figures 19, 20 and 21. The limits do not preclude successful data transmission at higher bit rates or longer transmission distances if a code other than NRZ is employed.<sup>13</sup> The limits do not guarantee time jitter percentages for bit rates and transmission distance which fall under the curve. Rather, the operating limits are valid when the receiver threshold is located at the center of the eye pattern, time skew between complementary outputs of the driver, is less than 1 nanosecond, voltage levels of the complementary outputs of the driver

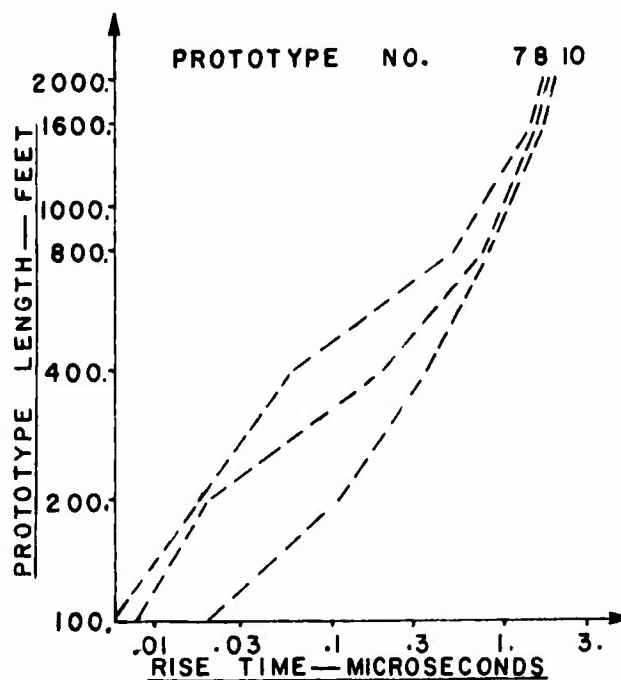


FIGURE 18—LENGTH VERSUS TIME.

are matched within 5% and balance of the shielded twisted pair is maintained within 5%.

Test results for the prototype cables tested in design conditions IIA, and IIIB, C are not presented as they are in agreement with the trends established for conditions IA, IIA and IIIA.

Design condition IA results: Variable (w/d), constant (D). Operating points or combinations of transmission distance and bit rate which lie between the operating limits for 0% and 20% peak-to-peak time jitter would nominally provide less than 20% peak-to-peak jitter. For example, in figure 19, each prototype cable could function with less than 20% peak-to-peak jitter at 1 MHz bit rate and

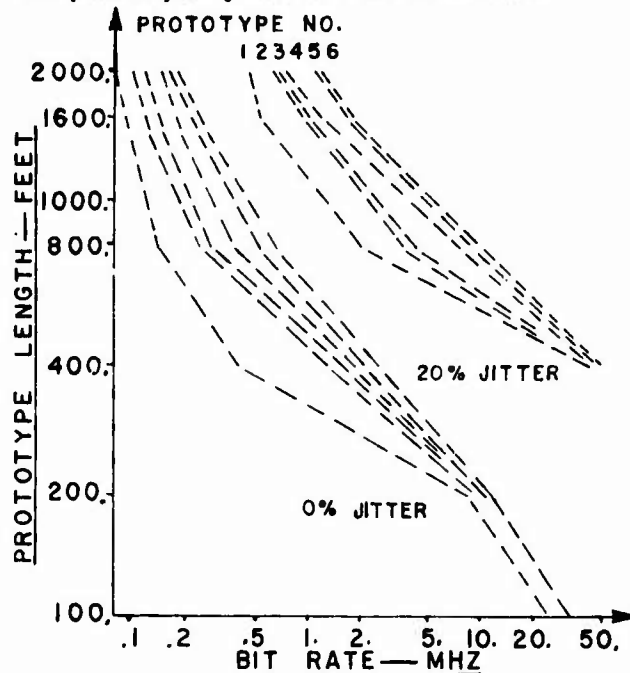


FIGURE 19—LENGTH VERSUS BIT RATE.



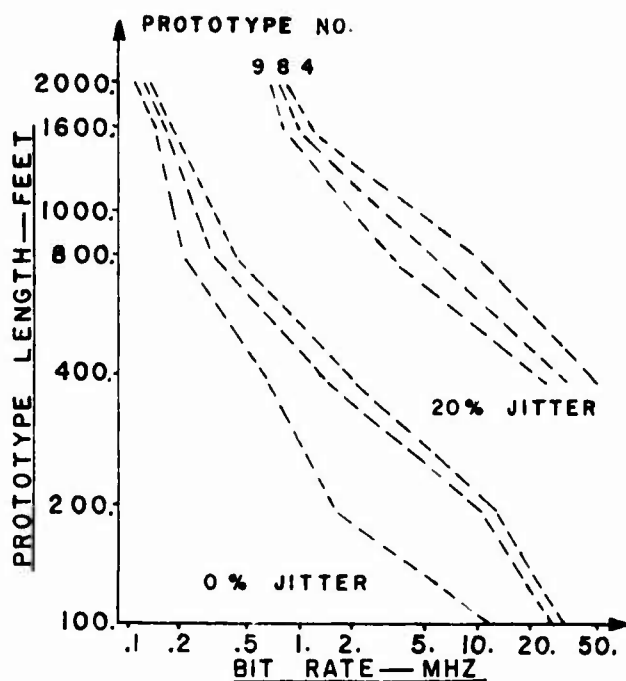


FIGURE 20—LENGTH VERSUS BIT RATE.

1000 feet transmission distance. The transmission distance and bit rate at 0% or 20% peak-to-peak jitter is greater for the prototype cable with greater impedance. For a transmission distance of 2000 feet prototype #6 with 165 Ohm impedance would allow more than double the bit rate possible with prototype #1 which has 68 Ohm impedance.

Design condition IIIA results: Variable (w,d), constant (d). Figure 20 indicates that bit rate and transmission distance can be increased simply by increasing the insulation wall thickness while keeping the conductor diameter constant. This corresponds to increasing the impedance of the cable.

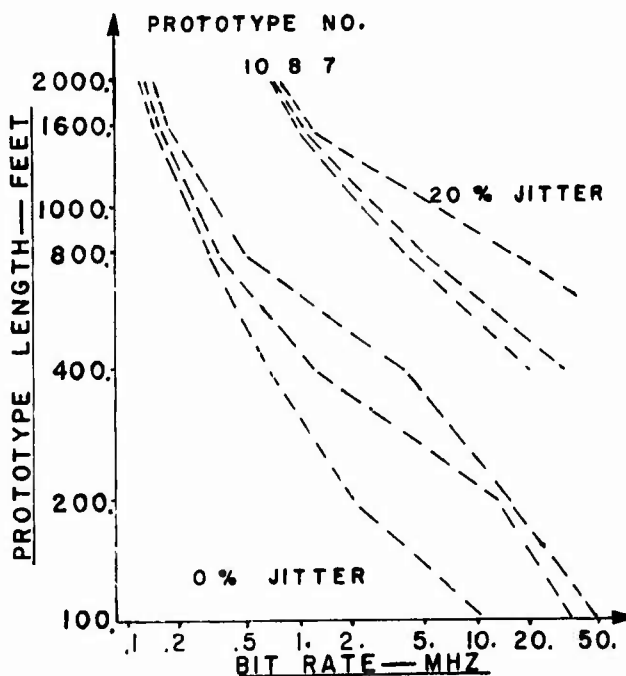


FIGURE 21—LENGTH VERSUS BIT RATE.

Design condition IIA results: Variable (D), constant (d/w). The data plotted in figure 21 indicates that transmission distance and bit rate can be increased by increasing the conductor diameter while keeping the cable impedance constant. The amount of improvement is dependent on the transmission distance. For a transmission distance of 400 feet, prototype cable #7 (with #18 AWG conductor) allows approximately 5 times the modulation rate possible with prototype #10 (24 AWG conductor). For 1600 feet and 2000 feet transmission distances the #18 AWG conductor provides only marginally higher bit rate capability.

#### SELECTION OF OPTIMAL CABLE

Among the many factors involved in the selection of the optimal cable the signal attenuation and bit rate versus transmission distance capability are of paramount importance. Though not considered here, the physical and electrical characteristics required by the cable application, as well as standards imposed by appropriate industry or government agencies, must be evaluated when determining the optimal twisted pair cable.

This paper has reported the results of laboratory measurements of signal attenuation and bit rate versus transmission distance for a selection of prototype cables. Based on this data the following general guideline is recommended.

- A. To insure low attenuation at high frequencies, shielded twisted pair cable should:
  - (1) Specify Mead's proportioning ratios. For cable similar to the prototype cables the ratio of insulation wall thickness to uninsulated conductor diameter should be approximately 1.0.
  - (2) Specify an insulation material with a low, stable dielectric constant and low power factor. Solid polyethylene is an excellent choice for many applications.
  - (3) Specify conductors which have high conductivity. For skin effect limited current, silver coated conductors have approximately 105% of the conductivity of bare copper conductors.
- B. To obtain high bit rate versus transmission distance capability the shielded twisted pair cable design should also:
  - (1) Specify the cable impedance to be as high as is compatible with the line driver - receiver requirements.
  - (2) Specify the largest diameter conductor compatible with obtaining the highest allowed impedance.

It should be noted that the design requirements for low attenuation and those for fastest rise time are somewhat in conflict. According to Mead's theory there is a definite ratio of insulation wall thickness, (w), to conductor diameter, (d), which will give lowest or optimum attenuation. This has been substantiated by the laboratory measurements. However, the laboratory measurements of rise time indicate the larger the (w/d) ratio the shorter the rise time. The data transmission application will determine whether low signal attenuation or short rise time is required of the shielded twisted pair cable.

### CONCLUSION

The two aspects of optimal design which have been treated give an accurate account of the capabilities of shielded twisted pair cable for balanced transmission of digital data. New cable designs will be influenced by these results.

The continuing demand for this type cable in many digital data applications should provide impetus for further work. In particular, a theoretical explanation of rise time dependence on transmission length, and the cable parameters, impedance, capacitance, and attenuation would be most helpful in predicting the bit rate versus transmission distance capability of this type cable. Additional laboratory analysis with digital codes other than "NRZ" would be of interest because higher bit rates and longer transmission distances may be achievable.

The laboratory analysis for this paper produced a considerable amount of test data which will be invaluable as a customer service tool for digital data transmission applications.

### ACKNOWLEDGEMENTS

The author gratefully acknowledges the dedication of the Technical Research Center staff in preparing the prototype cables and in performing the laboratory analyses.

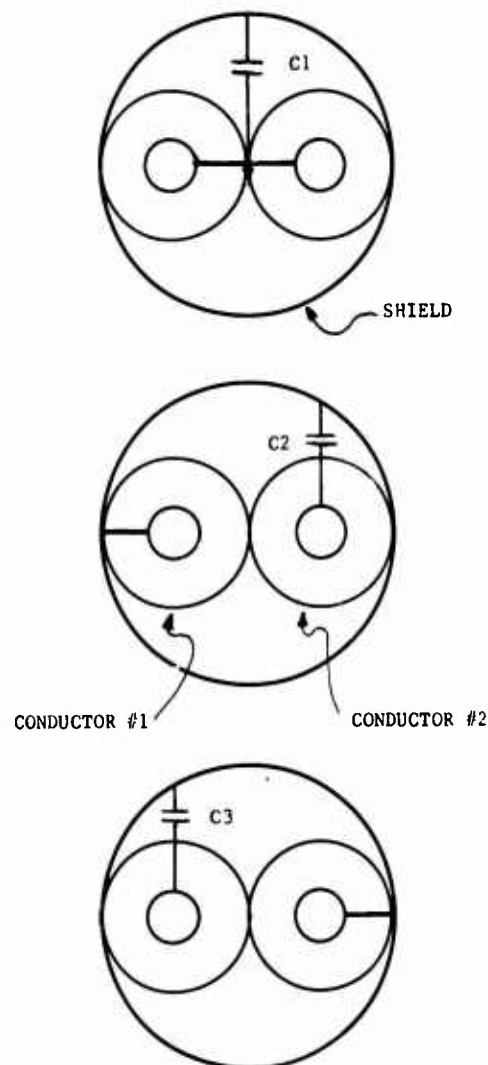
### REFERENCES

1. Thomas, R. J., "Choosing Coaxial Cable for Fast Pulse Response", *Microwaves*, November, 1968.
2. Mead, S. P., U. S. Patent No. 2086629, July 13, 1937.
3. Skilling, H. H., "Electric Transmission Lines", McGraw-Hill, p 310.
4. Mead, S. P., U. S. Patent No. 2086629, July 13, 1937.
5. Mead, S. P., U. S. Patent No. 2086629, July 13, 1937.
6. Martin, R. L., "Ultrahigh Frequency Engineering", Prentice-Hall, p 185.
7. Mead, S. P., U. S. Patent No. 2086629, July 13, 1937.
8. AN-22 Integrated Circuits for Digital Data Transmission, "Interface Integrated Circuits", National Semiconductor Corporation, 1974.
9. True, K. M., "The Interface Handbook", Fairchild Semiconductor, Chapter 4, 1975.
10. True, K. M., "The Interface Handbook", Fairchild Semiconductor, Chapter 4, 1975.
11. True, K. M., "The Interface Handbook", Fairchild Semiconductor, Chapter 4, 1975.
12. True, K. M., "The Interface Handbook", Fairchild Semiconductor, Chapter 4, 1975.
13. True, K. M., "The Interface Handbook", Fairchild Semiconductor, Chapter 4, 1975.



John W. Kincaid received the MSEE and BSEE degrees from the University of Oklahoma in 1967 and 1966, respectively. He is a Product Development Engineer in the Electronic Division Product Development Department and is chiefly engaged in the design of shielded cable for POS and other computer based systems.

### APPENDIX A



Capacitance: Cable capacitance is calculated from the following expression:

$$C = \frac{2 \cdot (C_2 + C_3) - C_1}{4} \quad \text{pf/ft}$$

where  $C_1$ ,  $C_2$ , and  $C_3$  are determined with a parallel capacitance bridge.

Capacitance Unbalance: percent capacitance unbalance is calculated from the following expression:

$$\% \text{ Unbalance} = 100 \cdot (C_2 - C_3) / C$$

Resistance Unbalance: percent resistance unbalance is calculated from the following expression:

$$\% \text{ Unbalance} = 100 \cdot (R_1 - R_2) / R_1$$

where  $R_1$  is the resistance of conductor #1 and  $R_2$  is the resistance of conductor #2.

Impedance: impedance is calculated from the following expression:

$$Z = 101600 \cdot (V \cdot C)$$

where  $C$  is the cable capacitance and  $V$  is the percent velocity of propagation. A measurement technique for  $V$  is given on page 8 of Bulletin E104, "The Measurement of Cable Characteristics", 1966, General Radio Company.

# GLASSFIBRE ARMoured PIC-TRUNK CABLE ASSEMBLED WITH CONNECTING PLUGS

H.G. Dagefoerde

P. Gregor

G. Thoennessen

AEG-TELEFUNKEN KABELWERKE AG

Development Center

4330 Muelheim/Ruhr

West Germany

## Summary

This paper introduces a new PIC-trunk cable system designed for minimizing field work. Design possibilities for glassfibre armouring to attain the tensile strength required are discussed. Cables fitted with plugs enable connections to be made rapidly and easily without sealing boxes. Measures are described for manufacture of drum lengths which can be connected to form line sections without balancing being necessary. Results of complete line systems are discussed. Possible applications for broadband transmission are stated.

## Introduction

A large proportion of the costs for the installation of a cable transmission line are accounted for by the time-consuming work outside the plant, which must be carried out by trained personnel. Extensive automation and rationalization measures have been introduced in the manufacture and burying of the cables. However, today this has scarcely been possible for the connection and balancing work, because of the considerable difficulties met in the field.

These facts led to our concept of developing cables which require no balancing in the field, and to fit the cable ends with connecting plugs to restrict field work to plugging the connectors together. A further advantage is a reduction in the installation time, and thus a reduction in the installation costs. In addition, it is possible to commission the transmission line immediately following installation.

## Task

As compared with conventional cables, high demands have to be made on the mechanical and electrical properties of these new cables for realization of the overall concept.

The installation and maintenance of a high-grade PIC-trunk cable line with a minimum

number of personnel calls for a cable of robust design which is easy to handle. High tensile strength must be accompanied by the lowest possible weight to ensure that the cables can easily be laid even with difficult terrain conditions.

Plug connections for cables instead of coupling boxes can be regarded as an optimum simplification of field work only when balancing work can also be eliminated. This calls for extremely small capacity unbalances. No local concentrations of unbalance must be present within the drum length, in order to obviate the need for balancing for both voice and carrier frequency operation. These high demands can be met only by PIC cable.

The requirements made on balance-free telephone cables, and the possibilities of their manufacture were reported on at the 22nd IWCS (1973).

A decisive demand made on plastic-core cables is adequate protection against the ingress of moisture.

On the one hand, this demand is made even more severe by the fact that the filler must not have any adverse effect on the transmission properties of the cable, and on the other it must be possible to locate any defect which allows water to enter through the wall of the sheath.

In total, these demands led to the following design for a 24-pair cable, which takes the paper-lead carrier-frequency cable in the German long-distance network as a basis.

## Cable Design and Manufacture

Copper conductors with a diameter of 0.9 mm and foamed-polyethylene insulation are stranded to form star-quads in accordance with German requirements. Three star-quads are located in the centre of the cable, and these are surrounded by nine star-quads. The moisture barrier is a copolymer-coated aluminium strip, which surrounds the cable core

longitudinally. The inside of this aluminium strip is covered with a glassfilament strip featuring a very high tensile strength value. These glass-filaments constitute the tensile armoring of the cable. At certain intervals, the spaces between the wires forming the cable core are filled with polyurethane foam. The outer sheath of the cable is of polyethylene, and is firmly bonded to the aluminium strip. Watertight plugs are fitted to the cable ends.

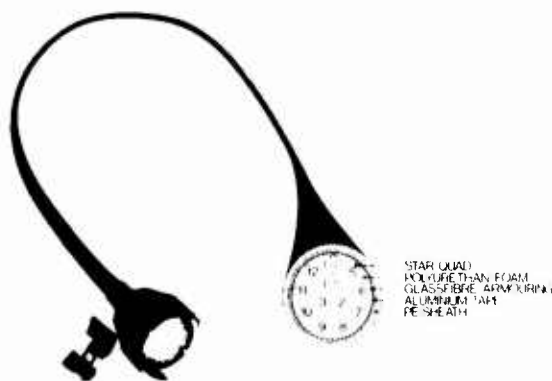


Fig. 1

Fig. 1 shows cable end with plug; illustration of the cable cross-section.

Maximum demands are made on all work cycles involved in cable manufacture. Machines of modern design are absolutely essential.

For example, the cores are insulated in electronically controlled lines to guarantee the required high uniformity of the foamed polyethylene insulation as regards diameter and degree of foaming. The star-quads are produced in precision stranding machines with a short lay. Only in this way, and by careful selection and matching of the lay lengths of the star-quads and of the layers, can the low and uniform capacity unbalances required for freedom from balancing be attained. The injection of polyurethane foam at definite intervals, the introduction of the aluminium tape with its strip of glassfibre as a moisture barrier, and the extrusion of the polyethylene sheath are carried out in one operation, also using an electronically controlled machine. The high quality of the star-quads permits dependable quality control using statistical methods.

#### Mechanical Properties

Mechanical properties are of special importance in the case of cables with plugs. This aspect has been taken into account by the development of a new plastic sheath with fibreglass armoring. The mechanically robust cable sheath has the task of protecting the core from the high tensile forces generated during cable installation, and of protecting

the core against corrosion. In addition, it is light, and corrosionproof itself.

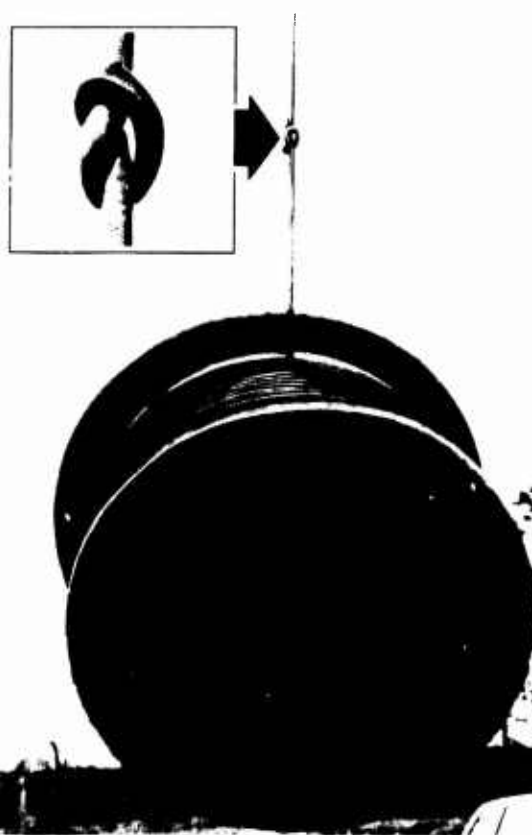
**Tensile strength.** The excellent tensile strength of the sheath stems from the use of glassfilaments as armoring elements.

Glass has greater tensile strength than steel. However, bundles of glassfilaments generally have relatively poor tensile strength values, as the individual filaments are not uniformly loaded under tensile stresses, and thus break.

The glassfilament armour for the cable sheath under discussion comprises bundled glass filaments, the bundles themselves being bonded together to suppress this unfavourable mechanism: the tensile load is distributed evenly among all filaments.

The normal tendency to disintegrate under tensile stresses is eliminated and the tensile strength is substantially improved.

Glassfilaments have such low elongation properties that a cable armoured with them would be rigid. This drawback can be obviated by slightly corrugating the bundles of glass-filaments.



Worst case test for glassfibre armoring (weight of drumlength = 41 % of breaking load)

Fig. 2

As illustrated in Fig. 2, the armoring does not rupture even when there is a knot in the cable; a drum with 500 m of cable can be suspended from the knotted cable.

The stress-strain diagram of the fibreglass reinforced sheath of a long-distance cable of the type

A-02YF(ZgL)2Y 24x2x0.9

is shown in Fig. 3.

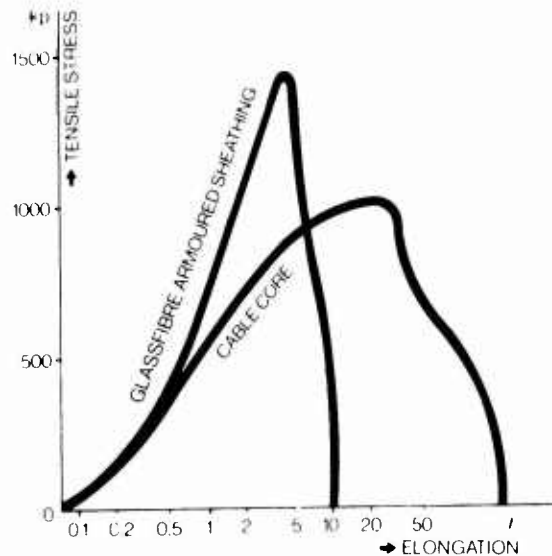


Fig. 3

The breaking strength is 1.4 t. The stress-strain curve of the cable core is also plotted in the diagram. The steeper slope of the curve for the tensile sheath clearly shows that this absorbs the greater part of the tensile force. The cable core is stressed only in the elastic range.

Weight, outside diameter, bending diameter. The use of glassfilaments as tensional elements in conjunction with a plastic sheath provides an elegant solution for an easily handled cable. This becomes apparent when this design is compared with conventional designs for high-tensile cables.

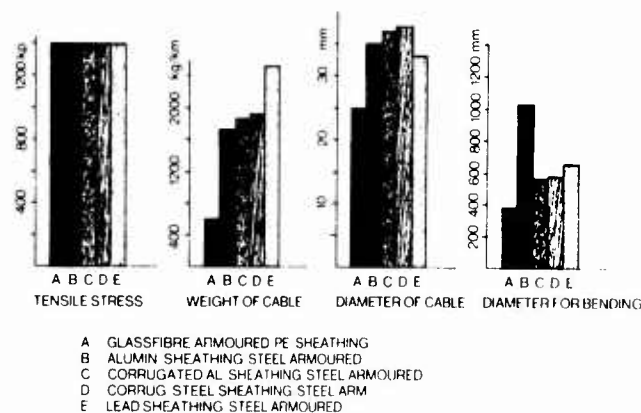


Fig. 4

Fig. 4 compares the cable weights, the outside diameters, and the minimum permissible bending diameters of 4 steel-armoured cables with those of fibreglass-armoured cable. All cables have the same cable cores and tensile strength values. It will be noted that the glassfilament armour offers optimum values for all compared criteria.

#### Protection against Moisture in the Cable Core

New methods have been developed not only for the design of a high-tensile sheath, but also for protection of the cable against the ingress of water.

It is generally recognized that cables insulated with plastics sheaths must be protected against the ingress of water. A metallic moisture barrier in the cable sheath is in keeping with the state of the art, in the same way as filling of the spaces in the cable core to prevent the ingress of water should the cable be damaged.

The standard practice of petro-jelly fillings is not applied for cables fitted with connecting plugs. Following several years of development work, it was preferred to fill spaces with polyurethane foam. As compared with petro-jelly fillings, polyurethane foam results in only an insignificant increase in the cable weight. Also, polyurethane foam does not cause any significant increase in mutual capacitance. The filler material has no aging problems, and does not negatively affect the long-term stability of the capacity unbalances. This is particularly important in the case of cables used at higher frequencies, i.e. with carrier frequencies. Foam filling of the cable core is not carried out continuously, but interrupted rhythmically at short intervals to yield alternate lengths of approx. 50 cm of filled and unfilled sections.

The purpose of this intermittent filling is to allow water to penetrate into only a limited section of the cable should the sheath suffer extraneous mechanical damage, so that monitoring of the cable and localization of the fault are possible.

Suitable procedures for this are the measurement of the insulation resistance with a bridge method if test wires with artificially perforated insulation are located in the cable core, or the pulse measurement method. The local increase in the mutual capacitance in the water filled chamber causes a sudden increase in the characteristic impedance, with a reflection factor of 14%, for example, in the cable mentioned here. This increase can be localized with a pulse echo meter.

Monitoring can be carried out as a routine procedure. This is expedient to ensure that an accumulation of unrecognized minor defects does not cause total failure of the complete line in the course of time, which may happen to fully filled cables.



## Connection System

These waterproof, plastic-insulated long-distance cables, armoured with fibreglass, are produced in lengths of 500 m. The connecting plugs at the ends of the cables are also corrosion-resistant, waterproof, and resist tension. They are made of plastics, and have a low weight.

The fibreglass armouring of the cable is inserted into the plugs and firmly connected with the plug casing by casting-in an epoxy resin compound. The complete plug connection has a tensile strength of more than 800 kp. Since the plug casing is filled with epoxy resin it is completely waterproof. The plugs are also resistant to vibration, shock, and impact. The connected plugs can later be covered with thermo-shrink tubing (Fig. 5).



Fig. 5

This prevents unauthorized access, and provides additional mechanical strength. The plugs have 52 poles. The crossfork contacts generate a high specific contact pressure; each of the four contact legs is independently sprung. As the plugged cables are intended for use at carrier frequencies and for PCM transmission, the wiring plan of the plugs is so designed that the geometry of the cable is retained.

The plug and the socket of the connectors are identical, so that the cables can be laid in any direction.

Accessory line equipment has also been developed to match the cables. Fig. 6 shows a coil piece with plugs for loaded lines. Sleeves for carrier-frequency amplifiers or PCM regenerators can also be fitted with plugs. Stub cables are used for the connection of exchange equipment.



Fig. 6

## Transmission Properties

If a trunk cable line is to permit installation without balancing or field work, even the drum lengths must feature excellent properties.

### Quality characteristics of drum lengths.

Fig. 7 shows the cumulative frequency of the capacitance unbalance of 40 lengths measured at 800 Hz.

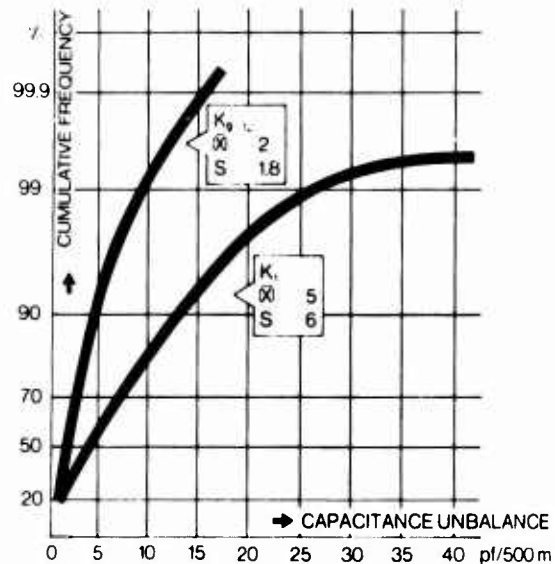


Fig. 7

The low mean values ( $k_1 = 5$  pF/500 m and  $k_2 = 2$  pF/500 m) guarantee the serviceability of the cables for high-quality transmission systems. The capacity unbalance amplitude along the length of the cable is checked by means of a pulse measuring method to check that it oscillates within narrow limits around the zero value.

The capacity unbalances and crosstalk attenuation are theoretically linked thus:

$$FEX [dB] = 20 \log \frac{8}{\omega Z k}$$

The crosstalk attenuation values measured at 120 kHz, shown as a cumulative frequency in Fig. 8, are even better than the capacity unbalance measurements, made at 0.8 kHz in view of the low accuracy in the zero-range, would indicate.

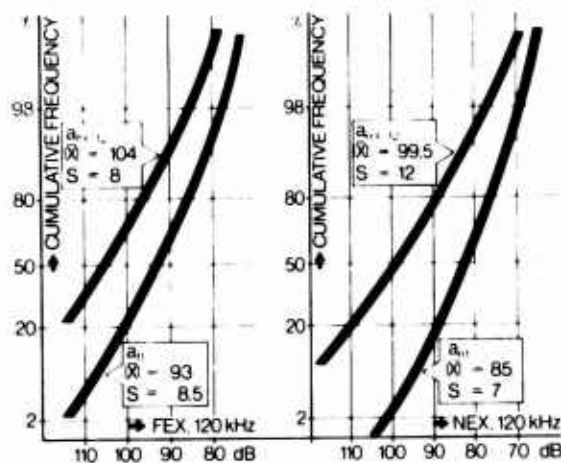


Fig. 8

In order to avoid fluctuations in the characteristic impedance and capacitive reflection points along the line, the mutual capacitance values of the drum lengths should vary only slightly (Fig. 9).

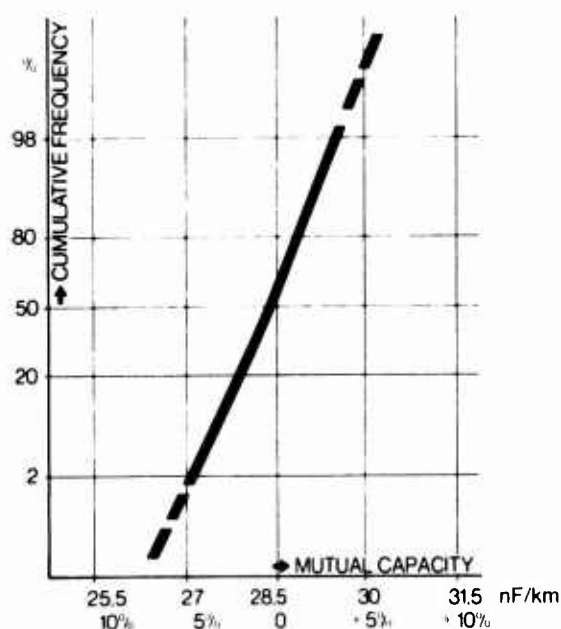


Fig. 9

These requirements were met in good degree. The deviation of the mean from the specified value is approx. 0.8%. Only a few individual values show deviation of max. 6%.

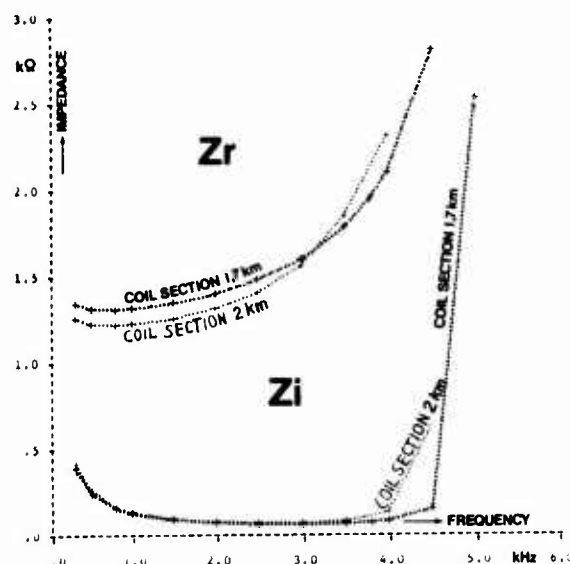
Line characteristics. The characteristic impedance for the cable in the voice frequency range (VF) is calculated from the values of the mutual capacitance and the d.c. loop resistance as follows:

$$|Z| = 1/2 \sqrt{\frac{R}{2\omega C}} = 554.2 \sqrt{\frac{1}{f}}$$

$Z$  in Ohm;  $f$  in kHz

The characteristic impedance values calculated with this formula were confirmed by measurements on a 30 km line.

The ripple on the measured  $Z$ -curve was better than 1%. Due to the low variation of the mutual capacity and loop resistance, the frequency-dependent factors impedance (Fig. 10) and line attenuation can be calculated with a computer for various loading systems.



Computed Impedance  $Z_r$  and  $Z_i$  of loaded lines

Fig. 10

The impedance of a line loaded with 80 mH (coil spacing = 2 km) was measured, and was found to attain the theoretically calculated values with an accuracy of better than 1%. There was no ripple on the impedance due to the uniformity of the mutual capacitance of all drum lengths in the line.

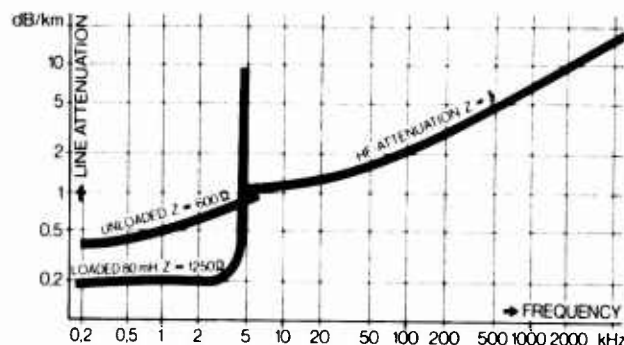


Fig. 11

The attenuation values in the VF range for unloaded and loaded lines and the line attenuation for RF transmission up to 6 MHz are shown in Fig. 11.

Quality characteristics of the line. Fig. 12 shows the far-end crosstalk FFX and the way it develops when coil sections are successively connected to form a long-distance line.

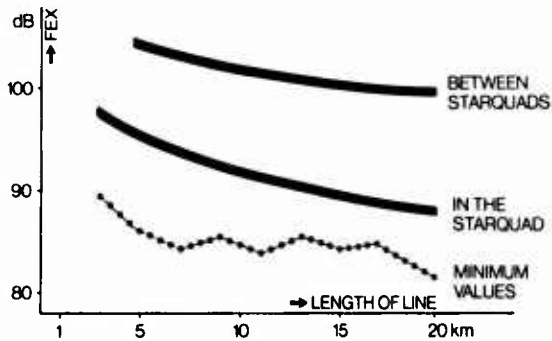


Fig. 12

Sections of 4 drum lengths each were successively connected with loading coils. It proved possible to maintain the normal line specifications easily without additional balancing work.

The line results were determined using a PCM30 regenerator field, in this case consisting of 12 cables with plugs (6 km). The crosstalk results up to 4 MHz are shown below as frequency-governed mean values (Fig. 13).

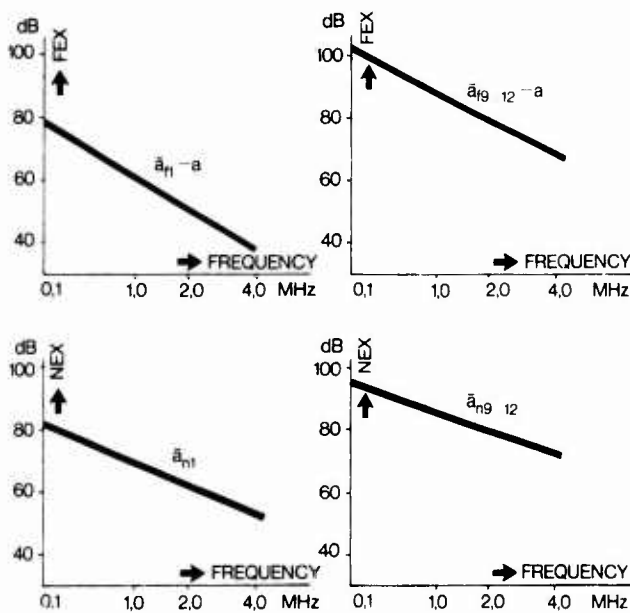


Fig. 13

Although the cable had no screening to separate the two directions of transmission, duplex operation (PCM30 and videophone) is possible in all neighbouring combinations. As far as possible, only one transmission direction should be operated in any one

star-quad.

#### Suitable Transmission Systems

Cables fitted with plugs permit easy assembling of cable lines without additional balancing work. The electrical uniformity of the cable is so good that the cables can be used without any further work for low frequency, carrier frequency, or PCM transmission following installation and connection of the drum lengths by means of the plugs.

In the case of voice frequency transmission, the cables can be used in either loaded or unloaded mode. Due to the low mutual capacitance, economical coil spacing of 2 km with side circuit loading coils of 80 mH can be obtained within the critical frequency. The ready-for-use coil pieces are also equipped with connecting plugs, so that they need not be assembled in the field.

Voice frequency transmission lines with these cables exhibit values for near- and far-end crosstalk attenuation which meet the requirements of the Federal German Post Office and the Federal German Railways for balanced trunk lines.

Connected unloaded lines are suitable for carrier frequency operation up to 120 kHz. Depending on requirements, up to 100% flexibility, e.g. in conjunction with the German 12-channel transmission system Z 12, is possible without additional balancing. For CF systems with higher frequencies concentrated balancing is possible to increase far-end crosstalk attenuation.

Digital transmission systems, e.g. 30-channel PCM with a transmission rate of 2.048 Mbit/sec can be used without limitation on these cable lines with commercially available regenerators. The necessary PCM regenerators are mounted in boxes, which can be fitted with plug connections. Experiments on a 20 km long transmission line have shown that combined operations are possible without mutual interference, one part of the circuits being occupied by 30-channel PCM and the other by a 120 kHz CF system.

#### Economic and Future Aspects

Special manufacturing methods are necessary for the production of the described glassfibre armoured PIC trunk cables assembled with connecting plugs. In addition, the high-tensile glass-armoured sheath and the plug fitting operations represent a further cost element in the production of the cables. The field work carried out by individuals in the field is transformed into controlled production routines in the plant. Consequently, there is no need for highly qualified personnel in the field, and manual operations in the field are reduced to an absolute minimum: the increased costs for cable

manufacture can be compensated, particularly taking into account the steadily rising labour costs of today.

In addition, the use of cables with connecting plugs offers several other advantages: this is apparent even in the planning stage of a transmission line, since no balancing specifications are necessary, and the cables need not be grouped. The normal planning and storage of materials for balancing elements, splicing and so on, can be dispensed with. Connecting plugs completely eliminate errors when the cables are assembled to form a line.

As there is no need for testing or measuring operations, the line can be put into operation as soon as the cables have been buried and the plugs connected.

If the cable is damaged, the line can be repaired later at a more suitable time. The hollow spaces formed by the intermittent filling with polyurethane foam allow immediate fault detection, but the axial spread of the water is prevented. If necessary, whole lengths or short pieces can be exchanged without balancing being necessary.

Precise localization of the defect is also simplified by the fact that it is possible to simply disconnect a plug connection in the near vicinity for a short period of time without any long interruption in line service.

Further economic advantage are offered by the suitability of these cable lines for operation at higher frequencies. Lines for low-frequency transmission can readily be converted for carrier frequency or PCM operation. There is no need for subsequent balancing for CF operation. The only operations necessary are the removal of the coil pieces and replacement by CF amplifiers or PCM regenerators, which are also fitted with plugs. Due to these cost- and labour-saving measures, the transmission capacity of a cable system can be expanded from 24 low-frequency channels to 288 channels with 12-channel CF or 360 channels with 30-channel PCM transmission. This equals an expansion of the cable system transmission capacity by the factor 12 or 15.

Simple and low-cost installation; tensile capacity offered by fibreglass armouring; short installation time; reliable operation with various frequencies; higher-quality transmission methods; these advantages make the cable with connecting plugs eminently suitable for a wide range of applications.

Apart from these advantages in countries where labour costs are high, the use of cables with connecting plugs means that high-quality cable transmission lines can also be installed even when no trained personnel is available for the work in the field. A final example of the efficiencies of cables with connecting plugs is in emergencies where it is necessary to set up reliable multi-pair cable systems extremely rapidly.

#### Acknowledgements

This paper is a result of team effort. We earnestly thank the individuals with a special mention to D.S. Parmar for his contribution to glassfibre application.



Dr. G. Thönneßen  
(Speaker)

AFG-TELEFUNKEN KABELWERKE  
Aktiengesellschaft  
Development Center  
W. Germany

22-28 Sommerfeld  
433 Mülheim/Ruhr-Saarn

Dr. G. Thönneßen finished his studies at Technische Hochschule Aachen in 1964. After a 3 years employment as a development engineer for CF-measuring instruments, he returned to Technische Hochschule Aachen, where he graduated as Dr. Ing. in 1971. Since that time he is a member of the development staff of the AFG-TELEFUNKEN KABELWERKE.



H.G. Dageförde is Head of the development of symmetrical communication cables section of the AEG-TELEFUNKEN KABELWERKE. As a Dipl.-Ing. of the Technische Hochschule Aachen, he joined Kabelwerk Duisburg (now a subsidiary company of AEG-TELEFUNKEN) in 1952. Since then he is engaged in testing, quality control, installation and development of communication cables.



P. Gregor studied at the Ingenieurschule Duisburg. He joined Kabelwerk Duisburg, now a part of AFG-TELEFUNKEN KABELWERKE, in 1966. Since then he is engaged as a development engineer in the department of telecommunication cables.

# MECHANICAL CHARACTERIZATION OF CABLES CONTAINING HELICALLY WRAPPED REINFORCING ELEMENTS

by

T. C. Cannon & M. R. Santana  
Bell Laboratories  
Norcross, Georgia

## SUMMARY

In this paper, the general system equations which describe the mechanical characteristics of a cable having one or more helically wrapped reinforcing elements are developed. These equations relate the cable moment and axial load to axial strain and cable untwist. The equations are applied to a cable of interest. The theoretical predictions and the experimental measurements generally agree to within ten percent. In a cable deployment situation, the frictional forces acting on this particular cable should be sufficient to resist the tension-induced twisting torque; therefore, cable untwist under load should be small and an accurate characterization of the cable's behavior should be obtained by invoking a zero twist assumption.

## 1. INTRODUCTION

Helical wrapping, of one form or another, is often found in cable construction. The wrapping may take the form of metal armor wires, tapes, plastic ribbons, binders or perhaps tensile reinforcing elements. For whatever purpose, the wrapping is an integral part of the cable and contributes to its mechanical properties. This report studies how helically wrapped elements influence the tensile and torsional characteristics of a cable.

The first portion of this report concerns itself with developing the general system equations for cables containing one or more helical elements. These equations are then used to predict the mechanical behavior of a newly designed cable. As a check on the theory, laboratory experiments are devised and carried out. The resulting data are then compared with the theoretical predictions.

## 2. ANALYSIS

The cable system equations will be derived by first developing the kinematic relations for a cable having a single layer of helically wrapped elements and then extending the theory to multiple layers. Combining the kinematic relations with cable load equations results in the general cable system equations.

## 2.1 Kinematics of Deformation

Figure 1 shows a section of a reinforced cable. The trajectory of one reinforcing strand is traced over the surface of the cylinder. The quantity,  $R$ , is defined as the distance between the center of the cable's core and the center of an armor strand.

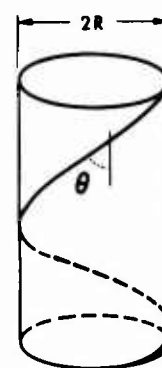


FIGURE 1

TRAJECTORY OF AN ARMOR WIRE  
OVER THE CABLE'S CORE.

Figure 2a shows a developed view of the surface along which the strands lie. The lay length is represented by  $l$  and the lay angle by  $\theta$ . The length of strand necessary to complete one wrap of the cable is defined as  $l_s$ . Figure 2b shows the cable after being subjected to a tensile load. In general, the strand will stretch and this elongation will be denoted as  $\delta l_s$ . Simultaneously, there will occur a diametric contraction of the core,  $2\delta R$ , and a twisting of the cable,  $\phi$ , turns per foot. The net result is that the

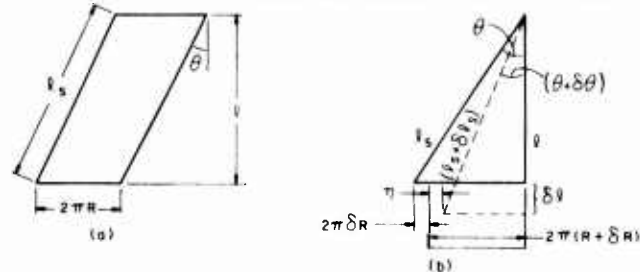


FIGURE 2

DEVELOPED VIEW OF THE ARMORED SURFACE



original element (solid lines) is transformed into the deformed element (dashed line) in Figure 2b.

The following geometrical relations describe the new configuration

$$(\ell_s + \delta\ell_s) \cos(\theta + \delta\theta) = (\ell + \delta\ell) \quad (1)$$

$$\tan(\theta + \delta\theta) = \frac{2\pi(R + \delta R) - \eta}{(\ell + \delta\ell)}, \quad (2)$$

where the twist arc length is given by

$$\eta = \phi\ell(2\pi R) \quad (3)$$

Combining (1), (2) and (3) leads to an expression relating the axial and strand elongations to the twisting of the cable

$$(2\pi R)^2 (1 - \phi\ell + \frac{\delta R}{R})^2 =$$

$$\ell_s^2 (1 + \frac{\delta\ell_s}{\ell_s})^2 - \ell^2 (1 + \frac{\delta\ell}{\ell})^2 \quad (4)$$

Making use of geometric identities, (4) may be reduced to

$$\begin{aligned} \frac{2\delta\ell_s}{\ell_s} + \left(\frac{\delta\ell_s}{\ell_s}\right)^2 &= \cos^2\theta \left[ 2\frac{\delta\ell}{\ell} + \left(\frac{\delta\ell}{\ell}\right)^2 \right] \\ &+ \sin^2\theta \left[ -2\phi\ell - 2\phi\ell \frac{\delta R}{R} + \frac{2\delta R}{R} \right. \\ &\left. + (\phi\ell)^2 + \left(\frac{\delta R}{R}\right)^2 \right] \quad (5) \end{aligned}$$

Equation (5) is the basic expression interrelating the various deformations of the cable. There is a nonlinear dependence of  $\delta\ell_s$  on  $\delta\ell$ ,  $\phi$  and  $\delta R$ . A convenient linear approximation may be obtained by neglecting products of small terms. Doing this (5) becomes

$$\left(\frac{\delta\ell_s}{\ell_s}\right) = \cos^2\theta \left(\frac{\delta\ell}{\ell}\right) + \sin^2\theta \left(-\phi\ell + \frac{\delta R}{R}\right) \quad (6)$$

Recognizing that

$$\frac{\delta\ell_s}{\ell_s} = \epsilon_s$$

$$\frac{\delta\ell}{\ell} = \epsilon_c$$

(6) may be written as

$$\epsilon_s = \epsilon_c (\cos^2\theta - v^* \sin^2\theta) - (\ell \sin^2\theta) \phi, \quad (7)$$

where  $\epsilon_s$  is the strand strain,  $\epsilon_c$  is the axial cable strain and  $v^*$  is a pseudo Poisson's ratio for the cable and is a measure of its diametric contraction. Mathematically  $v^*$  is given by:

$$v^* \equiv - \frac{(\delta R/R)}{(\delta\ell/\ell)} \quad (8)$$

Equation (7) is the fundamental linearized relation describing the deformation of the cable strands.

## 2.2 Multiple Layers of Helically Wrapped Material

The single layer kinematic equations will now be extended for the case of more than one layer of helical elements.

For small deformations, the strain experienced by the  $i$ th strand layer,  $\epsilon_{si}$  wrapped at a lay angle  $\theta_i$  is given by

$$\epsilon_{si} = \epsilon_c (\cos^2\theta_i - v_i^* \sin^2\theta_i) - \phi(\pi R_i \sin 2\theta_i), \quad (9)$$

where  $\epsilon_c$  represents the axial strain of the cable,  $v_i^*$  is the diametric contraction that the cable experiences at the strand location,  $R_i$  is the radial location of the strand layer, and  $\phi$  is the untwist turns experienced per unit length of the cable when it is loaded. For multiple strand layers an untwist sign convention must be adopted. A right hand lay angle will be defined as positive and hence  $\theta_i$  will be either a positive or negative number, depending on whether the strand has a right or left hand lay. A clockwise twist of the cable about its axis is defined as positive. This is illustrated in Figure 3.

## 2.3 Cable Load Equations

Using the above convention, the twisting moment developed on a cable is readily computed. Defining clockwise twisting moments as positive, the moment generated by the  $i$ th strand layer is

$$M_i = T_{si} R_i \sin\theta_i - \phi(n_i J_{si} G_{si} \cos^2\theta_i), \quad (10)$$

where  $T_{si}$  is the tension supported by the  $i$ th strand layer,  $n_i$  is the number of strands

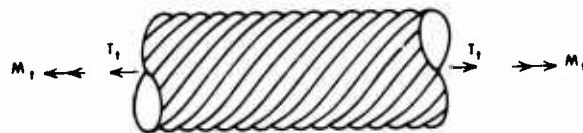


FIGURE 3  
RESULTANT CABLE MOMENT



in the  $i$ th layer,  $J_{si}$  and  $G_{si}$  are the strand's moment of inertia and torsional rigidity, respectively. Writing (10) in terms of the strand elastic modulus,  $E_{si}$ , and area,  $A_{si}$  results in

$$M_i = (n_i E_{si} A_{si} R_i \sin \theta_i) \epsilon_{si} - \phi (n_i J_{si} G_{si} \cos^2 \theta_i). \quad (11)$$

The total cable moment equals the sum of the moment contributions from each of the strand layers plus that of the core. (Here core refers to all other elements of the cable that are not helically wrapped.) Hence

$$M_t = -\phi J_c G_c + \sum_{i=1}^m \left[ \epsilon_{si} (n_i E_{si} A_{si} R_i \sin \theta_i) - (n_i J_{si} G_{si} \cos^2 \theta_i) \phi \right], \quad (12)$$

where the subscript "c" refers to core properties, and  $m$  is the number of strand layers. Finally, using (9) to eliminate  $\epsilon_{si}$  yields

$$M_t = \epsilon_c \left[ \sum_{i=1}^m (\cos^2 \theta_i - v_i^* \sin^2 \theta_i) (n_i E_{si} A_{si} R_i \sin \theta_i) - \phi \left\{ J_c G_c + \sum_{i=1}^m \left[ (n_i J_{si} G_{si} \cos^2 \theta_i) + \pi R_i^2 \sin 2\theta_i (n_i E_{si} A_{si} \sin \theta_i) \right] \right\} \right] \quad (13)$$

Equation (13) is the generalized moment relation. The general tension relation is the other equation needed to complete the system.

The total axial load carried by the cable is the sum of the core load and the strand load. This is

$$T_t = T_c + \sum_{i=1}^m T_{si} \cos \theta_i$$

or

$$T_t = (E_c A_c) \epsilon_c + \sum_{i=1}^m (n_i E_{si} A_{si} \cos \theta_i) \epsilon_{si}. \quad (14)$$

Again using (9) to eliminate  $\epsilon_{si}$  leads to the general expression for  $T_t$

$$T_t = \epsilon_c \left[ E_c A_c + \sum_{i=1}^m (\cos^2 \theta_i - v_i^* \sin^2 \theta_i) \times (n_i E_{si} A_{si} \cos \theta_i) - \phi \left[ \sum_{i=1}^m (\pi R_i \sin 2\theta_i) (n_i E_{si} A_{si} \cos \theta_i) \right] \right] \quad (15)$$

Equations (13) and (16) describe the mechanical behavior of cables containing helically wrapped elements. In the following section these equations will be used to characterize the performance of an experimental cable of interest.

### 3. APPLICATION OF THEORY

For convenience (13) and (16) will be written in the abbreviated form

$$\left. \begin{aligned} M_t &= C_1 \epsilon_c - C_2 \phi \\ T_t &= C_3 \epsilon_c - C_4 \phi \end{aligned} \right\} \quad (16)$$

where the coefficients,  $C_i$  are defined as

$$C_1 \equiv \sum_{i=1}^m (\cos^2 \theta_i - v_i^* \sin^2 \theta_i) (n_i E_{si} A_{si} R_i \sin \theta_i) \quad (17)$$

$$C_2 \equiv J_c G_c + \sum_{i=1}^m \left[ n_i J_{si} G_{si} \cos^2 \theta_i + \pi R_i^2 \sin 2\theta_i \times (n_i E_{si} A_{si} \sin \theta_i) \right] \quad (18)$$

$$C_3 \equiv E_c A_c + \sum_{i=1}^m (\cos^2 \theta_i - v_i^* \sin^2 \theta_i) \times (n_i E_{si} A_{si} \cos \theta_i) \quad (19)$$

$$C_4 \equiv \sum_{i=1}^m (\pi R_i \sin 2\theta_i) n_i E_{si} A_{si} \cos \theta_i \quad (20)$$

The coefficients  $C_1$ ,  $C_2$ ,  $C_3$  and  $C_4$  were computed for an experimental cable. The cable consisted of a cable core, helically wrapped strands of fibrillated polypropylene twine, helically wrapped graphite yarns, and a low density polyethylene (LDPE) jacket. The polypropylene strands were wrapped with a left hand lay at a 16.0° lay angle. The graphite strands were wrapped with a right hand lay at a 4.4° lay angle.

A summary of the material properties of the cable components is given in Table I.

Table I  
MATERIAL PROPERTIES OF CABLE COMPONENTS

Component	Tensile Modulus, E, and Shear Modulus, G (PSI)	Total Cross-Sectional Area (in <sup>2</sup> )
Cable Core	E = $10 \times 10^6$	$1.38 \times 10^{-3}$
Polypropylene	E = $0.33 \times 10^6$ G = $0.118 \times 10^6$	$2.23 \times 10^{-2}$
Graphite	E = $18 \times 10^6$ G = $7.2 \times 10^6$	$2.04 \times 10^{-3}$
LDPE	E = $.35 \times 10^5$ G = $.12 \times 10^5$	$4.52 \times 10^{-2}$

In using (17), (18) and (20) the subscripts "1" and "2" will refer to the polypropylene and the graphite respectively. The subscript "c" will refer to the combined properties of the cable core and the LDPE sheath. Experience has shown that a characteristic value for  $v_1^*$  is about 0.5.

Using elementary theory of elasticity, the moments of inertia were computed to be:

$$\begin{aligned} J_{PE} &= .996 \times 10^{-3} \text{ in.}^4 \\ J_{CGC} &= 1.66 \text{ (in.-lb.)/(turns/foot)} \quad (21) \\ J_{s1} &= 3.18 \times 10^{-6} \text{ in.}^4 \\ J_{s2} &= 4.60 \times 10^{-9} \text{ in.}^4 \end{aligned}$$

The corresponding torsional rigidities are:

$$\begin{aligned} n_1 J_{s1} G_{s1} &= (5 \times 3.18 \times 10^{-6} \times 1.18 \times 10^5)/12 \\ &= 0.156 \frac{\text{(in.-lb.)}}{\text{(turns/foot)}} \quad (22) \end{aligned}$$

$$\begin{aligned} n_2 J_{s2} G_{s2} &= (12 \times 4.6 \times 10^{-9} \times 7.2 \times 10^6)/12 \\ &= 3.3 \times 10^{-2} \frac{\text{(in.-lb.)}}{\text{(turns/foot)}} \quad (23) \end{aligned}$$

Substituting (21), (22) and (23) and the parameters displayed in Table I into (17), (18), (19) and (20) yielded values for  $C_1$ ,  $C_2$ ,  $C_3$ , and  $C_4$ . These numbers are:

$$\begin{aligned} C_1 &= 1.77 \times 10^2 \text{ (in.-lb.)/(in./in.)} \\ C_2 &= 5.85 \text{ (in.-lb.)/(turns/foot)} \\ C_3 &= 5.80 \times 10^4 \text{ (lb.)/(in./in.)} \\ C_4 &= 89.4 \text{ (lb.)/(turns/foot).} \quad (24) \end{aligned}$$

Having computed these coefficients, certain predictions can now be made about the cable's behavior.

An important cable parameter is its tensile modulus,  $T/\epsilon_c$ . The tensile modulus may be computed under two conditions: (1) twist restrained ( $\phi = 0$ ) and (2) unrestrained ( $M_t = 0$ ). From (8) these values are:

$$(T_t/\epsilon_c) \Big|_{\phi=0} = C_3 = 5.80 \times 10^4 \text{ (lb.)/(in./in.)} \quad (25)$$

$$(T_t/\epsilon_c) \Big|_{M_t=0} = C_3 - \frac{C_4 C_1}{C_2} \quad (26)$$

$$= 5.53 \times 10^4 \text{ (lb.)/(in./in.)}$$

The two numbers differ by 4.9 percent.

A second important cable parameter is the twisting moment generated when the cable is heavily loaded. Excessively large twisting moments may necessitate the utilization of special cable pulling equipment. From (16) the twisting moment is:

$$\begin{aligned} M_t \Big|_{\phi=0} &= 1.77 \times 10^2 \epsilon_c \text{ (in.-lb.)/(in./in.)} \\ &\quad \phi=0 \end{aligned}$$

A reasonable upper limit on  $\epsilon_c$  is approximately 0.5 percent. Hence

$$(M_t)_{\max} \approx 0.88 \text{ (in.-lb.)}. \quad (27)$$

This number is small and consequently the twisting moment should not have a noticeable effect on the cable pulling equipment.

When the cable is not twist restrained, dynamic loading can cause the cable to form kinks and fail.<sup>1</sup> This tendency increases for cables having relatively small torsional rigidities. Thus the ratio of generated torque to resisting modulus becomes important. (This ratio is in terms of turns per foot.) From (16) the twist of the unrestrained cable is computed to be:

$$\phi = C_1 \epsilon_c - C_2 \phi$$

or

$$\left( \frac{\phi}{\epsilon_c} \right) = \frac{C_1}{C_2} = 30.2 \text{ (turns/foot)/(in./in.)}. \quad (28)$$

In order to access the accuracy of the theoretical predictions, several experiments were designed and carried out. This experimentation is discussed in the following section.

## 4. EXPERIMENTAL

### 4.1 Purpose

The intent of the experimental investigation was to check on the accuracy of the theoretical predictions. Specifically, it was desired to obtain a direct or indirect measurement of the two coefficients  $C_3$  and  $C_4$  and the ratio  $C_1/C_2$ .

### 4.2 Measurements Needed

All of the information sought can be found through cable tension testing. From (16) it is seen that

$$C_3 = \left( \frac{T_t}{\epsilon_c} \right) \bigg|_{\phi=0} \quad (29)$$

This ratio can thus be determined by applying a tensile load on a cable whose ends are restrained from rotating and measuring the ratio of axial load to strain.

With a different setup the quantities  $C_4$  and  $C_1/C_2$  can be determined. If the cable ends are free to rotate, the system equations become

$$\begin{aligned} 0 &= C_1 \epsilon_c - C_2 \phi \\ T_t &= C_3 \epsilon_c - C_4 \phi \end{aligned}$$

Solving for the desired parameters yields

$$\left( \frac{C_1}{C_2} \right) = \left( \frac{\phi}{\epsilon_c} \right) \bigg|_{M_t=0} \quad (30)$$

and

$$C_4 = \frac{(C_3 \epsilon_c - T_t)}{\phi} \quad (31)$$

Thus, the measurements required in order to determine  $C_4$  and  $(C_1/C_2)$  are axial load, strain, and angle of twist.

### 4.3 Experimental Setup

Figure 4 shows a sketch of the setup used for the experiments. A 2000 lb ratchet winch was connected to a force gauge by way of a wire rope. The other end of the force gauge was connected to a radial bearing swivel which in turn was connected to a Kellems grip. The cable was loaded through the Kellems grips attached to its ends. The stationary end of the cable was prevented from rotating.

Strain measurements were made with a ten foot flexible steel gauge. One end of the gauge was directly attached to the cable. The movement of the other end of the gauge relative to a point on the cable provided a measure of the cable elongation.

### 4.4 Experimental Procedure

The cable was loaded under two conditions. In one set of tests the swivel bearing allowed one end of the cable to rotate as load was applied. In the other testing, the swivel joint was removed and the cable was prevented from twisting. For both cases the load and strain were recorded incrementally. Twist measurements were made either incrementally or at extremal load points, depending on measuring feasibility.

It was anticipated that  $\phi$ , the cable twist per foot, would be small. Accordingly, it was originally planned to test long lengths of cable in order to increase the amount of cable twist and thereby reduce the error in measuring  $\phi$ . A cable length of 180 feet was chosen for the initial test.

Trial tests conducted prior to the actual experimentation yielded valuable information which resulted in some alterations in the experimental procedure. When under no load the cable rested in a long wooden tray. As load was applied the cable tended to raise itself off the tray and form a catenary. Prior to lift off, the frictional forces between the cable and the tray were large enough to resist the twisting action of the cable. Hence for long cables it was difficult to make accurate measurements of  $\phi$ . On the other hand, for short cables (approximately thirty feet) lift off occurred after only a few pounds of tension and  $\phi$  could be measured more accurately. It was thus decided to make  $\phi$  measurements on short cable lengths.

Another phenomenon observed was the uncertainty in the neutral, or zero twist, position of the cable. If a length of cable is twisted about its longitudinal axis (in either the clockwise or counterclockwise directions), it will undergo an initial plastic rotation before developing an elastic restoring moment. The amount of plastic rotation separating the elastic restoring regions will be referred to as the play. This cable play represents the amount of uncertainty in determining the neutral position of the cable. It was speculated that the play was a result of internal damping. Testing of different cable lengths showed the play to be inversely proportional to length.

In order to remove the play uncertainty from the twist measurements the following routine was followed. First, the cable was loaded until the high slope region of the load-elongation curve was reached. At this point the load was maintained constant while the play was removed. This was done by twisting the cable in the direction opposite to the untwisting motion until the cable would self restore. The loading of the cable was then resumed and the cable untwist and strain were recorded from that point on. (After the maximum load was reached, a similar procedure was followed to check on the cable twisting as the load was removed. Before the cable was

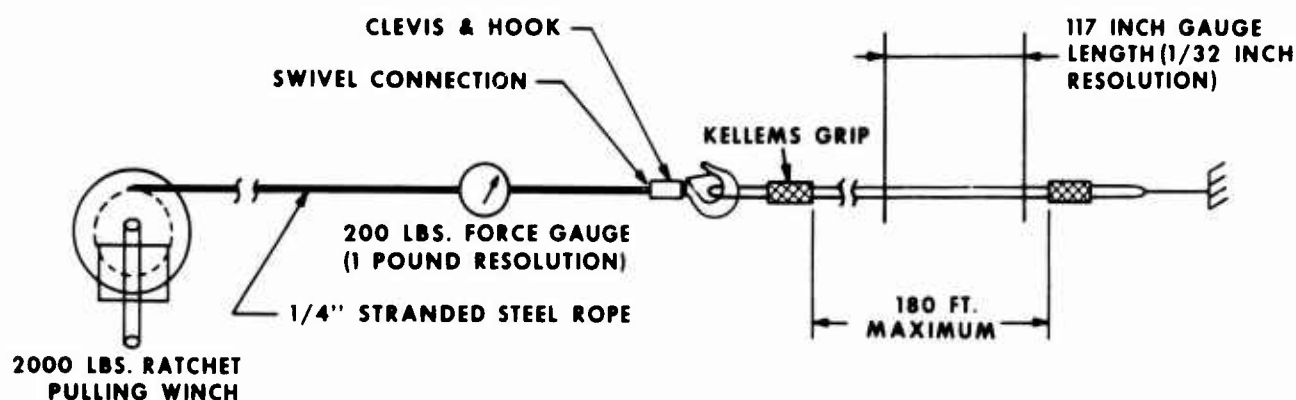


FIGURE 4. EXPERIMENTAL SETUP

unloaded, the uncertainty was removed by untwisting the cable until it would self restore. Both measurements yielded identical results.)

In all of the cable testing it was observed that there was no twisting tendency until after the high slope region of the load elongation curve had been reached. This was the anticipated response since the high slope region signals the point where the graphite begins to take significant load and the graphite loading is responsible for cable twist.

##### 5. RESULTS AND CONCLUSIONS

The results of the testing are presented in Figure 5 and Tables II and III. Figure 5 shows the load-strain curves for the cable with free and fixed end conditions. Consistent with theory, the fixed end cable has a higher tensile modulus than the free-end.

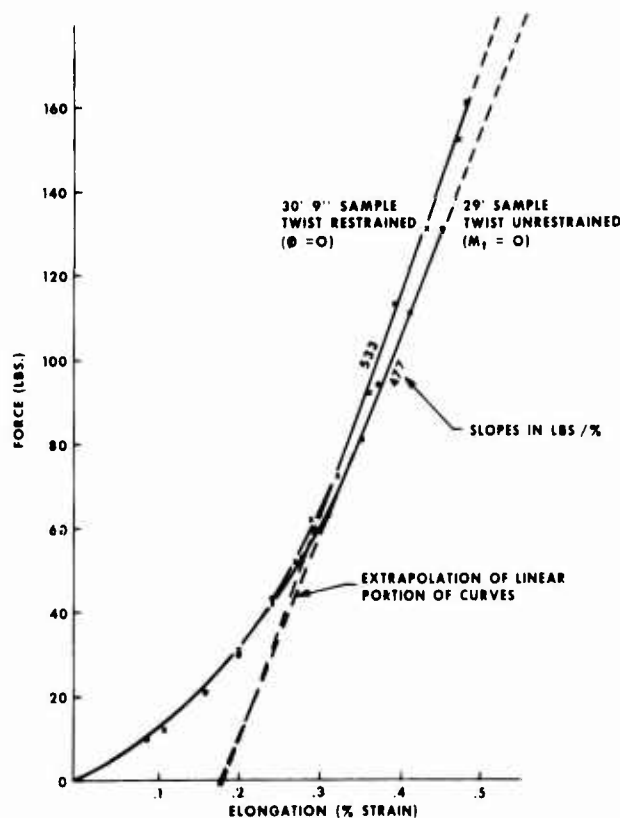


FIGURE 5 LOAD-STRAIN BEHAVIOR OF THE CABLE

TABLE II  
SUMMARY OF CABLE TWIST MEASUREMENTS

Sample Number	Sample Length (ft.)	Number of Runs	Max. Cable Twist $\theta_{max}$ (Turns/ft.)	Min. Cable Twist $\theta_{min}$ (Turns/ft.)	Avg. Cable Twist $\theta_{ave}$ (Turns/ft.)	Max. Cable Tension (lbs.)	Differential Cable Strain (in./in.)
1	15.79	2	.087	.079	.081	140	.00270 to .00285
2	15.79	3	.079	.071	.077	140	.00270 to .00285
3	14.17	1	.079	.079	.079	140	.00275 to .00302
4*	30.75	1	0	0	0	160	.00270 to .00300

\* Twist restrained

The twist measurements are summarized in Table II. Three different samples were tested and all three agree fairly well. During the testing it was noticed that the initial loading of a specimen tended to yield larger axial strains than subsequent runs. This was attributed to a structural looseness that became worked out as the cable was cycled. In any case, all of the data agreed to within ten percent.

TABLE III  
SUMMARY OF EXPERIMENTALLY AND THEORETICALLY  
DETERMINED CABLE PARAMETERS

Sample Number	$C_3 = \frac{T_t}{\epsilon_c} \Big _{\phi=0}$ ( $\frac{\text{lbs.}}{\text{in./in.}}$ )	$\frac{T_t}{\epsilon_c} \Big _{M_t=0}$ ( $\frac{\text{lbs.}}{\text{in./in.}}$ )	$\frac{C_1}{C_2} = \frac{\phi}{\epsilon_c} \Big _{M_t=0}$ ( $\frac{\text{Turns/ft.}}{\text{in./in.}}$ )	$C_4 = \frac{C_3 \epsilon_c - T_t}{\phi} \Big _{M_t=0}$ ( $\frac{\text{lbs.}}{\text{Turns/ft.}}$ )
1	—	49,100 to 51,800	29.1 to 30.7	47 to 143
2	—	49,100 to 51,800	27.0 to 28.5	51 to 155
3	—	46,400 to 50,900	26.2 to 28.7	83 to 252
4*	53,300 to 59,200	—	—	—
Theory	58,000	55,300	30.2	89.4

\* Twist restrained

Table III compares the experimentally determined cable parameters with theoretical predictions. All four quantities determined agree well with theory. There is a large uncertainty in the experimental determination of the quantity  $C_4$ . The coefficient  $C_4$  is proportional to the difference between  $C_3$  and  $(T_t/\epsilon_c) \Big|_{M=0}$ . These quantities are the

slopes of the load-elongation curve for the twist restrained and unrestrained cases respectively. In determining  $C_4$ , it is required that the difference between these two large slopes be found. This operation causes the uncertainty in  $C_4$ . The net effect is that a consistent and accurate measurement of  $C_4$  becomes difficult. However, the theoretical predictions fall within the range of the experimental determinations.

The theoretical and experimental values for  $C_3$  agree to within ten percent. The theoretical computation of the tensile modulus for a cable with free ends exceeds the measured value by about ten percent. Here, it is felt that an overestimation of the contribution of the core is responsible.

The final quantity determined, the untwist of the cable, was found to agree well with the theoretical prediction. The first cable tested had a measured value of  $(C_1/C_2)$  from 29.1 to 30.7 (turns/ft.)/(in./in.) compared to a predicted value of 30.2. The agreement was not as close, but still good, with the other two samples. The third sample was tested only once and the cable's structural looseness may have masked some of its torsional characteristics.

A point mentioned earlier, and worth reiterating, is that the frictional forces that acted on the cable when it was allowed to rest in the long wooden tray were sufficient to resist the tension induced twisting torque. Thus the cable behaved as if its ends were restricted from turning. In a cable deployment situation it is suspected that similar restricting forces will exist. Accordingly, cable untwist under load should be small and a more

accurate characterization of the cable's behavior should be obtained by invoking the zero twist assumption.

Summarizing, the theoretical predictions and the experimental measurements generally agree to within ten percent. For the case where significant differences do exist it is believed that these differences arise from limitations on the resolution of the experimental data. Thus it is felt that the theory presented herein accurately describes the cable mechanics. Further, the testing procedure used appears to be sufficient in order to characterize the cable. In future tests, this procedure may be expanded to include direct measurements of the twisting moment.

## REFERENCES

1. J. J. Myers, Handbook of Ocean and Underwater Engineering, (New York: McGraw-Hill, 1969), 1st Edition, Chapter 5, p. 9.



Thomas Cannon received his BS, MS and PhD degrees in Aeronautical Engineering from Purdue University. After graduation in 1970 Tom began work at Bell Telephone Labs in the Safeguard Division. He has since worked in the Ocean Systems Division and has been working in the Loop Transmission Division since October of 1974.



Manuel R. Santana received his BS degree in Electrical Engineering in 1970 from the University of Hartford and his MS degree in Electrical Engineering in 1971 from Georgia Institute of Technology. Since 1970 he has worked on cable design and development in Bell Telephone Laboratories' Loop Transmission Division.

# RELATING THE TWIST DETECTION MEASUREMENTS OF TWISTED PAIRS TO THEIR CROSSTALK PERFORMANCE

by  
H. W. Friesen  
Bell Telephone Laboratories, Inc.  
Norcross, Ga.

## ABSTRACT

The desirability of a more complete understanding of crosstalk behavior in multipair cable has led to a procedure for relating pair orientation and separation as a function of distance along the cable to the crosstalk coupling between that combination of pairs. The measurement procedure is non-destructive. The cable is simply pulled through a "twist detection head assembly, (TDH)".

Pair twist information is obtained by exciting the pair of interest with an audio frequency current. The resultant field is detected on the outside of the cable by means of tuned coils inside the TDH as the cable is pulled past the coils. Pair separation is determined by measuring unit orientation and assuming nominal unit dimensions. In a typical recording arrangement, twist length data for two pairs, stranding lay of the units they are in and the cabling lay is obtained in a single pass by means of frequency multiplexing. The information is recorded on an audio tape recorder. Demodulation and conversion to digital form takes place when the recording is played back.

A digital computer is used to compute the coupling from the twist data by means of a formula for the magnetic coupling between two twisted pairs inside a shield. This so called "twist coupling function" is compared with the coupling function obtained from near-end crosstalk measurements. The agreement between the two coupling functions for like twist combinations is quite remarkable.

In the case of like twists the need for keeping pairs well separated in order to keep crosstalk low is demonstrated. One of the examples shows that the twisting process can be so accurate that the number of twists for two pairs in 2600 feet can be the same to within a fraction of a twist length.

## I. INTRODUCTION

Crosstalk in multipair cable is a very complicated phenomenon. This is due to the fact that fields in wire pairs are not tightly confined to the wires of the individual pairs but interact with other pairs in the same cable. A second reason is that the location of wires inside a multipair cable cannot be precisely predicted from design information of the cable. This re-

sults in the crosstalk behavior being quite random.

Crosstalk is a performance limiting factor in several carrier systems such as T1, T1C, T2 and voice frequency systems with repeater gain. It appears that overall system costs could be reduced in such systems if cable crosstalk could be reduced without significantly increasing cable costs. To achieve this crosstalk reduction, or even know if it is possible, requires a better knowledge of the relationship between the physical cable structure and the resultant crosstalk performance.

The subject of this presentation is that of obtaining measurements of various geometric quantities such as pair angle, stranding angle and cabling angle and relating those measurements to the corresponding crosstalk performance. The basic measurement procedure is non-destructive in that the cable is simply pulled through a twist detection head assembly (TDH).

## II. DIRECT CROSSTALK EQUATIONS

The basic crosstalk circuit being studied is shown in Figure 1. Only direct crosstalk is being considered. Figure 1 shows two pairs with the same characteristic impedances,  $Z_0$ , and propagation constants,  $\gamma$ . If a

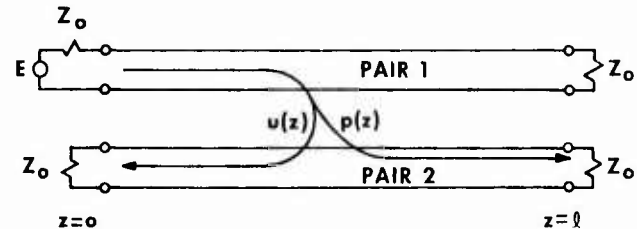


FIGURE 1  
DIRECT CROSSTALK CIRCUIT

signal is launched at the transmitting end ( $z=0$ ) of pair 1, some of it will propagate to point  $z$  in the cable incurring an  $e^{-\gamma z}$  propagation effect, couple over to pair 2 via the near end coupling function  $u(z)$  and return to the transmitting end having incurred another  $e^{-\gamma z}$  propagation effect. The expression summing up this kind of coupling over the whole cable length is given by Equation (1) and is known as the near end crosstalk equation.<sup>1</sup>

$$N(\omega) = j\omega \int_0^l e^{-2\gamma z} u(z) dz \quad (1)$$



Similarly, some of the signal launched at the transmitting end of pair 1 in Figure 1 propagates to location  $z$ , couples over via the far-end coupling mechanism  $p(z)$  and propagates to the receiving end of the pair 2. The far-end crosstalk equation<sup>1</sup> sums up this kind of behavior over the whole cable length as indicated by

$$F(\omega) = j\omega e^{-\gamma l} \int_0^l p(z) dz \quad (2)$$

The coupling functions  $u(z)$  and  $p(z)$  can be expressed in terms of the sum and difference respectively of the electromagnetic and electrostatic components of coupling as denoted by

$$u(z) = 1/2[Y_0 L_{12}(z) + Z_0 C_{12}(z)] \quad (3)$$

$$p(z) = 1/2[Y_0 L_{12}(z) - Z_0 C_{12}(z)] \quad (4)$$

In the above equations  $L_{12}$  and  $C_{12}$  are the inductive and capacitive pair to pair coupling components respectively. The amplitude of these quantities is mainly a function of wire separation of the individual pairs and pair separation, being proportional to the former and inversely proportional to the latter. Twisting the pairs causes  $L_{12}$  and  $C_{12}$  to oscillate, principally, at the sum and difference of the pair twist frequencies.<sup>2</sup> This greatly reduces the crosstalk, as can be seen by noting that Equations (1) and (2) are basically integrals of  $u(z)$  and  $p(z)$  respectively

Much of this presentation pertains to relating the coupling functions obtained from twist measurements to those obtained from near-end crosstalk data. The nature of near end crosstalk is such that frequency domain data,  $N(\omega)$ , can be transformed into distance domain information,  $u(z)$ . A useful expression for this computation can be found in reference 3. This method of computing the coupling function yields essentially the same coupling variations with distance along the cable when the measurements are made at one end of the cable as when they are made at the other end.<sup>3</sup>

### III. TWIST DETECTION TECHNIQUE

The twist detection technique involves exciting the pair or circuit of interest with an audio frequency current. The field produced by the current is a dipole field as is depicted in Figure 2. Tuned coils external to the cable are used to detect the polarity and strength of the magnetic field relative to the coil orientation. Two coils mounted on the X axis, connected in an additive mode, and two more coils on the Y axis, also connected in an additive mode, yield an estimate of the sine and cosine respectively of the angle of a line drawn through the two members of the pair relative to the X axis.

If the pair is perfectly twisted, is pulled past the coils at a constant speed,

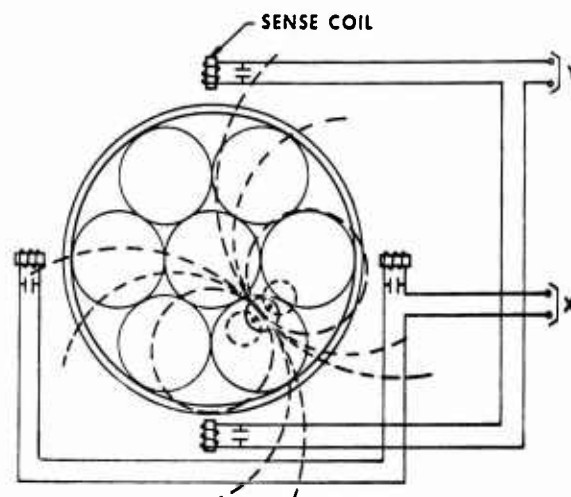


**FIGURE 2**  
**DIPOLE CURRENT FIELD RESULTING FROM EXCITING PAIR WITH AUDIO FREQUENCY CURRENT**

and the pair is always on the axes of the X and Y coils, perfect sine and cosine waveforms are observed on the X and Y axis coils. The typical response for a pair moving about within the cable cross section as well as rotating is more complex.<sup>4</sup> Various compensation and correcting techniques have been devised. Also, the coil response decreases with decreasing twist length. The present TDH has shielding sufficient for detecting 1" twists and longer in 50 pair cables.

The cable is pulled past the coil configuration at a constant line speed by means of a caterpillar capstan. Typical line speeds for up to 100 pair cable are in the 50 to 100 ft./min. range.

Much of the twist detection work to date has been carried out on a 52 pair LOCAP cable.<sup>5</sup> The 52 pair design consists of seven 7-pair units and three interstitial pairs. The units are not fully stranded but are oscillated back and forth. Figure 3

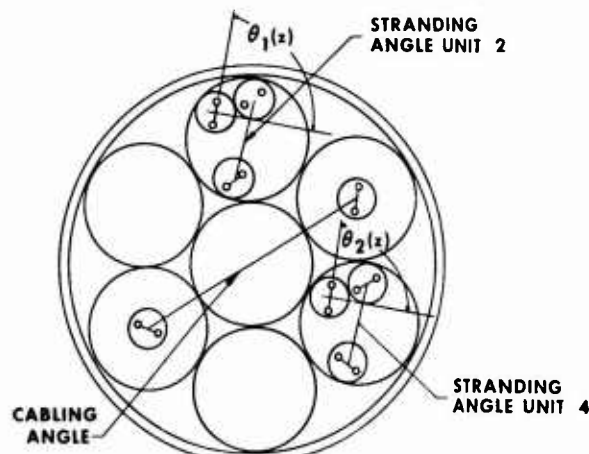


**FIGURE 3**  
**CROSS SECTION OF LOCAP CABLE SHOWING ANGLES THAT MUST BE MEASURED**

is a cross section view of such a design showing the pairs involved in twist measurements for a typical pair combination. In all, five different angles must be measured as a function of distance to allow calculation of the coupling between a layer pair of one unit and layer pair of a second unit. Twist measurements of the two pair angles, the stranding angles of the units they are in and the cabling angle allow one to compute the actual wire locations with respect to the center of the cable and in turn the coupling function. Such a calculation assumes that pairs and units stay in the proper positions relative to other pairs and units. The stable six around one lay-up of the LOCAP cable is good from this standpoint. This calculation also assumes nominal wire separation, unit diameter, etc.

Frequency multiplexing is used for the five circuit detection system. The present set of frequencies range from 9 to 11 kHz. They are well enough separated to allow separation by means of filters with a Q of 200 and close enough together to pass through the single tuned detection coils.

The present method of obtaining the twist data involves recording the twist data for the five circuits simultaneously on a stereo tape recorder and subsequently playing back and digitizing the information one circuit at a time. The recording circuitry is depicted in block diagram form in Figure 4. A package containing the five battery powered signal sources is mounted on either

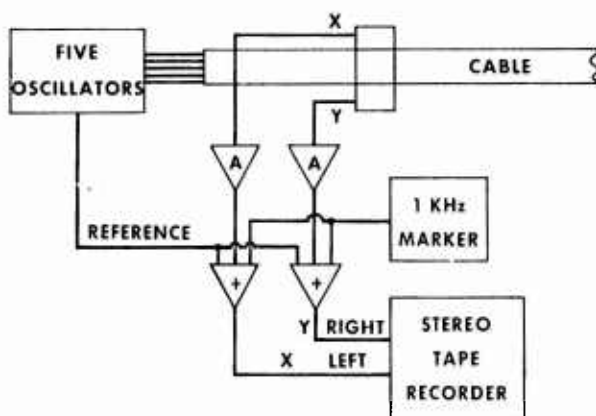


**FIGURE 4**  
BLOCK DIAGRAM OF RECORDING CIRCUIT

the takeup or payout reel. The present circuitry applies up to 40 ma. current to each of the five circuits. This package also supplies five reference frequencies which are one half the corresponding oscillator frequencies. These reference frequencies are brought out via slip rings. The X and Y signal components are amplified and combined with the reference and 1kHz marker signal and recorded on a stereo tape recorder.

The playback circuitry for the 10 kHz twist signals is shown in Figure 5. The

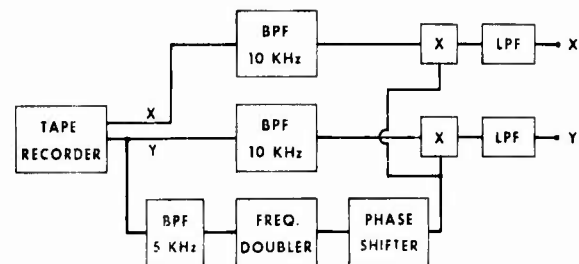
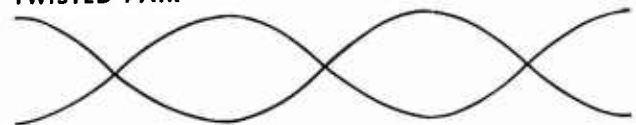


**FIGURE 5**  
BLOCK DIAGRAM OF PLAYBACK CIRCUIT FOR 10 KHz TWIST SIGNALS

other frequencies are accommodated by switching in the corresponding band pass filters. The signal processing involves demodulating the X and Y signals by multiplying them with the audio oscillator signal that was used to excite the pair and low pass filtering. The audio oscillator signal is obtained from the appropriate reference frequency recorded on the tape by squaring the reference to obtain a double frequency version and phase shifting the resultant to the extent needed to optimize outputs X and Y. The output of this circuitry is processed further in digital form.

The signals involved in the twist detection procedure are illustrated in Figure 6. The upper-most waveform is a representation of a one and one half twist section of helically twisted pair. The signal due

#### TWISTED PAIR



#### DETECTED SIGNAL



#### REFERENCE SIGNAL



#### PRODUCT



**FIGURE 6**

#### SIGNALS INVOLVED IN TWIST DETECTION

to the current applied to that pair, appearing at the TDH is represented by the second waveform. This is a double sideband suppressed carrier signal (DSBSC). This signal is multiplied by the reference signal, which is a square wave version of the signal used to excite the pair at recording time. The result is the product waveform which when

lowpass filtered represents the pair shown at the top.

#### IV. TWIST ANGLE COMPUTATIONS

Twist data processing typically begins with computation of the twist angle from the X and Y components of twist data. This would be easily accomplished if the signal were simply the sine or cosine of the twist angle as it would be under ideal conditions. In that case the  $\arctan Y/X$  would be a good estimate of the twist angle. Various sources of distortion prevent use of such a simple approach. The solid curves of the top two graticles of Figure 7 are typical of actual X and Y twist data obtained for a 3.5" twist length cable pair. This is a

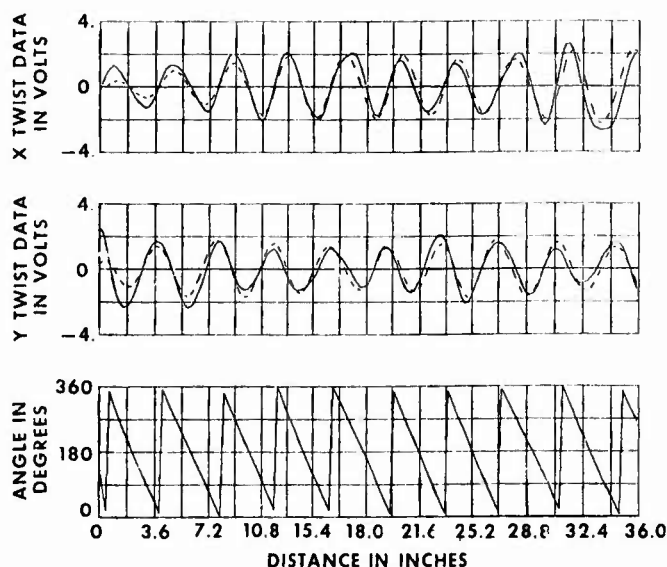


FIGURE 7  
X-DATA, Y-DATA AND COMPUTED TWIST ANGLE  
36 INCH LENGTH OF PAIR 13 (3.5 INCH TWIST LENGTH)

layer pair in one of the layer units of the LOCAP cable. Both the X and Y data show some amplitude variation with distance. The amplitude is modulated in accordance with the cable lay of 36 inches. This modulation has an 18 inch period with X being maximum amplitude when Y is at a minimum, etc. The X and Y data also exhibit a small amount of noise which can be attributed to sources such as mechanical vibrations at recording time and various electrical sources.

Various methods of computing the twist angle from data such as this have been tried. An approach which has proven to be quite reliable involves filtering and using a method about to be described. The dashed curves in the upper two graticles of Figure 7 are results obtained by using a single tuned digital filter with a Q of about 3. This filter removes the noise and most of the harmonic content but allows most of the twist length variation to be retained. Using the filtered X values, an estimate of the twist angle can be calculated by means

of the expression  $\theta_x = \arctan \frac{\Delta X}{X\eta\Delta Z}$ , where  $\eta$

is the average radian twist frequency and  $\Delta Z$  is the sample spacing. Similarly, an estimate based on Y data can be calculated

by means of  $\theta_y = \arctan \frac{Y\eta\Delta Z}{\Delta Y}$ . The average

of these two values turns out to be a good estimate. This result is shown in the bottom graticle of Figure 7. The individual estimates  $\theta_x$  and  $\theta_y$  are so much alike that the difference between the two would barely be observable on the graph had they been included along with the average. The  $\theta_x$  and  $\theta_y$  approach has several advantages over just using one of the two. An error in  $\eta$  (which could result from capstan speed variations during twist length measurement) is compensated for by using the average. Also, the precessing and recessing effects due to pair movement as well as rotation within the cable cross section are removed because Y data recesses when X data precesses and visa versa. Similar procedures can be used for computing the twist angle of the other pairs, the angle of the units and the cabling angle.

The movement of a pair within the cable can be determined by combining the information obtained from the cabling and stranding circuits with the pair twist angle. The expression for computing the X component of position for a wire center for a layer pair in a layer unit of the cable being considered here is

$$X_w = R_c \cos(\theta_c + n_c \pi/3) + R_s \cos(\theta_s + n_s \pi/3) + R_p \cos \theta_p \quad (6)$$

where  $R_c$ ,  $R_s$  and  $R_p$  are the center of cable to center of layer unit mean radius, the center of unit to center of pair mean radius and center of pair to center of wire radius respectively.  $\theta_c$ ,  $\theta_s$  and  $\theta_p$  are the cabling, stranding and pair angles respectively.  $n_c$  is the number of units separating the unit of interest from the cabling circuit where positive is counterclockwise.  $n_s$  is the number of pairs separating the pair of interest from the stranding circuit. The Y component of position is given by a function similar to Equation (6) except that sine functions are used. The coordinates for the mate are obtained by reversing the sign of the last term in Equation (6). Figure 8 is a polar plot of the results of such computations for a short length of cable. The line segments connect the center of one wire to its mate. The distance between two cusps corresponds to one-half twist length (1.75"). In this case the pairs rotate in the clockwise direction and cabling is counterclockwise, (right hand twist and left hand cabling). The spiral-like path of the pair is due to the cabling which has a 3 ft. period. The radius of the path changes because of unit oscillation. Only about 6 ft. of a 30 ft. oscillation period is involved here; however a substantial change in radius has occurred.

Figure 8 demonstrates the ability to track the position and orientation of a cable pair in a non-destructive manner. In

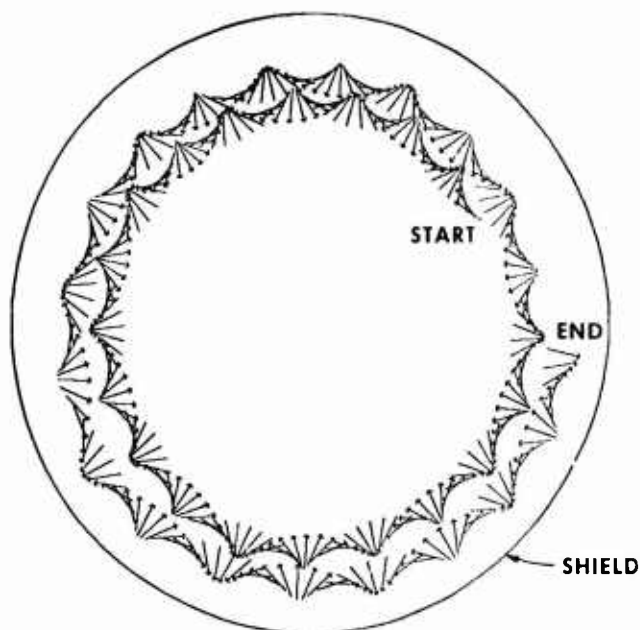


FIGURE 8

**POLAR DISPLAY OF PAIR 13 SHOWING TWISTING, STRANDING AND CABLING EFFECTS**

order to show two pairs, the cabling effect can be removed simply by subtracting the cabling angle from the stranding and pair angles. This has the effect of keeping unit position fixed. Figure 9 shows such a plot for only a fraction of a twist length for pairs 13 and 27. It shows pair separation as well as orientation for this short segment. To a first order approximation, coupling between two pairs is proportional to  $\frac{a^2}{d^2} \cos(\theta_1 - \theta_2)$ , where  $a$  is wire separation,  $d$  is pair separation and  $\theta_1$  and  $\theta_2$  are the two twist angles. In this case, the pairs are rotating in an in-phase manner so as to maximize the coupling. This phase relationship is sometimes maintained for long distances when pairs have nominally like twist lengths causing the coupling to be cumulative.

It is of interest to plot data such as that shown in Figure 9 for a longer portion of cable. Figure 10 is such a plot for about 9 ft. of cable. It is not possible to follow the phasing between the two pairs in this illustration. However, this plot shows that both units have appreciable oscillation. It shows that one of the units has rotated a greater distance than the other one in this portion of cable. Also, unit 4 displays some preferred unit positions or nonuniform rotation rate. Twist measurements such as these can reveal some interesting aspects of cable structure.

**V. COMPUTATION OF NEAR END COUPLING FROM TWIST DATA**

To compute the near end coupling function from actual twist data it becomes necessary to relate such quantities as the coupling inductance and capacitance,  $L_{12}$

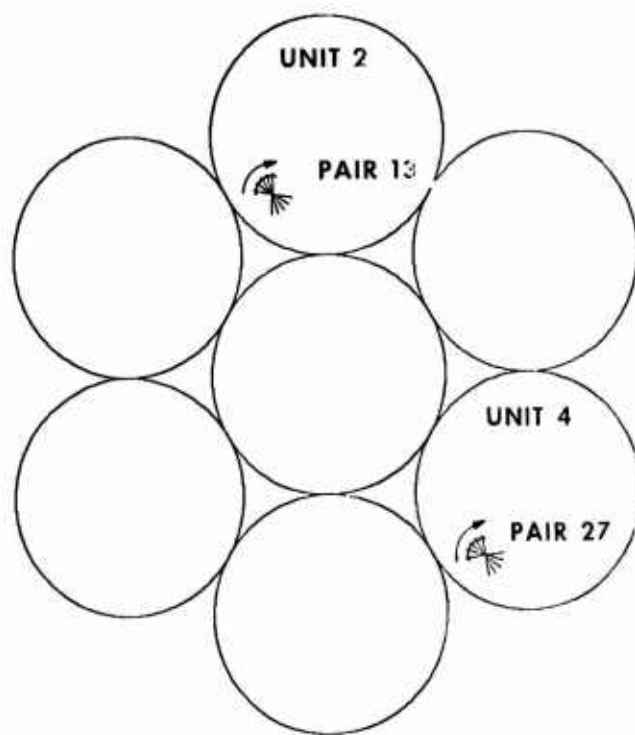


FIGURE 9

**PAIR ROTATION FOR TWO PAIRS WITH CABLING EFFECT REMOVED**

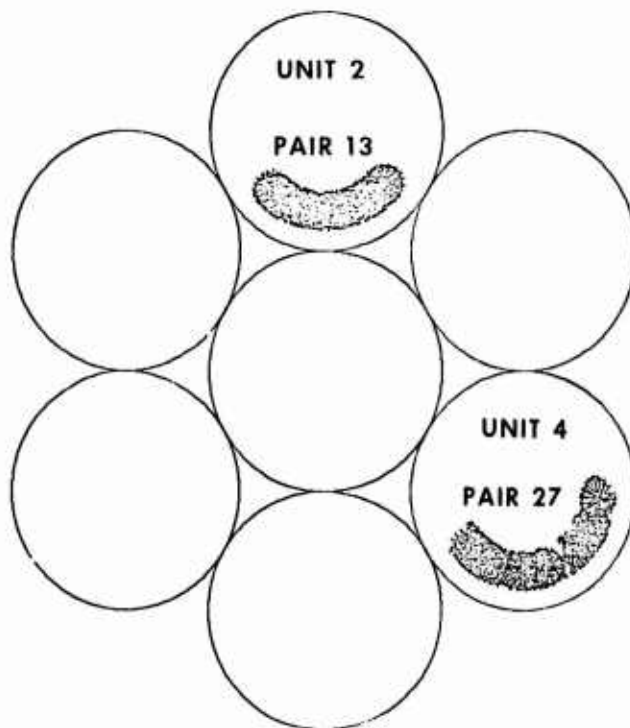


FIGURE 10

**PAIR POSITION FOR 9 FT. LENGTH OF CABLE SHOWING UNIT OSCILLATION**

and  $C_{12}$  of Equations 3 and 4 to geometric and material parameters. The pair combinations to be considered are well separated like twist combinations, where  $C_{12}$  is small, hence an expression for  $L_{12}$  only is all that is needed.

The first attempts to compute a near end coupling function from twist data involved multiplying the cosine of the difference of the two twist angles by a coefficient derived by S. O. Rice.<sup>6</sup> This coefficient was based on two pairs of zero conductor diameter in free space with parallel axes and like twists in the same direction. The "twist coupling function," TCF, based on this model, after being low pass filtered to the same resolution as that available for a coupling function computed from crosstalk data, XCF, was found to have a somewhat smaller rms value. Some structural differences were also noted. The shielding effects of intervening pairs for well separated pairs would lead one to expect that the XCF should be smaller instead.

A more refined model was next developed which took into account the effect of the shield on coupling. A formula for the inductive coupling taking the image of the disturbing pair due to the shield into account was derived by N. A. Strakhov.<sup>8</sup> This derivation was based the same assumptions made by Rice.<sup>6</sup> In addition, it assumed very long (infinite) twist lengths. The result of this derivation is

$$L_{12}(z) = -\frac{\mu}{2\pi} \frac{a^2}{R_o^2} \left[ \frac{1}{P} \cos(\theta_1 + \theta_2) + \frac{1}{A} \cos(\theta_1 - \theta_2 + \phi) \right] \quad (7)$$

where  $\theta_1$  and  $\theta_2$  are the pair angles measured by the TDH,  $a$  is the interaxial wire separation value for the two pairs,  $\mu$  is the magnetic permeability, and  $R_o$  is the shield radius. Also

$$P = S_1^2 + S_2^2 - 2S_1S_2 \cos W_1,$$

$$A = S_1^2 S_2^2 - 2S_1S_2 \cos W_1 + 1$$

and

$$\phi = \tan^{-1} \frac{2S_1S_2 \sin W_1 - S_1^2 S_2^2 \sin 2W_1}{1 - 2S_1S_2 \cos W_1 + S_1^2 S_2^2 \cos 2W_1}$$

where  $S_1$  and  $S_2$  are the center of shield to center of pair distances for pairs one and two respectively, divided by shield radius and  $W_1$  is the angle extending from a radial line to pair 2 to a radial line to pair 1. The first like twist combinations for which TCF's were computed were center of unit to center of unit combinations where the units are separated by one unit (refer to Fig. 3). For these combinations both the coefficient of the difference of twist angles term and the phase shift are constant. Substituting the dimensions for the LOCAP cable into Equation (7) and dividing by  $2Z_o$  (340 $\Omega$ ) results in a coupling coefficient for the difference of angles term of .0116  $\mu$ -sec/mi. and a phase shift  $\phi$  of 35°. The sum of the twist angles term in Equation (7) is oscillatory with a period much shorter than the wavelengths of interest here and can be discarded.

\*Nominal values ( $a = .08"$ ,  $S_1 = S_2 = .67$  and  $W_1 = 120^\circ$ ) were assumed for this calculation.

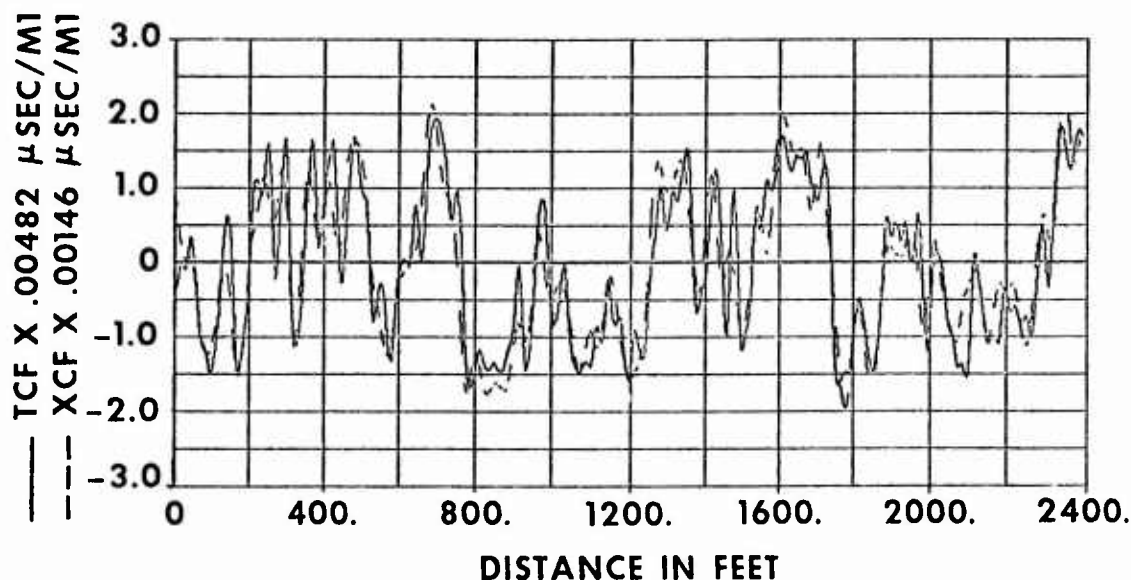


**FIGURE 11**  
**COUPLING FUNCTION COMPARISON BASED ON IMAGE**  
**EFFECT OF SHIELD FOR CABLE 183814 PAIRS 8-22**



The coupling function computed from twist data for a combination of pairs can be compared to the one computed from the near end crosstalk data for those pairs on the basis of rms amplitudes as has already been indicated. It is also desirable to have a measure of structural similarity. A useful figure of merit can be obtained for the structural agreement by computing the mean square of the difference (MSD) for the whole length of the two estimates normalized by their rms values. To gauge the meaning of this number note that the MSD can range from zero to two, the latter value occurring when one function is the negative of the other. Another gauge of MSD numbers comes from calculations of MSD between an XCF obtained from near end crosstalk data from one end of a cable and an XCF obtained from the other end. Such calculations were made for 20 pair combinations from a cable of comparable length with MSD's ranging from .06 to .20.<sup>7</sup> Thus, a reasonable evaluation of these numbers is that MSD's under .2 represent excellent agreement, MSD's in the .2 to .4 range represent good agreement, while MSD's above .4 represent poor agreement.

Twist coupling function calculations were made on three center of unit to center of unit combinations, where the units are separated by one, in each of two cables. The results, after low-pass filtering to the same resolution as that available from crosstalk, for pairs 8-22 of cable 183814 are shown in Figure 11 along with an estimate of the crosstalk coupling function obtained from crosstalk data. The two estimates have been scaled relative to their rms amplitude to allow better visual comparison. The two estimates agree quite well from a structure standpoint throughout the whole cable length. The multipliers for the vertical scale differ for the two traces. The TCF estimate multiplier is about 3 times as large as the XCF multiplier. Most of this difference is probably due to shielding of intervening pairs.

The results for the 6 center of unit to center of unit combinations and one layer pair to layer pair combination are summarized in Table 1. They show that the TCF values based on the shield model are about three times larger than the XCF values for all seven combinations. The MSD values obtained using the shield model are in the excellent and good range (less than .3) for all seven combinations. TCF computations using the Rice model were made for three combinations in the first cable. The rms values based on this model are all considerably smaller than the XCF values. The MSD values are all higher than the ones obtained when using the shield model indicating that this model does not fit as well from a structural standpoint.

The XCF rms values for cable 477220 are somewhat higher than those in the first cable.\* Part of this is due to the small twist frequency difference and unfavorable phasing between the pairs of the combinations studied in cable 477220 as discussed in the following paragraph. Also the combinations in the first cable exhibited a more extensive unit oscillation capture. Oscillation capture is beneficial to crosstalk; however, further discussion of it is beyond the scope of this paper.

One of the aspects of like twists observed during the course of this work is the extent to which the pairs have like twists. In Figure 11 the coupling functions maintain a given polarity for several hundred feet in various regions. This is due to the number of twists in the two pairs being very nearly alike over those regions. A plot for the difference between  $\theta_1$  and  $\theta_2$  was obtained for the whole cable length with the result that one pair had approximately one more twist per 1000 feet of cable.

\*Note that the TCF rms value could be as large as .0116 if the pairs were phased in the worst possible way ( $\theta_1 - \theta_2 + 35^\circ = 0$ ) for the whole cable length.

TABLE I: Comparison of Crosstalk Coupling Function (XCF) and Twist Coupling Function (TCF) Computations

	Shield Model			Rice Model	
	XCF rms $\mu$ sec./mi.	TCF rms $\mu$ sec./mi.	Mean Sq. Difference	TCF rms $\mu$ sec./mi.	Mean Sq. Difference
<u>Cable 183814</u>					
Pair 8-22	.00146	.00481	.185	.00087	.337
Pair 8-36	.00151	.00531	.181	.00105	.364
Pair 22-36	.00155	.00533	.259	.00100	.397
Pair 13-27	.00176	.00400	.214		
<u>Cable 477220</u>					
Pair 8-22	.00189	.00636	.212		
Pair 8-36	.00228	.00620	.294		
Pair 22-36	.00274	.00634	.179		



The far-end crosstalk which is simply the integral of this function multiplied by  $w$  is greatly reduced because of this difference of only a few twists. Several of the six combinations being considered here were found to have twist differences of less than one twist length and as a consequence, considerably stronger crosstalk. The XCF and TCF plots for pairs 8-22 in cable 477220 displayed a definite positive bias for the whole cable length. The far end crosstalk was 25 dB stronger than that for the same combination in cable 183814. In this case, a plot of the twist difference angle ( $\theta_1 - \theta_2$ ) indicated the two pairs had the same twist frequency to within one twist in 5,000 (approximate number of twists in cable length).

## VI. CONCLUSION

This work demonstrates the ability to make measurements of pair twist geometry and compute accurate estimates of the coupling function from such information. The multifrequency twist detection system performs quite favorably. To date recordings have been made on cables with up to 50 pairs. Extension to cables with several hundred pairs appears possible at this point. The number of frequencies could probably be doubled to ten yielding more information per recording pass.

The coupling function computations for like twist combinations demonstrate the influence of the shield on crosstalk for well separated pairs. They also indicate that strong crosstalk can result when twists are very much alike. Extension of the coupling function computation to different twist combinations should be attained as advances are made in theory and data processing techniques.

## REFERENCES

1. Campbell, G. A., "Dr. G. A. Campbell's Memoranda of 1907 and 1912," B.S.T.J., October, 1935

2. Strakhov, N. A., "Crosstalk on Multipair Cable - Theoretical Aspects," National Telecommunications Conference, November, 1973.
3. Friesen, H. W., "Experimental Verification of Near End Crosstalk Equation for Balanced Telephone Cable Pairs," National Telecommunications Conference, November, 1973.
4. Friesen, H. W., September, 1973, Unpublished data, Bell Laboratories.
5. Setzer, D. E. and Windeler, A. S., "A Low Capacitance Cable for the T2 Digital Transmission Line," International Wire and Cable Symposium, December, 1970.
6. Rice, S. O., "Mutual Inductance Between Twisted Pairs," February, 1943, Unpublished Bell Laboratories Document.
7. Friesen, H. W., "A Comparison of ACCS Crosstalk Data with Models of Direct Crosstalk and the Calculation of a Near End Coupling Function, November, 1976 "Unpublished Bell Laboratories Document.
8. Strakhov, N. A., "Magnetic Coupling Between Two Pairs in a Shield," February, 1975, Unpublished Bell Laboratories Document.



Harold W. Friesen  
Bell Laboratories  
Atlanta, Georgia

Harold W. Friesen received his MEE from New York University in 1965. He obtained his BSEE degree at the University of Colorado in 1963. He joined Bell Laboratories in 1963 as a Member of Technical Staff. Hal has worked on various projects related to multipair cable in the Transmission Media Laboratory. He is a member of I.E.E.E.

ECONOMIC ANALYSIS  
OF  
PROTOTYPE CABLE DESIGNS

J. L. McL. Fairfield

General Cable Corporation  
Lawrenceburg, Kentucky

ABSTRACT

Advances in cable design and manufacturing technique coupled with today's highly volatile material prices, have created the need to explore more thoroughly the economic interrelationship of foamed insulants, foamed filling compound and conductor material substitutions.

These relationships are explored with the help of a simple computer model.

INTRODUCTION

Economies in material cost can accrue through developments in three areas:

- (1) Cellular insulants.
- (2) Cellular filling compound.
- (3) Conductor material substitution.

and fourthly, any combination of these three elements.

The approach taken in trying to identify the impact on material costs derived from manipulating these parameters was as follows:

1. Develop equations that allowed all material costs to be represented as a function of the diameter of the single insulated conductor, for each gauge and pair count.
2. Identify what the single diameter over insulation would have to be to satisfy today's design specifications related to resistance, mutual capacitance and voltage breakdown; given variations in conductor material, degree blow of insulant and specific inductive capacitance of filling compound.
3. Having developed steps one and two, program the results to form a computer model that permits proposition analysis of these changes as they relate to corporate sales mix.

1. COST EQUATIONS

Base equation

$$\text{COD} = 2 D\sqrt{N} \quad \text{---EQ 1}$$

This equation used to find the core diameter of a cable (COD) given the pair count (N) and diameter of the single conductor (D) is empirically accurate only to  $\pm 5\%$  due to different compression factors inherent in each gauge. However, the error introduced by this inaccuracy is not great due to the fact that the model is designed to show comparative material cost changes rather than absolute material costs.

Area of Core

$$\begin{aligned} &= \frac{\pi}{4} (2D\sqrt{N})^2 \\ &= \pi D^2 N \end{aligned} \quad \text{---EQ 2}$$

Area of Insulated Conductors

$$\begin{aligned} &= \pi \frac{D^2}{4} 2N \\ &= \pi \frac{D^2 N}{2} \end{aligned} \quad \text{---EQ 3}$$

Area of Void or Filling Compound

$$\begin{aligned} &= \text{Equation 2} - \text{Equation 3} \\ &= \pi D^2 N - \pi \frac{D^2 N}{2} \\ &= 1.57 D^2 N \end{aligned} \quad \text{---EQ 4}$$

Area of Insulation

$$\begin{aligned} &= \frac{\pi}{4} (D^2 - d^2) 2N \\ &= 1.57 N (D^2 - d^2) \end{aligned} \quad \text{---EQ 5}$$

From equations one through five, it is possible to calculate the material volumes of any cable as a function of the single insulated diameter. Having obtained these volumetric equations, the weight of each material may be calculated.

## WEIGHT EQUATIONS

### Conductor Weight

- Equation 3 - Equation 5
- $1.57 D^2 N - 1.57 N (D^2 - d^2)$
- $1.57 N d^2$  = Crosssectional area.
- lbs. per 1000' feet
- $1.57 N d^2 W_1 A) \times 12,000$  ..EQ 6
- )
- or )
- )
- $W_1 B)$

### Insulation Weight

- Equation 5
- $1.57 N (D^2 - d^2)$
- lbs. per 1000' feet
- $1.57 N (D^2 - d^2) W_2 (1 - B_1) \times 12,000$  -EQ 7

### Core Wrap Weight

From circumference derived for equation 1 plus overlap factor.

- $$= 2\pi(D\sqrt{N} + I_2) \left( \begin{matrix} W_3A \\ \text{or } \\ W_3B \end{matrix} \right) \times 12,000 \quad \text{---EQ 8}$$

### Shield Weight

From circumference derived for equation 1 plus overlap and diameter build up constants

- lbs. per 1000' feet
- $(\pi(2D\sqrt{N+K_1})+L_2)W_4 \times 12,000$  -EQ 9

## Filling Compound Weight

From equation 4

- 1.57 D<sup>2</sup>N
- lbs. per 1000' feet
- 1.57 D<sup>2</sup>N W<sub>5</sub> x 12,000 -EQ 10

However, an important consideration with filling compound is that its specific gravity (S.G.) will change as its specific inductive capacitance (S.I.C.) changes. A fairly accurate representation of the relationship between S.I.C. and S.G. can be derived from the law of mixtures.

$$L_N E_R = V_1 L_N E_1 + V_2 L_N E_2 \text{ (Lichtenecker's formula)}$$

**Where**

- $E_R$  = Resultant S.I.C. of mixture  
 $E_1$  = S.I.C. of component one  
 $E_2$  = S.I.C. of component two  
 $V_1$  = Percent volume of component one  
 $V_2$  = Percent volume of component two  
 $L_N$  = Natural log

Hence, for an air hydrocarbon mixture

- $E_R$  = Variable approximately 1 through 2.3  
 $E_1$  = Approximately 2.3  
 $E_2$  = Air = 1  
 $V_1 \& V_2$  = 100 through 1 percent  
 $V_1 + V_2$  = 100

Therefore,  $E_R$  can be related to the specific gravity of the mixture by substituting  $V_1$  &  $V_2$  values used in the Lichtenecker formula to derive  $E_R$  values into equation 11 below.

$$SG_R = \frac{V_1}{V_1 + V_2} \times SGV_1 \quad \text{---EQ 11}$$

**Where**

- SG<sub>R</sub> = Resultant specific gravity
- SGV<sub>1</sub> = Specific gravity of V<sub>1</sub>

## Jacketing Compound Weight

From circumference derived from equation 1 plus diameter build up constants, corrugation constants, and wall thickness variables.

**Simplifies to:**

- lbs. per 1000' feet
- $\frac{\pi}{4} (2D\sqrt{N} (T-K_2) + T^2 - K_2^2) W_6 \times 12,000$  -EQ 12

## 2. GENERATION OF SINGLE INSULATED DIAMETERS FOR VARIOUS CONDITIONS

2.1 Calculation of diameter over dielectric (D) for solid insulant surrounded by a medium of varying specific inductive capacitance given a final cable mutual capacitance of 83 nano farads/mile.

The accepted equation to calculate mutual capacitance of an air core cable is

$$MC = \frac{19.4 \times E_{eff}}{\log_{10}(1.5 S/d)} \quad \text{-Ref. 1}$$

Where

MC = Mutual capacitance in nano farads/mile.

$E_{eff}$  = Dielectric constant of air polyethylene mixture.

S = Center to center spacing of conductors.

d = Conductor diameter.

Resolving the above to "S" for a MC of 83.

$$S = \frac{d}{1.5} \text{ Antilog}_{10} \frac{(19.4 E_{eff})}{83} \quad \text{-EQ A}$$

But from Windeler's paper.

Ref. 2

S = D + a

Where

D = DOD

S = Center to center spacing

a = Air gap

resolving graph in that paper

$$\begin{aligned} a &= 15 (D-20) 1.85 \\ S &= 115D - 4.85 \end{aligned}$$

substituting into equation A and resolving to D.

$$D = \frac{1}{1.15} (4.85 + \frac{d}{1.5} \text{ Antilog}_{10} \frac{19.4 E_{eff}}{83}) \quad \text{-EQ B}$$

Now having derived a formula to give D in terms of conductor diameter and  $E_{eff}$  for a given MC of 83 nano farads per mile, the next logical step is to find  $E_{eff}$  for a given S.I.C. of filling compound then substitute these figures into equation "B" and hence develop DOD's for respective conductor diameters and S.I.C.'s of filling compounds.

Now from the paper given by R. C. Mildner, et al

-Ref. 3

$$E_{eff} = \frac{C_f}{C} \times 1.75$$

Where

$E_{eff}$  = Resultant S.I.C. of mixture  
C<sub>f</sub> = Mutual reading of filled cable  
C = Mutual reading of same dry cable

Also

$$C_f = C \frac{E_f(1+R)}{1+R E_f}$$

Where

$$R = \frac{E_a - 1}{E_p - E_a}$$

$E_a$  = Effective S.I.C. of unfilled cable

$E_p$  = S.I.C. of filling compound

$E_f$  = S.I.C. of filling medium

Substituting

$$E_{eff} = \frac{E_f(1+R)}{1+ E_f R} \times 1.75 \quad \text{-EQ C}$$

Having obtained  $E_{eff}$  values from equation C, they may be substituted into equation B to derive diameters over dielectric (DOD) for various filling compounds.

Doing so it is found that these derived diameters do in fact closely relate to those used in practice.

Now the last problem to resolve is to develop the logic to enable various degrees of insulation blow to be incorporated into the model.

This step was approached both theoretically and empirically.

From the Phillips Cable paper

Ref. 4

$$C = \frac{736E}{\log_{10} D/d} \quad \text{-EQ D}$$

Where

C = Pico farads per 100 feet  
E = S.I.C. of insulant  
D = Diameter over dielectric  
d = Conductor diameter

Also from the same paper

$$\% \text{ Blow} = \frac{2.25-E}{.014} \quad \text{-EQ E}$$

Substituting equation "E" into equation "D"

$$D = d \frac{\text{Antilog } 736 (2.25 - .014B)}{C} \quad \text{-EQ F}$$

Now from equation "F" it can be seen that for a given percent blow "B" and a given pico farads per foot the diameter of the single insulated conductor could be calculated.

Therefore, the remaining problem is to find a means of predicting the pico farads per foot requirement to meet a fixed 83 nano farads per mile given variations in the S.I.C. of the filling compound.

There are two ways to do this:

First, theoretically-take the solid diameters derived from equation "B" and substitute these values into equation "D" and therefore derive pico farad per 100 foot values.

Secondly, determine pico farad per 100 foot values from empirical data available.

In order to meet 83 nano farads per mile, filled cable specifications require a single capacitance of 54 pf/100 ft. and the filled cable has an S.I. C. of approximately 2.3; whereas, dry cable specifications call for a single capacitance of 71 pf/100 ft. and the finished cable has a final effective S.I.C. of approximately 1.75.

Now if there was to be a linear relationship between the final cable S.I.C. and the single pf/foot then  $\frac{71}{54} \times 1.75$  should closely approximate 2.3; in fact, it calculates to 2.3 exactly; this relationship has been indicated by other empirical data but I must stress that we are dealing with a hypothesis rather than a theory.

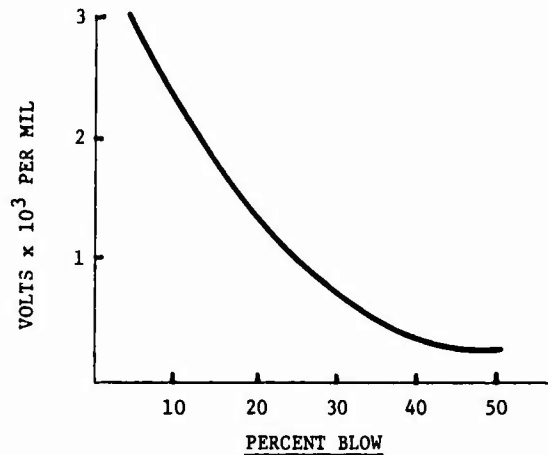
Given the choice between these two methods, the empirical approach was chosen because it gave good results at either end of the spectrum while the theoretical approach was less accurate when compared to known data.

Now, we are finally in a position to calculate varying single insulated diameters given various degrees of blow of both filling compound and insulation and hence these diameters can be used in equations 6 through 12 to calculate the cost of any cable one could wish to design.

Finally, the last parameter that should be included in the model is that of voltage breakdown, Figure I shows the relationship between degree blow and withstand voltage per mil of medium density polyethylene insulation.

**FIGURE I**

Graphic relationship of withstand voltage per mil compared to % blow.



This graph resolves to the equation

$$V = \frac{D-d}{2} \frac{(-381 + 31,128)}{B}$$

Where

- V = Withstand voltage per mil
- D = Diameter over insulation
- d = Conductor diameter
- B = % Blow

This equation is included in the model as memoranda in order to give an indication of the robustness of the construction being examined.

### 3. INTERROGATION OF MODEL

Having developed and programmed the model, it is now possible to interrogate it with questions that previously were at best answered by long and tedious calculations and in some cases, unanswerable. For example, it is possible to calculate quite accurately the relative merits of propositions as diverse as:

80¢ copper using a 30% insulation blow and a filling compound having an S.I.C. of 1.2 and S.G. of .3 and a cost of \$1.20 per lb.

As against

36¢ aluminum using a 50% blow and a filling compound having an S.I.C. of 1.8 and S.G. of .7 and a cost of 40¢ per lb.

Moreover, the print out would not cover just one or two standard cable sizes but the full product line weighted to show the effect of sales mix and would also show the voltage breakdown for each gauge and each proposition.

For the sake of interest, here are nine simple propositions using a fictitious product sales mix for 22 AWG cable and copper conductors only. Cost of filling compound has been ignored and insulation cost per pound fixed for both solid and foam.

#### Proposition 1

- (a) Solid Insulation
- (b) S. I. C. of filler 1.8

#### Proposition 2

- (a) Solid Insulation
- (b) S. I. C. of filler 1.4

#### Proposition 3

- (a) 30% Blown Insulation
- (b) S. I. C. of filler 2.3

#### Proposition 4

- (a) 30% Blown Insulation
- (b) S. I. C. of filler 1.8

#### Proposition 5

- (a) 30% Blown Insulation
- (b) S. I. C. of filler 1.4

#### Proposition 6

- (a) 40% Blown Insulation
- (b) S. I. C. of filler 2.3

#### Proposition 7

- (a) 40% Blown Insulation
- (b) S. I. C. of filler 1.8

#### Proposition 8

- (a) 40% Blown Insulation
- (b) S. I. C. of filler 1.4

#### Proposition 9

- (a) 50% Blown Insulation
- (b) S. I. C. of filler 2.3

TABLE I

THE PERCENTAGE OF MATERIAL SAVINGS DERIVED FROM PROPOSITIONS 1-9 USING SOLID INSULATION AND P. J. FILLING COMPOUND AS THE BASE COST FOR FILLED CABLE

Material	Base \$ 10 <sup>6</sup>	Prop 1 % Saved	Prop 2 % Saved	Prop 3 % Saved	Prop 4 % Saved	Prop 5 % Saved	Prop 6 % Saved	Prop 7 % Saved	Prop 8 % Saved	Prop 9 % Saved
Insulant	2.4	18	33	58	64	68	70	74	76	78
Mylar	.3	6	14	17	19	21	20	21	24	23
FPA	2.2	4	11	13	13	17	14	17	22	22
Filler (Vol.)	1.4	14	26	33	38	42	40	42	48	46
Jkt.	3.4	7	14	14	18	20	18	20	23	21
Total \$	8.3	.876	1.550	2.203	2.491	2.749	2.660	2.893	3.162	3.139
Total % \$ Savings On All Material	0	10.4	18.6	26.5	30.0	33.1	32.0	34.8	38.1	37.8

NOTE (1) FILLING COMPOUND HAS BEEN CALCULATED ONLY IN TERMS OF VOLUME BECAUSE OF THE UNKNOWN PRICE STRUCTURE OF LOW S.I.C. FILLING COMPOUNDS.



As can be seen from Table I the percent savings on non-conductor costs varies considerably depending on the proposition.

The model can also be used to accurately reflect freight costs and to some extent predict changes in labor cost due to design changes.

#### CONCLUSION

The model has proven quite accurate in predicting material costs for existing cable constructions and is helpful in predicting the material cost of prototype designs. However, its greatest value lies in the fact that it may be used to indicate the cost benefit of possible research programs and thereby increase the effectiveness of research effort.

#### APPENDIX

##### Symbols for Cost Equations

COD	=	Core Diameter
d	=	Diameter of Conductor
D	=	Diameter of Insulated Single
N	=	Number of pairs in a cable
B <sub>1</sub>	=	% Blow of Insulation
L <sub>1</sub>	=	Constant=Overlap of Core Wrap
L <sub>2</sub>	=	Constant=Overlap of Shield
K <sub>1</sub>	=	Diameter Build Up Due to Core Wrap
K <sub>2</sub>	=	Diameter Build Up Due to Core Wrap and Shield & Corrugation Factor If Needed
K <sub>3</sub>	=	Length Corrugation Factor May Also Be Used, Dependent on C.P.I. and Corrugation Depth
T	=	2 x Jacket Thickness + 2 x Corrugation Factor + K <sub>2</sub>
W <sub>1A</sub>	=	Lbs. per Cubic Inch of Copper
W <sub>1B</sub>	=	Lbs. per Cubic Inch of Aluminum
W <sub>2</sub>	=	Lbs. per Cubic Inch of Polyethylene
W <sub>3A</sub>	=	Lbs. per Square Inch of Mylar
W <sub>3B</sub>	=	Lbs. per Square Inch of G.R.P.
W <sub>4</sub>	=	Lbs. per Square Inch of Shield Material
W <sub>5</sub>	=	Lbs. per Cubic Inch of Filling Compound
W <sub>6</sub>	=	Lbs. per Cubic Inch of Jacketing Compound

#### REFERENCES

1. G. S. Eager, Jr., I. Kolodny, L. Jachimowicz, D. E. Robinson, "Transmission Properties of Poly. Insulated Telephone Cables at Voice and Carrier Frequencies", AIEE Summer and Pacific General Meeting and Air Transportation Conference - Seattle, Washington 6/21-26/1959, 59778
2. A. S. Windeler, "Design on Poly Insulated Multipair Telephone Cable", AIEE Summer and Pacific General Meeting and Air Transportation Conference - Seattle, Washington 6/21-26/1959, 59793
3. R. C. Mildner, K. F. Nacke, E. W. Veasey, P. C. Woodland, "New Approaches to Fluid Blocking" 1969, Obtainable from Dow Chemical Company.
4. S. M. Beach, D. F. Cretney, J. Ruskin, "Cellular Polyethylene Insulation Fully Filled Cable With High Dielectric Strength", Phillips Cables - Vancouver



Julian Fairfield  
General Cable Corporation  
Lawrenceburg, Kentucky 40342

J. L. McL. Fairfield is at present Plant Superintendent of the Lawrenceburg facility of General Cable. Born in 1947 in Portsmouth, England, he graduated as a Chartered Accountant in 1971, completed a post graduate degree in Industrial Administration at the University of Aston in 1972 and has since then worked in the communications cable industry in England, Canada and the United States.

# A CRITIQUE OF MILITARY WIRE MAXIMUM TEMPERATURE RATINGS

by

R. P. Fialcowitz  
Douglas Aircraft Company  
McDonnell Douglas Corporation  
Long Beach, Ca 90846

## Summary

Many electrical and physical performance tests for the evaluation of military specification wires are conducted at room temperature. If certain specification wires are tested at their claimed maximum temperature rating, significant degradation in a number of these values is observed. This is considered objectionable. The temperature rating of wire should be that range in which wire can be employed without taking extraordinary installation precautions. This situation can be corrected by originating a uniform method, applicable to all aerospace wires, that will establish a realistic temperature rating.

## Discussion

Most papers presented at this meeting describe new developments or successful solutions. This paper, however, discusses a problem that has been present in the aerospace industry for many years, and one that has been studiously ignored. In fact, the only thrust of this paper is to convince the reader that the problem does exist.

In each military wire specification, a particular number is listed and labeled "Temperature Rating." A position can be taken that there is no adequate definition in the aerospace wire industry for that term, nor is there a uniform method of establishing it.

Some concurrence with this opinion is presented in a recent paper by Reed and Perkins.<sup>(1)</sup> In announcing the development of TEFZEL, the authors admitted: "The determination of a rating is always difficult and generates controversy . . ." Temperature rating is one of the most critical and definitive numbers associated with the use of a wire, and we live with a system that is accepted as "difficult" and "controversial."

It has been stated that there is no adequate definition for the term. Standard paragraph 6.1.1 found now in all the applicable military specifications states: "Temperature ratings as specified in specification sheets pertaining to this specification represent the maximum permissible operating temperature of the conductor. The maximum ambient temperature should be the rated maximum conductor temperature of the wire diminished by the operating rise in temperature of the conductor."

This is not a definition; rather, it is a use instruction. It refers only to a condition existing in the conductor. It permits a particular combined temperature to occur continuously in a conductor. Conductors, of course, are insulated, and presumably this insulation will also experience some percentage of this temperature. Is there an implication that the insulation will be unaffected by that temperature?

Further investigation of the literature reveals another explanation of "temperature rating." The recently published Brand-Rex Wire and Cable Engineering Guide<sup>(2)</sup> provides the following definition: "Temperature Rating . . . The maximum temperature at which an insulating material may be used in continuous operation without loss of its basic properties." This definition is, of course, not original. Variations of the wording can be located elsewhere, for instance, in a paper by Buschman.<sup>(3)</sup>

Upon study, the definition really says very little. Its most significant qualification is the limiting of the properties under consideration to the "basic" ones. But are we all agreed as to which of the electrical and physical properties are "basic"? And what is meant by "loss"? Is it partial or total loss? Is it the first sign of detectable loss in any of the properties? Or is it the first detectable sign of loss in the final property? Is it a percentage of loss? 10 or 20 percent? Is it the same percentage for all the properties?

A typical military specification sheet, MIL-W-81381/12, may be examined. With the exception of the temperature and voltage ratings, every number cited in the "Additional Requirements" has a corresponding specific test procedure associated with it in the body of the specification. The rating of 600 volts (rms) is that mythical number that could be the subject of a historical study of its own. There is no test to ascertain that MIL-W-81381/12 wire is indeed 200°C, and there is no standard test cited that was used to originally establish that rating. An argument might be presented that the life cycle test pertains to the temperature rating. But where is the justification? Where in the specification is the test procedure that convinces the user that 500 hours at 230°C is the equivalent of a continuous 200°C?

Sufficient testing of this construction was conducted to convince Elliot<sup>(4)</sup> that a rating of 230°C would be tolerable. What chance does this construction have of ever being rated at 230°C? None as long as there is no standard method of establishing the rating.

As we all know, 200°C was assigned to MIL-W-81381/12 by no particular tests. The assumed rating of the weakest constituent, fluorinated ethylene propylene (FEP), was given to the construction as a whole. And despite the fact that FEP has had its rating for a long time, how was it established?

Throughout the literature of wire temperature rating, there is a corollary of "aging." Years ago, the commercial wire industry in attempting to assign a temperature rating to wire, seems to have been concerned only with age. In studying the early versions of the old AIEE Standards 1,<sup>(5)</sup> the following statement can be found: "The question of how hot an insulation can be operated can be answered only on the basis of how long it is desired to have it last."

This very restricted viewpoint is not fully repeated in many of the subsequent classical papers. Campbell and Brancato<sup>(6)</sup> in 1963 refer to attendant physical degradation of the plastic, as does Elliot<sup>(4)</sup> in 1972. An ASTM subcommittee is currently working on a method to establish a "Temperature Index" for wire. Their unpublished drafts cannot be quoted, but early versions appeared to recognize the existence of viscous flow characteristics of the insulation and excluded this feature from their objective. All the above literature utilizes the reduced physical condition as an end point for their accelerated aging tests. However, all recent work does seem to be limited to the original AIEE thought that aging need be the only criterion for establishing temperature rating.

It is curious that although insulations do have admittedly limited life at elevated temperatures, there is no acknowledgment in the military specifications. Heslop and Frisco<sup>(7)</sup> in 1973 claimed no more than 10,000 hours of life at 260°C for the wire that eventually became

MIL-W-81044/20. There is no corresponding limitation in that specification sheet.

### Test Results

It will be noted that a consistent sequence of wire types was not used in the following test data. This was deliberate to avoid undesired comparisons between the wire specification sheets themselves. The wires represented are not under criticism. Many are yielding outstanding performance in current service. What is being discussed is their maximum permissible temperature exposure. Only enough values are utilized to demonstrate detectable effects on the physical and electrical performances.

### Tensile Strength

The primary physical property is, of course, tensile stress. All the following physical performance tests are just other manifestations of this basic characteristic. An Instron tensile tester with temperature chamber was used to investigate insulation slugs for the wires shown in Figure 1. Average tensile stress at room temperature is compared with that recorded at maximum rated temperature.

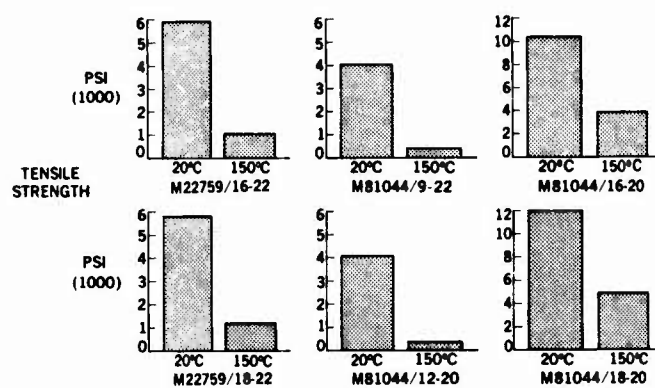


FIGURE 1. LOSS IN ULTIMATE TENSILE STRENGTH AT RATED TEMPERATURE

### Elongation After Aging

Two wire types were aged for 2000 hours at their rated temperature of 150°C. The wire specimens, with conductor intact, were 5 inches in length and unstressed. The exposure was not continuous, however, and the samples were allowed to cool undisturbed to room temperature 12 times during the 2000 hours. Figure 2 approximates the percentage difference between the unaged control samples (100 percent) and the 2000-hour aged specimens. The Instron tensile tester was used at room temperature for all runs. It should be noted that 2000 hours is not an excessive length of time in the life of most air vehicles.

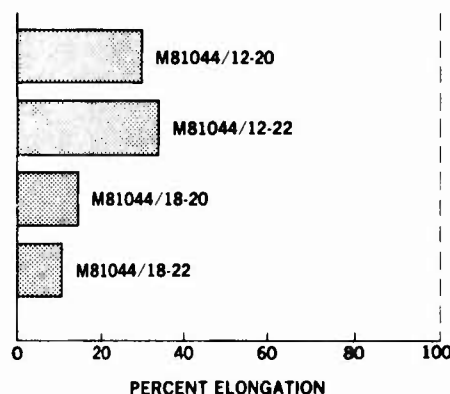


FIGURE 2. REDUCTION IN ELONGATION AFTER 2000 HOURS AT RATED TEMPERATURE (150°C)

### Static Cut-Through

Static cut-through represents the only test in this series which attempted to follow the performance of the wire types between the temperature regime of 20 to 150°C. The Underwriters Laboratories 90-degree anvil was used as a cutting edge, and a weight of 4 pounds employed. Samples were stabilized in an oven for 1 hour before applying the load. A 2500-volt potential was imposed between the anvil and the specimen conductor.

It can be questioned if any of the wires represented in Figure 3 would be seriously considered for application if they displayed cut-through resistance of approximately a few seconds at room temperature. In actual service, what is so privileged about 150°C that condones this level of performance?

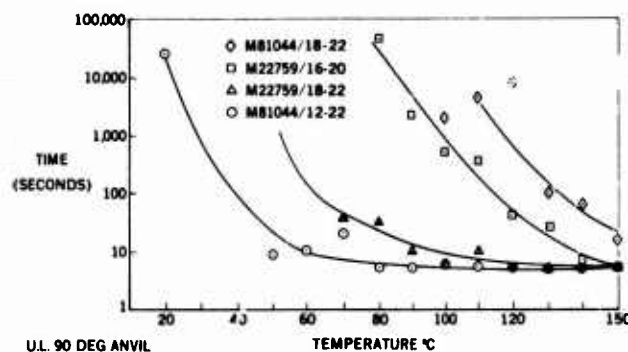


FIGURE 3. STATIC CUT-THROUGH

### Scrape

A G.E. scrape machine was not available for this investigation; a substitute, therefore, had to be improvised. Again, the Underwriter's Laboratories 90-degree anvil was used. It was held perpendicular to the wire and scraped lengthwise along it for a distance of 1.5 inches. This shape proved effective and provided very reproducible data. It was determined no appreciable weight was needed, the 342 grams being the bearing load statically computed from the jig arm. The temperature in the test specimens was obtained by current heating. The temperature level was monitored by removing a 1/4-inch slug of insulation, birdcaging the conductor, and burying a thermocouple lead in the strands. After pulling the strands back into position, the area was covered with tape. Considerable confidence was held that true temperature levels were reached due to the outstanding stability on the Acromag digital readout.

Scrape is essentially a variation of cut-through, and it is almost redundant to list it. One deficiency of Figures 4 and 5, however, is that they do not really convey the observed impression of the soft, buttery consistency of some of these insulations at their rated temperatures.

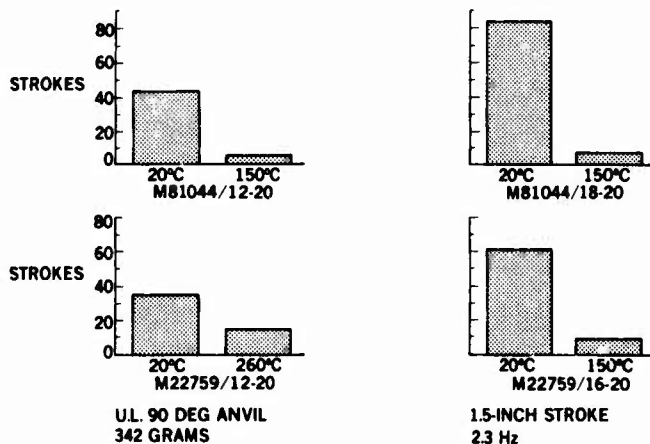


FIGURE 4. REDUCTION IN SCRAPE RESISTANCE

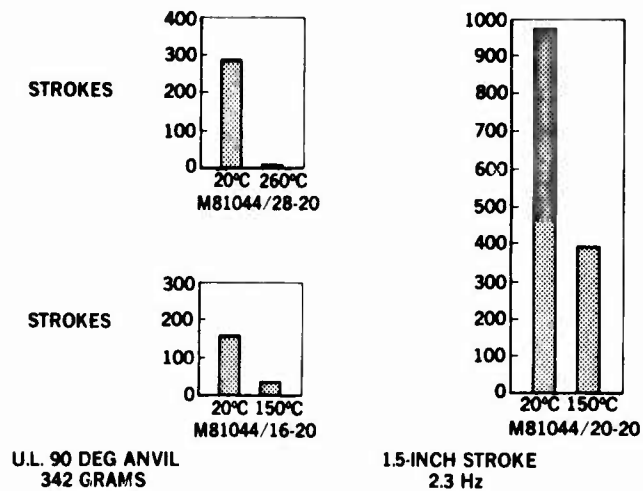


FIGURE 5. REDUCTION IN SCRAPE RESISTANCE

#### Scrape After Aging

Lengths of the wire that had been aged for 2000 hours at their rated temperature were scraped on the above described apparatus. These runs were all made at room temperature. A curious inconsistency can be noted in Figure 6. These two widely differing plastic systems yielded opposite results. Specimen M81044/18 was little affected in scuffing resistance by its 2000-hour exposure. Specimen M81044/12, on the other hand, quickly crumbled under the anvil.

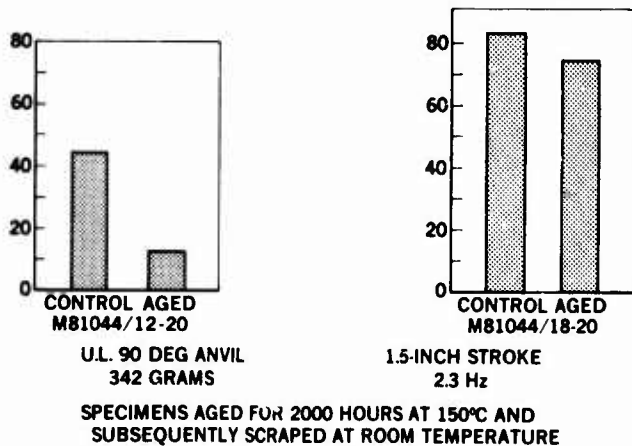


FIGURE 6. SCRAPE OF AGED SPECIMENS

#### Solderability

Efforts were made to wet the strands of these 2000-hour aged specimens with solder. Figure 7 illustrates typical solder rejection.



TINNED PLATED COPPER CONDUCTORS AGED AT 150°C FOR 2000 HOURS

FIGURE 7. TYPICAL SOLDER REJECTION

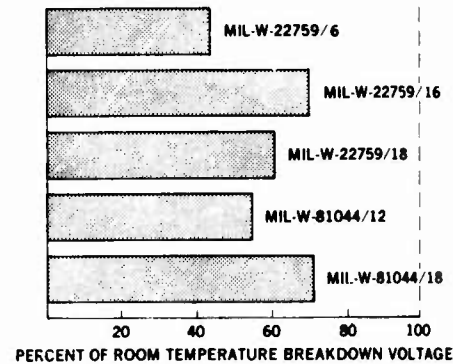


FIGURE 8. REDUCTION OF BREAKDOWN VOLTAGE AT RATED TEMPERATURE

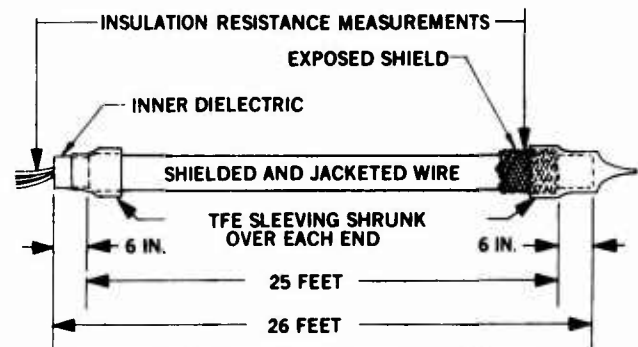


FIGURE 9. INSULATION RESISTANCE TEST SPECIMEN

TABLE 1  
INSULATION RESISTANCE

WIRE TYPE	OHMS PER 1000 FEET AT ROOM TEMPERATURE	MAXIMUM RATED TEMPERATURE (°C)	OHMS PER 1000 FEET AT RATED TEMPERATURE
M22759/6	$1.00 \times 10^{16}$	260	$1.6 \times 10^9$
M22759/16	$3.80 \times 10^{10}$	150	$4.0 \times 10^7$
M81044/16	$1.25 \times 10^{12}$	150	$1.4 \times 10^8$
M81044/9	$0.65 \times 10^{12}$	150	$0.57 \times 10^8$

#### Insulation Resistance

Again, due to the elevated temperatures utilized, a dry test specimen had to be developed. A shielded and jacketed construction was adapted as defined in Figure 9. Test results are listed for four wire types in Table 1. This test actually represents the greatest percentage falloff of a property cited herein. By examining the exponents, it can be noticed the insulation resistance at rated temperature is in the vicinity of 1 percent or less of the room temperature value.

It is conceded that the absolute values of the breakdown voltages and insulation resistance at these rated temperatures are still far superior to anything required in service. But it should not be ignored that these accompany the degradation in physical values defined in the preceding charts.

### Conclusion

To repeat the principal statement of this paper, there is no uniform, standard method to establish the temperature rating of aerospace wire. Moreover, it is difficult to visualize arguments in favor of not immediately developing such a procedure.

Figure 6, showing the inconsistency of performance in scrape after longtime aging, points out the inadequacy of using only one test condition to define rating. The final procedure will probably be a series of performance tests.

The one test condition, cut-through, in which an effort was made to follow the performance of the wire throughout the temperature regime of 20 to 150°C, reveals a feature that might be utilized in the eventual method. The data are preliminary and cursory, but a knee can be discerned in some of the curves. More detailed investigation may confirm this tendency in other tests: shallow falloff of performance with rising temperature, until a softening is reached, and then rapid degradation thereafter. A judicious averaging of these "knee" points may be used to set the maximum temperature rating.

In any event, from the wire user's point of view, wire temperature rating should be that temperature range in which wire can be used without taking any extraordinary installation precautions and have it last the intended life of the vehicle.

### References

1. "Tefzel" ETFE Fluoropolymer: Temperature Rating and Functional Characterization, J. C. Reed and J. R. Perkins, Proceedings of 21st International Wire and Cable Symposium, Atlantic City, N. J., Dec 1972
2. Brand-Rex Wire and Cable Engineering Guide, E. F. Low, Publication WC-74, 1974
3. What Every Engineer Should Know About High Temperature Wire and Cable, F. X. Buschman, Electronic Industries, Jan - Feb 1959
4. A Standardized Procedure for Evaluating the Relative Thermal Life and Temperature Rating of Thin-Wall Airframe Wire Insulation, D. K. Elliot, Lockheed-California Company, Paper C72265-7, Feb 1972
5. AIEE Standards 1, Pars 385-393, Feb 1954,
6. Determination and Application of Thermal-Life Characteristics of Aerospace Wires, F. J. Campbell and E. L. Brancato, U. S. Naval Research Laboratory, Insulation Magazine, Oct 1963, pp 17-22, and Nov 1963, pp 23-30
7. Performance Evaluation of Polyarylene Wire Insulation, W. R. Heslop and L. J. Frisco, Proceedings of 22nd International Wire and Cable Symposium, Atlantic City, N.J., Dec 1973



Mr. Fialcowitz graduated in 1952 with a B.S. degree from the U.S. Merchant Marine Academy, Kings Point, N.Y. Since 1962, he has been an electrical components engineer at Douglas Aircraft Company, Long Beach, California. He is a member of the SAE A2H and A2X Subcommittees.

## A NEW FAULT LOCATOR FOR COAXIAL CABLE

K. Asada  
Nippon Telegraph and Telephone Public Corporation  
Tokyo, Japan

T. Naruse H. Yasuhara M. Oguchi  
The Fujikura Cable Works, Ltd.  
Tokyo, Japan

### 1. Summary

Among various troubles of coaxial cables, the dielectric weak point is one of those faults which are relatively difficult to locate. This paper is concerned with an instrument for locating a dielectric weak point from one end of a cable without destroying the cable. It is designed with special emphasis laid on easy operation and transportation and high measuring accuracy. With regard to measuring errors, our theoretical study agreed with the experimental results well.

### 2. Introduction

Quick and accurate detection of a cable's fault location is extremely important for establishing a reliable cable system. High-capacity transmission system by coaxial cables has become common. As a result, quick and accurate measurement of a fault location has become essential to cope with any abnormality not only during manufacturing process but also during construction, including laying and splicing works, and during maintenance.

Cables can have various troubles. This device is used when the dielectric strength between the inner conductor and the outer conductor of a coaxial cable deteriorates and a discharge starts at some voltage below the specified level. Up to now, various methods for measuring such a faulty location have been proposed. When a faulty point is completely or almost completely short-circuited, it can be located fairly well by the bridge method or by the pulse reflection method. However, a faulty point is not easy to locate when its dielectric strength is not far below the specified voltage level. Such a faulty point can be located either by using a high voltage bridge for starting discharge at the faulty point or by using a bridge after fault burning with high voltage, or by discharging a faulty point with high voltage pulses and to know the distance to a discharge point through measurement of the time required for two-way pulse reflection trip.

Each of these methods has some defects. For example, the high voltage bridge method causes the unstability of the measuring and furthermore, the cable is in some case, destroyed by carbonizing or the melting of the fault point. The fault burning method also damages a cable and requires a high voltage power source of considerably large capacity. The high voltage pulse method requires pulses of small width to ensure high

resolution. For this reason, measurements are seriously influenced by the attenuation of a line. Therefore, this method is not suitable for a long line.

The method to be described here is that D.C. voltage is to be affected to make the fault point to discharge. The pulse counter measures the propagation time of its surge. It thus allows to measure the distance to a discharge point directly by only one discharge. This method requires neither experiences nor skills. It can locate a faulty point accurately and easily without giving a serious damage to a cable.

### 3. Principle of Measurement and Operation

FIG.1 shows the external view of the measuring equipment and terminal box. This instrument consists of a high voltage supply, a differential circuit, a counter and a display, etc., as shown in FIG.2. Connect a faulty cable to this instrument and depress the Measure Button, and the voltage from the high voltage supply will rise gradually at a pre-set speed.

After a while, a dielectric breakdown will occur and flash discharge will be generated at the dielectric weak point B. Surge current is propagated to the both sides of a cable. The surge that is propagated to the remote end C is absorbed by the termination connected at the end of the cable. The surge to be propagated to the measuring end A reaches the point A after the time lapse of  $\tau_1 = l/v$  ( $l$ : Distance to the fault point,  $v$ : velocity of propagation of e.m. waves in a cable). If the impedance of the point A is larger than that of the cable, this surge will return to the faulty point B.

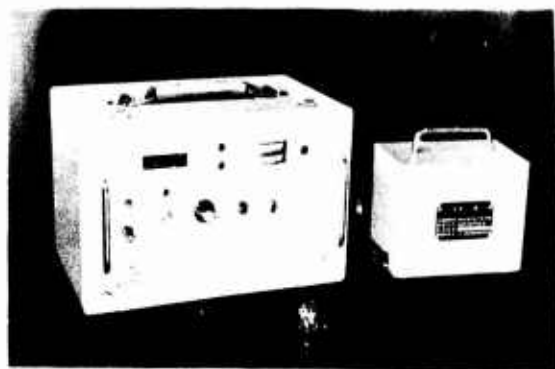


FIG.1 EXTERNAL VIEW OF THE FAULT LOCATOR



On the other hand, the discharging period at the point B is far longer than the time  $\tau_2 = 2l/v$  required for the surge to make a two-way trip between A and B. Since the point B has low impedance during this period, the surge that returns to B is reflected again and reaches A after  $\tau_3 = 3l/v$  with its polarity inverted. Similarly, this oscillation is repeated while being attenuated. This phenomenon can be observed as FIG.3.1 at the impressing point A.

Since this instrument has a differential circuit to simplify signal processing, an alternately positive and negative pulse row, as shown in FIG.3.2 is obtained at D. Therefore, the distance to the faulty point can be obtained by measuring the time interval of positive and negative pulses ( $\tau = \tau_3 - \tau_1 = 2l/v$ ) if the pulse propagation speed in a cable is known.

The pulse row is separated into positive and negative components by the differential circuit, converted into logic level and is used as start and stop control signals for the input gate of the counter. The time interval of pulses is  $\tau = 2l/v$ . If the frequency  $f$  of a reference oscillator is selected as

$$f = n/2 \quad (1)$$

the distance to the faulty point is obtained by the following equation. The counter's indication is put as  $n$ .

$$l = v \cdot n \cdot 2f = n \quad (2)$$

In other words, the counter's indication directly shows the distance  $l$  to the faulty point.

This instrument is to be operated by the following steps:

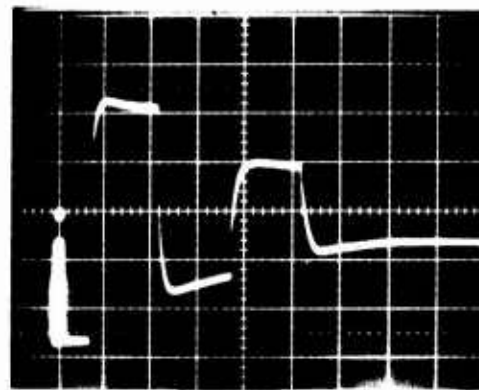


FIG.3-1 PULSE SHAPE AT "A", X; 10μsec/div  
Y; 500 v/div

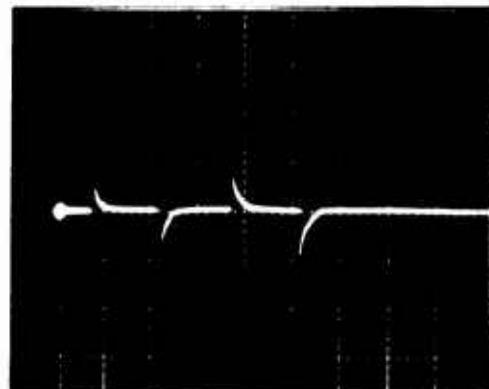


FIG.3-2 PULSE SHAPE AT "D", X; 10μsec/div  
Y; 50v/div

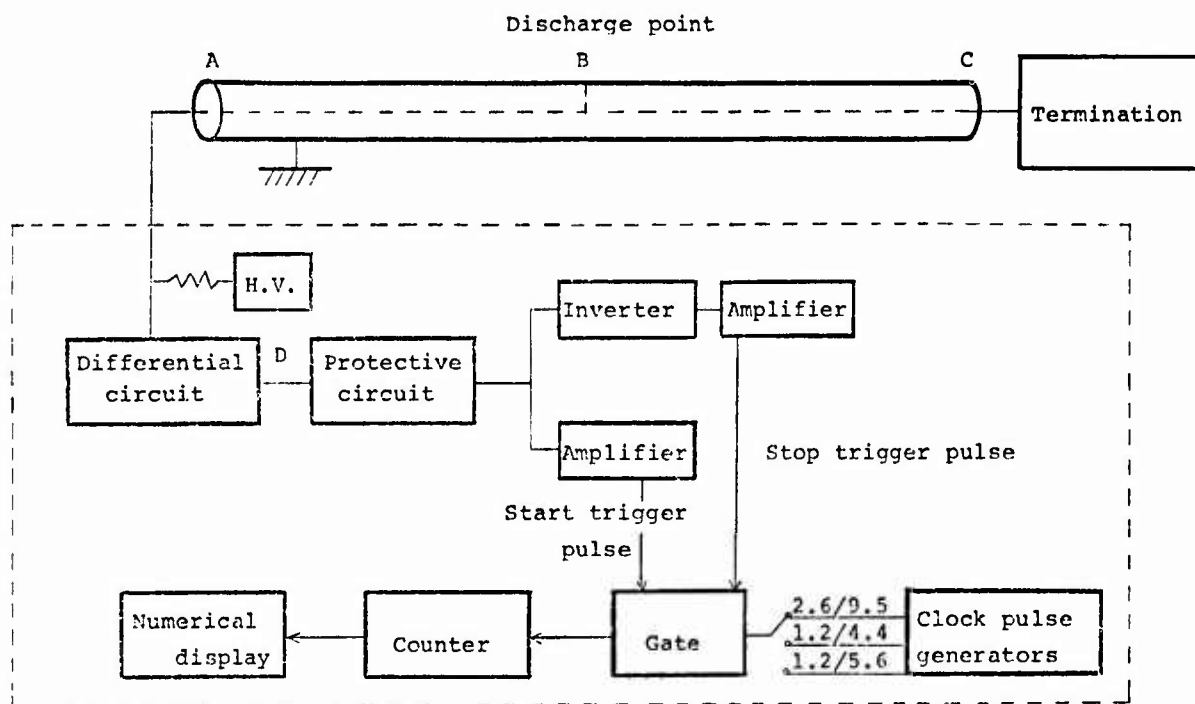


FIG.2 BLOCK DIAGRAM OF FAULT LOCATOR

- (1) Before connecting the instrument to a cable, set the dial to power check with the cord tip left open and make sure that a power source is normal.
- (2) Set cable select dial to a "Lamp Check" range and press "Measure Button". If the measurement system is normal, display "8888" on the display.
- (3) Connect a faulty cable to the instrument with its end terminating.
- (4) "Abnormal Lamp" will light up in case of any abnormality. The distance to a faulty point will be indicated on the display.

#### 4. Measuring Limits and Measuring Errors

TABLE 1 shows the repeater spans of long distance coaxial cable transmission systems used in Japan and the standards of dielectric strength of various cables. Since this instrument was designed to measure a faulty point within one repeater span without disassembling, the following design targets were set. With a coaxial cable of 2.6/9.5 mm, a faulty point with discharge voltage of DC 500 V - 3000V can be measured up to 5000 m. With a coaxial cable of 1.2/4.4 mm, a faulty point with discharge voltage of DC 500V - 2000V can be measured up to 2500 m accurately without switching.

##### 4.1 Measuring limits

In principle, measurements are possible as long as the discharge pulse reaching the input terminal of the instrument is above certain operating voltage and start the amplifier. Discharge pulse arriving at the input terminal is proportional to discharge voltage and is attenuated as propagated through a cable. Therefore, discharging pulse does not reach the operating voltage when discharge voltage is low and attenuated heavily by the cable. This is the measurement limit of a remote faulty point.

Operating voltage should not be too low to prevent errors attributable to various noises and impedance irregularities of cable.

On the other hand, discharge pulse and reflected pulse cannot be distinguished well when the distance to a weak point is extremely short. The resolution of discharge pulse

and reflected pulse can be increased by shortening the time constant of the differential circuit. In this case, the differential circuit will take out the high frequency components of pulse alone. As a result, the effective attenuation of pulse increases. This will be undesirable for the measurement of remote faulty points. Therefore, optimum values for C and R of the differential circuit must be selected in consideration of the above factors.

##### 4.2 Causes of errors

The major causes of errors are listed below.

- (1) Error due to scatter in the rising time of transistor for receiving start and stop pulse
- (2) Error due to scatter in phase constant of cable
- (3) Error due to difficulty of distinguishing between discharge pulse and reflected pulse in case of a faulty point located extremely close to a measurement end
- (4) Error due to delay of the stop side gate's operation caused by transmission distortion of reflected pulse in case of a faulty point located far from a measurement end

Other causes of error include the stability of a reference oscillator's oscillation frequency and the counter's digit error. Since a crystal oscillator is used as a reference oscillator and its stability is below  $10^{-5}$ , its effect can be ignored.

Among these factors, (1) can be controlled quite well by uniformizing transistor characteristics at the stage of instrument adjustment and by fine adjustments of the delay circuit.

The factor (2) is determined by the probabilistic scattering of the propagation constant of a coaxial pair and the difference in the lay ratio at the time of stranding and the temperature characteristics of phase parameter. The following results are the measured phase parameters of the 2.6/9.5 mm coaxial cable recently manufactured in Japan.

min. = 21.658 + 0.257 f (rad/km)  
 ave. = 21.724 + 0.267 f (rad/km)  
 max. = 21.801 + 0.287 f (rad/km)  
 Temperature: 10°C f: frequency (MHz)

		2.6/9.5mm Cox	1.2/4.4mm Cox
Repeater Spacing (Ave.)	4-MHz systems	9 Km	3.8 Km
	12-MHz systems	4.5 Km	2 Km
	60-MHz systems	1.5 Km	-
Dielectric Strength	Factory length	DC 3000V 2 Min.	DC 2000V 1 Min.
	After installation	DC 3000V 2 Min.	DC 1500V 1 Min.

TABLE 1 REPEATER SPACING OF THE COAXIAL CABLE SYSTEMS AND THE SPECIFIED VALUE OF THE DIELECTRIC STRENGTH OF COAXIAL CABLES

At high frequency, the scatter may be attributed to the coefficient of the first term. The standard deviation  $\sigma_0$  is 0.2% and the difference between the maximum and the minimum is 0.66%. These measurements were taken with about 250 m long cables. For a long line, cables differing in phase parameter are more likely to be randomly connected to obtain a 5,000 m, parameter scatter will decrease. If twenty cables are connected to obtain a 5,000 m long line, standard deviation  $\sigma$  will be  $\sigma_0/\sqrt{20}$ . The temperature modulus of  $\beta$  is not large. But these errors can hardly be avoided.

The factor (3) depends on the time constant of the differential circuit of the instrument's input terminal, as discussed before. Since the time constant is limited by the relation with a measuring distance, error due to this factor is limited.

The factor (4) is inevitable since the propagation function of a cable has a frequency characteristic. Its effect is large when discharge voltage is low and the distance to a faulty point is large. This error can be decreased by attaching an equalizer. However, it is not realistic to use a wide-band equalizer for this purpose when the error is within certain allowable range.

These measuring error characteristics depend on the distance to a faulty point and cable type, discharge voltage and instrumental error.

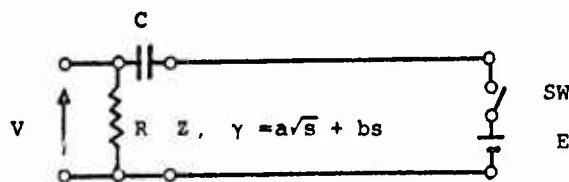
#### 4.3 Analysis of discharging pulse waveform

Let us obtain the state of discharge pulse propagating through a cable analytically.

An equivalent circuit is shown in FIG.4. We assume a cable's propagation parameter as:

$$\gamma = a\sqrt{s} + bs$$

$$s = j\omega, \omega = 2\pi f$$



- Z; Characteristic Impedance of the Cable
- $\gamma$ ; Propagation Parameter
- C; Capacitance of the Differential Circuit
- R; Resistance of the Differential Circuit
- SW; Switch
- E; DC. Power Supply
- V; Voltage

FIG.4 EQUIVALENT CIRCUIT

When the switch is turned on at the time  $t = 0$ , the voltage  $V(s)$  received at the input terminal of the instrument is as given below:

$$V(s) = \frac{RE}{s \left\{ \left( R + \frac{1}{sC} \right) \cosh \gamma l + Z \sinh \gamma l \right\}} \quad (3)$$

$$= \frac{2RE e^{-(a\sqrt{s}+bs)l}}{(R+Z)(s+\Omega_1)} \sum_{n=0}^{\infty} \left[ -\Gamma \frac{s+\Omega_2}{s+\Omega_1} e^{-2(a\sqrt{s}+bs)l} \right]^n$$

$$\Gamma = \frac{R-Z}{R+Z}, \Omega_1 = \frac{1}{C(R+Z)}, \Omega_2 = \frac{1}{C(R-Z)}$$

$$R \neq Z$$

(4)

The right member of the multinomial expression indicated discharge pulse, reflection and re-reflection pulse....., respectively. It is significant to note the waveform of the discharge pulse of the first term ( $n=0$ ) and the reflection pulse of the second term ( $n=1$ ). Their reverse transforms are given as

$$v_0(t) = \frac{REal}{\sqrt{\pi(R+Z)}} \int_{bl}^t \frac{\exp[-\Omega_1(t-\tau) - \frac{a^2 l^2}{4(\tau-bl)^2}]}{(\tau-bl)^{3/2}} d\tau \quad (5)$$

$$v_1(t) = -\frac{RE\Gamma \cdot 3al}{\sqrt{\pi(R+Z)}} \times \int_{3bl}^t \frac{\exp[-\Omega_1(t-\tau) - \frac{9a^2 l^2}{4(\tau-3bl)^2}]}{(\tau-3bl)^{3/2}} d\tau - \frac{RE\Gamma \cdot 3al(-\Omega_1 + \Omega_2)}{\sqrt{\pi(R+Z)}} \times \int_{3bl}^t \frac{(t-\tau) \exp[-\Omega_1(t-\tau) - \frac{9a^2 l^2}{4(\tau-3bl)^2}]}{(\tau-3bl)^{3/2}} d\tau \quad (6)$$

FIG.5 - FIG.8 show the results of the numeric calculation for 2.6/9.5 mm coaxial cables. The distance to discharge point and R of the differential circuit were taken as a parameter leaving  $(R+Z)C$  constant. In these graphs,  $RE/(R+Z)$  is normalized by 1. FIG.5 shows that discharge pulse overlaps with reflection pulse when the distance to a discharge point is short. And it shows that the larger R is better as for the wave distortion due to overlapping. FIG.6 shows the relation between peak values of the pulses and distance to the faulty point for some value of R. In this case the larger R is better than the smaller one, too. FIG.7 shows the pattern of the discharged pulse and reflected pulse at each distance. And FIG.8 shows the relation between error and distance to a weak point at each discharge voltage. The operating voltage is assumed to be 3V, and R is 1000 $\Omega$ . It shows the experimental values agree well with the theoretical results.

The dynamic receiving range is obtained from these calculated values.

Dynamic range due to distance 38 dB

Dynamic range due to difference in discharge voltage 16 dB

Then the maximum ratio of the two pulses is calculated to be 54 dB. In other words, theoretically speaking, the internal line uniformity must be at least 54 dB in the severest test condition, or else, it is impossible to distinguish a discharge pulse from a reflection pulse occurred at the nonuniform point of the cable. But, in our

experiment, it is found that this instrument can locate the discharge point correctly, if there are some irregularities about 20 dB measured with 10 ns pulse echo tester. This seems to be explained by rapid attenuation of high frequency components of discharge pulse during transmission through a line. It is found that even a considerably large irregularity in a line gives no influence on the measurement of a discharge point.

The measurement accuracy of a remote faulty point can be improved further by referring FIG.8 as a calibration curve. To measure a faulty point within the distance of 20 m, about 20 m long coaxial cord with known propagation velocity can be attached to the input terminal and an adjustment can be made later. In other words, the distance to a cable's faulty point can be obtained by the following equation. Where  $l_c$  and  $v_c$  are cord length and pulse propagation velocity in cord respectively.

$$l = n - \frac{v}{v_c} l_c \quad (7)$$

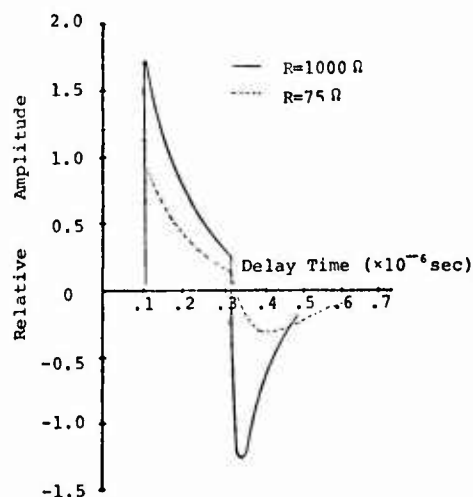


FIG. 5 PULSE SHAPE WHEN THE DISTANCE TO A DISCHARGE POINT IS SHORT

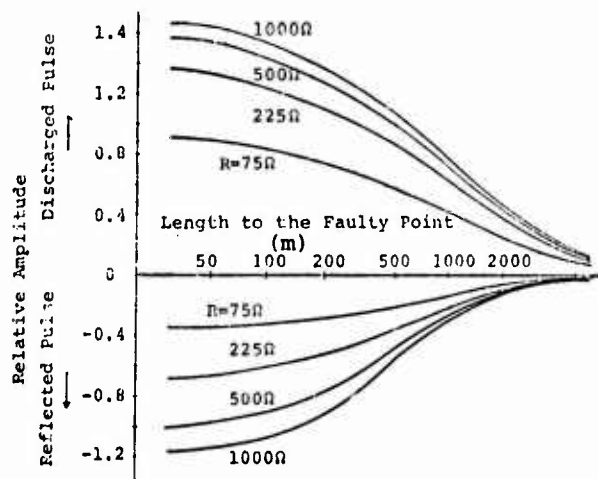


FIG. 6 PEAK VALUE OF THE PULSE VS. DISTANCE TO THE DISCHARGE POINT

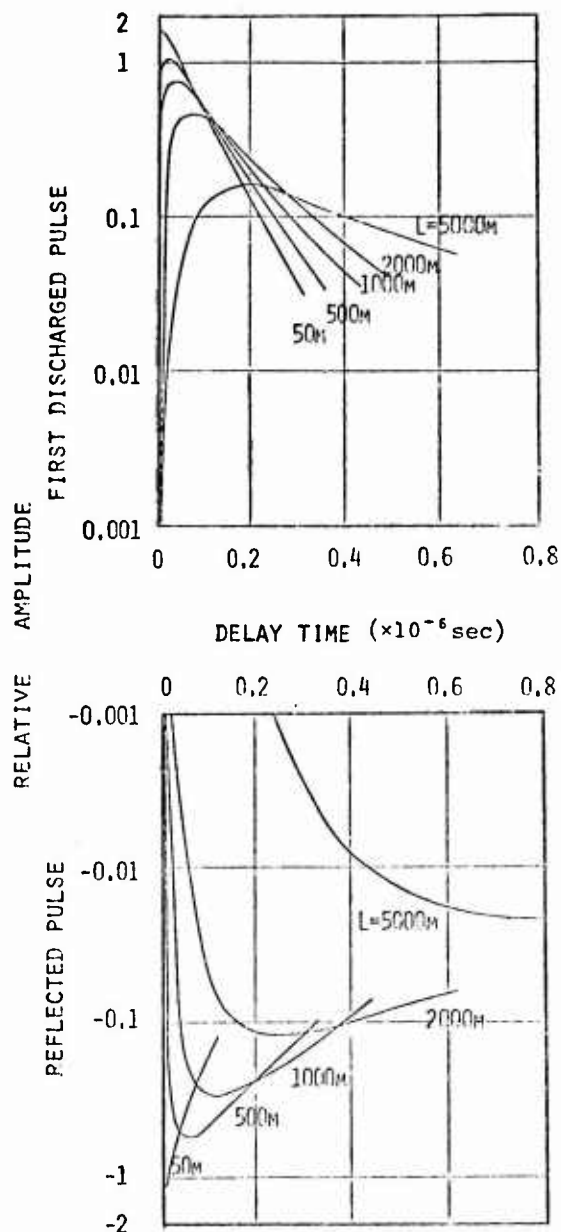


FIG. 7 PULSE WAVEFORM FOR SOME DISTANCE

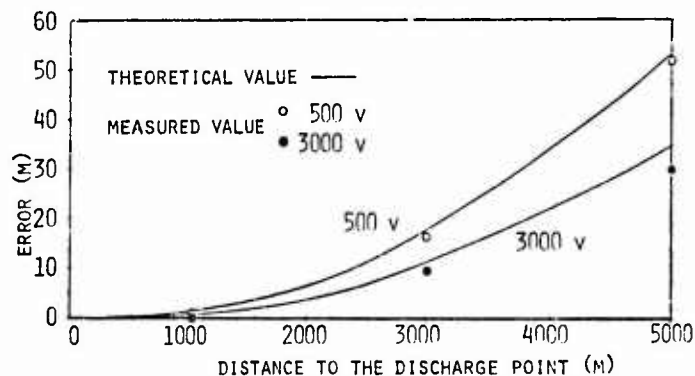


FIG. 8 ERROR VS. DISTANCE TO THE DISCHARGE POINT

## 5. Performance

This instrument is designed to ensure easy maintenance work at the field. The major features are listed below:

- (1) It is small and light. A high voltage power supply is built into this instrument. A maintenance worker can take measurements with this instrument alone. Since it weighs less than 10 kg, it is easy to carry.
- (2) It works with any of the three types of power source; namely, AC 100V, DC 12V power source (automobile's battery) and a built-in dry batteries (1.5V x 10).
- (3) It requires no adjustment. Operators only have to specify a cable to be measured with the cable selection switch and to depress "Measure Button".
- (4) The distance from the measuring end to a weak point is digitally displayed in meter to allow direct reading.
- (5) The high voltage generator circuit works only while "Measure Button" is being depressed. When "Measure Button" is released, voltage falls and the charge in a cable is automatically discharged to ensure safety.

The main performances of this instrument and the terminal box are shown in TABLE 2.

This instrument was subjected to a temperature and humidity test, an impact test and an vibration test as environmental tests under normality in these tests.

	2.6/9.5mm Coaxial Cable	1.2/4.4mm Coaxial Cable
Measuring limits	30 5000m	30 2500m
Output Voltage	Max. 3000V	Max. 2000V
Accuracy	100m	± 3m
	100m	± 2%
Electric Source	AC 100V, DC 12V, Dry Battery (1.5Vx10)	
Dimension	H 220mm x W 320mm x L 240mm	
Weight	10Kg	

TABLE 2.1 PERFORMANCES OF FAULTY LOCATOR

Dielectric Strength	DC 3000V 5 min.
Input Impedance	75 ± 10% at 2.5 MHz
Dimension	H 150mm x W 110mm x L 170mm
Weight	3 Kg

TABLE 2.2 PERFORMANCES OF TERMINAL BOX

## 6. Conclusion

This instrument is made use of the propagation time of the current surged from a discharge point with applying DC high voltage to a cable. And it permits stable measurement without carbonizing and melting a discharge point. Recently developed digital technique was fully used to realize easy operation.

Several units of this instrument are being subject to field testing. It is to be used by Nippon Telegraph and Telephone Public Corporation for maintenance in the near future.

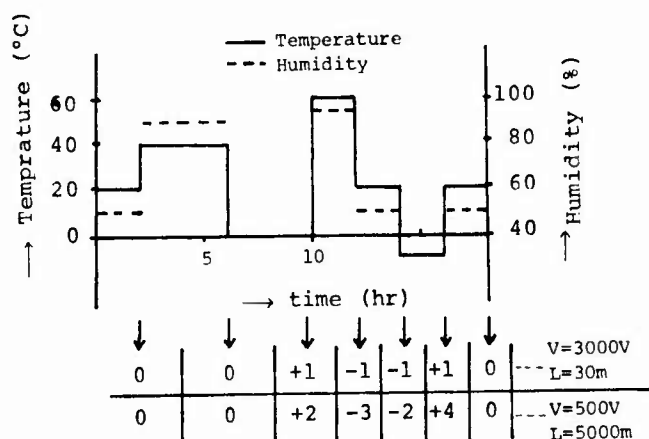


FIG. 9.1 TEMPERATURE AND HUMIDITY TEST

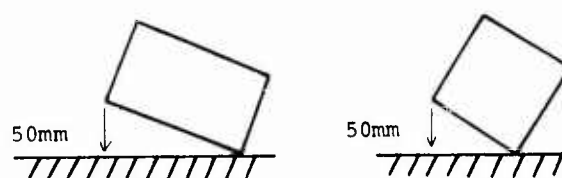


FIG. 9.2 IMPACT TEST

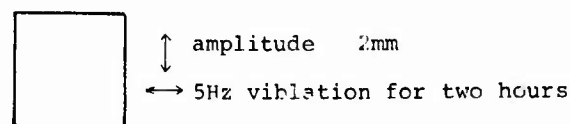


FIG. 9.3 VIBRATION TEST

## 7. Acknowledgment

The authors wish to thank to the people at NTT and the Fujikura Cable Works, Ltd. who contributed to the development of the equipment and the commercial tests of it.

### Reference

1. Japanese PAT. NO. 14502 The Fujikura Cable Works, Ltd.
2. Y. Negishi et al. "High frequency Characteristics of 2.6/9.5 mm coaxial cable" IECEJ paper of technical group on Communication Systems. (CS74-140) 1974



KAZUO ASADA

Staff Engineer of the Engineering Bureau, Nippon Telegraph & Telephone Public Corporation 1-1-6, Uchisaiwai-cho, Chiyoda-ku, Tokyo, Japan.

Mr. Asada received his B.E. degree in electrical engineering from Keio University in 1963. He then joined N.T.T. and is now engaged in the development of outside plant as well as long distance telecommunication systems. He is a member of the Insutitute of Electronics Communication Engineers of Japan.



TOSHIHIDE NARUSE

Assistant Chief, Telecommunication Cable Research & Development Dept., The Fujikura Cable Works, Ltd., 1440 Mutsusaki, Sakura-shi, Chiba-ken, Japan.

Mr. Naruse reveived his B.E. and M.E. degrees in electrical engineering from Waseda University in 1963 and 1965 respectively. He then joined the Fujikura Cable Works, Ltd. and has been engaged in research and development of telecommunication cable. He is a member of the Institute of Electronics and Communication Engineers of Japan.



HIKARU YASUHARA

Senior Engineer, Telecommunication Cable Research & Development Dept., The Fujikura Cable Works, Ltd., 1440 Mutsusaki, Sakura-shi, Chiba-ken, Japan.

Mr. Yasuhara received his B.E. degree in electronics engineering from Tokyo University in 1966. He then joined the Fujikura Cable Works, Ltd. and has been engaged in research and development of telecommunication cable. He is a member of the Institute of Electronics and Communication Engineers of Japan.



MUNESUKE OGUCHI

Senior Engineer, Telecommunication Cable Manufacturing Engineering Section of Sakura Plant, The Fujikura Cable Works, Ltd., 1440 Mutsusaki, Sakura-shi, Chiba-ken, Japan.

Mr. Oguchi received his P.E. degree in electrical engineering from Toyo University in 1967. He then joined the Fujikura Cable Works, Ltd. and has been engaged in Engineering and development of telecommunication cable. He is a member of the Institute of Electronics and Communication Engineers of Japan.



## PRECISION INSERTION LOSS MEASUREMENTS AND DATA ANALYSIS ON MULTIPAIR CABLE

J. Kreutzberg and T. D. Nantz  
Bell Laboratories  
Atlanta, Georgia

### SUMMARY

An analysis procedure is described which yields multipair cable transmission properties and geometric and material parameters over the 100 Hz to 15 MHz band from accurate measurements on 2-3 thousand feet of cable in the 10 KHz to 15 MHz band. Accuracies obtainable are 0.3 percent or better for the transmission properties and 1-2 percent for the geometric and material properties. Dissipation factor is estimated to 10 percent or better.

#### 1. Introduction

The objective of this paper is to show how, from a limited set of measurements on a representative length of multipair telephone cable, a full characterization of cable transmission and material properties can be obtained. This is accomplished by accurate transmission measurements, appropriate estimation and substantial computation.

First, a few terms should be defined. By accuracy, of course, we mean closeness to truth and not resolution. By transmission properties, we refer to the primary and secondary constants listed in Figure 1 and not to crosstalk and other unbalance effects.

Measured transmission properties of cables include effects of the measurement setup. In the case of primary constant measurements, these are primarily propagation effects due to cable length. Secondary constant measurements are primarily influenced by termination mismatch to the measuring set. In both cases the measurement data needs to be processed to remove the test setup effects and yield the true primary and secondary constants which characterize the transmission properties of a cable independently of its environment of use. It is these eight true properties that we are working to quantify. First, it should be stated that it is only necessary to determine any four of the eight desired parameters. The remaining four can then be accurately computed.

It is important to characterize a cable in relatively long lengths primarily because that's how it is used. Extrapolating long length behavior from short length measurements can be hazardous. However, a compromise must be made between length and measurement frequency band. Two to three thousand feet seems a good compromise for measurements in the 10 KHz to 15 MHz band. Also, the importance of accurate measurement of cable length cannot be overemphasized.

What properties can be measured accurately in lengths of a few thousand feet? Insertion loss and phase are obvious choices. Since measurement results are strongly influenced by the test set source and terminating impedances, the measurement data will have to be processed to convert from insertion loss and insertion phase to the desired attenuation and phase constant. The primary constants are measurable, but with varying accuracies due to propagation effects. Of these, capacitance is the easiest to measure accurately, particularly for cables with polyolefin insulation where dielectric constant is flat over the frequency range of interest. In lengths to 3000 feet, capacitance propagation effects are small.

Dissipation factor, which is a measure of the cable insulation loss, is directly related to conductance through capacitance and can be estimated from the shape of insertion loss or attenuation versus frequency by suitable curve fitting and computation. Fortunately, the effect of dissipation factor on the computed results is small so some inaccuracy in its estimation is acceptable. A ten percent error in the estimation of dissipation factor

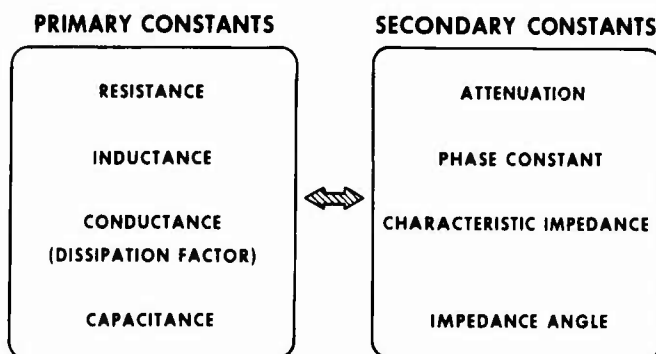


Figure 1

at the 1000 microradian level will produce no more than a half percent error in extracted resistance. Effects on the other properties are negligible.

We have now identified three parameters to be measured, insertion loss, insertion phase, and capacitance, and a fourth, dissipation factor, that can be estimated with sufficient accuracy. These, together with measurement of test set impedance will permit conversion from insertion loss and phase to attenuation and phase constant and computation of the remaining transmission parameters over the entire measurement frequency band.

## 2. Measurements

How is this done? We measure insertion loss and phase with a Computer Operation Transmission Measuring Set<sup>1</sup> (COTMS) as seen in Figure 2.



Figure 2

The set uses a microbel comparison technique and is capable of insertion loss and phase measurement in the 50 Hz to 1 GHz range. Generator and detector impedances are 50 ohms coaxial. Loss accuracy is 0.01 db in 20 db over the 10 KHz to 15 MHz band. Corresponding phase accuracy is 0.2 degrees in 360. Since telephone cables are used in the balanced mode, unbalanced to balanced transformers are used to change modes and provide some degree of impedance matching. The basic circuit is shown in Figure 3.

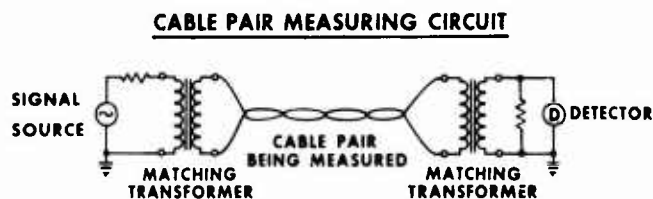


Figure 3

By making an insertion loss measurement on a highly accurate resistance standard that is flat with frequency, Figure 4, we can extract the complex generator and detector impedance versus frequency. In this process, it is assumed that the generator and detector impedance are equal.

## TEST SET IMPEDANCE MEASURING CIRCUIT

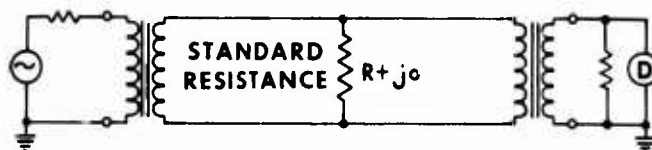


Figure 4

Next, capacitance measurements are made at 1 KHz on a General Radio 1683 RLC Bridge. We measure the direct capacitances to mate and ground, compute the mutual capacitance and correct for propagation effects. This is done to an accuracy of 0.2 percent. For cable pairs with polyolefin insulation, capacitance is constant over the frequency band of interest. The mutual capacitance measured at low frequency can be accurately used at all frequencies. For pulp and PVC insulated pairs, capacitance change with frequency can be modeled, so, given low frequency capacitance, capacitance at other frequencies can be readily estimated. DC resistance is measured to an accuracy of 0.2 percent.

## 3. Transmission Parameters in the Measurement Band

Cable transmission loss is composed of two components, a series resistive component associated with the copper loss increasing in the megahertz region with the square root of frequency and a shunt dissipative component associated with the dielectric loss increasing directly with frequency. These relationships are shown in Figure 5.

## HIGH FREQUENCY CABLE ATTENUATION COMPONENTS

<u>RESISTIVE</u>	<u>DISSIPATIVE</u>
$\text{ATTEN} \approx \frac{\text{RES}}{2} \sqrt{\frac{\text{CAP}}{\text{IND}}}$	$+ \frac{\text{PHASE CON} \cdot \text{DISFAC}}{2}$
$\approx a + b \sqrt{f}$	$+ cf$
$\text{DISFAC} \approx \frac{2 \cdot cf}{\text{PHASE CON}}$	

Figure 5

By polynomial curve fitting to the insertion loss measurement data over an appropriate frequency band, say 0.4-12.0 MHz, these two components can be separated and quantified. Dissipation factor can then be computed from the direct frequency term,  $\omega l$ , and the measured insertion phase. This process extracts an effective dissipation factor which may be different from the insulating material loss properties. If the cable pair being analyzed has sufficient unbalance to cause mode conversion or if the pair is driven with a significant longitudinal component, any non-square root of frequency contribution due to these causes will influence the extracted dissipation factor values. For typical cables, we estimate this technique extracts effective dissipation factor to an accuracy of at least 10 percent which is more than adequate for computation of the other transmission properties to accuracies commensurate with the insertion loss and phase measurement accuracy.

The computation of the extracted primary and secondary constants is performed in an iterative loop from the above data as shown in Figure 6.

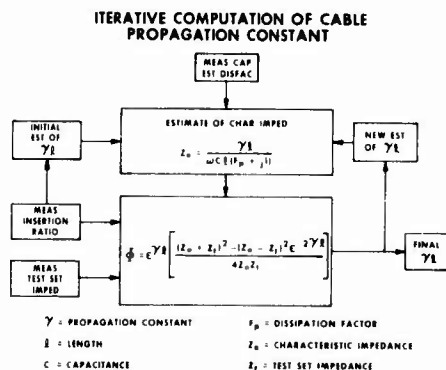


Figure 6

The insertion ratio,  $\Phi$ , of a uniform transmission line of length  $l$  with characteristic impedance,  $Z_0$ , and propagation constant  $\gamma$  inserted between a generator and detector of impedance  $Z_t$  is given by the central equation. If  $Z_0$  and  $Z_t$  were known, we could solve for  $\gamma l$  directly. However, since  $Z_0$  is not known, we must use an iterative technique. The measured value of insertion ratio is used as an initial value for propagation constant.  $Z_0$  is then estimated from that and the measured capacitance and estimated dissipation factor. This  $Z_0$  is then used to compute a correction factor to  $\gamma l$  based on mismatch. The loop is iterated until the change in  $\gamma l$  from the  $i$ th step to the  $(i+1)$ th step is suitably small (typically .05%).

This technique works fine at higher frequencies (generally above 100 KHz) where the mismatches are small and the initial guess quite close. However, in the lower frequency region, convergence does not always result because the initial guess obtained from the measured insertion loss may not be close enough to the final value to assure convergence. In order to solve this problem, the

following is done. For the two highest frequencies, the technique described above is used. Usually these are in the megahertz range and convergence is assured. Then for each frequency below the two highest, the initial guess at  $\gamma l$  is obtained by a straight line extrapolation of the previous two higher frequencies. This change in the process of obtaining an initial estimate leads to convergence down to about 10 KHz for cables in 2000-3000 ft. lengths.

If the iterative process used to compute attenuation and phase constant is itself iterated on dissipation factor, a better estimate of dissipation factor is obtained. Two passes through the process is sufficient.

With propagation constant determined, we have attenuation and phase constant directly, being just the real and imaginary components, respectively. This is shown in Figure 7. From propagation constant and characteristic impedance, we compute distributed resistance and inductance.

#### COMPUTATION OF CABLE RESISTANCE AND INDUCTANCE

$$R + j\omega L = \gamma \cdot Z_0 \quad \text{where} \quad \gamma = \alpha + j\beta$$

$$Z_0 = |Z_0| \angle \theta$$

$$R = \text{Re}(\gamma \cdot Z_0)$$

$$L = \frac{\text{Im}(\gamma \cdot Z_0)}{\omega}$$

$\alpha$  = ATTENUATION       $\theta$  = ANGLE CHARACTERISTIC IMPEDANCE  
 $\beta$  = PHASE CONSTANT       $R$  = RESISTANCE  
 $|Z_0|$  = MAGNITUDE CHARACTERISTIC IMPEDANCE       $L$  = INDUCTANCE  
 $\omega = 2\pi f$

Figure 7

#### 4. Low Frequency Transmission Parameters

To this point, then, we have shown how the primary and secondary transmission parameters of multipair cable pairs can be extracted from insertion loss and phase and capacitance measurements from 10 KHz to 15 MHz. Our goal, however, is to characterize cables over the entire transmission band of interest to the telephone engineer, namely from 100 Hz and below to 15 MHz. To extend our characterization down to the lowest frequency of interest, we employ intelligent extrapolation and interpolation. Though we can measure and compute to 10 KHz, we believe the measurement results are noisy below about 40 KHz. It remains to estimate transmission properties below 40 KHz.

Low frequency inductance is nominally linear below about 100 KHz. A least squares linear fit to the extracted inductance data is made in the 40-100 KHz band and the slope and zero frequency intercept are determined. Inductance at any frequency between 40 KHz and DC can now be computed to about one percent. By suitable cubic curve fitting between the measured DC resistance and the 40 KHz resistance and their slopes, resistance can be estimated to better than one percent over the low frequency range.

A linear least squares fit to extracted dissipation factor versus log frequency in the 0.1-1.0 MHz band gives a reasonable basis for extrapolating dissipation factor down to the lowest frequency of interest. A minimum value of 200 microradians is allowed, which is representative of high quality commercial polyolefins.

With the four primary constants now defined over the entire frequency band of interest, the secondary constants can be computed using the equations in Figure 8, giving the full range of transmission parameters over the band. With sufficient replication of the measurement process over different gages and pair counts, a statistical data base can be built.

#### COMPUTATION OF CABLE SECONDARY CONSTANTS

$$\alpha = R_0 \sqrt{\omega C(R + j\omega L)(F_p + j)}$$

$$\beta = \text{Im} \sqrt{\omega C(R + j\omega L)(F_p + j)}$$

$$|Z_0| = \left| \frac{(R + j\omega L)}{\omega C(F_p + j)} \right|$$

$$\angle Z_0 = \frac{\text{ARCTAN} \frac{\omega L}{R} - \text{ARCTAN} \frac{1}{F_p}}{2}$$

Figure 8

#### 5. Extraction of Material and Geometric Properties

At this point, we have satisfied the needs of the telephone system designer and some of the needs of the cable designer for cable characterization information. However, for the cable designer who is interested in cable transmission models to predict transmission performance of arbitrarily specified new designs, the effect of material properties and cable geometry needs to be related to the transmission properties.

Specifically, the relationships between physical properties such as pair conductor diameter, conductor conductivity, pair spacing, insulation diameter, and dielectric constant and the transmission properties need to be quantified. Unfortunately, firm theoretical relationships for these parameters for multipair cable do not exist at this time, so we need to resort to empirical techniques.

Conductor diameter can be measured at the cable ends with a micrometer or can be estimated from direct current resistance measurements by assuming a conductor material conductivity. Or conductivity can be determined experimentally from accurate resistance measurements and weighing of a carefully measured short length. Wire spacing of a pair can be computed from the zero frequency inductance intercept. Diameter over the dielectric can best be determined from production line measurements or on a shadowgraph from cable cross section samples.

Determination of dielectric constant is more complicated because it is non-uniform within the cable core. The conductors of a pair are generally closer to each other than they are to the conductors of the other pairs surrounding them. Also, the insulation and fill space around the pairs are different and, hence, have different dielectric constants. However, estimation of dielectric constant is amenable to computation. We have a computer program that solves Laplace's Equation in two dimensions for multiple circular conductors, with circular insulation and a circular overall shield. By arranging the insulated conductors appropriately in this model, a configuration simulating a pair in a multipair cable can be realized. Figure 9 shows the basic geometrical relationships.

#### MULTIPAIR CABLE PHYSICAL CHARACTERISTICS

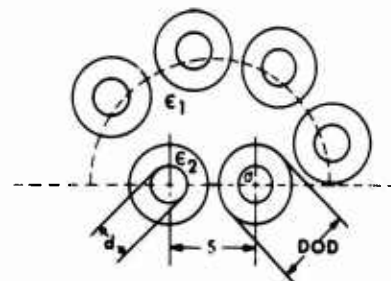


Figure 9

The conductor diameter,  $d$ , diameter over the dielectric,  $DOD$ , conductor spacing,  $S$ , and dielectric constants of the conductor insulation,  $\epsilon_2$ , and surrounding area,  $\epsilon_1$ , are specified. Then, by appropriately adjusting the positions of the conductors forming the shield around the pair being modeled, the measured direct capacitances can be duplicated and the corresponding effective dielectric constant obtained.

We now have reasonable estimates for the basic material properties and the pair geometry associated with a particular set of transmission measurements. Using similar data from a variety of cables, empirical models to predict transmission properties of multipair cable can be constructed for a reasonably broad range of input parameters. Thus, we have satisfied the remaining needs of the cable designer.

#### CABLE DATA ANALYSIS FLOW DIAGRAM

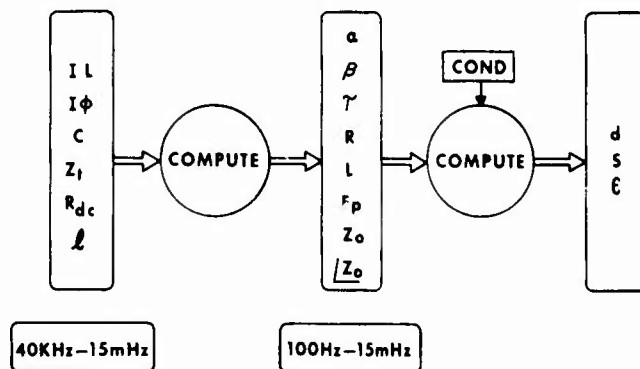



Figure 10

## 6. Summary


In summary then, Figure 10, we have shown how all of the transmission parameters and material and geometric information from multipair cables can be obtained over a wide band from a limited set of measurements and some knowledgeable estimation. Typical accuracies for the various measured and extracted parameters range from around 0.3 percent for the extracted transmission parameters to one to two percent for the dimensional and material property extractions. Dissipation factor is extracted to 10 percent or better.

## References

1. Anderson, R. E., "Computer Controlled Cable Measurements," 21st International Wire and Cable Symposium, December, 1972.



J. Kreutzberg graduated with a B.S. in Physics from Northwestern University in 1949, and received his M.S. in EE from John Hopkins in 1962. He has been employed by Bell Laboratories since 1956, and has worked on the development of L-carrier coaxial cable, ocean cable and multipair cable. In his present position as supervisor of the Computation and Measurements Group at Bell Labs Atlanta Location, he is responsible for electrical measurements and analysis of Bell System wire and cable products.



T. D. Nantz received the BSEE from the University of Pennsylvania in 1968, and the MSEE from Northeastern University in 1972. He is currently a Member of Technical Staff at Bell Laboratories engaged in measurement of transmission and crosstalk properties of multiple cable.

## DESIGN AND OPERATIONAL CHARACTERISTICS OF CABLE PRESSURE TELEMETRY SYSTEM

Y. Goto, M. Kusunoki

Nippon Telegraph & Telephone Public Corporation  
Tokyo, Japan

### Summary

Even when cable systems are constructed according to standards, experiences show that circuits may be put out of service because of failures in cable sheaths or splices. Circuit trouble due to the water penetration may be avoided by keeping the cable under gas pressure.

However, the number of gas leakages is rising year by year, in proportion to the increment of pressurized cable installations and manpower required to repair the gas leaks occupies a large portion of the cable maintenance. A cable pressure telemetry system was developed under NTT auspices to reduce the manpower needed for locating gas leakage points and to shorten the time required to repair the gas leaks in pressurized cables. This system consists of gas pressure supervisory and display equipment (center equipment), which is installed in a telephone office, and gas pressure sensors (pressure transducers), which are enclosed in the cable splices.

Commercial testing of this system is now under way at four telephone offices in Tokyo and in Tokai, Kyushu and Hokkaido areas and has shown satisfactory operation so far. This paper gives an equipment outline and field trial results.

### Introduction

The pressurization method for telecommunication cable maintenance was introduced in NTT in 1947, and it has been most effective in giving early warning of troubles which affect service. However, the number of gas leaks is rising year by year in proportion to the increase of pressurized installations. In 1974, there were about 18,800 such troubles (16.3/year·100 km sheath length).

Repair work for these gas leaks — gas leak point locating and failure repair work — requires an average of 6 man-days. Locating the gas leak point requires 5 man-days and takes as much as two days elapsed

time. Therefore, saving of manpower used in this locating work is the principal objective.

Gas leak point locating work, as practiced today by NTT, is as follows:

When a gas leak is detected by a contact manometer installed at the cable end or by gas flow alarm unit attached to the gas source, repair men begin measuring the gas pressure in the cable along the cable route, using mercury manometers. Measured values are plotted on a gas pressure distribution diagram to determine the leakage point. In this method, gas pressure measurements are carried out simultaneously at three or more points. At least 30 minutes are required for one measurement. This process is repeated along the cable route, changing the measuring points. In each set of measurements, the first measurement point is the same as the last point of the preceding set. During this process, gas pressure in the cable continues to fall. Hence, the measured pressure value must be corrected at every set of measurements. Therefore, this method is not very accurate, considering the time and manpower required. Recent restrictions on work in the manholes along roads, especially in urban areas, makes the problem more serious.

In 1971, NTT started its basic study on the most effective method of locating gas leakage points, at the Ibaraki Electrical Communication Laboratory. In 1972, cable pressure telemetry equipments were manufactured for trial use and, in 1973, field trial of these equipments was carried out. Results showed that the basic equipment characteristics and the gas leakage point locating accuracy almost fulfilled the requirements, only a few modifications being needed. Then, reliability tests on the equipments were carried out. Commercial tests of the system using the modified equipments are now under way.

### System Construction

The cable pressure telemetry system consists of a gas pressure supervisory and display equipment (center equipment), which



is installed in a telephone office, and gas pressure sensors (pressure transducers), which are enclosed in the cable splices. An outline of this system is shown in Fig.1.

The center equipment normally operates in an automatic mode and monitors the status of the cable gas pressure all the time.

Gas pressure sensors are installed at certain intervals according to the types of cables to which they are applied and the cable route construction.

In the following sections, a detailed description of these equipments is given.

unit is powered all times. A selective filter unit responds to the scanning signal from the center equipment and turns on the power switching unit. D.C. voltage from the center equipment is supplied to the voltage stabilizer unit and stabilized voltage is supplied to the current supply unit and the voltage-current transducer unit.

A gas pressure sensor unit consists of a bellows and a pair of semi-conductor strain gauges, as shown in Fig.4. Gas pressure is continuously exerted onto a bellows which expands until it applies force to the measuring lever, balancing

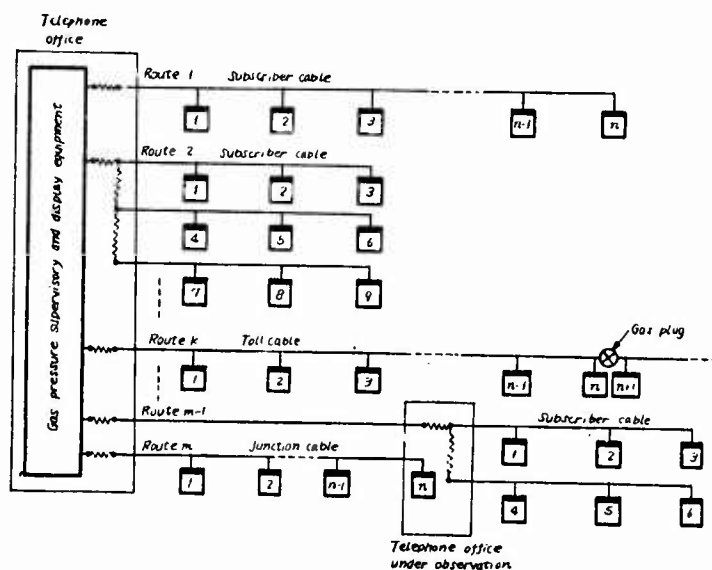


Fig.1 Cable pressure telemetry system

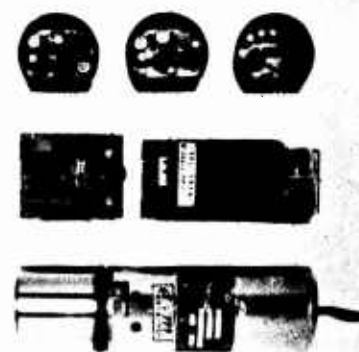


Fig. 2 Gas pressure sensor external view

### Cable Pressure Telemetry System Equipments

#### Gas Pressure Sensor

The gas pressure sensor converts the gas pressure into an electric current proportional to the gas pressure. An external view of the gas pressure sensor is shown in Fig.2 and a blockdiagram is shown in Fig.3.

The gas pressure sensor operational sequence is as follows:

An individual frequency, ranging from 382.5 Hz to 982.5 Hz with 30 Hz spacing between them, is allocated to each gas pressure sensor. The response circuit

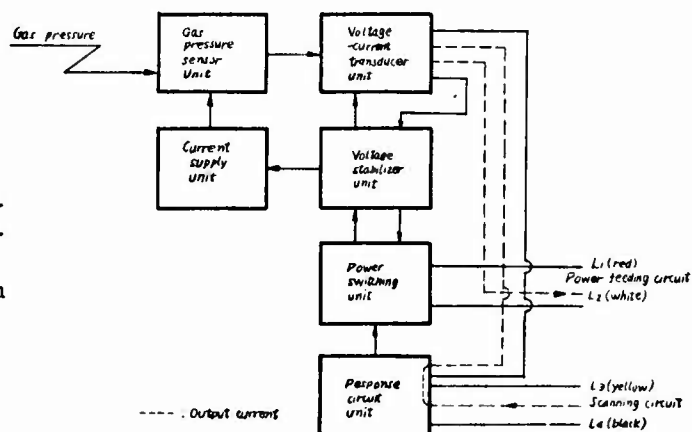


Fig.3 Gas pressure sensor blockdiagram

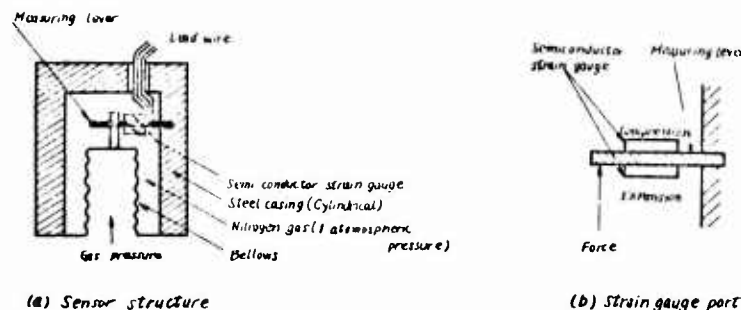


Fig.4 Gas pressure sensor construction

with the bending elasticity of the lever. The strain of the lever due to the force conveyed from the bellows is converted into resistance change of the semi-conductor strain gauge on the measuring lever.

The pair of strain gauges forms a circuit, as shown in Fig.5, and is supplied with constant current  $I$  from the current supply unit. If the electric resistances of the respective strain gauge change by  $r$  in direction opposite to each other due to a change in gas pressure, differential voltage

$$V_d = 2I \cdot r$$

is generated between the strain gauges.

The differential voltage is transduced into the constant current through the voltage-current transducer unit and a cur-

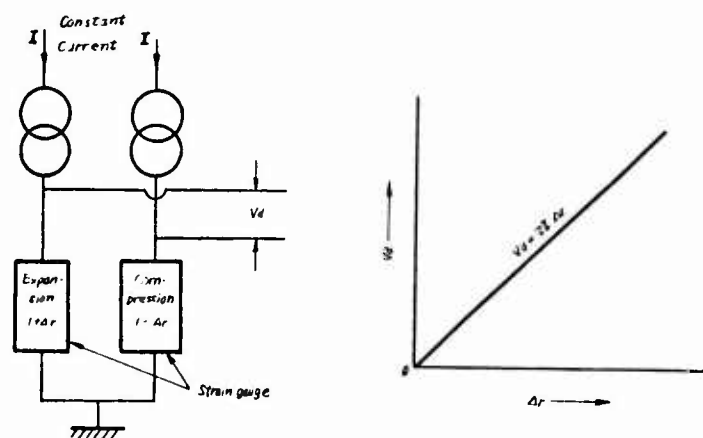


Fig.5 Constant current bridge circuit

ent proportional to gas pressure is transmitted to the center equipment.

The sensor spacing, taking into account the gas leak point locating accuracy, is less than 1.5 km for junction and toll cables. In the case of local underground cable, sensors are installed about 500 meters from a telephone office, at the end of the cable route and at an intermedi-

ate point, because the length of local underground cable is usually less than 4 km in Japan. If there is a branched cable, which is more than 200 meters long, an additional sensor is installed at the end of the branched cable. With this spacing, the pinpointing accuracy is expected to be within one span between manholes (100 - 150 meters).

#### Gas Pressure Supervisory and Display Equipment

Gas pressure supervisory and display equipment (center equipment) is installed in the telephone office or at the cable maintenance center, gas pressure sensors being connected to this equipment by a leased circuit.

An external view and a blockdiagram of the gas pressure supervisory and display equipment are shown in Figs. 6 and 7.

This equipment consists of a power feeding unit, supervisory and logic unit, display unit and memories for correction and alarm point. Gas pressure signals from the gas pressure sensors are computed in the supervisory and logic unit, comparing them with the predetermined value held in the memory unit, and displayed or printed out by the display unit.



15576

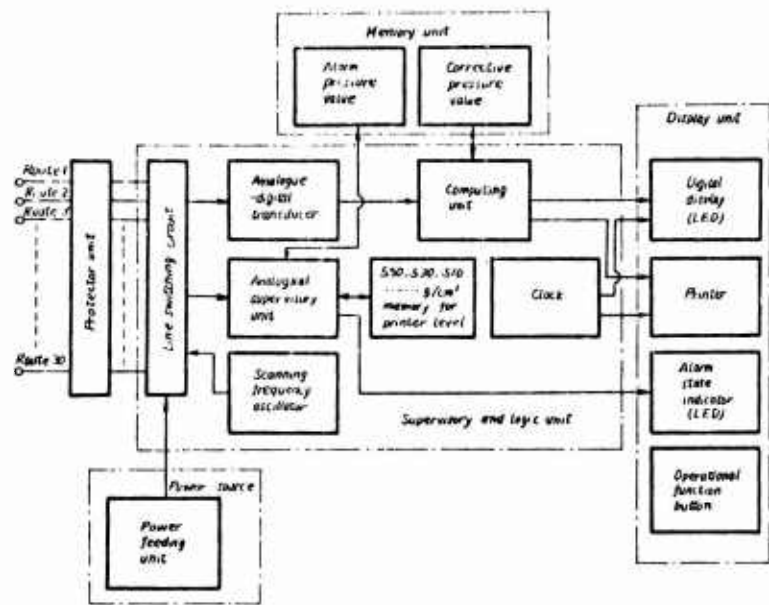


Fig.7 Gas pressure supervisory and display equipment blockdiagram

Fig.6 Gas pressure supervisory and display equipment (center equipment)

This equipment has the following functions:

(1) Power feeding function

As IC's are used in each gas pressure sensor, three-wire power feeding system consisting of + and - metallic circuit wires and a return phantom on two metallic wires is employed. The supplied power voltage is +60 volts and -20 volts, with respect to the phantom line.

(2) Scanning function

A scanning signal at a frequency ranging from 382.5 Hz (CH 1) to 982.5 Hz (CH 20) at 30 Hz spacing is sent out in turn for all cable routes. All the cable routes are scanned simultaneously. The sending time for each frequency is 2 seconds, and scanning pauses for the next 2 seconds. Therefore, a scanning frequency is sent out every four seconds and the whole cycle of scanning 20 channels takes 80 seconds. (See Fig.8) Normally, the center equipment is operated in an "automatic mode". If required, the operating mode is switched

to "manual mode" whereby any desired route can be scanned individually.

(3) Gas pressure display function

In the 80 seconds scanning cycle, the scanning frequency current is sent out in turn for 2 seconds at 2 second intervals. During the latter half of the 2 second scanning time, the cable route is scanned sequentially by line switching circuit. The response signal from each route is compared with the predetermined standard voltage, print out level or alarm level, in the comparator circuit in the analogical supervisory unit. (See Fig.8)

- a) If the gas pressure is normal in every cable route, the 80 seconds comparison cycle is repeated.
- b) When gas pressure falls below a predetermined value (for example, 550 g/cm<sup>2</sup>) in any cable route, the analogical supervisory unit memorizes the faulty cable route, and, in the next 80 seconds, the gas pressure of only the faulty cable route is precisely measured sequentially from CH 1 to CH 20, the measured value is transduced into a digital signal and the value is automatically printed out, together with date, time, route number and gas

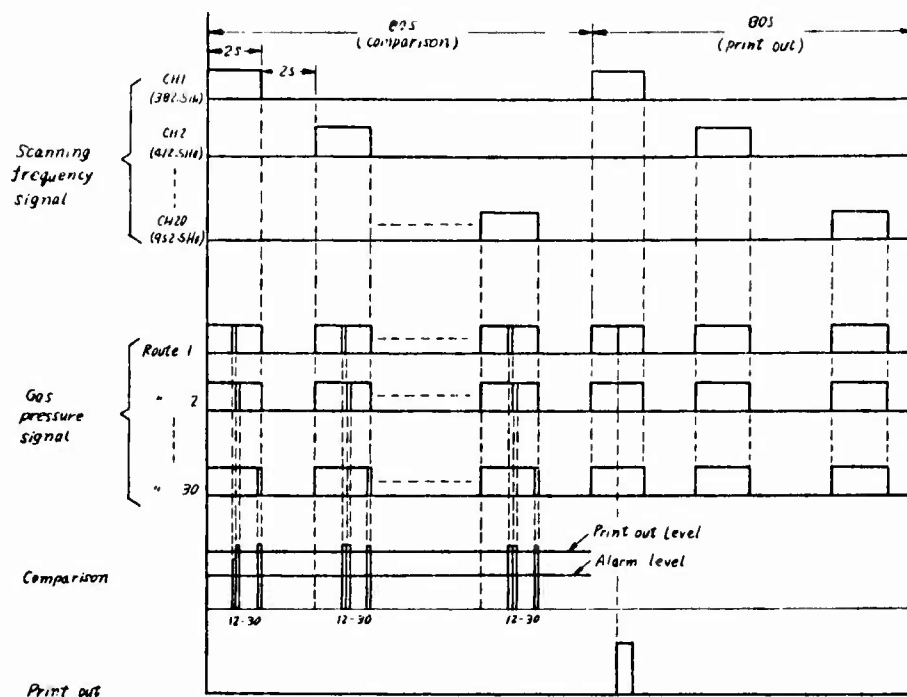


Fig. 8 Center equipment time chart

pressure sensor channel number. In the next 80 seconds, gas pressure in every cable route is scanned and compared again as in the normal condition. These operations are repeated every 20 g/cm<sup>2</sup> drop.

This operational procedure is adopted in order to reduce spotting error.

When required, the gas pressure distribution along any chosen cable route can be manually displayed and printed out.

If there is an error in the displayed pressure value, due to aging of the gas pressure sensor, it can be corrected, before being displayed, within a range of  $\pm 15$  g/cm<sup>2</sup>. The corrective pressure value is memorized in the memory unit.

#### (4) Alarm function

When the gas pressure falls below the alarm value (300 g/cm<sup>2</sup> for local cable, 400 g/cm<sup>2</sup> for toll cable), an alert is indicated by the equipment and, as a result,

repair work is initiated. The gas pressure distribution along the cable route is also printed out.

#### Principal Specifications

Principal specifications of the equipments are shown in Table 1.

#### Result of Accelerated Degradation Test

Accelerated degradation tests, as shown in Table 2, are carried out on the gas pressure sensor. The results showed that variations in the response were within  $\pm 2.5$  g/cm<sup>2</sup>.

Table 1 Principal Specifications

	Items	Specifications	Characteristics of equipments for commercial testing
Gas pressure sensor	Rotation characteristics (variation from standard value)	Less than $\pm 2$ g/cm <sup>2</sup> (when rotated around standard axis by $\pm 90^\circ$ and $180^\circ$ )	+ $90^\circ$ : -0.14 (0.19) * 180°: 0.46 (0.23) - $90^\circ$ : 0.40 (0.21)
	Inclination characteristics (variation from standard value)	Less than $\pm 2$ g/cm <sup>2</sup> (when inclined from horizontal level by $\pm 5^\circ$ )	+ $5^\circ$ : 0.32 (0.17) - $5^\circ$ : -0.38 (0.13)
	Vibration characteristics (variation from standard value)	Less than $\pm 3$ g/cm <sup>2</sup> (when vibrated at a frequency of 600/m with an amplitude of 1.0 mm in up-and-down and side-to-side directions)	0.25 (0.21)
	High pressure characteristics (variation from standard value)	Less than $\pm 2$ g/cm <sup>2</sup> (when pressure of 1.0 kg/cm <sup>2</sup> is imposed for 1 minute)	at 200 g/cm <sup>2</sup> : 0.22 (0.14) at 400 g/cm <sup>2</sup> : 0.19 (0.13) at 600 g/cm <sup>2</sup> : 0.16 (0.14)
	Measuring range	0 - 800 g/cm <sup>2</sup> (relative pressure)	
	Maximum permissible pressure	1,500 g/cm <sup>2</sup> (relative pressure)	
	Accuracy (15 $\pm$ 2 C; 0 - 800 g/cm <sup>2</sup> )	Less than $\pm 2$ g/cm <sup>2</sup>	at 200 g/cm <sup>2</sup> : 199.9 (0.49) at 400 g/cm <sup>2</sup> : 399.8 (0.46) at 600 g/cm <sup>2</sup> : 600.3 (0.60)
	Temperature characteristics (variation from the value at 15 $\pm$ 2 C)	Less than $\pm 3$ g/cm <sup>2</sup> (when temperature is changed by $\pm 10^\circ\text{C}$ )	at 400 g/cm <sup>2</sup> : + $10^\circ\text{C}$ : 0.75 (0.64) - $10^\circ\text{C}$ : 0.92 (0.67)
	Shape, size	Cylindrical, less than 50 mm $\phi$ x 200 mm	
	Weight	Less than 800 g	
Gas pressure supervisory and display equipment	Number of sensors to be connected	600 (20 CHx30 routes)	
	Permissible line loop resistance	1,000 ohm	
	Power source	AC 100 volts, 800 VA	
	Shape, size	Rectangular 800 mm 450 mm 1,800 mm (w) (d) (h)	

\*The value in parentheses is the standard deviation.

Table 2 Accelerated Gas Pressure Sensor Degradation Tests

Items	Test Method	Number of Repetitions
Vibration test	Frequency 600 cycle/min. Amplitude 1.0 mm	$10^6$
Heat cycle test	Temperature range - $5^{\circ}\text{C}$ ~ $35^{\circ}\text{C}$ Frequency 4 cycle/day	100
High temperature test	Temperature - $5^{\circ}\text{C}$ , $80^{\circ}\text{C}$ Period of one stage 2 hours	10
Repeated pressure test	Pressure range 0 ~ $800\text{ g/cm}^2$ Period of repetition 20 seconds	$10^3$
High pressure imposition test	Pressure $1,500\text{ g/cm}^2$ Imposition time 30 minutes	10

#### Gas Leakage Point Estimation

##### Accuracy

In order to determine variations in cable pressure distribution when gas leakage trouble occurs on a pressurized cable, measurements are carried out by attaching a 0.2 mm gas leak valve to the cable. Results showed that, in eight cases out of thirteen, the leakage point estimated by this system almost coincided with the actual point of leakage. In the other five cases, the error in the estimates was within one manhole spacing (about 100 - 150 meters).

Hence, in view of the fact that most gas leakages occur at a cable-splice point, it is satisfactory that errors in pinpointing should be within a manhole spacing.

An example of the measured pressure distribution along a cable route is shown in Fig.9.

#### Gas Pressure Sensor

##### Reliability Estimation

The reliability of one pressure sensor can be estimated at less than 1,900 FIT.

In most underground subscriber's cable, three gas pressure sensors are required. Therefore, using the above reliability

value, the failure for each cable route can be estimated at 0.05/route·year. This value is less than one twentieth of cable faults.

#### Conclusion and Future

##### Prospect

A cable gas pressure telemetry system, which enables gas pressure distribution in each cable to be constantly monitored from the telephone office by setting gas pressure sensors at intervals of about 1.5 km in each cable, has been developed.

Commercial tests of this system have been going on since February, 1975 in four telephone offices in Tokyo and in Tokai, Kyushu and Hokkaido areas. About 20 cables are connected for each system in the commercial test.

By using this system, pressure distribution of up to 30 cable routes can be constantly monitored from the telephone office, and, if a route of the center equipment is assumed to be divided into four sub-routes, as shown in Fig.10, 120 cable routes can be monitored.

When gas leakage occurs in any cable route, approximate pinhole size and leakage location can be estimated and repair urgency can be determined from the pressure distri-



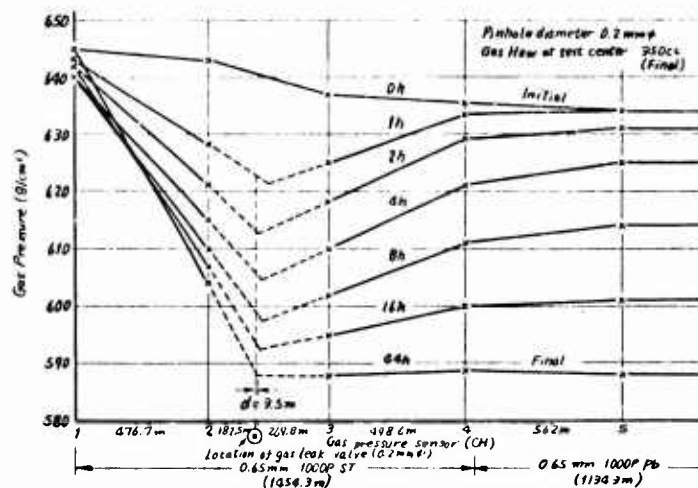


Fig. 9 Cable pressure distribution variation as related to elapsed time

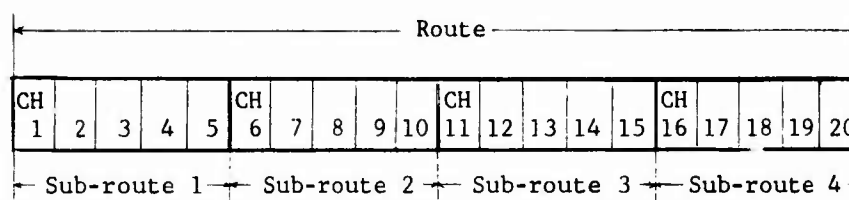


Fig. 10 Sub-route composition

bution data obtained while the gas pressure is continuing to drop, thus enabling the maintenance work to be carried out according to trouble priority.

In order to improve the efficiency of pressurized cable maintenance, in big cities, studies are now being made on a method of centralizing maintenance.

An outline of the proposed system is shown in Fig. 11.

A remote terminal is installed in every telephone office. It has almost the same functions as the center equipment described in this paper, except that a coder is attached in place of the display unit.

The remote terminal is scanned by the center equipment every 20 or 30 minutes

through a 50 ~ 200 bit/s digital circuit. If gas leakage is detected by one of the remote terminals, cable pressure distribution along the leaky cable route is printed out in the center equipment.

The center equipment is installed in a Pressure Cable Supervisory Center, which is allocated to every Urban Telecommunication Division. When the cable pressure falls below the alarm level, the gas leakage point location is indicated in Pressurized Cable Supervisory Center by plotting the measured gas pressure along the cable route. Then, the order for repair work is dispatched to the Cable Maintenance Center.

Since the gas leakage point location can be determined with good accuracy, when the gas pressure approaches the final gas pressure level value indicated in Fig. 9,

100,000 man·days, which is required every year for locating the gas leakage point, is expected to be saved.

This system will be very useful for labor saving and rationalization of pressurized cable maintenance work.

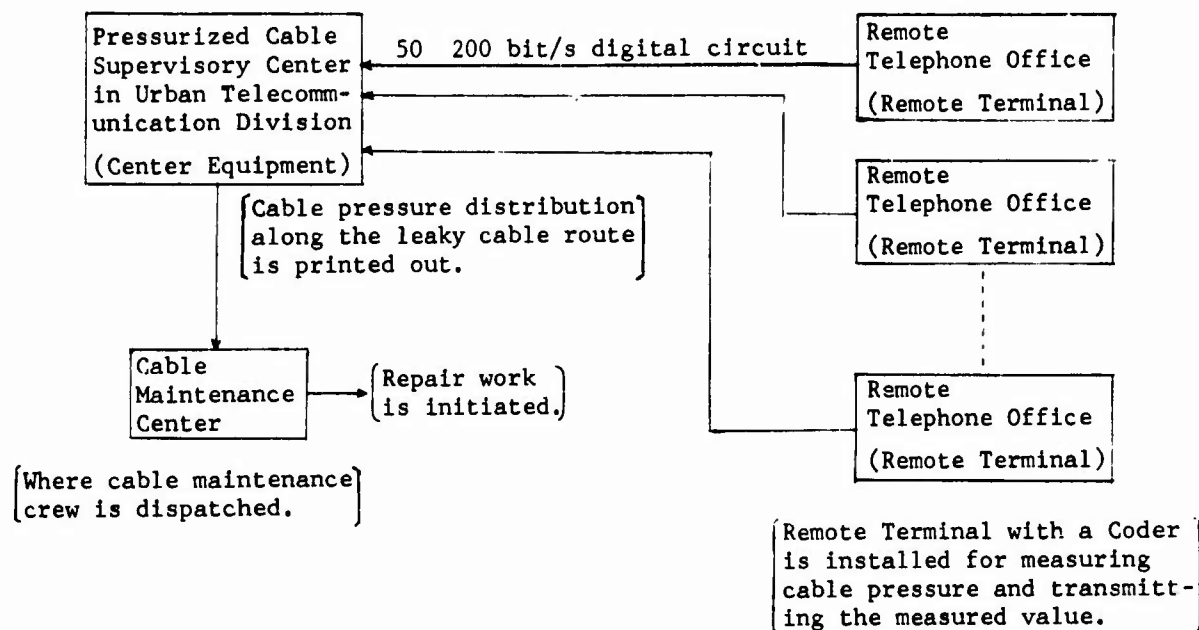


Fig. 11 Centralized cable pressure telemetry system



YUKIO GOTO

Nippon Telegraph &  
Telephone Public  
Corporation

1-1-6 Uchisaiwai-  
Cho, Chiyoda-Ku,  
Tokyo, Japan

Yukio Goto is Staff Engineer, Outside Plant Division, Engineering Bureau, NTT, and is now in charge of development of outside plant, especially gas pressurization system.

He received B.E. degree in telecommunication engineering from Osaka University in 1965, and is a member of the Institute of Electronics and Communication Engineers of Japan.



MICHIHIKO KUSUNOKI

Nippon Telegraph &  
Telephone Public  
Corporation

Shirane, Shirakata,  
Tokai-Vill.,  
Ibaraki Pref., Japan

Michihiko Kusunoki is Staff Engineer, Outside Plant Development Division, Ibaraki Electrical Communication Laboratory, NTT, and is engaged in the development of the structure of underground and overhead telephone lines.

He is a member of the Institute of Electronics and Communication Engineers of Japan.

# CORROSION STUDIES ON SHIELDING MATERIALS FOR UNDERGROUND TELEPHONE CABLES

## PART I: DEVELOPMENT OF TEST METHODOLOGY

T. S. Choo  
Dow Chemical U.S.A.  
Freeport, Texas

### Abstract

Efforts to define a sensitive and realistic laboratory test methodology to study corrosion of telephone cable shielding materials are described. The instrumentation chosen for corrosion rate measurement is similar to modern electrochemical methods successfully being used on a real-time basis by the chemical process and pipeline industries. Synthetic soil solutions based on analyses of the National Bureau of Standards/Rural Electrification Administration field test sites are used as the test media.

Initial data on electrochemical corrosion and galvanic corrosion due to dissimilar metals, differential aeration, and stress are presented for several shielding materials. The results are in reasonably good agreement with selected data from the NBS/REA field trials. Direction of further test development is discussed.

### Introduction

Telephone cables represent about one-third of plant investment and are expected to have a 40-year service life. Electrically continuous and properly grounded metallic shields are essential for safe and noise-free cable operation. Most cables being installed today are buried directly in soil - a complex biological, chemical and physical environment. The outer polyethylene jacket of such cables may be subject to damage from the rigors of installation, rocks, rodents, lightning, frost and dig-ins. The underlying metallic shields can thereby be exposed to soil water and the attendant potential for corrosion. Therefore, the ability of a shielding material to resist corrosion can determine, to a significant extent, technical functionality of a cable throughout the service life required for adequate return on investment.

From the standpoint of corrosion resistance, the most helpful guide for selection of shielding materials would be well documented data on service experience of the operating companies. Unfortunately, such data are almost non-existent. Present-day economics often dictate that an inoperative cable simply be abandoned rather than recovered for examination. Therefore, many corrosion problems remain buried. In these circumstances, it is difficult to justify development of the qualified staff and sophisticated equipment necessary to isolate and identify shield corrosion failures. Consequently, most operating companies have had to rely on other sources and tests for corrosion evaluation of shielding materials.

A number of field tests have been conducted by various agencies in representative soils of the U.S. The most comprehensive of these tests to date are the efforts sponsored jointly by the National Bureau of Standards (NBS) and the Rural Electrification Administration (REA).<sup>1,2,3</sup> Data from this program have been valuable and helpful. However, all field tests have an inherent disadvantage in that several years are required to reach significant conclusions. Also, the expense of including enough samples to attach a reasonable level of statistical significance to the results is usually prohibitive. This leaves the reproducibility of results open to question. These factors underscore the need for a short-term laboratory test procedure which could not only screen materials but predict shield corrosion resistance in various soil environments.

At the outset of the present study, three key areas of test methodology were identified: (1) method of corrosion rate measurement, (2) test environments or media, and (3) sample preparation techniques. It was decided to explore potentiostatic linear polarization as a corrosion rate measurement tool<sup>4</sup> since the chemical process and pipeline industries have developed sufficient confidence in this method to use it on an in-line, real-time basis. These industries have realized cost savings and safer working conditions as a result. Efforts to define the test media resulted in generation of synthetic soil solutions based on the chemistry of the NBS/REA test sites. The environments were later extended to include differential aeration. Variation in sample preparation was kept to a minimum so that reproducibility of the test methodology could be investigated.

### Electrochemical Corrosion Rates From Polarization Data

#### Theory and Principles

When metal corrodes in a solution, current is produced in much the same manner as a dry cell battery. Metal goes into solution freeing electrons at anodic areas; the electrons flow through the metal to cathodic areas. At the cathode surfaces the electrons are taken up by acceptors such as hydrogen ion ( $H^+$ ) to form hydrogen gas. These microscopic batteries on the surface of a corroding metal are called local-action cells. By this process, current can continue to flow as long as there are a corroding metal, a conductive solution (electrolyte), and continuous electrical and ionic paths.

The electrons which flow through the bulk metal between the local anodes and cathodes make up what is known as the corrosion or local-action current. While it is impossible to insert a meter into this circuit and measure the corrosion current directly, it is possible to do so indirectly. This is based on the fact that there is a measureable relationship between the corrosion current and the effect of an externally applied current on the condition of the metal surface, i.e. its potential. This indirect measurement of corrosion current is the basis of polarization techniques.

In making a polarization measurement, a source of external current is connected between an auxiliary electrode and a corroding metal of known surface area, called the test electrode. This applied current is added to the corrosion current and slightly alters the corrosion conditions (the corrosion potential) at the metal surface. This process of altering the surface condition is called polarization, and the test electrode is said to be slightly polarized.

In order to determine how much polarization of the metal surface has occurred due to the applied current, the test electrode is compared to a reference electrode which is unpolarized. This comparison is made by measuring the potential difference between the test and reference electrodes before and during the time the applied current is flowing between the test and auxiliary electrodes. A schematic drawing illustrating this is shown in Figure 1.<sup>5</sup>

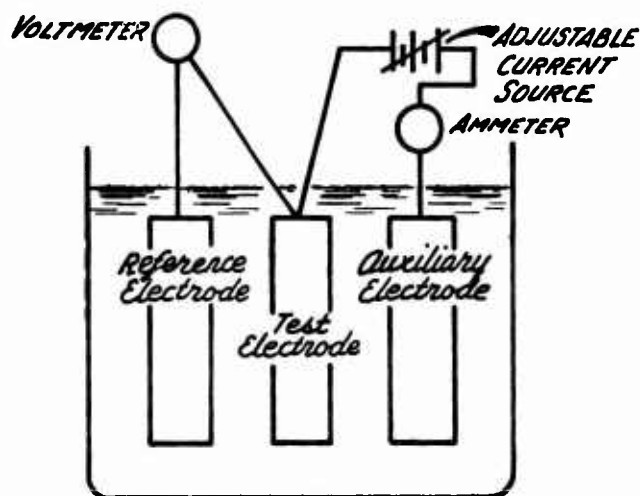


FIGURE 1. SCHEMATIC LAYOUT OF CORROSION RATE METER

The linear polarization technique which has been selected for this study is based on the fact that the change in potential varies linearly with applied current in the region very near the corrosion potential. For a test electrode of known area this relationship can be expressed by the following equation:

$$I_{cor} = \frac{\Delta I}{\Delta E} K_1 \text{-----(1)}$$

Where:  $I_{cor}$  = corrosion current density (microamps/cm<sup>2</sup>)  
 $\Delta I$  = applied current density (microamps/cm<sup>2</sup>)  
 $\Delta E$  = shift in potential from some reference (mV)  
 $K_1$  = A proportionality constant (mV)

If the potential difference ( $\Delta E$ ) is kept constant at a given value, e.g. 10 mV, equation (1) can be reduced to:

$$I_{cor} = \Delta I \cdot K_2 \text{-----(2)}$$

Corrosion rate can be calculated from weight loss per unit time. Substituting the weight loss from Faraday's Law, corrosion rate in mils per year (mpy) of penetration can be obtained by the following equation:

$$CR(\text{mpy}) = 0.129 I_{cor} e/D \text{-----(3)}$$

Where:  $CR(\text{mpy})$  = corrosion rate (mils per year)  
 $I_{cor}$  = corrosion current density (microamps/cm<sup>2</sup>)  
 $e$  = equivalent weight of metal (grams)  
 $D$  = density of metal (grams/cm<sup>3</sup>)

Equations (2) and (3) can be combined to:

$$CR(\text{mpy}) = 0.129 \cdot \Delta I \cdot K_2 \cdot e/D = \Delta I \cdot K_3 \text{----(4)}$$

It can be seen that a current meter reading on the test electrode of known surface area can now be calibrated to directly indicate corrosion rate in mils per year.

#### Corrosion Rate Meter

Electrochemical corrosion rates were measured with a Petrolite® Corrosion Rate Meter M-1010 CIY having a saturated calomel reference electrode and a platinum auxiliary electrode. The microammeter was calibrated so that the current required to produce 10 mV polarization on a mild steel test sample having a 9 cm<sup>2</sup> surface area could be read directly as mils per year (mpy). When metals other than mild steel were used, the microammeter readings were adjusted for changes in exposed surface area of the test electrode and equivalent weight and density of the metal as indicated in equation (4).

#### Synthetic Soil Solutions

Solutions having substantially the same chemical compositions and pH's as the water extracts of soils from the NBS/REA test sites were used as the test media. Table I summarizes the properties of the soils as reported by Gerhold et al.<sup>6</sup> Three solutions representing sandy loam (site A, pH 8.8), clay (site C, pH 4.0), and tidal marsh (site G, pH 7.1) were selected. Properties of these synthetic solutions are recorded in Table II.

TABLE I. PROPERTIES OF SOILS AT NBS/REA TEST SITES

Site Ident.	Soil	Location	Internal drainage of test site	Resistivity (a) (ohm - cm)	pH	TDS (b)	Composition of water extract (parts per million)							
							Ca	Mg	Na + K as Na	CO <sub>3</sub>	HCO <sub>3</sub>	SO <sub>4</sub>	Cl	NO <sub>3</sub>
A	Sage Moor sandy loam	Toppenish, Wash.	Good	400	8.8	7,080	108	23	1,960	0.0	5,002	216	330	6
B	Hagerstown loam	Loch Raven, Md.	Good	5,200	5.8	(c)	---	---	---	---	---	---	---	---
C	Clay	Cape May, N.J.	Poor	300	4.0	14,640	540	754	2,242	0.0	0.0	6,768	3,529	118
D	Lakewood sand	Wildwood, N.J.	Good	30,000	7.3	(c)	---	---	---	---	---	---	---	---
E	Coastal sand	Wildwood, N.J.	Poor	55	7.1	11,020	302	329	3,230	0.0	55	1,133	5,765	31
G	Tidal marsh	Patuxent, Md.	Poor	300	7.1	11,580	140	165	2,392	0.0	0.0	1,709	3,259	37

(a) Resistivity determinations made at the test site with Shepard Canes.

(b) TDS, total dissolved solids--residue dried at 105°C.

(c) Analyses not made for soils at sites B and D because of the very low concentrations of soluble salts in these soils.

TABLE II. PROPERTIES OF SYNTHETIC SOIL SOLUTIONS

Solution Identification	Soil	pH	Ca	Mg	Chemical composition (parts per million)				
					Na	HCO <sub>3</sub>	SO <sub>4</sub>	Cl	NO <sub>3</sub>
A	Sandy Loam	8.8	7	20	2420	4207	215	314	7
C	Clay	4.1	598	716	2200	0	6480	3413	116
G	Tidal Marsh	7.1	166	152	2350	0	1776	3212	35

#### Experimental Procedure

The shielding materials selected for test development purposes were bare and plastic clad aluminum, copper, black and tin plate steel, and plastic clad tin plate steel. The test electrodes were one inch (2.54 cm) wide and two inches (5.08 cm) long with a 1/4 inch x 6 inch (0.635 cm x 15.24 cm) neck. Specimens were washed with acetone to clean and degrease. Beeswax was used to mask the neck area so that only about 0.0625 in<sup>2</sup> (0.403 cm<sup>2</sup>) of unmasked neck was exposed to the test media. The corrosion cells contained 900 cc of solution and were kept at room temperature without agitation. The nominal thickness and exposed area of metal for each material are listed below:

TABLE III. DESCRIPTION OF TEST ELECTRODES

Shielding Material	Metal Thickness		Exposed Area (cm <sup>2</sup> )
	(mm)	(mils)	
Aluminum	0.203	8	26.5
Copper	0.127	5	26.4
Tin Plate Steel	0.152	6	26.4
Black Plate Steel	0.152	6	26.4
Plastic Clad Aluminum	0.203	8	0.310
Plastic Clad TPS	0.152	6	0.232

Corrosion rates of the shielding materials in the three synthetic soil solutions were measured at the outset and then weekly for one month. Potentiodynamic polarization curves were run during the fifth week. Then the specimens were removed for examination.

#### Results and Discussions

In order to facilitate understanding of the quantitative data generated by the corrosion rate meter, qualitative descriptions and discussions on test samples are presented first.

**Qualitative Results.** Figures 2, 3 and 4 show condition of the samples after five weeks in synthetic soil solutions A, C and G. For the metals commonly used as electrostatic shielding - namely aluminum, copper, and plastic clad aluminum - the plastic clad aluminum was affected least by corrosion in all three solutions. Plastic clad aluminum did not show any signs of corrosion in solution A on visual inspection. In solutions C and G, there were small areas of edge corrosion, but the flat surfaces were not affected.



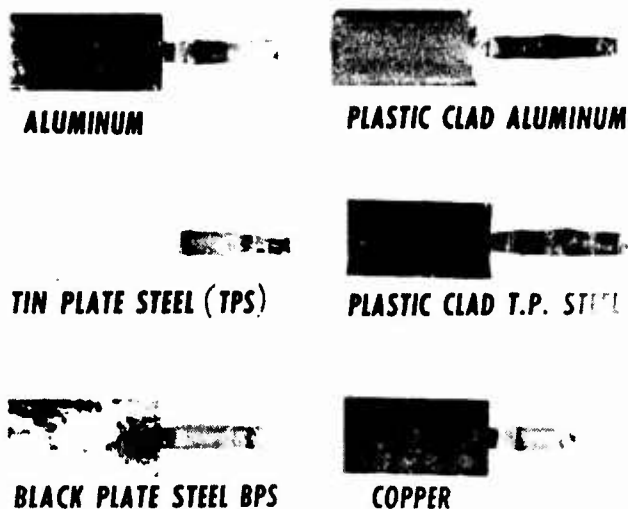


FIGURE 2. TEST SAMPLES AFTER 5 WEEKS IN SOLUTION A

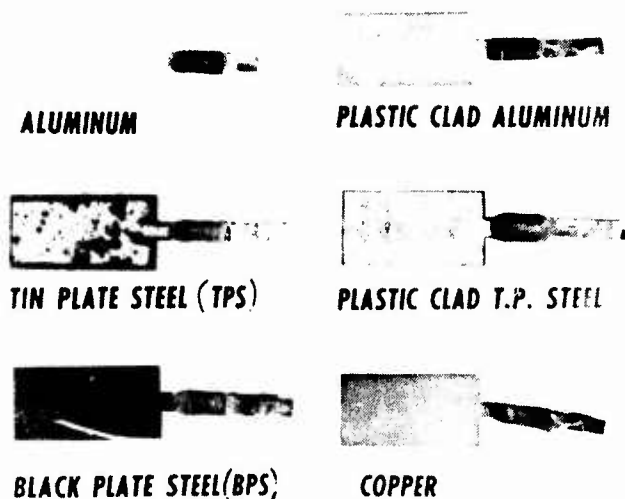


FIGURE 3. TEST SAMPLES AFTER 5 WEEKS IN SOLUTION C

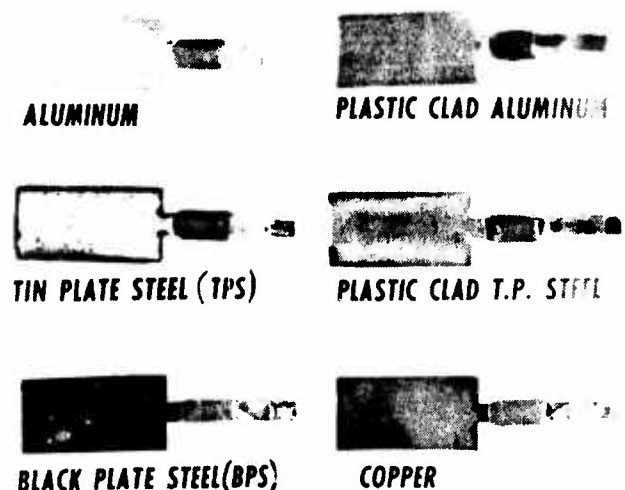


FIGURE 4. TEST SAMPLES AFTER 5 WEEKS IN SOLUTION G

Bare aluminum changed color to grayish-black in solution A. There was no indication of pitting on the flat surfaces. However, the metal was severely corroded in solution C with numerous pits and some perforations. The flat surfaces were covered with chalky corrosion products. Pitting was also present in solution G, but the severity was less than found in solution C. At the neck area in solution G, crevice corrosion was evident under the beeswax.

The copper sample in solution A was dark brown. There were many dark orange spots on the flat surfaces, indicating localized corrosion. The metal surface in solution C was dull and rough. Significant thinning of the sample was observed near the neck area; the sample could not be held horizontally without bending. However, there was no sign of pitting. In solution G, green patina was found on the copper but corrosion appeared to be uniform.

Among the three steel products commonly used for armoring, black plate steel was the most susceptible to corrosion in all three solutions followed by tin plate and plastic clad tin plate respectively. Black plate steel was relatively unaffected in solution A except for a few large areas of localized corrosion. Dark brown corrosion products were present on these areas. In solutions C and G, black plate had suffered severe uniform corrosion attack. Loosely adhering dark brown corrosion products were found, but there was no indication of deep pitting or other localized corrosion.

Tin plate steel was virtually unchanged in solution A except in some areas where the tin had lost its luster. In solution C, edges of the tin plate were severely corroded. The tin coating was totally consumed on scattered areas with a buildup of reddish-brown corrosion products. In solution G, the most noticeable corrosion was observed on the edges of the sample. The tin was discolored and had many pits.

Except for some localized corrosion on the edges, plastic clad tin plate steel was unaffected in solution A. In solutions C and G, corrosion was confined to the edges; reddish-brown corrosion products were present at these locations. Some of the corrosion products were deposited on the outside of the plastic coating. It appeared that solution G was the most corrosive environment for plastic clad tin plate steel.

**Quantitative Results.** The currents applied between the test and auxiliary electrodes to produce 10 mV polarization of the test samples are reported in Table IV. Corrosion rates in mils per year were calculated using equation (4) and are shown in Table V.

Although measured currents for bare aluminum in all solutions were significantly greater than that for plastic clad aluminum, the order reverses when current densities are calculated - due to the ratio of exposed surface areas. That such differences exist at

TABLE IV. CURRENT REQUIRED TO PRODUCE 10mV POLARIZATION (Microamps)

	<u>Aluminum</u>	<u>Copper</u>	<u>Plastic Clad Aluminum</u>	<u>Black Plate Steel</u>	<u>Tin Plate Steel</u>	<u>Plastic Clad T. P. Steel</u>
<u>SANDY LOAM (A)</u>						
1 Day	4.4	7.2	0.55	1.3	0.39	2.0
1 Week	2.0	6.6	0.22	0.39	0.11	0.11
2 Weeks	0.61	12	0.17	3.7	0.06	0.06
3 Weeks	0.39	21	0.11	7.0	0.06	0.02
4 Weeks	0.44	22	0.11	22	0.06	0.06
<u>CLAY (C)</u>						
1 Day	33	78	2.8	510	50	11
1 Week	12	42	0.77	340	53	10
2 Weeks	8.3	29	0.44	300	62	6.8
3 Weeks	5.0	46	0.50	250	44	6.8
4 Weeks	4.4	43	0.33	230	40	5.0
<u>TIDAL MARSH (G)</u>						
1 Day	5.0	6.1	0.33	110	31	11
1 Week	3.5	4.4	0.11	94	22	11
2 Weeks	1.2	2.8	0.03	88	23	12
3 Weeks	0.55	6.7	0.11	94	24	13
4 Weeks	0.33	23	0.06	77	24	15

TABLE V. CORROSION RATE ADJUSTED FOR EXPOSED AREA (MPY)

	<u>Aluminum</u>	<u>Copper</u>	<u>Plastic Clad Aluminum</u>	<u>Black Plate Steel</u>	<u>Tin Plate Steel</u>	<u>Plastic Clad T. P. Steel</u>
<u>SANDY LOAM (A)</u>						
1 Day	0.25	0.44	2.7	0.07	0.020	14
1 Week	0.11	0.41	1.1	0.02	0.007	0.77
2 Weeks	0.03	0.75	0.81	0.23	0.003	0.38
3 Weeks	0.02	1.3	0.54	0.43	0.003	0.15
4 Weeks	0.02	1.4	0.54	1.5	0.003	0.38
<u>CLAY (C)</u>						
1 Day	1.9	4.8	14	31	3.1	78
1 Week	0.69	2.6	3.8	21	3.3	74
2 Weeks	0.48	1.8	2.2	18	3.8	45
3 Weeks	0.28	2.9	2.4	17	2.7	48
4 Weeks	0.25	2.7	1.6	15	2.5	35
<u>TIDAL MARSH (G)</u>						
1 Day	0.28	0.37	1.6	6.8	1.9	78
1 Week	0.20	0.27	0.54	4.8	1.4	78
2 Weeks	0.06	0.17	0.14	5.4	1.4	85
3 Weeks	0.03	0.41	0.54	4.8	1.5	93
4 Weeks	0.02	1.4	0.27	4.8	1.5	100

**TABLE VI. AVERAGE CORROSION RATE AND PROJECTED SERVICE LIFE**  
(one-inch wide samples)

	<u>Aluminum</u>	<u>Copper</u>	<u>Plastic Clad Aluminum</u>	<u>Black Plate Steel</u>	<u>Tin Plate Steel</u>	<u>Plastic Clad T. P. Steel</u>
<u>SANDY LOAM (A)</u>						
Average Corrosion Rate (mpy)	0.086	0.85	1.1	0.45	0.007	3.1
Projected Service Life (yrs)	47	2.9	440	6.7	420	160
<u>CLAY (C)</u>						
Average Corrosion Rate (mpy)	0.72	2.9	4.7	20	3.1	56
Projected Service Life (yrs)	5.5	0.85	100	0.14	1.0	9.0
<u>TIDAL MARSH (G)</u>						
Average Corrosion Rate (mpy)	0.12	0.53	0.62	5.7	1.5	88
Projected Service Life (yrs)	34	4.7	800	0.5	2.0	5.7

all for the same metal may be explained in terms of the energy states of the exposed areas. For example, slit edges, having been stressed, are at a higher energy level as compared to flat surfaces and are therefore less resistant to corrosion.

As can be seen in Table V, most samples had high initial corrosion rates which tended to decrease with time. In general, initial corrosion rates are expected to be high and unstable as a passive film of corrosion product is being formed on the metal surface. This creates, for example, the situation in solution A where bare aluminum has lower corrosion rates than copper. However, these passive films are very thin (ca. 100Å) and fragile and are subject to damage by abrasion, dissolution, or cracking.<sup>7</sup> In such instances, the corrosion rate will rise while the film is being reformed.

Since functional longevity is an important factor in selection of shielding materials, projected service lives of one inch wide samples were calculated using averages of the corrosion rates as reported in Table V. These results are shown in Table VI. The service lives of bare metal samples were calculated by dividing the half-thickness of each sample in mils by its average corrosion rate, since corrosion could occur at both surfaces of the sample. For the plastic clad metals, the

half-width of each sample in mils was divided by its average corrosion rate.

Bearing in mind that the data in Table VI represent only the chemical effects of the solutions, there is reasonable agreement between the laboratory and NBS/REA tests. The projected service lives of aluminum, copper and tin plate steel in solution C were 5.5, 0.85 and 1.0 years respectively. The corresponding service life (or years to electrical discontinuity) from the NBS/REA field tests were 2, 3, and 1 years respectively in site C.<sup>8</sup> Some data reversals were noted, but the general correspondence between laboratory and NBS/REA studies is considered good for corrosion-type testing, particularly in solutions C and G. The most notable reversal concerns performance of copper in solution A and will be subject to further study.

While electrochemical corrosion studies give very interesting results on the behavior of materials in selected environments, they represent an idealized situation in that the materials are isolated from galvanic effects which usually occur under service conditions. Therefore the test methodology has been extended to include three common galvanic phenomena which are known to have significant impact on shield service life.

## Galvanic Corrosion Due To Dissimilar Metals

### Theory and Principles

Shields of telephone cables are bonded and grounded at intervals along their length. The types of metals used for bonding and grounding clamps and grounding rods are often different from the shielding materials. Also, certain designs of cable sheaths incorporate dissimilar metals to obtain both electrostatic shielding and mechanical armoring protection. In these circumstances, the potential for galvanic corrosion exists and must be considered.

Dissimilar metals have different potentials when immersed in an electrolytic solution. If the metals are connected electrically, this potential difference serves as the driving force to produce current flow and, therefore, corrosion. Since the magnitude of current flow in this situation can be greater by a decade or more than that for uncoupled metals, corrosion of the anodic metal can proceed at a much faster rate as compared to electrochemical corrosion rates discussed earlier. Corrosion current flow between coupled metals can be measured directly by insertion of an appropriate instrument such as a zero resistance ammeter (ZRA) into the circuit.

### Experimental Procedure

The galvanic couples selected for this test were aluminum/tin plate steel, plastic clad aluminum/tin plate steel, and aluminum/copper, and galvanized steel/aluminum. One inch (2.54 cm) by seven inches (17.78 cm) long strips of different test materials were cleaned with acetone, placed in corrosion cells containing about 900 c.c. of synthetic soil solutions, and coupled electrically. The solutions were kept at room temperature without agitation. The actual area of exposure was about one inch (2.54 cm) by three inches (7.62 cm); there was no masking with beeswax. Galvanic corrosion current readings were made at different time intervals for eight weeks using a zero resistance ammeter.

### Results and Discussions

**Qualitative Results.** Figures 5, 6, and 7 show conditions of the test couples after eight weeks in synthetic soil solutions A, C and G. In the aluminum/tin plate steel couples, both the aluminum and the tin plate steel were virtually unaffected in solution A. The bare aluminum changed color to grayish-black, indicating the presence of a passive film. In addition, noticeable corrosion was found at the solution and air interface with a deposit of voluminous, chalky corrosion products. The corrosion at this interface is attributed to a differential aeration cell. The tin had lost its luster. In solution C, the aluminum was almost discontinuous at the solution and air interface. There was a number of perforations on the flat surfaces of the metal. Corrosion was confined to the edges of the tin plate steel, with a build-up of reddish-brown corrosion products. The tin coating was practically unchanged except for several pits on the



FIGURE 5. TEST SAMPLES AFTER 8 WEEKS IN SOLUTION A



FIGURE 6. TEST SAMPLES AFTER 8 WEEKS IN SOLUTION C

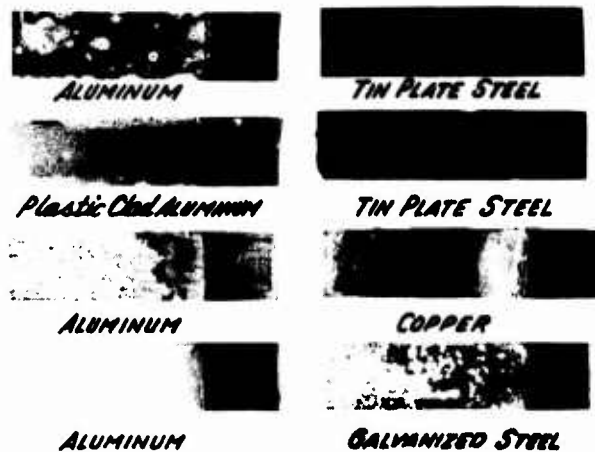


FIGURE 7. TEST SAMPLES AFTER 8 WEEKS IN SOLUTION G

flat surfaces. In solution G, a number of holes were developed on the flat surfaces of the aluminum due to corrosion; other areas were practically unchanged. The tin plate steel was in good condition except for corrosion at the edges.

In the plastic clad aluminum/tin plate steel couples, the plastic clad aluminum was not affected by corrosion in solution A except for several areas of localized corrosion on one edge. The tin plate steel had lost its luster throughout the exposed areas. In solution C, the plastic clad aluminum was unchanged except for corrosion at the edges while the edges of the tin plate steel were severely corroded. The tin coating was totally consumed on scattered areas with a build-up of reddish-brown corrosion products. In solution G, the corrosion on the plastic clad aluminum and the tin plate steel was confined to the edges.

In the aluminum/copper couples, the copper was unaffected in all three solutions except for certain areas of discoloration. The aluminum became discontinuous at the solution and air interface in solution A. The flat surfaces of the metal were virtually unaffected. In some areas, a grayish-black film was found. In solution C, the corrosion of the aluminum was so severe that large areas of the metal were completely consumed. Pits and perforations were found throughout the flat surfaces; voluminous, chalky corrosion products were accumulated at these areas. In solution G, numerous pits and perforations were present on the flat surfaces. Powdery corrosion products were found at these locations.

In the galvanized steel/aluminum couples, the aluminum was unaffected in all three solutions except for the changes in color to various shades of gray. In solution A, the galvanized steel had lost its luster. The zinc coating was totally consumed in certain areas. In solution C, the entire surfaces of the galvanized steel were covered with bulky, flour-like corrosion products. In solution G, chalky corrosion products were present on scattered areas of the flat surfaces.

Quantitative Results. The galvanic current readings on the test couples are recorded in Table VII. Many couples had high initial current readings which tended to decrease with time. In general, galvanic current readings on the aluminum/copper couples were the highest, those on the plastic clad aluminum/tin plate steel the lowest. Aluminum was usually anodic to other metals except for galvanized steel. However, several of the couples had changed the anode/cathode polarity, i.e. the direction of current flow, at least once during the test.

Copper coupled to aluminum caused severe corrosion on aluminum in all three solutions. The severity of corrosion in this couple is due to the greater potential difference between aluminum and copper, as compared to other aluminum couples of Table VII, and the relative insensitivity of copper to polarization. Therefore, there is relatively little decrease in the galvanic current readings of the copper couples with time.

TABLE VII. GALVANIC CORROSION CURRENT (Microamps)

ANODE:	ALUMINUM	PLASTIC CLAD ALUMINUM	ALUMINUM	GALVANIZED STEEL
CATHODE:	TIN PLATE STEEL	TIN PLATE STEEL	COPPER	ALUMINUM
<u>SANDY LOAM (A)</u>				
1 Day	110	10	310	16
1 Week	82	6.8	230	130
3 Weeks	19	5.1	240	58
4 Weeks	26	7.9	130	26
8 Weeks	48	27	240	(1.8)*
<u>CLAY (C)</u>				
1 Day	(72)	(14)	310	160
1 Week	(28)	13	680	41
3 Weeks	33	24	460	38
4 Weeks	35	27	510	36
8 Weeks	42	22	410	25
<u>TIDAL MARSH (G)</u>				
1 Day	0.2	(0.07)	610	17
1 Week	86	52	490	(6.6)
3 Weeks	48	28	420	26
4 Weeks	40	28	380	26
8 Weeks	34	28	240	17

\* ( ) Indicates changes in the anode/cathode polarity.

On the other hand, the aluminum coupled to galvanized steel was protected at the expense of the zinc coating on the galvanized steel. It should be noted, however, that the aluminum became anodic to the galvanized steel after eight weeks in synthetic soil solution A. It appears that as the zinc coating is consumed due to corrosion, the underlying steel is exposed. Since steel is cathodic to aluminum, it is not surprising to observe a change in the polarity of the aluminum and galvanized steel couple.

The galvanic current readings have been averaged, where appropriate, to determine the corrosion rates of the aluminum anodes of the test couples. The projected service lives of the aluminum were calculated using the average corrosion rates and are reported in Table VIII. No calculations were made for the aluminum/galvanized couples because aluminum was usually the cathode. The projected service life of the aluminum anode coupled to copper is 0.8 years in solution C. This prediction is in agreement with the NBS/REA field test data. Eight mil (0.203 mm) aluminum shield coupled to copper was electrically discontinuous, due to dissipation of the metal by corrosion, in the ring and window areas within a year in site C.<sup>9</sup>

Galvanic corrosion on the aluminum and tin plate steel couple was serious. The NBS/REA field test data on an aluminum/steel shield design are supportive of the laboratory data. The outer steel and inner aluminum shields at the ring were electrically discontinuous on the cable specimen exposed for three years at site C.<sup>10</sup> Laboratory data indicate a ten year life in this case. (Table VIII).

#### Galvanic Corrosion Due To Differential Aeration

##### Theory and Principles

When a piece of metal is placed in an electrolyte which has a concentration gradient of dissolved oxygen, the portions of the metal exposed to higher concentrations of oxygen are cathodic to portions in lower oxygen concentrations. This galvanic situation is known as a differential aeration or oxygen concentration cell.

Since the concentration of oxygen in the soil is not uniform and the outer cable jacket is subject to damage, the potential for corrosion of the shield due to differential aeration is present and must be considered. Soil water can enter the cable sheath at the jacket opening and migrate along the sheath between the jacket and shield. Oxygen dissolved in the soil water is consumed by corrosion reactions and is replenished by diffusion from the surrounding soil. Since the polyethylene jacket is a substantial barrier to diffusion, an oxygen concentration gradient is established in the soil water; water near the jacket opening is oxygen-rich relative to water between the jacket and shield. Thus the shield near the jacket opening is cathodic to surrounding areas and a differential aeration cell is established.

TABLE VIII. AVERAGE CORROSION RATE AND PROJECTED SERVICE LIFE OF ONE-INCH WIDE ALUMINUM ANODE

ANODE:	ALUMINUM	PLASTIC CLAD ALUMINUM	ALUMINUM
CATHODE:	TIN PLATE STEEL	TIN PLATE STEEL	COPPER
EXPOSED AREA: (cm <sup>2</sup> )	39.1	0.361	39.1
<u>SANDY LOAM (A)</u>			
A.C.R.* (mpy)	0.63	14	2.5
P.S.L.** (yrs)	6.4	37	1.6
<u>CLAY (C)</u>			
A.C.R. (mpy)	0.40	20	5.2
P.S.L. (yrs)	10	24	0.8
<u>TIDAL MARSH (G)</u>			
A.C.R. (mpy)	0.46	32	4.7
P.S.L. (yrs)	8.6	16	0.9
* A.C.R. - AVERAGE CORROSION RATE			
** P.S.L. - PROJECTED SERVICE LIFE			

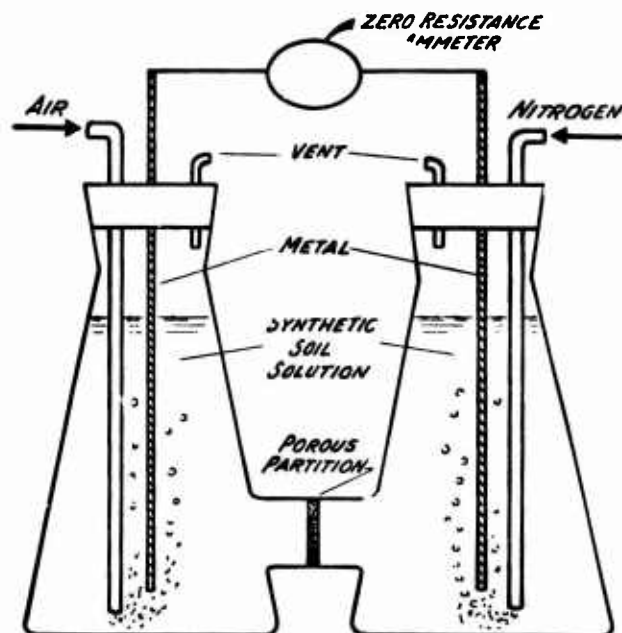


FIGURE 8. DIFFERENTIAL AERATION CELL



Some investigators<sup>11</sup> consider differential aeration as one of the most important and prevalent reasons for corrosion damage of metals in soil.

#### Experimental Procedure

One inch (2.54 cm) by nine inch (22.86 cm) strips of a metal were cleaned with acetone and placed in separate compartments of a differential aeration cell as shown in Figure 8. Two strips were then connected through a zero resistance ammeter (ZRA) to monitor current flow. Both compartments of the cell contained the same synthetic soil solution, but were separated by a porous partition of frit. The types of metal and exposed anodic areas in contact with electrolyte are listed in Table IX. The cell was activated by bubbling air and nitrogen into the separate compartments at a rate of about one cubic foot per hour (271 c.c. per minute). The current flow between the electrodes was recorded as a function of time for one hour.

#### Results and Discussions

Current readings, corrosion rates (from equation (3)), and projected service lives are reported in Table IX. The current readings were recorded after one hour of cell activity, by which time the cells appeared to have stabilized.

All shielding materials tested were susceptible to varying degrees of corrosion due to differential aeration. In general, aluminum was the most affected followed by black plate steel and copper. However, aluminum was most susceptible in solution A while solution G had the greatest impact on black plate steel.

The NBS/REA data indicate that almost all cable samples experienced some degree of corrosion of shields under the polyethylene jacket one-half inch from the ring or window areas of jacket opening. The corrosion of the shields in these areas can be attributed to differential aeration.

Comparison of the corrosion rates measured under differential aeration versus electrochemical corrosion illustrates the importance of the oxygen gradient on shield corrosion. For example, the corrosion rate for bare aluminum in solution A under differential aeration is 10 mpy. The corresponding (1 day) rate for aluminum under only electrochemical corrosion is 0.25 mpy. The oxygen gradient caused a 40 fold increase.

An apparent anomaly occurred again in the case of copper. Corrosion rates actually decreased in solutions A and C under differential aeration as compared to electrochemical corrosion. This is an interesting and possibly important effect which warrants further investigation, especially in light of the current concern with the corrosion of copper concentric neutrals in power cable.

TABLE IX. DIFFERENTIAL AERATION CORROSION  
(one-inch wide samples)

	<u>Aluminum</u>	<u>Copper</u>	<u>Plastic Clad Aluminum</u>	<u>Black Plate Steel</u>	<u>Plastic Clad T. P. Steel</u>
Exposed Area (cm <sup>2</sup> )	39.1	38.9	0.361	39.0	0.271
<u>SANDY LOAM (A)</u>					
Corrosion Current (Microamps)	910	16	24	23	2.9
Corrosion Rate (mpy)	10	0.18	29	0.27	4.9
Projected Service Life (yr)	0.4	14	17	11	100
<u>CLAY (C)</u>					
Corrosion Current (Microamps)	81	51	8.6	55	24
Corrosion Rate (mpy)	0.88	0.60	10	0.65	41
Projected Service Life (yr)	4.5	4.2	49	4.6	12
<u>TIDAL MARSH (G)</u>					
Corrosion Current (Microamps)	88	56	1.3	820	110
Corrosion Rate (mpy)	0.96	0.66	1.6	9.6	190
Projected Service Life (yr)	4.2	3.8	320	0.31	2.6

## Other Galvanic Cells

Galvanic cells can be created simply by differences in the metallurgical composition and surface condition of a metal and by gradients in environmental factors such as temperature or ion concentration. In almost all cases, that portion of a single metal at a higher impurity level, stress, or temperature would be anodic to the rest of the metal. Since shielding materials are subjected to significant mechanical stress during cable manufacture, installation and service, a simple test was conducted to determine the order of magnitude of the galvanic cell created by the stress.

A strip of bare aluminum one inch (2.54 cm) wide by seven inches (17.78 cm) long was stretched 10% using an Instron® Tensile Tester. This sample was connected electrically to an unstretched aluminum strip of the same dimensions and the couple was immersed in solution A for eight weeks. A control couple having two unstretched aluminum samples was maintained in solution A for the same period of time as a reference. The surface area of each strip exposed to electrolyte was 39.1 cm<sup>2</sup>.

At the end of the test period, a zero resistance ammeter was used to measure galvanic current. Current flowing in the couple having the stretched strip was 18.6 microamps as compared to 0.22 microamps measured in the control couple. This 85 fold difference indicates that stress can have a major effect on shield corrosion resistance. It also suggests that further testing on dissimilar metal couples should be conducted on corrugated samples to more accurately analyze potential for corrosion.

## Conclusions

1. A sensitive and realistic corrosion test methodology is being defined. The methodology can be used to screen and predict relative corrosion resistance of telephone cable shielding materials in a range of soil environments. Laboratory corrosion test data are in reasonably good agreement with trends observed in the NBS/REA field tests.
2. A comprehensive evaluation of shielding materials for corrosion resistance requires that galvanic actions due to dissimilar metals, differential aeration, and mechanical stress be considered. The data indicate that these factors may override effects of electrochemical corrosion and constitute the major determinants of service life.
3. All of the common shielding materials experienced varying degrees of corrosion in the several different soil solutions. In general, plastic clad metals had a better resistance to the types of corrosion investigated than the corresponding bare metals.

4. Aluminum suffered severe corrosion when coupled to copper in all three solutions. Galvanized steel protected the aluminum until the zinc coating was consumed. Consideration should be given to such galvanic effects during the selection of materials for grounding rods and bonding clamps.
5. Data reversals were encountered during testing, especially with copper. The test methodology appears to have potential as a tool for further investigation of these anomalies.

## Future Activities

In addition to studies on the data anomalies involving copper, further test refinements are planned. Long term effects of differential aeration at varied gas feed rates will be studied. Attempts will be made to measure corrosion rates of samples coated with filling and flooding compounds. The data base in galvanic corrosion due to mechanical stress will be expanded.

## Acknowledgements

The author wishes to thank C. G. Arnold for his technical advice, K. E. Bow, T. H. Lyon and R. C. Mildner, for their helpful guidance and suggestions, W. G. Lewis for the data in Table VI, E. L. Greene, G. E. Sealy and E. W. Veazey for photographs and figures, and J. Jackson for typing. He also wishes to thank the management of the Dow Chemical Company for permission to publish this work.

## References

1. G. A. Lohsl and M. Romanoff, "Corrosion Evaluation of Shielding Materials for Direct Burial Telephone Cables," 17th International Wire and Cable Symposium, Atlantic City, New Jersey, December, 1968.
2. G. A. Lohsl and M. Romanoff, "Progress Report on Corrosion Evaluation of Shielding Materials for Direct Burial Telephone Cables," 18th International Wire and Cable Symposium, Atlantic City, New Jersey, December, 1969.
3. W. F. Gerhold, J. P. McCann, and W. E. Williamson, "Report on Corrosion of Underground Telephone Cable Shielding Materials in Soil Environments after Exposure for Four Years," Paper 87, National Association of Corrosion Engineers, Chicago, Illinois, March, 1974.
4. National Association of Corrosion Engineers Publication 3D170, "Modern Electrical Methods for Determining Corrosion Rates." Prepared by NACE Task Group T-3D-1 on Instruments for Corrosion Rate Measurements.

5. Petrolite® Corrosion Rate Meter Automatic Model M-1000 Series Operating and Maintenance Manual, p.2.
6. Gerhold et al., p. 31.
7. U. R. Evans, The Corrosion and Oxidation of Metals, E. Arnold, Ltd., London (1960) p. 153.
8. Gerhold et al., p. 25, 26.
9. Ibid., p. 25.
10. Ibid., p. 27.
11. E. Schaschl and G. A. Marsh, "Some New Views on Soil Corrosion," Materials Protection, Vol. 2, No. 11, p.8.

## Biography



T. S. (Sam) Choo is a Senior Research Chemist in the Specialty Products R&D Laboratory, Olefin Plastics Department, Dow Chemical U.S.A. He is chairman of the National Association of Corrosion Engineers Task Group T-10C-3 on Corrosion of Lead and Other Metallic Sheaths. He is also a member of the teaching staff of the Appalachian Underground Corrosion Short Course held annually at West Virginia University. Mr. Choo received an A.B. in Chemistry from Dartmouth (1968) and an M.B.A. from Case Western Reserve University (1971).

# OXIDATIVE STABILITY OF HIGH-DENSITY POLYETHYLENE CABLES

B.S. Bernstein and F.N. Lee  
Phelps Dodge Cable and Wire Company and  
Phelps Dodge Communications Company  
Yonkers, N.Y. 10702

## Summary

Several high density polyethylene-insulated wires for air core telephone cable were examined after various oven-aging times at 125°C; DSC oxidation induction (OIT) times (at 200°C) and weight changes were monitored. A correlation was observed between the onset of significant weight change and zero OIT; the correlation was confirmed over the 105°-190°C oven-aging temperature range with insulated wires for one HDPE. An Arrhenius plot of the air oven-aging thermal life is linear between 105-150°C, with deviation starting at about 150°C up to 190°C. (the highest temperature tested). Activation energies and projected cable lives for (a) oven-aging induced weight changes, (b) DSC monitoring of oven-aged samples, and (c) DSC testing of un-aged samples, are compared. DSC testing of un-aged cables project to longer cable life than does non-blooming oven-aging conditions (a and b); the latter two techniques yield identical results, within experimental error.

## Introduction

Projection of cable life can be made by several test procedures including one of the following methods: (a) measuring the oxidative induction time (OIT) of the insulation by differential scanning calorimetry (DSC) or differential thermal analysis (DTA) at temperatures above the insulation melting range ( $T_m$ )<sup>1</sup> and then projecting cable life to lower temperatures; (b) measuring insulation weight (or other physical property changes) upon circulating air oven-aging below the insulation melting temperature range, and projecting cable life to lower temperatures<sup>2</sup>. In some cases, pre-conditioning of samples by forced blooming (to induce antioxidant exudation) prior to air oven-aging has been performed<sup>3</sup>.

The DSC or DTA test is employed for its relative ease and rapidity; OIT measurements usually require less than one hour at appropriately chosen test temperatures. The OIT values so obtained reflect the effectiveness of the antioxidant employed and the concentration in the insulation. Therefore, DSC or DTA testing provides a convenient means for routine quality control testing of the antioxidant concentration in cable insulations. The oven-aging test is more time consuming, but appears to possess certain

advantages; sample geometry, the test temperature range, and the gas environment during oven-aging are closer to some of the more severe cable service conditions. High density polyethylene-insulated cables require oven-aging periods ranging from several months to a year or more (depending on the apparent antioxidant effectiveness and concentration) to reach the oxidative-degradation inception time at about 20°C below its melting point. Therefore, the oven-aging test is not suitable as a rapid quality assurance method.

Since the DTA or DSC-OIT procedure provides a suitable means of measuring residual antioxidant activity, we have employed this method to evaluate sample previously subjected to air oven-aging at various temperatures. In addition, comparison of cable life projections by the conventional DTA or DSC-OIT, and air oven-aging methods have been made. In this paper, we report our results of work performed in these areas with air core HDPE-insulated cables.

## Experimental

### Materials

Air-core telephone wires (No. 19 and 22 AWG) insulated with three different commercial high density polyethylene resins were employed for testing. These are designated as A, B and C respectively; antioxidant and copper deactivator were tetrakis (methylene-3 (3', 5'-di-*t*-butyl-4'-hydroxyphenyl) propionate) methane (Irganox 1010) and OABH respectively. Antioxidant and metal deactivator were present in the materials as received (approximately 0.1% level). Colors employed and DSC melting peak temperatures (referred to herein as melting point) for each resin grade are listed in Table I.

Table I

Colors and DSC Melting Point for  
HDPE Insulated Air-Core Cables  
Employed in this Study

HDPE Compound	A	B	C
Colors Tested	Blue, Violet	Green, White	Violet,Grey Yellow, Brown
Melting Points (°C)	129	129	129

## Procedures

(a) Equipment: A Perkin Elmer Model 1B Differential Scanning Calorimeter was employed for OIT determinations. Blue M air circulating ovens having air circulation rates of about 250 CFM, were employed for all aging tests.

(b) Air Oven-Aging at 105°C and 125°C: For the oven-aging test procedure<sup>2</sup>, two coils of each color of each resin grade were aged; one was 18 feet in length for weight change measurements, and the second was 10 feet in length for DSC-OIT tests. The separated coils were suspended from the top wall of the oven by hooks prepared from the same insulated wires. Weight changes, examinations for cracking, and OIT's at 200°C were monitored once each week. The cracking test was visual, and consisted of twisting two inches of wire (cut from the coil) into a pigtail prior to examination. For the DSC test (see d, below) two mm. long samples from the middle portion of the pigtail were employed.

(c) Air Oven-Aging at 150°C-190°C: Above 150°C, a modified oven-aging procedure was employed. Two foot samples of each insulated wire specimen were placed in a sinusoidal pattern in two-inch O.D. aluminum pans (each sample being tested in duplicate). For 200°C OIT monitoring, one-inch of insulated wire was removed from the end of each specimen; two mm. long samples were cut from the middle sections for testing at regular intervals that varied between several hours to one week, depending upon oven-aging temperature.

(d) DSC-OIT Test: For oxidation induction time measurements<sup>4</sup> after each oven-aging period, the test temperature was 200°C. To extrapolate cable life at lower temperatures, DSC-OIT tests on un-aged specimens were performed over the 170°C to 205°C range.

## Results and Discussion

I. Oven-Aging of A, B, and C HDPE Insulated Wires at 125°C: In Figures 1 and 2, weight and relative OIT changes for all colors of A, B, and C insulated wires aged at 125°C are plotted against oven-aging times. From the weight change vs. time curves, the following consecutive pattern of changes can be noted:

(a) A very slight initial weight drop (less than one percent) during the first two weeks.

(b) A period of relatively constant weight which is about nine to ten weeks for insulations A and B and five weeks for in-

sulation C.

(c) A small weight increase for most the HDPE-pigment combinations.

(d) Finally, a large weight loss, which occurs after nine to twelve weeks for insulations A and B, and six weeks for insulation C.

The relative OIT changes, however, follow a different pattern; they decrease in an essentially continuous manner with oven-aging time to zero OIT value. The time required for zero OIT appears to coincide with either (c) or (d) above.

In evaluating the combined weight and OIT change curves, the following explanation of events appears reasonable:

(a) The initial weight drop is probably due to the degassing of absorbed and/or adsorbed volatile material<sup>3</sup>. (Antioxidant vaporization would not explain the small weight loss as its level is too low).

(b) The insulation weight remains relatively constant during the consumption of antioxidant. The OIT curves do not indicate the exact antioxidant level within the insulation wall.

(c) When the antioxidant is completely consumed, or nearly so (as indicated by zero OIT value), the auto-oxidative chain reaction starts to gain momentum by accumulating the polymeric hydroperoxide<sup>5</sup>. This may result either after the complete depletion of antioxidant or in the presence of a small amount of antioxidant inadequate to suppress the auto-oxidation process. The small weight gain prior to the steep weight loss is probably an indication of peroxide accumulation. (The A violet and B green insulations were exceptions; it is believed that this is due to experimental error). Due to the reproducibility limitations of the OIT measuring technique, it is not possible at this time to determine conclusively whether the zero OIT point coincides with the onset of weight gain or the onset of weight loss.

(d) The final weight loss reflects the degradation process inside the insulation. Chain cleavage is likely occurring at this stage.

It should also be noted that some samples exhibited cracking (as indicated by the zigzag arrow in Figures 1 and 2) during the interval between the onset of weight gain and loss; it is very likely that in addition to peroxide accumulation, some chain cleavage is simultaneously occurring during this period.

These results indicate that a fairly good correlation between zero-OIT and oven-aging is

attainable for the HDPE resin/pigment combinations. One of these resin systems was then studied in further detail over a broader temperature range.

II. Oven-Aging of C HDPE Insulated Wires Between 105°C and 190°C: In Figure 2 through 7, the weight and relative OIT changes are plotted as a function of oven-aging time. By comparing these figures, the following results are observed:

(a) The weight changes at different temperatures follow the same general pattern as at 125°C, i.e., an initial weight loss, a period of relatively constant weight, a slight weight increase and, finally, the sharp weight drop. However, the weight increases just prior to the sharp weight drop are more frequently not observed at higher temperatures (relative to the lower temperatures). This is likely due to more rapid antioxidant consumption and oxidative degradation rates at the higher temperatures.

(b) For HDPE C at 105°C and 125°C, the zero OIT point corresponds reasonably well with the onset of the weight gain prior to the sharp weight drop for all four colors studied. At higher temperatures (150-190°C), the coincidence of these two points is less apparent. However, the qualitative correlation between the weight change and the OIT decay still exists. This correlation shows that there is a potential advantage in using a combination of OIT plus weight change measurements as a monitoring device for oven-aging tests. Judging from the relative OIT value at any particular oven-aging time, the end point for oven-aging tests may be estimated.

(c) OIT decay appears linear with time at 150°C, 170°C, 180°C, and 190°C as shown in Figures 4-7. However, OIT decay is non-linear with time at the lower temperatures (105°C and 125°C, i.e., below the melting peak temperature of 129°C of the C insulation as shown in Figures 2 and 3). In Figures 8-10, the logarithm of OIT is plotted against oven-aging time for the C insulated wires at 105°C and 125°C. (A and B HDPE insulations are shown at 125°C in Figure 11 for comparison). Straight lines were observed in all cases up to 10% or less of the initial OIT values. The different OIT decay patterns observed for temperatures above and below the melting peak temperature may imply that the consumption of antioxidant follows different mechanisms in the solid and molten states.

The apparent linear OIT decay rate in the molten state implies that antioxidant consumption during, both, oven-aging above  $T_m$  and OIT testing at 200°C, occurs by a simi-

lar mechanism. This can be explained for zero, first and second order reactions in the following manner:

Zero Order:

$$C_{oa} = -k_{oa} t_{oa} + k'_{oa} \quad (1)$$

$$C_{oit} = -k_{oit} t_{oit} + k'_{oit} \quad (2)$$

First Order:

$$C_{oa} = \text{Exp}-(k_{oa} t_{oa} + k'_{oa}) \quad (3)$$

$$C_{oit} = \text{Exp}-(k_{oit} t_{oit} + k'_{oit}) \quad (4)$$

Second Order:

$$C_{oa} = 1/(k_{oa} t_{oa} + k'_{oa}) \quad (5)$$

$$C_{oit} = 1/(k_{oit} t_{oit} + k'_{oit}) \quad (6)$$

$C_{oa}$  = antioxidant concentration during oven-aging

$C_{oit}$  = antioxidant concentration during OIT testing

$k_{oa}$  = reaction rate constant of antioxidant decay during oven-aging

$k_{oit}$  = reaction rate constant of antioxidant decay during OIT testing.

$t_{oa}$  = oven-aging time

$t_{oit}$  = OIT testing time

$k'_{oa}$  = integration constant for antioxidant decay during oven-aging

$k'_{oit}$  = integration constant for antioxidant decay during OIT testing

When the initial antioxidant concentrations are the same, and when antioxidant decay via oven-aging and OIT tests follow similar mechanisms, then for any order reaction,  $C_{oa}$  must equal  $C_{oit}$  and  $k'_{oa}$  must equal  $k'_{oit}$ . Therefore, the time required for the HDPE insulation to reach the same final antioxidant concentration by both methods must satisfy the following equation:

$$k_{oa} t_{oa} = k_{oa} t_{oit} \quad (7)$$

The actual OIT which was measured after each oven-aging interval can be related to  $t_{oit}$  as follows:

$$\text{OIT} = t_{oit}^0 - t_{oit} \quad (8)$$

Where  $t_{oit}^0$  is the time required for reaching essentially negligible antioxidant level from the initial antioxidant level, via OIT testing at 200°C. By substituting



(8) into (7) the following equation is obtained:

$$k_{oa} t_{oa} = k_{oit} (t_{oit}^0 - OIT) \quad (9)$$

When OIT or  $(OIT/t_{oit}^0)$  is plotted against  $t_{oa}$  (oven-aging time) a straight line with a negative slope should be obtained, and this is experimentally observed in Figures 4 to 7.

As noted earlier, the non-linear OIT decay in the solid state during oven-aging tests implies that the mechanism of antioxidant consumption differs from that in the molten state. To support this argument, different combinations of equations 1, 3, 5 and 2, 4, 6 other than the above have been examined; no further linear relationships could be obtained between OIT's and oven-aging times. Some combinations do result in logarithmic or near logarithmic functions, however, it is premature to try to relate the oven-aging and OIT tests to any specific reaction mechanism at this time.

#### III. DSC Testing of HDPE C at Various Temperatures; Extrapolation of Cable Life:

Oxidative Induction times of HDPE C insulated wires were obtained via the DSC test performed at temperatures ranging from 170°C to 205°C. The results were plotted against the inverse of absolute temperature and are shown in Figure 12. Results indicate the following:

(a) A single straight line was obtained for the yellow, brown and grey colored wires; the violet wires provide a parallel straight line, with a higher reaction rate.

(b) The activation energy obtained from the slope of the straight lines is 37.2 kcal/mole; this is quite close to the apparent activation energy for Irganox 1010/OABH decay in low density polyethylene<sup>6</sup>.

(c) Extrapolation of this straight line implies a cable life of 189 years at 70°C, and thousands of years at 40°C.

IV. Extrapolation of Cable Life from Oven-Aging Data by Weight Monitoring: The oven-aging life times were plotted against the inverse of the absolute temperature for all C insulated wires aged from 105°C to 190°C and are also shown in Figure 12. Where possible, the time required for the onset of the sharp weight gain (noted as Phase C of Section I) was taken as the thermal life. Results indicate the following:

(a) A straight line was obtained between 105°C and approximately 150°C.

(b) The activation energy calculated from this straight line is 23.4 kcal/mole.

(c) The plot starts to show non-linear character at approximately 150°C and above. The slope increases and may perhaps ultimately overtake the slope for the DSC data.

(d) Extrapolating the straight line between 150°C and 105°C to lower temperatures provides apparent cable life-times of 12 years at 70°C and 304 years at 40°C.

#### V. Comparison of Thermal Life Estimates by Oven-Aging vs. DSC-OIT Monitoring of Oven-Aging.

As noted above, zero OIT time requirements via oven-aging correspond fairly well with the onset of weight gain, and the OIT decay curves appear to follow a defined function (linear above  $T_m$  and logarithmic below  $T_m$ ). These OIT decay patterns suggest that short-term OIT decay data may be adequate for end point extrapolation, via the appropriate function. To test this possibility, OIT decay data for HDPE-C at 150°C (linear function, see Fig. 4) and 105°C and 125°C. (logarithmic functions, see Figs. 2 and 3) were extrapolated to the end points of the oven-aging tests. For the latter, one minute OIT results were employed (due to the impossibility of extrapolating back to zero OIT). By plotting oven-aging end points obtained in this manner vs. the inverse of the absolute temperature, apparent projected cable lives of 11 years at 70°C and 274 years at 40°C, and an  $E_a$  of 23.3 kcal/mole were obtained. This compares favorably with the weight monitoring approach (12 years at 70°C, 304 years at 40°C, and  $E_a$  at 23.4 kcal/m). It should be noted that the deviations between the data are greater by the extrapolation method as compared to the weight monitoring of air oven aging specimens; however, this problem could be overcome by employing a sufficient number of replications.

#### VI. Comparison of Thermal Life Estimates by Oven-Aging and DSC-OIT Methods:

In sections III and IV, cable life estimates were obtained using circulating air oven-aging (105-190°C) and DSC-OIT (170-205°C) techniques. From this data, it is seen that the DSC-OIT method over-estimates the cable life (relative to the oven-aging method) by a factor of roughly 16 at 70°C and even more at 40°C.

The possible factors involved that could account for this difference in cable life projections include (a) antioxidant blooming phenomena, (b) test temperature range differences, (c) sample geometry and size, and (d) gas environment during testing. These factors are discussed below.

(a) Antioxidant Blooming Effect: It is known that antioxidant blooming from PE in-

sulation takes place at low temperature; e.g. 70° for LDPE<sup>6</sup> and 50-70°C for LDPE and HDPE<sup>3</sup>. Howard<sup>6</sup> has discussed the factors affecting migration in some detail, and emphasizes that temperature is the key; migration takes place only below the melting range and may be most prominent at 50-70°C, at least for LDPE. It is to be noted that all oven-aging (and DSC) data reported herein for HDPE were obtained at a minimum temperature of 105°C, well above the temperature at which blooming might be anticipated (again at least for LDPE). From data of Roe, Bair, and Gieniewski<sup>7</sup>, we have estimated that the solubility of Irganox 1010 in LDPE (about 50% crystallinity) is approximately 0.015% at 70°C and 0.40% at 105°C. If one assumes that the solubility in HDPE is 1/3 of that in LDPE at an equivalent temperature, then one could anticipate approximately 0.13% solubility in HDPE at 105°C. This is still greater than the actual antioxidant concentration (about 0.1%) prior to wire extrusion. Therefore, while the possibility of antioxidant blooming under these test conditions cannot be unequivocally excluded, it does not appear likely, and this factor alone is not adequate to explain the different activation energies and cable life projections.

(b) Temperature: The temperature effect is demonstrated from both the OIT decay curves (Figures 2-7) and the Arrhenius plot of thermal aging life time vs. absolute temperature (Figure 12). As discussed in Section II-C, the OIT decays linearly with oven aging time above, and non-linearly below the melting peak temperature. This implies the possibility of different antioxidant decay mechanisms in the two different temperature zones. In Figure 12, the significant non-linear character of the Arrhenius plot was also developed around 150°C. This further supports the hypothesis that there are two different antioxidant decay mechanisms for the two temperature zones; therefore, the projected thermal life is also anticipated to be temperature zone dependent.

(c) Sample Size and Geometry: The effect of sample dimensions on DSC-OIT results was considered and examined during the course of this work. In Figure 13, the OIT as a function of oven aging time at 115°C is shown for both 19 and 22 AWG HDPE C insulations. The OIT difference between these two gauge wires having the same insulation-pigment combinations, was observed to increase as the oven-aging time increased; thinner insulation walls lead to more rapid antioxidant decay. This demonstrates the surface nature of the antioxidant consumption reaction during the oven-aging test. Decker, Mayo, and Richardson<sup>8</sup> have previously demonstrated the surface nature of the oxidation process in LDPE samples by oxygen

absorption experiments. This mode of antioxidant consumption renders the sample size and geometry as important factors in developing data for thermal life estimates.

Furthermore, we have observed that the wire insulation for oven-aging tests maintains its original shape up to 150°C and then exhibits some spreading at higher temperatures, at the point of contact between the specimen and the aluminum pan. Insulation spreading is not very great at 150°C, but, visually, appears to increase as the temperature increases. The OIT test samples, which are much smaller in size and different in shape, than the oven-aging test samples, also had more surface contact with the copper pan due to their greater spreading relative to the oven-aging test samples at equivalent temperatures. The larger surface to volume ratio for the OIT test samples (vs. oven-aging test samples) would cause more rapid antioxidant consumption.

In the 170°C-190°C temperature region of Figure 12, the two Arrhenius plots are relatively parallel to each other; however, the oven-aging curve is always below the OIT straight line. This indicates that the OIT test displays faster antioxidant decay than the oven-aging test in this temperature region. This difference in reaction rate is believed due at least partially, to the sample geometry and sample size differences for the two techniques. (Of course, the copper catalytic effect<sup>5</sup> during the OIT testing cannot be neglected).

(d) Gas Environment Effect: No experiments have been performed to attempt to clarify the effect of circulating air vs. circulating oxygen (if any) on the projected thermal life. However, the oxygen absorption data of HDPE wire between 120°C-160°C reported by Chan<sup>9</sup>, allows the calculation of an activation energy of 33 kcal/mole.

This value is considerably higher than 23.4 kcal/mole obtained from the oven-aging data between 105°C and 150°C (Figure 12) reported herein. The main difference between these two procedures is gas environment. Our specimens were exposed to circulating air while Chan's were kept inside a pure oxygen atmosphere. This indirect evidence may suggest that the gas environment is also a factor in projecting thermal life. This area requires further investigation.

Overall results indicate that, despite the potential limitations to the test technique, the use of the DSC-OIT test to monitor the circulating air oven-aging treatment, provides comparable cable life estimates to weight changes alone. The results reported herein also provide further in-

sight into the decay mechanism.

### Conclusions

1. Circulating air oven-aging of HDPE insulated air core cables leads to weight changes involving four phases: (a) an initial weight drop, (b) a period of relatively constant weight, (c) a small weight increase, and (d) a large weight loss. It is believed that these phases correspond to (a) degassing of volatiles, (b) antioxidant consumption, (c) onset of oxidation with polymeric hydroperoxide formation, and (d) chain cleavage.

2. Measurement of relative antioxidant levels, via DSC-OIT monitoring during these four phases indicates a continuous reduction in antioxidant concentration through phase C.

3. Zero OIT has been observed to coincide with either the onset of phase (C, weight gain), or phase (d, sharp weight loss). This behavioral pattern was observed for air oven-aging over the 105°C-125°C range. At higher temperature, (150-190°C), the agreement between the two end points exhibits some deviation, believed due to the rapid antioxidant consumption, which increases the relative experimental error.

4. An Arrhenius plot of the air oven-aging behavior is linear between 105°C-150°C;  $E_a$  is calculated to be 23.4 kcal/mole, and projected cable life is 12 years at 70°C and 304 years at 40°C. The Arrhenius plot deviates from linearity at about the 150°C range up to 190°C, the highest oven-aging temperature employed.

5. Comparison of Arrhenius plots of weight monitoring data vs. extrapolated DSC-OIT monitoring data for air oven-aging between 105°C and 150°C, reveals that it is not possible to accurately distinguish between cable life projections and  $E_a$  between the two techniques.

6. Conventional DSC-OIT testing of unaged cables over the 170-205°C range yields a linear Arrhenius plot.  $E_a$  is calculated to be 37.2 kcal/mole, and projected cable life is 189 years at 70°C and thousands of years at 40°C.

7. The Arrhenius plot of the air oven-aging data and the related OIT decay curves indicate that a different antioxidant decay mechanism is likely above and below  $T_m$ .

8. Differences in cable life projections are reviewed in terms of antioxidant blooming effects, temperature ranges, samples sizes, and geometry, and the gas environment.

### References

1. H.E. Bair, 31st Annual Technical Conference of the Society of Plastics Engineers, Pgs. 106-109, (1973)
2. GT&E Manufacturing Specification #8502 (paragraph 9.4.2), (1972)
3. G.A. Schmidt, Proceedings of 22nd International Wire and Cable Symposium, Atlantic City, N.J. Pgs. 11-22 (1973)
4. Western Electric Manufacturing Standard 17000, Section 1230, 5.2.B, (August 4, 1971)
5. W.L. Hawkins, "Polymer Stabilization", Chapter 1, Wiley Interscience, (1972)
6. J.B. Howard, Proceedings of 21st International Wire and Cable Symposium, Atlantic City, N.J. Pgs. 329-41 (1972)
7. R.J. Roe, H.E. Bair, and C. Gieniewski, Polymer Preprints, 14 (1) 530-36 (1973).
8. C. Decker, F. Mayo and H. Richardson, J. Polymer Science 11, 2879-98 (1973)
9. M.G. Chan, Proceedings of the 23rd International Wire and Cable Symposium, Atlantic City, N.J. Pgs. 34-45 (1974)

### Acknowledgement

The authors wish to thank Dr. M.C. Biskeborn of Phelps Dodge Communications Company for many helpful comments during the course of this work, Mr. A. Geppert of GTE-Automatic Electric Laboratories, and Mr. R.M. Morgan of Phelps Dodge Communications Company for stimulating interest in this area, and Ms. J. Goller for performing most of the test measurements.



BRUCE S. BERNSTEIN was formerly Assistant Director of Research & Development at Phelps Dodge Cable & Wire Company, Yonkers, New York. He joined Phelps Dodge in 1972 after fifteen years of diversified industrial experience in the Polymer industry. During his career, he was concentrated on the technical aspects of plastics, elastomers, paper and fibers. He attended City University of New York, has an M.S. in Organic Chemistry from Iowa State University, and attended Stevens Institute of Technology and Brooklyn Polytechnic Institute.

His areas of interest include: (a) cross-linking techniques for polymeric materials, (b) radiation effects and stabilization of polymers, (c) adhesion phenomena, (d) grafting onto polymeric materials, and (e) fluid transmission through polymers.



PANG-NAN LEE is a Staff Chemist responsible for the Analytical Instrumentation group in the Research & Development department of Phelps Dodge Cable & Wire Company. He received a Ph.D. in physical chemistry from the University of Rhode Island in 1968, and performed post doctoral studies at Northwestern University, Baylor University and the University of Texas from 1968 to 1972. He joined Phelps Dodge Cable & Wire Company in 1973.

His interests include: (a) polymer radiation chemistry, (b) polymer surface, and bulk properties, and (c) application of modern analytical instrumentation to material property studies.

Fig. 1 Relative weight and OIT changes during oven aging of HDPE - A & B insulated air core telephone cables at 125°C.  
A = 24 AWG; B = 19 AWG  
o - Weight % change, • - OIT % change  
--- cracking point

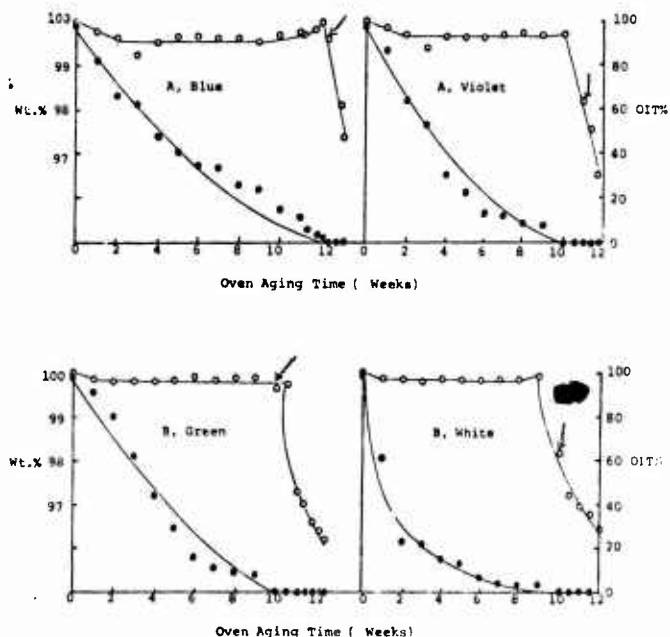


Fig. 2 Relative weight and OIT change during oven aging of 22 AWG HDPE-C insulated air core telephone cables at 125°C  
o-----Wt.% change, e-----OIT% change  
~---cracking point

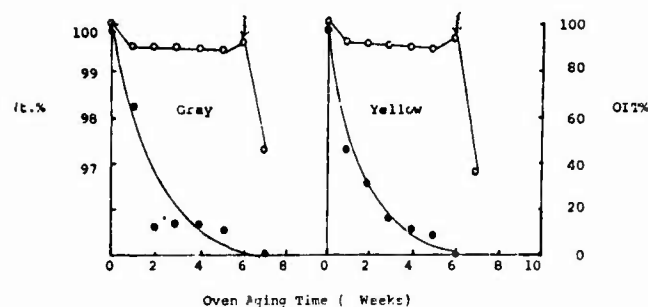
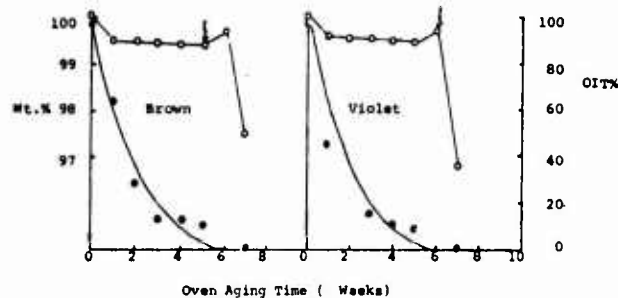


Fig. 3. Relative weight and OIT change during oven aging of 22 AWG HDPE-C insulated air core telephone cables at 105°C  
o-----Wt.%, e-----OIT%  
~---cracking point

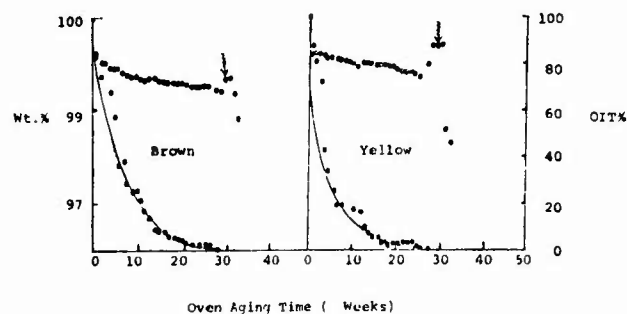
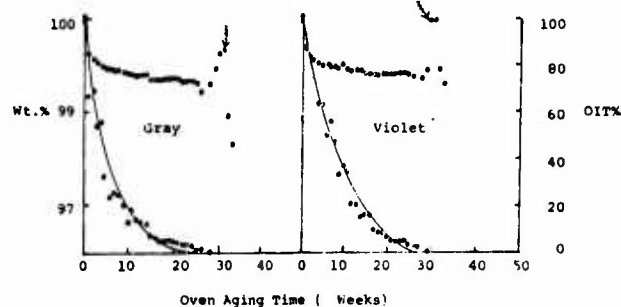


Fig. 4. Relative weight and OIT change during oven aging of 22 AWG HDPE-C insulated air core telephone cables at 150°C  
o-----Wt.% e-----OIT%

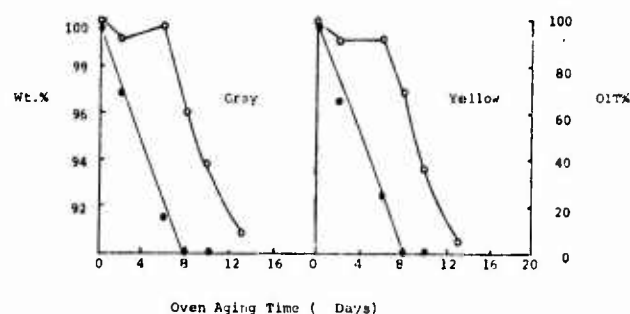
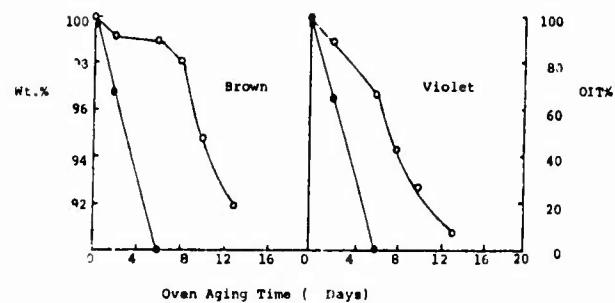


Fig. 5. Relative weight and OIT change during oven aging of 22 AWG HDPE-C insulated air core telephone cables at 170°C  
o-----Wt.%, e-----OIT%

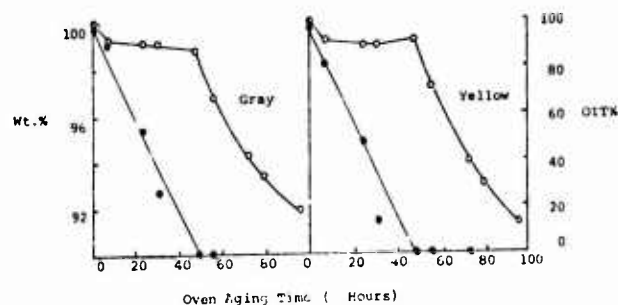
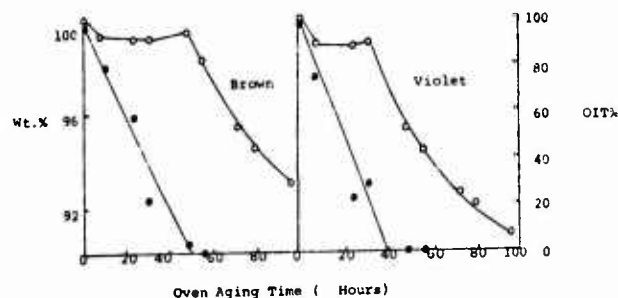


Fig. 6. Relative weight and OIT change during oven aging of 22 AWG HDPE-C insulated air core telephone cables at 140°C  
 o-----Wt.%, ●-----OIT%

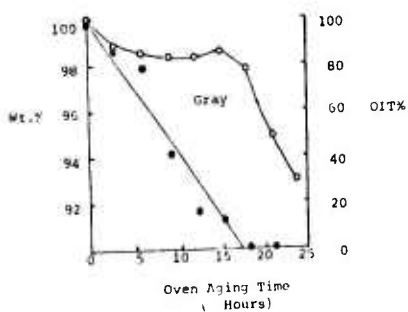
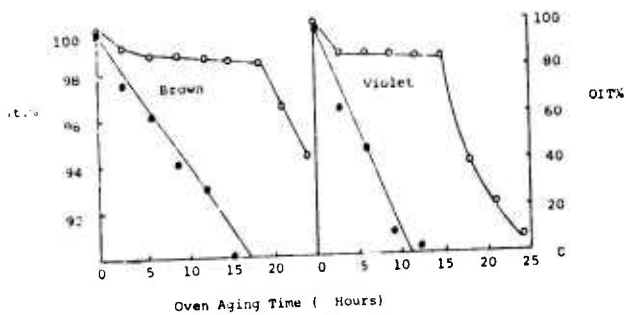


Fig. 7. Relative weight and OIT change during oven aging of HDPE-C insulated telephone cables (22 AWG., air core) at 190°C  
 o - Wt. %, ● - OIT%

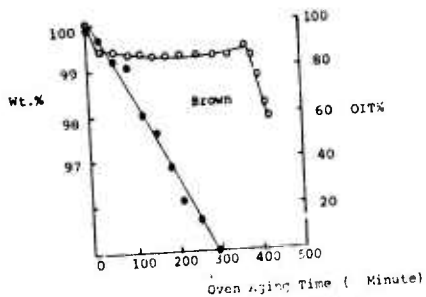
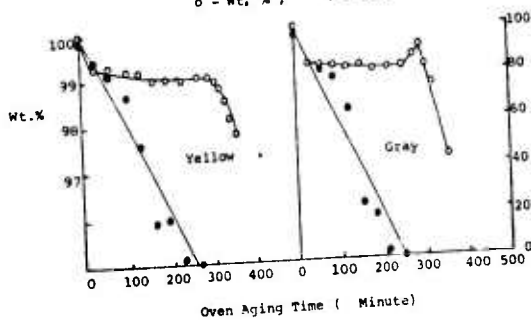


Fig. 6. Logarithm of OIT vs. oven aging time at 105°C, for 22 AWG HDPE-C insulated air core telephone cables

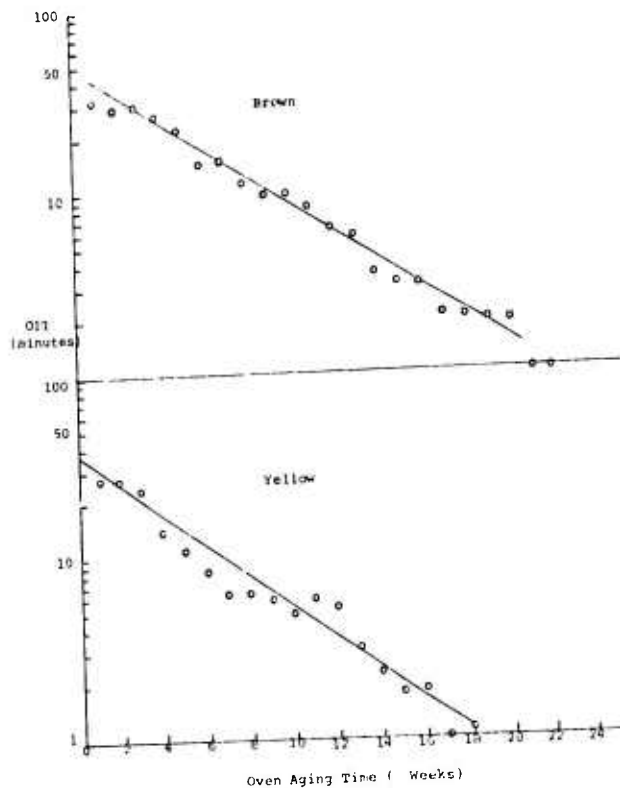


Fig. 9. Logarithm of OIT vs. oven aging time at 105°C for 22 AWG HDPE-C insulated air core telephone cables.

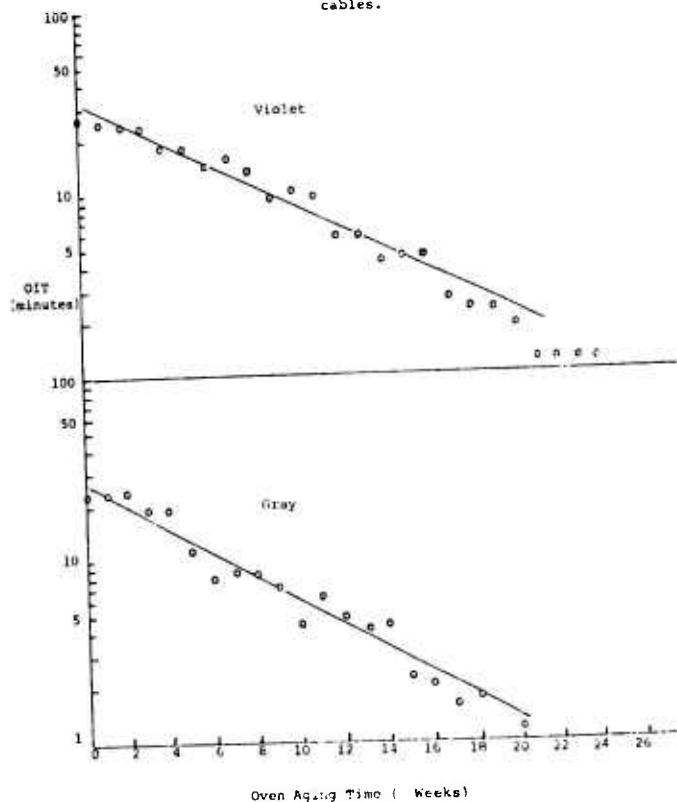




Fig. 10. Logarithm of OIT vs. oven aging time at 125°C for 22 AWG HDPE-C insulated air core telephone cables.

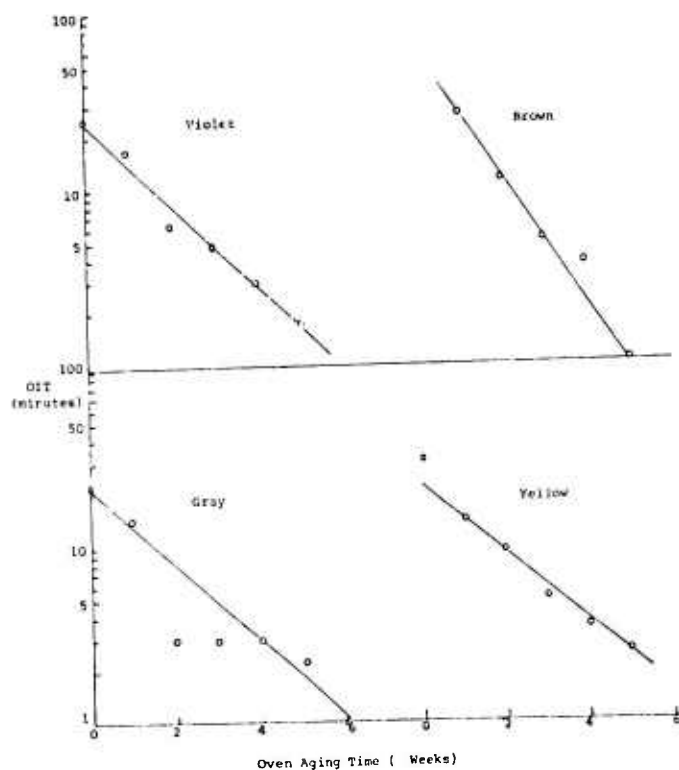
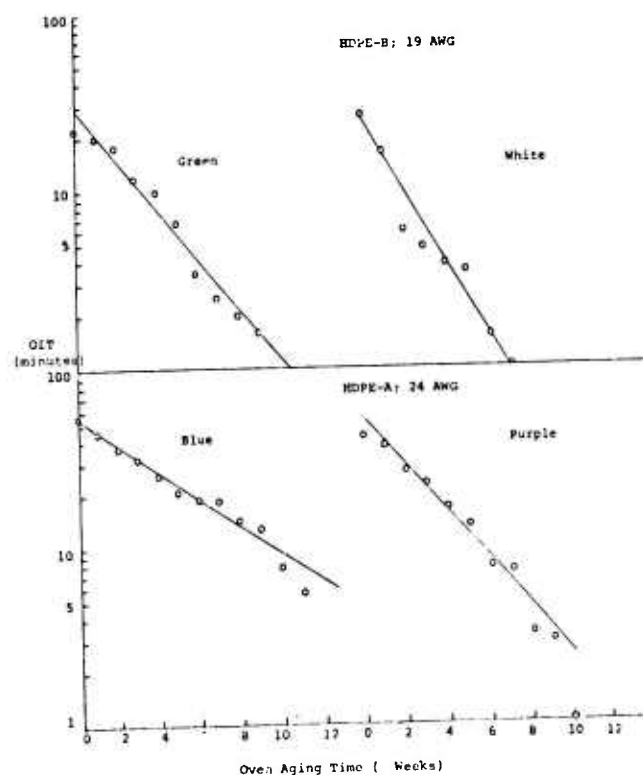


Fig. 11. Logarithm of OIT vs. oven aging time at 125°C for HDPE insulated air core telephone cables.



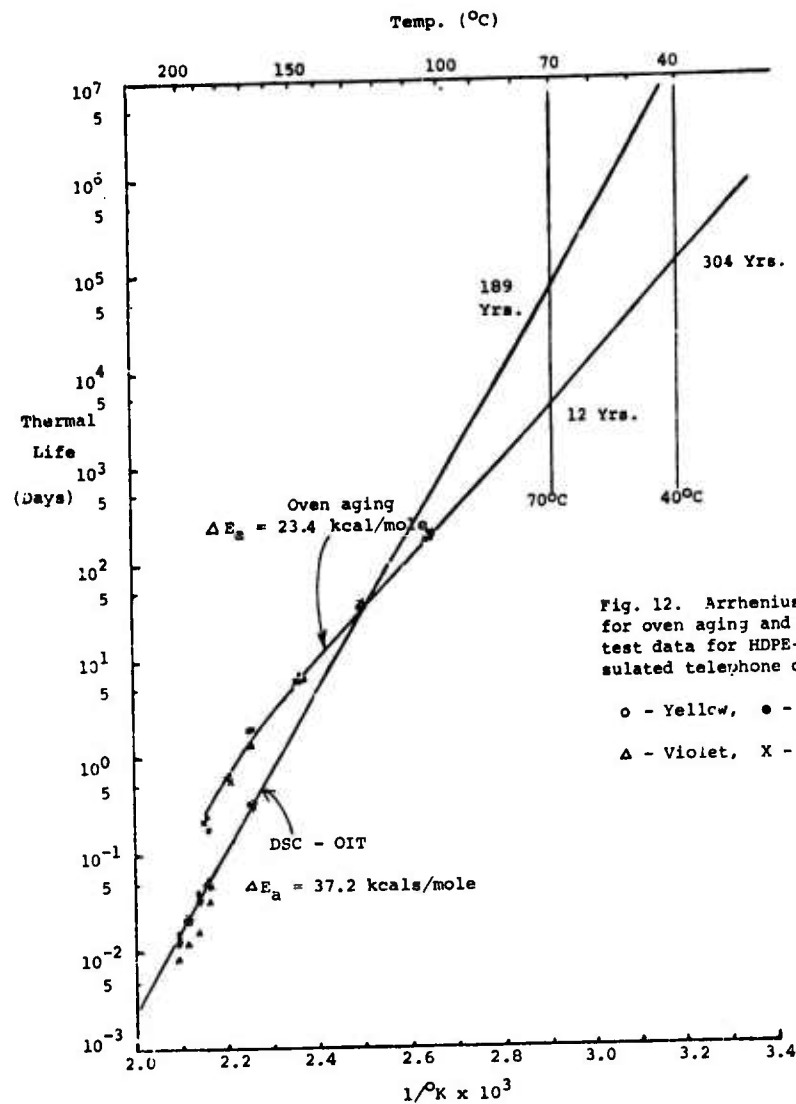
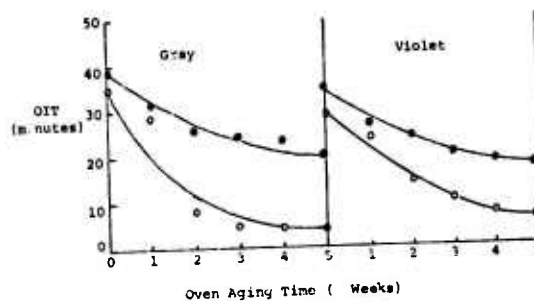


Fig. 12. Arrhenius plot for oven aging and DSC-OIT test data for HDPE-C insulated telephone cables

○ - Yellow, ● - Brown  
 △ - Violet, X - Gray

Fig. 13. Effect of wire gauge on DSC-OIT after air oven aging of HDPE-C air core cables at 115°C.

● 19 AWG  
 ○ 22 AWG



# LOW TEMPERATURE BRITTLINESS OF LOW DENSITY POLYETHYLENE FOR CABLE JACKETS

by

K. YAMAGUCHI, H. KISHI  
H. TAKASHIMA and S. OTOMO  
Ube Industries, Ltd.  
Tokyo, Japan

## SUMMARY

A reproducible testing method for evaluating the low density polyethylene for cable jacket which had very low brittleness temperature was established. This test method was essentially same as ASTM D746 except that surface notched specimens were used. The notching apparatus and measuring method of notch depth are described. In order to control the notch depth and its uniformity, the microscope observation was used.

Using this testing method, the effective factors on brittleness temperature of polyethylene for cable jacket were investigated. Several factors which affects the low temperature properties of cable materials are discussed.

A new low density polyethylene which has good low temperature characteristics as well as excellent properties for cable jacket was developed and commercialized.

## INTRODUCTION

The low temperature characteristics among various essential properties such as environmental stress crack resistance (ESCR) and weathering resistance is one of most important properties of low density polyethylene for cable jacket.

Many apparatuses for measuring the brittleness temperature of plastics have been proposed. The apparatus developed by Smith et al<sup>1)</sup> and standardized in present form of ASTM D746<sup>2)</sup> is widely used. The brittleness temperature of the high molecular weight low density polyethylene for cable jacket measured by ASTM D746 is lower than -80°C. But cable jacket is not actually used at such very low temperature and sometimes fails at much higher temperature than estimated by ASTM method. The measurement at such low temperature causes the mechanical problem of apparatus, the difficulty of temperature control and the scattering of testing results. So it can not be effectively used for the quality evaluation of cable jacketing material. In order to overcome these difficulties, the method using notched specimens for the test at higher temperature which can eliminate the fluctuation caused by specimen preparation had been proposed.<sup>3)4)5)</sup>

The surface notched specimens were used in this testing, because the notch is similar to a scratch or a cut of cables in the field and also it raises brittleness temperature remarkably. In the early stage of development, the brittleness temperature measured with surface notched

specimens widely fluctuated. Then it was found that the fluctuation was mainly due to the scattering of notch depth. The notch depth could be measured by a microscope with scale in eyepiece. To keep the notch depth constant, an idea of an air cylinder which presses the specimen on a razor blade at constant pressure was introduced. An improved apparatus using this idea was developed by a testing machine maker. This apparatus was found to be successful in getting more reproducible results.

The brittleness temperature of polyethylene and polyethylene cable jacket is dependent on manufacturing conditions, thermal history and surface damage. Several effects on brittleness temperature of polyethylene were investigated by newly developed testing method.

The most essential matter to increase the low temperature characteristics of cable jacket is to use the material which has very low brittleness temperature. As the cable jacketing compound of ethylene homopolymer which was used in the past, was inferior in ESCR and low temperature characteristics, the material which has better properties was required. In order to fulfil the above requirements, an ethylene vinylacetate (EVA) copolymer cable jacketing compound which has better properties not only in ESCR and low temperature brittleness but also weather resistance, resistance to chemicals, mechanical strength and processability was newly developed and commercialized.

## TESTING METHOD

### Description of Sample and Apparatus

The sample used in this testing was the low density polyethylene for cable jacket "UBEC 600V6" which was newly developed and had very good low temperature characteristics as shown later.

The apparatus for brittleness temperature test in ASTM D 746 was used and its striking member was motor driven. The clamp and specimen were set as shown in Fig 1. The distance from the edge of clamp to surface notch was effective on brittleness temperature (Fig 2). In order to fix the distance to 2 mm, the distance from specimen edge to notch was set at 14.5 mm because the length of specimen in clamp was 12.5 mm. Since the notch depth was most effective as shown in Fig 3, a semi-automatic notching apparatus<sup>6)</sup> which was shown in Fig 4 was used. It consists of the parts which fix a razor blade to the predetermined height and control the pressure as well as time that specimens are

pressed on razor blade. The height of razor blade can be set by the screw with scale. The pressure was controlled by the pressure of air cylinder and the time was set by the timer which controls the opening and closing of double solenoid valve.

\* The apparatus is commercially available from Toyo Seiki Seisaku-sho Ltd. (Tokyo)

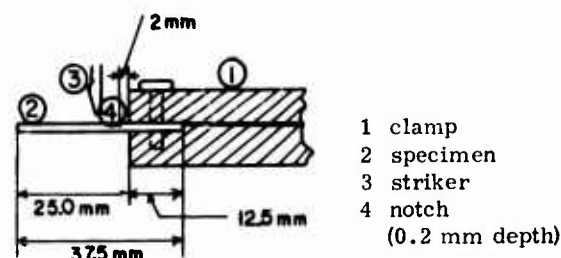


Fig. 1 Dimension of specimen and clamp

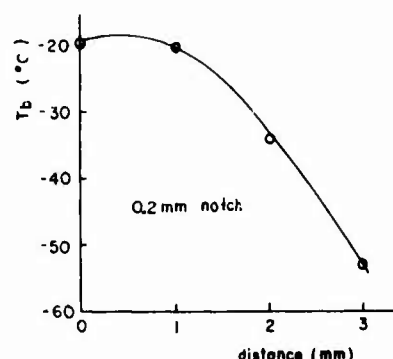


Fig. 2 Effect of the distance from notch to clamp edge on brittleness temperature

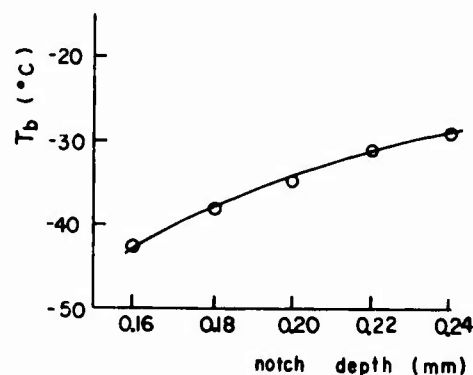


Fig. 3 Effect of surface notch depth at about 0.2 mm on brittleness temperature

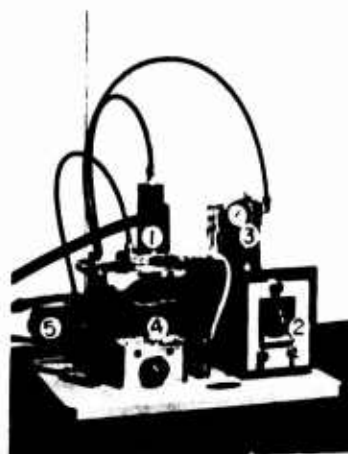


Fig. 4 Notching apparatus

- 1 air cylinder
- 2 timer
- 3 pressure gauge
- 4 razor blade and specimen

#### Measurement Procedure

Polyethylene granules were homogenized by milling and molded at  $165 \pm 5^\circ\text{C}$  into  $1.91 \pm 0.25$  mm sheets. In order to get constant cooling rate, the melting sheet was taken out from the press, and then backing plates was detached before sample was quenched in water of  $25 \pm 2^\circ\text{C}$ .

As the brittleness temperature using notched specimens was found not influenced by specimen cut methods (Table 1), the die cut were used in this investigation.

Table 1 Effect of specimen cut method on brittleness temperature

cut method	brittleness temperature
die cut	$-35.2^\circ\text{C}$
razor cut	$-34.0^\circ\text{C}$
guillotine cut	$-33.9^\circ\text{C}$

A razor blade was set at about 0.2 mm height, then a couple of specimens were notched. The specimens were cut apart along the notches, and each depth was measured by the microscope with scale in eyepiece. If the depth was not at  $0.200 \pm 0.005$  mm, the height of razor blade was reset. This procedure was repeated until  $0.200 \pm 0.005$  mm notch depth was attained. Several specimens were notched after razor blade setting for a confirming that all of the notch depth are within  $0.200 \pm 0.010$  mm, then all specimens were prepared.

Failure was defined as the easy bend to an angle of 90 deg. in the impact direction. The brittleness temperature was determined by calculation because the values by calculation method (ASTM standard method) were conformed with those determined by graphic method.

## Reproducibility of Results

The first criterion of acceptability for a proposed quality evaluation test is a good reproducibility of results. In the earlier stage when the notch depth and uniformity could not be controlled and molding conditions and the distance from clamp edge to notch were not strictly constant, the results fluctuated among measuring blocks.

The 12 testing results of UBEC 600V6 were shown in Table 2. The overall average brittleness temperature was  $-34.83 \pm 1.34^\circ\text{C}$ . This level of reproducibility proves that this method can be used for the evaluation of cable jacketing material.

The average notch depth of each run was controlled within  $0.200 \pm 0.010$  mm and overall average notch depth was  $0.1967 \pm 0.0051$  mm. The notch depths of failed and unfailed specimens at each stroke were measured. The overall average notch depth of failed specimens was 0.1970 mm and that of unfailed specimens was 0.1969 mm, which shows no tendency between notch depth and specimen failure.

Table 2 Reproducibility of brittleness temperature ( $T_b$ ) of UBEC 600V6

notch depth (mm)				
Tb	ave.	stand. dev.	ave. (fail)	ave. (unfail)
-37.0	0.1947	0.0070	0.1953	0.1946
-35.6	0.2000	0.0040	0.2006	0.2013
-33.2	0.1928	0.0050	0.1913	0.1941
-36.4	0.2004	0.0021	0.2013	0.1997
-36.2	0.1938	0.0035	0.1950	0.1934
-34.4	0.1955	0.0055	0.1953	0.1979
-35.8	0.1943	0.0060	0.1957	0.1922
-35.4	0.1936	0.0052	0.1911	0.1925
-34.0	0.1990	0.0050	0.2007	0.1982
-33.8	0.1992	0.0071	0.2009	0.1980
-33.0	0.1965	0.0051	0.1940	0.1981
-33.2	0.2026	0.0052	0.2026	0.2025
average	-34.83	0.1967	0.1970	0.1969

average of  $T_b$ :  $-34.83$   
standard deviation: 1.34

## EFFECTIVE FACTORS

### ON BRITTLENESS TEMPERATURE

It is supposed that the brittleness temperature of the cable jacket is influenced by, for instance, the following factors. Firstly, cable jacket is subjected to the exposure under severe environment, which implies there might be the change of crystalline and molecular structure and also the surface damage is expected. Secondly, the processing conditions affect the residual strain, molecular and crystalline structure. Thirdly, the cable structures such as aluminium seam part of colligation and bonded jacket cable, are ready to damage the jacket. In this part, several factors are chosen and their effect on the brittleness temperature are discussed.

## Effect of Carbon Black.

Carbon black which is incorporated with weather resistant polyethylene for cable jacket influences the brittleness temperature depending on its amount and its particle size. As shown in Fig 5, the addition of 2.6 % carbon black raised brittleness temperature by about  $10^\circ\text{C}$  and the furnace type carbon widely used at present deteriorates by about  $2^\circ\text{C}$  in comparison with the channel type carbon which was once prevalent has become very minor at the moment due to by the air act law.

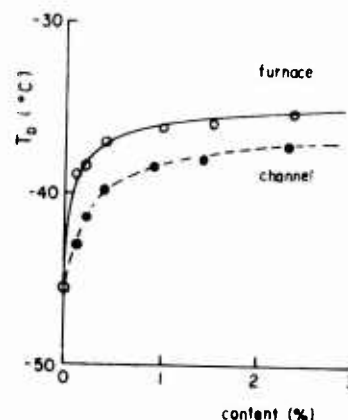


Fig. 5 Effect of carbon black type and content on brittleness temperature

## Effect of Extrusion

The effect of extrusion on brittleness temperature was measured. The compounds which were extruded at various temperatures were compression molded into sheets. The brittleness temperature and melt index of the sheets were shown in Table 3. From these results, both the brittleness temperature and melt index of extrudate were the same as those of original, which means the effect of extrusion degradation on brittleness temperature is negligible.

Table 3 Effect of extrusion of material on brittleness temperature

temperature ( $^\circ\text{C}$ )	$T_b$ ( $^\circ\text{C}$ )	melt index (g/10min)
original	-34.3	0.13
180 $^\circ\text{C}$	-33.8	0.13
210 $^\circ\text{C}$	-34.0	0.14
240 $^\circ\text{C}$	-35.0	0.13
270 $^\circ\text{C}$	-32.0	0.12

## Notch Effect

As mentioned in the testing method and shown in Fig 6, the notch effect on brittleness temperature was very significant when unnotched specimens

were used, the brittleness temperature of UBEC 600V6 was lower than  $-110^{\circ}\text{C}$ . But only 0.1 mm surface notch raised it to about  $-60^{\circ}\text{C}$  and 0.5 mm notch (1/4 specimen thickness) to about  $-5^{\circ}\text{C}$ . The fracture surface of various specimens observed by an electron microscope are shown in Fig 7. These figures show that the failure of unnotched specimen takes place in the state of brittleness and that the center of specimen is imposed by the complicated stress. The deeper was the notch, the higher became the failure temperature. In this case, polyethylene adjacent to the end of notch was elongated and failed but the successive failure was proceeded in brittle state.

#### Brittleness Failure from the Seam of Bonded Jacket

The results of low temperature impact test of bonded jacket with UBEC 600V6 and ethylene homopolymer for cable jacket were shown in Table 4. 1lb weight was dropped from 3 feet height on to the seam of aluminum at various temperature according to REA specification. 6) The cables were cut and cracks at the edge of aluminum were observed. The small size cable cracked at higher temperature. This might be due to high impact energy per unit area. As shown in Fig 8, though the cracks occurred from the edge of aluminum at relatively higher temperature, the fracture surface shows the brittleness failure. Table 4 also shows the brittleness temperature measured with notched specimen ( $T_b$ ) and the failure temperature of specimen which was bonded aluminum on polyethylene and whose aluminum edge was placed at the position of the notch ( $T_b(A)$ ). These results show that the cables made of the material which has lower brittleness temperature have also good low temperature characteristics.

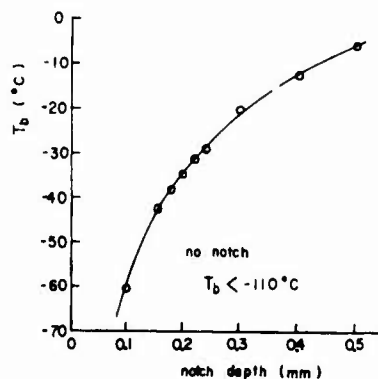


Fig.6 Effect of surface notch depth on brittleness temperature

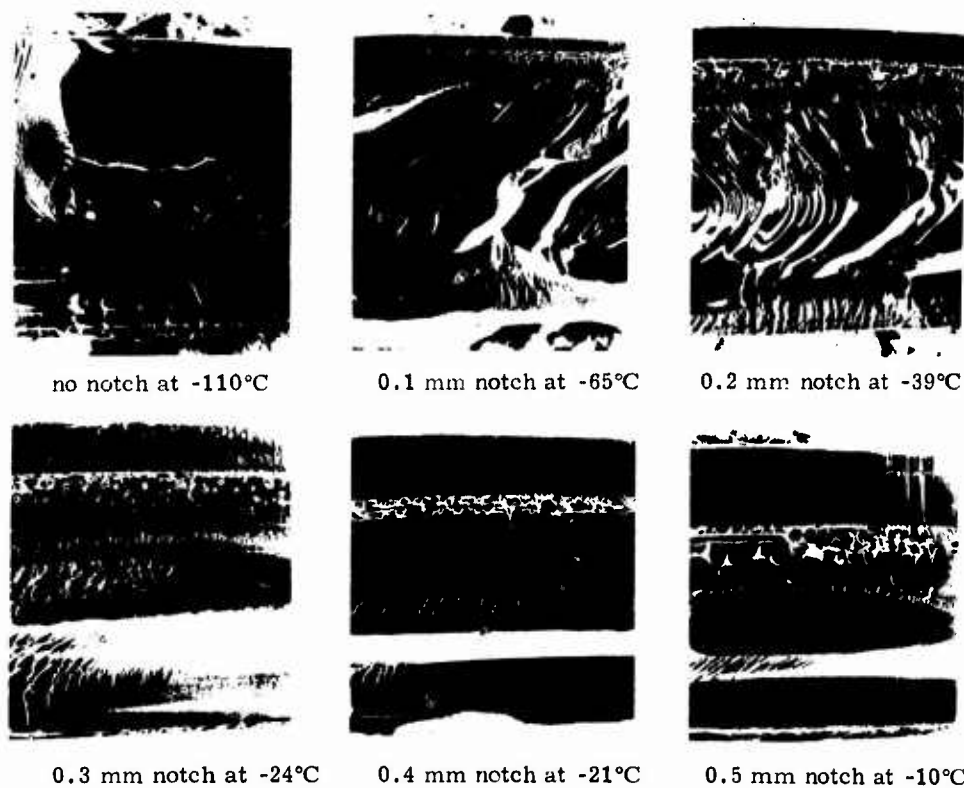


Fig.7 Micrograph of fracture surface by electron microscope. Specimens were struck from up to down of micrograph



Table 4 Brittleness temperature and low temperature impact test of bonded jacket

	UBEC 600V6	ethylene homopolymer compound
T <sub>b</sub> (°C)	-34.8	-18.5
T <sub>b(A)</sub> (°C)	-38.4	-21.5
low temperature impact (failure %)		
small size cable		
-20°C	0	4
-30°C	17	44
-40°C	29	62
medium and large size cable		
-20°C	0	0
-30°C	0	0
-40°C	0	5



Fig. 8 Micrograph of fracture surface which occurred by weight falling impact test of bonded jacket. The crack initiates from aluminum edge and stop in the middle of specimen thickness.

#### Effect of Heat and Weathering

The maximum temperature of cable is supposed to be about 60~70°C in the warm district. Cable jacket is usually exposed in high temperature and sunshine for a long time and sometimes it is subjected to higher temperature heat treatment in such case that cable is jointed. The brittleness temperature was slightly raised by 18 hours heat treatment up to 90°C but it was extremely raised at higher temperature treatment than 90°C(Fig. 9). By annealing at high temperature, the crystallinity or density increases and the crystalline is rearranged, therefore the polyethylene becomes more brittle. The weathering effects in carbon arc weathermeter and out door exposure were shown in Fig. 10. The brittleness temperature rose slightly in the short time exposure, but thereafter it did not change so much in this exposure period. The thermal history in outdoor exposure and carbon

weathermeter estimated from the shoulder of DSC thermogram was 50~60°C and 65~75°C, respectively.<sup>7)</sup> The results show that the slight increase of brittleness temperature in the short period is due to heat but the noticeable increase does not occur until polyethylene begins to degrade.

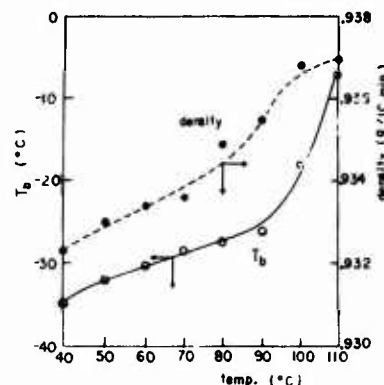


Fig. 9 Effect of heat treatment on brittleness temperature

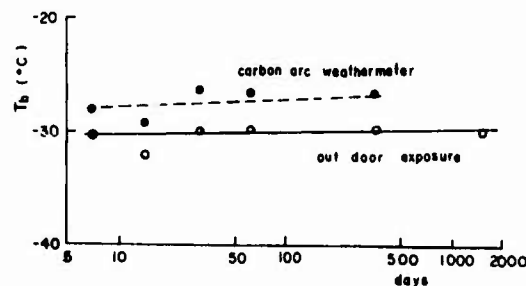


Fig. 10 Effect of weathering in weathermeter and out door exposure.

#### PROPERTIES OF NEW COMPOUND

The cable must be used for a long time, so that it is desired to improve the reliability of cable jacket. The new cable structure such as bonded jacket which influences on the low temperature characteristics was developed. Moreover, the production of channel carbon was stopped because of air pollution and furnace carbon, which is slightly inferior to channel carbon in ESCR and low temperature characteristics, had to be used. For these reasons, it was required to develop a compound which contains furnace carbon and possesses high ESCR and low brittleness temperature. In order to fulfil the requirement, an EVA copolymer for cable jacket, UBEC 600V6 was developed. In Table 5, the properties of UBEC 600V6

are shown comparing with ethylene homopolymer compound. From the results of Table 5 and various testing of low temperature brittleness, this compound is superior in low temperature characteristics. It showed no ESC under severe conditioning and processing degradation. The weather resistance in xenon arc weathermeter is shown in Table 6. This shows that no indication of degradation was detected until 8000 hours. As already shown in Fig. 9, noticeable increase of brittleness temperature was not also detected in carbon arc weathermeter until 8000 hours (330 days). Besides ESCR and brittleness temperature, this compound is excellent in mechanical properties, electrical properties, resistance to chemicals, processability and so on which are essential for cable jacketing compound.

### CONCLUSION

The testing method of brittleness temperature was established by the use of surface notched specimens and the control of the followings:

- depth and uniformity of notch
- distance from clamp edge to notch
- molding temperature and cooling rate

Cable jackets sometimes fail at considerably high temperature because of surface damage, defects of cable structure and thermal history at high

temperature. For these reasons, in order to increase the reliability of cable jacket, it is essential to use the material which has low brittleness temperature and attention has to be paid to the design of cable structure, processing and handling.

Based on these information, a new cable jacketing compound UBEC 600V6 was developed and successfully commercialized.

### REFERENCES

- 1) E. F. Smith, F. J. Dienes  
ASTM Bulletin NO 154, 46 (1948)
- 2) ASTM D746-72  
Brittleness Temperature of Plastics and Elastomers by Impact.
- 3) E. A. W. Hoff, S. Turner  
ASTM Bulletin NO 225, 58 (S957)
- 4) P. N. Bestelink, S. Turner  
ASTM Bulletin NO 231, 63 (1956)
- 5) S. Turner  
British Plastics 31, 526 (1958)
- 6) REA Specification p22 june (1967)
- 7) H. Takashima, Y. Nitta and A. Itakura  
TRANS. I. E. E. J. 94-A, 241 (1974)

Table 5 Properties of UBEC 600V6

	UBEC600V6	UBEC600
polymer type	EVA copolymer	homo- polymer
carbon black type	furnace	channel
content (%)	2.6	2.6
melt index (g/10min)	0.13	0.25
tensile properties		
yield strength (kg/cm <sup>2</sup> )	95	95
break strength (kg/cm <sup>2</sup> )	250	250
elongation (%)	650	650
ESCR at 50°C (F50, hr)		
145°C, 1hr, 5°C/hr	not fail	0.5
70°C, 18 hr	not fail	10
brabender mix		
at 160°C, 1hr		
and 70°C 18hr	not fail	0.1
brittleness temperature		
unnotch (°C)	<-110	-103
0.2 mm notch (°C)	-34.8	-23.8
electrical properties		
dissipation factor at 1 MHZ	6.5 x 10 <sup>-3</sup>	1.3 x 10 <sup>-3</sup>
dielectric constant		
at 1 MHZ	2.52	2.56

\* commercial name of ethylene homopolymer cable jacketing compound

Table 6 Watherability of UBEC 600V6 in xenon weathermeter

time (hrs)	MI (g/10min)	strength (kg/cm <sup>2</sup> )	elongation (%)	brittleness at -60°C
original	0.13	230	610	0/5
2000	0.13	215	630	0/5
4000	0.11	205	600	0/5
6000	0.12	215	615	0/5
8000	0.15	215	600	0/5



Koji Mamaguchi  
UBE Industries, Ltd.  
7-2, Kasumigaseki 3-chome,  
Chiyoda-ku, Tokyo, Japan

Koji Yamaguchi is presently the manager of technical department, petrochemicals division, UBE Industries, Ltd. He received his B.S. degree in fuel engineering from Kyoto University in 1949. He joined UBE Industries, Ltd. in the same year and worked for 10 years at the Central Research Laboratory in Ube, then for three years at the Department for Planning in Tokyo. In 1963, he joined the construction of UBE's first high pressure polyethylene in Chiba. Since then he has been the chief of the research and development activities of UBE polyethylene, polypropylene and polybutadiene.



Hidehiro Kishi  
UBE Industries, Ltd.  
7-2, Kasumigaseki 3-chome  
Chiyoda-ku, Tokyo, Japan

Hidehiro Kishi is presently an assistant manager of technical department, petrochemicals division, UBE Industries, Ltd. He received a B.S. degree in applied chemistry from Kyushu University in 1959 and joined UBE Industries, Ltd. in the same year. Initially he worked at Ube fertilizer Plant. He has been engaged in the research and development of high pressure polyethylene and polypropylene, since 1963.



Hideaki Takashima  
UBE Industries, Ltd.  
8-1 Goi Minamikaigan  
Ichihara, Chiba, Japan

Hideaki Takashima is presently a staff engineer of technical department, petrochemicals division, UBE Industries, Ltd. He received B.S. degree in applied chemistry from Nagoya University in 1965. He joined UBE Industries, Ltd. in the same year, and has been engaged in research and development of high pressure polyethylene and polypropylene.



Susumu Otomo  
UBE Industries, Ltd.  
8-1 Goi Minamikaigan  
Ichihara, Chiba, Japan

Susumu Otomo is presently a staff engineer of technical department, petrochemicals division, UBE Industries, Ltd. He received B.S. degree in industrial chemistry from Yamaguchi University in 1970. He joined UBE Industries, Ltd. in the same year, and has been engaged in research and development of high pressure polyethylene.

# COMPARISON OF TEST METHODS FOR DETERMINATION OF STABILITY OF WIRE AND CABLE INSULATION

by

E. T. Kokta  
Bell Laboratories  
Murray Hill, New Jersey 07974

## Summary

Predicting the lifetime of Bell System wire insulation in the field is of the utmost importance to insure adequate service life. Many test methods are used: differential thermal analysis, oxygen uptake, and physical cracking. This paper discusses the principles of these methods, their advantages, limitations, and interchangeability.

## Introduction

Recent field failures of low-density polyethylene wire insulation<sup>1</sup> have led to an extended program on material stabilization together with an attempt to improve our ability to predict the lifetime of Bell System wires in the field. This paper discusses the principles of several test methods, their advantages and limitations, and whether or not they can be used interchangeably.

Basically, two types of tests are used: higher temperature methods represented by thermal analysis (220-180°) and oxygen uptake (150-110°), and a lower temperature method illustrated by physical cracking in pedestals or forced-air ovens.

Experience has shown that both types of test methods are essential for obtaining complete information about the oxidative stability of a sample. Short-term, high-temperature tests are needed for quality control purposes, while the longer term, lower temperature testing is necessary for accurate prediction of service life.

## Experimental

### Preparation of Samples

Samples for this study were made from duPont's unstabilized, high-density polyethylene and different combinations of antioxidants and copper deactivators. Mixing was achieved by milling at 160°C for not more than four minutes. The milled samples were then extruded onto a 22 AWG copper wire<sup>2</sup> using a Welding Engineers' 0.8-inch twin-screw extruder with a length-to-diameter ratio of 24:1. Barrel and crosshead temperatures were maintained at 425 °F, screw speed at 80 rpm, and head pressures at 1600 psi. The wire speed was 180 feet per minute, and the insulation thickness was maintained at 6.0±0.5 mils. The conductor was preheated to 400°F using a Walco preheater modified for low speeds.

### Test Methods

Thermal Analysis - The oxidative stability of polyethylene insulation is conveniently measured by thermal analysis (Figure 1). When

performed at high temperatures (180-220°C), this test requires a short time.

In the method used in the present work, a sample is arranged in an aluminum pan lined with a copper disc and placed in the thermocouple position, heated in helium to a desired temperature (220, 210, 200, and 190°C were used in this experiment), and held at that temperature in oxygen until the exotherm occurs. A typical thermogram is shown in Figure 2. The induction time determined from the exotherm by extrapolation is the measure of the oxidative stability of a sample. A zero induction time is considered as indicating that all the stabilizers initially present have been exhausted at the temperature of testing. Some residual stability may be present at lower temperatures.

The instruments used for this study were an E. I. duPont 990 Thermal Analyzer equipped with a DSC cell and an R. L. Stone Thermal Analyzer with a DTA cell.

Oxygen Uptake - A second method frequently used is oxygen uptake. This method has been described in detail by Hawkins et al.<sup>3</sup> As Figure 3 shows, a sample is placed in a glass tube filled with oxygen and connected to a buret containing mercury. The tube is inserted into a constant-temperature bath (temperatures of 150, 130, and 110°C were used in this experiment) and readings taken periodically as the sample absorbs oxygen. The induction time is determined by plotting buret readings against time, and this procedure generates a curve quite similar to that produced by thermal analysis (Figure 4).

Oxidative Stress-Cracking - The stress-cracking method detects physical failures of wire insulation aged at different temperatures in pedestals or ovens. A typical Bell System B-type pedestal dome complete with base plate is shown in Figure 5.

Pedestals like this are actually used in the field to protect cables at junctions from which wires are led to a house. In this experiment heated pedestals were used to simulate an environment to which wires might be exposed in service. Aging temperatures of 110, 100, 90, 80, and 70°C were used. Custom-made heating mantles were used to heat the pedestal domes. Each pedestal had its own temperature controller and high-temperature alarm system. In oven aging a standard forced-air oven at 70°C was used. To initiate cracking, wires were twisted into so-called "pigtailed" and visually examined for cracks.

### The Effect of Solubility

It has been observed by J. B. Howard and H. M. Gilroy<sup>4</sup> that data from high-temperature test

methods for low-density polyethylene (LDPE) occasionally tend to produce misleading information when extrapolated to lower temperatures. This is partly due to an abrupt change in the solubility of stabilizers in LDPE near its melting point (around 80°C). Above this temperature most stabilizers remain reasonably soluble in the polymer, but below it the solubility is sharply decreased to a level of a few parts per million. The result is that most stabilizers partially diffuse out of the polymer and are lost<sup>5,6</sup> (Figure 6). Although the loss rate of stabilizers from a solid polymer is smaller from high-density polyethylene (HDPE),<sup>7,8</sup> one of the objectives of this study was to determine whether HDPE behaves similarly to LDPE.

Because of this solubility phenomenon, testing at lower temperatures is necessary to obtain a realistic evaluation of service life at field temperatures.

#### Advantages and Limitations of Test Methods

Some characteristics of the three test methods discussed in this paper are summarized in Table I. The thermal analysis method requires a short period of time to produce results. Only a small quantity of material is needed for testing, and a sample is prepared in a matter of seconds. Material in a variety of forms can be tested by this method - pellets, molded films, powder, or wires. Of these four most used forms, molded films and powders give the most reproducible results because in such samples stabilizers are well dispersed within the polymer. Pellets and wires are less homogeneous, so in these cases the reproducibility is somewhat lower.

In this method a sample is tested in the molten state, a procedure which reduces the reliability of the data for lifetime prediction purposes. For this reason and also because of the short time needed to obtain results, the thermal analysis method is probably best limited to use for quality control purposes.

Oxygen uptake experiments are usually carried out at lower temperatures than thermal analysis. Often the temperatures used are well below the melting region of polyethylene. A larger sample (~10g) is needed, and the forms most widely used are films or wires, although powders and pellets can also be accommodated. Preparation of a sample is rather elaborate and requires some time. This method is slower in producing results than thermal analysis because of the lower temperature used. Testing at lower temperatures, which takes a long period of time, requires a sealed system to avoid leaks in connecting tubes which frequently occur due to oxidation. Unlike thermal analysis, oxygen uptake is mostly used for screening of samples since the elaborate preparation and the long time it requires to produce results render the method inconvenient for quality control use.

An outstanding advantage of both thermal analysis and oxygen uptake methods is that a curve containing kinetic information is generated in each case.

The stress-cracking method is much slower than the above two, but because the sample is tested in a solid state, the testing conditions more closely resemble the field environment. Therefore, the data can be used for lifetime prediction. A disadvantage of this method is that a large sample (>10g) is needed, and preparation of a sample (molding, extruding) is necessary prior to testing. It is impossible to test powders or pellets. The reproducibility of results is quite good, but a clear definition of a crack has to be made prior to testing since cracks occur in different forms.

#### Interchangeability of Test Methods

Since the three methods described above are all used concurrently in testing samples for the Bell System, it is important to know how they compare and indeed whether they test the same phenomenon, i.e., thermal oxidation of the polyolefin.

As discussed earlier in this paper, the bases for each of the three test methods are slightly different; and therefore, some discontinuities may be expected if the data are plotted together.

An example of data points from all three methods is shown in Figure 7. Sample A is stabilized with a ternary system containing 0.1 percent of an oligomer of 2,2-4-trimethyl-1,2-dihydroquinoline, 0.05 percent distearyl thiodipropionate, and 0.05 percent dibromooxanilide. It can be seen that the thermal analysis induction time points (220, 210, 200, and 190°C) and the oxygen uptake time points (150, 130, and 110°C) fall onto a straight line. On the other hand, the line through the points plotted from the cracking data at lower temperature shows a slope different from the high-temperature line, and the extrapolated lifetime from the cracking data line is shorter than that obtained from the induction time/oxygen uptake data line. Some of the different factors affecting the results obtained from each test method are discussed below.

In the oxygen uptake method, the sample is in a static closed system. Thus all of the stabilizers or their reaction products remain in the system. The sample may or may not be tested in the molten state, since both higher and lower temperatures are used.

In the thermal analysis method, the sample is flushed constantly with oxygen, which might be expected to remove stabilizers. However, as the sample is always tested in the molten state, a high solubility is maintained.

The samples for the cracking test are exposed to very slow air changes caused by convection in pedestals and to more rapid air circulation in the forced-air ovens. This air may carry away some of the stabilizers, especially if they diffuse to the surface at the lower temperatures. This would, of course, leave the sample less protected from oxidation. This probably explains why pedestal aging appears to be a more severe test than the oxygen uptake method and explains the discrepancy between the data obtained from these tests in



Figure 7. The cracking method cannot test samples at temperatures higher than 110°C, so the results obtained from this test better represent the conditions of a practical application.

It might be argued that the pure oxygen atmosphere used in the oxygen uptake test should accelerate degradation relative to the pedestal or oven test where air forms the atmosphere. Apparently this effect is outweighed by other differences such as those discussed above.<sup>6</sup> This argument is further supported by the cracking data obtained from a 70°C forced-air oven. The point designated as "oven cracking point" in Figure 7 falls far below the line through the pedestal cracking points, which indicates that in the 70°C oven the sample cracked some 50,000 hours earlier than the extrapolated pedestal data show for 70°. This is probably a result of the rapid air change which would encourage the maximum volatilization of antioxidants from the samples. The forced-air oven is consequently the most severe of the tests examined.

Another factor that might explain the differences in data points found between the cracking test and the thermal analysis and oxygen uptake is the observed phenomenon that sometimes cracking is surface-initiated and can occur before a total loss of stabilizers is established by higher temperature methods. It should also be mentioned that there is another important difference between the thermal analysis, oxygen uptake, and stress-cracking methods: In thermal analysis and in oxygen uptake tests at higher temperatures, the samples are in the molten state during testing; and therefore, the stabilizers are well dissolved within the polymer.

The same trends as discussed above were observed in many other samples - for example, in Sample B (Figure 8) stabilized with 0.1 percent tetrakis [methylene-3(3',5'-di-tert.-butyl-4'-hydroxyphenyl)propionate] methane, 0.05 percent thiodiethylene bis (3,5-di-tert.-butyl-4-hydroxy) hydrocinnamate, and 0.05 percent salicyloyl amine triazole. Samples A and B both showed large differences in data points between the high-temperature and the low-temperature test methods.

#### Conclusions

As Figure 8 shows, the differences in data obtained from the three test methods are real and do not depend on the stabilization system of the sample. It is concluded that the thermal analysis method is very useful for quality control purposes, while the oxygen uptake is best suited for screening new stabilizer combinations. However, these two methods are not accurate for extrapolation and prediction of the lifetime because they tend to give results which are too optimistic. Cracking tests produce more realistic results but because of the lower temperatures involved take a longer time and thus are not very useful for quality control or screening purposes.

#### Acknowledgments

The author wishes to acknowledge helpful discussions with H. M. Gilroy during the course

of this work. The author would also like to thank L. D. Loan, M. G. Chan, and W. H. Starnes for their comments on this manuscript and W. M. Martin for his assistance in setting up the oxygen uptake test.

#### References

1. J. B. Howard, Proc. 21st Int. Wire and Cable Symp., Page 329 (1972).
2. M. G. Chan and R. A. Powers, Proc. 33rd ANTEC, Page 292 (1975).
3. W. L. Hawkins, R. H. Hansen, W. Matreyek, and F. H. Winslow, J. Appl. Polymer Sci. 1, 37 (1959).
4. J. B. Howard and H. M. Gilroy, "Some Observations on the Long-Term Behavior of Stabilized Polyethylene," Polymer Eng. and Sci. 15, 268 (1975).
5. H. E. Bair, Polymer Eng. and Sci. 13, 435 (1973).
6. R. J. Roe, H. E. Bair, and C. Gieniewski, J. Appl. Polymer Sci. 18, 843 (1974).
7. M. G. Chan, Proc. 23rd Int. Wire and Cable Symp., Page 34 (1974).
8. P. N. Lowell and N. C. McCrum, J. Polymer Sci. A-2 9, 1935 (1971).



Elena Kokta is a member of the Plastics Chemistry, Research and Development Department at Bell Laboratories, Murray Hill, New Jersey. She received a B.A. degree in chemistry from Fairleigh Dickinson University in 1973 and joined Bell Laboratories immediately thereafter. At present she is engaged in the development and application of polyolefins for wire and cable.



## DTA SCHEMATIC

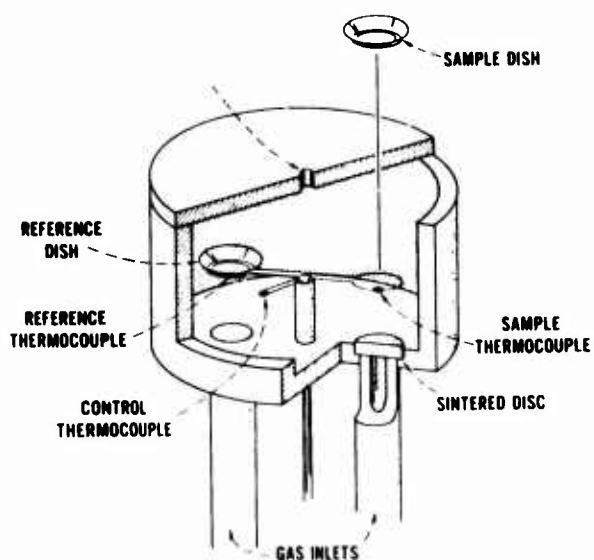


Figure 1

## Typical Oxygen Uptake Curve

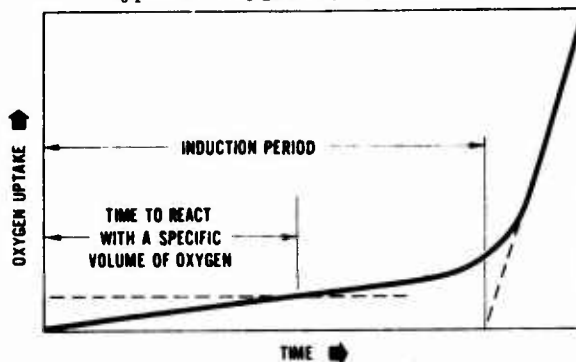


Figure 4

## TYPICAL DTA THERMOGRAM

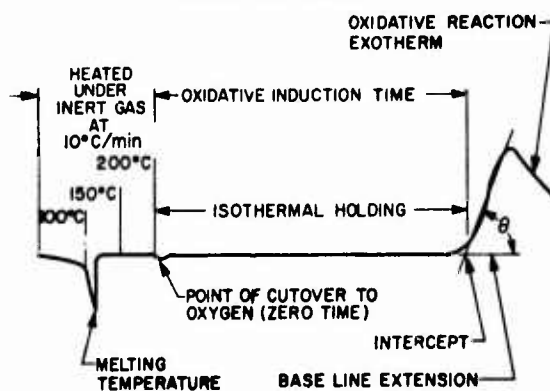


Figure 2

## Oxygen Uptake Schematic

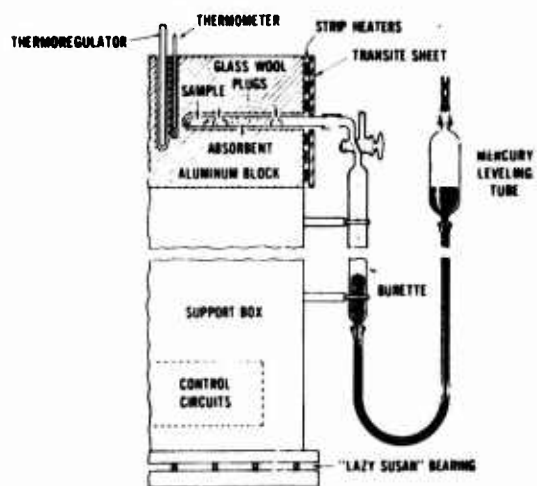


Figure 3

## PEDESTAL AGING OVEN

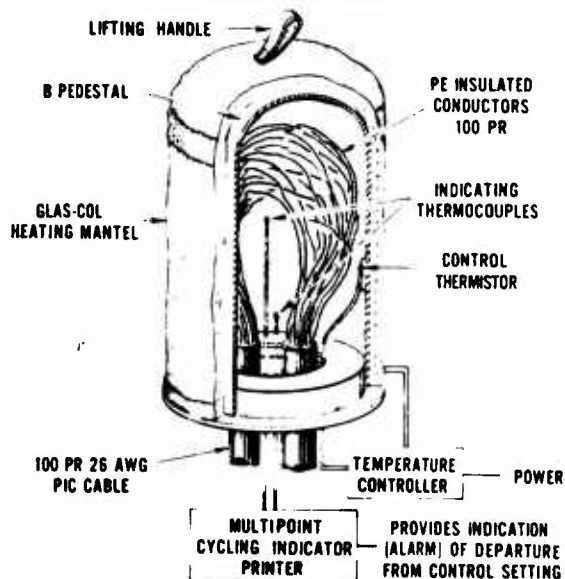


Figure 5

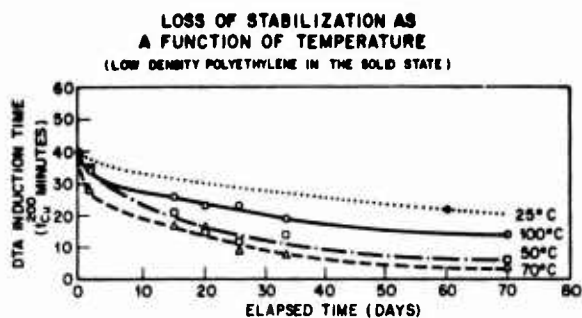


Figure 6

#### Advantages and Limitations of Test Methods

	DTA	OXYGEN UPTAKE	STRESS-CRACKING
TEMPERATURE RANGE	180°-220°C	110°-150°C	50°-110°C
TESTING TIME RANGE	MINUTES-HOURS	HOURS-DAYS	MONTHS-YEARS
SAMPLE DURING TESTING	MOLTEN	MOLTEN-SOLID	SOLID
SAMPLE PREPARATION	SIMPLE	TIME CONSUMING	SIMPLE
SAMPLE SIZE	VERY SMALL (mg)	LARGER (0.1g)	LARGE (>10g)
ATMOSPHERE	OXYGEN	OXYGEN	AIR
REPRODUCIBILITY	FAIR	GOOD	GOOD
APPARATUS COST	VERY EXPENSIVE	MODERATELY EXPENSIVE	INEXPENSIVE
BEST USED FOR	QUALITY CONTROL	SCREENING	LIFE-TIME PREDICTING

Table I

#### Interchangeability of Test Methods

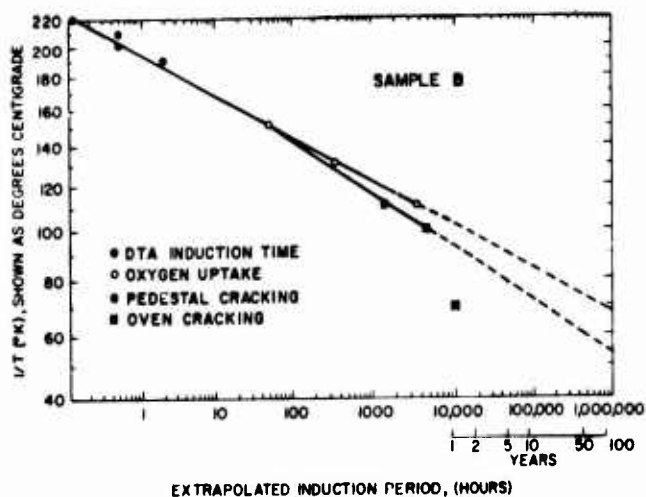


Figure 8

#### Interchangeability of Test Methods

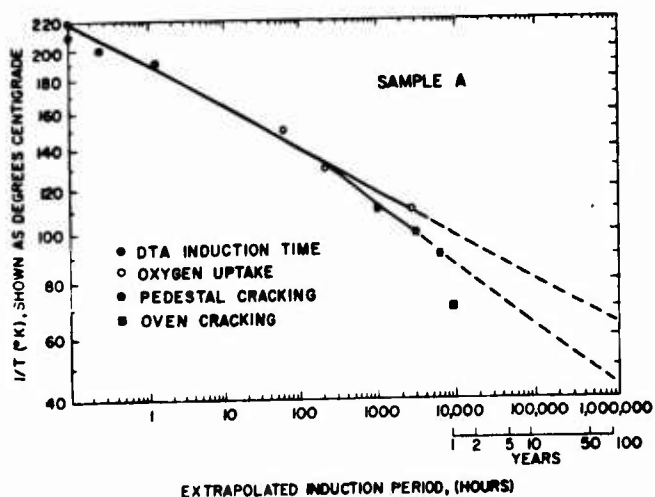


Figure 7

# IMPROVED TELEPHONE JACKET COMPOUNDS

by

Sherman Kottle and R. B. McAda  
Dow Chemical U.S.A.  
Freeport, Texas

## SUMMARY

Work undertaken to obtain a better understanding of the fundamental properties of ethylene copolymer telephone jacket compounds has led to the identification of a new series of products of improved performance toward the processing and environmental influences to which such compounds are subject.

## INTRODUCTION

The low density polyethylene compounds which are used in telephone cable jackets are specialized materials uniquely formulated for this application. Many of the scientific and engineering requirements have been defined through the efforts of Bell Laboratories.<sup>1</sup> The major factors affecting the extrusion of cable jackets are oxidative and thermal stability under shear in extrusion equipment. The major environmental factors to which such compounds must be resistant in service are the effects of stress cracking agents and the effects of ultraviolet light and oxygen. They must also maintain adequate physical properties over a broad temperature range.

Most of the high stress crack low density polyethylene jacket compounds of commercial importance have utilized ethylene-vinyl acetate copolymer (EVA) to secure stress crack resistance which is superior to that exhibited by unmodified polyethylene. At the time of the development of these compounds, in the early 1960's, EVA copolymers were the most economical low crystallinity ethylene polymers available. The potential usefulness of other ethylene copolymers was demonstrated, but few large volume applications resulted.<sup>2</sup> Work was begun in our laboratories several years ago to re-examine the usefulness of copolymers of ethylene with acrylic esters in the cable jacket area.

## EXPERIMENTAL PROCEDURES

The materials described in Table I were synthesized in our laboratories on a commercial or semi-commercial scale. The samples described as jacket compounds were formulated to contain appropriate concentrations of antioxidants and 2.5 wt-% of type N-110 furnace black. The carbon black was omitted in samples F and G which were used to perform accelerated ultraviolet light (UV) tests. All the jacket compounds had nominal melt indexes of 0.3 dg/min under the conditions of the standard ASTM D-1238 test. Copolymer samples J and K contained approximately 25% by weight of comonomer and were free of additives. They were used in investigating

ccopolymer stability, where the comonomer concentration in the jacket compounds made such observations difficult.

TABLE I

### MATERIALS TESTED

Designation	Description	Comonomer	Carbon Black
A	Compound	Vinyl Acetate	Yes
B	Compound	Isobutyl acrylate	Yes
C	Compound	N-Butyl acrylate	Yes
D	Compound	Ethyl acrylate	Yes
E	Compound	Methyl acrylate	Yes
F	Compound	Vinyl acetate	No
G	Compound	Isobutyl acrylate	No
J	Copolymer	Vinyl Acetate	No
K	Copolymer	Isobutyl acrylate	No

Low temperature brittleness testing (LTB) was performed by means of the impact apparatus used for ASTM D-746, with liquid nitrogen as the coolant for a methylcyclohexane medium. Standard methods were used for comparison of physical properties to standard industry specifications. Dynamic mechanical tests were made using a low frequency torsion pendulum.<sup>3</sup>

Thermal stability was investigated through the use of a technique which can be described as thermal volatilization analysis (TVA).<sup>4</sup> Although somewhat analogous to thermogravimetric analysis (TGA), the TVA technique is capable of many orders higher sensitivity. In TVA analysis milligram quantities of a sample are heated in vacuum at temperatures which are linearly increased with time. By means of a system of high vacuum pump, pressure transducer, and calibrated leak, an X-Y recorder is made to record the relative rate of evolution of gaseous products as a function of temperature.

Processing stability was investigated by means of milling experiments performed in a Brabender Plasti-Corder®. Samples were milled, then removed for further testing.

Environmental stress crack resistance (ESCR) was measured by means of the bent-strip test (ASTM D-1693). The milled samples were also used for infrared analysis and for oxidation resistance tests.

Specimens were tested for oxidative stability by the use of an automatic recording oxygen up-take instrument manufactured in our laboratories. Tests were conducted at a temperature of 200°C under one atmosphere pressure of oxygen. The data were obtained in terms of a recording of oxygen volume consumed as a function of time. The oxidative induction period was defined as the time, in minutes, required for the onset of autocatalytic oxidation.

Ultraviolet light resistance tests were performed on ASTM type C tensile bars prepared from compression molded sheets 0.125 inch thick. Two types of tests were performed. One group of samples was exposed on outdoor roof racks at a 45° angle, facing south, at our laboratories in Freeport, Texas. Another group was tested under accelerated conditions through the use of an apparatus of our manufacture which uses General Electric type RS sunlamps. Standard ASTM methods were used to evaluate the degree of retention of tensile properties and melt index changes.

## RESULTS AND DISCUSSION

### Low Temperature Performance

The LTB results are shown in Table II. The results were found to be very dependent on the concentration of comonomer. The data given in Table II represent compositions which were judged practical in terms of over-all property balance. By performing a great many tests it was possible to ascribe F<sub>50</sub> temperature ranges to several of the compositions. Typical results for the EVA and EIBA (ethylene-isobutyl acrylate) samples are shown in Table III.

TABLE II

#### LOW TEMPERATURE BRITTLINESS

Sample	Breaks at -76°C/ Number of Specimens
A	2/30
B	0/30
C	2/30
D	0/30
E	1/30

TABLE III

#### LTB F<sub>50</sub> Ranges

Sample	F <sub>50</sub> Temperature, °C
A	-98 to -110
B	-103 to -114

Only slight differences were found in the dynamic mechanical spectra of compounds A and B in the temperature range of -150 to +70°C. In view of this, data were obtained on copolymer samples J and K in which the comonomer concentrations were 5-6 times greater than in compounds A and B. Torsional modulus and damping curves for the EVA copolymer are shown in Figure 1. There is a pronounced transition evident at -22°C, as well as smaller ones normally found in polyethylene at approximately -130°C and +70°C. The major damping peak is believed to occur in the temperature region in which the polymer is changing from a flexible state to a glassy, more brittle, state.<sup>3</sup> Figure 2 shows that the corresponding peak temperature is centered at -32°C for the EIBA polymer. Even lower transition temperatures were found in other acrylates. It is known from observations on rubber reinforcement of brittle polymers that the desirable criteria for the rubber are: a very low temperature glass transition, general chemical compatibility, and some degree of phase separation.<sup>5</sup> The results obtained in this work suggest that the improvement in LTB of acrylate jacket compounds may be explained the same way.

### Thermal Stability

Since the ester comonomers are minor components in terms of concentration in the final cable compounds, thermal stability was investigated through the use of the copolymers as model polymers. Thermal volatilization curves on copolymers J and K, EVA and EIBA, respectively, are shown in Figures 3 and 4. EVA exhibits dual maxima in degradation rate, centered at 320 and 420°C. It is well known that the pendant acetate groups of EVA copolymers quantitatively degrade to produce acetic acid and leave the main polymer chain with vinyl unsaturation.<sup>6</sup> The higher temperature decomposition peak may be ascribed to degradation of the polymer 'backbone' from the appearance in the mass spectrum of the gases of a wide variety of hydrocarbon fragments.

The single, broader maximum for the EIBA was identified, as shown in Table IV. These analyses were performed by rapidly raising the sample temperature from ambient to the value shown, instead of programming at 10°C per minute as in the TVA scans. It is reasonable to assume from the results of these isothermal experiments that the volatile products shown in Table IV correspond to the left-hand, center, and right-hand side of the broad, single peak in the TVA thermogram of the EIBA copolymer.

**TABLE IV**  
**ANALYSIS OF VOLATILE PRODUCTS**

Temperature, °C	Predominant Compounds Present
200	Isobutylene, carbon dioxide
320	Isobutylene, carbon dioxide, hydrocarbons
400	Hydrocarbon fragments

Loss of comonomer was also observed directly on fully-formulated compounds by means of tests performed in an electrically heated Brabender. Forty-gram samples were milled with a rotor speed of 125 rpm and an initial head temperature of 154°C. The plastic temperatures achieved during milling for time periods up to 3 hours remained between 216°C and 230°C. After individual samples were milled for various times, they were analyzed by infrared for retention of comonomer. To overcome the difficulty of thickness measurement of thin infrared specimens (since the samples contained approximately 2.5 wt-% carbon black) the infrared analyses were based on the use of a polyethylene carbon-hydrogen band as an internal standard. The results are graphed in terms of retention of VA and IBA, respectively, in Figure 5. The data show that the acrylic ester jacket compound retained 86% of its comonomer, while the EVA compound retained only 65% of its VA, after 3 hours of milling. The compound containing EIBA was demonstrably more stable, in accord with the results of further degradation tests described below.

#### Resistance to Shear Degradation

All compounds were tested by a series of procedures designed to simulate the cable-making process steps of jacket extrusion, slow cooling of reels of cable, and the environmental stress crack testing of finished jackets. The simulation involves shearing of the polymer in an oil-heated Brabender, annealing of a molded sheet made from the milled sample, and subsequent ESCR testing. In our experiments the standard conditions of 154°C initial head temperature and 125 rpm rotor speed were used. In addition to the standard 1 hour time, tests were done with other samples for extended milling times of 2, 3, and 4 hours. The ESCR data are not tabulated here because all products tested exhibited no failures after 1, 2, or 3 hours of milling. Some of the acrylic ester compounds were able to endure 4 hours of milling before showing ESCR deterioration.

Since the milling step is primarily an oxidative experience, the samples used for ESCR tests were also examined for oxidative stability. The results are summarized in Table V for EVA and EIBA compounds contain-

**TABLE V**  
**EFFECT OF BRABENDER MILLING ON OXIDATIVE STABILITY**

Compound	A		B	
Antioxidant, ppm	1,150	600	875	1,150 1,500
Milling Time, hours	Oxidation Induction Period, Minutes @ 200°C			
0	26	18	22	24 29
1	20	12	17	24 25
2	15	6	12	14 20
3	10	5	7	11 14

ing various concentrations of a proprietary antioxidant. The results of these tests indicate that the oxidative stability of the acrylic ester compound is at least equivalent to that of the EVA product. The results of extrusion testing were entirely analogous, but less dramatic, since 1 hour of milling has been demonstrated in our laboratory to be equivalent to several extrusion passes.

#### Ultraviolet Light Resistance

The major factor governing the UV resistance of telephone jacket compounds is the incorporation of a suitable amount and type of carbon black.<sup>10</sup> Nevertheless, UV resistance tests were performed on samples F and G which were prepared to be otherwise identical in composition to samples A and B, except for omission of the carbon black. The findings regarding the relative stabilities of EVA and EIBA compounds toward changes in melt index, tensile strength, and elongation are shown in Figure 6. The results indicate that the compounds are equivalent.

#### General Physical Properties

Examination of the general physical properties which are commonly used in characterizing black low density polyethylene telephone jacket compounds revealed that the acrylate compounds were equivalent to those of presently used vinyl acetate compounds. Table VI summarizes the more pertinent data.

#### CONCLUSIONS

Black polyolefin copolymer telephone jacket compounds based on acrylic ester-ethylene copolymers have been developed which offer the promise of being superior to conventional vinyl acetate compounds in regard to stability and low temperature performance.

TABLE VI  
GENERAL PHYSICAL PROPERTIES

Compound	A	B	C	D	E
Melt Index, dg/min	0.22	0.25	0.35	0.33	0.35
Tensile Yield, psi	1400	1300	1320	1350	1370
Ultimate Tensile, psi	1950	1900	1900	2000	2100
Ultimate Elongation, %	600	650	500	550	550
LTB @ -76°C (Failures/No. Specimens)	2/30	0/30	2/30	0/30	1/30
Process Degradation Stress Crack Resistance (Failures/No. Specimens in 24 Hours)					
1 hour milling	0/10	0/10	0/10	0/10	0/10
2 hour milling	0/10	0/10	0/10	0/10	0/10
3 hour milling	0/10	0/10	0/10	0/10	0/10

#### ACKNOWLEDGEMENTS

The authors wish to acknowledge the contributions of T. E. McMillan, R. C. Williams, D. P. Flores, M. C. McGaugh, and G. E. Waples, for experimental observations and polymer preparations. This work was done while the authors were members of the Texas Division Research Department, Dow Chemical U.S.A.

#### REFERENCES

1. J. B. Howard in R.A.V. Raff and K. W. Doak, "Crystalline Olefin Polymers", pp 47-104, Interscience, New York, 1964.
2. R. F. Smith, R. C. Mildner, and E. W. Veazey, "Copolymer Compositions for the Wire and Cable Industry", Proceedings of the 11th Annual Wire and Cable Symposium, 1962.
3. S. G. Turley and H. Keskkula, Journal of Polymer Science: Part C, 14, 69 (1966).
4. M. C. McGaugh, and S. Kottle, Polymer Letters, 5, 719 (1967).
5. E. M. Fettes and W. N. Maclay, Journal of Applied Polymer Science: Applied Polymer Symposia, 7, 3 (1968).
6. J. Kaczaj and R. Trickey, Analytical Chemistry, 41, 1511 (1969).
7. Anon., "The Score on Weatherability", Modern Plastics, 44, 86 (1967).



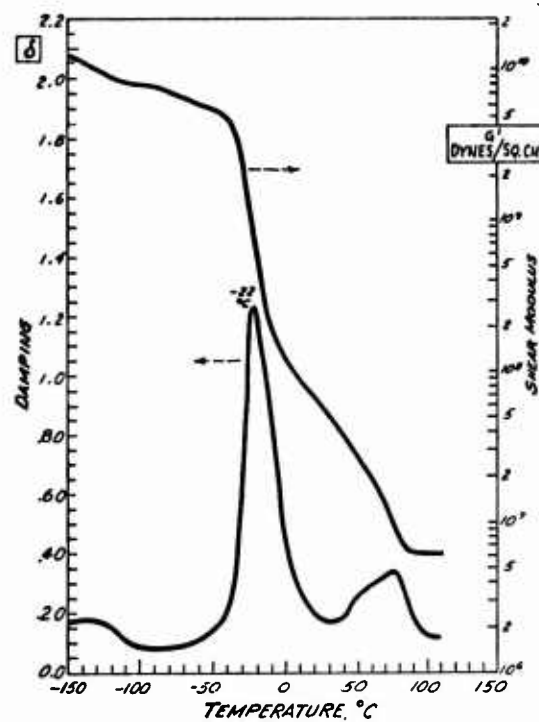


FIG. 1 MECHANICAL SPECTRUM OF EVA COPOLYMER

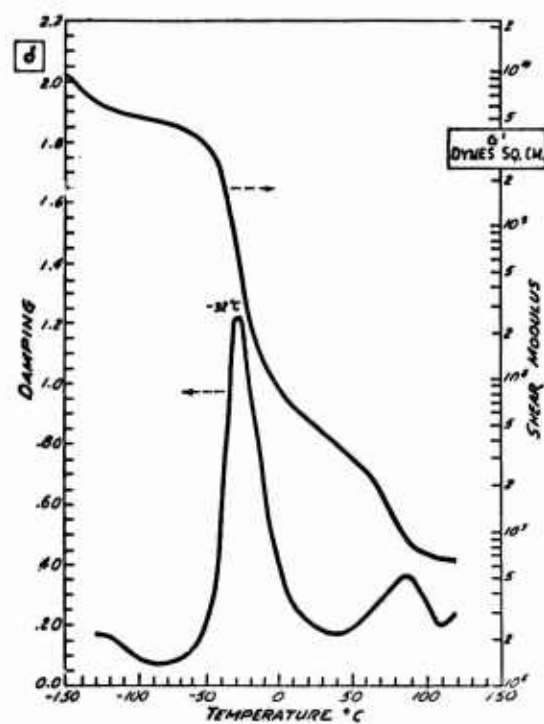


FIG. 2 MECHANICAL SPECTRUM OF EIBA COPOLYMER

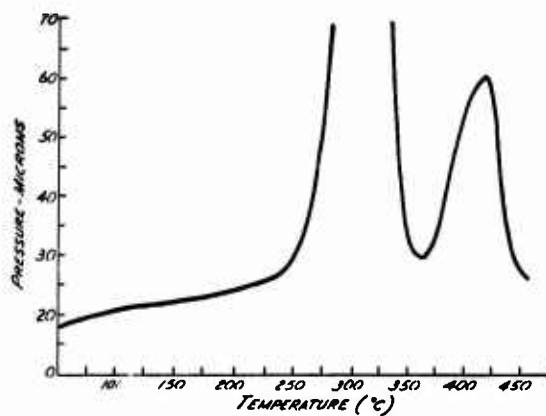


FIG. 3 THERMAL VOLATILIZATION ANALYSIS OF EVA COPOLYMER

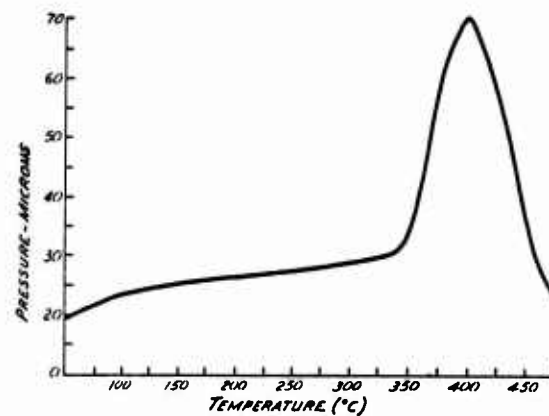


FIG. 4 THERMAL VOLATILIZATION ANALYSIS OF EIBA COPOLYMER

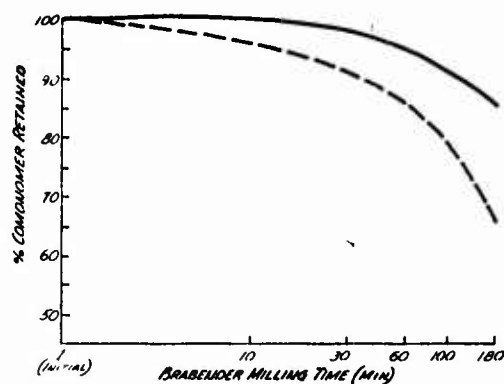


FIG. 5 COMONOMER RETENTION IN MILLED SAMPLES (---EVA Compound, —EIBA Compound)

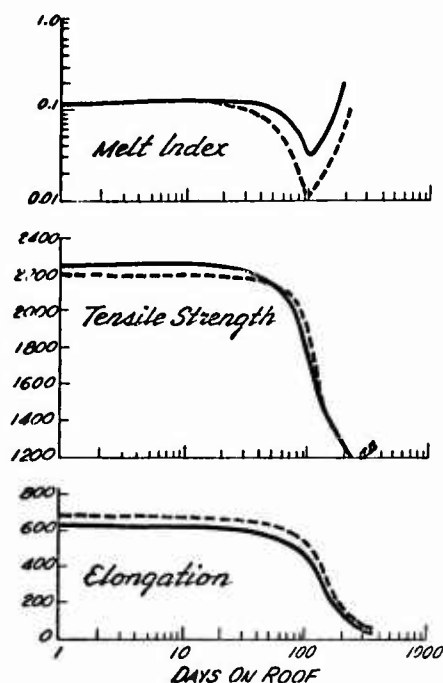


FIG. 6 ROOF AGING RESULTS (---EVA Compound, —EIBA Compound)



Sherman Kottle is Research Manager of the Specialty Products Laboratory, Olefin Plastics Department, of Dow Chemical U.S.A. He received the Ph.D. degree in chemistry from the University of Texas (Austin) in 1954.



Bernie McAda is the Supervisor of chlorinated solvents laboratories in the Texas Division Production Department of Dow Chemical U.S.A. He is the holder of a B.S. in chemistry from Lamar University conferred in 1964.

OXIDATIVE STABILITY STUDIES ON CELLULAR HIGH DENSITY  
POLYETHYLENE INSULATION FOR COMMUNICATIONS WIRE

D. D. O'Rell and A. Patel

CIBA-GEIGY CORPORATION  
Ardsley, New York 10502

SUMMARY

The effects of chemical blowing agents on the thermal oxidative stability of high density polyethylene (HDPE) in contact with copper have been examined. The initial phase of the study was designed to isolate the effect of the blowing agent from other variables associated with cellular insulation. This was accomplished by blowing various HDPE formulations in a controlled manner, removing the cell structure by milling and then preparing solid copper screen laminate samples containing no visible voids. Using these samples, it was found that virtually all blowing agents when used at 0.5% caused a significant reduction in the 200°C DTA induction times compared to similar formulations containing no blowing agents. The detrimental effect could be overcome by increasing the concentration of the antioxidant. In the second phase of the study, the performances of various stabilizer systems were examined using both cellular and solid HDPE insulated wire. In this phase of the study, the solid HDPE insulated wire was more thermally oxidatively stable than the cellular insulated wire containing the same stabilizer package. The thermal oxidative stability of the chemically blown HDPE wire insulation was improved by increasing the antioxidant concentration. The use of MDA-1 alone offers a viable alternative to the present multi-component systems.

INTRODUCTION

Within the last few years, there has been an increasing emphasis placed on developing the necessary technology, equipment, etc., for the production and use of cellular insulation. The recently witnessed raw material shortages and the subsequent price increases for polyolefins, particularly high density polyethylene, and in addition to other factors including improved electrical properties, have tended to accelerate the development of cellular insulation.

Despite the increasing emphasis on producing and installing cellular insulation, only limited data have been published comparing the relative stabilities of cellular insulation versus the presently used solid insulation. Recent published data<sup>1</sup> indicates that expanded HDPE insulation has a much lower DTA induction time than solid HDPE insulation when evaluated in the presence of copper. Also, 120°C oxygen uptake data<sup>2</sup> shows expanded HDPE insulated wire to be inferior to solid HDPE in thermal stability. These above findings can be well supported by our results which show that expanded HDPE insulation is less stable than solid HDPE insulation. The actual cause of lower stability of expanded HDPE insulation or the mechanism of chemical changes, if any, is unknown. However, one may postulate that the lowered stability of HDPE insulation may be due to the interaction of free radicals, generated by the blowing agent, with the polymer or with the antioxidant in an oxidizing mode and thereby introduce oxidation initiators and/or reduced the antioxidant concentration. It is also conceivable that trace decomposition products of the blowing agent could serve as oxidation initiators.

Previous work<sup>3</sup> has shown that the decomposition of azodicarbonamide at 190°C in paraffin oil yielded 34% gaseous products, 27% urazole, 34% biurea and 5% cyanuric acid. It is not entirely clear what effect the residual solid by-products would have on the

thermal stability of expanded HDPE insulation, but it has been suggested that they may also contribute to the instability of cellular HDPE.

EXPERIMENTAL

PREPARATION OF COPPER SCREEN LAMINATES

Procedure A - The specified stabilizer system plus 0.1% dioctylphthalate, 0.5% zinc oxide and 0.5% blowing agent were incorporated into a minimally stabilized wire grade high density polyethylene (DuPont 5496) by milling on a two-roll mill at 149°C (300°F) for 5 minutes. The milled stock was cut into 25 gram pieces, placed in a 10.2 cm x 10.2 cm x 0.32 cm (4" x 4" x 0.120") mold and heated in a compression mold at 232°C (450°F) for 5 minutes to effect blowing of the resin. The foamed resin was remilled at 149°C (300°F) for 5 minutes to remove the cell structure and the void-free stock was compression molded at 193°C (380°F) into void-free 0.03 mm (10 mil) thick films. The copper screen laminates were prepared by compression molding clean copper screen between two 0.03 cm thick polyethylene films at 193°C (380°F) for 3 minutes.

Procedure B - The specified stabilizer system (0.1% Antioxidant-1 + 0.1% MDA-1) and indicated decomposition product were incorporated into a minimally stabilized wire grade high density polyethylene (DuPont 5496) by milling on a two-roll mill at 149°C (300°F) for 5 minutes. The milled stock was compression molded at 232°C (450°F) for 5 minutes, re-milled as above and compression molded again at 193°C (380°F) into 0.03 mm (10 mil) thick films as indicated in Procedure A above. The copper screen laminates were prepared by compression molding clean copper screen between two 0.03 mm thick polyethylene films at 193°C (380°F) for 3 minutes.

PREPARATION OF INSULATED WIRE SAMPLES

Initial Compounding: The specified stabilizer system plus 1% titanium dioxide were dry blended into a minimally stabilized wire grade high density polyethylene (DuPont 5496) and extruder compounded at 199°C (390°F) to yield pellets approximately 3 mm in diameter by 3 mm long.

Solid HDPE Insulated Wire: The pellets obtained above were extruder coated onto 22 AWG copper wire using a 25 mm (1") 24:1 L/D extruder equipped with a constant pitch gradual transition metering screw and a wire coating crosshead.

The crosshead temperature ~254°C (490°F) was maintained. The speed of the wire coating line was 39 meters (130') per minute. The wire was pre-heated using a hot air gun at 260°C (500°F) to assure adequate adhesion. The thickness of the solid HDPE insulation was 0.35 mm (14 mil) thick.

**Expanded HDPE Insulated Wire:** The pellets obtained as above were dry blended with 0.5% Celogen AZNP-130 and extruder coated onto 22 AWG copper wire using the same extruder as described above. The wire coating cross-head was maintained at 210°C (410°F) and 197 kg/cm<sup>2</sup> (2800 psi) pressure. The speed of the wire coating line was 27 meters (90') per minute. The copper wire was preheated using a gas flame to assure proper adhesion. The cellular coating on the wire was 0.35 mm (14 mil) thick.

#### TESTING PROCEDURES

**Differential Thermal Analysis:** Circular samples of copper screen laminates or short length of wire which could be easily fitted into the DTA dishes were cut in a reproducible method. The samples were placed in aluminum pans, positioned in the cell and heated to 200°C under nitrogen. Oxygen was introduced when the samples equilibrated at 200°C and the time to exotherm was measured. The results were run in duplicate.

**Petroleum Jelly Exposure:** Wire samples 30 cm (12") long were dipped into Witco 13C petroleum jelly maintained at 115°C (239°F) for one second. The samples were oven aged for 10 days at 70°C (158°F), wiped free of all petroleum jelly and formed into pig tails.

**Oven Aging at 120°C (248°F):** The copper screen laminates or pigtailed wire samples were oven aged at 120°C (248°F) and visually examined daily for embrittlement, cracking or decomposition. The failure times are based on the results of five replicates.

#### DISCUSSION

In the first phase of this study, an attempt was made to isolate the chemical effect(s) of blowing agents on the performance of selected stabilizer systems from the physical factors which could effect the thermal stability of cellular insulation, e.g., cell structure, percent voids, uniformity of cell size, and also from the effect of petroleum jelly exposure. This was accomplished by milling the additives in HDPE, blowing the resin under controlled conditions, removing the cell structure by milling a second time and then preparing copper screen laminate samples. The differential thermal analysis (DTA) data in Table 4 indicates that the use of 0.5% of reagent grade azodicarbonamide as a blowing agent reduces the DTA induction time. Interestingly, all blowing agents evaluated, gave very nearly the same DTA value, which was considerably lower than the DTA times for the samples containing no blowing agent (Table 5). The reduction in the DTA induction times does not appear to be restricted to azodicarbonamide compounds since the same effect was also observed with sulphonylhydrazides or hydrazide based blowing agents as well.

Earlier publications<sup>1</sup> suggested the solid decomposition by-products of azodicarbonamide could be responsible for the reduced thermal stability of cellular insulation. However, the data in Table 6 suggests that these products have little effect on thermal stability as measured by oven aging at 120°C, when evaluated singly and in the absence of any blowing agent. An additional point suggesting that the decomposition products are not significant is the observation that sulphonylhydrazide based blowing agents have the same effect as azodicarbonamide but do not yield the same solid by-products.

The adverse effects of azodicarbonamide on the thermal stability of the copper screen laminate samples can be compensated for by increasing the antioxidant concentration as shown in Table 7. In this instance, the addition of 0.1% Antioxidant-1 to the initial system containing 0.1% Antioxidant-1 and 0.1% MDA-1 doubled the DTA induction time and was comparable to the control containing no azodicarbonamide. Increasing the antioxidant concentration to 0.3% more than tripled the DTA induction time compared to the original value of 25 minutes.

The second phase of this study involving wire prepared in-house again showed the detrimental effect of azodicarbonamide on both DTA induction time and oven aging life-time at 120°C. The data presented in Table 8 show a very close correlation with the results obtained earlier using the copper screen laminates. Again the thermal stability of the cellular insulation is about one-third that of the solid insulation and that the DTA induction time can be improved by increasing the antioxidant concentration. The sample of commercially prepared wire which was included in this study was considerably less stable than any of the samples prepared in-house. This wire has not been characterized in terms of stabilizer system, blowing agent, etc. The performance of MDA-1 alone as both antioxidant and metal deactivator appears to have special merit.

Present indications suggest the use of cellular insulation will be restricted to petroleum jelly filled cables. Previous work has shown the thermal stability of either solid or cellular insulated wire was reduced when the wires were exposed to petroleum jelly. This was also observed in this program as shown in Table 9. The two main points to be derived from the data in Table 9 are (1) cellular insulation is less stable than solid insulation and (2) exposure to petroleum jelly reduces thermal stability. The use of higher levels of antioxidant improves the stability of the system both before and after petroleum jelly exposure. The use of 0.2% MDA-1 appears to offer a good alternative to the present two component systems (antioxidant + metal deactivator).

The concentration/performance profile for MDA-1 presented in Table 10 indicates that 0.2% is a very viable concentration level, while 0.1% MDA-1 is probably too low a concentration to be useful.

In the course of this study, many other stabilizer systems were evaluated by both DTA and oven aging at 120°C and the failure times are plotted in Figure 1. An analysis of these points using a least squares linear equation shows there is a very poor correlation between these two tests. The full implications of this observation have not been investigated, but it would suggest that DTA induction times for new stabilizer systems should not be the sole criteria for evaluating a new stabilizer system.

#### CONCLUSIONS

1. The thermal stability of high density polyethylene insulation is reduced when a blowing agent is added to the system.
2. The adverse effect of the blowing agent on the thermal stability of cellular HDPE can be overcome by using higher levels of antioxidant.

3. The use of MDA-1 alone, at about 0.2%, offers a viable alternative to the present two component stabilizer systems and appears to be less sensitive to petroleum jelly exposure than the two component systems.
4. The use of DTA induction time does not appear to be a viable method for estimating the performance of new stabilizer systems and other tests should be used to establish performance.

#### ACKNOWLEDGMENTS

A special acknowledgment is given to Dr. Peter Klemchuk for his guidance throughout this study.

We would like to express our sincerest thanks to Mr. John Windus, who performed most of the experimental work and to Mrs. Mary Trojak, whose help in preparing the manuscript was invaluable.

#### REFERENCES

- 1 - M. Robinson, Society of Plastics Engineers, Tech. Papers, Vol. XXI, p. 390 (1975).
- 2 - B. D. Gesner and R. J. Harmel, *ibid*, 286 (1975).
- 3 - R. A. Reed, British Plastics, October 1960, p. 470.

#### ADDITIVES USED IN THIS STUDY

Antioxidant 1: Tetrakis[methylene-3(3',5'-di-tert-butyl-4-hydroxyphenyl)propionate]/methane.

Antioxidant 2: Thiodiethylene bis(3,5-di-tert-butyl-4-hydroxy)hydrocinnamate.

MDA 1: N,N'-Bis(3,5-di-tert-butyl-4-hydroxy-hydrocinnamoyl)hydrazine.

MDA 2: N,N'Dibenzal oxalyldihydrazide.

Blowing Agent 1: Fical EP-A

Blowing Agent 2: Fical EP-D

Blowing Agent 3: Celogen AZ-130

Blowing Agent 4: Celogen AZNP-130

Blowing Agent 5: Celogen AZ-199

Blowing Agent 6: Celogen CB

Blowing Agent 7: Celogen RA

#### BIBLIOGRAPHY

D. O'Rell

Dr. Dennis O'Rell received his B.S. degree in Chemistry from California State University in 1964 and his Ph.D. in Organic Chemistry from the University of Oregon, Eugene, Oregon in 1970. He has worked as a Laboratory Supervisor in Polymer Additives Department, Plastics and Additives Division of CIBA-GEIGY CORPORATION for four years.

A. Patel



Mr. A. Patel received his B.S. degree in Dyes and Intermediates Technology from the University of Bombay (India) in 1965 and his M.S. in Polymer Science from the University of Akron in 1969. He is now a research and development chemist, working on polymer stabilization in the Polymer Additives Department, Plastics and Additives Division of CIBA-GEIGY CORPORATION.

Mr. Patel is a member of the American Chemical Society and the Society of Plastics Engineers, Inc.

Table 1

Effect of Copper on DTA Times of Experimental Expanded and Solid HDPE Insulations<sup>1</sup>

<u>Samples</u>	<u>200°C t* AL, Min. Conductor In</u>
Solid HDPE/0.1% IRGANOX 1010/0.1% OABH	30
Expanded HDPE/0.1% IRGANOX 1010/ 0.1% OABH/0.8% Fical	5
Expanded HDPE/0.1% IRGANOX 1010/ 0.1% OABH/0.6% Kempore	15

\* Average of 3 Samples

<sup>1</sup> - M. Robinson, Society of Plastics Engineers, Technical Papers, Vol. XXI, 390 (1975).

Table 2

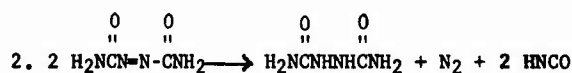
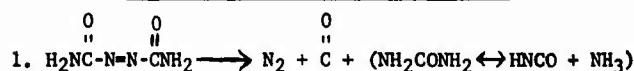
Hours to Failure for Petrolatum Treated Wires  
Exposed to Oxygen at 120°C<sup>2</sup>

	Petrolatum Treated		
	Untreated	Witco #12 + 0.2% AC B	Witco #12 + 0.2% AO C
Solid High Density Polyethylene	1886	616	814
Cellular Expanded High Density Polyethylene	872	102	504

2 - B. D. Gesner and R. J. Harmel,  
Society of Plastics Engineers,  
Technical Papers, Vol. XXI,  
286 (1975).

Table 3

Decomposition of Azodicarbonamide



The non-gaseous fragments of the decomposition of the  
azodicarbonamide recombine to form the following  
identified compounds:

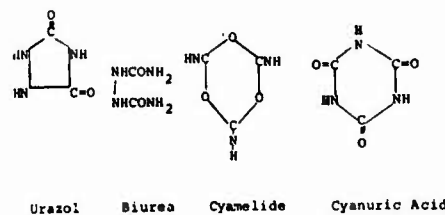


Table 4

Effect of Blowing Agent on Thermal Stability of  
Copper Screen Laminates (No PJ Exposure)

Stabilizer System	200°C DTA Induction Time* (Min.)	
	No Blowing Agent	0.5% Azodicarbonamide (Reagent)
0.1% Antioxidant-1 + 0.1% MDA-1	60	25
0.1% Antioxidant-1 + 0.1% MDA-2	34	25
0.1% Antioxidant-2 + 0.1% MDA-1	48	19
0.1% Antioxidant-2 + 0.1% MDA-2	30	18

\* Averages of two replicates

Table 5

Effect of Various Blowing Agents on 200°C DTA  
Induction Times for HDPE -  
Copper Screen Laminates<sup>a)</sup> (No PJ Exposure)

0.1% Antioxidant-1 + 0.1% MDA-1	200°C DTA Induction Time <sup>b)</sup> (Minutes)
No Blowing Agent	60
Azodicarbonamide (Reagent Grade)	25
Blowing Agent 1	13
Blowing Agent 2	19
Blowing Agent 3	24
Blowing Agent 4	21
Blowing Agent 5	25
Blowing Agent 6	26
Blowing Agent 7	26

a) Prepared by Procedure A

b) Averages of two replicates

Table 6

Effect of Solid Decomposition Products of  
Azodicarbonamide on Thermal Stability  
of Copper Screen Laminates<sup>a)</sup>

0.1% Antioxidant-1 + 0.1% MDA-1 +	Hours to Embrittlement <sup>b)</sup> at 120°C
None	2400+
0.25% Urazol	2400+
0.25% Biurea	2400+
0.25% Cyanuric Acid	2400+

a) Formulation does not contain  
dioctylphthalate or zinc oxide.

b) Averages of two replicates



Effect of Increasing Antioxidant Concentration  
on Thermal Stability of Copper Screen Laminates<sup>a)</sup>  
(No PJ Exposure)

a) Prepared by Procedure A  
b) Averages of two replicates

### Effect of Blowing Agent on the Thermal Stability of HDPE Insulated Wire (No PJ Exposure)

\* Averages of two replicates

### Effect of Blowing Agent on Thermal Stability of Cellular HDPE Insulated Wire

\* Averages of five replicates

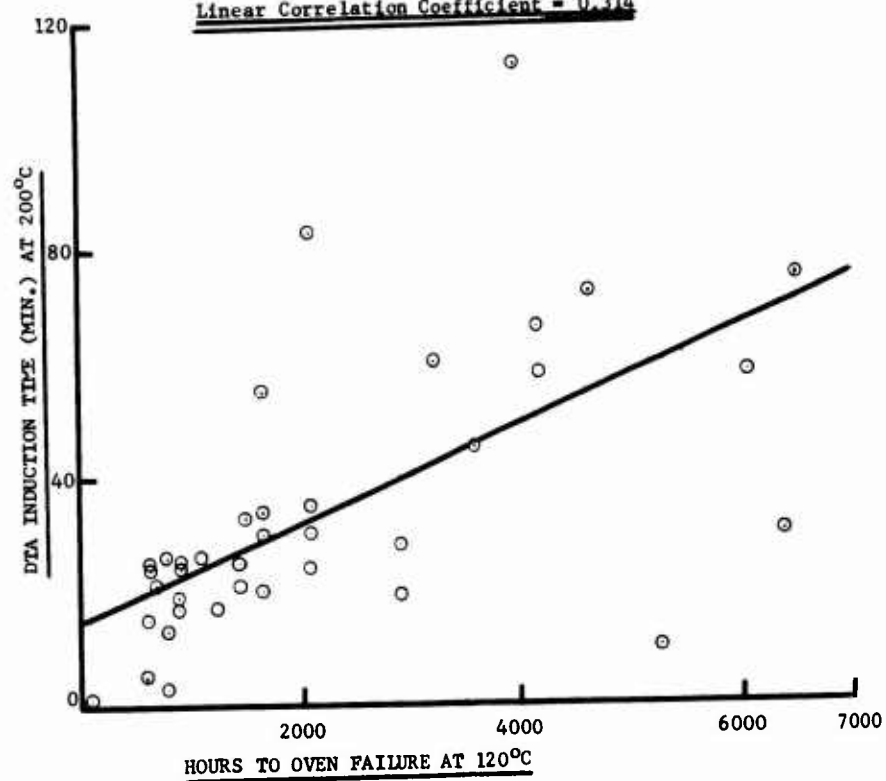
### Concentration/Performance Profile for MDA-1 in Cellular HDPE Insulation

\* Averages of five replicates

FIGURE 1

Correlation Between Induction Time at 200°C and  
Oven Aging Failure at 120°C

Linear Correlation Coefficient = 0.314



## THE BARE BASE ELECTRICAL SYSTEM

JOHN E (JACK) WIMSEY  
USAF Ground Equipment SPO  
Aeronautical Systems Division  
Wright Patterson Air Force Base Ohio

### ABSTRACT

The Air Force Bare Base program amounts to an instant, do-it-yourself Air Base, deployable anywhere in the world. It provides the air mobile equipment and facilities for operation of five squadrons, up to 4500 men, in 72 hours. The Bare Base electrical system is the first known air mobile system having high voltage generation and transmission (primary) and a transformed low voltage (secondary) distribution at the using points. It features a "hard wire" equipment safety grounding conductor from the generator to the very last piece of using equipment. The primary or high voltage portion is 4160V, three phase-three wire-grounding 60Hz and the secondary or low voltage portion is 120/208V three phase-four wire-grounding-60Hz. This electrical system meets all requirements of the National Electric Code and OSHA for mobile systems and equipment. It provides maximum standardization of equipment and operation while providing maximum flexibility of layout and capacity. There are practically no fixed distances in the layout. Two lengths of one size cable and one length of a second size cable replaced 14 sizes and over 67 lengths of cables previously used. The system utilizes approximately 98 miles of high voltage cable; 93 miles of 60-amp 4 conductor type G secondary cable; 20,550 60-amp connectors; 0.4 miles of 200-amp 4 conductor type G secondary cable; and 412 200-amp connectors. The cables are all industry standard, and the connectors are military standard.

### INTRODUCTION - BARE BASE

The Air Force Bare Base Program amounts to an instant, do-it-yourself air base deployable anywhere in the world. The concept of a "Bare Base" is not new. The Air Force has had to operate from essentially unprepared sites in every conflict. We then put in a massive and expensive effort to construct or upgrade the facility to minimum livability. This has left concrete and steel monuments to our construction skill many places in the world.

Over the years, the aircraft, armament and support equipment was becoming increasingly more complex, requiring more highly skilled personnel and greatly increased standards for operations, maintenance and housekeeping. Rapid deployment of these sophisticated systems to remote areas of the world, for limited periods of time, was envisioned more and more as a necessary capability. The DOD budgets would no longer permit large expenditures for construction of conventional facilities in a foreign land which would be used for a short period of time and then abandoned. The earlier attempts to provide air mobile facilities were unsuccessful.

With these considerations, in 1965, a new program was initiated to develop an air mobile system for support of modern tactical fighter aircraft. It was designated the Bare Base Program because of the proposed use of "Bare Bases" throughout the world - for build-up into complete tactical operating installations. The system was to rotate Newton's Law - "What goes in, comes out".

The Bare Base concept starts with runway, aircraft parking area, a source of water, and nothing else as shown in Figure 1. Over 1000 sites meeting these criteria exist all over the world. The Bare Base Equipment System provides the relocable, air transportable equipment and facilities to convert this site into a fully functioning air base supporting operational missions within 72 hours of the first cargo aircraft touchdown as shown in Figure 2. It has a capacity for Five Squadrons and 4500 men. The system provides everything from "Abodes to Commodes", i.e. shelters, utilities, environment control, vehicles, medical, food service and airfield lighting. The system is a flexible, building block type which can be varied according to the location where it is to be deployed, the mission to be performed and duration of the deployment. The Bare Base Equipment may be used globally, in all seasonal environments and related climatic conditions within the temperature range of minus 25°F to plus 125°F. All equipment is designed for transport in C-130 aircraft. It may also be transported by truck, rail or ship.

The backbone of the Bare Base Equipment System is the four standardized shelters shown in Figure 3. The base of all the shelters or their shipping containers forms a 463L Pallet for use in the 463L Materials Handling System (Aircraft Roller Conveyor Materials System). Approximately 1000 shelters, in various combinations are used for a full Five Squadron Deployment.

### BARE BASE ELECTRICAL SYSTEM

An Air Mobile Electrical System meeting the requirements for Bare Base did not exist. If 120/208 Volt Diesel Engine Generator Sets were used, a fully deployed Bare Base would have required over 250-200 KW sets. At an airlift capability of four per C-130 aircraft load, this approach was quickly discarded. The only 2400/4160 Volt Generators in existence were beyond airlift capability of any aircraft. The Bare Base Program therefore designed the following system:

#### System Description.

The Bare Base electrical system is an air mobile system having high voltage generation and transmission (primary) and a transformed



FIGURE 1. BARE BASE SITE

low voltage (secondary) distribution at the using points. It is the heart and blood supply of the Bare Base. It features a "hard wire" equipment safety grounding conductor from the generator to the very last piece of using equipment. The primary or high voltage portion is 4160V, three phase-three wire-grounding-60Hz and the secondary or low voltage portion is 120/208V, three phase-four wire-grounding-60Hz. This electrical system meets all requirements of the National Electric Code and OSHA for mobile systems and equipment. The Bare Base electrical system consists of the following:

- a. High voltage generators
- b. Primary Distribution System (High Voltage) consisting of:
  1. Power distribution and control stations known as contactor control cubicles (CCC)
  2. Primary power distribution cables
  3. Primary Power Cable Reel Pallets
- c. Secondary Distribution System (Low Voltage) consisting of:

1. Transformer/Distribution boxes known as secondary distribution center (SDC)
2. Mission Essential Power Generators (MEP)
3. Secondary Power Cable Assemblies
4. Mission Essential Power (MEP) Cable Assemblies
- d. Remote area lighting sets (RAL)

The Bare Base electrical system is diagrammed in Figure 4. An examination of this diagram shows that although the generators are three phase 2400/4160V, wye-connected, the power is transmitted in delta using only the 4160V portion to the primary side of the SDC. A further examination of the diagram shows that the equipment safety ground is continuous from the generator through to the last piece of using equipment in a shelter. Note that ground rods are used only at the generators, CCCs and SDCs. Studies have shown that additional ground rods do not provide additional reliability, and since this Bare Base electrical system is designed for world-wide operation, this "hard wire" grounding provides the highest possible degree of safety

## BARE BASE SYSTEM



### LEGEND:

- |                            |                                |
|----------------------------|--------------------------------|
| 1 Refueling Site           | 8 Food Service Complex         |
| 2 Hospital                 | 9 Base Maintenance Vehicles    |
| 3 Personnel Shelters       | 10 Latrine                     |
| 4 Aircraft Hangar          | 11 Electrical Power Generation |
| 5 General Purpose Shelters | 12 M-Series Vehicles           |
| 6 Maintenance Shelters     | 13 Water Plant                 |
| 7 Billets                  |                                |

FIGURE 2 - BARE BASE EQUIPMENT DEPLOYED

# BARE BASE SHELTER SUMMARY

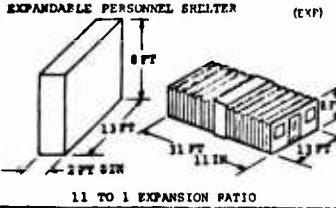
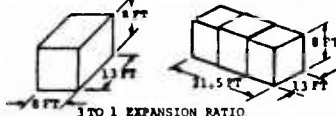


SHELTER PICTURE		CONSTRUCTION	FUNCTION	WEIGHT	REMARKS	ERECTION TIME
SHIPPING	EXPANDED					
		<b>Expandable Wall -</b> Polyvinyl Chloride Coated Kraft Paperboard Sandwich With a Urethane Foam Core  <b>End Walls -</b> Fiberglass Skins With Impregnated Balsa Core  <b>Center Section &amp; Floor -</b> 1/8" Aluminum Skin/Paper Honeycomb Core Sandwich Panel	Administration Office  Billeto  Food Preparation & Storage  Aircrew Alert  Aircrew Operations	Empty-28500  Payload-15000  Total-43500	Airlift-9 Per C-130  The Base of 3 Shelters Form A 463L Pallet	4 Manhours
		<b>Walls, Ceilings, &amp; Floors</b> 1/8" Aluminum Skin/Paper Honeycomb or Foam Core Sandwich	Aircraft Maintenance, Base Maintenance  Kitchen  Latrine	Empty-40000  Payload-85000  Total-12,5000	Airlift 3 Per C-130  Base Is a 463L Pallet	4 Manhours
		<b>Modular Design:</b> Double Hinged Aluminum Beams  <b>Panel -</b> 1/8" Aluminum Skin With Paper Honeycomb Core Sandwich	Storage  Laundry  Dining Hall  Chapel  Briefing Facility  AGE Maintenance	Empty-10,0000  Payload-0  Total-10,0000	1 Shipping Container  Airlift - 1 Per 463L Pallet  4 Per C-130	100 Manhours
		Same as General Purpose Shelter With Interchangeable Parts	Aircraft Maintenance  Weapons Loading  Jet Engine Shop  Vehicle Maintenance	Empty-36,0000  Payload-0  Total-36,0000	Airlift - 1 Per C-130  4 Shipping Containers  Containers Form Entrances	300 Manhours

FIGURE 3.

in installation and use for a mobile electrical system. The primary portion is shown in Figure 5 and the secondary portion is shown in Figure 6. There are no fixed distances to the system, it can be varied to fit any site. The Bare Base Electrical system is capable of accepting 4160V base or commercial power at the CCC's or SDC's. The SDC's can also accept 120/208V-three phase-4 wire-60Hz power and distribute to the shelters or using equipment. The Bare Base Electrical System as well as all Bare Base equipment used standardized terminal identification and wire color coding as follows:

Gen. Term. Mark-ing	Term. or Contact	Cond-uctor Circuit	Wire Color
L <sub>1</sub>	A	Phase A	Black
L <sub>2</sub>	B	Phase B	Red
L <sub>3</sub>	C	Phase C	Blue
L <sub>0</sub>	N	Neutral	White
G (or Gnd)	G	Safety grounding	Green

## High Voltage Generators

The generator sets (Figure 7) are 750KW, 2400/4160V, three phase-four wire-60Hz gas turbine engine sets which are wheel mounted.

The sets are 96 inches wide, 98 inches high, 241 inches long and weigh 19,700 pounds.

The sets come complete with switch gear, controls, output power conductors (high voltage) and fuel hoses. The sets are powered by a continuous duty JP or diesel fueled gas turbine engine. The sets are fully enclosed, with weatherproof access panels to all areas. Each set is capable of operation under autonomous local or remote control, or units may be operated in multiples of two or more under local or remote control. The generator sets may be connected singly or in multiples of up to four to a common external fuel supply using a specially provided fuel manifold connection. The generator sets are connected to the electrical system through the CCCs using three separate 5KV, cross linked polyethylene (XLP) insulated #1/0 copper power conductors and one insulated #2 copper grounding conductor. The power and grounding conductors are stored in the generator sets for deployment and are installed manually. Although not shown in Figure 4, for parallel operation of two or more sets, it is normally required for stability that all of the generator neutrals be connected together with 5KV insulated #1/0 wire. The generator sets are towable by most Bare Base vehicles. The generator sets are air transportable in a C-130 aircraft and are type designated A/E24U-11. Five to eight generator sets provide the power for a 4500 man base without air conditioning. Fifteen to eighteen generator sets are used when the base is air



# BARE BASE ELECTRICAL SYSTEM

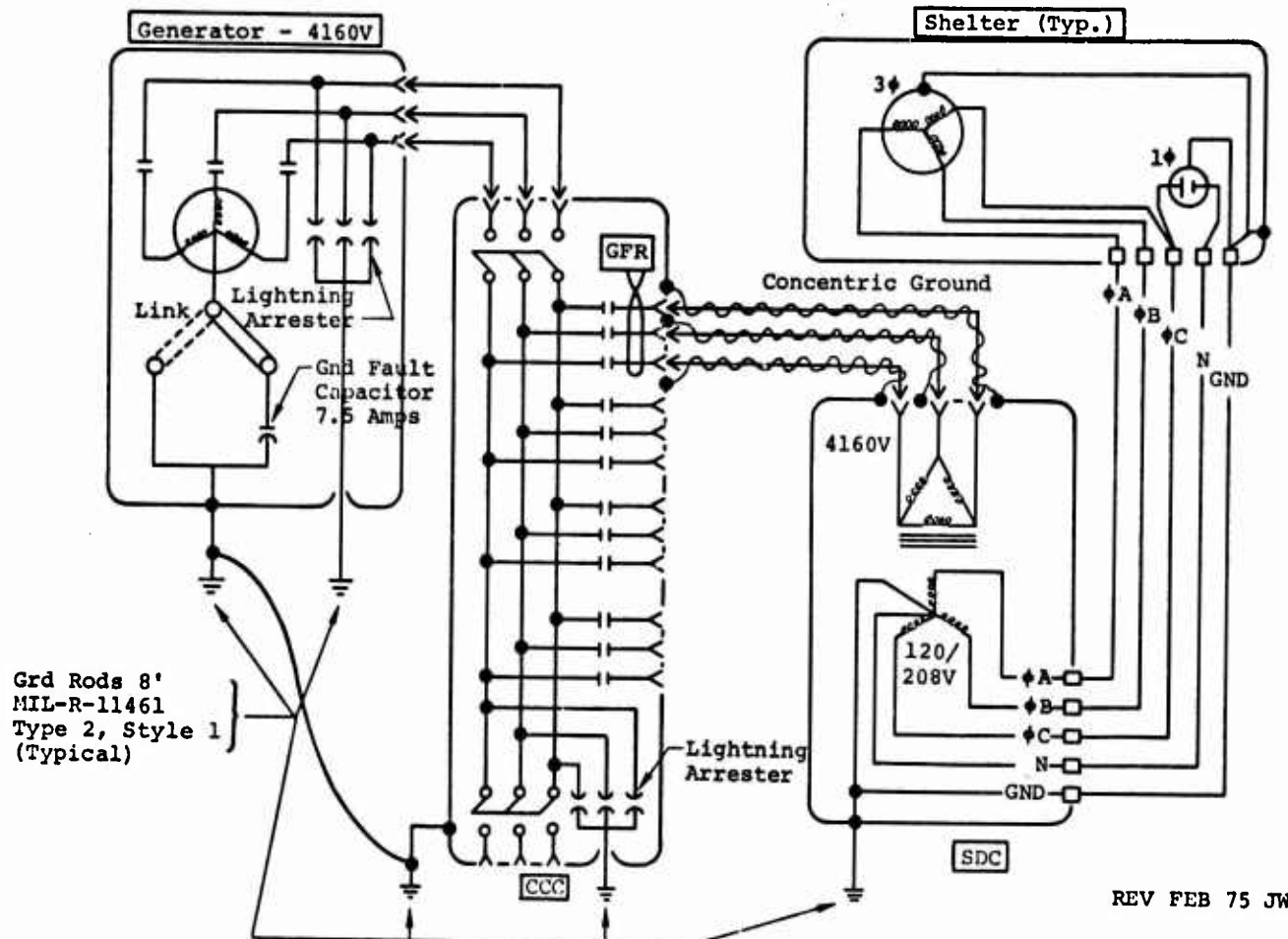


FIGURE 4.

conditioned.

## Primary Distribution System

The Primary Distribution System controls and transmits the 4160V power from the generators to the Secondary Distribution System as shown in Figure 5. It consists of the following components:

1. **Contactor Control Cubicle.** The contactor control cubicle (CCC) Figure 8 is a skidmounted, 4160V, three phase-three wire-60Hz power distribution and control station. The cubicle is 108 inches wide, 95 inches high, 45 inches deep and weighs 6340 pounds. Each CCC is equipped with four each fused three-phase contactors (electrically operated high voltage switches), connected to a common bus. Each end of the bus is provided with a mechanical disconnect switch. Each contactor is equipped with a relay to clear ground faults in the high voltage (primary) distribution system. Each contactor is provided with terminals for

connection of generators and/or primary distribution cables. For direct access to the bus, two sets of terminals are provided at each end. Contactors and the bus terminals may be used as power inputs or power outputs, permitting adaptation to local Bare Base requirements. The operator's station is tent protected. Numerous interconnection combinations are possible for power transfer between generators, CCCs commercial power sources, and Bare Base loads. Two control panels removed from generators may be mounted in a CCC: CCC panels are removable and may be installed with generator control panels in a separate equipment rack for remote operation. See Figure 9. The equipment rack is 85 inches wide, 70 inches high, 30 inches deep and weighs 850 pounds. An equipment rack will hold up to four generator and two CCC panels. For air transportability, one CCC fits a 463L pallet with capacity left for one equipment rack or other items. Two equipment racks will fit a 463L pallet.

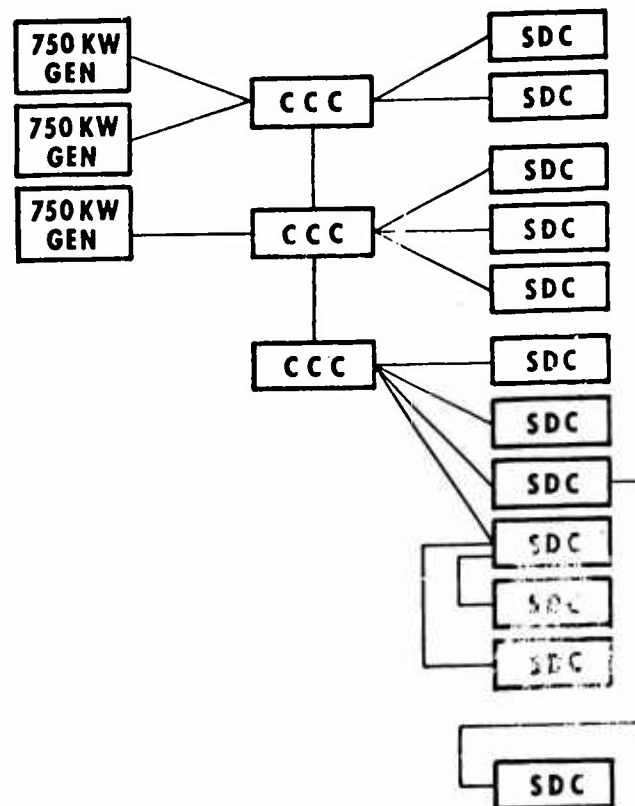


FIGURE 5. PRIMARY HIGH VOLTAGE GENERATION/TRANSMISSION SYSTEM, TYPICAL LAYOUT

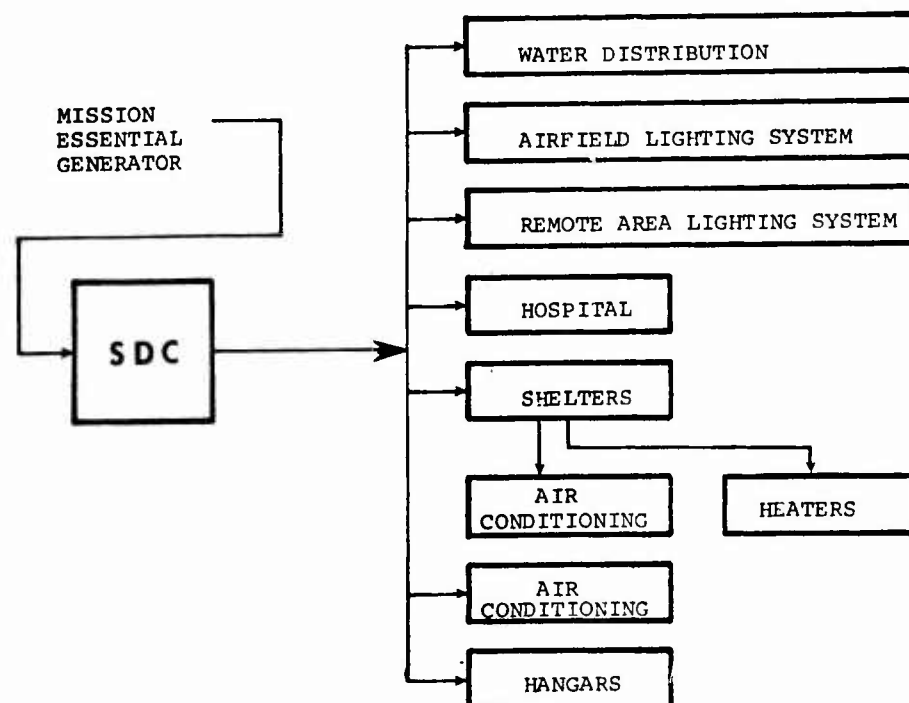


FIGURE 6. SECONDARY LOW VOLTAGE DISTRIBUTION SYSTEM COMPONENTS AND INTERFACES

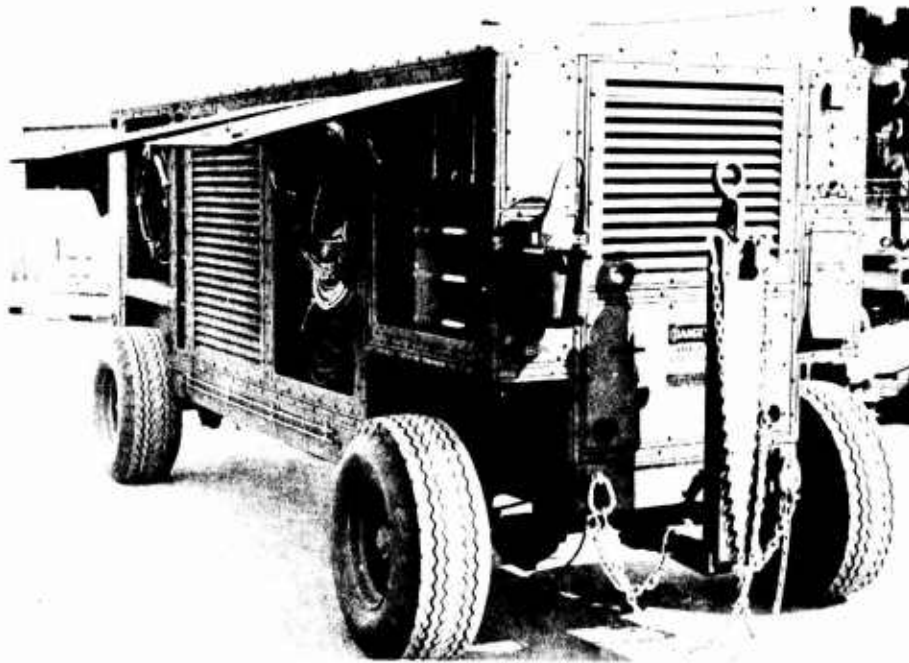


FIGURE 7. BARE BASE 750KW GENERATOR

2. Primary Distribution Cable. Primary distribution cables (high voltage) are used for transmission of power between CCCs and the SDCs. The original primary cable procured consisted of four separate #1/0 aluminum conductor cables rated 5KV and using cross linked polyethylene (XLP) insulation. Three are used as phase conductors and the fourth was used as a grounding conductor. These have been abandoned. The primary cables now provided consist of three separate #1/0 aluminum conductor cables rated 5KV, with XLP insulation and having a 1/3 concentric neutral serve. See Figure 10. The three conductors are used as the phase conductors and the three concentric neutrals are paralleled to serve as the equipment safety ground (also called the grounding conductor). If the deployment is for less than 30 days the primary cable may be left on top of the ground and would be removed on pull-out. For longer deployments and other special conditions, the cable is buried 18 to 24 inches deep. Buried cable is abandoned upon pull-out as cable damage, recovery effort and electrical checkout make it uneconomical to consider.

3. Primary Cable Reel Pallets. Primary cable reel pallets (see Figure 11) which are essentially cable reeling machines are used for storing, transporting and paying out of the primary cables. The cable reel pallets hold three reels, phase A, phase B and phase C for simultaneous payout. The cable reel pallets with reels are 84 inches long, 54 inches wide, 54 inches high and weigh 5000 pounds. Each reel holds approximately 3800 feet of cable. Two cable reel pallets fit on one 463L pallet for air shipment. For installation on deployments, the cable reel pallets are

mounted on a truck, forklift or other conveyance while cables are simultaneously payed out from all of the reels. When the end of a reel is reached, the cable is field spliced using standard commercial underground cable splices and the run is continued. If the cable has not been buried during the deployment, the cable reel pallets can be used for recovering the primary cable.

#### Secondary Distribution System

The secondary distribution system transforms the primary power to 120/208V - three phase-four wire-grounding-60Hz power and distributes it to the various load centers. It also provides Mission Essential power to critical loads. A typical load section of the secondary distribution system (Figure 6) is shown in Figure 12.

The original concept as tried in "Operation Coronet Bare" in Oct 1969 had the shelters surveyed out around the secondary distribution centers (SDC). The SDCs were sized to the load of the shelters. When air conditioners were used, an additional SDC was required and the air conditioners were connected to it. The secondary cables were sized to the loads, and were cut to length for the particular grouping. Fourteen different sizes and 67 different lengths of secondary cables were used. This resulted in the SDCs and the shelters, or other load type equipment, being dedicated to a specific grouping and having a very fixed location. Additionally, the secondary cables were wound on reels, the reels were numbered with the shelter and the SDC number and were then loaded on 463L pallets for airlift. Many aircraft loads of cable reels would arrive at a deployment and "Pandemonium

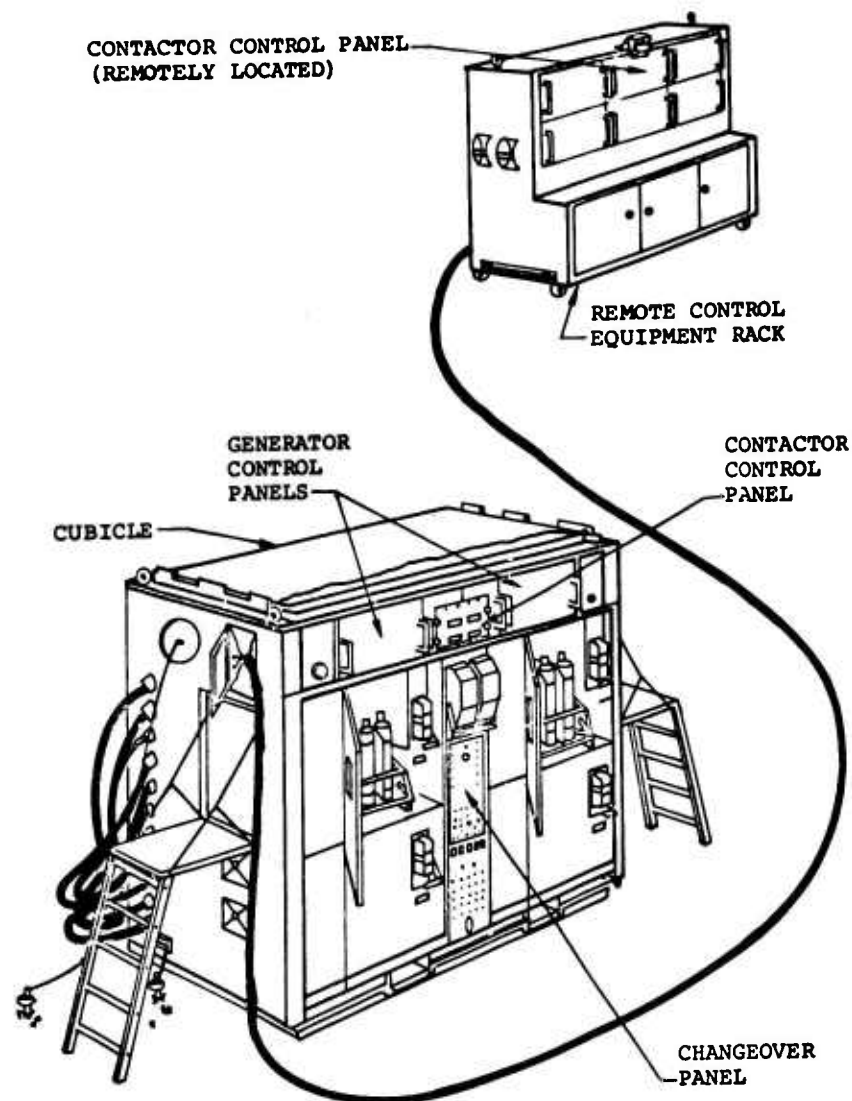
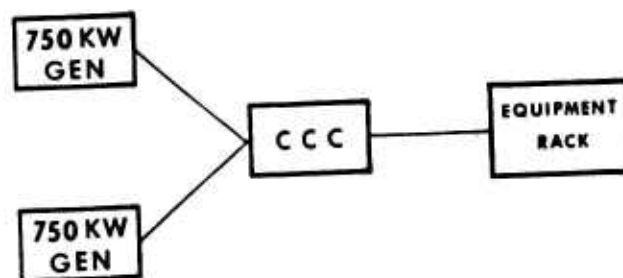


FIGURE 8. CONTACTOR CONTROL CUBICLE



GENERATOR CONTROLS  
MAY BE LOCATED AT:

1. GENERATOR
2. CCC
3. EQUIPMENT RACK

CCC CONTROLS MAY  
BE LOCATED AT:

1. CCC
2. EQUIPMENT RACK

FIGURE 9. GENERATOR AND CCC CONTROLS

# HIGH VOLTAGE CABLE

## STANDARD COMMERCIAL CABLE

- 5000 VOLT UNDERGROUND DISTRIBUTION
- 1/0 ALUMINUM CONDUCTOR
- 1/3 CONCENTRIC GROUND



FIGURE 10.

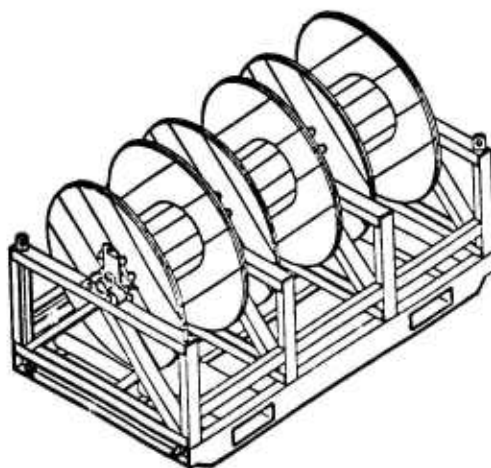


FIGURE 11. PRIMARY CABLE REEL PALLET

## SECONDARY DISTRIBUTION SYSTEM

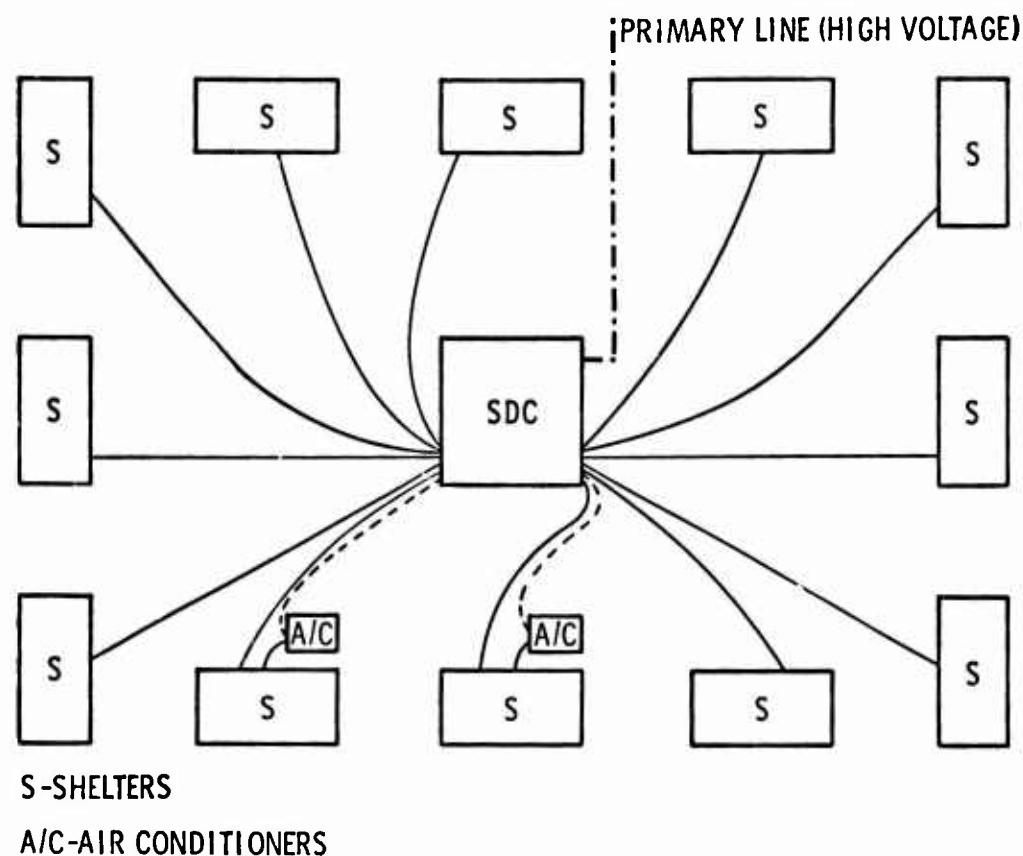


FIGURE 12.

Supreme" resulted with everyone looking for his particular cable reel.

Another problem surfaced as a result of the "Coronet Bare" test - the connectors for the secondary cables. The various shelters and equipment were being designed by different contractors or agencies, where the designers had a choice of male or female connectors with either pins or sockets. The end result was two male connectors, of the same manufacturer, facing each other or a male and female connector facing each other but both having sockets. The troops in the field soon fixed this by finding connectors that would mate, cut the cables and spliced them. There was not enough electrical tape, so a new type connector was developed as shown in Figures 13 and 14. The secondary distribution system was redesigned as follows:

a. All new SDCs were standardized in size and MIL-STD-Class L connectors were used.

b. Old SDCs were retrofitted with Class L connectors.

c. All new shelters and equipment were provided with Class L connectors.

d. All old shelters and equipment were retrofitted with Class L connectors.

e. All old secondary cables were scrapped.

f. New secondary cables were provided having two lengths in 60 amp 3 phase size and one length of 200 amp 3 phase size.

g. Class L power receptacles were provided on the shelters for the air conditioners so that they could be connected to the shelter or when needed, to the SDCs.

h. A fifty and a hundred foot 60 amp cable was placed in each shelter.

i. Two fifty and four one hundred foot 60 amp cables were stored in each SDC as spares.



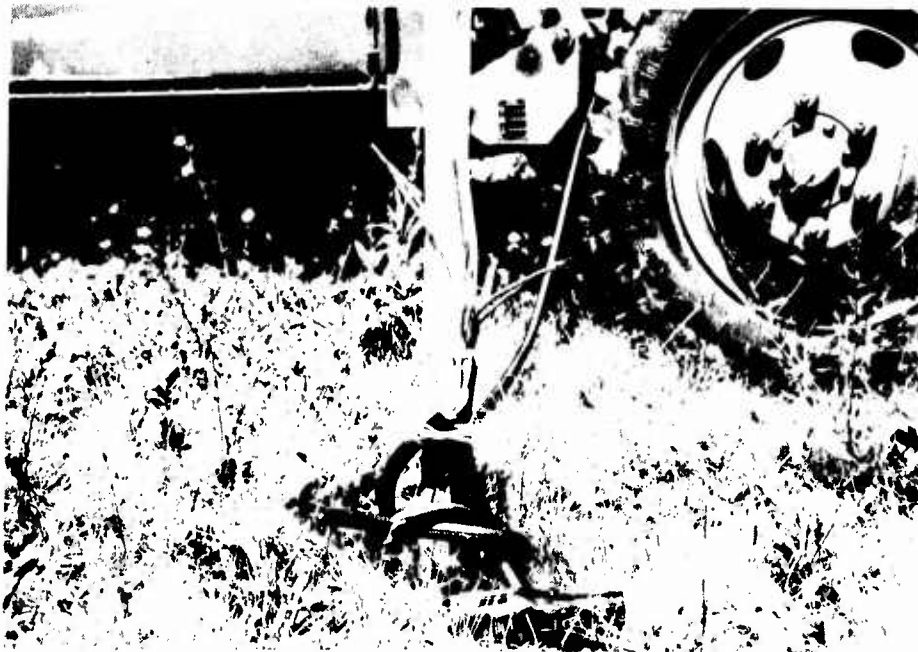


FIGURE 13. CABLE SPLICE - CABLE TIED AROUND STAKE,  
CONDUCTORS STRIPPED BACK - WIRES TWISTED TOGETHER



FIGURE 14. PEPSI-COKE CONNECTOR (MODEL 7UP)  
CABLE SPLICE USING SOFT DRINK BOTTLES AS INSULATORS

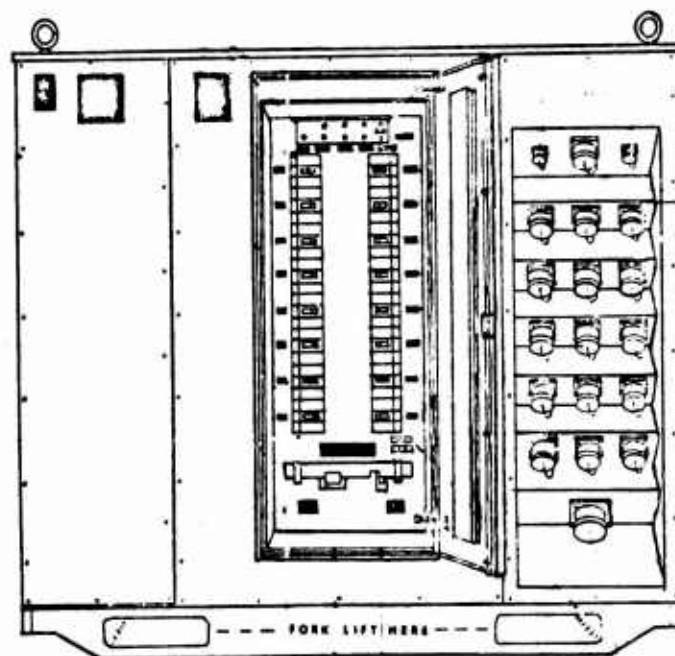


FIGURE 15. 150KVA SDC-OPERATING CONTROLS AND INDICATORS

The revised secondary distribution system as shown in Figure 12 allowed the shelters to be set out by the forklift operator and required only one standard SDC even with air conditioning. The air conditioners were connected to the shelter unless the load exceeded 60 amps in which case spare cables from the SDC were used to connect the air conditioner directly to the SDC. If a shelter was positioned too far from an SDC, one of the spare cables could be connected to the cables from the shelter and the power could be provided to that shelter. This revised system provided maximum flexibility as shelters and SDCs were no longer dedicated, there were no fixed distances, there were no misfits of connectors, and there was free airlift of the cables. Also the logistics of the cable assemblies was greatly reduced.

The secondary distribution system now consists of the following components:

1. Secondary Distribution Center. The secondary distribution center (SDC), see Figure 15, is essentially a transformer/distribution box where the 4160V, three phase-three wire-grounding-60Hz primary power (high voltage) is transformed to 120/208V, three phase-four wire-grounding-60Hz secondary power (low voltage) and is delivered to output receptacles through circuit breakers. See Figure 4. Although not indicated on Figure 4, each SDC has the capability of feeding primary power (high voltage) to two other SDCs as shown in Figure 5. The new 150 KVA size SDC is a skid-mounted enclosure containing primary power (high voltage) input connections, the power distribution transformers and associated distribution circuitry and 16 Military Standard Class L 120/208V, three phase-four wire-grounding-60 amp receptacles. The SDC is 84 inches long,

48 inches wide, 74 inches high and weighs 5000 pounds. The high voltage section of each SDC consists of three sets of three "load break" bushings, one for each phase. Each of the three primary cables plugs into a bushing by use of a molded elbow connector (load break connector). These elbow connectors can be easily installed in the field with standard equipment that is used by commercial power companies. One set of bushings feeds directly into the bus of the high voltage switch. This set of bushings is used only for incoming power which can be disconnected at the source. Each of the other two sets of bushings is connected to a "load break" portion of a high voltage switch. These two sets of bushings are normally used for outgoing power to other SDCs. Parking bushings are also provided for each set of bushings. The fused portion of the high voltage switch feeds the SDC transformer. The concentric neutrals (or grounding conductor) must be connected to the ground bus of the SDC. An SDC also contains a military standard Class L 120/208V, three phase-four wire-grounding-200 amp power input receptacle for receiving mission essential power (MEP) from MEP generators. See Figure 6. The MEP is required during Bare Base erection, dismantling and in case of primary power failure, to provide secondary power to critical loads essential to the Bare Base mission. Special interlocks are provided so that either primary power (high voltage) or MEP (low voltage) can be fed into the SDC but that both cannot be fed in at the same time. Some older SDCs were procured in 45, 75, 100, 112.5, 150 and 200 KVA capacity having from 8 to 20, 60 amp power receptacles. Two SDCs fit on one 463L pallet for air transport.

2. Mission Essential Power Generators. Mission essential power (low voltage) is

**CABLE ASSEMBLY - 120/208V - 3 $\phi$   
4 WIRE - GROUNDING 60 Hz - 60 AMP**

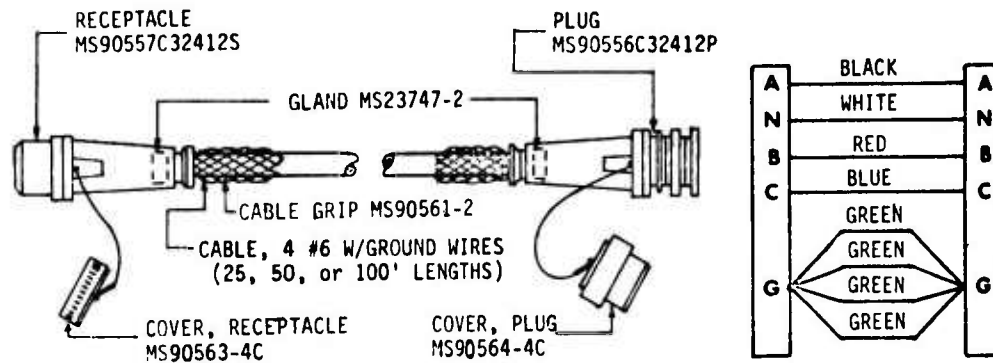


FIGURE 16. SECONDARY CABLE ASSEMBLY

**FOUR CONDUCTOR TYPE G**

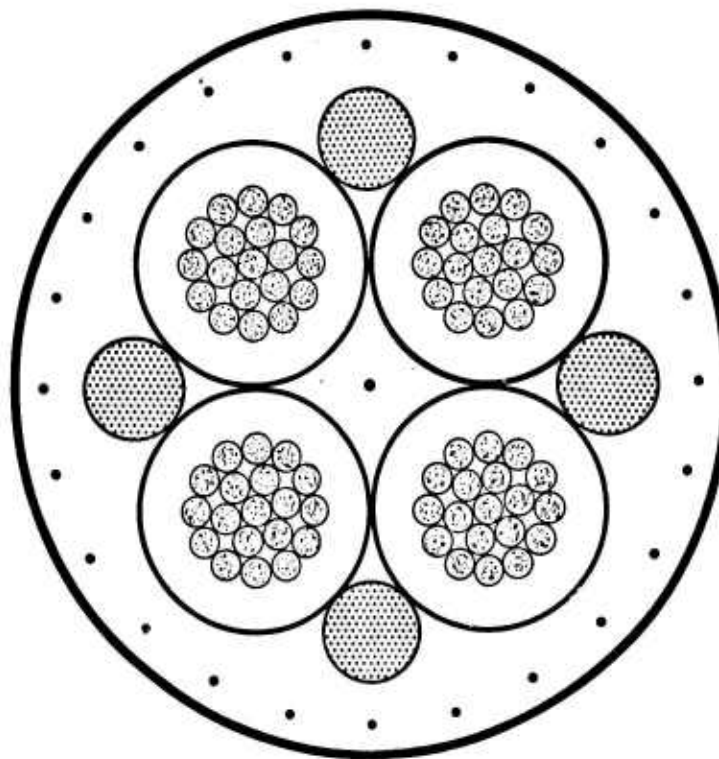


FIGURE 17.

120/208V, three phase-four wire-grounding-60Hz, 200 amp power delivered to the SDC by Air Force type MB-17 generators having 60 KW capacity. DOD Model MEP-006A generators also rated 60KW may be substituted. Both of these generator sets are diesel driven sets. The sets are approximately 87 inches long, 36 inches wide, 59 inches high and weigh 5000 pounds. The sets may be either skid-mounted or wheel-mounted.

**3. Secondary Power Distribution Cable Assemblies.** Secondary power distribution cable assemblies are used to connect the shelters and other equipment to the SDCs. The cable assemblies are standardized 50 and 100 foot assemblies USAF 72284-50 and 72284-100 power cables. See Figure 16. These cable assemblies use an industry standard safety cable known as 4 conductor type G where the grounding conductor is divided into four smaller conductors that are placed in the interstices of the power conductors so that mechanical penetration of the cable will result in a phase to ground fault before a phase to phase fault can occur. See Figure 17. The 60 amp cable has four #6AWG (133 strand) conductors with four #12AWG (37 strand) grounding wires. Conductor insulation is vulcanized ethylene-propylene-rubber (EPR) or a blend of EPR and XLP, and the grounding wires are insulated with the same materials but are not vulcanized. The cable jacket is a double pass, fiberglass reinforced, chloro-sulfonated-polyethylene (Hypalon). This is an industry standard cable for mine, quarry and construction use. The connectors used on the cable assemblies are the US Army ECOM developed DOD standard MIL-C-22992, Class L, 120/208V, three phase-four wire-grounding-60Hz, 60 amp connectors which are keyed for voltage, frequency and amperage and cannot be connected to the wrong power without a serious and deliberate attempt. See Figures 18 and 19. The connectors will mate with any 120/208V, three phase-four wire-grounding-60Hz, 60 amp equipment of Bare Base as well as any equipment of DOD using this same power and connectors. Cables are distributed for storage and shipment among SDCs, shelters, RALs and other equipment.

**4. Mission Essential Power Cable Assemblies.** The Mission Essential Power Cable assemblies are used to connect the Mission Essential Generators to the SDCs. See Figure 20. The MEP cables are standardized 25 foot USAF 72303-25 power cables. The MEP cables are constructed the same as the secondary distribution cables except that the conductors are four #4/0 AWG (427 strand) with four #4AWG (133 strand) grounding wires and the connectors are 200 amp Class L. The MEP cables are stored and shipped with the MEP generators.

#### Remote Area Lighting Sets

Remote area lighting sets, Figure 21, (RAL) are provided for dispersed area lighting. The sets are 84 inches long, 48 inches wide, 48 inches high and weigh 2500 pounds. Light fixtures, lamps, support poles, RAL cables, and electrical control equipment are all

packaged in containers for storage and shipment. Upon deployment, power is routed from SDCs to the RAL container with secondary distribution cables. Four 375-foot RAL cables are routed from each RAL container with lights positioned on the container and twelve at 125-foot intervals along the RAL cables. Two lamp fixtures using 200 Watt, Self-Ballasted Mercury Vapor PAR-38 Bulbs are used on each pole. A photoelectric cell and switches at the container control RAL operation.

#### TOTAL BARE BASE ELECTRICAL SYSTEM

The total equipment for the Bare Base Electrical System will provide for simultaneous equipping of one 4500 man deployment with air conditioning and one 4500 man deployment without air conditioning. The equipment is summarized in Table I and the cables and connectors are summarized in Table II and III.

#### CONCLUSION

A representative sample of the Bare Base Electrical System was tested during April and May 1975 in connection with Gallent Shield's 75 exercise. Other than some minor servicing problems with the High Voltage Generators, there were no other servicing problems and no failures of any part of the Bare Base Electrical System.

The Bare Base Electrical System is an Air Mobile system providing maximum standardization of equipment and operation while providing maximum flexibility of layout and capacity. There are no fixed distances in the layout. The complete system, or portions of it are suitable for all Department of Defense ground equipment. Use of this equipment by the services would guarantee intermatibility anytime equipment from one service is required to operate with equipment from another service. This system is also adaptable for civilian use.

#### REFERENCE

1. New Safety in Power Connectors. E.A. Ryan and S.R. Kinney, Proceedings E.C.S.G. Connector Symposium pp 129-143 October 1972.

#### ACKNOWLEDGEMENTS

The author extends his grateful appreciation to all people who gave technical assistance or supplied the equipment, without which this system and this paper would not be possible. In particular, Mr. A.R. Jeffers - Aeronautical Systems Division, U.S. Air Force, Mr. Edward A. Ryan - U.S. Army Electronics Command, Mr. Jack Kerr - U.S. Navy Electronics Command, Mr. Robert W. Tonar - Defense Electronics Supply Center; and to all of the personnel of the following organizations who assisted in this program: The Bare Base SPO at WPAFB Ohio; Defense Electronics Supply Center, Dayton, Ohio; Defense Industrial Supply Center, Philadelphia, Pa.; Bendix ECD, Sidney, New York; Amphenol Connector Division, Broadview, Ill.; Matrix Science Corp, Torrance Ca; ITT Cannon, Canada; Pico Crimping Tools Co, Sante Fe Springs, Ca.; ITT Royal Electric



FIGURE 18. MIL-C-22992 CLASS L CONNECTORS

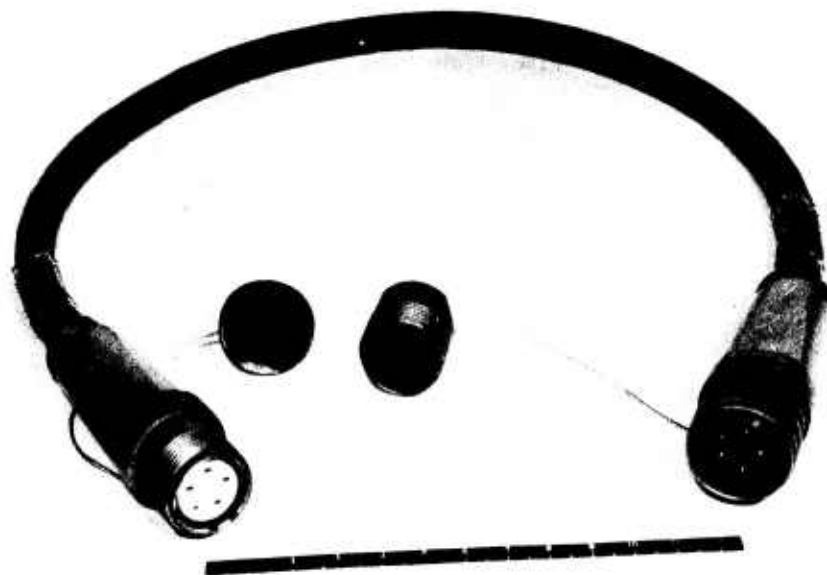


FIGURE 19. STANDARD CABLE ASSEMBLIES USING CLASS L CONNECTORS

**CABLE ASSEMBLY - 120/208V - 3 $\phi$   
4 WIRE - GROUNDING 60 Hz - 200 AMP**

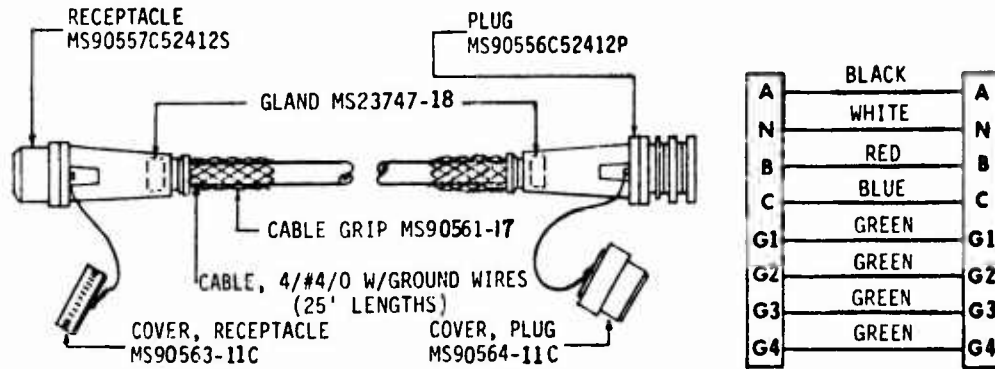


FIGURE 20. MEP CABLE ASSEMBLY

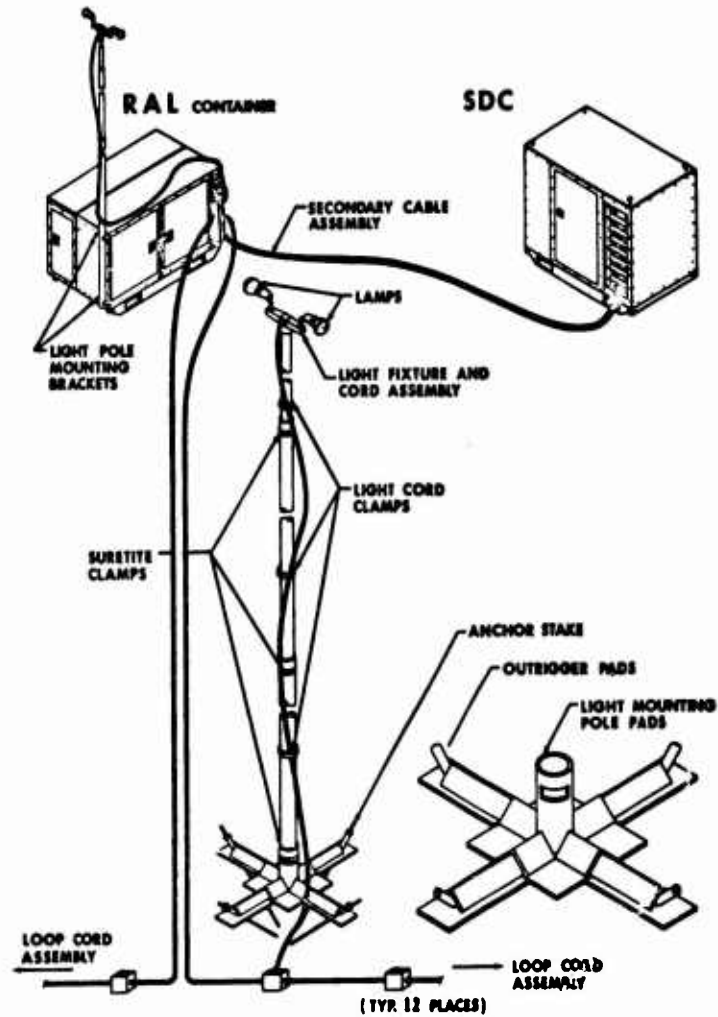


FIGURE 21. REMOTE AREA LIGHTING SET (RAL)



### BARE BASE ELECTRICAL SYSTEM EQUIPMENT

GENERATORS 750KW 4160 VOLT	26	SECONDARY DISTRIBUTION CENTERS (SDC)	
CONTACTOR CONTROL CUBICLES (CCC)	14	NEW TYPE 150 KVA	94
EQUIPMENT RACKS FOR REMOTE CONTROL	11	RETROFITED OLDER TYPE	
CABLE REEL PALLETS WITH 3 REELS ON EACH	44		
		45 KVA	17
		75 KVA	16
		100 KVA	43
MEP GENERATORS 60 KW 120/208V	66	112.5 KVA	10
		150 KVA	12
REMOTE AREA LIGHTING SETS	32	200 KVA	3
			<u>101</u>

TABLE I

### BARE BASE ELECTRICAL SYSTEM HIGH VOLTAGE CABLE

PRIMARY CABLE 5KV, #1/0 ALUMINUM WITH 1/3 CONCENTRIC NEUTRAL  
 SINGLE CONDUCTOR 517,500 FT OR 98.01 MILES  
 3-CONDUCTOR DISTRIBUTION LINES 172,500 FT OR 32.67 MILES

TABLE II

### BARE BASE ELECTRICAL SYSTEM CABLE ASSEMBLIES AND CONNECTORS

SECONDARY CABLE ASSEMBLIES 120/208V-3 PHASE-4 WIRE GROUNDING, 60Hz-60 AMP (CABLE-4 CONDUCTOR #6 TYPE G)

<u>LENGTH</u>	<u>TOTAL QUANTITY</u>	<u>AMOUNT OF CABLE USED</u>
50 FT	3135	163,020 FT OR 30.87 MILES
100 FT	2979	303,858 FT OR 57.55 MILES
25 FT EQUIPMENT CABLES	975	<u>26,325 FT OR 4.99 MILES</u>
		TOTAL 493,203 FT OR 93.41 MILES

#### CONNECTORS - 60 AMP

MS90555	POWER RECEPTACLES	4,986
MS90556	LINE PLUGS	7,089
MS90557	CABLE RECEPTACLES	6,114
MS90558	EQUIPMENT PLUGS	<u>2,362</u>
	TOTAL	<u>20,551</u>

MISSION ESSENTIAL POWER CABLE ASSEMBLIES 120/208V-3 PHASE-4 WIRE-GROUNDING, 60Hz-200 AMP (CABLE - 4 CONDUCTOR #4/0 TYPE G)

25-FT LENGTH - TOTAL QUANTITY 73  
 AMOUNT OF CABLE USED 1,972 FT OR 0.37 MILES

#### CONNECTORS - 200 AMP

MS90555	POWER RECEPTACLES	70
MS90556	LINE PLUGS	73
MS90557	CABLE RECEPTACLES	73
MS90558	EQUIPMENT PLUGS	<u>196</u>
	TOTAL	<u>412</u>

TABLE III

Division, Pawtucket, RI; ETS-Hokin and Galyan Electric Co., San Diego, Ca.; Solar Division of International Harvester Company, San Diego, Ca. and Alcoa, Conductor Products Co., Wayne, Pa.

#### BIOGRAPHY



John E. (Jack) Wimsey  
Chief, Standardization Engineering  
USAF Ground Equipment SPO  
Wright-Patterson Air Force Base, Ohio

Mr. Wimsey graduated from Marquette University with a Bachelor of Civil Engineering degree in 1943. He served in the US Army and Air Force in Aerial Photomapping. He was later assigned to Wright-Patterson Air Force Base as a project engineer for the development of geodetic and aerial photomapping equipment.

In 1946 he returned to Wright-Patterson Air Force Base as a civilian project engineer for development and standardization of Mapping and Photographic Equipment. In 1956 he was promoted to handling policy on Standardization and Procurement engineering. During 1960 to 1962 he served as an engineering investigator for the Inspector General. From 1963 to 1970 he served as Senior Engineer managing Procurement and Standardization Engineering for Systems and Ground Equipment. From 1970 to July 1975 he served as Chief Standardization Engineer for the Base Equipment System Program Office. Since July 1975 he has served as Chief, Standardization Engineering, Ground Equipment SPO.

Mr. Wimsey is presently managing projects initiated by the Office of the Assistant Secretary of Defense (I & L) for the standardization of electric power cables and distribution systems for the entire Department of Defense. He prepared the Specifications and Standards manual used by the Air Force and assisted in the preparation of the DOD Standardization Manual 4120.3M.

# HARNESS CONNECTOR SYSTEM

by  
Don Doty, AMP Incorporated  
Harrisburg, Penna.

## ABSTRACT

Insulation Displacing Mass Wire Termination, as pioneered by AMP Incorporated in the CHAMP Connector line of products has entered the "Second generation." Years ago, we realized that in order to successfully apply "Displacement" to the board based electronic market, the product family, including printed circuit edge connectors, cable-to-board connectors, in-line and in-out connectors, would have to be capable of randomly mass terminating the different wire types; solid, stranded and fused stranded, either in the form of discrete wires or the varieties of flat flexible cable. Additionally, the products must have the capability to *randomly* accommodate a large range of wire gauges, typically 14 thru 20 AWG or 18 thru 26 AWG in the above wire types. Further, individual contact points must be capable of mass terminating multiple wires of the same gauge and, finally, there must be a commonality of applicator tooling; i.e. a universal applicator tool for single insertion manual mass wire termination, semi- or fully automatic, must be able to *randomly* mass terminate all of the above products in one positional increments in all of the above wire types, gauges and multiples.

This paper deals primarily with a "State of the Art" concept and to illustrate this capability, the specific product family described is a series of .156" C/L Connectors which have been developed using this system.

Shown in Figure 1 are:

- (1) Printed Circuit Edge Connector for 1/16" single-sided P. C. Boards.
- (2) Post Receptacle Connectors for .045<sup>2</sup> or .045 dia. or .031 X .062 posts.
- (3) Hermaphroditic In-Line or In-Out Connectors.

Features common to *all* of the above products:

1. Available in one position increments from 2 thru 24 positions.
2. .156 center-to-center spacing.



Figure 1. A Family of Connector Products.



Figure 2. Pistol Grip Single Wire Insertion Tool.

3. Available with or without mounting ears.
4. Wire termination can *randomly* accommodate #18 thru #26 AWG solid, stranded or fused stranded wire.
5. In #20 thru #26 AWG, the wire termination can accept two wires of the same gauge per contact.
6. Capable of terminating Co-AX and drain wire.
7. .055" maximum insulation diameter, two wires.  
.110" maximum insulation diameter, single wires.

The photographs above illustrate two levels of applicator tooling; a pistol grip single wire insertion tool, and terminating bases and head for manual assembly of "Wind-in" or "Lay-in" form board type cable harnesses. Feasibility of fully automated, programmed cable harness machines has been established.

It is important to note that commonality of applicator tooling has been stressed in this system. The same universal tool accepts all of the connector types, in any of the positional increments available.

Electrical checkout of the form board type of tooling is accomplished by inserting the connector to be terminated into its counterpart, located in the termination base. In the case of the edge connector, an extender board is used on the back of the form board and is pre-wired to check the functions desired.

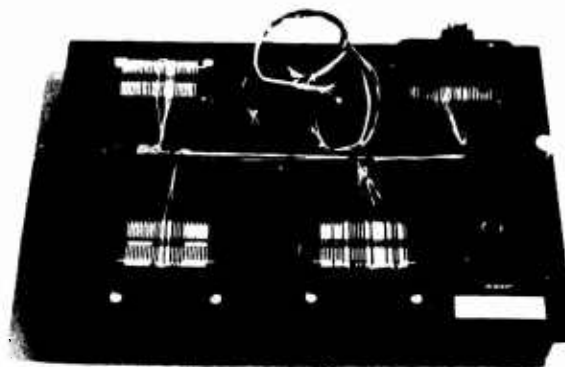


Figure 3. IDMWT of Form Board Cable Harnessing.

## THE SYSTEM:

For comparison purposes, the following reviews the steps in constructing a cable harness by standard "Wind-in" techniques as contrasted to the new mass wire termination system:

### Typical Steps Required by Present Harness Assembly Techniques:

1. Wind-in wires on "nail-type" form board.
2. Lace cable, stitching individual wire breakouts for subsequent contact termination.
3. Cut wire ends to length.
4. Remove cable from form board, transport to next station.
5. Strip individual leads for contact termination, transport to next station.
6. Crimp on individual contacts, transport to next station.
7. Insert individual contacts into connector housings, transport to next station.
8. Inspect and check out finished harness.

## MASS TERMINATION APPROACH:

1. Insert connectors into tool bases on form board. (Connectors engage contacts of programmed check-out circuit on back of form board.)
2. Wind-in wires complete, secure main cable branches.
3. Mass terminate with upper tool section.
4. Ringout finished cable assembly and remove from form board.

All of the previously required transports, high failure incidence points, have been eliminated as well as the majority of time-consuming steps.

A harness, for which actual standard hour rates were available, was chosen as a basis for comparison. A harness board was built to make the same harness, except that only one color of wire was used, and the application tooling bases were mounted on the assembly board. The harness was then wound a number of times in order to determine when the assembler had reached the learning curve stabilization point. Then each step of the assembly was timed so that an average time could be calculated. The harness that was chosen for this study had only P. C. Board edge connectors; it is understood that most typical harnesses would also have other types of connectors.

## PRESENT METHOD-LAY-IN OF PRE-TERMINATED LEADS:

1. Measure, cut and strip both ends of 143 leads/harness with a quantity of 1,000 leads per run for each lead, for making 1,000 harnesses, on an Artos CS-6 wire stripping machine.

Lead Length Range	Total Quantity of Leads	Production Rate
4.5"-15"	3M leads	0.362 hrs/M leads
15"-31"	88M leads	0.694 hrs/M leads
31"-48"	51M leads	1.031 hrs/M leads
48"-64"	1M leads	1.361 hrs/M leads

TOTAL TIME  
1.09 hrs  
61.11 hrs  
52.58 hrs  
1.36 hrs

2. Bench terminate the following leads:
 

Doubly terminate 85M leads	X 1.667 hrs/M leads	141.70 hrs
Singly terminate 58M leads	X 0.833 hrs/M leads	48.31 hrs
Doubling of (2) leads into one terminal		64.44 hrs
29M terminals	X 2.222 hrs/M terminals	
3. Lay the 143 pre-terminated leads per harness onto the harness assembly board and make up 1,000 harnesses.
 

8.2 sec./lead X 143 leads/harness X 1,000 harnesses	325.72 hrs
---	------------
4. Pick up a connector housing and insert the leads into the following connector housings
 

13 terminals/connector X 2 connectors/harness X 6.3 seconds/terminal X 1,000 harness	45.50 hrs
15 terminals/connector X 1 connector/harness X 6.3 seconds/terminal X 1,000 harnesses	26.25 hrs
17 terminals/connector X 4 connectors/harness X 6.3 seconds/terminal X 1,000 harnesses	119.00 hrs
21 terminals/connector X 1 connector/harness X 6.3 seconds/terminal X 1,000 harnesses	36.75 hrs
22 terminals/connector X 1 connector/harness X 6.3 seconds/terminal X 1,000 harnesses	38.50 hrs
23 terminals/connector X 4 connectors/harness X 6.3 seconds/terminal X 1,000 harnesses	161.00 hrs
5. Plug the 13 connectors onto the test cards on the harness assembly board. Press the continuity test button on the harness assembly board and check for wiring errors.
 

Insertion Time: 4.0 sec./conn. X 13 conn./harness X 1,000 harnesses	14.44 hrs
Test Time: 1.0 sec./lead X 143 leads/harness X 1,000 harnesses	39.72 hrs
6. Place 55 tie wraps around the harness and pull up tight by hand. Use the hand tool for final tightening and cutting off the excess tails.
 

12.2 sec./tie X 55 ties/harness X 1,000 harnesses	186.39 hrs
---	------------

7. Remove the harness from the harness assembly board.  
 36.0 sec./harness X 1,000 harnesses 10.00 hrs  
 Total time per 1,000 harnesses 1,373.86 hrs  
 Total time per harness  
 1,373.86 hrs/M harnesses/1,000 harnesses = 1.37386 HRS/harness = 82.43 minutes/harness

#### PROPOSED METHOD—USING HARNESS CONNECTOR SYSTEM:

- |   | TOTAL TIME                          |
|---|-------------------------------------|
| 1. Time to load connector housings onto the harness assembly board application tooling bases and to close bases.<br>18 pos. conn. = 7.8 sec./conn. X 6 conn./harness = 46.8 sec./harness<br>24 pos. conn. = 8.0 sec./conn. X 6 conn./harness = 48.0 sec./harness<br>15 pos. pin conn. = 7.8 sec./conn. X 1 conn./harness = 7.8 sec./harness | 0.78 min.<br>0.80 min.<br>0.13 min. |
| 2. Average time to wind harness (after the learning curve stabilization point) 29 min./harness  | 29.0 min.                           |
| 3. Place the inserter tool into the application tooling base. Push the handle forward to insert the leads into the terminals and to shear the excess lead loops. Remove the inserter tool and proceed to the next base or lay the tool down.<br>7.8 sec./conn. X 13 conn./harness = 101.0 sec./harness                                      | 1.68 min.                           |
| 4. Open the movable comb on the application tooling base. Pull out the excess sheared wire loops.<br>7.0 sec./conn. X 12 conn./harness = 84 sec./harness  | 1.4 min.                            |
| 5. Press the continuity test button on the harness assembly board and check for wiring errors.<br>1.0 sec./lead X 143 leads/harness = 143.0 sec./harness  | 2.38 min.                           |
| 6. Pick up the strain relief clips, out of the storage bins, and place one on each of the 13 connector housings.<br>5.0 sec./conn. X 13 conn./harness = 65.0 sec./harness   | 1.08 min.                           |
| 7. Place 45 tie wraps around the harness and pull up tight by hand. Use the hand tool for final tightening and for cutting off the excess tails.<br>12.2 sec./tie X 45 ties/harness = 549.0 sec./harness  | 9.15 min.                           |
| 8. Remove the harness from the harness assembly board.<br>36.0 sec./harness<br>Total time per harness   | 0.60 min.<br>47.00 min.             |

#### RESULTS OF COMPARISON:

Total assembly time:  
 (Present Method) = 82.43 minutes per harness  
 (New Method) = 47.00 minutes per harness  
 Total Labor Savings = 35.43 minutes per harness  
                               = 0.59 hours per harness

Estimated labor rate = \$11.35/hour for direct labor  
                               plus benefits plus overhead

Total labor cost savings:  
 \$11.35/hr X 0.59 hrs/harness = \$6.70/harness

Conservative cost savings per termination:  
 (\$6.70/harness)/(244 terminals/harness) = \$0.027 = 2.7¢/termination

Illustrations 1 thru 8 show in sequence the steps involved in completing a typical wind-in cable using this "State of the Art" approach.

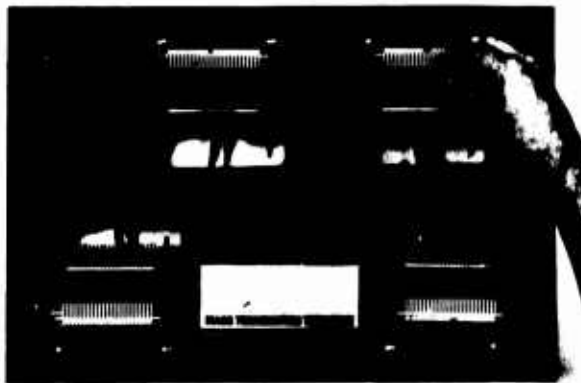


Figure 1. 41122—Install connector on extender boards in bases.

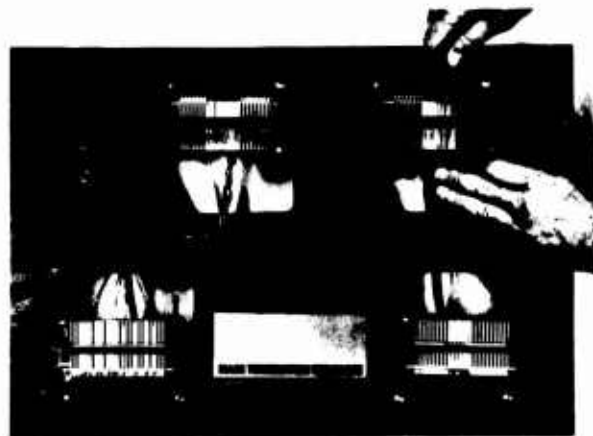


Figure 2. 41127—Wind-in or Lay-in wires.

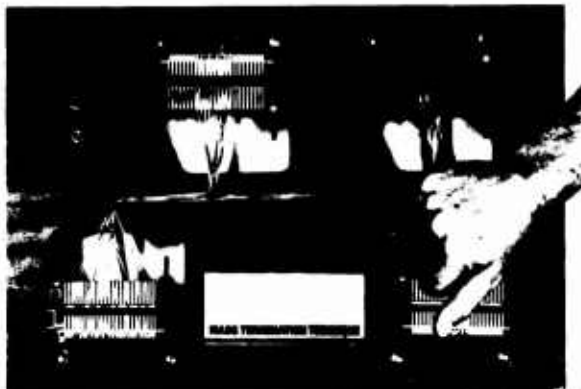


Figure 3. 41120—Mass terminate with universal applicator tool.

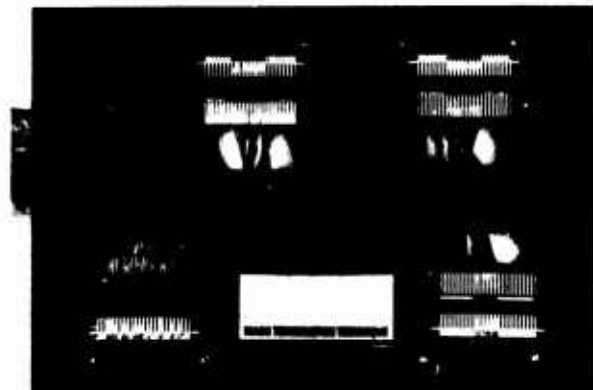


Figure 4. 41128—Open bases and energize test circuit.

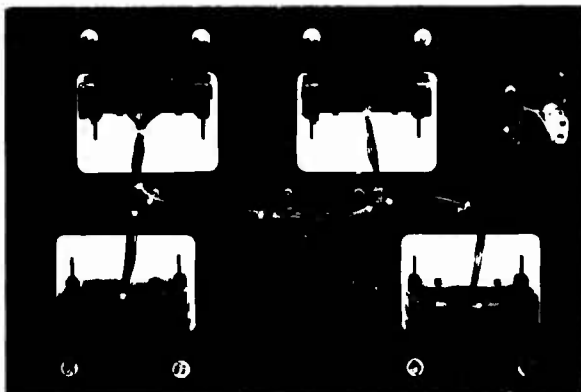


Figure 5. 41117—Back of form board showing pre-wired test circuit.

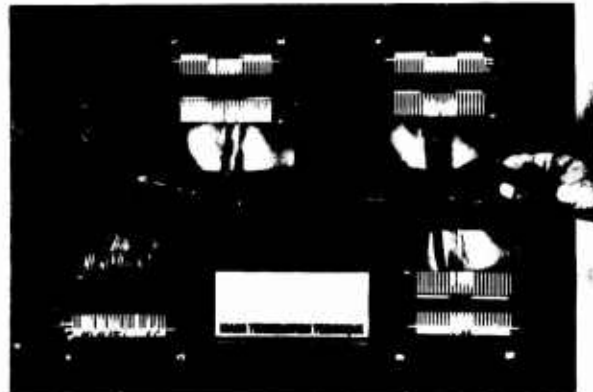


Figure 6. 41123—Cable tie connector breakouts.



Figure 7. 41126—Install strain relief covers.

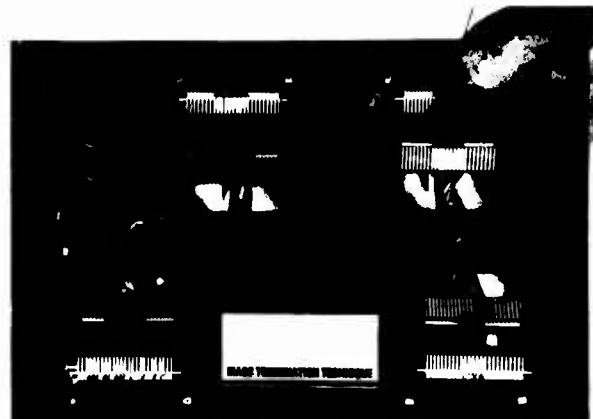


Figure 8. 41125—Remove completed and tested harness from form board.



Donald J. Doty is Manager of Development Engineering, Communications Products Division, AMP Incorporated. A graduate of Rutgers University with a Bachelor of Science Degree in Engineering, he has more than 20 years experience in the design and manufacture of electronic component and equipment, including microwave and UHF components, and printed circuits.



## ENGINEERING FOR CABLE INSTALLATION

V. W. Pehrson  
General Cable Corporation  
Colonia, New Jersey

### Summary

Cable plows have been in general use for the past two decades but were used extensively for installation of toll cables in the Bell System since the early 1930's. The construction and the handling of cable plows have, however, imposed some difficulties for cable and these, along with the impact of filled cable, are discussed.

Duct installation of long cable lengths necessitates more exacting engineering and planning to avoid needless risks. These installations are, in many cases, complicated by intermediate manholes and/or bends. The basis and methods of calculation of pulling lengths, or tensions, and handling practices in intermediate manholes are discussed.

### Introduction

The evolution of communication cable design, the development of installation equipment, the introduction of new materials and the innovation of new devices all have an impact on cable installation methods and practices. Although this is the essence of progress it is very seldom that a development takes place that is all on the plus side of the ledger. While it may be a very significant advancement on the whole, it may also have some weaknesses or detrimental aspects which must be dealt with in practice.

This is a discussion of practices and, to some extent, of equipment used in placing buried or duct cables with the objective of outlining good practices, pointing out some risk areas or means of identifying risks and to suggest methods of handling that will minimize the risks involved.

### Cable Plowing

The concept of buried cable installation by plowing was introduced many decades back. One of the very early installations, if not the first, was the installation of a telegraph cable along a railroad track by a plow pulled by a locomotive. Nystrom<sup>1</sup> reported in 1931 the development of a cable plow and plowing more than 300 miles of steel tape armored lead sheathed toll cable by Southwestern Bell Telephone Company. In 1950 Royal<sup>2</sup> stated that a large portion of the coaxial and balanced pair toll circuits in the Bell System plant is enclosed in cable that has been buried in a plowing operation. There has been a great deal of progress through the years. Today there are more sophisticated cable plows designed to be pulled by a locomotive, there are plows designed to be pulled behind tractors, plows designed to be attached to tractors and there are plows designed as an integral part of a tractor. There are static plows, vibratory plows and even plows of a somewhat different design which have been developed for underwater cable installation.

Installation of buried cables by plowing burgeoned in the mid 1950's accompanying the development of pedestals for splicing and terminating. This type of installation, which was relatively inconspicuous and offered both cost savings and greater freedom from storm damage, as compared with aerial cables or open wire pole lines, stimulated the spread of telephony into the rural areas of the United States. Over the past few years the widespread adoption of filled cable for buried installations has imposed some new aspects on this method of installation.

The changes mentioned above are in the interest of progress but they have also imposed a few problems for which allowances must be made during installation. Table 1 shows gross package weight (i.e. cable and reel) of several popular sizes of cable illustrating the greater weights of the increased standard lengths of filled cable.

The pay offs of most cable plows have no provision for any power control of the pay off reel so that during the normal plowing operation the power to accelerate and turn the reel is from tension in the cable, unless it is turned manually. A number of users have recognized this problem and provide a man to turn the reel or to provide a slack loop of cable ahead of the plow.

The tension required to turn the reel under steady state conditions is well within the strength limitations of the cable. There are, however, no steady state conditions in a plowing operation. First of all, when the plow starts the reel must be accelerated from a stop to the plowing speed. Then, any changes in reel speed, necessitated by changes in speed of the plowing or by the attitude of the plow due to uneven terrain, can either tension the cable to accelerate the reel or develop a slack loop in the cable. Under the latter condition the reel slows up, and when the accumulated slack is used up, the cable reel must again be accelerated to accommodate the plowing speed, usually with a severe jerk of the cable. This is not a new condition, merely a continuing one. What has changed is that reels of cable, with longer lengths and filled with a water-proofing compound, have become heavier.

The design of cable plows has not in all cases been in the best interest of the cable, possibly because of engineering or economic compromises. The recommended minimum bending radius for cable is 10 times the cable diameter and the maximum recommended bearing pressure or sidewall pressure is 150 pounds per foot. The radius at the bottom of the cable chute in some plows is much less than 10 times the diameter of the largest cables they can accommodate. There is no real problem in designing cable chutes to conform with this criteria and plow manufacturers should not have difficulty furnishing them with such a radius.

Table 1

Package Weights  
22 AWG PIC

Cable Size (pairs)	Unfilled Cable		Filled Cable		Weight Ratio (multiples)
	Standard Length (feet)	Total Weight cable & reel (pounds)	Standard Length (feet)	Total Weight cable & reel (pounds)	
12	5000	870	6000	1095	1.25
25	5000	1325	6000	1800	1.36
50	3000	1390	6000	3430	2.47
75	3000	1955	6000	4700	2.40
100	3000	2575	3000	3130	1.22

Some plowing equipment has rollers to support the cable between the cable reel mounted at the front of a tractor and the rear mounted cable plow. Some of these are as small as 4.5 inches in diameter. They are obviously intended as guide rollers, and if the cable passing over them is not under tension they are satisfactory as guides or supports for the cable as it passes over the tractor. In practice, however, unless a slack loop is pulled off the reel, or the reel is turned by some means to preclude any significant tension in the cable, it can be subjected to the jerking mentioned above. Such jerking will bend the cable over far too small a radius and can subject the cable to very high bearing pressures over the rollers.

It is difficult to estimate the peak tensions which can result from such jerking. A report was received of a momentary cable tension of over 600 pounds at the start of a plowing operation, measured by connecting a dynamometer between the end of the cable and an anchor. This of course measured the tension at the exit of the plow chute where it would be somewhat greater than over the rollers above.

An illustration of this set of conditions is shown in Figure 1. It is assumed the tension is 600 pounds at the exit of the chute and a 100 pr 22 AWG filled PIC cable which has a diameter of 1.4 inches is being installed. Assume the radius of bend in the chute is 10 times the cable diameter which is 14 inches or 1.17 feet. The effect of cable weight in this instance is negligible so the bearing pressure against the wall of the chute is:<sup>3</sup>

$$P = T/R \quad (1)$$

Where:

P = bearing pressure, pounds per foot

T = tension, pounds

R = radius, feet

Substituting,

$$P = 600/1.17 = 513 \text{ pounds per foot}$$

This shows that though the minimum bending radius is observed the momentary tension is such that the side-wall bearing pressure is far in excess of 150 pounds per foot, which is the maximum recommended.

The tension at the roller directly above the cable chute of the plow can be calculated by

means of the formula for belt friction, which is sometimes called the capstan formula:<sup>4</sup>

$$T_2 = T_1 e^{k\theta} \quad (2)$$

Where:

$T_2$  = tension at exit of bend, pounds

$T_1$  = tension at entrance of bend, pounds

e = base of natural logarithms

k = coefficient of friction

$\theta$  = angle of contact, radians

To solve for  $T_1$  this equation can be rewritten:

$$T_1 = T_2 / e^{k\theta} \quad (3)$$

It will be assumed that bend in the chute has a 90 degree or 1.57 radian included angle, and that the coefficient of friction is 0.3, which is a figure sometimes used for belt friction over a flat pulley.

Then, with the tension of 600 pounds at the exit of the chute:

$$T_1 = 600 / e^{0.3 \times 1.57} = 375 \text{ pounds}$$

and the bearing pressure against a 4.5 inch diameter roller, i.e. 2.25 inch, or 0.1875 feet radius, is:

$$P = 375 / 0.1875 = 2000 \text{ pounds per foot.}$$

This is over 13 times greater than the maximum recommended bearing pressure for a cable and, in addition, the cable is bent around a radius that is far smaller than the minimum recommended. This excessive bending and pressure may occur several times over different rollers before the cable goes through the chute and is placed in the ground.

The big question is, has the cable been damaged by this abuse, and if it has, how much has it been damaged? Plowing is, to a great extent, a blind operation and sheath damage can easily get into the ground unnoticed but can usually be detected by shield to ground resistance measurements. Other types of trouble may show up at a later date, and it is extremely difficult to determine the cause after a period of time.

The introduction of filled cable has brought with it some new considerations in installation. The objective of filling cable, is to eliminate all voids in a cable and thus leave no paths for moisture migration. With no voids in the cable it is incompressible. This is contrasted to unfilled PIC cable, in which approximately 50 per cent of the volume of the cable core is air or gaseous voids; consequently unfilled cable is compressible to some extent.

If a circular configuration is deformed, either its circumference must be increased or its area reduced. In the case of filled cable the area cannot be reduced, so if it is deformed the circumference must increase, which is to say the jacket must stretch. An example of this is shown in Figures 2 and 3. Figure 2 shows a 3 inch diameter circle which has a circumference of 9.43 inches and a cross sectional area of 7.07 square inches. If this is deformed to an ellipse with a minor diameter of two inches (2/3 that of the circle) and if this is a filled cable, its cross sectional area would remain unchanged so the circumference must increase to 10.94 inches as shown in Figure 3. This is an increase in circumference of 1.51 inches, or 16 percent. This may not be the exact shape which a cable will deform, but it illustrates the phenomenon.

Because the jacket of filled cables must stretch to permit them to deform, they offer much greater resistance to deformation than unfilled cables. When they are subjected to sufficient force, however, they will deform and if there is a substantial amount of deformation the jacket will probably split. The cause of the deformation is somewhat beside the point, except that a sudden deforming force, as if from an impact, is more injurious to the cable.

This has happened to reels of cable which were bumped during shipment. There have been reports of jackets splitting when cable was deformed by pressure against a guide roller of a cable plow due to jerking. This has been borne out in simulated plowing tests in the laboratory. There is also evidence that cables have been crushed when the plow has been jounced or deflected by hitting a boulder, causing the jacket to split.

When the cable sheath is subjected to internal pressure the jacket is reinforced by the shielding tape. The point of little or no reinforcement, however, is at the edge of the overlap of the shield. The seal tends to open up and subjects the jacket adjacent to the overlap to localized circumferential stretching, and the split sheaths this author has seen have occurred along that line. This is illustrated in Figure 4. Those observed have been from approximately 6 to 14 inches in length, which indicates a very localized loading.

As mentioned above, some operating companies have recognized the tension problem and have avoided it by such procedures as paying off the cable on the ground ahead of the plow from a separate reel carrier or by having a man walk ahead of the plowing prime mover and pull a 15 to 20 foot loop of cable off a tractor mounted reel. This is an added cost, but is not as expensive as damaged cable. A powered automatic reel tender would be a great advantage and it is hoped that a satisfactory one will become available.

It is believed there will always be some risk when plowing cable in rocky terrain. This can

probably be minimized by pre-ripping and finding a diversionary route which will avoid the boulders or marking where boulders are encountered so that special treatment can be given such as trenching the local area with a backhoe.

#### Duct Installation

Along with the larger diameters of ducts that are currently being installed and the larger cables that are being pulled into them, there is increasing interest in longer pulling lengths as a means to reduce construction and splicing costs, but it must be realized that with longer pulling lengths the requirement on the engineering, the handling, the techniques and the material used become more exacting. When large cables are involved it becomes increasingly important that proper practices are employed so that installation can be accomplished without damage to the cable. The following discusses some of the factors that influence the maximum cable lengths that can be pulled without undue risk, and provides information that, it is hoped, will not only contribute to refinements in installation practices, but will also give a better insight as to what can be done safely.

It is a general practice in the cable industry, whether for power cable or communication cable, to limit pulling tension to 10,000 psi on the cross section of annealed copper to which the pull is applied. The value of 0.008 lb. per circular mil approximates the load of 10,000 psi and though the two are not precisely the same, they are used interchangeably in tension calculations. This limitation is stated in the Underground Systems Reference Book<sup>5</sup>, but the recognition of it predates this publication. The reason for this limitation is illustrated by the stress-strain curve for annealed copper shown in Figure 5. Note that the curve has a knee at approximately 10,000 psi and that tensions exceeding this involve considerable elongation of the conductor for relatively small increase in tension. This tension, calculated for both wires of a pair of the popular gauge sizes, and with a bit of rounding is shown in Table 2.

Table 2

#### Permissible Pulling Tension Per Pair

	(pounds)
19 AWG	20
22 AWG	10
24 AWG	6.4
26 AWG	4.0

It is pointed out, however, that for larger size cables it is necessary to push some of the pairs back into the cable to insert the pulling bolt. The percentage may vary slightly from one cable size to another and possibly from one manufacturer to another, but approximately 40 percent of the pairs are pushed back and 60 percent are clamped in the eye. A diagram of a typical pulling eye is shown in Figure 6. Table 3 shows permissible pulling tensions for popular sizes of stalpeth, based on 60 percent of the pairs clamped in the eye.

Table 3  
Stalpeth  
Permissible Pulling Tensions

<u>19 AWG</u>			
<u>Cable Size</u> <u>No. of Pairs</u>	<u>Diameter</u> <u>(Inches)</u>	<u>Weight</u> <u>(Pounds/Foot)</u>	<u>T max</u> <u>(Pounds)</u>
200	1.9	2.2	2400
300	2.2	3.2	3600
400	2.6	4.2	4800
450	2.7	4.7	5400
550	3.0	5.7	6600*
<u>22 AWG</u>			
300	1.7	1.7	1800
400	2.0	2.3	2400
450	2.1	2.5	2700
600	2.4	3.3	3600
900	2.8	4.8	5400
1100	3.1	5.8	6600*
1200	3.2	6.3	7200*
1500	3.5	7.8	9000*
<u>24 AWG</u>			
600	1.9	2.1	2300
900	2.3	3.1	3450
1200	2.6	4.1	4600
1500	2.9	5.0	5750
1800	3.1	5.9	6900*
2100	3.4	6.9	8050*
2400	3.6	7.8	9200*
<u>26 AWG</u>			
600	1.5	1.4	1440
900	1.8	2.0	2160
1200	2.0	2.6	2880
1500	2.3	3.2	3600
1800	2.5	3.8	4300
2100	2.6	4.4	5050
2400	2.8	5.0	5750
2700	3.0	5.5	6500
3000	3.1	6.1	7200*
3600	3.4	7.4	8650*

\*Because of practical considerations in pulling cables into ducts, a maximum tension of 6500 pounds is recommended even though some cables will withstand higher tensions.

The tension required to pull cable into a straight duct is:

$$T = Lwk \quad (4)$$

Where:

T = tension, pounds

L = length, feet

w = weight of cable, pounds per foot

k = coefficient of friction

The only factor in this equation that is difficult to determine accurately is the coefficient of friction "k". It is a simple matter to make a laboratory

determination of the coefficient of friction between cable sheaths and various duct materials, with and without lubricants. The values obtained by measurement under laboratory conditions will, however, be the minimum coefficient that can be expected and which, in most cases, will be quite optimistic when compared with "effective" coefficients determined from pulling tensions measured in actual installations.

It is essential, when pulling long lengths of cable, to have knowledge of the "effective" coefficient of friction and to control the factors which have a bearing on it insofar as practical, so as to know what tensions can be expected realistically. The "effective" coefficient of friction is defined as the relationship between a cable weight and the force required to pull it into a duct, and it

must be determined empirically. This force may include several contributions that are not strictly due to weight times the coefficient of friction but these are difficult to separate from the coefficient in a measurement, so it is convenient to include them in the "effective" coefficient.

These contributions may include:

1. Dirt or contamination, particularly in old ducts.
2. Lubrication. In a long duct run lubrication can be applied at the feeding end but it is difficult to achieve effective lubrication throughout the length of the duct because the lubricant is wiped from the cable as it slides into the duct and is thus not distributed uniformly throughout the length of the duct. This means that the coefficient of friction can differ in different portions of the duct depending on the amount of lubrication, and it is usually less effective in long ducts.

3. Deviations of a duct from a straight line. This will cause the cable to bear against the duct wall in a direction dependant on the direction of the deviation, and the pressure against the duct wall will increase with cable tension resulting in greater friction.

A cable under tension and lying on a flat surface will form a straight line. Any directional deviations of a duct which will deflect a cable under tension from a straight line will result in a force in pounds per foot equal to  $T/r$  (equation 1) as mentioned in the discussion of plowing. It can be seen that as tension increases due to longer pulling lengths, the contribution of friction at each pressure point is increased. This side wall bearing pressure can be added vectorially to the cable weight to obtain the total pressure. This will, except where the curvature is such the cable tends to lift, have the same effect as increasing the cable weight, but it will be apparent as an increase in the coefficient of friction. It is pointed out that though the effects of minor changes in alignment are generally considered negligible when pulling high voltage power cable into steel pipes,<sup>3</sup> it must be remembered that with welded steel pipes the inadvertent variations from a straight line are very small and also that the coefficient of friction used in engineering these installations has been determined empirically from field data. Even where duct systems are engineered to be straight, they may deviate from a straight line due to construction inaccuracies or settling of the ground during back filling or after construction is completed. When pulling short lengths of cable where tensions are relatively low, the effect of minor deviations from a straight line are generally negligible, but as tensions increase with cable length and particularly as cable diameters approach duct diameters, nonlinearities in a duct can materially increase tensions. As an example, a 1500 pair 24 AWG stalpeth cable which weighs 4.9 pounds per foot is to be pulled into a duct. The permissible pulling tension for this cable is:

$$T_{\max} = \text{Number of pairs} \times 0.6 \times \text{permissible tension per pair.}$$

$$T_{\max} = 1500 \times 0.6 \times 6.4 = 5760 \text{ pounds}$$

Let us arbitrarily assume, for purposes of illustration, that this duct has a horizontal non-

linarity with a radius of 500 feet at a point where the cable tension is 4500 pounds. The side bearing pressure due to tension is equal to:  $P_t = T/r$  (equation 1) where  $P_t$  denotes pressure due to tension in pounds per foot.

Hence:

$$P_t = \frac{4500}{500} = 9 \text{ pounds per foot}$$

The resultant pressure ( $P_r$ ) of the horizontal component due to tension and the vertical component due to cable weight is:

$$P_r = \sqrt{P_t^2 + w^2} \quad (5)$$

$$= \sqrt{9^2 + 4.9^2} = 10.2 \text{ pounds per foot}$$

This is considerably different than the pressure due to the 4.9 pounds per foot cable weight which would be used in calculating pulling tensions in what is considered an essentially straight section. It is realized that these minor deviations may occur in any plane with effects corresponding to the direction and radius of curvature of the deviation and also that the condition is not applicable to the entire length of the duct. It illustrates, however, that minor deviations from a straight line have an effect on side bearing pressure, and consequently on pulling tension, which cannot easily be predetermined, but which will exhibit itself in the "effective" coefficient of friction.

It is pointed out that published cable diameters are nominal diameters as measured by a diameter tape and are subject to manufacturing tolerances, and also unfilled cables may deform somewhat from the reeling and unreeling operations before they are installed in a duct. The maximum caliper diameter may be significantly larger than the tape diameter. It is felt that for straight ducts, the duct diameter should be at least one half inch, or 15 percent, larger than the cable, whichever provides the greater clearance, and even more clearance would be prudent if there are bends in the duct which would result in substantial side bearing pressure. Pulling eye diameters are larger than the cable but, except in very small cables, should not exceed cable diameter by more than 10 percent.

In addition to cable deformation, it has been found that fiber and plastic ducts are sometimes out of round. They have been found seriously out of round under roadways, presumably from either compacting operations preparatory to paving, or compacting from traffic after completion of the roadway. Joints in concrete or tile duct will sometimes drop leaving an offset.

If there is any question that fiber or plastic ducts may be out of round, or that sectional ducts may be slightly offset, or that the duct may be contaminated or obstructed, or if the cable diameter approximates 85 percent of the duct diameter, a mandrel should be pulled through the duct prior to making the cable pull. The mandrel should be within 1/4 inch of the nominal diameter of the duct and should be larger than the cable pulling eye. The short mandrels available commercially are useful but a stiff mandrel five to six feet long is preferable because it can give warning of an abrupt nonlinearity or an offset duct section. Any evidence of silting will indicate the necessity of cleaning.



Pulling tensions for polyethylene jacketed cables have been measured in the Bell System under a variety of conditions and they have determined coefficients of friction from these measurements. The following values are listed in a Bell System Practice.<sup>6</sup>

Table 4

Duct Material	No Lub	Lubricant <sup>7</sup>	
		B or C Lub	D Lub
Concrete	0.6	0.42	0.25
Fiber	0.47	0.44	0.25
Fiber Cement	0.50	0.50	0.25
Plastic	0.43	0.38	0.18

Bell Laboratory representatives have advised that the coefficients calculated from measured values of pulling tension covered a range of values, of which those listed above are 75 percentile figures. This is to say that 25 percent of their cable pulls would be expected to involve coefficients higher than those listed. These coefficients will not necessarily be valid for all ducts. Duct conditions will vary even with the best of construction practices due to the practical engineer- and construction trade-offs which are dictated by economics, and by soil conditions, hence it is urged that operating companies measure and record cable pulling tensions and determine effective friction coefficients empirically from the tension data, as a basis for their engineering. It is suggested that along with the pulling tension the data should include cable diameters, cable weight, type of cable, duct diameter and material, location and radius of all bends, length of pull, grade involved (uphill, level or downhill) and type and method of lubrication.

There are a few points in setting up and pulling the cable which are important, and though they are shown in most underground cable placing practices they will be repeated here. The reel should be set up on the same side of the manhole as the duct into which the cable will be fed, so that the direction of curvature of the cable coming off the top of the reel, going through the feeding tube and into the duct is not changed. If there are bends in the duct the reel should be set up at the manhole closest to the most severe bend if at all practical. In order to take advantage of minimum pulling tensions it is good practice to make calculations in both directions of pull, particularly if there are multiple bends.

Pulling should be very slow until at least two feet of cable are in the duct then the pulling speed should be fast enough to keep the cable and the reel moving smoothly, but not so fast that feeding cannot be safely controlled. With straight ducts and good conditions at all manholes, including any intermediates, higher speeds can be safely used but should not exceed 100 feet per minute. Thirty feet per minute is a good minimum to maintain uniform movement of the cable and reel, with 80 to 100 feet per minute reasonable when conditions are good;<sup>3, 8</sup> however, the speed should be reduced when the cable approaches the pulling manhole.

If it is necessary to stop the cable between manholes, the tension should be maintained

on the winch line if possible. When starting again it must be kept in mind that both the static friction and the inertia of the cable must be overcome, so the tension must be increased gradually until the cable begins to move.

#### Bends

Where bends are designed into the duct, the location and radius of curvature of the bend is known and the effects of the bends on pulling tensions can be calculated. This is essential for accurate calculations.

Equation 2 is sometimes used for an approximate calculation of tension around bends. This equation neglects the cable weight, but on calculations involving light weight cable where bend radius and the tension are such that the cable weight is small in comparison to the sidewall pressure it can be used without great error. With heavy cables and large radius bends, or if pulls are in a direction where duct wall pressure adds directly to cable weight, such as convex bends, the error could be significant.

The most common problems, however, involve horizontal bends since, except for bends at risers, which are usually in connection with short pulls, most bends of any significance are substantially horizontal. Rigorous equations have been developed for calculating tensions around horizontal bends. One equation, developed by Buller<sup>9</sup> is also shown in Reference 5. Expressed in terms of tension the equation is:

$$T_2 = wR \sinh \left( k\theta + \sinh^{-1} \frac{T_1}{wR} \right) \quad (6)$$

or in terms of equivalent length is:

$$L_2 = \frac{R}{k} \sinh \left( k\theta + \sinh^{-1} \frac{L_1 k}{R} \right) \quad (7)$$

Where:

$T_2$  = tension, pounds at exit from bend

$T_1$  = tension, pounds at exit from bend

$L_2$  = equivalent length, feet at exit from bend

$L_1$  = equivalent length, feet at entrance of bend

$k$  = effective friction coefficient

$R$  = radius of bend, feet

$\theta$  = angle of bend, radians

$w$  = weight of cable, pounds per foot

Equivalent length is defined as the length of straight duct which would result in tension equivalent to the bend.

Equations were developed independently by Rifenburg<sup>3</sup> which are somewhat more involved but are reducible to that shown above. This reference also shows equations for pulling tensions in vertical concave and convex bends and for both up hill and down hill vertical offsets.

These equations can be programmed on a programmable hand held calculator such as the Hewlett

Packard HP-65 as well as larger scientific computers, and when programmed their solution is easy and their complexity, relative to the approximate formula, is not a matter of consequence. Graphical solutions<sup>9</sup> have been developed for these equations by Buller, Rifenburg<sup>3</sup> and Bosworth.<sup>10</sup> Their use, however, is more involved than the use of a calculator and, though they are reported to have at least slide rule accuracy if properly made and scaled, they are less accurate than the calculator. An additional advantage of the calculator for design purposes is that once it is programmed calculations for alternate route lay-outs can be readily made to select the most advantageous one as far as cable installation is concerned.

The calculation should begin with the tail load,  $L_0$ , equivalent to pulling 50 feet of cable into the duct. If calculating equivalent length, which has certain conveniences, the 50 feet is merely added to the initial straight section of duct to become  $L_1$ .  $L_2$  is then calculated as the equivalent length at the exit of the bend. Succeeding straight sections and bends are calculated progressively. The tension at the end of the duct section can be calculated from the equivalent length by equation 2,  $T = Lwk$ , or, possibly more convenient for duct design purposes, the maximum equivalent length is:

$$L = \frac{T \max}{wk} \quad (8)$$

The side bearing pressure should be calculated at the exit of the most critical bend and should not exceed 150 pounds per foot. This however, might prove excessive for single bore conduit unless it is properly encased in concrete. With unit pressure in this range the contribution from the cable weight is not significant and the sidewall pressure is calculated by equation 1.

In most cases manhole spacing is determined by the need for branch splices in some, but not necessarily all, of the cables in a duct bank. Since this spacing is usually less than maximum length of plastic sheathed cable that can be pulled, the installation of long lengths will, in these instances, necessitate pulling through intermediate manholes.

When duct mouths are on exactly opposite sides of the manhole and the ducts are in line with each other on the opposite sides, i.e. no change in direction either horizontally or vertically, the cable can be pulled through the manhole without risk of snubbing on the duct mouths. If the ducts at the opposite ends of the manhole have a significant offset or are out of alignment with each other there is risk of snubbing at the duct mouths and possibly damaging cable unless the tension through the intermediate manhole is light. If there is a long pull or a bend which results in high tension at the intermediate manhole, and offsets or misalignment exists, the pull-through should be avoided.

Cable pulls through intermediate manholes should not be planned unless all of the following conditions are met:

1. Calculated pulling tensions based on knowledge of the duct layout and/or previous experience, indicates that maximum tension for the two or more manhole sections are within the permissible limits for the cable and the pulling line.

2. The length of cable on the reel is adequate for the two or more manhole sections involved, with allowances for racking in intermediate manholes and for splicing and waste.

3. Adequate equipment is available to handle the reel size involved, and that winch line and winch are adequate for the length and pulling force.

4. Suitable racking equipment is available.

5. Intermediate manholes are straight through, i.e. no branch splices planned.

6. The ducts at each end of the manhole are well aligned.

#### Racking in Manholes

Where cable is pulled through an intermediate manhole it is necessary to develop slack to properly rack the cable. A prerequisite to developing slack in an intermediate manhole is to make provision in the adjacent manholes. This may necessitate anchoring the cable in one of the adjacent manholes if it is preferable or essential that the slack come from one direction.

The cable in the manholes from which the slack may come must be supported in a straight line from the duct mouth for a sufficient length so the cable can move into the duct without restriction and without risk of damage at the duct mouth.

Various methods have been used to pull slack into a manhole, some of which are regarded as makeshift. Luffing grips over the cable at each end of the manhole, with a chain hoist between them to pull the slack, have often been used, but when a substantial force is needed to pull the slack there is risk of moving the cable sheath relative to the core and possibly damaging the cable. Racking jacks are available and are often used in combination with cable bending shoes to gain slack by jacking the cable into position by forcing it away from the opposite wall of the manhole.

A more sophisticated tool is a slack puller consisting of four bending shoes on a framework with a linkage between them arranged so that a chain hoist can be connected between two lever arms.<sup>11</sup> Slack is gained by pulling the lever arms together, forcing an offset into the cable and positioning it for racking.

Whatever method of pulling slack and racking the cable is used, it is important that approximately four inches of straight cable extend from each duct mouth to preclude the possibility of cable damage at the duct mouth should the cable in the duct contract from temperature drop.

#### Conclusions

##### Cable Plowing

1. The cable should have minimal tension when passing over guide rollers and as it enters the plow chute.

2. The radius of curvature in the plow chute should be a minimum of 10 times the diameter of the largest cable it will accommodate.

3. It is advisable to pre-rip in rocky terrain and to take appropriate measures where boulders are encountered.

#### Duct Installations

1. Cable tension should be limited to 10,000 pounds per square inch of the copper cross section that is clamped in the pulling eye.

2. Friction coefficients shown herein are submitted as a guide, but it is recommended that operating companies measure pulling tensions and empirically determine friction coefficients in their own ducts.

3. Ducts should be a minimum of one-half inch or 15 percent larger than the cable, whichever provides the greater clearance.

4. Pulling tensions or equivalent lengths should be calculated for bends in the duct. Where the location and radius of the bend is not known, long cable pulls should not be attempted unless experience has shown conditions to be satisfactory.

5. Side wall pressure should not exceed 150 pounds per foot.

6. Pulling through intermediate manholes should not be attempted unless all conditions are suitable.

7. Care should be taken in racking in intermediate manholes so the cable is not kinked nor bent too sharply, and so that the cable sheath is not unduly stressed.

#### References

1. Nystrom, C. W., "Tape Armored Telephone Toll Cable," AIEE Transactions, March, 1932.
2. Royal, W. C., "Modified Tape Armor and Lepeth Sheath Cable," Bell Laboratories Record, Vol XXVIII No. 6, June, 1950.
3. Rifenburg, R. C., "Pipe-Line Design for Pipe-Type Feeders," AIEE Transaction, Vol 72, Part III, P. 1275.
4. Miriam, J. L., "Mechanics," Second Edition, Part II, John Wiley and Sons, Incorporated, P. 1284.
5. Underground Systems Reference Book, Edison Electric Institute, New York, 1957.
6. Bell System Practices, Section 919-240-100 Issue 2, December 1974, "Conduit System Design."
7. A T & T Specification AT-7437.
8. General System Practices, Section 628-100-201, Issue 1, August 1966, "Installation, Placing Cable in Main Conduit, Underground Cable." Copyright 1966 - Automatic Electric Company.
9. Buller, F. H., "Pulling Tension During Cable Installation in Ducts or Pipes," General Electric Review, August, 1949.

10. Bosworth, D. W., Discussion of R. C. Rifenburg "Pipe Line Design for Pipe-Type Feeders," AIEE Transactions, Vol 72, Part III.

11. General System Practices, Section 081-325-101, Issue 1, April 1970, "Puller, Slack, Cable, Manhole." Copyright 1970 - Automatic Electric Company.



V. W. PEHRSON

Mr. V. W. Pehrson received a BS degree in Electrical Engineering at Iowa State University in 1949. He was employed after graduation by General Cable Corporation. After assignments in the Research Laboratory and the Manufacturing Department, he was transferred to the Application Engineering Department in 1954. He is presently Chief Engineer, Communications Operation, General Cable Corporation and Vice President, Electrack, Incorporated.

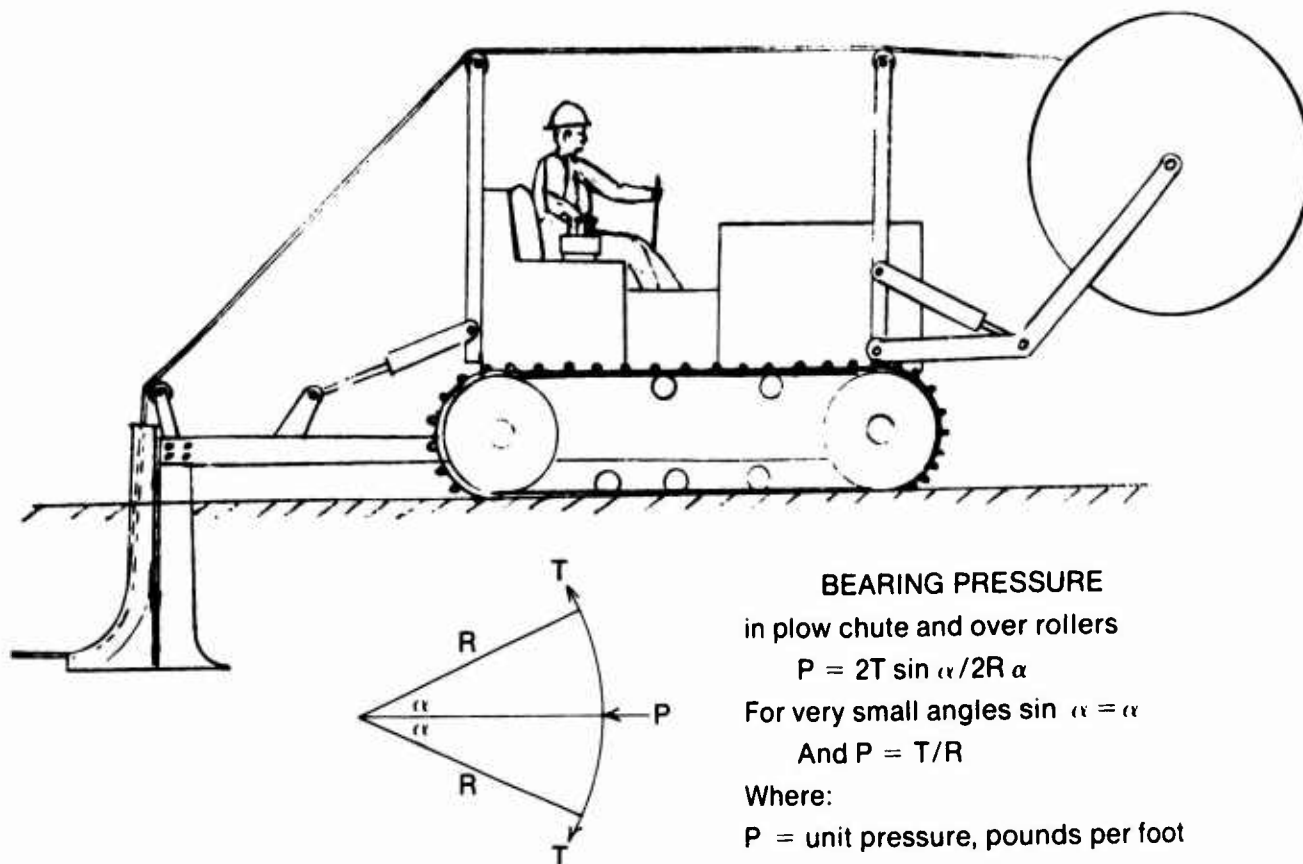


FIGURE 1

### BEARING PRESSURE

in plow chute and over rollers

$$P = 2T \sin \alpha / 2R \alpha$$

For very small angles  $\sin \alpha \approx \alpha$

$$\text{And } P = T/R$$

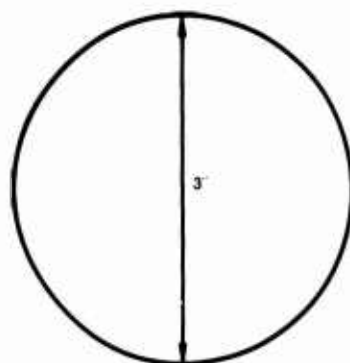
Where:

$P$  = unit pressure, pounds per foot

$T$  = tension, pounds

$R$  = radius, feet

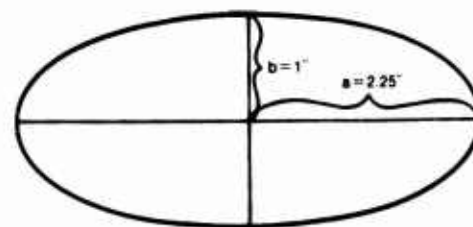
$\alpha$  = angle, radians



$$\text{Circumference} = \pi d = 9.43 \text{ inch}$$

$$\text{Area} = \frac{\pi d^2}{4} = 7.07 \text{ sq. in.}$$

FIGURE 2



Assume a 3 inch diameter circle is deformed to an ellipse with a 2 inch minor diameter (2/3 that of the circle) but maintaining the same area.

$$\text{AREA} = \pi ab = 7.07 \text{ sq. in.}$$

$$\text{with } b = 1 \text{ inch}$$

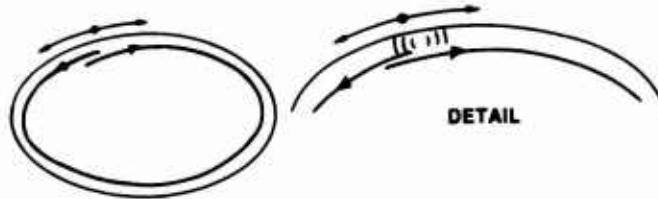
$$a = \frac{7.07}{\pi} = 2.25 \text{ inch}$$

$$\begin{aligned} \text{CIRCUMFERENCE} &= 2\pi \sqrt{\frac{a^2 + b^2}{2}} \\ &= 2\pi \sqrt{\frac{2.25^2 + 1^2}{2}} \\ &= 10.94 \text{ inch} \end{aligned}$$

In relation to the 3 inch diameter circle, the circumference is:  
 $10.94 - 9.43 = 1.51$  inches greater,  
 or 16% greater than the circle.

FIGURE 3

### WHEN THE SHEATH STRETCHES



The jacket is reinforced by the shield as a result of adhesion and friction.

In filled cables the weak point in the shield is the overlap where adhesion is reduced by the presence of filling compound which is essential to prevent moisture migration.

When adhesion in the shield overlap is overcome the shield can slide on itself at the overlap which concentrates the stretching of the jacket at that point.

With the stretching concentrated in a small fraction of an inch it can exceed the elongation properties of the jacket and it will part in a line over the shield overlap.

FIGURE 4

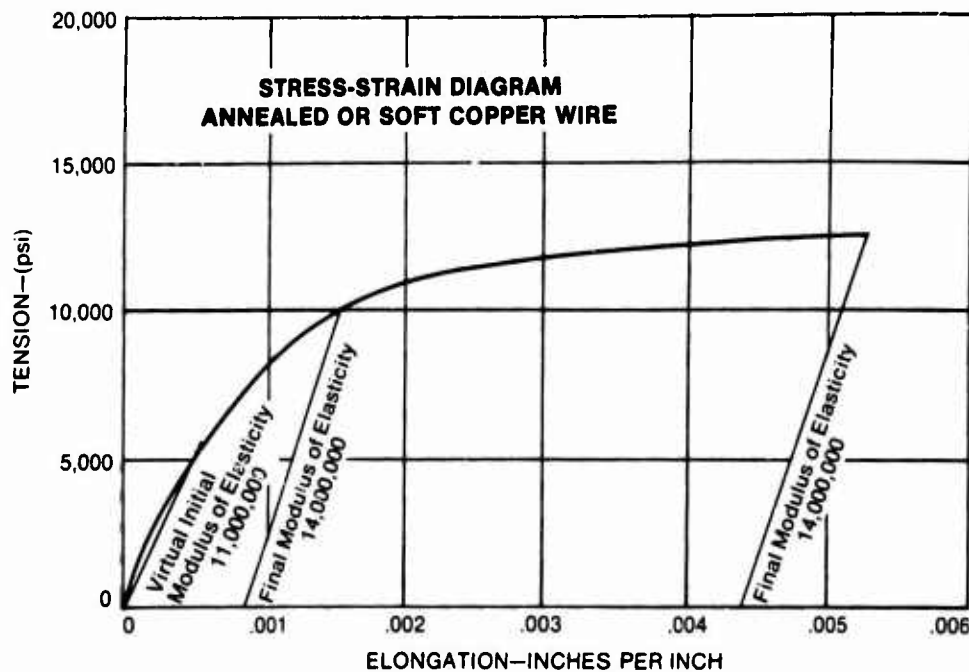
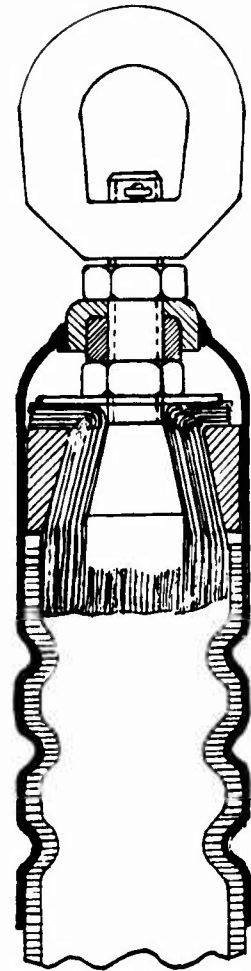


FIGURE 5



PULLING  
EYE

FIGURE 6

## UNDER CARPET POWER AND COMMUNICATION WIRE SYSTEM

by  
**James Fleischhacker**  
**AMP Incorporated**  
**Harrisburg, Penna.**

In the construction of modern open-area office space, a major design problem is to economically provide electric power and communication services to interior locations. As the use of color-keyed carpeting to separate work areas becomes more widely used due to its flexibility and low maintenance costs, the elimination of expensive duct work and raceways by laying a flat cable wiring system directly on the primary floor becomes a possibility. The successful manufacture of flat-conductor cable as pioneered by NASA<sup>1-5</sup> as part of the space program further supports such an endeavor.

The major limitation to such a system is that it does not service the ceiling lighting circuits. The expected advantages of this system, however, are lower initial cost (through elimination of raceways) and ease of rearrangement.

A trial installation of the under-carpet system was conducted in a 3400 square foot sales office area. It included 18 floor mounted and three baseboard-mounted duplex outlets, and 24 key-phone sets. Three steps were involved in the installation. First, flat power cables were run from the wire closet to the desired outlet locations, and a steel-fault current shield laid over the cable to provide mechanical and electrical protection. Second, flat communication cables were run over the power cable to several telephone outlet locations. Finally, carpet was laid over the area, with openings cut in it to expose the cable terminations. Power outlets and key sets were connected to these points.

### POWER CABLING

Four parts made up the power cabling assembly: a transition from round wire to flat cable, flat cable tee tap assemblies, duplex outlets, and a fault-current shield.

#### Transition

Primary power was provided by a commercially available GFI (ground fault indicator) protected breaker panel. Three flat cable circuits were interfaced to the round wire from the panel at barrier blocks as shown in Figure 1.

The flat cable configuration, developed by Parlex Corporation and NASA-Huntsville, consisted of three 14 AWG copper conductors (600 X 6 mils) laminated between two five-mil Mylar jackets. This configuration passes UL 719 and UL 83 requirements.<sup>5</sup>

Three main cable runs were extended from the wire closet to the office area by taping the cable to the concrete floor. Right angle corners were made by folding the cable back on itself (Figure 2).

The folded double thickness in these areas was undetectable once the carpet was in place.

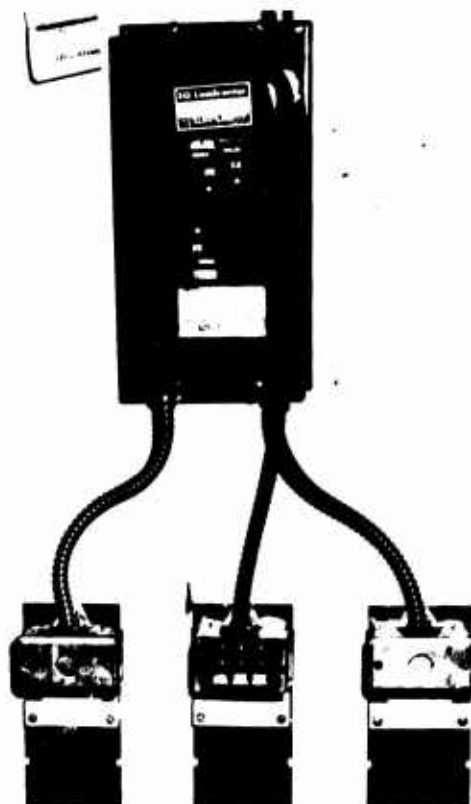


Figure 1. Barrier Blocks

#### Tee Tap Assembly

To provide power at the duplex outlet locations, tee joints were tapped into the three main cable runs. The taps consisted of three terminals bonded to a Mylar carrier (Figure 3). The tooling used to apply this assembly was a fixture plate to position the cables and tap-

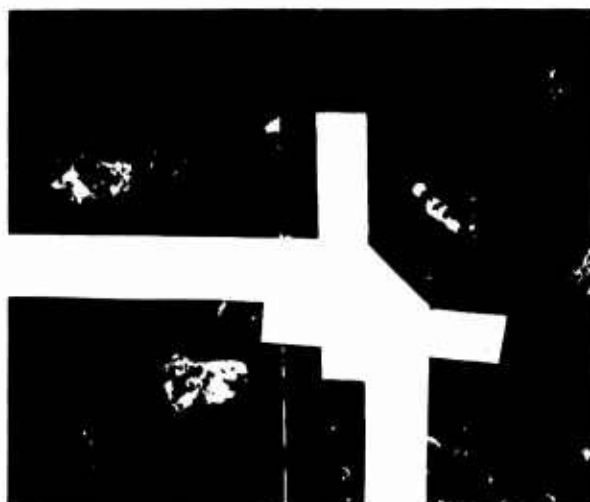


Figure 2. Folded Corner



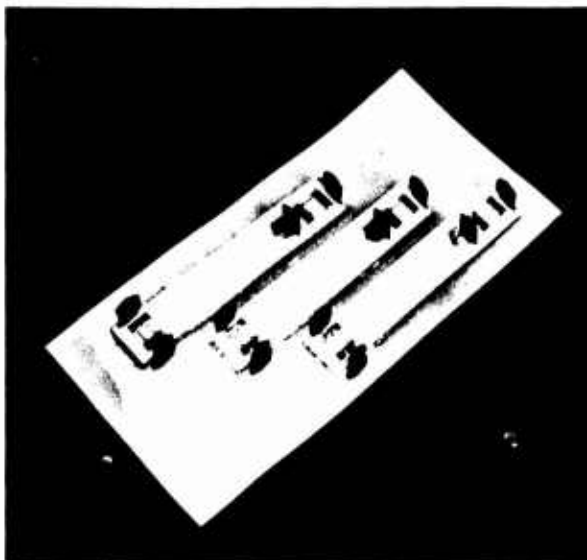


Figure 3. Tee Tap Assembly

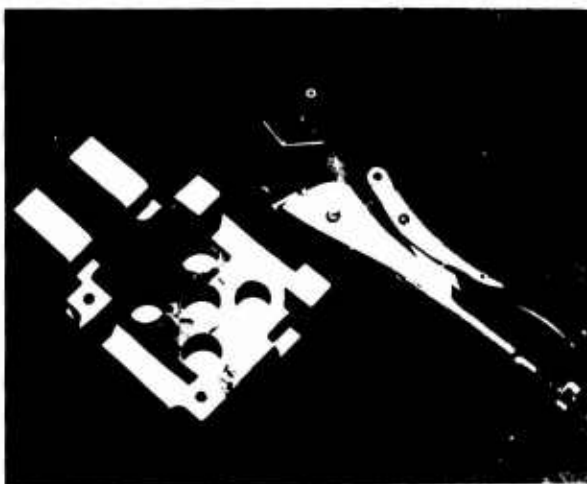


Figure 4. Applicator Tooling

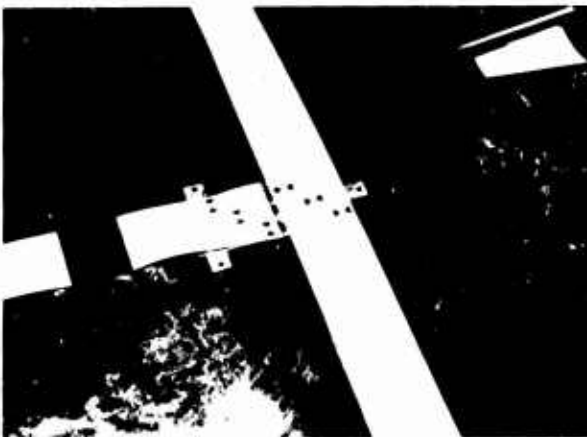


Figure 5. Tee Joint

#### TERMINAL AND CRIMPING SEQUENCE

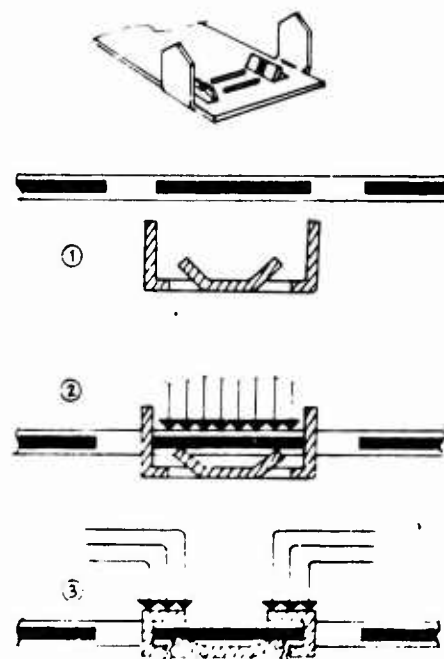


Figure 6. Terminal Crimping Sequence

assembly, and a modified vise grip to crimp the terminals (Figure 4). A finished tee joint is shown in Figure 5. Mylar was taped over the joint to insulate it.

The insulation displacing terminal and the crimping sequence that was developed to terminate the power cable is illustrated in Figure 6. In the crimping sequence, the cable is positioned over the terminal assembly and the fixture plate forces the large lances through the cable insulation. The visigrip is then used to crimp the large lances over. The crimping action forces the cable to depress the four contact lances. These skive the Mylar insulation from the bottom of the conductors, wipe the copper, and form a stored energy, gas tight, redundant joint. A microphotograph of the crimp is shown in Figure 7. The crimp has been current-cycle tested at



Figure 7.



Figure 13. Communication Cable Congestion



Figure 14. CHAMP Terminated Cable.



Figure 15. Communication Runs

laid on top of the power cables, running at right angles where possible to facilitate these movements.

The 25 pair communication cables were mass terminated on both the office and wire closet ends by using the CHAMP connector and tooling.<sup>6</sup> A terminated

cable is shown in Figure 14. The connectors were placed at the desired outlet locations and the cables were run back to the wire closet (Figure 15). A mating CHAMP connector provided transition to round wire in the closet. The round wire was terminated line-by-line in standard 66 blocks.

## CARPETING AND CONNECTING

With all cabling in place, the floor was coated with adhesive and six foot wide carpet was installed. The base plates were visible as lumps under the carpet. Guided by feel, the installer first cut on the narrow sides of the rectangular base plate and then cut across a keyed long side. As the cable always approached the base block from the non-keyed long side, there was no danger of cutting the cable while cutting the carpet. Folding back the carpet exposed the base plate as shown in Figure 16.

Standard duplex outlets were equipped with pigtail leads terminated with pre-insulated quick connect terminals. These in turn mated with the tabs that had been crimped to the power cable (Figure 17). The carpet flap was tucked into a divided compartment in the trim box. This keeps the carpet, which could have conductive anti-



Figure 16. Base Plate Exposed



Figure 17. Quick Connect Pigtails

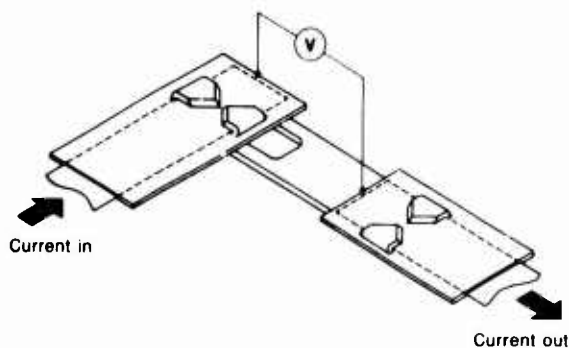


Figure 8. Resistance Testing

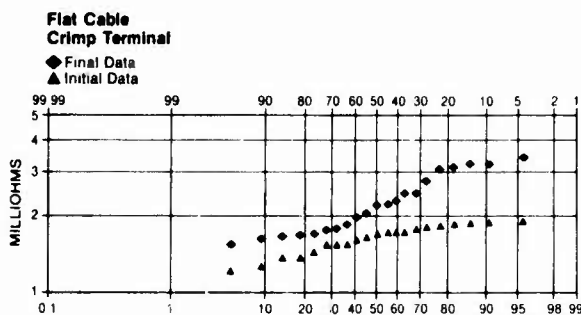


Figure 9.

40 amperes with equal "on" and "off" periods of 15 minutes.

Four wire resistance measurements were taken across the tap as shown in Figure 8. The initial and final resistance distributions (Figure 9) show a maximum increase of two milliohms after 512 current cycles.

#### Duplex Outlets

Terminations to the duplex outlets were made at the ends of the tee runs by use of tab terminals and base plates. This assembly is shown in Figure 10. The terminals were crimped to the cable as before, but in this application a tab protruded from the crimp area for con-

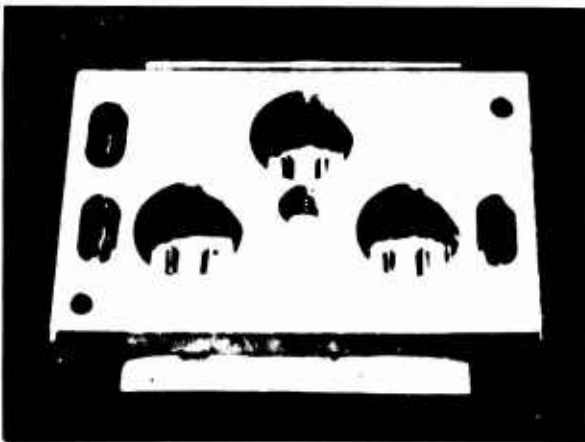


Figure 10. Duplex Termination



Figure 11. Installed Duplex Base

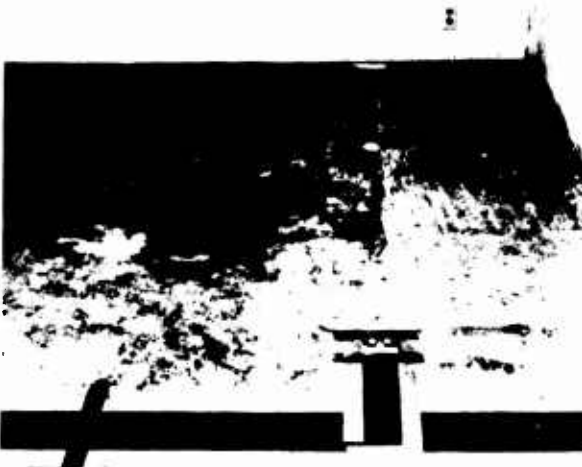


Figure 12. Fault-current Shield

necting to the duplex outlet by means of a pigtail lead. The base plate provided mechanical protection for the terminals and was attached to the concrete floor by a ram set rivet. An installed assembly is shown in Figure 11.

#### Fault-current Shield

A six-inch width of adhesive-backed, eight-mil steel was laid over the power cabling. This both secured the cabling and provided mechanical protection. The shield also was grounded back through the breaker panel to provide protection against electrical hazards such as piercing of the cable by a sharp metal object. The shield also aided in fairing over the cable edges and made them virtually undetectable under the carpet. Figure 12 shows a circuit run with the shield in place.

#### COMMUNICATION CABLING

The communication cabling consisted of twenty-four runs of flat cable, primarily Western Electric PSEUDO TWIST. Since only three power circuits were required, the main wiring density was in the communication system. (This is graphically shown at the wire closet in Figure 13.)

Since these cables are moved more frequently than are the power cables, the communication cables were

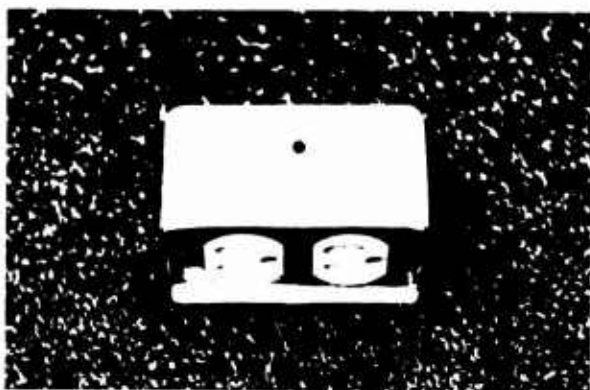


Figure 18. Completed Power Outlet



Figure 19. Completed Telephone Outlet

static fibers, separated from the hot side of the outlet. It also preserves the carpet flap so it can be placed back in position if the outlet location is ever moved. The telephone and power trim boxes were secured to the base plates with screws. Figure 18 shows a completed power outlet, and Figure 19 a completed telephone outlet.

## CONCLUSIONS

The trial installation demonstrated that an under-carpet wiring system is entirely feasible. Satisfactory cable, terminations and installation techniques were established. Furthermore, the expected benefits of labor and material savings can be realized.

One area that requires additional work is the capacitive coupling of the power conductor to the steel shield foil. The installed circuits fundamentally are distributed capacitors. This imports small leakage currents to the shield and can cause false tripping of the GFI's. This was overcome in the trial installation by using an off-setting lumped capacitor that fed a current equal to the leak current to the return side of the GFI.

Additional trial installations are necessary to again experience in using the system on a day-to-day basis and to establish confidence in the long term reliability of the system. We are continuing our development and testing to gain this experience.

## REFERENCES

1. W. Angele, "The Manufacture of Flat Conductor Cable." NASA TMX-64875, May 1974.
2. J. D. Hankins, "Temperature Rise of Flat Conductor Cable Installed Under Carpet." NASA TMX-64883, September, 1974.
3. J. D. Hankins and J. R. Carden, "Surface-Mounted Flat Conductor Cable For Home Wiring." NASA TMX-64887, August 1974.
4. J. D. Hankins, "Testing of a Flat Conductor Cable Baseboard System For Residential and Commercial Wiring." NASA TMX-64888.
5. R. W. Loggins and R. H. Herndon, "Testing of Flat Conductor Cable To Underwriters' Laboratories Standards UL 719 and UL 83." NASA TMX-64893, September 1974.
4. D. J. Doty and G. A. Patton, "Mass Wire Insulation Displacing Termination of Flat Cable." AMP Technical Paper prepared for NEPCON East, 1973.

James Fleischhacker graduated in 1966 from the University of Minnesota with a Bachelor's degree in Aeronautical Engineering and graduated in 1968 from MIT with a Master's degree in Mechanical Engineering. He worked for the Sandia Corporation and MIT prior to joining AMP Incorporated in 1970. He is Project Manager of the Advanced Development Laboratory.



INSERTION FORCES AND MECHANICAL STRENGTH  
CHARACTERISTICS OF 700-SERIES CONNECTOR INSTALLATIONS

by

A. T. D'Annessa, J. J. Blee, D. T. Smith  
Bell Laboratories

ABSTRACT

The use of the 700-3B slotted beam connector for splicing various size aluminum and copper telephone cable conductors is discussed and selected joint characteristics are described. The principal topics of interest include: connector forces, insulation piercing behavior, wire joint strength, and effects of component compliance during installation. Force-displacement profiles during conductor installations in the 700-3B and observations on subsequently dissected connectors provided much of the information on these topics.

INTRODUCTION

The 700-3B single-type connector (Figure 1) is used in outside plant waterproof telephone systems to join either copper or aluminum conductors.<sup>1</sup> Connections can be made with any combination of wire sizes ranging from 26 to 17 gauge without stripping insulation. The 700-3B is a three component connector consisting of a body, cap, and contact and is furnished to the craftsman as an assembled unit containing an encapsulant compound for moisture resistance. Connection is accomplished with either a plier type tool requiring prepositioning of each connector or a magazine load-type tool with parallel clamp faces (jaws).

This paper discusses the results of several studies concerned with the characterization of the 700-3B connector. These include (1) the insertion forces encountered during installation, (2) mechanical strength of connections, and (3) body and cap compliance effects on insulation forces and joint strength.

CONNECTOR FORCES

The insertion forces encountered during connection in the 700-3B were studied in order to:

1. determine typical forces involved in the cut-through of different insulations and the penetration and insertion of the conductor into the contact;
2. rank insulations in terms of their resistance to penetration and piercing by the contact element; and

3. evaluate the effects of installation temperature as it influences the behavior of the plastic components of connector and the insulation.

Experimental Technique

The force-displacement profile was recorded for each installation of interest. Each test consisted of a fully inserted single conductor in the center wire position, Figure 1, of the connector; thus, force data were obtained for connection into the front and rear slots of the contact. These installations were made in an Instron Model TM-S testing machine operated in the compression mode. A minimum of five replicate tests were conducted. The strain relief details of the cap component, Figure 1(a), were removed for these tests. This work was performed with 24 gauge copper conductor having the following insulations:

- a. Low density polyethylene for air core cable (LDPE)
- b. High density polyethylene for air core cable (HDPE)
- c. High density polyethylene for waterproof cable (WP-HDPE)
- d. Polypropylene for waterproof cable (WP-PP)
- e. Pulp
- f. Polyvinyl chloride (PVC)
- g. Irradiated polyvinyl chloride (IR-PVC)
- h. Polyvinyl chloride with cotton serving (PVC/C.S.)

The difference between HDPE and WP-HDPE is the diameter of the insulation; nominal diameters for these insulations are referenced in Figure 3. Earlier work (not reported here) showed that subtle variations in insulation-contact interactions were often overshadowed with larger diameter conductors but not with 24 gauge copper conductors.

A typical force-displacement profile, Figure 2, displays several discrete features.



The curves for various conductors and insulations had the same general characteristics but varied in slope and amplitude. The stage of insertion corresponding to each portion of the curve, Figure 2, was verified by interrupting the installation at points along the curve, dissecting the connectors and observing the partial connections under a microscope.

Of particular note, for the purposes of this paper, are the insulation piercing force and the maximum force associated with the insertion of the conductor. In addition, displacement data obtained from these curves were used in describing the effects of compliance and installation temperature.

#### Insulation Piercing Characteristics

The force for piercing the various insulations in ambient and 0°F temperature installations are shown in Figure 3. The piercing forces follow the tensile strength (also in Figure 3) of the insulations; high piercing forces are associated with high strength insulations. This relationship is maintained for both ambient and 0°F temperature installations.

#### Conductor Insertion

The force for insertion of the conductors into the contact wire slots, after the insulation is pierced, in ambient and 0°F temperature installations are shown in Figure 4. These data are arranged in order of decreasing ambient temperature insertion force; the forces associated with the installation of the bare conductor is included for reference. Although all of the conductors are 24 gauge copper, annealed to the same strength, it is clear that the prior insulation-contact interaction affects the force necessary to engage the conductor beyond the point where the insulation is pierced. With the exception of pulp insulated conductor, the conductor insertion forces tend to follow the trend in tensile strength of the insulations.

The insertion forces are lower at ambient temperature than 0°F except for the IR-PVC insulated conductor. However, even the bare conductor requires a significant increase in insertion force at 0°F which obviously cannot be attributed to an increase in insulation strength with decreasing temperature. This increase in conductor insertion force at low temperature is due to a decrease in compliance (increase in rigidity) of the polycarbonate connector components (cap and body). The effects of compliance are discussed in more detail in a later section. The more meaningful comparison of 0°F insertion forces for the varying insulated conductors (Figure 4) is with the 0°F bare conductor forces. Thus, the increases in conductor insertion forces at 0°F are significantly less when the compliance contribution of the polycarbonate is deleted.

#### Effect of Insulation on Conductor Insertion

Several points can be made in comparing insulation piercing data (Figure 3) with conductor insertion data (Figure 4). The data follow a logical sequence in that insulation piercing forces are lower than conductor insertion forces for the low strength insulations and comparable to or greater than insertion forces for the higher strength insulations. Of particular note is the effect of pulp on conductor insertion. The ambient conductor insertion forces with pulp are comparable to those encountered with the plastic insulations for waterproof cable and, for 0°F installations, the conductor insertion forces associated with pulp are as high as the forces encountered with the highest strength insulations.

All of the insulations provide additional resistance to insertion of the conductor. This additional resistance is due to effects associated with stripping away the insulation after the insulation is pierced during conductor insertion. Simultaneous with the metalworking of the conductor, the shoulders of the contact beams must strip away the insulation. The gathering, or piling, of insulation on the beam shoulders as they move through the conductor imparts a tearing action to the insulation. The resistance to this tearing action is the primary contribution of the insulation to forces measured during the conductor insertion interval. It follows that the insulation contribution to conductor insertion force would be greater with 26 gauge wire and less with 22 gauge or larger wire.

#### MECHANICAL STRENGTH OF JOINTS

The ambient temperature wire joint strength (load at failure) of 700-3B connections made at ambient and 20°F temperatures in a range of sizes of copper and aluminum conductors are shown in Figures 5 in normal distribution form. The joint failure loads were obtained directly from load-strain strip chart records on an Instron machine. The connectors were fixtured so that the conductors were pulled normal to the plane of the contact beams; the direction of pull is offset by the joggle of the wire through the strain relief of the connector. (The strain relief details were not removed in these tests.) Thus, the reported joint strengths include the contribution of the strain relief towards resisting failure of the connection.

#### Copper Conductors

The joint strengths of 19 and 24 gauge Cu do not vary significantly between ambient temperature and 20°F connections whereas, the 20°F connection for 26 gauge trend lower than ambient temperature ones. The latter variation is the result of the increased elastic response of the contact beams prior to penetration and piercing of the insulation. For the 26 gauge conductor, the beams spread

sooner in time at 20°F due to the low temperature strengthening of the insulation. The mechanical engagement of 26 gauge conductor by the contact beams is less than that experienced in ambient connections, and occasional joint failures occur by the wire pulling through the slots of the contact. However, there is no difference in the electrical characteristics of ambient and 20°F temperature connections in 26 gauge Cu.

The slopes of the lines in Figure 5, indicating standard deviation, are conductor size-dependent. Standard deviations increase with increasing conductor size (larger than 20 gauge) and are generally the same for 20 gauge and smaller conductors. With exception of the 26 gauge data, the standard deviations are the same for ambient temperature and 20°F connections; the high standard deviation for the 26 gauge, 20°F, data is due to the change in the mode of failure noted previously.

In summary, the mean wire joint strength of 700-3B copper connections is greater than the nominal ultimate tensile strength of the bare conductor. The mean strength of 17 gauge EC-Al connections compares with the nominal ultimate tensile strength of the bare conductor; whereas the mean joint strength for 20 gauge EC-Al connections is approximately 85 percent of the bare conductor strength.

#### Aluminum Conductors

Joint strength distributions for 20 gauge Al and 22 gauge Cu are shown in normal probability form in Figure 6. These plots are for two aluminum alloys (Stabiloy A and 8076), EC aluminum, and copper insulated with high and low density polyethylene. The data indicate that the joint strengths of 20 gauge aluminum conductors increase with increasing tensile strength and approach the strength of the equivalent resistance 22 gauge Cu conductor. The standard deviation of EC aluminum connections is slightly greater than those of the aluminum alloys while the alloys are comparable to 22 gauge Cu in this respect. It is significant that the mechanical reliability of aluminum joints can approach that of copper joints.

### PLASTIC COMPLIANCE EFFECTS

#### Material Properties

Connector bodies, Figure 1, made from high density polyethylene (HDPE) and low density polyethylene (LDPE) were compared with the standard plastic, polycarbonate (PC), to determine the effects of varying compliance (rigidity) materials. (The typical tensile moduli for these plastics are: PC- $3 \times 10^5$  psi, HDPE- $1 \times 10^5$  psi, and LDPE- $0.3 \times 10^5$  psi.) The results show that wire joint strength is directly dependent on the compliance characteristics of the plastic body, Figure 7. The standard plastic, PC, produces the highest joint strength distribution, HDPE the next highest, and LDPE the lowest. In addition, the standard deviation

in joint strength is least in connectors containing PC bodies and essentially the same in connectors containing the two polyethylene type bodies. These data clearly indicate the desirability of using a rigid plastic for the subject body design to minimize dynamic dimensional changes during installation.

#### Temperature Effects

The influence of temperature-related changes in PC plastic parts of the connector is revealed in Figure 8 which compares the normal distribution of insertion forces of ambient and 0°F temperature installations. These tests involved the insertion of bare 24 gauge Cu into the center wire position of 700-3B connectors. The PC body and cap parts were the only nonmetallic components; the moisture proofing sealant was omitted. The data show that temperature-dependent compliance of PC is a significant factor with respect to connector forces in low temperature installations. Referring to Figure 4, the temperature dependence of the insulations may actually be secondary to that of the PC components.

### SUMMARY AND CONCLUSIONS

1. Force-displacement profiles of connector installations contain discrete features associated with the interactions of the contact beams with the insulation and the conductor. Penetration and piercing of the insulation are readily distinguished from the deformation, metalworking, and insertion of the conductor.
2. Force-displacement profiles can be used to rank insulations by piercing characteristics and to evaluate design changes which influence insulation piercing and conductor insertion behavior.
3. A direct relationship was observed between insulation piercing forces and the tensile strength of the insulation. Conductor insertion forces are less dependent on tensile strength of the insulation and appear to be influenced by tear and cut-through characteristics.
4. The standard deviations in wire joint strengths of copper and aluminum connections do not vary significantly. Joint strengths of 20°F copper installations trend lower than ambient temperature installations; whereas the trend is opposite for aluminum.
5. Connector compliance variations due to temperature, geometry, and/or materials are important considerations with respect to connector forces and wire joint strength in the 700-3B. The rigid polycarbonate plastic is more desirable as a cap and body material than the less rigid polyethylenes.

#### REFERENCES

1. D. F. Frey, D. T. Smith, and J. P. Pasternak, "700 Series Connectors for Aluminum and Copper Telephone Cable Conductors," 21st International Wire and Cable Symposium-1972.



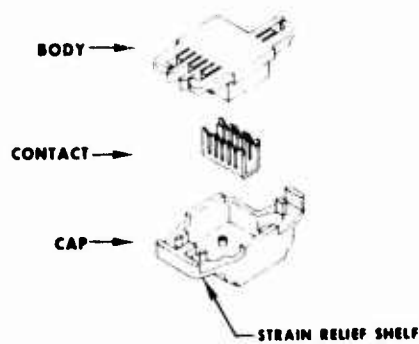
Donald T. Smith is a Senior Technical Associate in the Special Projects Group of Bell Laboratories at Atlanta, Georgia. He is a graduate of Wentworth Technical Institute and has been associated with development of connector systems from 1960 to present.



Anthony T. D'Annessa is a Member of Technical Staff in the Metallurgical Engineering Group of Bell Laboratories in Atlanta, Georgia, since 1972. Prior to this he was associated with metals joining and materials engineering developments in the aerospace industry. Mr. D'Annessa has the BWE and MSc degrees from The Ohio State University.



John J. Blee is an Associate Member of Technical Staff in the Metallurgical Engineering Group of Bell Laboratories in Atlanta since 1970. Mr. Blee received a B. A. degree from Rutgers College and has carried out graduate study at Rensselaer Polytechnic Inst. and Georgia Tech. His prior background was in the ocean cable protection area.



(a) ELEMENTS OF 700-3B CONNECTOR



(b) TYPICAL INSTALLATION OF WIRE IN CONTACT UNIT.  
Figure 1 - (Subcaptions as noted)

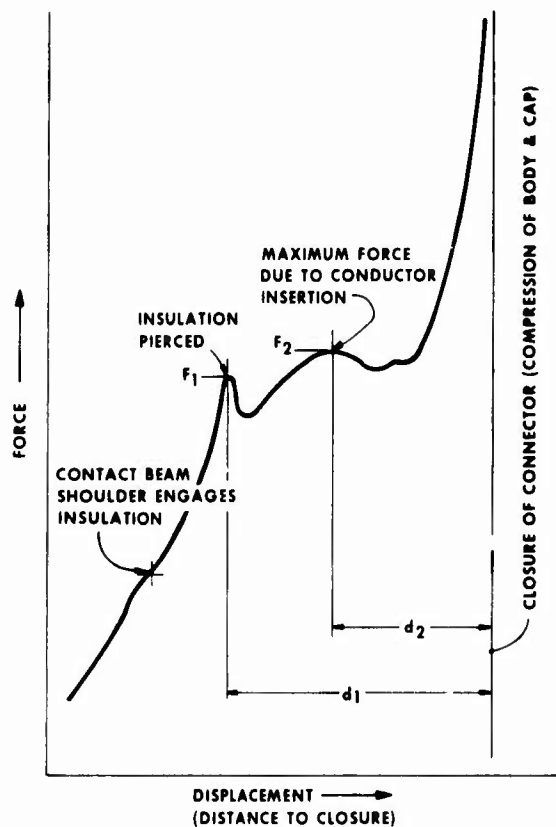


Figure 2 - Typical Force-Displacement Profile for 700-3B Connector Installation.

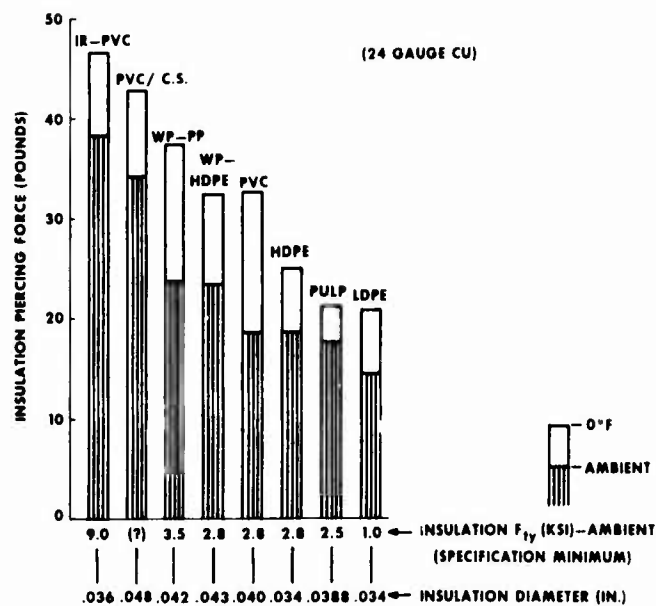


Figure 3 - Insulation Piercing Forces for 700-3B Connector.

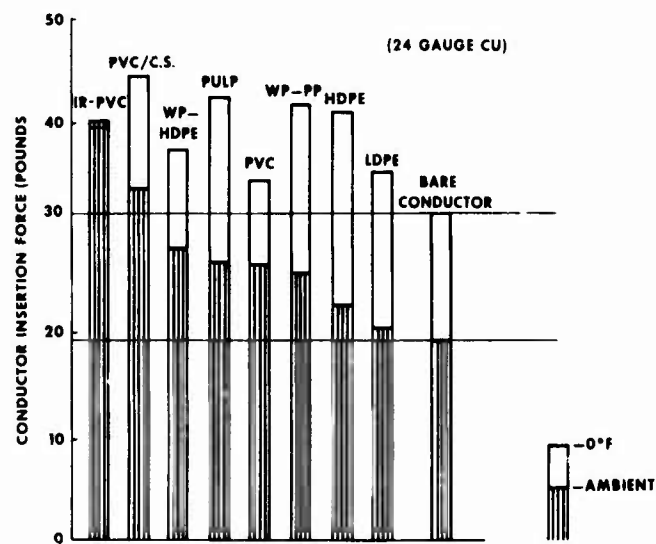


Figure 4 - Conductor Insertion Forces for 700-3B Connector.

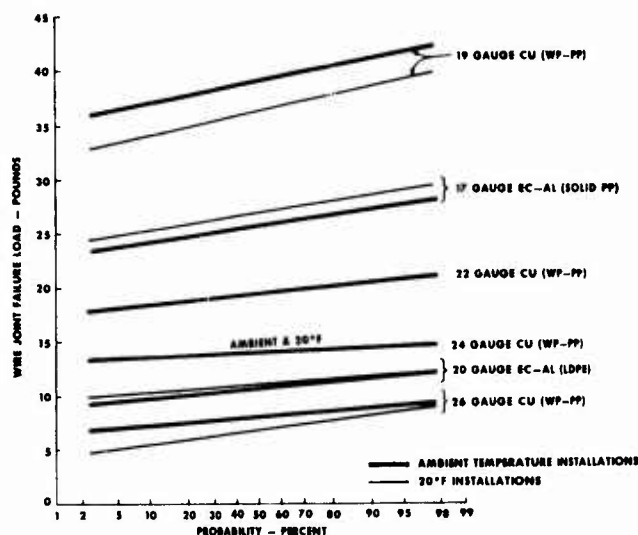


Figure 5 - Normal Distributions of Wire Joint Failure Loads for Copper and Aluminum Conductors Installed in the 700-3B Connector.

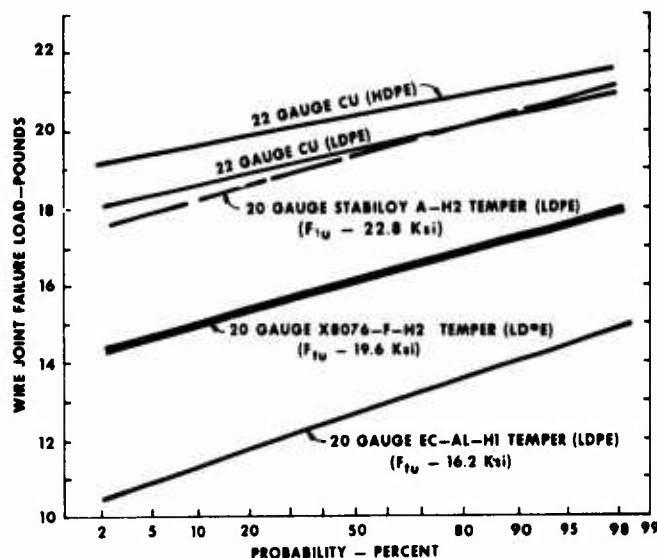


Figure 6 - Normal Distributions of 700-3B Connector Wire Joint Failure Loads Comparing 20 Gauge Aluminum with 22 Gauge Copper Conductor.

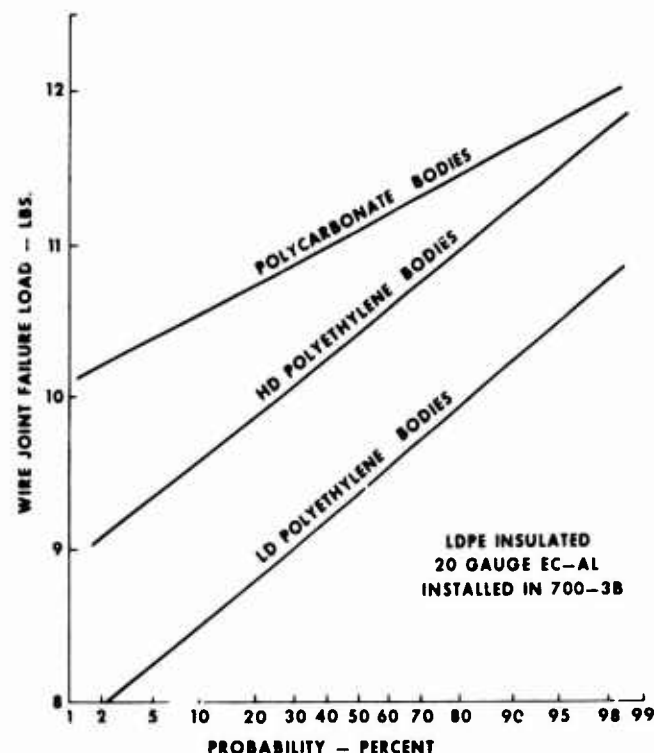


Figure 7 - Wire Joint Failure Load Variations Showing Effects of Varying Compliance (Rigidity) of the 700-3B Body Component by Plastic Material Substitution.

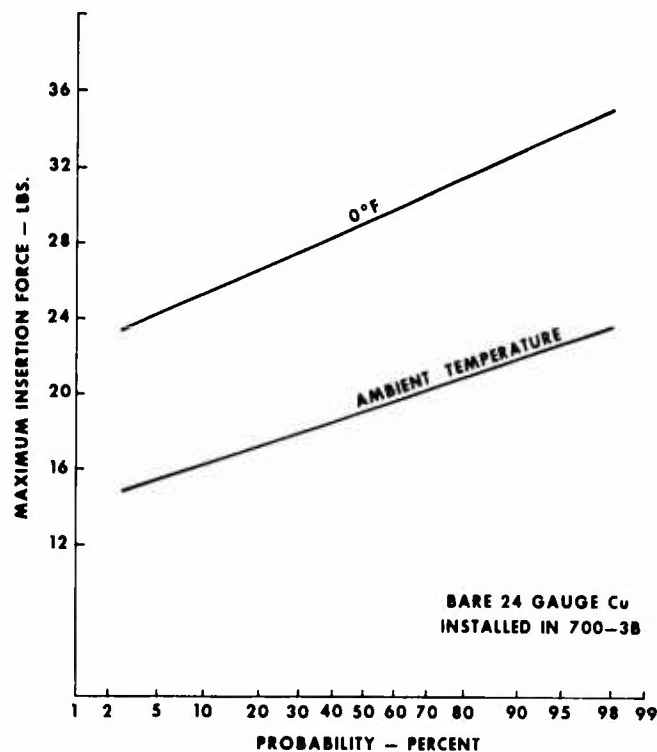


Figure 8 - Insertion Force Variations in 700-3B Connector Installations due to Temperature Effects on Polycarbonate Components.

## Advantages of Optical T-carrier Systems on Glass-Fiber Cable

John Fulenwider, GTE Laboratories, Waltham, Mass.  
George Killinger, GTE Service Corp., Stamford, Conn.

T-carrier gives 24, 96 and 672 voice circuits at the T1, T2 and T3 rates of 1.544, 6.312 and 44.736 megabits per second. T-carrier on twisted pairs at the T1 rate is now being used to provide many of the existing trunk circuits in telephone companies. Optical T-carrier on glass fibers at the T1, T2 and T3 rates offers great promise for economically providing many of the future trunk circuits. The potential of this new optical technology for use in interoffice trunking is examined below. The terms "T-carrier" and "PCM carrier" are used interchangeably in the remainder of this paper.

### Principles of Operation

The "new components" which are used in an optical T-carrier system are (1) light sources (2) glass fibers and (3) photodiodes.

A light source is a device which converts an electrical PCM signal (electrical pulses) to an optical PCM signal (light pulses). Present light sources include (1) light emitting diodes (LEDs) and (2) several types of lasers. For use in optical T-carrier systems, the light emitting diode is a solid-state device which generates wide-angle infrared light in a wavelength band typically centered about  $.85 \mu\text{m}$  (see Figure 1), or thereabouts--present commercial designs for these LEDs tend to have a center wavelength in the range of  $.8$ -to- $.9 \mu\text{m}$ . It appears that these light emitting diodes can be efficiently used as light sources for optical PCM carrier systems to be used in the telephone company environment--especially during the 1980-to-1985 time period. Short-duration light pulses at the T1, T2 and T3 rate can be generated by electrically pulsing a LED.

At a wavelength of  $1.06 \mu\text{m}$ , glass fibers generally have a lower value of attenuation than is obtained in the  $.8$ -to- $.9 \mu\text{m}$  wavelength band. A decrease in attenuation approaching  $1 \text{ dB/km}$  is sometimes obtained at the longer wavelength of  $1.06 \mu\text{m}$ . Light emitting diodes with a center wavelength of  $1.06 \mu\text{m}$  are now being developed. Certain types of lasers (including Nd:YAC lasers and semiconductor injection lasers) may eventually displace LEDs as light sources

for optical T-carrier systems because repeater spacing can be increased substantially, but the information given below pertains mainly to optical T-carrier systems using LEDs as light sources.

The PCM light pulses are attenuated as they travel down the glass fiber. There is also a "spreading" or "broadening" of the PCM light pulses as they travel down the glass fiber--so that a light pulse may "smear" into the following adjacent time-slot. If the following time-slot does not contain a light pulse, then a "bit error" may occur--that is, a "0" is sent in the following time-slot, but a "1" is detected.

When the light pulses at the T1 rate traveling in the fiber have been attenuated by  $45 \text{ dB}$ , or when pulse spreading exceeds one-half of a time-slot (assuming half-duty-cycle rectangular pulses), then the light pulses will enter a repeater to be "regenerated." In the repeater, the light pulses are directed to impinge on a photodiode. A photodiode is a solid-state device which converts the PCM light pulses into PCM electrical pulses (this function is called photodetection). The electrical pulses are amplified, detected and retimed. The retimed electrical pulses then drive a LED. The regenerated light pulses (from the LED), which have been amplified back up to their original amplitude, enter the next section of glass-fiber cable.

The  $45 \text{ dB}$  value for "loss in the glass-fiber cable between adjacent repeaters" at the T1 rate is thought to be realistic--and it is based on studies of the operation of recently-designed LEDs and non-avalanche photodiodes; noise generated in the photodiode lowers the signal-to-noise ratio, which tends to raise the error rate--and this limits the maximum  $\text{dB}$  loss which can be tolerated between adjacent repeaters. When loss in the glass-fiber cable between adjacent repeaters has a low value (much less than  $45 \text{ dB}$ ), pulse spreading somewhat in excess of one-half of a time-slot can probably be tolerated.

The half-life of commercial LEDs in the year 1980 is projected to be 10-or-more years (work is continuing to extend this half-life). Assuming that light power output does not degrade by more than  $3 \text{ dB}$  in ten years, this  $3 \text{ dB}$  degradation can be absorbed in the engineering design specifications by reducing "maximum loss between repeaters" by  $3 \text{ dB}$  (typically, a reduction in loss from  $48 \text{ dB}$  to  $45 \text{ dB}$  in the glass-fiber cable between adjacent repeaters at the T1 rate).

A multimode fiber can accept and transmit the light energy which enters the fiber at an angle (with respect to the fiber axis) which is less than the critical acceptance angle  $\theta_c$  of the fiber. Typically, about 1-to-2% of the light power from a LED is transmitted down the fiber. Figure 2 illustrates how a certain percentage of the light power from the LED is "accepted" by a multimode step-index fiber. The fiber acceptance angle has a value of  $2\theta_c$ , which is double the critical acceptance angle of the fiber.

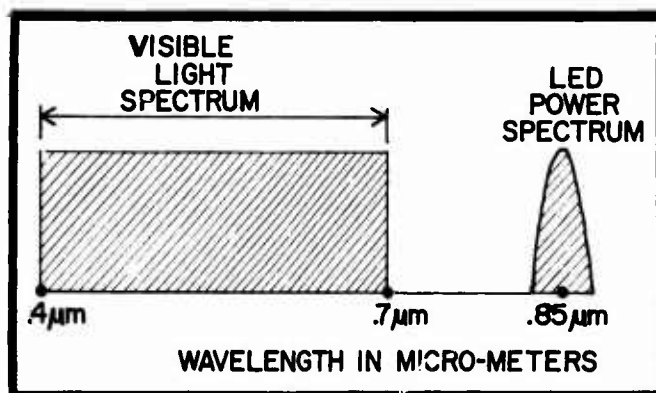


Figure 1. Typical LED power spectrum



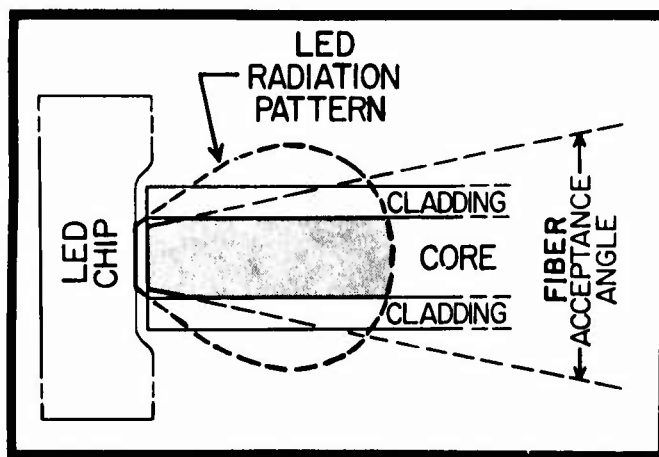


Figure 2. Acceptance of light power from a LED by a step-index fiber

Figure 3 illustrates the makeup of an optical T1 repeatered line. Light pulses are unipolar in a glass-fiber cable, while electrical pulses are bipolar in a twisted-pair cable. Existing channel banks can be used for an optical T1 line, but bipolar error detection will not be available with an optical T1 line. New office terminating repeaters and new line repeaters must be developed for an optical T1 repeatered line.

#### Glass Fibers in Cable

The diameter of a multimode glass fiber is typically 5 mils (.005 inches). Multimode glass fibers are classified as step-index fibers and graded-index fibers.

The step-index fiber (see Figures 4 & 5) has a glass core which carries the light power, with an approximate value of 1.5 for its index of refraction. A "cladding layer," with a slightly lower value for its index of refraction, surrounds the core. As can be seen in Figure 4, the light path of a propagating ray (mode) is made up of a series of straight-line segments--where each end of a path segment terminates on the boundary between the core and the cladding. When a divergent light ray strikes the interface between the core and the cladding, it is bent back (reflected) and continues traveling down the core (as is shown in Figure 4). Light rays which travel straight down the core (parallel to the center axis of the core) have a shorter path length than the light rays which are continually reflected back-and-forth as they travel down the core.

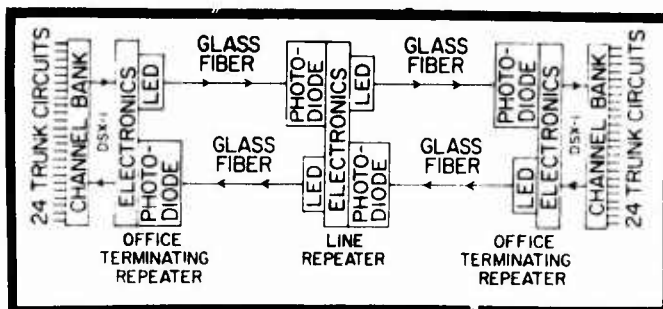


Figure 3. Optical T1 line on glass fibers

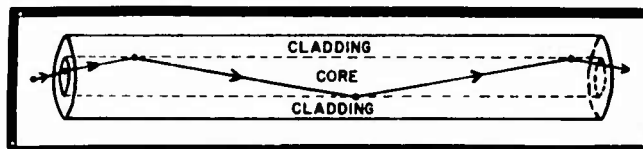


Figure 4. Light path in a step-index fiber

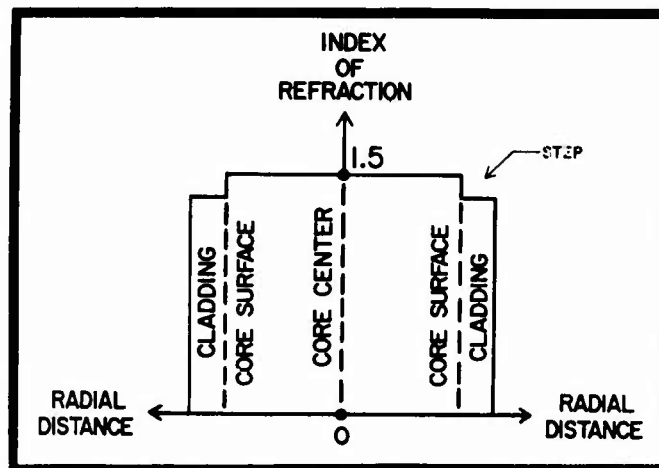


Figure 5. Index of refraction has a step profile in a step-index fiber

Light energy enters the end-surface of a step-index fiber at an infinite number of angles, but light energy is propagated within the core of a multimode fiber at distinct "grazing angles" (or angles of reflection)--due to interference effects. Only light rays which strike the core-cladding boundary at particular angles (corresponding to modes) are propagated within the core of a step-index fiber. Lower order modes correspond to small grazing angles, while higher order modes correspond to large grazing angles. The grazing angle of the highest order mode which is propagated in a step-index fiber is called the internal core-cladding critical angle of the fiber. A light ray which strikes the core-cladding boundary at an angle greater than the internal core-cladding critical angle is "lost" (will not be reflected). A multimode step-index fiber with a numerical aperture of .2 will typically propagate about 1500 modes within the core of the fiber.

Figure 6 shows the path of a light ray from a point light source traveling through the air and entering the end-surface of a step-index fiber at the critical acceptance angle  $\theta_c$ . This light ray may come from a LED or from another fiber. External light rays entering the fiber at an angle less than  $\theta_c$  will be transmitted down the fiber. Angle  $\theta_i$  is the internal core-cladding critical angle. In a practical optical system the air-gap may be absent between the light source and the fiber. In that case, one end of a "short-length coupling fiber" is bonded to the light emitting surface of the LED with an epoxy resin, and the other end of the coupling fiber is spliced to a fiber in a glass-fiber cable. The effects of an epoxy bond will not be considered here.

The numerical aperture (NA) of a step-index fiber is defined by the following formula:  $NA = \sin \theta_c$ . The angle  $\theta_c$  is the half-angle of an acceptance cone for which light rays will be accepted and transmitted

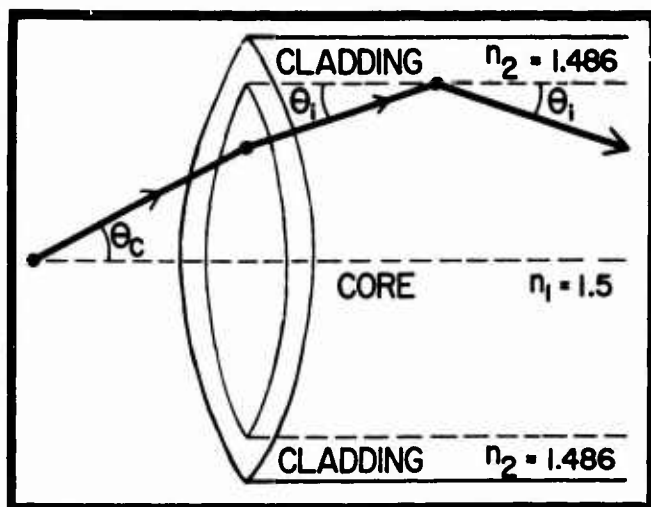


Figure 6. Critical angles of a step-index fiber

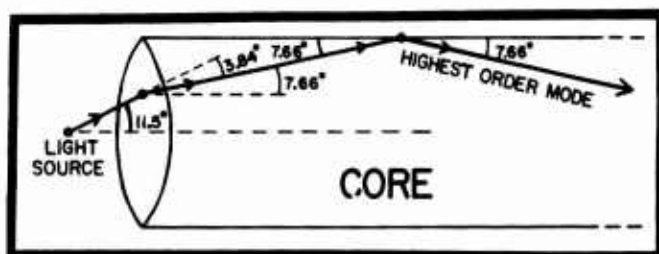


Figure 7. Highest order mode in the core of a step-index fiber

down the core. The parameters  $n_1$  and  $n_2$  (with assumed values of 1.5 and 1.486) specify the index of refraction in the core and in the cladding. The mathematical relationships for the step-index fiber shown in Figure 6 (which has a numerical aperture of .2) are as follows:

$$NA = .2 = \sqrt{n_1^2 - n_2^2} = \sin \theta_c = \sin 11.5^\circ$$

$$\theta_1 = 7.66^\circ \approx \frac{\theta_c}{n_1} = \frac{11.5^\circ}{1.5}$$

Figure 7 shows the core of a step-index fiber with a numerical aperture of .2, which has a critical acceptance angle of 11.5 degrees. Light striking the end-surface of the core at an angle which is not greater than 11.5 degrees (measured with respect to the axis of the fiber) will travel down the fiber. The highest order mode (which will be propagated) corresponds to a light ray which strikes the end-surface of the core at the critical acceptance angle of 11.5 degrees. This 11.5° light ray is refracted (bent) by 3.84 degrees as it enters the end-surface of the core from the air, so that the highest order mode has an angle within the fiber of 7.66 degrees--when measured with respect to the axis of the fiber.

For the step-index fiber shown in Figure 7, assume that the index of refraction in the core is 1.5 and the fiber length is 667 meters. With this index of refraction of 1.5, the speed of light in

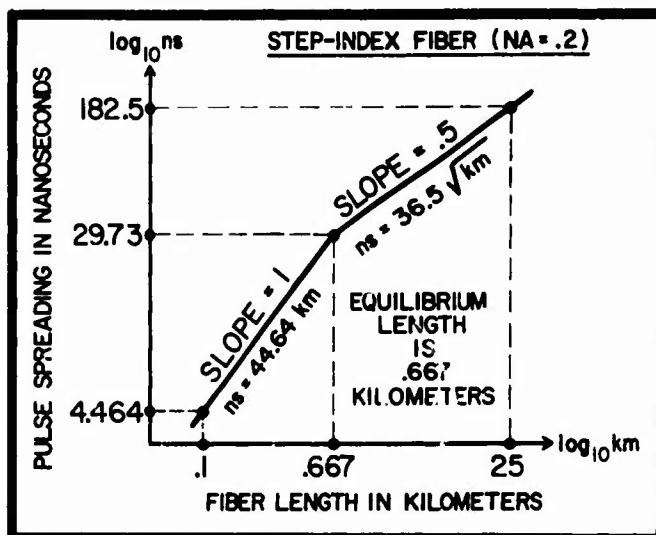


Figure 8. Log-log graph of pulse spreading

the core is 200,000 kilometers per second. The time required for light to travel end-to-end down the center of this fiber is 3.33 microseconds, and it is calculated as follows:

$$\frac{.667 \text{ km}}{200,000 \text{ km/s}} = 3.33 \mu\text{s}$$

Light which is traveling straight down the center of the fiber (at 0°) has a shorter path than light which is zig-zagging down the fiber at 7.66° (the highest order mode), and it will arrive sooner at the far-end of the fiber than the zig-zagging light. The percent difference in path lengths is .8928%, and it is calculated as follows:

$$100 \times (1.00 - \cos 7.66^\circ) = .8928\%$$

Pulse spreading in this 667-meter fiber is 29.73 nanoseconds, and it is calculated as follows:

$$.008928 \times 3.33 \mu\text{s} = 29.73 \text{ ns}$$

A light pulse tends to "spread out" or "broaden" as it travels down the fiber, and the amount of spreading increases with the length of the fiber. Pulse spreading increases in proportion to fiber length out to the equilibrium length--and beyond the equilibrium length, the pulse spreading increases in proportion to the square root of fiber length. The equilibrium length is assumed to be 667 meters for the step-index fiber shown in Figure 7. Pulse spreading as a function of fiber length is plotted in the "log-log graph" of Figure 8. From the log-log graph of Figure 8, the following two formulas for pulse spreading in nanoseconds (ns) as a function of fiber length in kilometers (km) can be mathematically derived.

$$ns = 44.64 \text{ km} \quad (\text{km} < .667)$$

$$ns = 36.5 \sqrt{\text{km}} \quad (\text{km} > .667)$$

Using these two formulas, pulse spreading has been recalculated, and it is plotted in the "linear graph" of Figure 9.

A step-index fiber will not have a perfect step profile at the boundary between the core and the

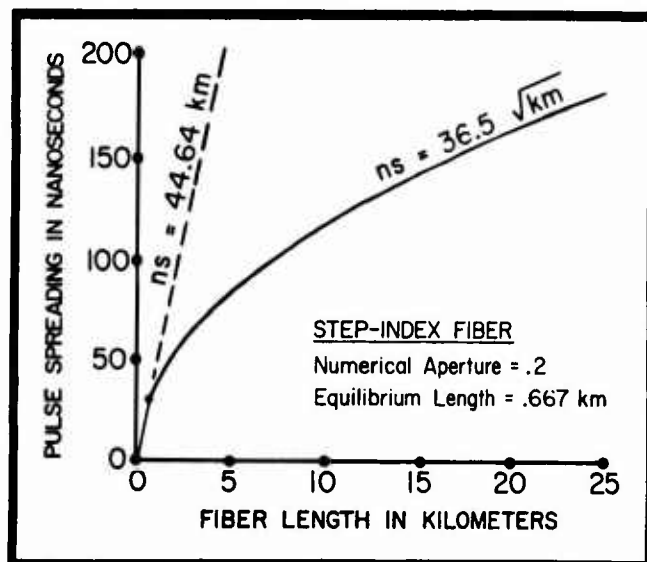


Figure 9. Linear graph of pulse spreading

cladding--but instead, there are irregularities and some "grading" at the boundary; and so the actual pulse spreading is somewhat lower than the theoretical model indicates (in some cases, up to 20% lower).

Figure 10 shows how a higher order mode travels in a graded-index fiber. There is a smooth bending of the light beam at each point on the path. The light beam winds its way back-and-forth (radially, as it travels down the fiber. In graded-index fibers, the index of refraction decreases with increasing radial distance from the center of the fiber (see Figure 11). The index of refraction has a maximum value at the center of the fiber, and a minimum value at the radial edge (surface) of the fiber. Speed of transmission of a light ray is inversely

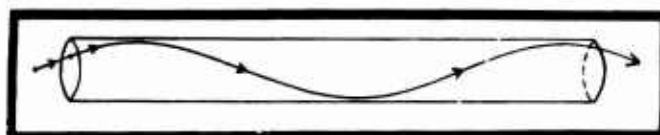


Figure 10. Light path in a graded-index fiber

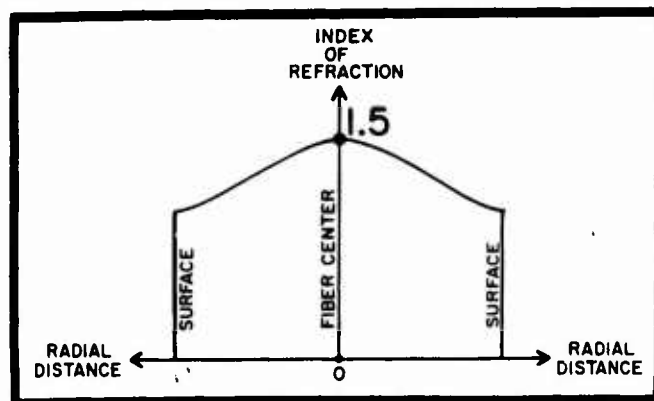


Figure 11. Index of refraction has a graded profile in a graded-index fiber

proportional to the index of refraction of the material in which the light ray is traveling, so that the light ray travels slower at the center of the fiber, and it travels faster in the more radial parts of the fiber.

The path length for a light ray traveling straight down the center of the fiber is shorter than the path length for a light ray which is zig-zagging back-and-forth as it travels down the fiber. However, the zig-zagging light ray travels faster as it swings out in the more radial parts of the fiber. By proper design of the grading pattern, it is possible to obtain net speeds for different modes which are approximately equal, so that pulse spreading is small.

Several "grading patterns" for index of refraction have been formulated for which the net speed of a light ray traveling straight down the center of the fiber is almost equal to the net speed of a light ray which is zig-zagging back-and-forth as it travels down the fiber. The pulse spreading in experimental graded-index fibers has recently been reduced to less than one nanosecond for a fiber length of one kilometer. When compared to the pulse spreading in a step-index fiber with the same numerical aperture, the pulse spreading in a graded-index fiber is reduced by a factor of 25-to-30. It is shown below that pulse spreading severely reduces repeater spacing at the T3 rate with step-index fibers, but has no effect with graded-index fibers.

Bending of the light beam can be explained in non-mathematical terms if it is assumed that the light ray shown in Figure 10 has a finite width. That part of the light ray which is nearer to the center of the fiber travels slower than that part of the light ray which is nearer to the radial surface of the fiber--because the index of refraction has a graded profile. These slight differences in speed of the more central and the more radial parts of the light ray causes the light ray to bend back toward the center of the fiber when the light ray is traveling in the radial portions of the fiber. When the light energy is traveling down a graded-index fiber, it is this "self-focusing" which prevents light energy from being lost out through the radial surface of the fiber.

At the present time, it is more difficult and more costly to make graded-index fibers than to make step-index fibers. Research and development efforts are making considerable progress in finding less costly methods of producing high quality graded-index fibers--which have low values for attenuation and pulse spreading. The cost of making graded-index fibers may break even with the cost of making step-index fibers by the year 1980.

By mid-year in 1975 it was possible to purchase 10 dB/km step-index and graded-index fibers from several companies at prices as low as \$1.50 per meter, and in lengths exceeding one kilometer.

Commercial low-loss glass fiber cable<sup>1</sup> having six buffered step-index fibers, with an initial selling price of \$13.50 per meter, was announced as an offering by a U.S. company in mid-1975. Since then, another company has indicated it will market a fiber cable--possibly by the end of 1975. Experimental fiber cable is being fabricated by several other companies, and additional commercial designs are likely to be forthcoming in the near future. Near-term commercial offerings may include (1) fiber cable with low-loss graded-index fibers, (2) fiber cable with lower values of attenuation and (3) fiber cable containing more than six fibers.

The cost of the glass fiber is projected to be \$.005 per foot by the year 1980. This cost of \$.005 per strand-foot of glass fiber is based on large-scale automated production of glass-fiber cable by the cable companies--which will be possible only if optical transmission hardware (terminals and repeaters) is also available in large quantities at competitive prices from the manufacturers (making entire systems feasible).

In addition to "first cost" considerations, the decreased susceptibility of glass-fiber cable to water damage, lightning and electromagnetic interference makes optical PCM carrier on fibers an attractive alternative to PCM carrier on twisted pairs as a means of providing many future trunk circuits in telephone companies.

#### Loss at Splices

Signal drop at a splice in a copper pair is negligible--that is, only a few millivolts. With this low loss, many splice points can be used when a copper-conductor cable is being placed. This is especially convenient because short sections of cable can be pulled into underground conduit (between manholes), and spliced in manholes between adjacent sections of the conduit. When a highway, street, railroad track, lake, river or other obstacle is encountered on a buried cable route, it is often convenient (or necessary) to splice the copper-conductor cable at this point (obstacle). In addition to the obstacles which require splice points in a buried cable route, additional splices may be required because of the length limitation on the amount of cable which can be shipped on a reel.

For conventional underground construction, where cables are pulled into conduit, typical spacing between splice points is 500 feet for large cables and 1000 feet for small cables. For buried cable routes, typical spacing between splice points is 1000 feet for urban routes and 2500 feet for rural routes.

Average loss for a splice in a multimode glass fiber has recently been reported at about .1 dB by several research groups. By the year 1980, it should be possible to consistently duplicate these research results under field conditions. A splice is most often formed by using a splicing connector (or coupler) which "butts together" the ends of two fibers in a semi-permanent arrangement. Total loss in the glass-fiber cable between adjacent repeaters in an optical T1 repeatered line is the sum of the loss in the glass fiber and the loss at the splice points, and is limited to 45 dB at the T1 rate when non-avalanche photodiodes are used. Pulse spreading in a multimode fiber has no effect on repeater spacing in an optical T1 repeatered line.

With an average loss of .1 dB at a splice point in a glass-fiber cable, and an average spacing between adjacent splice points of 2000 feet, the repeater spacing in miles is given in Figure 12 for an optical T1 repeatered line. The repeater spacing given in Figure 12 assumes that non-avalanche photodiodes are used in the optical repeaters, and that a signal-to-noise ratio of 21 dB (giving a repeater bit-error-rate of  $10^{-8}$ ) is required at the detector (photodiode) in the optical repeater.

When the more-expensive avalanche photodiodes are used in optical repeaters, then the values of repeater spacing given in Figure 12 can be increased by 20%--but the cost of avalanche photodiodes is too high at present to justify their use at the T1 rate.

Type of Fiber	Optical T1 Repeater Spacing in Miles	Number of Splice Points	dB Loss in Splices	dB Loss in Fiber
10 dB/km	2.75	7	.7	44.3
5 dB/km	5.42	14	1.4	43.6
2 dB/km	13.0	34	3.4	41.6

Figure 12. Repeater spacing in miles for an optical T1 line

#### Repeater Spacing

Repeater spacing at the T1, T2, and T3 rates--with non-avalanche photodiodes and avalanche photodiodes--is given below. The values of fiber loss given for glass-fiber cable do include the additional loss which may be present from microbending of fibers in the cable (considerable effort is being expended to minimize the microbending loss which will be present in commercial glass-fiber cable). An average loss of .1 dB per splice point, and an average spacing of 2000 feet between adjacent splice points, are assumed for the glass-fiber cable between optical repeaters. A signal-to-noise ratio of 21 dB at the detector (photodiode) is assumed, which gives a repeater bit-error-rate of  $10^{-8}$ . Pulse spreading between adjacent repeaters is limited to one-half of a time-slot (assuming half-duty-cycle rectangular light pulses)--which is 323.8, 79.2, and 11.18 nanoseconds at the T1, T2, and T3 rates. A 20 dB loss has been allowed for coupling a LED to a fiber, and the LED output power of light pulses (peak power) is assumed to be 2.5 milliwatts for commercial LEDs in the year 1980.

When non-avalanche photodiodes are used in optical repeaters, the total loss in the glass-fiber cable between adjacent repeaters is limited to 45 dB, 36 dB, and 24 dB at the T1, T2, and T3 rates. The bandwidth of a filter which passes a PCM electrical signal from a photodiode (detector) is wider at the higher bit rates, and more noise from the photodiode passes through the filter, so that a stronger PCM signal (less attenuation in the fiber) is required to obtain a signal-to-noise ratio of 21 dB at the higher bit rates. Figure 13 gives an allowable repeater spacing of 5.42 miles at the T1 rate, and .155 miles at the T3 rate, when 5 dB/km step-index fibers are

#### Repeater Spacing with 5 dB/km Step-Index Fibers

Type of Repeatered Line	Repeater Spacing in Miles	Allowable dB Loss in Cable	Actual dB Loss in Cable	Allowable Pulse Spreading in Nanoseconds	Actual Pulse Spreading in Nanoseconds
T1	5.42	45	45	323.8	108.5
T3	.155	24	1.25	11.18	11.18

Figure 13. Repeater spacing with 5 dB/km step-index fibers

### Repeater Spacing of an Optical T3 Line

Type of Fiber	Repeater Spacing in Miles	Allowable dB Loss in Cable	Actual dB Loss in Cable	Allowable Pulse Spreading in Nanoseconds	Actual Pulse Spreading in Nanoseconds
5 dB/km STEP-INDEX FIBER	.155	24	1.25	11.18	11.18
5 dB/km GRADED-INDEX FIBER	2.93	24	24	11.18	2.18

Figure 14. Repeater spacing of an optical T3 line

used. Pulse spreading in a step-index fiber severely restricts the allowable repeater spacing at the T3 rate. Figure 14 shows a repeater spacing of 2.93 miles at the T3 rate, and it is apparent that graded-index fibers are preferred at the higher bit rates. Figure 15 gives repeater spacing in miles with non-avalanche photodiodes for step-index and graded-index fibers.

At the T3 rate, only graded-index fibers will allow an acceptable repeater spacing. Equalization circuits can be used to partially compensate for pulse spreading in a step-index fiber at the higher bit rates, but the use of graded-index fibers is the preferred solution.

When avalanche photodiodes are used in optical repeaters, the total loss in the glass-fiber cable between adjacent repeaters is limited to 54 dB, 46 dB and 35 dB at the T1, T2 and T3 rates. Figure 16 gives repeater spacing in miles with avalanche photodiodes for step-index and graded-index fibers. An avalanche photodiode is presently about 10 times as expensive as a non-avalanche photodiode, and an elaborate bias circuit is required when an avalanche photodiode

	T1 Rate	T2 Rate	T3 Rate
1975 step-index fiber (.2 NA, 10 dB/km)	2.75	2.20	.155
1977 step-index fiber (.2 NA, 5 dB/km)	5.42	2.90	.155
1980 step-index fiber (.2 NA, 2 dB/km)	13.0	2.90	.155
1975 graded-index fiber (.2 NA, 15 dB/km, 2 nsec/km)	1.87	1.48	.99
1977 graded-index fiber (.2 NA, 5 dB/km, 1 nsec/km)	5.42	4.40	2.93
1980 graded-index fiber (.2 NA, 2 dB/km, 1 nsec/km)	13.0	10.6	7.20

Figure 15. Repeater spacing in miles with non-avalanche photodiodes

	T1 Rate	T2 Rate	T3 Rate
1975 step-index fiber (.2 NA, 10 dB/km)	3.30	2.90	.155
1977 step-index fiber (.2 NA, 5 dB/km)	6.48	2.90	.155
1980 step-index fiber (.2 NA, 2 dB/km)	15.2	2.90	.155
1975 graded-index fiber (.2 NA, 15 dB/km, 2 nsec/km)	2.21	1.93	1.44
1977 graded-index fiber (.2 NA, 5 dB/km, 1 nsec/km)	6.48	5.63	4.25
1980 graded-index fiber (.2 NA, 2 dB/km, 1 nsec/km)	15.2	13.2	10.3

Figure 16. Repeater spacing in miles with avalanche photodiodes

is used. The avalanche photodiode can be used to its greatest advantage at the higher bit rates (especially the T3 rate)--when low-loss graded-index fibers are being used.

The 2 dB/km value of fiber loss given for the year 1980 (in Figures 15 and 16) is for a wavelength of 1.06  $\mu$ m, and so it has been assumed that LEDs which operate at a wavelength of 1.06  $\mu$ m, and photodiodes with improved gain at 1.06  $\mu$ m, will be commercially available by the year 1980.

### Trunk Route Density

Trunk route density is defined as the number of voice circuits (trunks) in a trunk route. Figure 17 gives the cumulative distribution of toll connecting trunks by route density for GTE telephone companies.

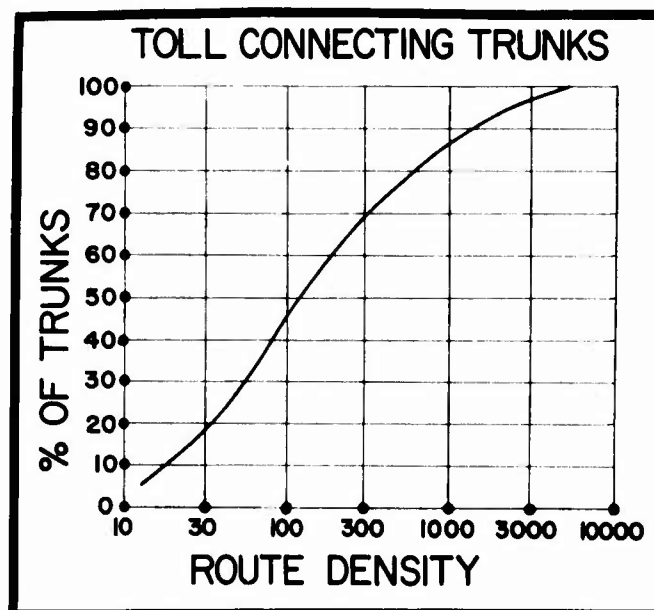


Figure 17. Distribution of toll connecting trunks by route density



Percentage of toll connecting trunks by number of trunks in routes can be determined from this distribution. For example, moving up the vertical line with route density labelled as 1000, the distribution curve is intersected at a value of 86%. This means that 86% of GTE toll connecting trunks are distributed in trunk routes with 1000-or-less trunks in each route, and 14% of GTE toll connecting trunks are distributed in trunk routes with 1000-or-more trunks in each route.

It appears that some optical T-carrier systems operating at the T3 rate will prove-in (economically) within GTE telephone companies. Within the smaller independent telephone companies, it appears that optical T-carrier systems operating at T2-or-lower rates (T1, T1C and T2) will economically handle most of the forecasted demand for future trunk circuits. If the demand for picture-telephone service or wide-band data services should increase dramatically during the next 20 years, then there will be a greater demand for optical T3 carrier.

Telephone companies often have access to routes (right-of-ways) where cable can be buried. Many buried cable routes consist of limited-width right-of-ways, with only enough space to bury one or two cables. When a buried cable contains graded-index fibers, then trunk circuits can be initially provided with optical T-carrier systems operating at the T1 rate (assuming that a small number of new trunk circuits are being added each year), and in later years the T-carrier can be upgraded to T2 or T3 operation as trunk route density continues to increase. This type of "expandability" will be especially attractive if the glass-fiber cable has a very long working life (50-or-more years). Shifting up to T3 operation on graded-index fibers is also attractive as a means to defer construction (placing) of new conduit when underground ducts in a trunk route become congested (full of cables). The additional circuit capacity of an optical T-carrier system on graded-index fibers, which is obtained by shifting operation up to the T3 rate, will tend to look even more attractive if current cost trends continue--labor costs for placing new cable are rising, while the cost of purchasing new carrier equipment is decreasing.

#### Optical PCM Trunk Circuits

If 2 dB/km glass fibers are used, then optical T1 repeater spacing can be 13 miles (68,640 feet). If microwave radio trunks are excluded, then about 42% of GTE-to-GTE interoffice trunks are in the length range of 5-to-13 miles (see Figure 18), and GTE-to-GTE trunks in the 5-to-13 miles range can be provided on 2 dB/km glass fibers without any line repeaters being used--with some cost savings (only 15% of GTE-to-GTE interoffice trunks are longer than 13 miles). If no line repeaters are required in a T1 line, then high quality trunks will be provided (the bit-error-rate for a T1 line without line repeaters is less than  $10^{-8}$ ). Also, these trunk circuits will be more reliable because no copper pairs are needed to power line repeaters--eliminating the possibility of shorted pairs, and doing away with lightning protection problems.

Many toll connecting trunks which are longer than 13 miles will pass (unswitched) through intermediate offices where optical line repeaters can be powered from local battery, so that copper conductors will not be needed for powering optical line repeaters on many toll connecting trunks which are longer than 13 miles. About 92% of GTE-to-Bell interoffice trunks have "trunk length within GTE boundaries" (in-boundary length) which is less than 13 miles. If GTE meets Bell at the GTE-Bell boundary with an optical PCM line

### CUMULATIVE DISTRIBUTION OF IN-BOUNDARY LENGTH FOR INTEROFFICE TRUNKS BY INTERCONNECTING COMPANIES

MICROWAVE RADIO TRUNKS ARE EXCLUDED  
INTRA-BUILDING TRUNKS ARE EXCLUDED

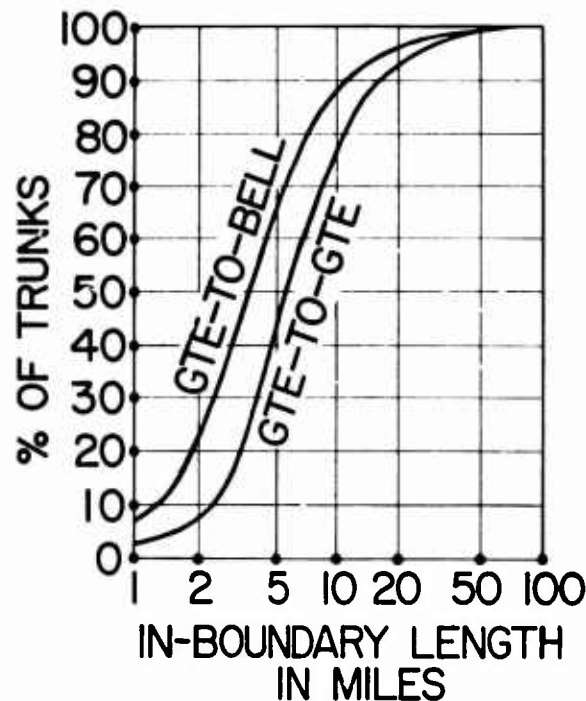


Figure 18. Distribution of interoffice trunks by in-boundary length in miles

on 2 dB/km glass fibers--to provide GTE-to-Bell interoffice trunks--then no optical repeaters will be needed within GTE boundaries in many of these GTE-to-Bell interoffice trunk routes (assuming optical operation along the entire end-to-end length of the GTE-to-Bell PCM trunks). Hence, copper conductors will not be used in many of the 2 dB/km glass-fiber cables which will be placed by GTE in GTE-to-Bell interoffice trunk routes. Sealing current will not be required in an optical span-line section which passes across (straddles) a GTE-Bell boundary (assuming optical operation along the entire end-to-end length of the GTE-to-Bell PCM trunks).

In an optical system, the PCM signal is transmitted over glass fibers and the repeater power is provided over a copper pair. The copper pair for repeater power is still susceptible to the effects of water and lightning. For greatest economy (lowest cost), a recent proposal has suggested that several optical line repeaters--at each repeater point (repeater location)--should be powered from a single pair of copper conductors. Figure 19 illustrates this concept of powering several optical line repeaters at each repeater point over one copper pair (this particular example is for illustration only, and is not meant to suggest a typical configuration for powering optical line repeaters).



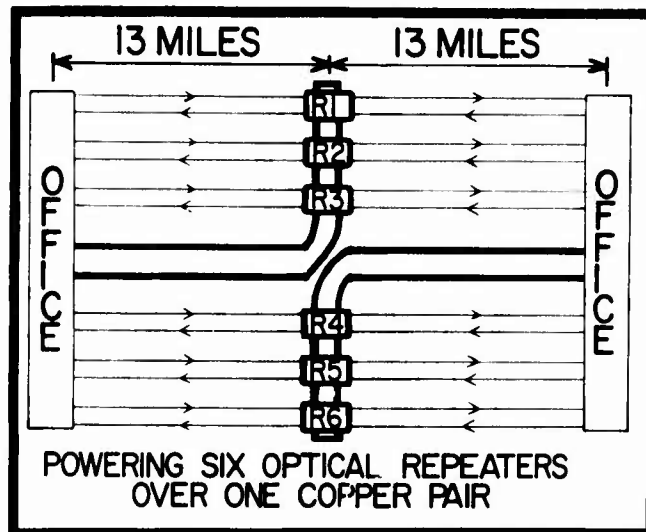


Figure 19. Powering six optical line repeaters at a repeater point over one copper pair

Figure 20 illustrates how 96 PCM circuits can be obtained over four T1 lines, and over one T2 line (CB = channel bank, OTR = office terminating repeater, LR = line repeater and M12 = multiplexer). The pair of M12 multiplexers used with the T2 line will cost \$6,000-to-\$8,000, but the number of glass fibers, line repeaters and office terminating repeaters are reduced by a factor of four. When the length of the trunk circuits is long, then there may be significant cost savings by using the T2 line.

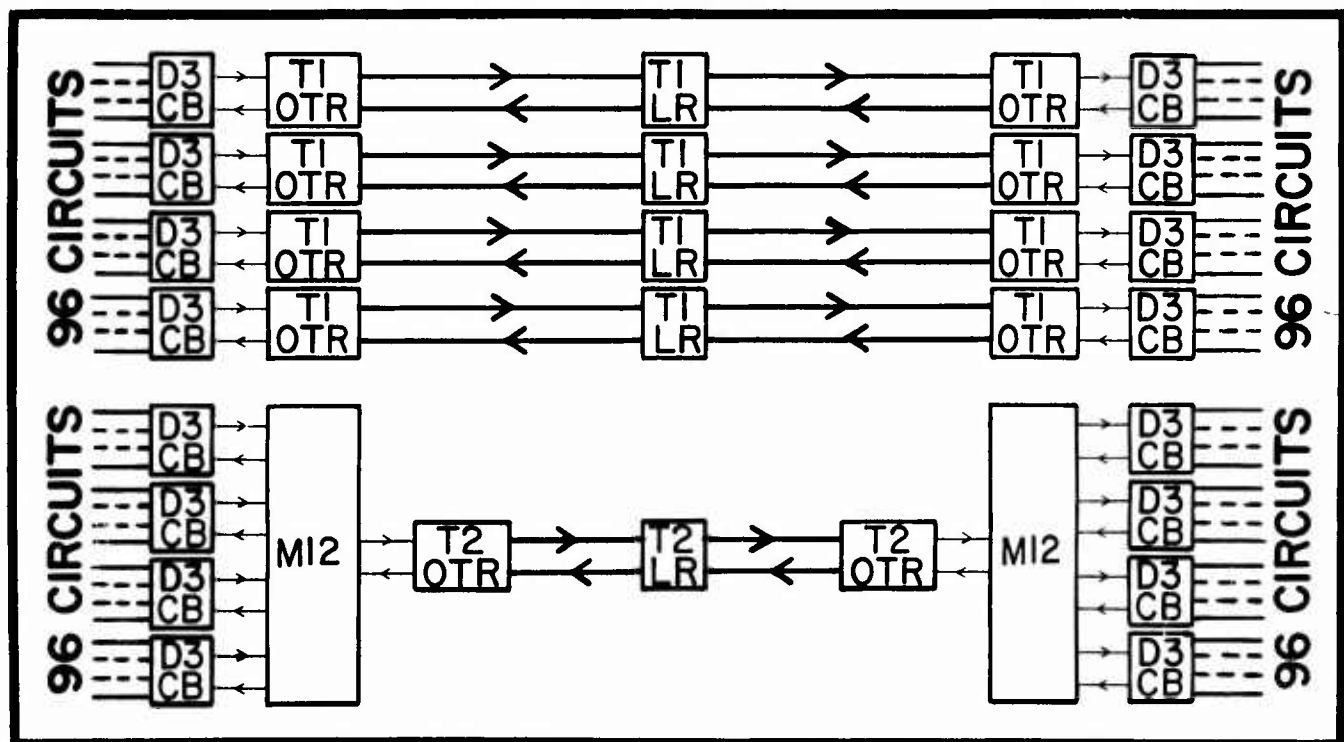


Figure 20. 96 PCM circuits on four T1 lines and one T2 line

#### First Cost Analysis of T-carrier

T-carrier systems on regular twisted pairs at the T1 rate are now being used for interoffice trunking. T-carrier systems on regular twisted pairs at the T1C rate (48 voice channels on two twisted pairs) are becoming available. Future T-carrier systems on regular twisted pairs at the T2 rate cannot be ruled out.

Most optical T-carrier systems on glass-fiber cable for interoffice trunking in the independent telephone companies (especially in the smaller companies) will operate at the T2-or-lower rates during the next 10 years. In a cost analysis of T-carrier for interoffice trunking in independent telephone companies, it appears that most optical T-carrier systems on glass fibers will be competing head-to-head with T-carrier systems on regular twisted pairs.

The 1980 cost of terminals, repeaters and multiplexers is assumed to be equal for optical PCM carrier on fibers and conventional PCM carrier on pairs--operating at the same bit rate. Although optical PCM repeaters require some additional components (LEDs and photodiodes) and some additional gain, it appears that less circuitry will be required for equalization and retiming of the PCM light pulses in optical repeaters.

A typical size for conventional 22-gauge filled screened trunk cable is 50 pairs. Twenty-five T1 repeatered lines can be provided in a 50-pair screened cable (at 100% fill), with a typical repeater spacing of 7200 feet. The "first cost" of providing 24 PCM circuits using a T1 line in a 50-pair screened cable and an optical T1 line in a 50-fiber cable will be calculated (when service life and maintenance cost

for fiber cable can be estimated, then it will be desirable to use present worth of annual charges in cost studies--rather than first cost). Cost of pairs and fibers to be used with a T-carrier system will be prorated on a per-system basis. When optical line repeaters are used, it is assumed that two optical line repeaters at each repeater point are powered over one 22-gauge pair (13 pairs are used to power the optical line repeaters in the 25 optical PCM lines).

Projected selling cost for cable in 1980 is \$.80 per foot for 50-pair filled screened cable, \$.70 per foot for 50-fiber cable and \$.80 per foot for 50-fiber cable with 13 pairs (for powering optical line repeaters). The 1980 cost for placing and splicing any one of these three cables is taken as \$.80 per foot. Hence, the 1980 in-place cost for cable is \$1.60 per foot for 50-pair cable, \$1.50 per foot for 50-fiber cable and \$1.60 per foot for 50-fiber cable with 13 pairs. It is assumed that fiber cable contains graded-index fibers with a loss of 2 dB/km. Prorated 1980 in-place cost of pairs and/or fibers to be used with a PCM line (T-carrier system) is \$.064 per foot for 50-pair cable, \$.060 per foot for 50-fiber cable and \$.064 per foot for 50-fiber cable with 13 pairs, assuming that 25 T1 lines will operate in the cable (cable cost is divided by 25 to prorate the cost of pairs and fibers to a per-system basis).

Estimated 1980 in-place first cost of 24 PCM circuits is shown in Figure 21 for circuit length up to 50 miles. At the T1 rate, optical PCM circuits on fibers have a lower value for estimated in-place first cost than PCM circuits on pairs--using the projected cable costs given above.

Estimated 1980 in-place first cost (prorated) of 24 optical PCM circuits on fibers at the T3 rate is also given in Figure 21. When circuit length is long, then estimated 1980 in-place first cost of 24 optical PCM circuits on fibers is considerably lower at the T3 rate than at the T1 rate. With a moderate trunk circuit growth rate, optical PCM operation at the T3

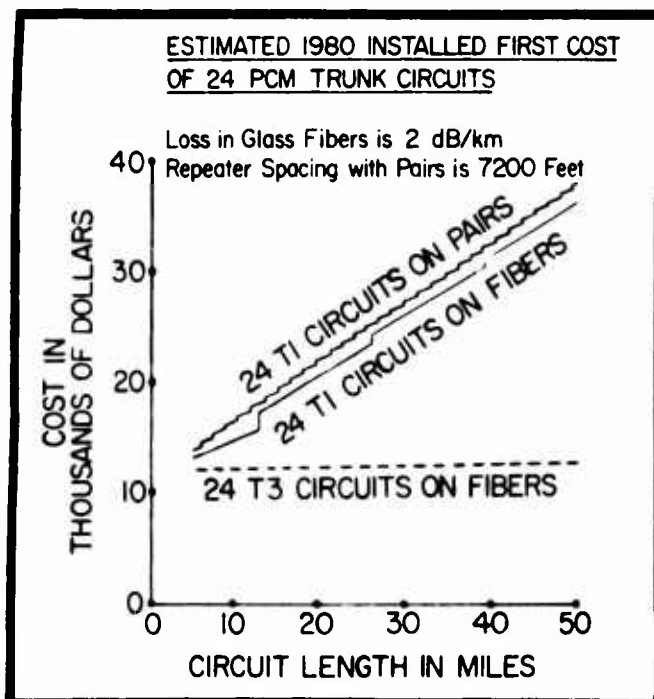


Figure 21. In-place cost of 24 PCM circuits

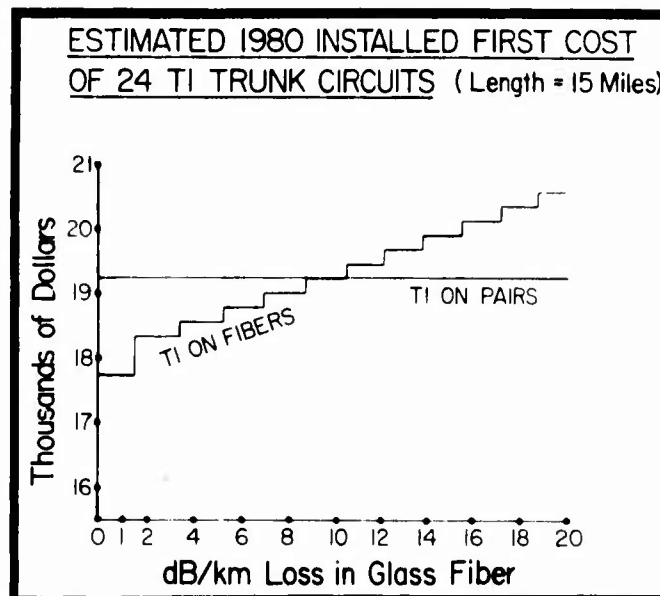


Figure 22. In-place cost of 24 T1 circuits

rate may not look quite as good when "present worth of annual charges" are being compared--because some investments (equipment costs) can be deferred for a period of time when the smaller-capacity optical T1 lines are being used.

With a circuit length of 15 miles and the projected cable costs which are given above, estimated 1980 in-place first cost of 24 optical T1 circuits on fibers is shown in Figure 22. Fiber loss varies from 0-to-20 dB/km. Estimated 1980 in-place first cost of 24 T1 circuits on pairs is shown for comparison. When fiber loss in dB/km is 8-or-less, the first cost of optical PCM circuits on fibers is lower than the first cost of PCM circuits on pairs.

Optical PCM carrier on glass-fiber cable gives a more reliable circuit, because it is immune to electromagnetic interference. The bit-error-rate of an optical PCM line with low loss fibers is decreased, because fewer line repeaters are used (fewer line repeaters also tends to increase the reliability of the optical line). For these reasons, it is expected that demand for optical T-carrier systems by telephone companies will appear when the projected fiber cable costs (given above) can be met, and when fiber loss in dB/km is 8-or-less (8 dB/km glass-fiber cable is now becoming available).

A fiber loss of 2 dB/km will be even more attractive--because of the additional cost savings, and because many trunk circuits can be provided over optical PCM lines without using optical line repeaters. When optical line repeaters can be eliminated, then no pairs are needed in the glass-fiber cable--and so the glass-fiber cable will be immune to the effects of water and lightning, which gives more reliable trunk circuits. Also, when optical line repeaters are not being used, then the glass-fiber cable can be buried adjacent to power cables (without separation)--and switching transients in the power cable will have no effect on the operation of the optical PCM lines.

### Equalization and Jitter in a T1 Line

The amplitude of the power spectral density of a bipolar electrical T1 signal has its maximum value at 772 kilohertz--and most of the signal power is contained in a frequency range (bandwidth) of roughly one megahertz about this center frequency of 772 kilohertz. The attenuation of a twisted pair varies considerably over this frequency range, and this results in distortion of the electrical T1 signal as it travels down the twisted pair--unless frequency equalization is used. The attenuation of a glass fiber is essentially flat over the baseband bandwidth of a unipolar optical T1 signal--and baseband frequency equalization for amplitude is not needed when glass fibers are being used.

Since a glass fiber is relatively immune to electromagnetic interference, "jitter" may be reduced when PCM light pulses are being transmitted on glass fibers, and the retiming of PCM light pulses may be more accurate and less complicated in optical repeaters than the retiming of PCM electrical pulses in conventional repeaters.

### Error Detection and Spare Span-Line Switching

A conventional T1 repeatered line alternates the polarity of the plus-and-minus electrical pulses which are transmitted down a cable pair. When two adjacent (non-zero) pulses are determined to have the same polarity, a "bipolar error" is detected. When the measured value of the bipolar error rate exceeds the "critical value" it (1) will trigger an alarm and (2) can cause spare span-line switching to occur.

Light pulses in a glass fiber are unipolar, and "bipolar error detection" is lost. Since a commercial PCM carrier system should have accurate error detection, a commercial optical T-carrier system may transmit "parity bits" for error detection.

Parity bits can be inserted (and checked) by M12 multiplexers for error detection on optical T2 lines. Parity bits can be inserted by M13 and M23 multiplexers for error detection on optical T3 lines. For error detection on optical T1 lines, parity bits may be inserted by channel banks (a "new code" is needed), or by T1 office terminating repeaters.

### Development & Evaluation of an Experimental Optical T1 System

Present plans call for an experimental optical T1 line to be installed and evaluated in GTE in 1976. This experimental system is being developed and evaluated as a joint project by GTE Laboratories, General Cable Corporation, GTE Lenkurt, GTE Service Corporation and a participating GTE telephone company. The knowledge gained from field evaluation of the experimental system will provide data to be used in the development of future cost-effective commercial optical PCM systems.

The experimental system will be evaluated (1) in the laboratory and (2) in the field. The laboratory evaluation will establish that there is proper operation and a high level of reliability in all transmission hardware of the experimental system. The field evaluation will verify the reliability and proper operation of the transmission hardware and the glass-fiber cable in the field environment of the telephone company--and evaluate field techniques for pulling fiber cable into ducts, splicing of fibers, etc.

### Conclusions

A considerable amount of time and effort is needed in the development of optical transmission hardware and glass-fiber cable. Although some problem areas remain to be worked out, development is proceeding at a rapid pace.

By the year 1980, optical PCM carrier operating on glass-fiber cable should be economically competitive with PCM carrier operating on twisted-pair cable as a means for providing many new circuits in the telephone company trunk plant. In addition to "first cost" benefits, commercial optical PCM carrier systems on glass fibers will provide higher quality trunk circuits--which are more reliable and require less maintenance than conventional PCM carrier systems on twisted pairs.

### References

1. F. L. Thiel, "Utilizing Optical Fibers in Communications Systems", 1975 IEEE International Conference on Communications, Volume II, page 32-1.

(Speaker)

John Fulenwider  
GTE Laboratories  
40 Sylvan Road  
Waltham, Mass. 02154



John Fulenwider is currently Senior Scientist, responsible for development of optical fiber transmission systems for telephone applications. He holds the B.S.E.E. and M.S.E.E. degrees from Northwestern University, and the Ph.D degree in electrical engineering from Stevens Institute of Technology.

He joined Sargent and Lundy, Chicago in 1952 and worked on designs of thermal electric generating systems. In 1955, he joined Booz-Allen Applied Research, Chicago and worked on systems analysis problems for military and industrial clients. He joined GTE Automatic Electric Laboratories, Northlake, Illinois in 1961. As Director of Research at GTE Automatic Electric Laboratories, he supervised the development of experimental stored program electronic switching systems. He was appointed Manager of Communication Laboratory at GTE Laboratories, Bayside, New York in 1968, responsible for development of experimental interactive terminals including printing data terminals and picture telephones.

He is a member of the Faculty of Northeastern University, state of the arts program, where he teaches courses on Optical Fiber Communication Systems and Data Communications Systems. He holds four U. S. Patents, with several patents pending.

(Co-author)

George Killinger  
GTE Service Corporation  
One Stamford Forum  
Stamford, Conn. 06904



# THERMOPLASTIC POLYESTER COPOLYMERS AND THEIR BLENDS WITH VINYLs FOR MOLDED AND EXTRUDED ELECTRICAL APPLICATIONS

Morton Brown  
E. I. du Pont de Nemours & Co.  
Elastomer Chemicals Department  
Wilmington, Delaware

## Introduction

A family of novel segmented copolyesters has been developed by the Du Pont Co. and introduced to the market place under the trademark "HYTREL." These polymers have many of the characteristics of rubbers, but are designed for processing on thermoplastic extruders and injection-molding machines. Since the commercial announcement a series of papers dealing with various aspects of copolyesters have been published.<sup>1-5</sup>

This paper reviews this group of commercially important copolyether esters derived from terephthalic acid (T), polytetramethylene ether glycol (PTMEG) and 1,4-butanediol (4G) having the generalized structure shown in Figure 1. The polymers possess a two-phase structure of continuous and interpenetrating crystalline and amorphous phases. The crystalline phase, designated 4GT in Figure 1, serves as thermally reversible tie-points which behave in a manner similar to chemical cross-links. The amorphous phase (PTMEG-T) contributes the elastomeric character to the polymer series. The relative proportions of the two phases determines the hardness, modulus, melting point, chemical resistance and permeability.

## Physical Properties

The two-phase structure of these copolyesters is shown in Figure 2, a thermogram by differential scanning calorimetry for a copolyester of 55 Durometer D hardness and which contains 58 wt. % of 4GT hard segments. The scan reveals two transitions, a glass transition ( $T_g$ ) of the amorphous phase at about  $-50^\circ\text{C}$  ( $-58^\circ\text{F}$ ) and a well-defined crystalline melting point at about  $200^\circ\text{C}$  ( $392^\circ\text{F}$ ). This combination of a low glass-transition temperature and a high crystalline melting-point is characteristic of these polyesters and is in part responsible for the broad service temperature range of this class.

Typical physical properties of copolyesters as a function of melt point and hardness are shown in Table I. Polymer properties can be varied widely, spanning the range from hard rubbers of 90 Durometer A to tough elastoplastics of 72 Durometer D. The entire family of copolyesters has solenoid brittle points below  $-70^\circ\text{C}$  ( $-94^\circ\text{F}$ ) and their low-temperature impact strength and toughness make them ideal candidates for low-temperature applications. They also have exceptional "hot strength" with the polymer at 58% 4GT still possessing a

tensile strength of  $13.8 \text{ MN/m}^2$  (2000 psi) at  $175^\circ\text{C}$  ( $347^\circ\text{F}$ ). Another example of their excellent thermal performance is indicated in Figure 3 which illustrates the effect of temperature on creep response at several tensile stress levels. Here creep strain is defined as the difference between the strain after 1000 hours at constant load and the strain after 1 minute.

## Heat and Chemical Resistance

Unstabilized copolyesters of this type are subject to degradation under dry heat conditions by oxidative attack on the polyether backbone. Commercial grades are supplied with phenolic or aromatic amine antioxidants<sup>6</sup> and a specially-stabilized composition is now available having a further 3-5X improvement in service life over the compound stabilized by an aromatic amine (Table II).

Table III summarizes the superior resistance of these copolyesters with different stabilized systems to ASTM No. 1 and No. 3 oils at  $150^\circ\text{C}$  ( $302^\circ\text{F}$ ). Competitive materials of similar modulus characteristics such as thermoplastic urethanes and plasticized nylon, generally fail in less than 1 week exposure at such temperatures.

## Environmental Resistance

The copolyesters of this class have inherent resistance to fungus and mildew and require no further stabilization. For protection against photo-degradation efficient UV absorbers, either chemical or pigmentary, are required. Properly stabilized, such compounds have retained 70% of their original tensile properties after 2 years of Florida exposure.

The hydrolytic stability of these polyether esters is very good at temperatures  $<70^\circ\text{C}$  ( $158^\circ\text{F}$ ). At higher temperatures hydrolytic stability can be significantly enhanced through the incorporation of polycarbodiimide stabilizers. A 55 Durometer D polymer stabilized in this fashion retained 64% of its original tensile strength and 98% of its original elongation after 6 months in boiling water.

## Processing

Characteristic of the entire class of polyether esters is the combination of a sharp melting point (Figure 2), a definite heat of fusion, a low melt-viscosity and a strong dependence of viscosity upon temperature. Figure 4 shows the apparent viscosity vs. shear rate relationship for

for a 55 Durometer D polymer at two melt temperatures. Note that at 225°C (437°F) the polymer viscosity is almost Newtonian over a broad shear range while at 215°C (419°F) a more typical melt flow curve is obtained with strong shear rate dependency. In both cases, however, the absolute value of the viscosity is low. Figure 5 shows the strong dependency of viscosity on melt temperature. For the 63 Durometer D compound a temperature variation of 28°C (50°F) causes a 5X variation in viscosity.

While the low viscosity of these copolyesters is of advantage in injection-molding, the strong dependency of viscosity upon temperature requires precise temperature control in extrusion applications to achieve proper control of caliper. This presents no problem to those already familiar with the extrusion characteristics of 6/6 nylon. Preferred screw designs have L/D ratios of at least 20, compression ratios of at least 3:1 and have a gradual compression zone comprising at least 1/3 of the screw length. The so-called polyethylene screw fills these requirements.

The entire series is mildly hygroscopic, absorbing about 0.3% moisture at equilibrium in 50% relative humidity. Safe processing requires levels of 0.1 max., a level easily achieved through the use of dehumidifying hopper driers.

#### Flame Retardancy

Additives to enhance flame retardancy of these polymers are available which increase the limiting oxygen index (ASTM-D-2863) to 30-32 and which have a flame resistance rating of VE-II by the UL-94 tests. Efforts are underway to prevent dripping during the test and thereby attain a VE-0 rating.

Flame retardant PVC compositions containing combinations of antimony oxide and phosphate ester plasticizers can tolerate the addition of up to 25% uncompounded copolyester without significant change in the limiting oxygen index or in the UL-94 test results.

#### Electrical Applications

Some representative electrical properties are shown in Table IV. The electrical properties of these polyesters show rather low sensitivity to moisture. The values for SIC and volume resistivity are comparable to those for nylon and polyurethane and are thus inferior to non-polar polyolefins and fluorocarbons. For this reason their use as insulators is limited to low-voltage, low frequency applications.

In addition to applications as an extruded jacket for oil-well logging cable, portable power cable and insulation for coiled cords, some injection-molded applications are shown in Figures 6-8. Figure 6 shows a snap-fit cable connector housing. It is injection-molded in one piece and is distinguished by its combination of high-temperature creep

resistance and low-temperature impact strength. Figure 7 shows an injection-molded panel connector cover. Both connector covers are molded with additive to give an oxygen index (ASTM-D-2863) of 26-27. Finally, Figure 8 shows a glass-filled composition as an electrical connector. Here the glass filler greatly improves the high-temperature creep characteristics and permits the assembly to maintain a tight connection at temperatures above 200°F.

#### Modification of Plasticized Polyvinyl Chloride

PVC compounders have long had goals to improve the following combinations of properties in their products.

1. Heat resistance
2. Low temperature flexibility and impact strength
3. Compression set resistance
4. Resistance to oils and fuels
5. Resilience
6. Non-migration of compounding ingredients

Generally, improvements are made through the use of plasticizers and compounding ingredients, or combinations thereof. By means of the addition of these thermoplastic copolyesters<sup>8</sup> all these properties can be improved, the degree of improvement being directly related to the level of copolyester used.

Blending studies with PVC compositions have been restricted to the 40 Durometer D copolyester. It melts at 176°C (even lower when solvated by plasticizer), a convenient temperature for PVC compounding. Higher-melting copolyesters have been used, but they must be fluxed at temperatures at the upper end of the PVC temperature processing range and so are not safely used.

While most of the laboratory data reported here are derived from Banbury-mixed compounds using pelletized copolyesters, powdered copolyesters have also been used successfully. Because of the large number of plastic processors using resins in the powdered form, one obvious advantage of using powdered polymers is the familiarity of processors with this particle form, as well as the ability to use such powders on plastic extruders, injection molders and other existing process equipment. The powdered form provides easier handling (free-flowing and pourable) and the uniform particle size provides quicker and more homogeneous dispersions at lower energy input than can be obtained through Banbury mixing.



First experiments in this field involved the blending of the 40 Durometer D copolyester with a general-purpose, fully-compounded flexible vinyl extrusion compound of 75 Durometer A. It was apparent (Table V) that amounts of polyester as low as 25% in the blend produced considerable improvement in tensile and tear strengths, flexibility, and impact resistance at low temperatures, as well as in heat distortion at 121°C. It is most significant to note that, although increasing amounts of copolyester increase the hardness and room-temperature torsional modulus of the blend, the low temperature flexibility is steadily improved by increasing levels of copolyester.

Similar blends have been prepared (see Table VI) using a 90 Durometer A vinyl compound for use in wire and cable jackets, characterized by a plasticizer combination providing permanence (low volatility and extractibility) as well as low temperature flexibility and resistance to heat distortion. Again, the addition of the copolyester further improves heat distortion, low temperature flexibility and provides sufficient permanence to greatly upgrade the performance after heat aging for 7 days at 121°C.

We have seen in the above cases the results of adding copolyester to a plasticized vinyl, and, in effect, maintaining the plasticizer/vinyl ratio constant. If a series of blends are prepared using instead a constant ratio of plasticizer to total resin (vinyl plus polyester), some very subtle effects can be observed. As an example, we have chosen the following basic formulation based on 30 phr of DOP based on total resin:

PVC Homopolymer	100-x parts
Copolyester (40 Durometer D)	x parts
DOP	30 parts
Epoxy Resin	5 parts
Whiting	20 parts
Ba-Cd Stabilizer	1.5 parts
Phosphite Stabilizer	0.5 parts
Stearic Acid	0.3 parts

and permitting x to vary from zero to 50. Results are summarized in Figures 9 through 12 wherein the data are presented as a function of x.

First, it is apparent that both hardness and modulus are determined primarily by the DOP/vinyl ratio, with the copolyester having little effect in this composition range (Figure 9). Increasing copolyester levels make the blend more flexible at both room temperature and at subnormal temperatures (Figure 10). As would be predicted, the increasing DOP/vinyl ratio in this series makes the blends less-resistant to oil and fuel extraction; swell values change from slightly positive levels to negative values, consistent with the presence of the monomeric plasticizer

(Figure 11). As shown in earlier work, brittle point is lowered with increasing copolyester content.

The most striking change in properties occurs in the heat distortion characteristics (Figure 12). Increasing copolyester levels will lower the heat distortion (ASTM D-1047, 121°C) value at 2000 g. load from over 60% with no copolyester to 18% where x = 50. Similarly, the heat distortion values at 500 g. load are reduced from above 20% to below 4% at x = 50.

This improvement in heat resistance is of great importance in the wire and cable industry. Generally, greater flexibility in PVC compounds can be realized only at the expense of heat distortion resistance. These copolyesters permit the formulation of lower Durometer PVC compounds of improved high and low temperature properties. Additional applications are under development which make use of the upgraded properties of PVC-copolyester blends.

#### Modification of Rigid Vinyl Compounds

Addition of small amounts of the lowest-melting 40 Durometer D copolyester to rigid vinyl compounds will enhance impact strength (Table VII) while improving extrusion and injection-molding characteristics (Table VIII). As little as 5 parts copolyester/100 of PVC lowers the equilibrium torque during mixing, lowers the viscosity and permits processing with a lower degree of shear heating. These characteristics have significance for diversified end products as wire and cable jackets and molded electrical connectors.

#### Summary

Polyether-ester copolymers have a combination of flexibility, toughness, oil and fuel resistance and resistance to environmental extremes which make them of interest for molded and extruded electrical goods. Important among these applications are cable jackets for specialty applications as well as injection-molded electrical connectors and covers.

Blends with flexible PVC extend the temperature use limits of vinyl, while blends with rigid PVC improve impact strength as well as processability.



## References

1. M. Brown, W. K. Witsiepe, Rubber Age 104/3 (1972) 35.
2. G. K. Hoeschele, W. K. Witsiepe, Angew. Makromol. Chemi 29/30 (1973) 265.
3. W. K. Witsiepe, ACS Polymer Preprints Vol. 13, No. 1, p. 588 (April 1972)
4. R. J. Cella, IUPAC International Symposium on Macromolecules, Helinski 1972, Preprint Vol. 4, p. 45.
5. G. K. Hoeschele, Polymer Eng. and Science, 14, 848 (1974)
6. M. Brown, Belg. Patent 794,028 Du Pont (1973); G. K. Hoeschele Belg. Patent 794,132 Du Pont (1973)
7. M. Brown, G. K. Hoeschele, W. K. Witsiepe U. S. Patent No. 3,835,098, Du Pont (1974)
8. R. W. Crawford and W. K. Witsiepe, U. S. Patent No. 3,718,715, Du Pont (1973)

## Biographical Note

Dr. Brown received his Bachelor's degree at Cornell University and his Ph.D. degree from M.I.T. He joined the Du Pont Company in 1957. After serving as a Research Chemist in both the Central Research Dept. and the Elastomer Chemicals Dept., he joined the Sales Division of the latter department and has been associated with HYTREL® polyester elastomer since its inception.



TABLE I

TYPICAL PROPERTIES OF COPOLYESTERS

DUROMETER HARDNESS,	92A	55D	63D	72D
MELTING POINT, °C.	176	202	212	218
SPECIFIC GRAVITY	1.15	1.20	1.22	1.25
TENSILE STRENGTH, MN/m <sup>2</sup>	38.9	43.5	46.9	41.3
ELONGATION AT BREAK, %	810	760	510	395
FLEXURAL MODULUS, MN/m <sup>2</sup>	44.1	206	345	517
IZOD IMPACT, NM/cm (NOTCHED)				
22°C.	>10.6	>10.6	>10.6	>10.6
-40°C.	>10.6	>10.6	0.5	0.4
GARDNER IMPACT, N-cm, -40°C.	>1810	>1810	1040	930
% VOLUME SWELL				
ASTM #3 OIL, 7d/100°C.	22.0	12.2	6.6	3.2

TABLE II

HEAT AGING CHARACTERISTICS OF 55 DUROMETER D COPOLYESTERS

TYPE OF STABILIZER	HEAT AGING TEMPERATURE		
	149°C	163°C	177°C
	DAYS TO FAILURE, 180° BLEND		
NONE	<1	—	—
HINDERED PHENOL	8	—	—
AROMATIC AMINE	17	8	3
SPECIAL STABILIZER SYSTEM	80	35	9

TABLE III

HOT OIL RESISTANCE OF 55 DUROMETER D COPOLYESTERS

(ASTM D-471)

	STANDARD GRADE (AROMATIC AMINE STABILIZED)	SPECIAL HEAT STABILIZED GRADE
ASTM NO.1 OIL/150°C		
1 WEEK		
TENSILE STRENGTH, MN/m <sup>2</sup>	17.1	33.5
ELONGATION AT BREAK, %	180	660
% VOLUME INCREASE	2.0	1.6
3 WEEKS		
TENSILE STRENGTH, MN/m <sup>2</sup>	DEGRADED	27.6
ELONGATION AT BREAK, %		630
% VOLUME INCREASE		1.5
ASTM NO.3 OIL/150°C		
1 WEEK		
TENSILE STRENGTH, MN/m <sup>2</sup>	16.6	29.8
ELONGATION AT BREAK, %	120	730
% VOLUME INCREASE	19.9	18.0
3 WEEKS		
TENSILE STRENGTH, MN/m <sup>2</sup>	DEGRADED	24.2
ELONGATION AT BREAK, %		320
% VOLUME INCREASE		18.3

**TABLE II**  
**ELECTRICAL PROPERTIES OF THERMOPLASTIC COPOLYESTERS**  
72°F (22°C)

	HARDNESS, DUROMETER D			
	ASTM-D	40	55	63
DIELECTRIC STRENGTH, VOLTS/mm	149			
50 % R.H.		3540	3320	3210
100 % R.H.		3410	2950	3090
POWER FACTOR, 10 <sup>3</sup> HZ, %	150			
50 % R.H.		0.66	0.82	0.80
100 % R.H.		0.77	0.87	0.91
SIC 10 <sup>3</sup> HZ	150			
50 % R.H.		5.97	4.6	4.84
100 % R.H.		6.01	4.9	4.96
VOLUME RESISTIVITY, OHM-CM	257			
50 % R.H.		2.25 × 10 <sup>13</sup>	5.6 × 10 <sup>13</sup>	1.43 × 10 <sup>13</sup>
100 % R.H.		1.11 × 10 <sup>13</sup>	3.0 × 10 <sup>13</sup>	1.01 × 10 <sup>12</sup>

**TABLE V**

**BLENDS OF COPOLYESTER (40 DURO.D) WITH COMPOUNDED VINYL (75 DURO.A)**

	A	B	C	D
PVC (75A)	100	75	60	50
COPOLYESTER (40 DURO.D)	—	25	40	50
HARDNESS, A DUROMETER	75	80	84	85
TENSILE STRENGTH, MN/m <sup>2</sup>	13.3	14.8	17.1	18.1
E <sub>B</sub> , %	175	200	280	380
BRITTLE POINT, °C	-38	-44	BELOW -60	BELOW -60
HEAT DISTORTION, % 121°C/2000 g. LOAD ASTM D-1047	15.6	8.5	8.3	5.5
TORSIONAL MODULUS, MN/m <sup>2</sup> 22 °C	6.4	6.55	6.92	7.85
-18 °C	366	152	99.1	58.6
TEAR STRENGTH, KN/m ASTM D-624 DIE C, 22°C	47.6	54.2	55.7	64.0
VERZELEY RESILIENCE, %	26	48	—	50.0

**TABLE VI**

**BLENDS OF COPOLYESTER (40 DURO.D) WITH COMPOUNDED VINYL (90 DURO.A)**

	A	B	C	D
PVC (90A)	100	75	60	50
COPOLYESTER (40 DURO.D)	—	25	40	50
HARDNESS, A DUROMETER	90	90	91	90
TENSILE STRENGTH, MN/m <sup>2</sup>	22.3	18.0	17.9	17.7
ELONGATION AT BREAK, %	280	345	540	650
BRITTLE POINT, °C	-50	BELOW -60	BELOW -60	BELOW 60
HEAT DISTORTION, % 121°C/2000 g. LOAD	15	11	7	4
TORSIONAL MODULUS, MN/m <sup>2</sup> 22 °C	12.7	11.3	13.8	15.2
-18 °C	398	214	114	55.8
BASHORE RESILIENCE, % AFTER 7 DAYS/121 °C	15	28	38	44
TENSILE STRENGTH, MN/m <sup>2</sup>	32.9	19.3	14.9	14.0
ELONGATION AT BREAK, %	220	290	390	520
BRITTLE PT. °C, FAILURE	-17	-50	BELOW -60	BELOW -60

**TABLE VII**  
**IMPACT STRENGTH OF PVC/COPOLYESTER BLENDS \*\***  
IZOD IMPACT STRENGTH, 0.32 cm., NOTCHED  
NM/cm., ASTM D-256

	72°F (22°C)	32°F (0°C)	0°F (-18°C)
COPOLYESTER 40 DURO D, PARTS/100 VINYL			
0	1.1	—	—
5	4.7	1.4	0.9
10	10.0	1.5	1.1
15	>10.6 (NB)	2.1	1.5
20	>10.6 (NB)	2.4	1.5

\*\* SEE TABLE VIII FOR COMPOSITION OF BLENDS

**TABLE VIII**

**COPOLYESTER (40D) AS A PROCESSING AID IN RIGID VINYL**

BRABENDER PLASTICORDER (1)				
COPOLYESTER PARTS/100 PVC	EQUIL. TORQUE, m-gm	TEMP. (°C)	DEGRADATION TIME, MINS.	VISCOSITY POISE (2)
0	1700	199	17	8800
5	1650	198	31	7300
10	1600	195	40	6800
20	1500	192	40	6100

COMPOUND: PVC HOMOPOLYMER 100  
COPOLYESTER 40D VARIABLE  
TIN MERCAPTIDE STABILIZER 1.45  
TIN CARBOXYLATE STABILIZER 1.45  
POLYETHYLENE WAX 0.35  
GLYCERYL MONOSTEARATE 3.4  
TITANIUM DIOXIDE 11.61

(1) BRABENDER PLASTICORDER CONDITIONS: 60RPM, 375°F (190°C)

(2) PISTON RHEOMETER CONDITIONS: 375°F (190°C), L/D = 16, 1400 SEC.

**FIGURE 1**

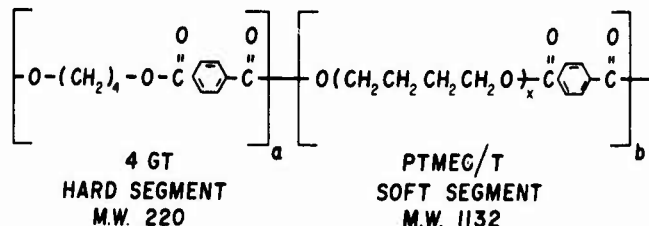


**FIGURE 2**  
DIFFERENTIAL SCANNING CALORIMETRY THERMOGRAM  
55 DURO. D COPOLYESTER

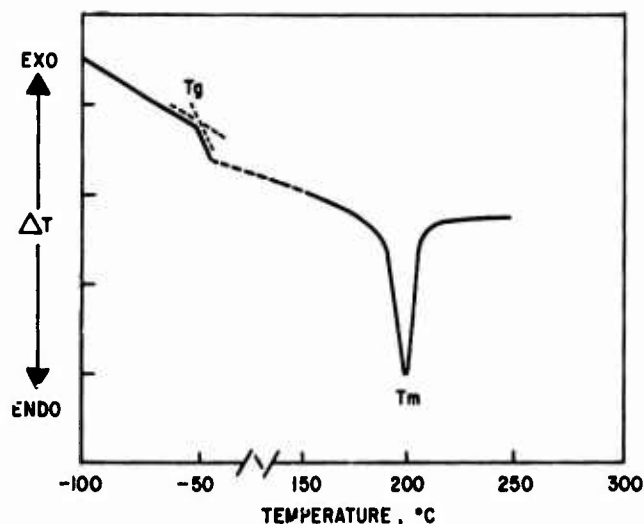


**FIGURE 4**  
APPARENT VISCOSITY VS. SHEAR RATE  
55 DURO. D COPOLYESTER  
L/D = 16

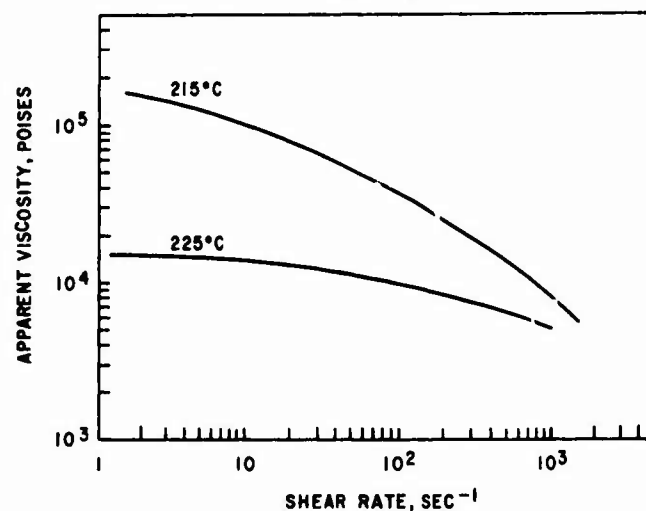


**FIGURE 3**  
EFFECT OF TEMP. ON CREEP RESISTANCE  
( 55 DUROMETER D COPOLYESTER )

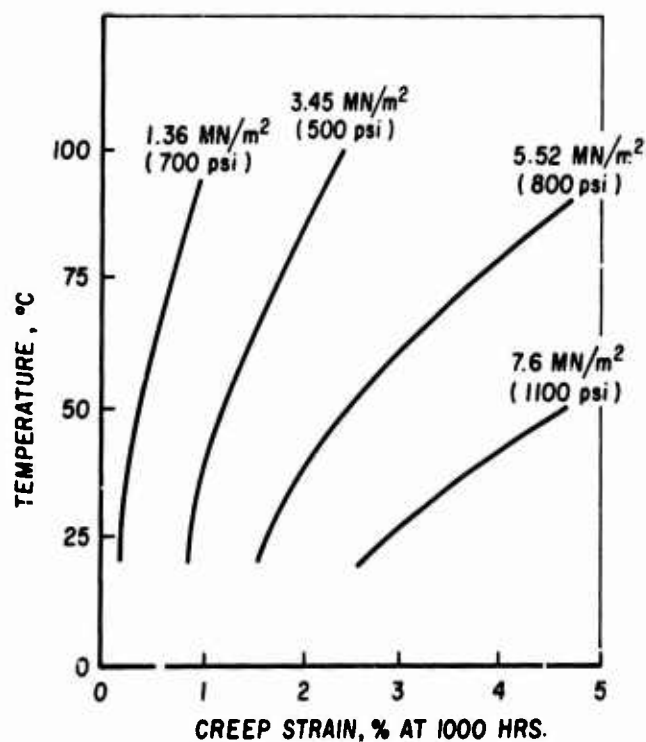


**FIGURE 5**  
VISCOSITY VS. TEMPERATURE

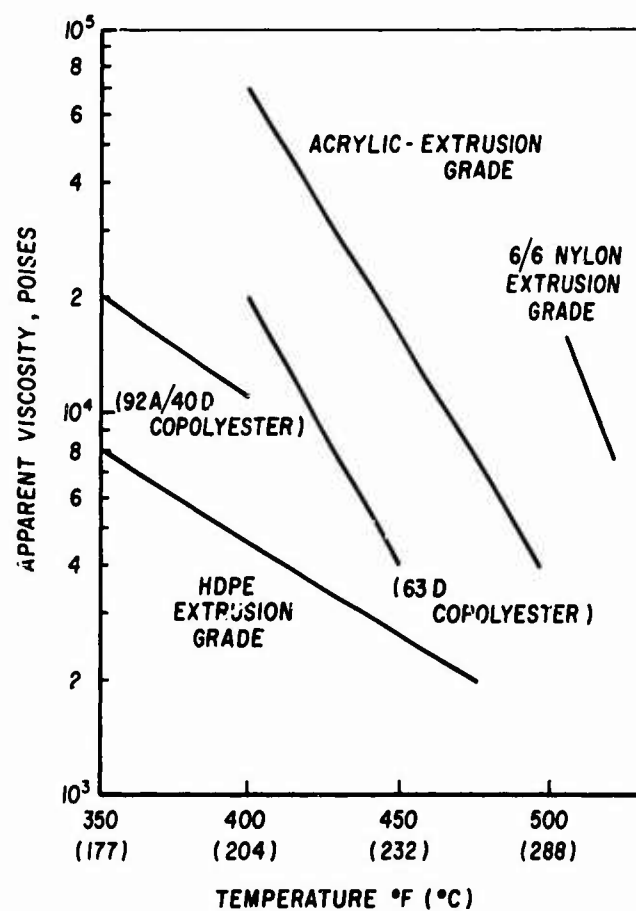


FIGURE 6  
SNAP-FIT CABLE CONNECTOR



FIGURE 8  
ELECTRICAL CONNECTOR  
( GLASS - FILLED COPOLYESTER )



FIGURE 7  
PANEL CONNECTOR COVER



FIGURE 9  
BLENDS OF PVC AND COPOLYESTER (40D)  
HARDNESS AND MODULUS VS. COMPOSITION

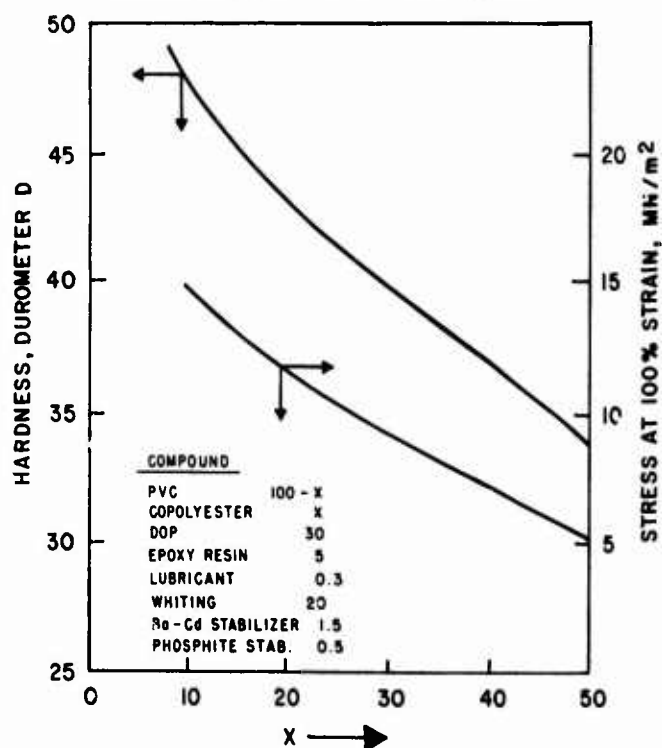


FIGURE 10

BLENDS OF PVC AND COPOLYESTER (40D)  
TORSIONAL MODULUS VS. COMPOSITION

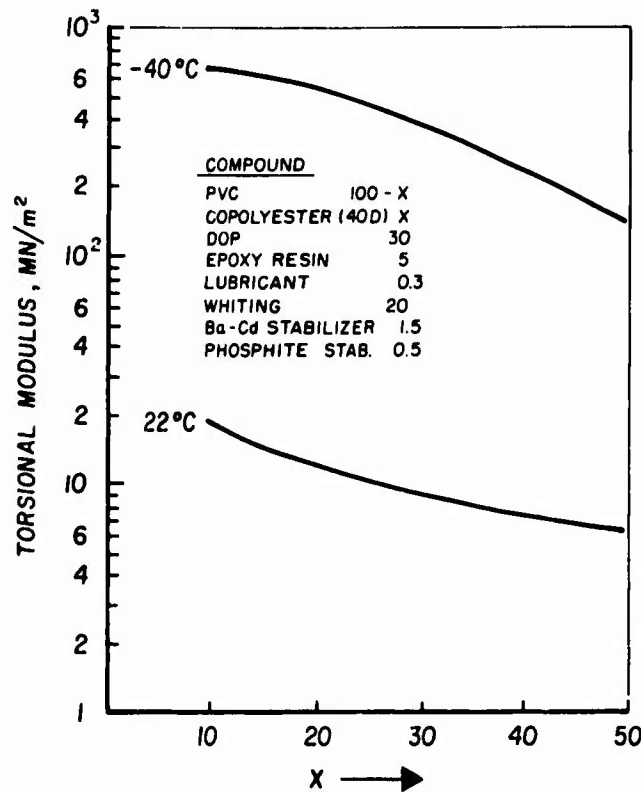


FIGURE 11

BLENDS OF PVC AND COPOLYESTER (40D)  
VOLUME SWELL VS. COMPOSITION

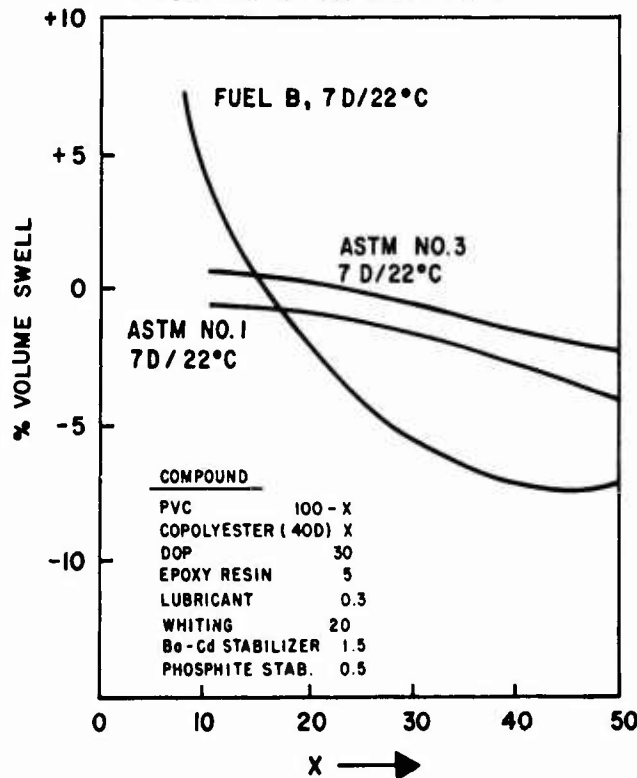
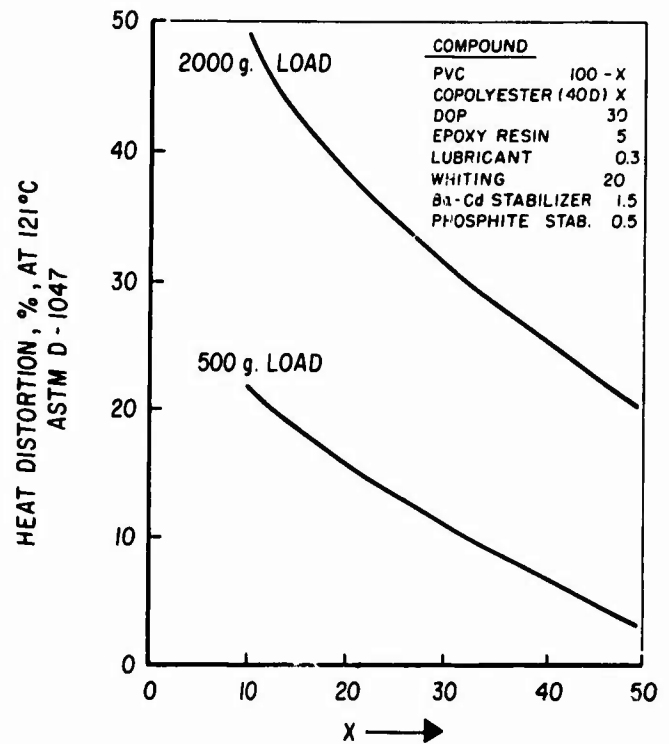


FIGURE 12

BLENDS OF PVC AND COPOLYESTER (40D)  
HEAT DISTORTION (ASTM-D-1047) VS. COMPOSITION



## ORGANO TITANATE COUPLING AGENTS FOR FILLED POLYMERS

S. J. Monte, G. Sugerman, P. D. Sharpe  
Kenrich Petrochemicals, Inc.  
Bayonne, N. J. 07002

### SUMMARY

- I. INTRODUCTION
- II. SIX FUNCTIONS OF MONOALKOXY TITANATE MOLECULE
  - A. Function 1 - Monoalkoxy
    - Titanate Filler Coupling Mechanism
    - Silane Filler Coupling Mechanism
    - Monomolecular Layer Formation
    - Chelate
    - Hydrolytic Stability
  - B. Function 2 - Transesterification
    - Cross-link and Viscosity Effects
  - C. Function 3 - Binding Group
    - Pyrophosphato Binding Group Function Explained
    - Flame Retardancy, Antioxidant, Thermal Stability Effects
  - D. Function 4 - Organic Backbone Type
    - R<sup>2</sup> Effect of Rheology
    - R<sup>2</sup> Functionality in Inorganic/Organic Composites - Thermosets and Thermoplastics
    - R<sup>2</sup> Chemical Internal Lube Effect on Filler Interface
    - Tear and Elongation
    - R<sup>2</sup> Contribution to Y Functionality
    - Number of Carbon Atoms in the Unsaturated Coupling Agent Linkage - Elongation Effect
  - E. Function 5 - Functional Group
    - Cross-link Performance
    - Effect of Number of Carbons in Unsaturate Linkage
    - Function Y Bonding of Substrates
  - F. Function 6 - Tri-Functionality
    - Trifunctionality and Inorganic Surface Energy Modification
    - A Comparison of Titanates and Silanes
- III. SIX FACTORS FOR SUCCESSFUL APPLICATION OF MONOALKOXY TITANATE COUPLING AGENTS
  - A. Factor 1 - Polymer Properties
  - B. Factor 2 - Filler Properties
  - C. Factor 3 - Titanate Properties
  - D. Factor 4 - Coupling Mechanism
    - How Other Compound Ingredients Effect Coupling
  - E. Factor 5 - Methods of Titanate Application
    - In Situ
    - Pretreatment
    - Inorganic Suppliers
    - Preparation of Fillers
  - F. Factor 6 - Processing

### IV. APPLICATIONS DATA

- A. Polypropylene
- B. HDPE
- C. LDPE
- D. Rigid PVC
- E. Flexible PVC
- F. Epoxy
- G. Polyester-Alkyd
- H. Thermoplastic Elastomers (TPE)
- I. CPE
- J. EPR
- K. EPDM
- L. Hypalon
- M. Silicone Rubber

### INTRODUCTION

The technology offered in this paper represents a new dimension in polymer technology for wire and cable. The reader is asked to discard all previous conceived notions concerning fillers and their effect on polymer rheology and performance.

The success of monoalkoxy organo titanate coupling agents stems from their effects on the interface wherein they provide a chemical bridge between the filler (inorganic) and continuous phase (organic polymer). Monoalkoxy titanates are unique in that they form monomolecular layers on the surface of the filler. The absence of polymolecular layers at the interface together with the chemical structure of the titanates create surface energy modification resulting in viscosity reductions in excess of coupling agents heretofore known. Tri-functionality of the coupling agent in the continuous phase plus the ability of titanates to cross-link via transesterification mechanism open many possibilities for titanate molecular modification and filled polymer systems optimization.

In this paper, we will discuss how monoalkoxy titanate coupling agents may be used in conjunction with inorganic fillers and organic polymers for optimum results.

Since monoalkoxy titanates have rather unwieldy chemical names, a shorthand letter code has been developed (See Table 1). Letter Codes will be used throughout the paper for brevity.

There are basically six functions intrinsic in the monoalkoxy titanate chemical structure and six factors to consider when applying these titanates to fillers and polymers.

Table 2 lists the major fillers used today and how two of the six functions of the titanate molecule effect coupling. Table 3 lists major polymers and how specific titanates and four of the six functions of the titanate molecule effect performance.



Table 1

<u>TITANATE LETTER CODE</u>	<u>DESCRIPTIVE NOMENCLATURE</u>		
TTS	Isopropyl Triisostearoyl Titanate	TB2NS-26	Isopropyl Di (Dodecylbenzenesulfonyl) 4-Amino Benzene Sulfonyl Titanate
TTA-2	Isopropyl Tri (Lauryl-Myristyl) Titanate	TTM-33	Isopropyl Trimethacryl Titanate
TSM2-7	Isopropyl Isostearoyl, Dimethacryl Titanate	TSN2C-37	Isopropyl Isostearoyl Di 4-Aminobenzoyl Titanate
TTBS-9	Isopropyl Tri (Dodecylbenzenesulfonyl) Titanate	TTOPP-38	Isopropyl Tri (Dioctylpyrophosphato) Titanate
TSA2-11	Isopropyl Isostearoyl Diacryl Titanate	TTAC-39	Isopropyl Triacryl Titanate
TTOP-12	Isopropyl Tri (Diisooctyl Phosphato) Titanate	TTOP-41	Isopropyl Tri (Dioctyl Phosphito) Titanate

Table 2

## TITANATE FUNCTION SELECTION FOR FILLER/INORGANIC COUPLING

CLASS	TYPE	MOISTURE CONDITION	TITANATE FUNCTION		
			R-O FUNCTION	X FUNCTION	
SILICAS	MINERAL	Sand	Dry	Monoalkoxy	As Desired
		Quartz	Dry	Monoalkoxy	As Desired
		Novaculite	Dry	Monoalkoxy	As Desired
SILICAS	SYNTHETICS	Wet Process Silica	Wet	Chelate	As Desired
		Fumed Colloidal Silica	Dry	Monoalkoxy	As Desired
		Silica Aerogel	Dry	Monoalkoxy	As Desired
SILICATES	MINERALS	Soft or Hard Clay	Wet	Monoalkoxy	pyrophosphato
			Wet	Chelate	As Desired
		Calcined Clay	Dry	Monoalkoxy	As Desired
		Mica	Dry	Monoalkoxy	As Desired
		Talc	Wet	Monoalkoxy	pyrophosphato
			Wet	Chelate	As Desired
			Dry	Monoalkoxy	As Desired
		Wollastonite	Dry	Monoalkoxy	As Desired
		Asbestos	Dry	Monoalkoxy	As Desired
			Dry	Monoalkoxy	As Desired
SILICATES	SYNTHETICS	Calcium Silicate	Dry	Monoalkoxy	As Desired
		Aluminum Silicate	Wet	Chelate	As Desired
CALCIUM CARBONATE	Chalk	Limestone	Dry	Monoalkoxy	As Desired
		Precipitated	Dry	Monoalkoxy	As Desired
		Zinc, Iron, Lead	Dry	Monoalkoxy	As Desired
METAL OXIDES	Titanium, Alumina, Magnesia	Hydrated Alumina	Dry	Monoalkoxy	As Desired
			Wet	Monoalkoxy	pyrophosphato
			Dry	Monoalkoxy	As Desired
		Acetates, Hydroxides	Dry	Monoalkoxy	As Desired
		Sulfates, Nitrates	Dry	Monoalkoxy	As Desired
FIBERGLASS	Manufactured Process		Wet	Chelated	As Desired
		Lamp Black	Dry	Chelated	As Desired
CARBON BLACK	Reinforcing		Dry	Chelated	As Desired

Table 3

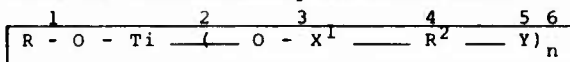
POLYMER TYPE	TYPE OF REACTIVITY	Function 2 + EFFECT	Function 3 X' EFFECT	Function 4 R' EFFECT	Function 5 Y EFFECT
<b>THERMOPLASTICS</b>					
Polypropylene HDPE LDPE Polybutylene	Van der Waal Entanglement			TTS	Impact
			TTOP-41	Antioxidant	TTOP-41
			TTOP-12	Flame Retardant	TTOP-12
			TTOPP-38	Moisture Resistance	TTOPP-38
					Impact
Polystyrene	Van der Waal Entanglement		TTOP-41 TTOPP-38	Antioxidant	TTS Melt Index Impact Melt Index Impact
PVC - Rigid	None		TTOPP-38	Flame Retardant	TTOPP-38
PVC - Flexible-Electrical	None		TTOP-12	Flame Retardant	TTOP-12
					Impact Low Temp. Flex.
PVC - Flexible-Non-Electrical	C1 Substitution		TB2NS-26S	Thermal Stability	TSN2C-37S Modulus TB2NS-26S Modulus
					TSN2C-37S Tear Strength Cross-link Tear Strength Cross-link
Nylon Polyamide-imide	Amino	TTOP-12	Cross-link	TTOP-12	Flame Retardant
				TTOP-12	Antioxidant
				TB2NS-26S	Thermal Stability
					Melt Index Impact Impact Impact Impact
					TSN2C-37S Cross-link TB2NS-26S Cross-link
PBT Polyacetal Polycarbonates	Trans-esterification	TSN2C-37S TB2NS-26S	Cross-link Cross-link	TB2NS-26S	Thermal Stability Flame Retardant Antioxidant
		TTOP-12	Cross-link	TTOP-12	Impact
				TTOP-41	Impact
PPO PPS	None		TTOP-12	Flame Retardant Antioxidant Antioxidant	TTOP-12 Impact Impact Impact
			TTOP-41 TTP-34		TTP-34
<b>THERMOSETTING RESINS</b>					
DAP Polyester	Olefinic	TTBS-9 TTOP-12	High	TTOP-12	Flame Retardancy
		TTAC-39S TTM-33S TSA2-11 TSM2-7 TTS	Viscosity Building		
		TTOP-41	None	TTOP-41	Antioxidant
					Impact
Cross-linkable Polyethylene	Olefinic				
					TTAC-39S TTM-33S TSA2-11 TSM2-7 Cross-link Cross-link Cross-link Cross-link
Epoxies	Epoxide	TTS TTBS-9	Viscosity Building Viscosity Gelling	TTOP-12	Flame Retardant Antioxidant
		TTOP-12	None	TTOP-12	Viscosity Reduction
		TTOP-41	None	TTOP-41	Viscosity Reduction
		Develop-mental	Prevent phase settling	Develop-mental	Viscosity Reduction
					Develop-mental Cross-link
Phenolics	Aromatic Unsaturation				TSN2C-37S TB2NS-26S TTP-34 TTS
					Impact Impact Cross-link Impact
					TSN2C-37S TB2NS-26S Cross-link Cross-link

Melamine Nylon Polyamides	Amino Substitution	TTOP-12	Moderate	TB2NS-26S TTOP-12	Thermal Stability Flame Retardant	TSN2C-37S TB2NS-26S TTOP-12 TTS	Impact Impact Impact	TSN2C-37S TB2NS-26S	Cross-link Cross-link
<b>ELASTOMERS</b>									
EPDM EPR CPE Polyisoprene CPE	Peroxide					TSA2-11 TSM2-7 TTS TTOPP-38	Elongation Elongation Viscosity Reduction	TTAC-39S TTM-33S TSA2-11 TSM2-7	Cross-link Cross-link Cross-link Cross-link
SBR EPDM Natural Rubber Nitrile Polybutadiene Polysulfide Hypalon	Sulfur			TB2NS-26S  TTOPP-38  TTOP-12	Thermal Stability  Flame Retardant  Flame Retardant	TB2NS-26S  TTS TTOPP-38  TTOP-12	Elongation  Rheology Higher Filler Loading Rheology	TSN2C-37S TSN2C-37S  TB2NS-26S	Tensile-up Modulus - Unaffected Tensile-up Modulus - Unaffected
We anticipate developing titanates for Sulfur Cured Systems which will build modulus and tensile with minimal effect on elongation. These will be amino and disulfide types.									
EPDM	Phenolic			TTP-34	Activation	TTP-34	Cross-link		
Hypalon Neoprene Hydrin	Metal Oxide					TSN2C-37S TB2NS-26S TTOP-12	Rheology Rheology Rheology	TSN2C-37S TB2NS-26S	Property Improvement Property Improvement
		TTOP-12	Toughness	TTOP-12	Flame Retardant	TTOP-12	Impact		
		TTBS-9	Toughness	TTBS-9	Thermal Stability	TTBS-9	Impact		
		TTOP-41	No Effect	TTOP-41 TTS	Antioxidant	TTOP-41	Impact Higher Filler Loading		
Polyester TPE	None			TTOP-12  TTOP-41	Flame Retardant  Antioxidant	TTOP-12  TTOP-41	Higher Filler Loading		
Urethanes	Chelated - 100 series with Hydroxyl and Amino Function under development.								

Tables 1, 2 and 3 point out the need for a discussion of these titanate molecule functions.

#### SIX FUNCTIONS OF MONOALKOXY TITANATE MOLECULE

The titanate molecule has six basic areas of functionality as shown below:



They are identified as follows:

- Function 1 - R - O - - Monoalkoxy
- Function 2 - - - - - Transesterification
- Function 3 - O - X<sup>1</sup> - - Binding Group
- Function 4 - - R<sup>2</sup> - - Organic Backbone Type
- Function 5 - - Y - - Functional Group
- Function 6 - - )<sub>n</sub> - - Trifunctionality

#### Function 1 - Monoalkoxy

Function 1 relates to the chemical coupling or linking of the titanate molecule via its alkoxy group to the surface of the inorganic. Monoalkoxy functionality has the following unique characteristics and advantages:

- The simple one-step reaction of the isopropoxy (CH-CH-O) portion of the titanate



with the free proton (H) provided by the inorganic. This reaction can be identified as the Titanate Filler Coupling Mechanism.

- Monomolecular layer formation which gives maximum wetting efficiency and de-agglomeration.

- Low energy levels to hydrolyze (react with free protons). This means that fillers react readily with titanates at room temperature.
- The size of the monoalkoxy group can be made longer to slow down its reaction rate in high moisture systems.
- Chelates can be designed to operate in aqueous systems. Chelation stabilizes against reaction with  $H_2O$ , introduces OH functionality and has no alcohol by-product when it reacts with the inorganic
- Hydrolytic Stability

#### Titanate Filler Coupling Mechanism

Figures 1 and 2 compare the Monoalkoxy Titanate and Trialkoxy Silane Filler Coupling Mechanisms.

#### Silane Filler Coupling Mechanism

It is evident from Figures 1 and 2 that

the titanate coupling mechanism precludes the formation of polymolecular layers. By comparison, "... only one of the silanol groups resulting from the hydrolysis of the silane reacts with the filler surface hydroxyl groups. The remaining hydroxyl groups may condense with adjacent silane molecules. It is also possible for the silane molecules to react with one another before they have a chance to react with the filler surface, thus reducing their effective coupling action. The most efficient method of using the silane is by premixing with the filler before addition to the elastomer. Coupling agent effectiveness is seriously reduced when it is added to the mix after the filler has been incorporated into the elastomer phase."<sup>1</sup> The minimization of the need for water and one third less alcohol formation in the titanate mechanism suggest better electricals.

Figure 1

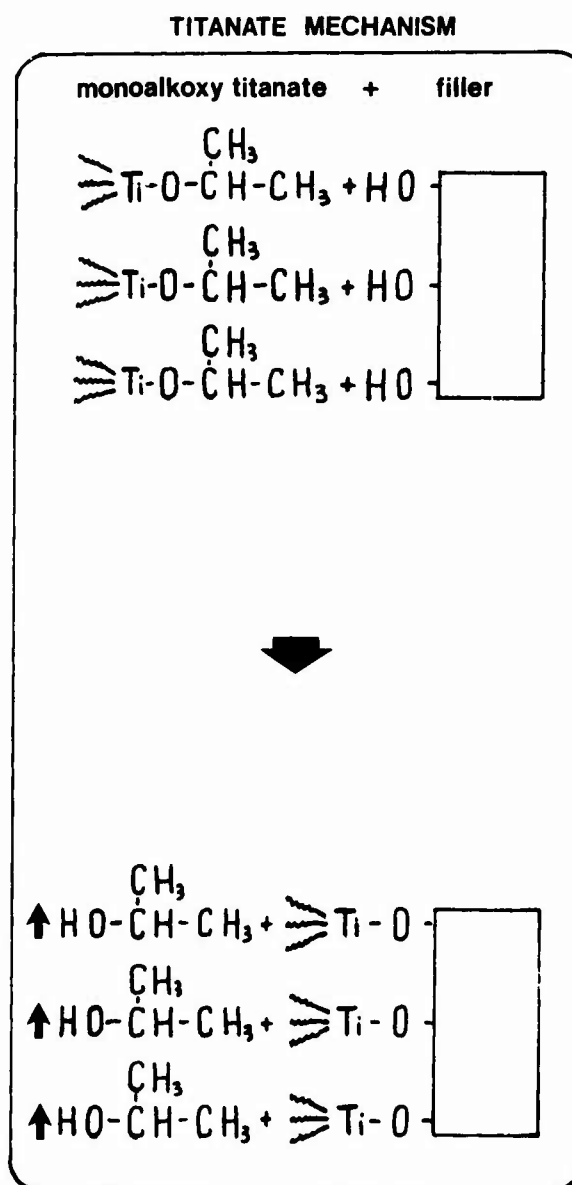
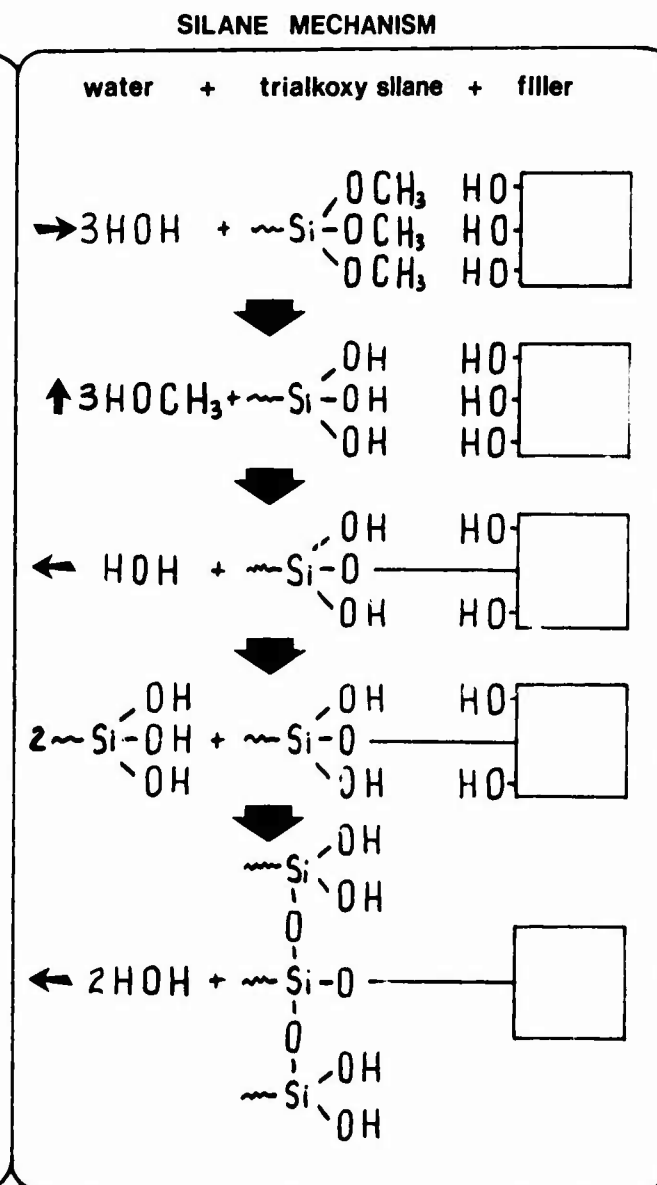


Figure 2



### Monomolecular Layer Formation

Table 4 shows the advantage of monomolecular layer formation in a zinc oxide dispersion.

Table 4 MONOALKOXY CHEMICAL STRUCTURE GIVES BEST WETTING AND STABILITY

ZINC OXIDE DISPERSION	
test formulation ingredients	parts by weight
inorganic — ZnO (-325 mesh, 5.3'/gm.)	90
Organic — Hydrocarbon Oil	7
Tri, Di & Mono Alkoxy Titanate	3

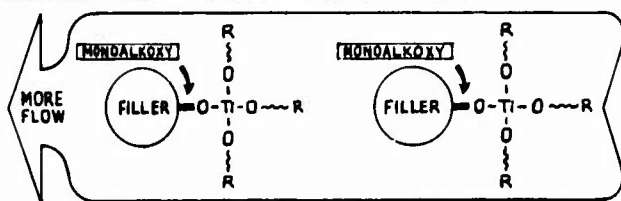
MEASURED ON NEEDLE PENETROMETER (ASTM TEST NO. D1321)  
HIGHER READING REFLECTS GREATER SOFTNESS AND WETTING

AGING, DAYS	TRI	DI	MONO
0	DOES	160	165
2	NOT	125	150
4	WET —	89	118
6	NO	85	115
8	READING	80	112

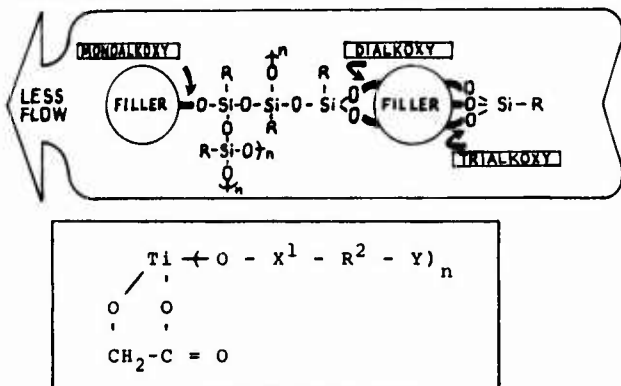
Figure 3 illustrates why monomolecular layer formation of monoalkoxy titanates give superior flow properties when compared to the polymolecular and multimolecular layer formation caused by trialkoxy silanes.

Figure 3

#### Monoalkoxy Titanates - Monomolecular Layer Formation On Filler



#### Trialkoxy Silanes - Multimolecular Layer Formation On Filler



### Chelate

The chelate effect on high moisture containing wet synthetic silica fillers such as HiSil 233 is shown in Table 5.

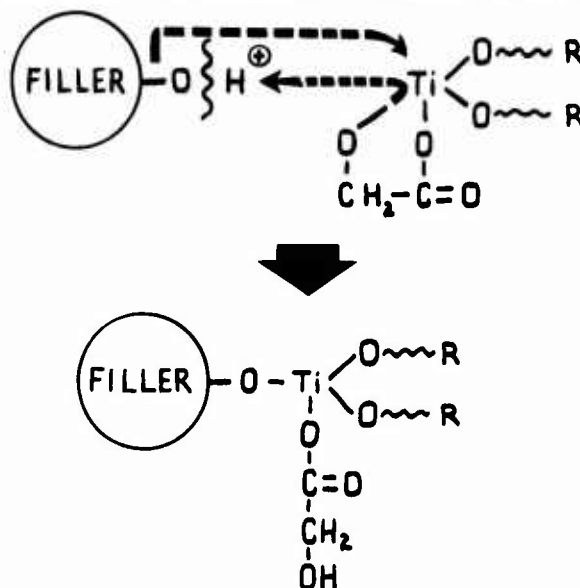
Table 5 ADVANTAGE OF CHELATE EFFECT ON HiSil 233

TEST FORMULATION: HiSil 233 — 20 PTS  
Mineral Oil — 80 PTS  
Titanate — 0.6 PTS

TITANATE	VISCOSITY
None	35,500
TTOPP-38	18,300
TTS	17,800
TTOP-12	13,500
TTOPI-41	13,300
TOP2G-112 (Chelate)	8,000

The chelated monoalkoxy titanate coupling mechanism is shown in Figure 4.  
Figure 4

### CHELATED MONOALKOXY TITANATE MECHANISM



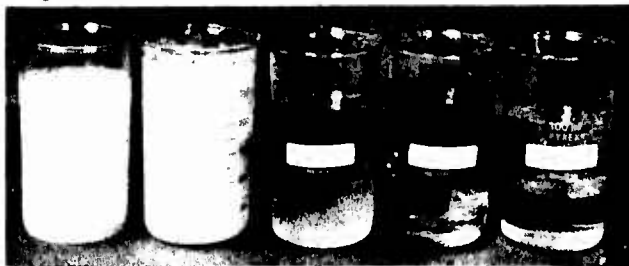
In summary, the method of manufacture of the filler and subsequent percentage moisture content determines which type titanate to use for maximum coupling efficiency as follows:

- monoalkoxy - inorganics with bonded moisture.  
dry process fillers which are mined and classified.  
water washed fillers which are dried by calcining. Calcining drives off free moisture. HOH present is atmospheric and has low percentage moisture content.
- monoalkoxy - pyrophosphato water washed fillers which are dried but not calcined. HOH present consists of atmospheric and free moisture and has moderate percentage moisture content.
- chelate - wet process filler with high surface area. HOH present consists of free moisture and high atmospheric moisture (due to surface area) and has high percentage moisture content.

### Hydrolytic Stability

Figure 5 illustrates the comparative hydrolytic stability of Vinyl Silane A-172, TetraIsoPropyl Titanate, TTA-2, TTS, and TTOPP-38.

Figure 5



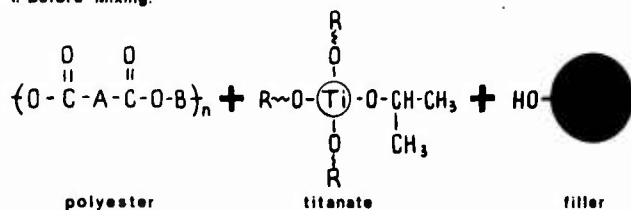




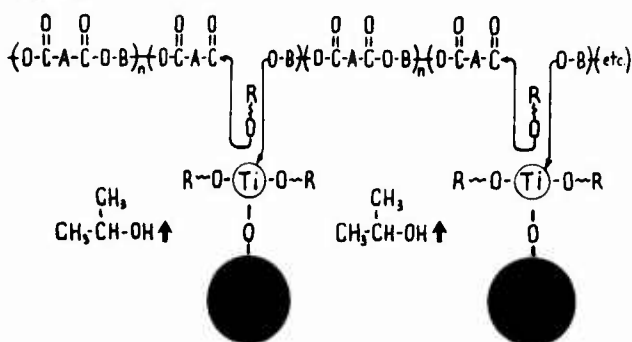
	1	2	3	4
CaCO <sub>3</sub>	60	60	70	70
Polyester	40	40	30	30
Ken-React TTOPi-41	—	0.6	—	0.7
Viscosity @ 92°F, cps	12,500	10,500	265,000	212,000

Figure 7

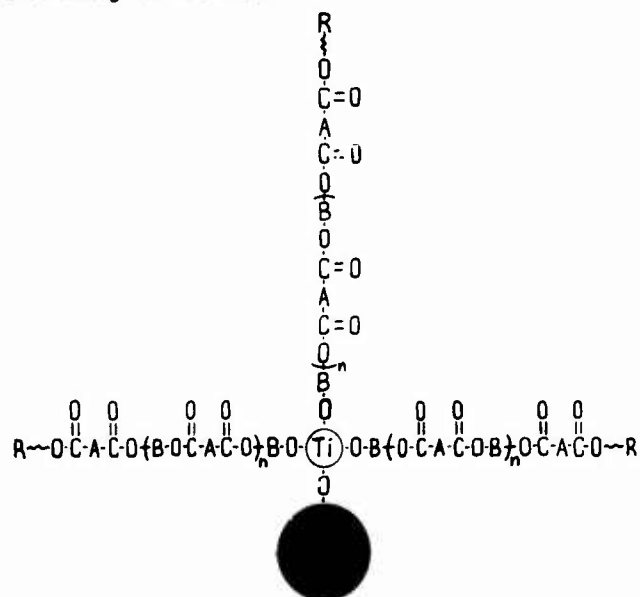
### 1. Before Mixing:



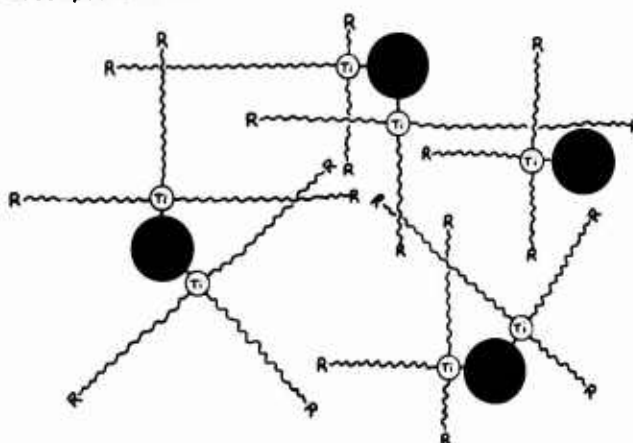
## 2. Mixing:



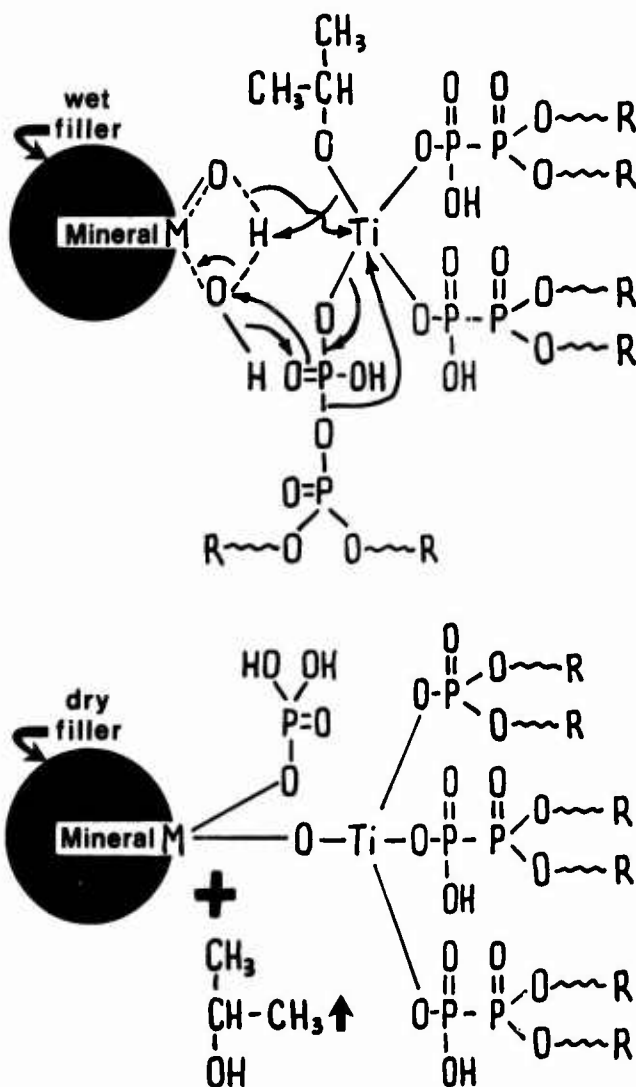
### 3. After Mixing - Unit Filler Effect:

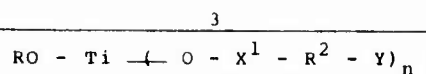


#### 4. Composite Effect:



### Pyrophosphate Moisture Absorption Mechanism In Hydrated (Wet) Mineral Filler





### Function 3 - Binding Group

The portion of the titanate molecule immediately adjacent to the titanium center affects performance as shown in Table 7.

The compounder can select a titanate which will give him the desired hydrolytic stability, thermal stability, transesterification activity and specific performance effects.

### Pyrophosphato Binding Group Function Explained

Table 8 shows the effect of increasing hydrolytic stability on the coupling efficiency of titanates in a water washed (non-calcined) clay filled mineral oil system. Although TTS and TTOP-12 are clearly superior to the control, TTOPP-38 is in a class by itself. This phenomenon is the result of the pyrophosphato water absorption mechanism of the TTOPP-38 molecules. The pyrophosphato moisture absorption mechanism is illustrated in Figure 11. (See Previous Page)

Table 7 BINDING GROUP PERFORMANCE EFFECTS

Binding Group Legend		PERFORMANCE EFFECTS					Specific Effects
Group	Structure	S Y M B O L	Hydrolytic Stability	Transester- ification Activity	Thermal Stability	S Y M B O L	
Alcoholate	-O-C-	A	Least Stable A	Inactive F	Least Stable B	A	Adhesion Promotion
Carboxyl	$\begin{array}{c} \text{O} \\ \parallel \\ -\text{O}-\text{C}- \end{array}$	B	B	Inactive E	A	B	Compatibility With Semi- Polar Materials
Sulfonyl	$\begin{array}{c} \text{O} \\ \parallel \\ -\text{O}-\text{S}- \\ \parallel \\ \text{O} \end{array}$	C	F	Active B	E	C	Thixotropic Agent For Epoxies and Polyesters
Phosphato	$\begin{array}{c} \text{O} \\ \parallel \\ -\text{O}-\text{P}-\text{O}- \\ \parallel \\ \text{O} \end{array}$	D	E	A	C	D	Contributes to Flame Retardancy Flexibilizer for PVC Viscosity Reducer in Epoxies Viscosity Builder in Polyesters
Pyrophosphato	$\begin{array}{c} \text{O} \quad \text{O} \\ \parallel \quad \parallel \\ \text{O}-\text{P}-\text{O}-\text{P}-\text{O}- \\ \parallel \quad \parallel \\ \text{O} \quad \text{O} \\ \text{O}-\text{H} \end{array}$	E	D	D	F	E	Absorbs Free Moisture Impact Improvement For Rigid PVC
Phosphito	$\begin{array}{c} \text{O} \\ \parallel \\ -\text{O}-\text{P}-\text{O}- \\ \parallel \\ \text{O} \end{array}$	F	C Most Stable	C Most Active	D Most Stable	F	Antioxidant Viscosity Reducer In Polyesters and Epoxies

Table 8 EFFECT OF VARIOUS TITANATES ON NON-CALCINED CLAY

	1	2	3	4
11 Catalpo Clay	30	30	30	30
Mineral Oil	70	70	70	70
KEN-REACT TTS	—	0.6	—	—
KEN-REACT TTOP-12	—	—	0.6	—
KEN-REACT TTOPP-38	—	—	—	0.6
Brookfield Viscosity, cps @ 25°C	19,000	8,200	5,200	700

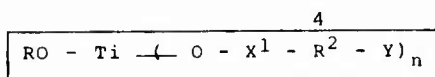
### Phosphato (X<sup>1</sup> Function) Flame Retardant Effect

Figure 12 shows a cast sand filled epoxy flooring compound having the following formula:

Resiplex 1628 Epoxy	-	65
Kenplast ES-2	-	35
Celanese 824 Hardner	-	20
3M Colorquartz #28	-	300
TTOP-12	-	3

After removing the flame, the carbon formed in the surface of the casting was wiped off and showed no ill effects.

Figure 12



### Function 4 - Organic Backbone Type

The molecular structure of the titanate backbone and its performance effects are shown in Table 9.

#### R<sup>2</sup> Effect on Rheology

The presence of a large number of carbon atoms on the titanate backbone creates surface energy modification on the inorganic interface which results in dramatic viscosity reduction. This effect is illustrated in Figures 13 through 21.

Table 9 — Organic Backbone Performance Effects


Backbone Type	Typical Structure	Performance Effects
Any Hydrocarbon	- R <sup>2</sup> -	<ul style="list-style-type: none"> <li>• Presence of large number of hydrocarbons modifies surface energy and reduces viscosity</li> <li>• Long chains impart tear strength</li> <li>• Makes fillers organophilic and hydrophobic</li> </ul>
Aliphatic Hydrocarbon	$\begin{array}{c} +\text{CH}_2\text{H}_2 \\ +\text{CH}_2\text{H}_n\text{CH}_2\text{CH}_3 \\ \text{CH}_3 \end{array}$	<ul style="list-style-type: none"> <li>• Provides Olefinic Compatibility</li> <li>• Provides long chains for Van der Waal bonding, polymer chain entanglement and stress-strain transfer for impact improvement</li> <li>• Isoparaffins liquify titanates which otherwise would be solid in neat state</li> </ul>
Aromatic Hydrocarbon		<ul style="list-style-type: none"> <li>• Provides Aromatic Compatibility</li> <li>• Potential Cross-link site</li> </ul>

Figure 13

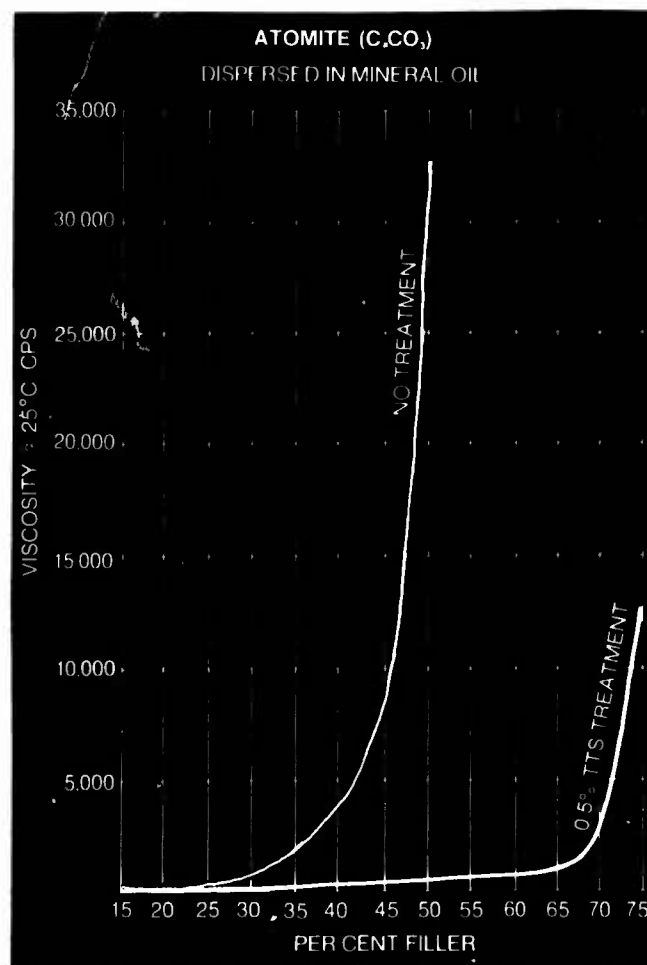


Figure 14

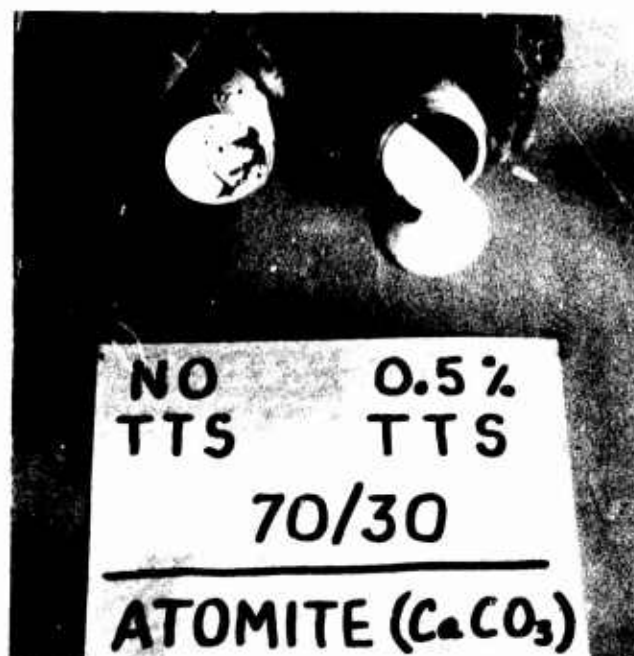


Figure 16

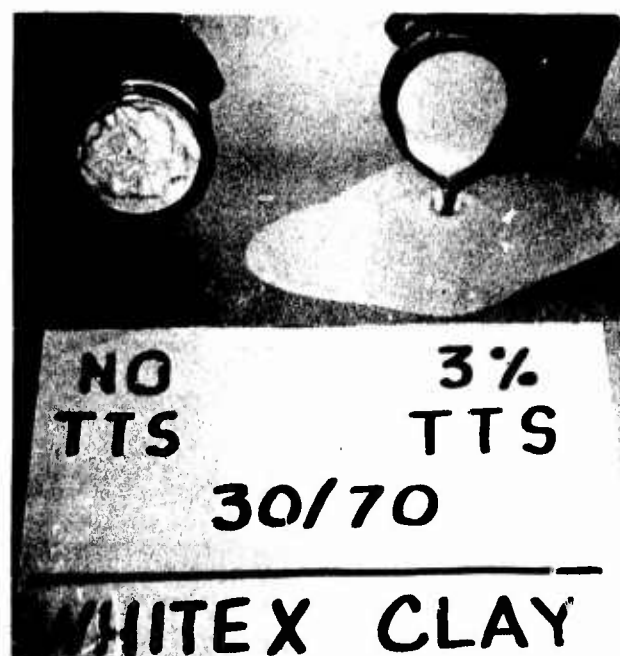


Figure 17

Figure 15

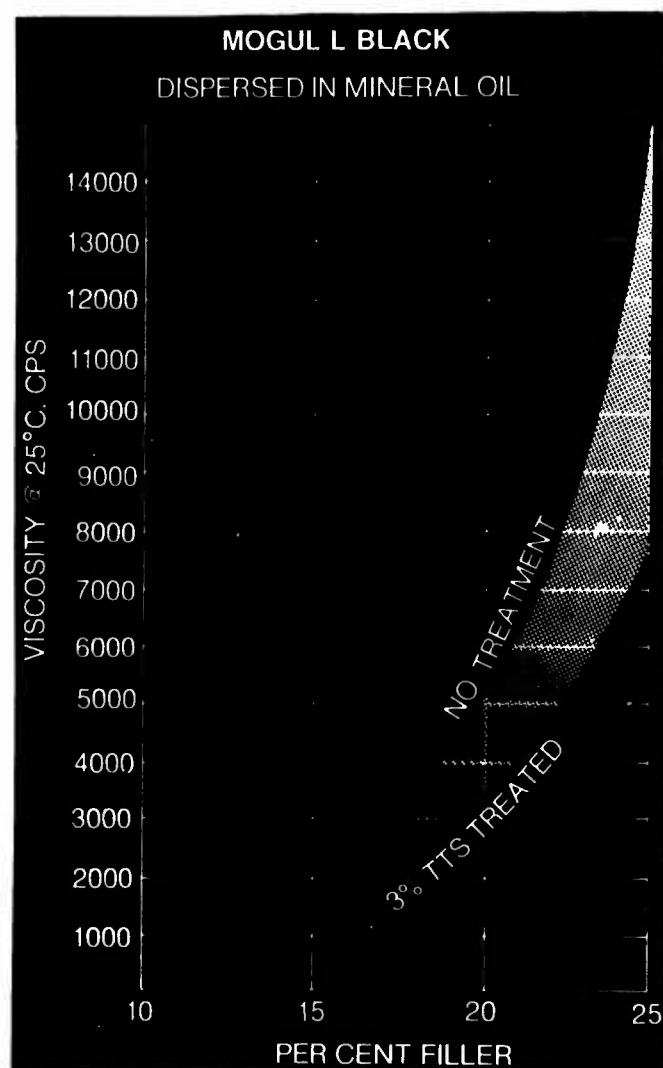
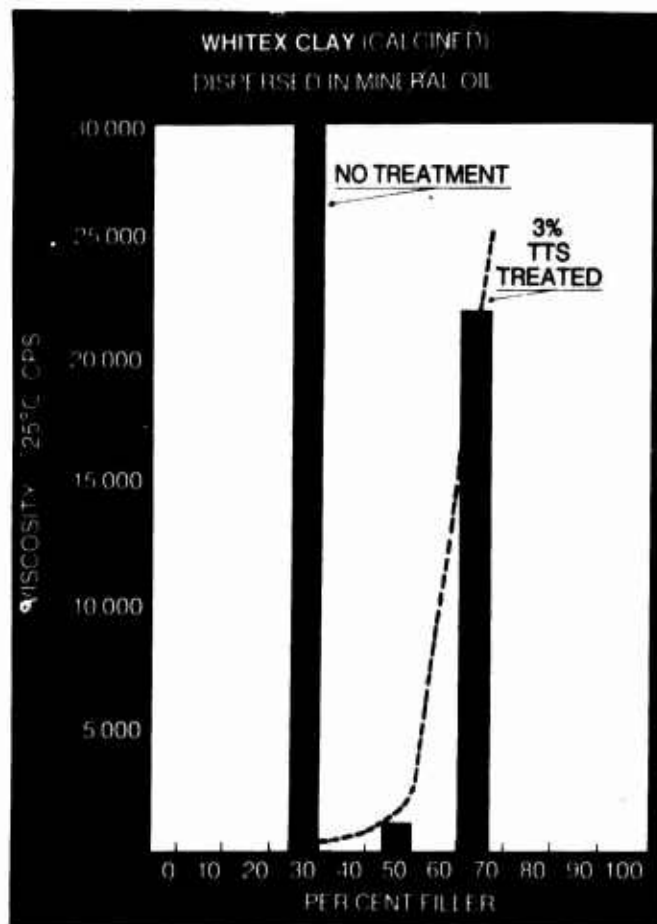


Figure 18

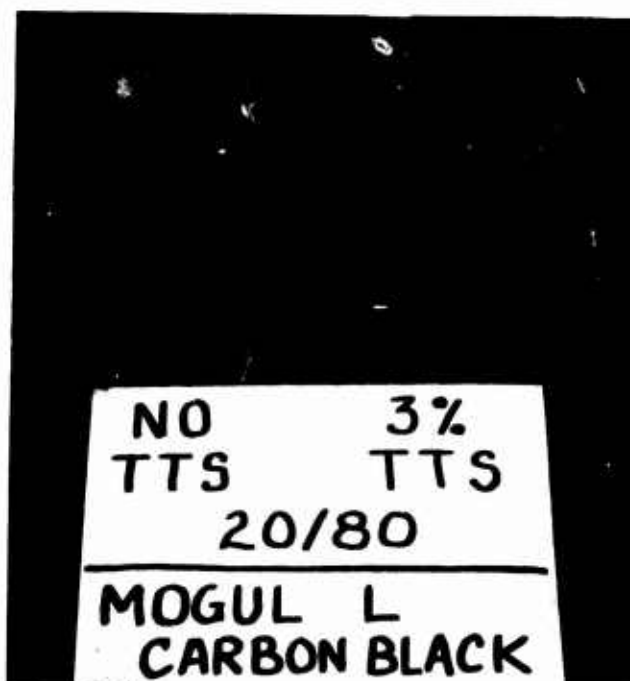


Figure 20

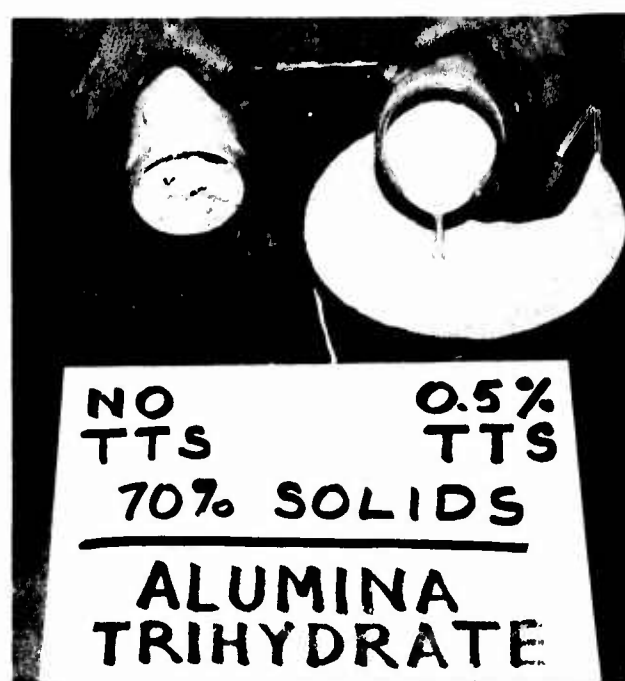


Figure 19

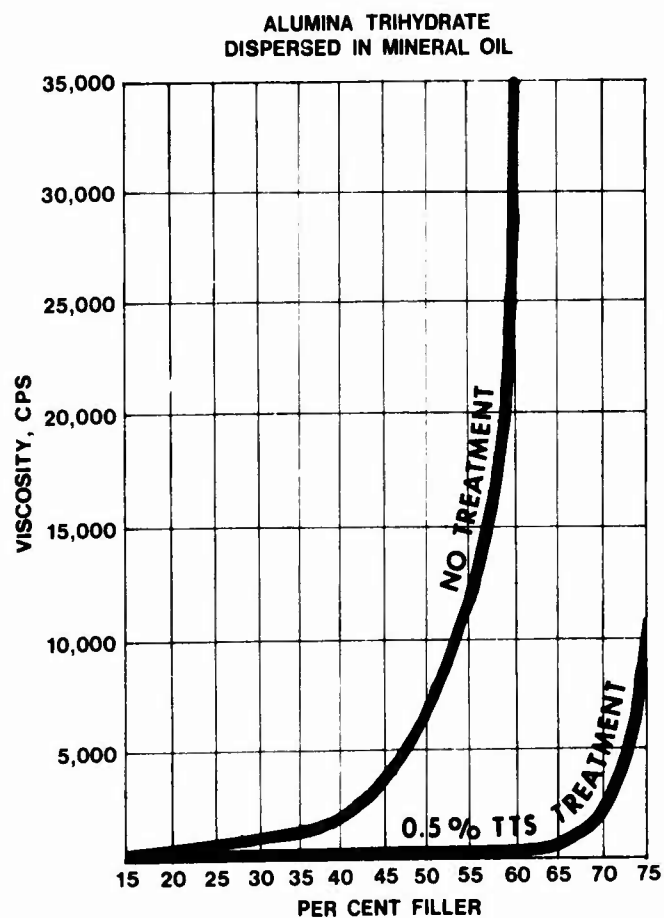
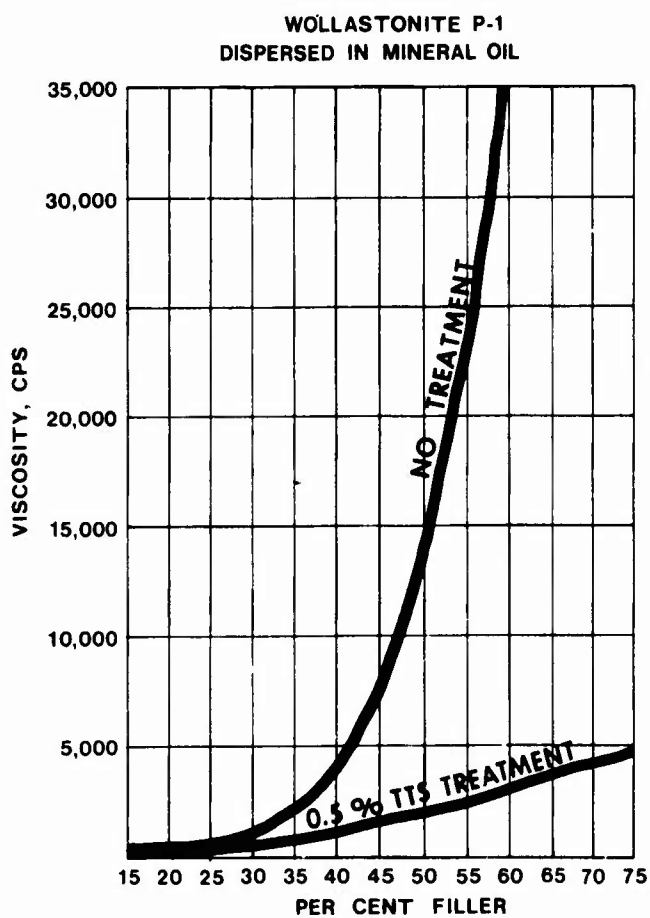


Figure 21



## R<sup>2</sup> Functionality in Inorganic/Organic Composites - Thermosets and Thermoplastics

Although we refer to the wire and cable industry, the rubber industry, the plastics industry, the coatings industry, etc., we really are dealing with inorganic/organic composites in two distinct systems - thermoset requiring cures and thermoplastics requiring no cure. The titanates are unique in that they can function broadly in both the thermoplastic and thermoset areas. As can be seen from Figure 22, the saturated long chains related to the R<sub>2</sub> function of the titanate allow for stress strain transfer via Van der Waal Entanglement which results in impact superior to virgin polymer, better melt flow and maintenance of tensile strength in ultra high filled thermoplastics.

Figure 22

### COUPLED FILLERS ARE COMMON TO BOTH SYSTEMS

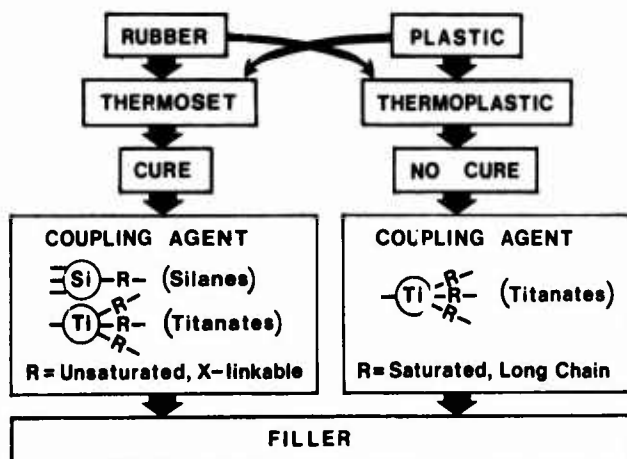
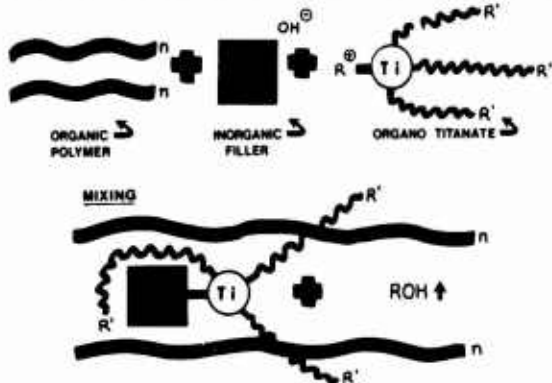


Figure 23 illustrates why and how titanate coupling agents dramatically improve impact and provide Van der Waal chain entanglement in filled thermoplastic polymer systems.

Figure 23

### COUPLING IN THERMOPLASTIC SYSTEMS WITH MONOALKOXY COUPLING AGENTS-TITANATES



### R<sup>2</sup> Chemical Internal Lube Effect On Filler Interface

In addition to the obvious function of the R<sub>2</sub> groups in thermoplastic systems, they can provide lubricity to any filled system such as a black filled nitrile rubber hose thermoset compound. Figure 24 illustrates the surface improvement of the extrudate with the use of TTS.

Figure 24



This lubricity or internal lube effect contributes the following additional benefits:

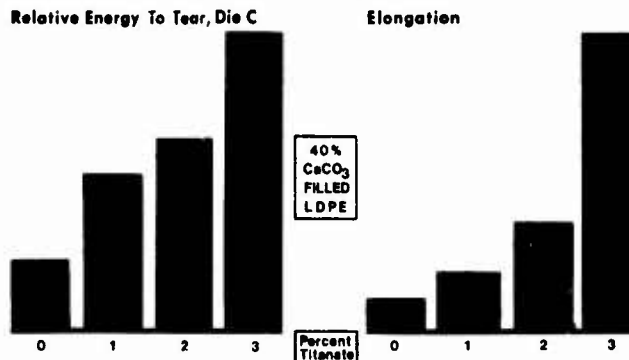
- Reduced Machine Wear
- Lower Mooney Viscosity
- Lower torque (energy) requirements during mixing
- Faster extrusion
- Shorter Banbury and mix cycles
- Reduced die wear
- Improved dispersion
- Improved electrical properties

This lubricity is obtained without fear of migration. The R<sup>2</sup> chain is chemically bound to the filler by covalent bonds.

### Tear and Elongation

In both the thermoplastic and thermoset systems, the presence of the long R<sub>2</sub> chains at the interface has flexibilizing and stress transfer functions which result in increased elongation and tear strength. This is exemplified in Figure 25, which shows the effect of TTS on 40% calcium carbonate filled low density polyethylene.

Figure 25





## R<sup>2</sup> Contribution to Y Functionality

In the past, the compounder has been forced to accept lower elongation in order to achieve acceptable modulus. Such is no longer the case. Titanates containing a mixture of say one Y group and two R<sup>2</sup> groups such as TS2M-6 now provide for densification of the cross-link network via the Y group resulting in higher modulus while simultaneously maintaining elongation via the two R<sup>2</sup> groups. High elongation data obtained from the use of titanates does not necessarily mean lack of cure.

Figure 26 illustrates the trialkoxy, monofunctional coupling mechanism of a single Y (vinyl) group silane such as A-172 in a filled thermoset system. This mechanism will result in high modulus and low elongation.

Figure 26

### COUPLING IN THERMOSET SYSTEMS WITH TRIALKOXY COUPLING AGENTS - SILANES

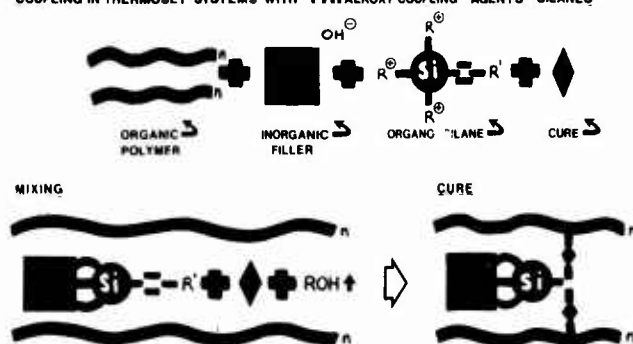
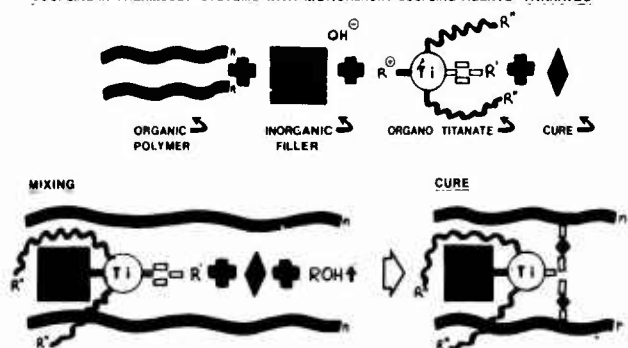


Figure 27 illustrates the monoalkoxy, trifunctional coupling mechanism of a single Y (methacrylic) group and two R<sup>2</sup> group titanate such as TS2M-6 in a filled thermoset system. This mechanism will result in a lower modulus and higher elongation when compared to the Vinyl Silane A-172 system - even though the degree of cross-link densification is similar.

Figure 27

### COUPLING IN THERMOSET SYSTEMS WITH MONOALKOXY COUPLING AGENTS - TITANATES



Equivalent cross-link densification systems can have dissimilar modulus and elongation because of the following principle reasons:

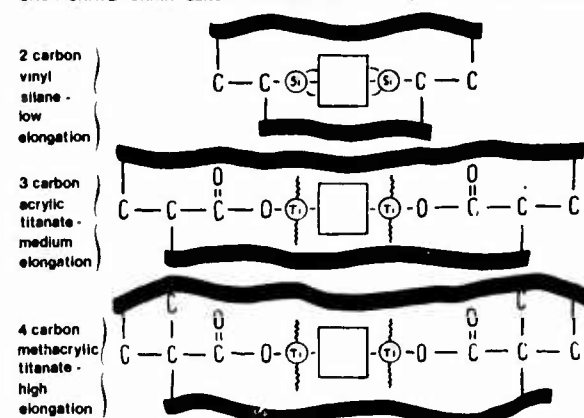
- The number of carbon atoms in the unsaturated linkage of the coupling agent
- The superplasticizer effect of long R<sup>2</sup> chains on the surface energy of the filler.

## Number of Carbon Atoms In The Unsaturated Coupling Agent Linkage - Elongation Effect

Figure 28 illustrates how the number of carbon atoms or length of the filler/cross-link chain result in different torque readings and elongation with the same number of cross-links.

Figure 28

### UNSATURATE CHAIN LENGTH EFFECT ON ELONGATION SILANE AND TITANATE



If higher modulus and lower elongation are desired, the compounder can go from a one methacrylic titanate (TS2M-6) to a one acrylic titanate (TS2A-10) to reduce the length of the cross-link chain. He can also increase the degree of cross-link densification by going to a "two Y group one R<sup>2</sup> group" titanate such as TSM2-7 or TSA2-11 or a "three Y group" titanate such as TTM-33 or TTAC-39S.

The use of TTAC-39S greatly increases the degree of cross-link as compared to A-172. However, the presence of nine carbon atoms trifunctionality (3) x acrylic (3 carbons) = 9 carbons still has a super plasticizer effect. Those schooled in the art know that a plasticizer lowers modulus and increases elongation.

For example, 3% TTS on CaCO<sub>3</sub> filler reduces tensile modulus in HDPE 40% as the phr level of filler is increased almost four-fold. At four times the filler loading, the tensile is unaffected while the melt flow increases and impact doubles.

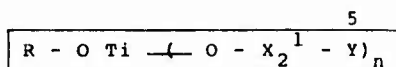
This data is shown in Table 10.

Table 10

### SUPER PLASTICIZER EFFECT LOWERS MODULUS

HDPE'	CaCO <sub>3</sub> '	TTS	Melt Index	Tensile psi'	Modulus psi	Impact Ft-lbs./in.
100	43	None	16.31	1961	217,927	0.531
100	150	4.5	17.81	1804	130,756	1.014

Therefore, although the degree of cross-link is higher due to triacrylic unsaturation availability (which normally would result in high modulus) the internal plasticization of the filler serves to counteract the acrylic modulus building effect. This is why triacrylic titanates such as TTAC-39S will show only slightly higher tensile modulus with corresponding higher elongation when compared to Vinyl Silane A-172 in a peroxide cured, clay filled EPDM compound. The higher degree of cross-link of the TTAC-39S will give 1 to 3 points higher Shore A hardness when compared to Vinyl Silane A-172. Although efforts have to be made to overcome the super plasticizer effect of titanates on modulus, the compounder gains numerous other process, flow and mechanical property advantages.



#### Function 5 - Functional Group

The functional group attached to the Organic backbone provides the following:

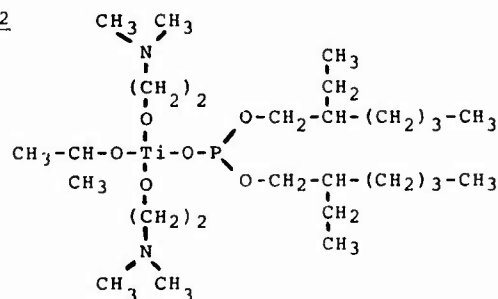
Type	Typical Structure	Performance Effects
Unsaturation	$\text{C} = \text{C}$  $-\text{CH} = \text{CH}_2$ $\text{CH}_3$ $-\text{CH} = \text{CH}_2$	<ul style="list-style-type: none"> <li>Provides unsaturation for peroxide and free radical cross-link.</li> <li>Methacrylics improve physicals.</li> <li>Acrylics give tighter cross-link networks and provide bonding.</li> </ul>
Amine	$-\text{NH}_2$	<ul style="list-style-type: none"> <li>Provides for sulfur cross-link</li> <li>Amino groups substitute react with</li> <li>Halogen to provide bonding.</li> <li>Cross-link with Esters</li> <li>Cures Epoxy and Filler.</li> </ul>
Hydroxyl	$-\text{OH}$	Typical Hydroxyl functionality effects
Hydrogen	$-\text{H}$	Nonreactive termination
Mercapto & Sulfide	Under Development	

Figure 29 shows the chemical structure of TN2PI-42 which cross-links epoxies by acting as a difunctional tertiary amine while simultaneously coupling with filler via the alkoxy group and reducing the viscosity via the phosphate functionality. Typically, 5% of TN2PI-42 replaces 10 to 50% of amine curing agents in Epon 828 or similar epoxies. It therefore acts as:

- A curative due to Y Function 5
- Viscosity Reducer due to  $\text{R}^2$  Function 4
- Antioxidant due to  $\text{X}^1$  Function 3
- Phase settling reducer due to  $\text{X}^1$  Function 2
- Filler Coupling Agent due to  $\text{R}-\text{O}$  Function 1
- Function 6 - n allows for the simultaneous presence of two Y groups and one  $\text{P}^2$  group.

Figure 29

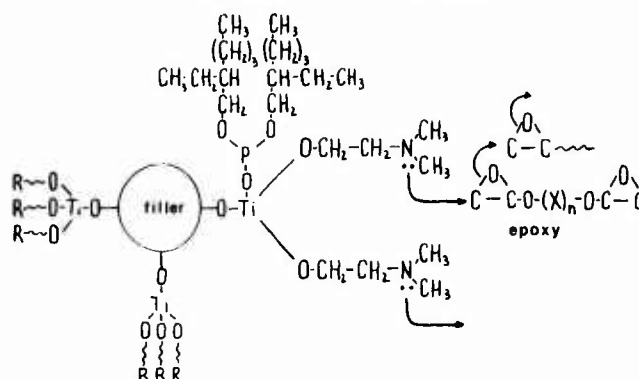
TN2PI-42



The mechanism for the action of this monoalkoxy titanate is suggested in Figure 30.

Figure 30

TN2PI-42 CURE OF FILLED EPOXY



#### Function Y Bonding of Substrates

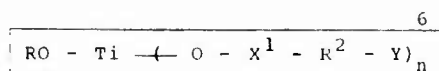
The acrylic functionality of TTAC-39S allows for the room temperature bonding of aluminum to aluminum. This is illustrated in Figure 31. Table 11 lists some titanate adhesion promoter suggestions.

Figure 31



Table 11

Adhesion Promotor Suggestions		
Substrate #1	Substrate #2	Suggested
<i>Polymer to Polymer</i>		
PVC	PVC	TSN2C-37S, TTN-22
EPR, EPDM (Sulfur Cure)	Nylon (6 & 66)	TSN2C-37S
EPR, EPDM (Sulfur Cure)	Polyester	TSN2C-37S
EPR, EPDM (Peroxide Cure)	Polyester	TTM-33S, TTAC-39S
SBR	Nylon, Polyester	TSN2C-37S
SBR, NR (Sulfur Cure)	EPDM	TSN2C-37S
Flouro Silicone	Silicone	TSM2-7, TSA2-11
<i>Polymer to Metal</i>		
PVC	Alum., Steel	TB2NS-26S, TSN2C-37S
Nylon	Alum., Steel	TTOP-12, TSN2C-37S
Polyester	Alum., Steel	TSN2C-37S, TTOP-12, TTAC-39S, TTM-33S
Polyethylene, PP	Alum., Steel	KEN-REACT TTS, TTOP-41
SBR	Alum., Steel	TB2NS-26S, TTP-34 & Hexa
Urethane	Alum.	TTAC-39S
Silicone	Steel	TTAC-39S, TTM-33S
Epoxy	Steel	TN2PI-42, KR-43
Hypalon	Copper	TB2NS-26S, TTOP-12, TTOP-38
<i>Metal to Metal</i>		
Nitrile	Copper	TB2NS-26S
Alum.	Alum., Steel	TTAC-39S
Steel	Steel	TTAC-39S, TTM-33S
<i>Composite to Metal</i>		
Concrete	Steel	TGM2-112, TTOP-38



#### Function 6 - Tri-Functionality

The tri-functionality or presence of three pendant organic groups has the following advantages:

- All functionality can be controlled to first, second or third degree levels. A control which is not possible with trialkoxy, monofunctional coupling agents which is typical of silanes.
- The probability of transesterification and thermoset cross-link via unsaturation, addition, or substitution mechanism is amplified.
- The probability of chain entanglement is enhanced due to a stearic molecular tri-anchor effect.
- As many as six phosphorous groups per mole of titanate can be placed monomolecularly at the inorganic interface to enhance flame retardant performance.
- Allows for the monomolecular deposition of a large amount of hydro carbon per mole of titanate. Surface energy is drastically modified resulting in dramatic viscosity reduction.
- High flaspoint titanates can be provided in the liquid state without the use of solvents. TSM2-7 is a liquid in the neat state with a flash point of 265°F. TTM-33 is a solid in the neat state. The addition of a non-flammable solvent creates TTM-33S with a flash point of 145°F which is in the same range as Vinyl Silane A-172.
- Hydrolytic Stability is greatly improved. Tri-Functional Titanates can be stored in standard containers without detriment to performance properties. Shelf life is excellent.

#### Trifunctionality and Inorganic Surface Energy Modification

The trifunctionality of the titanates allows even relatively short chains such as acrylates and methacrylates to reduce viscosity significantly since their total backbone carbon content is multiplied by a factor of 3. This is illustrated in Table 12 which compares a variety of monoalkoxy titanates as compared to a control and some representative silanes.

Table 12

#### VISCOSITY EFFECT OF VARIOUS TITANATE COUPLING AGENTS ON 0.5% TREATED CaCO<sub>3</sub>

TEST FORMULATION: CaCO<sub>3</sub> - 50.00 pts  
Mineral Oil - 50.00 pts  
Coupling Agent - 0.25 pts

CODE NAME	VISCOSITY, cps
Control	34,700
A-172 Silane	16,000
A-189 Silane	13,500
TTS	320
TTA-2	240
TSM2-7	230
TTBS-9	420
TSA2-11	310
TTOP-12	860
TB2NS-26	370
TB2NS-26S	280
TTM-33S	260
TSN2C-37S	330
TTOPP-38	180
TTAC-39S	410
TTOP-41	160

#### A Comparison of Titanates and Silanes

Table 13 compares the titanates and silanes using the features of the six functions as a basis.

Table 13

## THE TITANATE - SILANE DIFFERENCE

SYMBOL	ITEM	TITANATES R-O-Ti ( O-X'-R'-Y) <sub>n</sub>	SILANES (R-O) <sub>3</sub> -Si-R'-Y
R-O	Alkoxy Groups	one	three
	Alkoxy Chelate Capacity	yes	unstable
	In-situ Alcohol By-product		
	Elimination - if desired	yes	no
	Monomolecular Formation	yes	no
	Energy to Hydrolyze	low	moderate to high
	React with CaCO <sub>3</sub>	yes	limited
	Excessive Amounts Hurt Properties	frequently	occasionally
{	Transesterification -		
	X-link Polyester	yes	none
	X-link without Unsaturation	yes	no
X'	Binder Group Function	yes	none
	High Thermal Stability - if desired	yes	no
	Sulfonyl - Thixotrope	yes	no
	Phosphato - Flame Retardancy	yes	no
	Phosphito - Antioxidant	yes	no
R'	Length of R' Groups	long to short	short
	Viscosity Reduction	extreme	none to moderate
	Thermoplastic Impact Improvement	Superior - best known	none to moderate
	Flash Points	high to moderate	low
Y	Functional Groups	three	one
n	Tri-Functionality	yes	single
	Hydrolytic Stability	good to excellent	functionality good to poor
\$	Cost	\$2 to 5	\$2 to 5

#### SIX FACTORS FOR SUCCESSFUL APPLICATION OF MONOALKOXY TITANATE COUPLING AGENTS

A full treatment of the six factors has been published elsewhere.<sup>2</sup> However, some pertinent comments are made here concerning "Factor 4 - Coupling Mechanism" and "Factor 5 - Methods of Titanate Application".

##### Factor 4 - Coupling Mechanism

After selecting the proper titanate, simple guidelines are listed below to provide maximum coupling efficiency with the inorganic filler:

- Do not add surface active ingredients which will interfere or compete with the reaction of the titanate at the interface until coupling is achieved.
- Zinc oxide and stearic acid are surface active agents. Add them after the filler, polymer and plasticizer have been mixed together thoroughly.
- Most titanates transesterify and will react to different degrees with ester and polyester plasticizers. Therefore, add ester plasticizers after mixing has allowed coupling to occur. Petroleum derived plasticizers usually present no problem and can be used as a diluent to spread the small amount of titanate for better filler interaction and coupling.
- Titanates and Silanes can be used synergistically. However, they will compete for free protons at the filler interface. Cable compounds have been run with titanate treated clays and Vinyl Silane A-172 kickers with excellent results. However, treating Translink 37 or Burgess KE with TTAC-39S would be like putting on two pair of socks.

• Monoalkoxy titanates work best with dry and calcined inorganics.

• The presence of atmospheric moisture (0.1% to 2 or 3%) provides excellent reaction sites and is not detrimental.

• Bonded moisture such as Al<sub>2</sub>O<sub>3</sub>·3H<sub>2</sub>O provide excellent reaction sites.

• Free moisture (not bonded or atmospherically absorbed) presents problems for monoalkoxy mechanisms. For wet process fillers which are reasonably dry (i.e. water washed clays), pyrophosphato groups will insure monoalkoxy function success. For high surface area, wet fillers such as HiSil 233 - chelated alkoxy groups are preferred.

• Monoalkoxy titanates work best in organic systems.

• Chelated titanates (Ken-React 100 Series) work best in aqueous systems.

##### Factor 5 - Methods of Titanate Application

There are two methods of monoalkoxy titanate application:

In Situ - Added in the situation where all ingredients are brought together at time of mixing.

Pretreated - The inorganic and coupling agent are isolated and treated before coming in contact with the other ingredients at time of mixing. After pretreatment the decomposition point of the filler/titanate composite is raised to well over 800°F.

### In Situ Considerations and Advantages

- Economics - lowest raw material cost way to use titanates. Pretreatment equipment costs and processes are avoided.
- Flexibility- titanates and titanate levels can be altered as desired.
- Technique - certain polymer systems are straight forward and it is inherently difficult to make an error. In sensitive systems, consistent results will be obtained if applied according to good titanate coupling practice.
- Polymer - Sometimes best results are obtained by putting the titanate directly in the polymer.

### Pretreatment Considerations and Advantages

Pretreatment can be provided by the inorganic supplier or prepared in the laboratory.

#### Inorganic Supplier

- Economics - pretreatment equipment and processes are avoided.
- Technique - the filler and titanate are isolated to provide maximum coupling efficiency. Supplier is knowledgeable in coupling chemistry.
- Inorganic - treated inorganics "lock-in" that "factory fresh goodness". Atmospheric moisture attack is effectively blocked and the inorganic is made hydrophobic and organophilic. Inorganic properties are stabilized.

### Laboratory Preparation of Fillers

- Equipment - High shear mixers such as Henschel, Littleford or Waring Blender are excellent. Titanates react at room temperature so heat is not needed.
- Filler - Weigh out the desired amount to be treated.
- Titanate - Amount of titanate to be used is based on weight (or percentage) of filler - not the polymer. Optimum titanate loading to be applied to filler must be determined empirically for specific end-use. However, 0.1% to 3% of titanate on filler weight is the usual range evaluated. Three points (0.5%, 1% and

3%) will give a suitable performance curve for 2.0 to 3.0 gravity inorganics to determine optimum properties.

The titanate may be applied:

- neat directly to the dry filler in the fluidized state i.e. while the mixer is on.
- diluted in inert anhydrous (dry) plasticizer or alcohol (methanol, ethanol or isopropanol) and then added to dry filler. Do not add water to the titanates. This saves a water drying step and is not required nor recommended. This is contrary to silanes where a diluent containing a ratio of 10% water to 90% alcohol is recommended.
- coupled completely in alcohol solution and then dried. Solution coupling insures 100% molecular contact but is often impractical on a production basis. Furthermore, for most applications, simple dry blending is adequate and gives consistent reproducible results.

#### Treatment Procedure - Typical Waring Blender Operation

- Dump Filler into Blender
  - Turn Blender On
  - Feed titanate in uniformly over 30 second period
  - Post blend for 30 seconds to 1 minute
  - Filler is now pretreated
- Double time frames in production equipment to allow for geometric scale-up conditions as we do in our 3.5 and 11.5 cubic ft. Henschels and 26.1 cubic ft. Littleford high shear mixers. Ribbon Blenders require 10 to 20 times the mix cycle for equivalent results.

Note:

### APPLICATIONS DATA

The following applications data presented should not be construed as the best properties obtainable in any given polymer. The combination of specific end needs, various grades of a given type polymer, different types of fillers and combination of fillers represents a formidable applications testing undertaking for any one organization.

Some of the following data presented for a given polymer is reasonably extensive while other data is sparse. It is only intended to give you an indication of the potential of the monoalkoxy trifunctional titanate concept. Much work is yet to be done.

## A. Polypropylene

The effects of titanate coupling agents in filled polypropylene are dramatic. Table 14 lists the effects of TTS in calcium carbonate filled polypropylene. The impact strength of the 70% CaCO<sub>3</sub> - TTS system is 7.5 times stronger than virgin with melt flow similar to virgin. The 70% CaCO<sub>3</sub> system without TTS treatment had no flow.

Figure 32 shows injection mold plaques obtained from a run of 75% CaCO<sub>3</sub> filled polypropylene with and without TTS treatment. Although the photo may not show it entirely, the TTS plaque is smooth and glossy while the non-treated plaque is rough and could just be barely formed. When held to an intensive light, the untreated plaque was opaque while the TTS plaque was translucent.

Figure 32

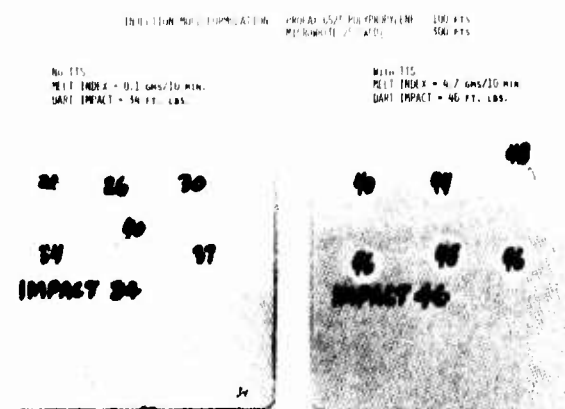


Table 14

EFFECT OF TTS ON FILLED POLYPROPYLENE

% CaCO <sub>3</sub>	% TTS(1)	Flexural Modulus	Drop weight Impact - Ft. lbs.	Mold Shrinkage (mils/in.)	Surface	Melt Flow (lb 230)
0	0	240,000	1.0	14-15	Good	5.00
70	0	550,000	1.5	10-11	Poor	0.00
70	0	530,000	1.8	10-13	Poor	0.07
70	3.0	380,000	7.5	11-12	Good	4.70

(1) % TTS based on weight of filler

## B. HDPE

Table 15 shows the effect of TTS on physical properties of mineral filled HDPE. Attempts above 30% filler without TTS were not tried since compounding becomes mechanically impractical at these levels.

Table 15 - Effect of TTS on Physical Properties of Mineral Filled HDPE

Formulation	Filler, %	TTS, % based on filler	Melt index, g./10 min.	Tensile strength, p.s.i.	Tensile modulus, ft.-lb./in. 10 <sup>3</sup> p.s.i.	Impact strength, ft.-lb./in. of notch
Control (HDPE only)	0	0	19.7	2,050	98.0	0.93
BaSO <sub>4</sub>	30	0	20.8	2,430	81.7	0.58
	30	3	22.0	2,460	49.0	0.60
	40	3	22.3	2,220	59.4	0.64
	50	3	22.3	2,060	63.3	0.76
	60	3	22.0	1,770	70.0	0.91
ASP-100 clay (aluminum silicate)	30	0	14.0	2,510	99.8	0.40
	30	3	12.9	3,020	133.2	0.60
	40	3	8.4	2,790	140.1	0.53
	50	3	1.5	2,490	145.3	0.45
	60	3	0	2,350	150.9	0.37
P-1 wollastonite (calcium metasilicate, CaSiO <sub>3</sub> )	30	0	16.5	2,330	72.2	0.56
	30	3	16.5	2,230	87.2	0.77
	40	3	16.5	2,020	106.0	0.81
	50	3	14.9	1,800	121.3	0.88
	60	3	12.0	1,610	130.8	0.93
CaCO <sub>3</sub> (Camel Tex)	30	0	16.3	1,960	217.9	0.53
	30	3	18.8	2,330	180.6	0.57
	40	3	18.4	1,730	163.4	0.78
	50	3	17.7	1,770	150.9	0.97
	60	3	17.8	1,800	130.8	1.01

## C. LDPE

Table 16 shows the superior wetting characteristics of the R<sup>2</sup> (Function 4) function of TTS as compared to conventional wetting agents.

Table 16 - CaCO<sub>3</sub> Dispersibility In LDPE

Additive	Torque, g./sq. m.						Melt index, g./10 min.	Particles per 144 sq. in.
	30 sec.	60 sec.	90 sec.	120 sec.	150 sec.	180 sec.		
None	2,000	2,000	1,900	1,750	1,750	1,750	0.27	312
Emcol H31-A <sup>a</sup>	2,150	1,400	1,150	1,000	1,000	1,000	2.30	6
Emcol 117 <sup>c</sup>	1,900	1,400	1,300	1,250	1,100	1,000	1.90	16
Glycerol monostearate	2,150	1,400	1,300	1,250	1,250	1,150	3.87	8
Emcol 116 <sup>c</sup>	1,900	1,400	1,300	1,150	1,150	1,100	1.69	20
Aluminum oleate	1,650	1,600	1,400	1,300	1,250	1,250	1.80	44
Aluminum stearate	1,900	1,400	1,300	1,250	1,250	1,250	1.60	32
Tween G5 <sup>d</sup>	2,500	1,500	1,250	1,000	900	900	1.25	7
Zinc stearate	1,900	1,650	1,400	1,150	1,150	1,050	2.30	44
Paricel 220 <sup>e</sup>	1,900	1,400	1,250	1,150	1,100	1,100	0.95	16
Ken-React TTS	1,250	900	900	900	750	750	4.17	16

a—Formulation: 9 parts of LDPE and 1 part of dry blend consisting of CaCO<sub>3</sub> (Camel-Tex) 70%, LD-501 28% and additive 2%.

b—LDPE 501, Exxon Chemical Co.

c—Witco Chemical Co.

d—Imperial Chemical Industries Ltd. (ICI).

e—Baker Castor Oil Co.



#### D. Rigid PVC

Table 17 demonstrates the efficacy of TTOP-12 and TTOPP-38 as impact modifiers in Rigid PVC. TTOPP-38 when used in conjunction with a fine  $\text{CaCO}_3$  (1-2 u) demonstrates a ninefold improvement in impact over untreated  $\text{CaCO}_3$  at the 40% filler level. It even surpasses virgin. TTOPP-38 is recommended for your further investigation for Rigid PVC.

Table 17

PVC	DS207	$\text{CaCO}_3$	TTOP-12	TTOPP-38	RELATIVE GARDNER IMPACT
100	1	—	—	—	100
60	1	40	—	—	12
60	1	40	0.4	—	51
60	1	40	1.2	—	79
60	1	40	—	0.4	108
60	1	40	—	1.2	13

#### E. Flexible PVC

Table 18 shows the super-plasticizer effect of TTOP-12 in calcium carbonate filled flexible PVC. It surpasses Omyalite 90T (a treated  $\text{CaCO}_3$ ) in performance and presents the possibility of either reducing ester plasticizer loadings or increasing filler loadings with no sacrifice in properties or processability.

Table 18

	1	2	3	4
PVC	100	100	100	100
DS 207	2	2	2	2
DOP	40	40	40	40
OMYALITE 90T - $\text{CaCO}_3$	60	—	—	—
OMYALITE 90 - $\text{CaCO}_3$	—	60	60	60
TTOP-12	—	—	0.6	1.8
MODULUS - 100%, psi	1665	1956	1720	1485
TENSILE STRENGTH, psi	2345	2365	2305	2120
ELONGATION, %	290	270	300	310
HARDNESS, SHORE A	94	94	94	92-93

#### F. Epoxy

Figure 33 demonstrates how TTOP-12 can prevent settling in granite filled epoxy. Table 19 shows that in addition to the prevention of settling this titanate reduced viscosity by 40%.

Figure 33



Table 19

	1	2
EPON 828	100	100
GRANITE FILLER	200	200
TTOP-12	—	2
BROOKFIELD VISCOSITY, cps @ 25°F	154,000	94,000

Shown below is the Base A portion of a proprietary polyamide cured epoxy room temperature cured epoxy paint system.

Base A	Non-Titanate	Titanate
Resypox 1628	607	607
TTOP-41	—	18
Solvent	285	285
Lecithin	8	8
Pine Oil	8	8
Flow Control Agent	4	4
$\text{TiO}_2$	300	300
Mg Silicate	170	670
Clay	150	650
$\text{BaSO}_4$	150	150
Cab-O-Sil	20	20
	1702 lbs.	2720 lbs.

TTOP-41 allowed double the total filler loading as compared to the prior art. In doubling the total solids loadings, the  $\text{TiO}_2$  content was held at the prior art level with beneficial effects of no increase in viscosity. These observations were drawn from the above work:

- Increased hiding and whitening power.
- Increased flexibility.
- Minimized chalking.
- Increased chemical resistance.
  - Concentrated HCL, nitric and phosphoric acids were applied to the drawdowns. The titanate treated film resisted attack while the untreated film deteriorated and dissolved.
- Increased thermal stability.
  - A three mil wet drawdown of the untreated and titanate treated paints were subjected to 250°F heat for 8 hours. The non-treated film thermally degraded while the titanate treated film was left unchanged.

In aromatic amide cured epoxy coatings (Bake System) the titanates allow the coatings formulator to pass current government regulations relative to low solvent levels. For example, prior art required the addition of a minimum of 40% solvent in order to incorporate one part of  $\text{TiO}_2$  to one part of unmodified liquid epoxy resin such as Resypox 1628 (Resin Corporation of America). Now with titanates such as TTOP-41, one part of  $\text{TiO}_2$  can be added to one part of unmodified liquid epoxy without any solvent.

In the prior art, grinding was required in order to disperse the  $\text{TiO}_2$  into the solvent and liquid epoxy resin. Now grinding is no longer necessary.

The above statements were made on the basis of user evaluations.

#### G. Polyester - Alkyd

Table 20 illustrates how TTOP-12 can reduce solvent levels, improve hardness, lower the bake temperature, and increase chemical resistance and provide other improvements in alkyds.

Table 20

**EFFECT OF KEN-REACT TTOP-12 ON AN ALKYD COATING****PIGMENT TO BINDER — 1:1 By Weight****FORMULATION:**

NV Weight	60%	
Vehicle	85%	Short Tail Oil Alkyd
	15%	Melamine
Pigment	95%+	TiO <sub>2</sub> (Non-Chalking, Rutile)
Catalyst		Toluene Sulfonic Acid
Titanate	1/2%	KEN-REACT TTOP-12 used on total paint

BAKE: 15 Minutes @ 275°F (100°F below normal practice)

SUBSTRATE: 17 Bonderite 1000

**TITANATE ADVANTAGES**

- reduced the vehicle in grind by 50%.
- increased the hardness from B to H at 1 mil dry film thickness.
- increased paint film resistance to pass 100 hours of 5% salt spray exposure. The film without KEN-REACT TTOP-12 had a 1/4 inch creepage at the scribe. With titanate the creepage was less than 1/8 inch which meets the product specifications.

**H. Thermoplastic Elastomers (TPE)**

Table 21 shows how TTS allows 50 ph. calcium carbonate addition to a TPE polymer system while increasing tensile strength by one-third and not affecting modulus, elongation or set at break. This shows that the titanate coupling agents do allow for high filler loadings in thermoplastic elastomers.

Table 21

**EFFECT OF TTS ON THERMOPLASTIC ELASTOMER**

	1	2	3
TPE Polymer System 69A	100	100	100
KEN-REACT TTS	—	1.5	—
CaCO <sub>3</sub> <sup>1</sup>	—	50	50
Hardness	61	68	72
100% Modulus	410	475	770
300% Modulus	580	660	1160
Tensile	1645	2170	2115
Elongation—Ultimate, %	780	755	660
Elongation—Set at Break, %	260	275	185

**I. CPE**

Water washed clays such as Catalpo Clay are widely used in CPE. Chlorowax 40 is a typical chlorinated plasticizer used in conjunction with CPE.

Table 22 illustrates the fivefold viscosity reduction obtained with the use of TTOPP-38 in the system. Work is continuing in this area.

Table 22

	1	2
Catalpo Clay	30	30
Chlorowax 40	70	70
KEN-REACT TTOPP-38	—	0.3
Brookfield Viscosity, CPS @ 25°C	90,000	18,000

NOTE: Chlorowax 40 (m.w. ca. 580) and CPE (m.w. ca. 30,000) both have 40% chlorine content and similar chemical structure.

**J. EPR**

Table 23 represents a comparison of vinyl silane with methacrylic and acrylic trifunctional titanates in a system containing both water washed clay and HiSil 233. The data clearly shows that the titanate coupling agents compete favorably on a head-on basis with the silanes. This work was done with available monoalkoxy titanates. Future chelated and pyrophosphato titanates with thermoset Y functionality pose tantalizing possibilities.

Table 23

**EPR CABLE JACKET—METHACRYLIC & ACRYLIC TITANATE VS VINYL SILANE**

Vistalon 40, Mistran Vapor—70; SP-33 Clay—70; HiSil 233 35; ZnO—5; Di-Cup R—2.5; Sulfur—0.3

# CARBONS	COUPLING AGENTS	1	2	3	4
0	Control—No Coagent	—	—	—	—
4x3	Methacrylic Titanate <sup>1</sup>	—	1.5	—	—
3x3	Acrylic Titanate <sup>2</sup>	—	—	1.5	—
2x1	Vinyl Silane <sup>3</sup>	—	—	—	1.5

Original Properties @ 70°F

20' Cure at 340°F

200% Modulus, PSI	240	325	445	405
300% Modulus, PSI	285	385	515	470
Tensile Strength, PSI	715	1020	1200	1075
Ult. Elongation, %	950	980	875	920
Shore A Hardness	70	74	77	75

1—Isopropyl trimethacryl titanate—100% solids—2.0 phr TTM-33S Usec.

2—Isopropyl triacryl titanate—100% solids—2.0 phr TTAC-39S Usec.

3—Vinyl-tris (2-methoxyethoxy) silane—100% A-172—Union Carbide Corp.

**K. EPDM**

The data in Table 24 and their bar graph plot in Figure 34 represent a comparative evaluation of Vinyl Silane A-172 versus TTM-33S and TTAC-39S in a calcined clay filled peroxide cured EPDM cable compound.

It appears that the original properties of the titanates could be improved by increasing the cure time. The titanates age very well as compared to vinyl silanes - in fact seem to indicate an edge in this respect. This is shown graphically in Figure 35.

Also, if one adjusts the plasticizer level, it appears that the monoalkoxy titanate could offer a wider range of tensile and modulus properties with significantly different elongations.

Mooney Scorch values show TTM-33S to be very scorchy; TTAC-39S to be processable. Further studies in this area are warranted.

Figures 36 and 37 are rheometer curves run at the 20 part and 10 part plasticizer levels. These show a higher cure rate for the titanate TTAC-39S; confirm the somewhat scorchy nature of TTAC-39S and suggest low compression set characteristics.

Table 24

EVALUATION OF KEN-REACT COUPLING AGENTS (TTM-33S and TTAC-39S) vs. A-172 VINYL SILANE IN EPDM																				
Vistalon 2504	100	100	100	100	100	100	100	100	100	100	100	100	100	100	100	100	100	100	100	100
AgeRite Resin D	1.5	1.5	1.5	1.5	1.5	1.5	1.5	1.5	1.5	1.5	1.5	1.5	1.5	1.5	1.5	1.5	1.5	1.5	1.5	1.5
Zinc Oxide 42-21	5	5	5	5	5	5	5	5	5	5	5	5	5	5	5	5	5	5	5	5
Sunpar 2280	20	15	10	5	—	20	15	10	5	—	20	15	10	5	—	20	15	10	5	—
Kenmix Red Lead/P 5/1	5	5	5	5	5	5	5	5	5	5	5	5	5	5	5	5	5	5	5	5
DiCup 40C	6	6	6	6	6	6	6	6	6	6	6	6	6	6	6	6	6	6	6	6
Whitex (1% A-172)	—	—	—	—	—	90	90	90	90	90	—	—	—	—	—	—	—	—	—	—
A-172	—	—	—	—	—	2	2	2	2	2	—	—	—	—	—	—	—	—	—	—
Whitex (1% KR-39S)	—	—	—	—	—	—	—	—	—	—	90	90	90	90	90	—	—	—	—	—
KR-39S	—	—	—	—	—	—	—	—	—	—	2	2	2	2	2	—	—	—	—	—
Whitex (1% KR-33S)	—	—	—	—	—	—	—	—	—	—	—	—	—	—	—	90	90	90	90	90
KR-33S	—	—	—	—	—	—	—	—	—	—	—	—	—	—	—	2	2	2	2	2
Whitex Clay	90	90	90	90	90	—	—	—	—	—	—	—	—	—	—	—	—	—	—	—
Original Properties	NO COUPLING AGENT					A-172					39S					33S				
20 min. cure @ 340°F	165	210	245	305	360	415	535	730	1130	1495	425	495	650	925	1165	360	405	505	565	830
200% Modulus, psi	200	235	270	355	385	710	875	—	—	—	605	705	855	1090	—	480	530	655	705	990
300% Modulus, psi	765	680	645	630	535	975	965	1075	1625	1690	870	855	960	1165	1285	840	840	960	1060	1070
Tensile Strength, psi	760	685	620	590	480	460	355	295	275	220	590	485	425	390	285	710	655	615	625	405
Ult. Elong. %	61	63	65	67	69	62	64	66	72	74	63	65	68	74	77	62	64	67	70	74
Shore A Hardness																				
Aged Properties 7 days @ 150°C																				
200% Mod. psi	385	555	560	590	650	530	640	820	1095	—	670	820	950	1170	1410	560	670	760	820	1340
300% Mod. psi	485	540	660	665	705	815	920	—	—	—	925	—	—	—	—	780	880	—	—	—
Tensile Strength psi	750	670	710	705	765	870	970	1090	1145	1340	980	1100	1135	1305	1485	860	980	938	940	1440
Ult. Elong. %	640	530	480	390	390	350	340	295	220	190	360	320	270	260	240	425	420	300	260	235
MOONEY Scorch @ 250°F	—	—	—	—	—	24	—	26	—	—	12	—	13	—	—	4	—	7	—	—
5 Pt. Rise, Min.	—	—	—	—	—	40.5	—	31	—	—	41	—	33	—	3	39	—	31	—	—
Mooney Plasticity @ 250°F																				
ML4-lb.-in.																				
Compression Set	70 hrs. @ 212°F					Cured 10 min. @ 340°F														
						32.4 - 34.8 - -					34.2 - 26.9 - -					- - - - -				

Figure 34

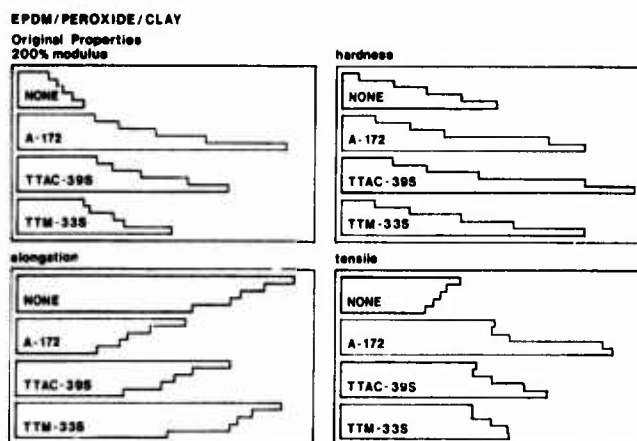


Figure 35

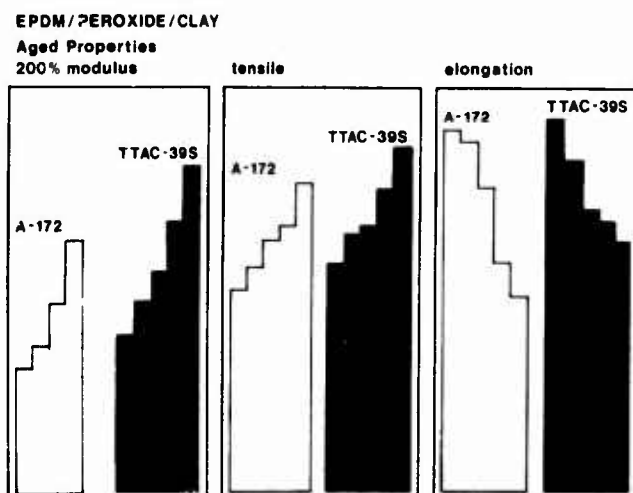


Figure 36

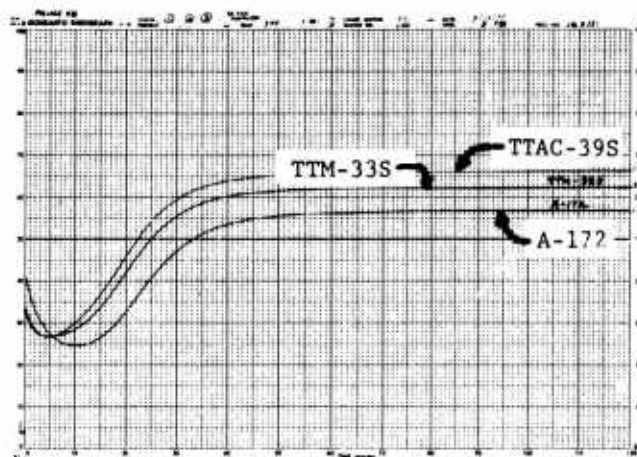
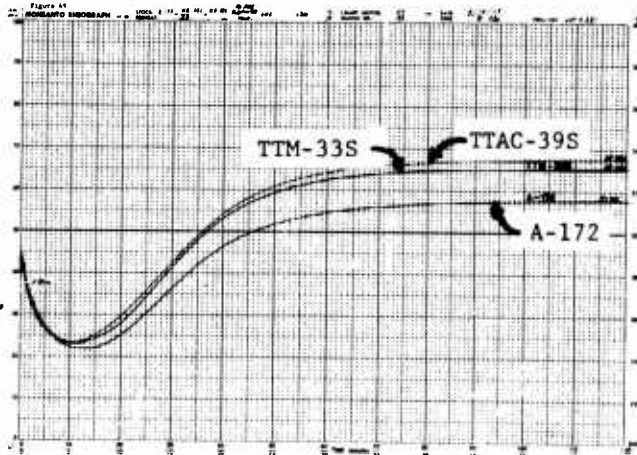


Figure 37



## L. Hypalon

Figure 38 illustrates the before and after effects of a soft clay filled Hypalon injection molded compound containing TB2NS-26. Prior to titanate treatment, the compound was running at a high rejection level. After the inclusion of TB2NS-26 into the compound, it eliminated rejects entirely.

Figure 38

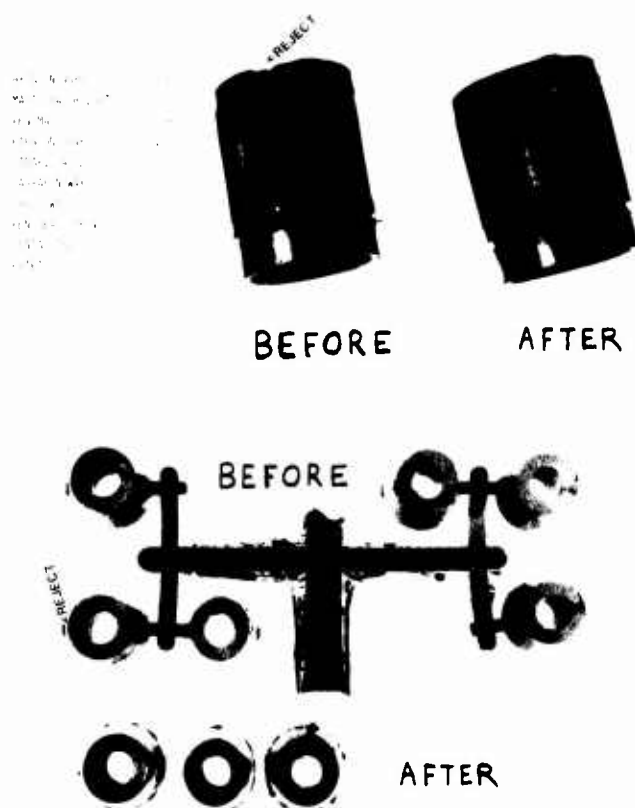


Table 25 shows the 40% reduction in Mooney viscosity one can obtain with the use of TTS. In addition, you will note the high elongations obtained with TTBS-9.

Table 25

EFFECT OF KEN-REACT TTS AND TTBS-9 ON SILICA FILLED HYPALON PROPRIETARY PRODUCTION RUN

	1	2	3
Hypalon 40	100	100	100
Silene D	80	80	80
DOP	40	40	40
Sulfur Cure System	Undisclosed		
KEN-REACT TTS	—	0.8	—
KEN-REACT TTBS-9	—	—	0.8
Cure: 30 min. @ 55 psi steam			
Mooney Viscosity	56	36	48
Scorch Time, min.	16	23	16.5
Tensile, psi	1415	1340	1230
Elongation, %	340	410	550
Hardness	82	80	78

Amino titanates would be expected to give similar rheology with higher physicals. The effect of Amino titanates on electrical properties has not been established. Caution should be exercised until they are.

## M. SBR

In Table 26 we show the very strong modulus response the titanates have on an oxidized Regal 300 carbon black. Work with untreated, standard grade blacks is in progress. This suggests more work in the treatment of oxidized blacks with titanates.

Table 26

SBR—CARBON BLACK SURFACE OXIDIZED WITH Ca(O Cl)<sub>2</sub>

SBR	100	100	100	100
Regal 300—1% Ca(O Cl) <sub>2</sub>	50	50	50	50
Zinc Oxide	4	4	4	4
Sulfur	2	2	2	2
Santocure NS	1	1	1	1
Stearic Acid	1	1	1	1
Kenplast RD	10	10	10	10
Neozone A	2	2	2	2
KEN-REACT TTNC-17	—	2	—	—
KEN-REACT TTNS-19	—	—	2	—
KEN-REACT TTP-34	—	—	—	2
Original Properties				
Cure 30 Min. @ 330°F				
300% Modulus, psi	740	1200	950	1660
400% Modulus, psi	1260	1930	1420	2540
Tensile, psi	2290	3145	2920	2680
Elongation, %	560	560	620	420
% Set at Break	12	13	12	3

## N. Silicone Rubber

Monoalkoxy titanate treatment of fillers facilitates the incorporation of high filler loadings, even in low shear polymers such as Silicone. The incorporation of high filler loadings without an increase in hardness has many subtle advantages. Reviewing physical properties alone without regard to the end application of the polymer compound may result in the investigator passing up some amazing benefits to be derived using titanates.

Table 27

NOVAKUP FILLED HTV SILICONE RUBBER MOLD COMPOUND

COMPOUND	1	2	3	4
Stauffer SWS-729	100	100	100	100
Novacite—No KEN-REACT	100	—	—	—
Novakup L-237—TTS—0.5	—	100	—	—
Novacite—TTOP-12—0.5	—	—	100	—
Novacite—TTM-33S—0.5	—	—	—	100
Varox	0.8	0.8	0.8	0.8
10 Minute Cure @ 300° F				
Tensile	—	460	500	410
Elongation	—	380	200	250
Tear, Die B	—	41	42	50
Hardness	—	60	65	55
15 Minute Cure @ 300° F				
Tensile	718	500	530	460
Elongation	178	350	210	280
Tear, Die B	65	40	38	37
Hardness	73	65	65	65
Number of Parts Produced By Mold Before Failure				
1/4" Section—Closed Duty System @ 850° F to 900° F	11	220	180	95

Table 27 shows a 100 phr filled Novacite (or Min-U-Sil) methyl vinyl siloxane polymer system which is used as a mold for making parts in a closed duty system at 850°F to 900°F. The use of monoalkoxy titanate on the Novacite to make Novakup type fillers had the following advantages:

1. Lowered compound cost
2. Made mixing easier
3. Increased Thermal Conductivity
4. Increased Mold life 2000%
5. 1/2% of TTS, TTOP-12 and TTM-33C made the stiff and boardy Silicone rubber stock soft and flexible. The compounder noted that he could have easily upped the physicals by adding another 50 phr filler.

### TABLE LIST

1. Monoalkoxy Titanate Letter Code
2. Titanate Function Selection For Filler/Inorganic Coupling
3. Suggested Titanate Selection Based on Four of Six Titanate Molecule Functions
4. Monoalkoxy Chemical Structure Gives Best Wetting and Stability
5. Advantage of Chelate Effect on Misch 233
6. Polyester Viscosity Reduction with TTOP-41
7. Binding Group ( $X^1$ ) Performance Effects
8. Effect of Various Titanates on Non-Calced Clay Viscosity
9. Organic Backbone Performance Effects
10. Effect of TTS on  $CaCO_3$  Filled HDPE
11. Titanate Adhesion Promotor Suggestions
12. Viscosity Effect of Various Titanate Coupling Agents on 0.5% Treated  $CaCO_3$
13. The Titanate - Silane Difference
14. Effect of TTS on  $CaCO_3$  Filled Polypropylene
15. Effect of TTS on Physical Properties of Mineral Filled HDPE
16.  $CaCO_3$  Dispersibility in LDPE
17. Effect of TTOP-12 and TTOP-38 on Impact Strength of  $CaCO_3$  Filled Rigid PVC - Relative Values for Screening Purposes Only
18. Effect of TTOP-12 on 2 Micron  $CaCO_3$  Filled PVC
19. Effect of TTOP-12 on Granite Filled Epoxy
20. Effect of TTOP-12 on an Alkyd Coating
21. Effect of TTS on  $CaCO_3$  Filled Thermoplastic Elastomer
22. Effect of TTOP-38 on Non-Calced Clay in Chlorinated Hydrocarbon
23. EPR Cable Jacket - Methacrylic & Acrylic Titanate vs Vinyl Silane
24. Evaluation of Titanate Coupling Agents (TTM-33S and TTAC-39S) vs A-172 Vinyl Silane in EPDM
25. Effect of TTS and TTBS-9 on Silica Filled Hypalon
26. SBR - Carbon Black Surface Oxidized With  $Ca(OH)_2$  - Titanate Treated
27. Novakup Filled HTV Silicone Rubber Mold Compound
14. Effect of 0.5% TTS Coagent Treatment on 70% Calcium Carbonate Filled Mineral Oil
15. Effect of 3% TTS on Whitex Clay (Calced) Dispersed in Mineral Oil
16. Effect of 3% TTS Coagent on 30% Calced Clay Filled Mineral Oil
17. Effect of 3% TTS on Mogul L Black Dispersed in Mineral Oil
18. Effect of 3% TTS Coagent on 20% Mogul L Black Filled Mineral Oil
19. Effect of 0.5% TTS on Alumina Trihydrate Dispersed in Mineral Oil
20. Effect of 70% Solids Alumina Trihydrate Dispersed in Mineral Oil
21. Effect of 0.5% TTS on Wollastonite P-1 Dispersed in Mineral Oil
22. Coupled Fillers Are Common To Both Systems
23. Coupling in Thermoplastic Systems with Monoalkoxy Coupling Agents - Titanates
24. The Internal Lubricant Effect of TTS Coagent on Black Filled Nitrile Rubber
25. Tear and Elongation Effects of TTS in 40%  $CaCO_3$  Filled LDPE
26. Coupling in Thermoset Systems with Trialkoxy Coupling Coagents - Silanes
27. Coupling in Thermoset Systems with Monoalkoxy Coupling Agents - Titanates
28. Unsaturate Chain Length Effect on Elongation - Silane and Titanate
29. TN2PI-42
30. TN2PI-42 Cure of Filled Epoxy
31. TTAC-39 Bonding of Aluminum to Aluminum
32. 75%  $CaCO_3$  Filled Polypropylene Injection Mold Plaques
33. Prevention of Phase Separation Using TTOP-12 in 67% Granite Filled Epoxy
34. EPDM/Peroxide/Clay Compound Properties with No Coupling Agent, A-172, TTAC-39S and TTM-33S - Original Properties
35. EPDM/Peroxide/Clay - Aged Properties
36. Monsanto Rheograph - 20 phr Plasticizer Level
37. Monsanto Rheograph - 10 phr Plasticizer Level
38. Effect of TB2NS-26 on Mold Flow of Clay Filled Hypalon

### FIGURE LIST

1. Titanate Filler Coupling Mechanism
2. Silane Filler Coupling Mechanism
3. Monoalkoxy Titanates - Monomolecular Layer Formation on Filler
4. Chelated Monoalkoxy Titanate Coupling Mechanism
5. Hydrolytic Stability
6. Titanate Transesterification Polyester Viscosity Options
7. Monoalkoxy Titanate/Filler Polyester Transesterification - Before Mixing
8. Monoalkoxy Titanate/Filler Polyester Transesterification - Mixing
9. Monoalkoxy Titanate/Filler Polyester Transesterification - After Mixing - Unit Filler Effect
10. Monoalkoxy Titanate/Filler Polyester Transesterification - Composite Effect
11. Pyrophosphate Moisture Absorption Mechanism in Hydrated (Wet) Mineral Filler
12. Phosphato Binding Group Contribution To Flame Retardancy
13. Effect of 0.5% TTS on Atomite ( $CaCO_3$ ) Dispersed in Mineral Oil

### REFERENCES

1. Dannenburg, Rubber Chemistry and Technology, Volume No. 48; Page 436.
2. TTS Bulletin KR-0975-2.  
  
"New Coupling Agent For Filled Polyethylene", Technical Feature, Modern Plastics, December, 1974, Sal J. Monte and Paul F. Bruins.  
  
"Coagent Improves Mixing, Boosts Physicals", Rubber World, January, 1975.

### CREDITS

Aluminum Company of America  
Alumina Trihydrate  
Burgess Pigment Co.  
Burgess KE  
Cabot Corporation  
Cab-O-Sil  
Mogul L Black  
Regal 300  
Celanese Chemical Corporation  
Celanese 825 Hardner



Cosden Oil & Chemical Co.  
Polystyrene  
Diamond Shamrock Chemical Company  
Chlorowax 40  
Chlorowax LV  
E. I. DuPont de Nemours & Company, Incorporated  
Hypalon  
Neozone A  
Engelhard Minerals & Chemicals  
ASP-100 Clay  
Exxon Chemical Company of U.S.A.  
Vistalon  
Freeport Kaolin Company  
Catalpo Clay  
Translink 37  
Hercules, Inc.  
DiCup R  
DiCup 40C  
Profax 6523  
J. M. Huber Corp.  
Paragon Clay  
Hughson Chemicals, Division of Lord Corp.  
Bonderite 1000  
Interpace  
Wollastonite  
Kenrich Petrochemicals, Inc.  
Ken-Mag  
Kenplast ES-2  
Kenplast RD  
Kenmix Red Lead/P - 5-1  
Littleford-Lodige  
Littleford Mixer  
Malvern Minerals Company  
Novacite  
Novakup  
3M Company  
3M Colorquartz #28  
Monsanto Company  
Santocure NS  
C. K. Mullins  
SP-33 Clay  
National Industries  
DS-207  
Pleuss Stauffer (North America), Inc.  
Omyalite 90  
Omyalite 90T  
PPG Industries, Inc.  
HiSil 233  
Prodex Henschel  
Henschel Mixer  
Resin Corp. of America  
Resypox 1628  
Rohm and Haas Company  
Paraplex G-33  
H. M. Royal  
Camel Tex  
St. Joe Minerals Corp.  
Zinc Oxide 42-21  
Shell Chemical Company  
Epon 828  
Stauffer Chemical Company  
Stauffer SWS-729  
Sun Oil Company  
Sunpar 2280  
Sylacauga Calcium Products  
Micro White 25  
Solem Industries, Inc.  
Hydrated Alumina  
Thompson Weinman & Company  
Atomite  
Whittaker, Clark & Daniels, Inc.  
Min-U-Sil  
Wyrough & Loser, Inc.  
E-TET-D 70  
Jesse S. Young Co.  
Whitex Clay

Union Carbide Corporation  
Vinyl Silane A-172  
A-189 Silane  
United Sierra Division, Cypress Mines Corp.  
Mistron Vapor  
R. T. Vanderbilt Company, Inc.  
AgeRite Resin D  
Varox



Sal J. Monte

B.C.E. - Manhattan College,  
1961  
M.S. in Polymeric Materials,  
Polytechnic Institute of  
New York, 1969

Executive Vice President, Kenrich Petrochemicals,  
Inc.  
Licensed Professional Engineer  
Chairman - Elect, New York Rubber Group



Gerald Sugerman

Ph.D. in Org.Chem., Fordham  
University, 1961  
M.S. in Anal.Chem., Fordham  
University, 1959  
B.S./BChE, CCNY, 1957

1974-Present Mgr. New Products Div., Kenrich  
Petrochemicals, Inc.  
1970-1974 Mgr. Research, Hexagon Labs Inc.  
1967-1970 Dir. Research, Chem. Systems Inc.  
1965-1967 Group Leader, Princeton Chem.  
Rsch.  
1960-1965 Rsch. Associate, Halcon Int'l.  
1957-1959 Rsch. Associate, N.Y. Downstate  
Med. Center



Paul D. Sharpe

B.A. in Chemistry,  
University of Alabama  
M.A. in Chemistry,  
University of Indiana  
Post Graduate Courses:  
John Hopkins  
Brooklyn Polytechnic  
Institute

Chemist, Quality Rubber Company, 1931-1934  
Chief Chemist, Acme-Hamilton Rubber Company,  
1934-1942  
Supervisor, Synthetic Rubber Polymer Plant  
(for Government), 1942-1945  
Senior and Staff Chemist, Mobil Oil Corp.  
1945-1971  
Technical Director, Kenrich Petrochemicals,  
Inc., 1971 - Present



## NYLON 66 FOR WIRE AND CABLE APPLICATIONS

Augustin Chen  
Celanese Plastics Company  
Summit, New Jersey

### Summary

This paper is to acquaint the wire and cable industry with Nylon 66 for wire and cable coating applications and to compare the property and processing characteristics of Nylon 66 with Nylon 6.

Based on the comparative properties and processing characteristics of Nylon 66 and Nylon 6, and after reviewing the results of evaluations at various wire manufacturers, it is believed that Nylon 66 is an excellent material candidate for wire and cable coating applications.

### INTRODUCTION

In view of the increasing interest in Nylon 66 for wire coating UL approved applications, this paper is intended to summarize the basic properties and processing conditions of heat stabilized Nylon 66 vs. heat stabilized Nylon 6.

In addition, important wire coating process parameters will be reviewed in its relationship to heat stabilized Nylon 66\*.

### UL WIRE DESIGNATIONS

The following are the definitions for UL wire designations:

Class T thermoplastic is acceptable for use up to 60°C (140°F).

Class TW thermoplastic is moisture resistant and acceptable for use up to 60°C (140°F).

Class THW is heat and moisture resistant and acceptable for use up to 75°C (167°F).

Class THH is highly heat resistant and acceptable for use up to 90°C (194°F).

Class TF is flexible, highly heat resistant and acceptable for use up to 90°C (194°F).

Class TFF is more flexible (compared to class TF), highly heat resistant and acceptable for use up to 90°C (194°F).

N is the designation meaning that the above wire types are nylon jacketed.

MTW means machine tool wire with THHN, THWN rating plus additional hot oil-resistance rating of 90°C.

\*Celanese Nylon 1003-1 manufactured by Celanese Plastics Company, and approved by UL for use in wire coating applications.

In summary, THWN type wire is PVC insulated wire, with a nylon jacket (over-coating), approximately 0.004" thick, which is moisture resistant and acceptable for use up to 75°C.

THHN type wire is PVC insulated wire with a nylon jacket (approximately 0.004" thick), which is acceptable for use up to 90°C.

The above two wire types are used extensively in the building construction industry. Other areas of use are Fixture Wire and Machine-Tool Wire and Cable.

### BRIEF HISTORY OF NYLON'S EVOLUTION IN THE WIRE AND CABLE INDUSTRY

#### A. Early History

Prior to the early 1960's, most nylon jacketed wire utilized Nylon 610, due to the low moisture absorption characteristics of that resin. At that time, the industry believed that moisture absorption would cause a reduction in the insulation properties of the wire. Subsequently, a Nylon 6 supplier demonstrated that as long as the primary wire insulation (PVC) was satisfactory, the moisture content of the nylon jacket had negligible effect on the insulation properties of the wire.

Nylon is used as a coating (0.003" - 0.01" thick) over PVC in THWN and THHN type wire for the following reasons:

1. Improved abrasion resistance.
2. Chemical resistance - especially to oil-based products.
3. High strength, which allows smaller diameter wire to be used.
4. High toughness, which allows considerable wire flexing without break.
5. Heat stability, which allows use at temperatures as high as 250°F continuously.
6. Low coefficient of friction - in many applications this reduces installation time (e.g., "Snaking" through conduits).
7. Reduction of plasticizer and stabilizer migration from the PVC insulation.

Based on economics (the expense of Nylon 610), it was only natural that once UL approval was obtained, many wire and cable manufacturers would and did switch to Nylon 6, where other specifications did not dictate otherwise.

## B. Present Industry Status

For the vast majority in the building construction industry, UL approval controls the type of wire to be used. Although both Nylon 610 and Nylon 6 formulations are presently approved, the majority of the wire product utilized is Nylon 6. Based on the formation generated to date, it is our opinion that Nylon 66 will perform equivalent or better than Nylon 6 in the approved wire coating applications. Celanese Nylon 1003-1 has been approved by UL for use in wire coating applications (THHN, THWN).

## B. Importance of UL Approval

Although a number of wire and cable coating applications do not require UL approval, it is estimated that they represent less than 10% of the total market. Examples of applications that do not require UL approval are push-pull cables, pulley cables, and wire insulation for "in-house" use or special applications.

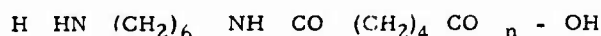
### WHAT IS HEAT STABILIZED NYLON 66 AND HEAT STABILIZED NYLON 6?

By definition, nylon is a generic term designating any long chain synthetic polymeric amide with recurring amide groups as an integral part of the main polymer chain.

The addition of a heat stabilizer increases the continuous use temperature of both Nylon 66 and Nylon 6 from 180°F to 250°F.

## Nylon 66

The chemical structure for Nylon 66 is the following.



Nylon 66 is manufactured by reacting equal amounts of hexamethylene diamine and adipic acid, in an aqueous solution to form hexamethylene diammonium edipate (nylon salt). Originally, the batch method was used to produce Nylon 66. With the advance in technology, the continuous process has been developed and employed by Celanese to produce the finest Nylon 66 available.

### Batch Process

In the batch process, the salts are fed into an autoclave, cooked and stirred until polymerization is completed. The batch is then dumped, chopped, ground, extruded into strands and chopped into pellets. Proper polymerization requires the accurate application of heat, both in temperature level and length of time. These factors are difficult to control in a mass of material which is inherently a poor conductor of heat. This is a tough way to get a uniform product and the product resulted from the batch process has pretty much defined the problems which have traditionally faced the nylon customer:

- Processing and property variations from batch to batch.
- Yellowness in the natural resins.

## Continuous Process

In the continuous process in which the salts are fed at a designed rate into the reactor so that it creates no holding time for the reactants. Since the resin mass moves amounts where heat level and duration can be closely controlled, the degree of polymerization of the final product can be more accurately established.

The continuous process produced a Nylon 66 which has reduced heat history (and therefore greater heat stability) and is whiter, cleaner and with greater uniformity in properties and processing characteristics. What this means is:

- Greater heat stability
- Greater property uniformity from lot to lot.

## Nylon 6

The chemical structure for Nylon 6 is the following:



Nylon 6 is manufactured by polymerization of Caprolactam, either by the batch or continuous process methods.

### THE PHYSICAL AND MECHANICAL PROPERTIES OF NYLON 66 AND NYLON 6

Key physical and mechanical properties of Nylon 66 and Nylon 6 are listed in TABLE I.

TABLE I

Physical and Mechanical Properties of Typical Nylon 66 and Nylon 6 for Wire Coating Applications

Property	HEAT STABILIZED NYLON 66		HEAT STABILIZED NYLON 6	
	Dry As Molded	Equilibrium Moisture @ 50% R.H.	Dry As Molded	Equilibrium Moisture @ 50% R.H.
Moisture Content, %	< 0.3	2.5	< 0.3	2.5
<u>Strength at 73°F</u>				
Tensile Strength, psi	12,000	11,000	11,500	10,000
Elongation at break, %	75	300	175	300
Tensile Yield Strength, psi	12,000	8,500	11,500	6,400
<u>Rigidity at 73°F</u>				
Flexural Strength, psi	17,000	6,100	16,000	5,800
Flexural Modulus, psi	420,000	185,000	395,000	140,000
<u>Impact and Toughness at 73°F</u>				
Izod Impact Strength ft.-lb/in. notch	1.0	2.1	1.1	4.0
<u>Thermal</u>				
Melting Point, °F	495	---	420	---
Specific Heat	0.4	---	0.4	---
Coefficient of Expansion in/in. °F	5x10 <sup>-5</sup>	---	4.6x10 <sup>-5</sup>	---
Heat Distortion, °F				
@ 100 psi	374	---	340	---
@ 264 psi	167	---	150	---
<u>Miscellaneous at 73°F</u>				
Specific Gravity	1.14	---	1.13	---

\*Celanese Nylon 1003-1

#### A. Mechanical Adhesion to PVC Coated Wire

There is no chemical bonding between the nylon jacketing and PVC insulation. Jacketing "tightness" is achieved through the thermal contraction and shrinkage of nylon upon cooling from its process melt temperature (related to melt point) to room temperature.

As the coefficient of thermal expansion for Nylon 66 and Nylon 6 are similar, it is expected that the substantially higher melting point of Nylon 66 (495°F vs. 420°F for Nylon 6), greater contraction would occur with a Nylon 66 jacket when cooling from its solidification point to room temperature. In addition, a slightly higher shrinkage rate for Nylon 66 (18 in/in vs. 13 in/in for Nylon 6; greater contraction would occur with a Nylon 66 jacket. This would induce higher mechanical bonding forces between the PVC insulation and the Nylon 66 jacket, achieving improved mechanical adhesion.

#### B. Heat Stability

##### Long Term

Both heat stabilized Nylon 66 and Nylon 6 offer equal long term heat resistance. Both nylons have a continuous end-use temperature of 250°F.

##### Short Term

For short term heat resistance (e.g., over-load conditions, soldering terminals close to the wire), Nylon 66 has a significant advantage due to its higher melting point (495°F as compared to 420°F for Nylon 6).

#### C. Moisture Absorption

The following data illustrates moisture absorption and dimensional characteristics of Nylon 66 and Nylon 6.

<u>Relative Humidities</u>				
	20%	50%	75%	100%
<u>Nylon 66</u>				
Moisture Gain, %	0.95	2.50	4.75	9.00
Dimensional Change, %	0.25	0.60	1.15	2.80
<u>Nylon 6</u>				
Moisture Gain, %	1.05	2.70	5.10	9.50
Dimensional Change, %	0.30	0.70	1.35	3.00

As moisture absorption results in dimensional growth, Nylon 66 has an advantage over Nylon 6 because of lower moisture absorption characteristics of the nylon jacketing after processing which will result in a higher mechanical bond strength between the jacket and the PVC insulation. This will reduce the tendency for wrinkle of the nylon jacket upon handling, such as assembly, re-spooling and bonding.

#### D. Cracking Resistance

Based on elongation (ability of the material to give) listed in TABLE I, it might be assumed that Nylon 6 offers slightly improved crack resistance compared to Nylon 66. However, after both nylons have

absorbed equilibrium moisture, their elongation is equivalent. It is our opinion that this property is of a major concern in predicting the cracking tendency of a coating.

Our field testing of UL approved heat stabilized Nylon 66 has resulted in a no crack situation compared to heat stabilized Nylon 6.

#### PROCESSABILITY

A higher heat profile (due to a 75°F higher crystalline melting point of Nylon 66) may be required to process Nylon 66. It should be pointed out however, that heat stabilized Nylon 66 has been successfully processed under heat stabilized Nylon 6 processing conditions.

During evaluations at various wire houses, it has been noted that Nylon 66 generates little or no smoke as the melt exits the die, while Nylon 6 wire coating grades (with or without plasticizers) generates considerable smoke. Although there has been no reported problem associated with Nylon 6 smoke generation, Nylon 66 has been classified as a "cleaner" compound by several wire houses.

Laboratory and field test data has concluded that the maximum recommended moisture content for Nylon to successfully wire coat is 0.15%. Several key process variables are discussed as follows:

#### A. Extruders Design

There are presently two basic types of extruders, non-vented and vented, available for wire coating applications.

An extruder is essentially a pump which has the function of uniformly delivered melted polymer through a breaker plate into a die which lays a coat on the wire. The extrusion of the wire coating is a steady state process and one of the key parameters is UNIFORM delivery of the melt to the die.

##### 1. Non-Vented Extruder

The non-vented extruder, Figure 1, is the most common extruder used in the wire coating industry. With proper screw design and heat control, both Nylon 66 and Nylon 6 can be satisfactorily processed, as long as the volatile level (moisture content) in the resin is lower than 0.15%.

##### 2. Vented Extruder

This type of extruder is not widely used by the wire coating industry, because of two stage compression screw is required which will result in the following disadvantages:

- Pressure surges in the melt which will result in non-uniform output at the die.
- Intermittent blockage of the vent which would require down-time to clean.

\*Celanese Nylon 1003-1, a heat stabilized non-lubricated Nylon 66.

However, there are several advantages for using a vented extruder:

- Nylon volatile level (moisture content) higher than 0.15% can be used in wire coating without pre-drying the material.
- Gases generated during the melting process are drawn out via the vent leaving a bubble or void free melt.

### B. Temperature Control

To successfully (because of the sharp melting point) extrude nylon for wire coating, sufficient heating elements are mandatory on the extruder, especially at the breaker plate. Accurate temperature control devices are recommended.

The importance of adequate heat control for nylons, both Nylon 66 and Nylon 6 should not be over emphasized.

### C. Processing Conditions

Typical processing conditions for Nylon 66 and Nylon 6 are listed in TABLE II.

FIGURE 1  
TYPICAL SINGLE "SCREW" EXTRUDER  
(NON-VENTED)

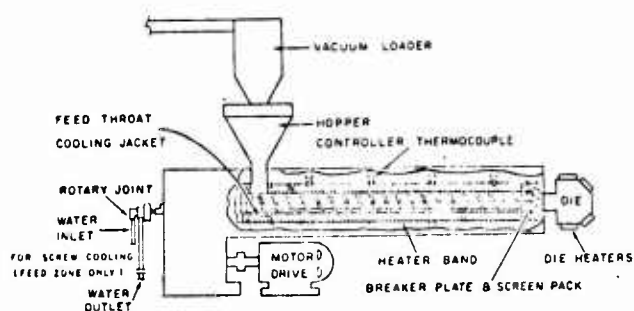


TABLE II  
Typical Processing Conditions

Machine:	2-1/2" Extruder	
L/D:	20/1 - 24/1	
Screw:	3 zone "Nylon" screw	
	3 zone	Nylon 66
Rear Zone	490 - 510°F	510 - 530°F
Rear Center Zone	500 - 540°F	530 - 550°F
Front Center Zone	510 - 540°F	530 - 560°F
Front Zone	530 - 550°F	540 - 570°F
Adaptor	550 - 570°F	560 - 580°F
Die	510 - 530°F	520 - 560°F
Melt Temperature	520 - 540°F	530 - 560°F
Water Bath	70 - 100°F	70 - 100°F
Take Off Speed	50 - 1200 ft/min	50 - 1200 ft/min
Jacket Thickness	0.003 - 0.010 in	0.003 - 0.010 in
Vacuum on hand	5 - 8 inches	5 - 8 inches

As shown in TABLE II, the processing conditions for extrusion wire coating, both types of nylon, are essentially identical with the exception being a slightly higher temperature profile for Nylon 66.

Typical processing conditions for Celanese Nylon 1003 which were experienced on various wire coating machines are listed in TABLE III - VIII.

Celanese Nylon 1003-1 (Nylon 66) is fully approved by UNDERWRITERS LABORATORIES, INC. for MTW (Construction B), TFN, TFFN, THWN and THHN type wire and cable including gasoline and oil resistance.

TABLE III

Extruder Mfr:	Davis Standard
Coating Line:	Tendon
Screw Diameter:	2-1/2
L/D Ratio:	24/1
Wire Size:	12" gauge

Cylinder Temperature Settings	
Rear Zone:	550°F
Rear Center Zone:	590°F
Front Center Zone:	580°F
Front Zone:	600°F
Adaptor Temperature:	460°F
Die Temperature:	585°F
Melt Temperature:	550°F
Water Bath Temperature:	75°F
Screw Rotational Speed:	20 RPM
Motor Load:	8 Amps
Screen Pack:	100 Mesh
Vacuum Pressure:	15 inches
Take Off Speed:	510 ft/min
Material Out-put:	40 lbs/hr

TABLE IV

Extruder Mfr:	Sterling
Coating Line:	Tendon
Screw Diameter:	2-1/2
L/D Ratio:	20/1
Wire Size:	10" gauge

Cylinder Temperature Settings	
Rear Zone:	530°F
Rear Center Zone:	540°F
Front Center Zone:	550°F
Front Zone:	540°F
Adaptor Temperature:	550°F
Die Temperature:	520°F
Melt Temperature:	530°F
Water Bath Temperature:	70°F
Screw Rotational Speed:	46 RPM
Motor Load:	42-44 amps
Screen Pack:	220 Mesh
Vacuum Pressure:	None
Take Off Speed:	400 ft/min
Material Out-put:	50 lbs/hr

TABLE V

Extruder Mfr:	Davis Standard
Coating Line:	Single
Screw Diameter:	2-1/2
L/D Ratio:	20/1
Wire Size:	14" gauge

Cylinder Temperature Settings	
Rear Zone:	540°F
Rear Center Zone:	560°F
Front Center Zone:	570°F
Front Zone:	580°F
Adaptor Temperature:	580°F
Die Temperature:	570°F
Melt Temperature:	570°F
Water Bath Temperature:	70°F
Screw Rotational Speed:	50 RPM
Motor Load:	18-20 Amps
Screen Pack:	300 Mesh
Vacuum Pressure:	None
Take Off Speed:	1000 ft/min
Material Out-put:	75 lbs/hr

TABLE VI

Extruder:	Entwistle
Coating Line:	Tendon
Screw Diameter:	2-1/2
L/D Ratio:	25/1
Wire Size:	14" gauge

Cylinder Temperature Settings	
Rear Zone:	540°F
Rear Center Zone:	540°F
Front Center Zone:	560°F
Front Zone:	570°F
Adaptor Temperature:	570°F
Die Temperature:	520°F
Melt Temperature:	540°F
Water Bath Temperature:	80°F
Screw Rotational Speed:	46 RPM
Motor Load:	19 Amps
Screen Pack:	100 Mesh
Vacuum Pressure:	15 inches
Take Off Speed:	360 ft/min
Material Out-put:	

TABLE VII

Extruder Mfr:	Produx
Coating Line:	Tendon
Screw Diameter:	2-1/2
L/D Ratio:	20/1
Wire Size:	12" gauge

Cylinder Temperature Settings	
Rear Zone:	530°F
Rear Center Zone:	545°F
Front Center Zone:	550°F
Front Zone:	560°F
Adaptor Temperature:	185°F
Die Temperature:	580°F
Melt Temperature:	510°F
Water Bath Temperature:	Air Cool
Screw Rotational Speed:	16 RPM
Motor Load:	12 Amps
Screen Pack:	180 Mesh
Vacuum Pressure:	None
Take Off Speed:	400 ft/min
Material Out-put:	

TABLE VIII

Extruder Mfr:	Reliance
Coating Line:	Single Extruder
Screw Diameter:	2-1/2
L/D Ratio:	5/1
Wire Size:	12" gauge

Cylinder Temperature Settings	
Rear Zone:	520°F
Rear Center Zone:	500°F
Front Center Zone:	500°F
Front Zone:	550°F
Adaptor Temperature:	
Die Temperature:	510°F
Melt Temperature:	510°F
Water Bath Temperature:	75°F
Screw Rotational Speed:	60 RPM
Motor Load:	45 Amps
Screen Pack:	160 Mesh
Vacuum Pressure:	7 inches
Take Off Speed:	850 ft/min
Material Out-put:	50 lbs/hr

J. L. Snyder and W. R. Hendricks  
Shell Development Company  
Houston, Texas

### SUMMARY

ELEXARTM thermoplastic rubbers represent a new class of commercially available block copolymer products specially designed for wire and cable applications. These materials represent a union of superior electrical properties with flexibility and toughness, in a product which can be processed with the speed and economy of a thermoplastic. Such qualities yield to the user the benefits of design versatility, product simplification, lower capital investment, and operating cost savings.

These rubbers are extremely versatile and with compositional variations, yield products with a wide variety of physical and mechanical properties to suit particular requirements. Products are available with Shore A hardness values from 60 to 95 and specific gravities from 0.9 to 1.2, all of which show the feel and flexibility expected of rubber. Tensile strengths of these materials range from 1500 to 3000 psi, tear strengths are greater than 400 pli, they have good thermal properties, resist oxidative and ozone degradation, and have withstood one year outdoor exposure in Florida with no loss in mechanical properties. Electrical properties of these new products are impressive; i.e., ELEXAR rubber grade 8431Z has a dielectric constant of 2.2, constant across the frequency range from 1 Hz to 100M Hz with a power factor of 0.000001 at lower Hz and 0 at 100M Hz.

These new block copolymer products have excellent resistance to water, alcohols, acids, and bases. Some ELEXAR rubber grades have oil resistance approaching that of compounded and vulcanized chloroprene as required by U.L.-62 standards. Other grades are flame modified to pass the horizontal or vertical flame tests. Products are being developed which will pass the tests required to obtain U.L. ratings of 125° and 150°C.

Compounds based on the styrene-ethylene butylene-styrene three block polymers are thermoplastic and can be readily processed with standard thermoplastic extrusion equipment, and at rates which compare favorably with other commercial thermoplastic polymers. They can also be injection molded for such applications as plugs, boots, harnesses, and connectors, offering significant cost savings over conventional cured products.

### Block Copolymers

Solution polymerization of styrene and butadiene or other monomers in a controlled manner can produce block polymer. These polymers have their constituent monomers arranged in pure block sequence. The block polymer under consideration here is composed of three blocks in the sequence, block polystyrene--block poly(ethylene-butylene)--block polystyrene, or S-EB-S. A comparison between this type of molecular construction and other common polymers is shown in Figure 1.

In a homopolymer such as polyethylene, one monomer is arranged more or less linearly in the polymer molecule. Subtle variations in the size, degree of branching or regularity of the molecule chain make important contributions to the overall physical properties of this type of polymer.

Random copolymers may be represented by styrene-butadiene rubber or SBR. This rubber contains styrene combined in a more or less linear and random fashion with butadiene. Molecules of this irregular composition and structure fit poorly together alongside one another. The mutual forces of attraction between chains remain small. Chain entangling is the predominant source of cohesion. For useful properties to be obtained, such a random copolymer must be subjected to a chemical crosslinking process.

When the constituent monomers of a polymer are now arranged in block sequences, a form of molecular orientation can take place in the solid due to mutual incompatibility. If the composition of an S-EB-S polymer contains about 30% styrene, the uniform styrene end blocks form a discrete dispersed phase, the so-called "domains". These domains will be submicroscopic, governed in size by the statistical chain length of a polystyrene end block. The center block or E-B component will form a continuous phase. A diagrammatic representation of this arrangement is shown in Figure 2. The polymer mass consists of two phases. One phase exists as polystyrene aggregates referred to as domains. These domains are dispersed in a continuous rubber matrix of ethylene-butylene polymer. Each individual S-EB-S molecule has its chain ends in a polystyrene domain and its center segment in the continuous poly(ethylene-butylene) phase. At subzero temperatures, the polymer remains flexible and rubbery because the continuous phase has a low second order or glass transition temperature (about -60°C). As the temperature is raised to service temperatures there is little change in the physical properties. The styrene domains remain hard and glass-like anchoring the ends of all the chains. In effect these PS domains act both as multiple cross-links and as bound filler particles.

At temperatures close to the glass transition temperature of PS (~100°C) the PS domains begin to change from the hard glassy state to a soft rubbery material. At higher temperatures these domains revert to a viscous fluid and can be disrupted by applied stress. The physical crosslinks of the domains are essentially eliminated and the polymer will flow under pressure. In effect, a material of very high molecular weight becomes one of very low molecular weight. On cooling the domains quickly reform again, immobilizing all the chain ends and re-establishing the three-dimensional elastomer network.

The absence of unsaturation yields resistance to ozone, U/V light and heat. Chemical resistance to corrosives and to some solvents is also good. Anything, however, which will swell or attack polystyrene can disrupt the domains and reduce the extent of physical cross-linking. The good electrical properties are due to the polymers low density, non polar monomers, and freedom from ionic contaminants.

In summary, the S-EB-S three block copolymer combines thermoplastic behavior, rubber-like character and molecular stability in a good dielectric.

### Processing and Properties of Block Copolymers

With the aid of modifying additives, readily processable grades for wire and sheathing can be



formulated. Representative are the four grades of material outlined in Table I covering a range of hardness from 65 to 95 Shore A units. These grades all show melt flow values typical of thermoplastics. The softer more rubber-like material, 8431Z, has a specific gravity of about 0.9, the harder stiffer more highly formulated grades have gravities of about 1.0 to 1.2.

#### Viscosity Behavior and Processing Conditions

All four grades are compounded and pelletized for easy extrusion. The data of Figure 3 illustrate that in the range of typical extrusion shear rates all compounds show viscosity-shear rate dependence--viscosity decreases rapidly with increase of shear rate analogous to polypropylene. In practice, this means that increasing line speed will not result in increasing head pressure.

Equipment used for the processing of polyethylene, polypropylene or PVC can normally be used to extrude block copolymer grades. Because of the domain linked network, uniform melts require more shear than can be obtained with very deep flighted low compression screws. The use of screen packs to increase the back pressure readily provides the added shear necessary to obtain a well plasticized melt.

Processing of three block copolymer compounds is best with a combination of temperature, back pressure, screw speed and die arrangement which results in the maximum shear immediately prior to the die. Both PVC and polyolefin dies have been used successfully, particularly if the tip is moved fairly far forward into the die. A set of typical operating conditions for the four grades is given in Table II. Based on experience to date, conventional wire extrusion coating lines work well with the block polymer compounds discussed here. The need for high shear to obtain good melt homogenization is stressed to avoid rough extrusion. Control over surface finish can be obtained with properly profiled cooling and use of proper melt and die temperatures.

#### Extruded and Molded Properties

In Table III are set forth some typical stress-strain data obtained on extruded block copolymer wire coating. The tensile strength of all grades is in the region of 2000 psi and the modulus at 200% extension is about 1000 psi. That for grade 8431Z, lowest in Shore A hardness, is somewhat lower. This grade also has the greatest elongation and exhibits the most rubber-like character--low deformation, high coefficient of friction, etc.

Additional properties of interest are listed in Table IV. The properties were determined on injection molded test pieces. In common with most polymers, injection molding of block copolymer grades imposes anisotropic behavior on the product. Where test results could be influenced by the direction of test, measurements were made in the flow or parallel direction to approximate extrusion behavior. The data of Table IV show that block copolymer compounds have acceptable tear strength, abrasion resistance, and water resistance. Stress crack resistance and low temperature flexibility are very good for all compounds.

#### Electrical Properties

The S-EB-S grades show a range of electrical properties from excellent to good. Dielectric constant ranges from 2.2 to about 2.8 depending upon the extent of compounding and is reasonably constant

over the range of frequencies from  $10^2$  to  $10^6$  Herz. The volume and surface resistivities are also in the range of a good dielectric. Highly modified, fire resistant S-EB-S grades are only modestly reduced in overall electrical properties. A summary of the electrical measurements is presented in Table V.

#### Solvent and Chemical Resistance

Chemical composition and structure of S-EB-S block copolymer determines the behavior toward chemical and physical attack. Modifying additives can exert some influence on environmental stability of the polymer. The hydrocarbon composition predicts good water resistance and this is found. Attack by other solvents and solutions is predicated on their chemical composition. Aqueous solutions, neutral or corrosive, have little effect nor do alcohols and glycols. Swelling in oils and similar fluids is also governed by their composition. Aromatic compounds are capable of disrupting the styrene domains and hence destroying the network, aliphatic materials are resisted. Some data on the resistance shown toward various solvents is given in Table VI.

#### Ozone, Oxygen and Weather Resistance

Ozone attack is seen mainly in stressed, unsaturated polymers. The S-EB-S block copolymers contain essentially no ozone sensitive unsaturation and show almost no reaction toward this gas. Oxygen is also non-reactive toward S-EB-S for much the same reason, there are simply no sensitive portions of the molecule capable of facile chemical combination with oxygen. A more practical measure of product stability is the determination of outdoor or weather resistance. Over a two-year period S-EB-S grades have shown excellent outdoor stability. Some results of ozone, oxygen and outdoor exposure are summarized in Table VII.

#### Thermal Resistance

Service life predictions based on oven aging data are fallable. The grades of block copolymer wire coating have good stability toward thermal oven aging. Data presented in Table VIII indicate the degree of resistance shown by these grades to oven aging. Short term, high pressure air bomb age resistance is excellent. These results together with the ozone and weather resistance already discussed suggest that the service life of wire and cable sheathed or insulated with block copolymer compound should be good. A portion of the compositional variables applied in these grades includes high temperature oxidation inhibitors and copper deactivator. These additions together with the inherently unreactive structure of S-EB-S promote overall thermal stability.

#### Flammability

As with all hydrocarbon, S-EB-S copolymer is flammable. With adequate amounts of flame retardant increasing degrees of flame resistance can be built into these materials. In Table IX some results of flammability tests are compiled. The 8431Z and 8421Z grades are not compounded for fire retardancy. These compounds show the degree of flammability found in most hydrocarbon polymers for example PE, PP, PS, or EPDM. Grades 8613Z and 8614Z do contain effective flame inhibitors. Stripped insulation of these grades from extrusion coated wire shows an increased oxygen requirement to maintain combustion. In real air of about 21% oxygen, 18 AWG wire coated with these grades has a self extinguishing, non dripping nature



depending upon mode of burning. The addition of enough fire retardant to gain this reduced flammability dilutes the domain network. Tensile strengths of the fire retardant grades are reduced by about 25 percent below those of the other grades.



BIOGRAPHY

NAME: John Leonard Snyder

BORN: Vancouver, British Columbia, Canada, 1923

SERVICE: Pilot, RCAF/RAF Bomber Command, 1942-1945

EDUCATION: University of British Columbia Vancouver, B.C., Canada  
BA, MSc, Organic Chemistry, 1951  
McGill University, Montreal. P.Q., Canada  
PhD, Wood Chemistry, 1953

CAREER: MacMillan and Bloedel, Vancouver, B.C.,  
Forest products applications and development, 1953-1955  
Shell Development Company, Houston, Texas  
Rubber and plastics applications and development, 1955-present

FAMILY: Married to Irene Marie with two daughters: Angela, 3 and  
Tiffany, 12 weeks.



BIOGRAPHY

W. R. Hendricks

A native of California, W. R. Hendricks attended College of the Pacific and served for three years in the Air Force during World War II. He joined Shell in 1945 at the Shell Development Company laboratories at Emeryville, California. He transferred to the Elastomers Technical Center at Torrance, California in 1956. He has since worked in both the Development and Applications Departments and is presently a member of the Elastomers Department of the Shell Development Company's Westhollow Research Center at Houston, Texas.

TABLE I

Four Grades<sup>a)</sup> of Block Copolymer Wire Coatings

Grade No.	8431Z	8421Z	8613Z	8614Z
Hardness <sup>b)</sup> , Shore A	65	89	94	95
Melt Flow <sup>c)</sup> , g/10	8	18	3	3
Specific Gravity	0.90	0.98	1.16	1.19

a) Grades of Shell ELEXAR<sup>TM</sup> thermoplastic rubber

b) Hardness measured on injection molded specimen

c) Condition G: 200 C, 5000g

TABLE II

## General Extrusion Conditions for Block Copolymer Grades

## Extrusion Equipment

Extruder Size	2½" - 3½"
Length: Diameter Ratio	20:1 - 24:1
Screw Type	Single Stage
Screw Compression Ratio	3:1 - 4:1
Die Type	Pressure or Tubing

## Temperature Profile

Hopper Zone	Cool - 121°C
Feed Zone	171 - 191°C
Middle Zone	205 - 218°C
Front Zone	218 - 232°C
Die	215 - 226°C
Melt Temperature	194 - 215°C
Screw Speed	60 - 80 rpm
Head Pressure	1500 - 2000 psi

TABLE III

Stress-Strain<sup>a)</sup> Properties of Extruded Block Copolymer Wire Coating

Grade No.	8431Z	8421Z	8613Z	8614Z
Hardness, Shore A	65	89	94	95
Tensile Strength, psi	2300	2700	1900	1800
Modulus at 200% Elongation, psi	300	900	1100	1000
Modulus at 400% Elongation, psi	800	1300	1400	1300
Modulus at 600% Elongation, psi	1200	2400		
Elongation at Break, %	700	625	450	425

a) Determined on insulation stripped from AWG 18 wire. ASTM D-2633.

TABLE IV

Physical Properties<sup>a)</sup> of Block Polymer Wire Coating

Grade No.	8431Z	8421Z	8613Z	8614Z
Hardness, Shore A	65	89	94	95
Tear Strength <sup>b)</sup> , pli	215	400	450	425
Abrasion Resist. <sup>c)</sup> , -cc/1000 cycles	0.14	0.25	0.41	0.42
Stress-Cracking <sup>d)</sup> 100% Igepal, 50°C 100% Igepal, 100°C	none none	none none	none none	none none
Water Absorption <sup>e)</sup> , 80°C, 7 days, mg/in <sup>2</sup>	4	5	7	7
Brittleness Temp <sup>f)</sup> , °C	-70	-70	-50	-50

a) Measured on injection molded specimens.

b) ASTM D-624 Die C.

c) Taber with H-18 stone, 1000g load.

d) ASTM D-1693.

e) ASTM D-570.

f) ASTM D-746.

TABLE V

Electrical Properties<sup>a)</sup> of S-EB-S Grades

Grade No.	8431Z	8421Z	8613Z	8614Z
Hardness, Shore A	65	89	94	95
Dielectric Const, K, at 10 <sup>2</sup> Hz	2.25	2.45	2.92	2.80
10 <sup>3</sup> Hz	2.25	2.43	3.03	2.80
10 <sup>4</sup> Hz	2.27	2.43	2.95	2.75
10 <sup>5</sup> Hz	2.20	2.43	2.61	2.80
10 <sup>6</sup> Hz	2.17	2.32	2.71	2.65
Dissipation Factor, D	0.0002	0.0008	0.005	0.005
Volume Resistivity, ohm-cm, 10 <sup>15</sup>	0.2	2.3	1.0	1.2
Surface Resistivity, ohms, 10 <sup>15</sup>	0.5	6.4	1.2	2.9
Arc Resistance, sec	64	69	74	65
Dielectric Strength, V/mil	900	600	500	500

a) Measured on injection molded specimens

TABLE VI

Resistance<sup>a)</sup> of S-EB-S Grades to Solvents and Oils

Grade No.	8431Z	8421Z	8613Z	8614Z
Hardness, Shore A	65	89	94	95
Percent Retention	T <sub>B</sub> E <sub>B</sub>	T <sub>B</sub> E <sub>B</sub>	T <sub>B</sub> E <sub>B</sub>	T <sub>B</sub> E <sub>B</sub>
ASTM #2 Oil 20 hr, 121°C	15 100	35 80	50 55	55 55
Motor Oil 48 hr, 100°C	20 92	45 55	60 45	60 65
Transmission Fluid 48 hr, 100°C	20 28	50 50	50 60	80 65
Brake Fluid 48 hr, 100°C	93 110	94 90	80 90	80 70
Gasoline 48 hr, 100°C	18 30	41 40	40 25	40 25
Antifreeze 48 hr, 100°C	84 89	95 90	94 84	100 85
Methanol 48 hr, 100°C	86 92	95 95	95 95	95 95

TABLE IX

Flammability of S-EB-S Wire Coating

Grade No.	8431Z	8421Z	8613Z	8614Z
Hardness, Shore A	65	89	93	95
Limiting Oxygen Index <sup>a,b)</sup>	18	18	25	30
Horizontal Burning, Wire <sup>c)</sup> , sec. , drip	Burns	Burns	>30 No	>15 No
Vertical Burning, Wire <sup>c)</sup> , sec. , drip	Burns	Burns	Burns No	>15 No

a) Percent oxygen in O<sub>2</sub>/N<sub>2</sub> mixture to maintain flame. ASTM D-2863.

b) On stripped insulation.

c) Extrusion coated AWG 18 bare copper with 30 mil wall.

a) Injection molded test pieces immersed in fluid.

TABLE VII

Ozone, Oxygen and Weather Resistance<sup>a)</sup> of S-EB-S Grades

Grade No.	8431Z	8421Z	8613Z	8614Z
Hardness, Shore A	65	89	94	95
Ozone, 100 pphm, 60°C, 1000 hr <sup>b)</sup>	no cracks	no cracks	no cracks	no cracks
Oxygen <sup>c)</sup> , 300 psi, 80°C, 150 hr Percent Retention, T <sub>B</sub> /E <sub>B</sub>	100/90	100/90	95/90	95/90
Weathering, Arizona 45° South, 24 mos., Percent Retention T <sub>B</sub> /E <sub>B</sub>	100/105	105/100	95/100	90/105

a) Measured on injection molded specimens.

b) Strip 1" x 4" x 0.075" bent double, ASTM D-1171.

c) ASTM D-572.

TABLE VIII

Thermal Resistance<sup>a)</sup> of S-EB-S Grades,  
Percent Retention of T<sub>B</sub>/E<sub>B</sub>

Grade No.	8431Z	8421Z	8613Z	8614Z
Gardness, Shore A	65	89	94	95
Air Oven, 30 days, 125°C	95/95	90/80	85/95	85/90
Air Oven, 30 days, 136°C	80/110	88/85	115/75	105/65
Air Oven, 7 days, 160°C	110/105	95/75	84/50	81/50

a) Samples aged were dumbbells from injection molded specimens.

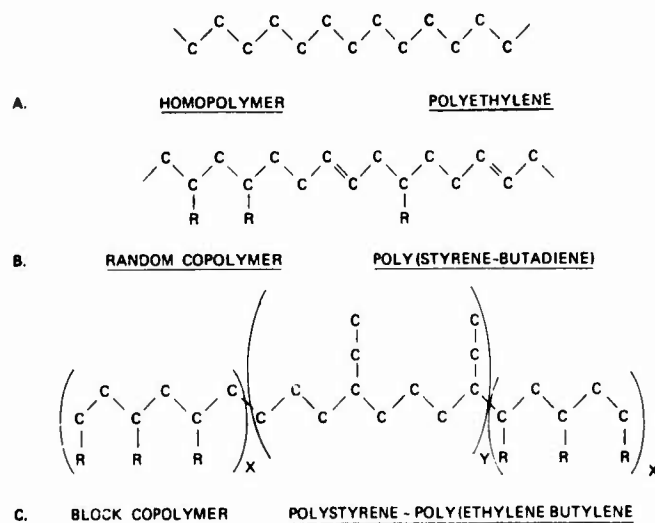
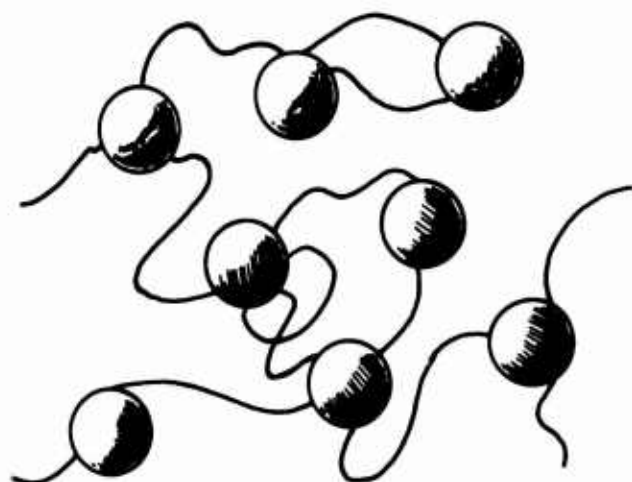


Figure 1. Schematic Structure of Some Polymers



POLYSTYRENE DOMAIN



POLY(ETHYLENE-BUTYLENE) CONTINUUM

**Figure 2. Two-Phase Model of S-EB-S Block Copolymers**

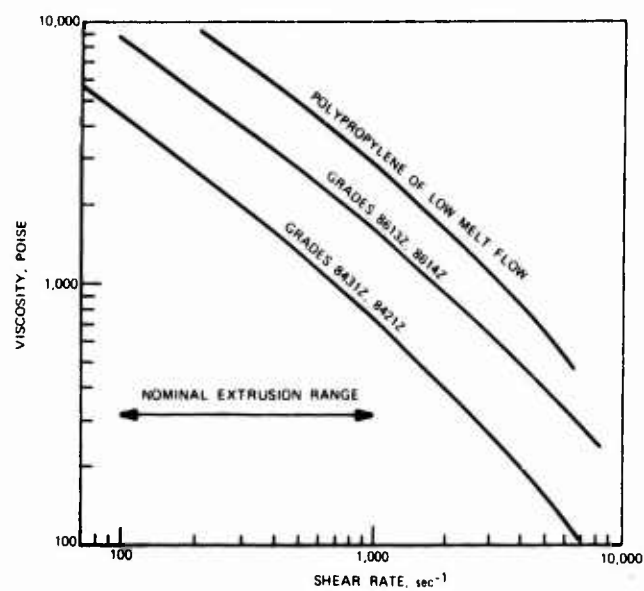


**Figure 3. Viscosity Shear Rate Relationships  
(200°C)**

## POLYMER ALLOYS FOR FLEXIBLE CABLE JACKETING

Fred Roesler

John McBroom

Tenneco Chemicals, Inc.  
Organics and Polymers Division

### Introduction

PVC is usually made flexible by using monomer and/or polymeric plasticizers. The former are esters of aromatic and/or aliphatic acids and alcohols of four to thirteen carbon atoms. Polymeric plasticizers are polycondensation products of aliphatic acids and glycols, and provide a degree of permanence unavailable with monomeric types. The concomitant reduction in performance of such properties as flexibility and processing are accepted sacrifices that accompany the use of some polymeric plasticizers. Often these losses can be minimized by blending PVC with other polymers to form alloys. This work is not intended to show the development of a new product but to show the versatility of PVC and alternate ways of making it resistant to some forms of deformation. The solid plasticizers (polymers) cited can broaden the use range of PVC in such areas as non-contaminating cable jacketing by demonstrating some unique uses heretofore unavailable with an all-liquid plasticized system.

In a number of applications, PVC is used adjacent to other materials, and migration of liquid plasticizers (phthalates, adipates, azelates, etc.) to the surface or into the other material will lead to a loss of physical properties. Migration of plasticizer from PVC jacketing to polyethylene insulation after extended service can cause a serious reduction in its performance in electrical applications and render the cable unsuitable for its intended use. Another example is the use of PVC jacketing in conjunction with acrylic or polystyrene lighting fittings, where a migrating plasticizer can cause crazing of the associated product. The effect is dependent on the interaction between the plasticizer and the second material caused by increased mobility of the plasticizer molecules due to temperature, humidity, migration, etc. In this kind of situation, nonmigratory polymeric plasticizers are usually recommended but even the best will often migrate under conditions of intense pressure, heat, etc. One method of overcoming this is to plasticize PVC with a polymer or polymer/polymeric plasticizer combination (such as chlorinated polyethylene, nitrile rubber or ethylene interpolymer copolymers) that cannot migrate.

### Experimental

The control selected for this work is the standard monomeric plasticizer DOP. This was done to provide a base point for determining plasticizing efficiency. The secondary control is a medium molecular weight polymeric plasticizer. The polymers used as plasticizers were added in the amount thought to provide the same plasticizing efficiency as the monomeric and polymeric plasticizers. In some cases, it will be noted that the

plasticizing efficiency is greater than desired but this is in the realm of the experiment. The work leading to the selection of the various formulas for the polymer blends was quite lengthy and a dissertation on each would be necessary for the explanation. Therefore, it was decided to provide information on the formulations that were most similar in performance or showed some improvement of performance over the monomeric/polymeric systems. The polymers used in the preparation of these alloys are commercial, readily available and have some compatibility with PVC. It should be noted, for instance, that some polymeric plasticizer was used in the CPE and nitrile rubber blends. This was done to provide the efficiency, processability and practical use of the compound. Secondly, it was necessary to use a filler in the nitrile formulation; this was done to reduce nerviness in the finished compound. The formulations used are in Table I; all test procedures are contained in Table II.

### Discussion

#### Efficiency

One specific grade for each of the four polymers was selected from the standpoint of compatibility with PVC and ease of processing. Formulations were prepared by dry blending and milling on a two-roll laboratory mill. Press polished plaques were prepared and specimens conditioned and tested in accordance with the test procedures in Table II. A cursory investigation of the data indicates that the nitrile rubber is a more efficient plasticizer followed closely by the ethylene interpolymer. However, it should be recalled that the nitrile rubber does contain some polymeric plasticizer which accounts for the better plasticizing efficiency of this formulation. On the other hand, the ethylene interpolymer and polyurethane are used as the sole plasticizers for the PVC. The former demonstrates a plasticizing efficiency similar to high molecular weight polymeric. The polyurethane would have better performance if it were compounded with a polymeric plasticizer. This may sound contradictory in view of ultimate elongation properties observed for the PVC/polyurethane combination, but it must be remembered that both of these polymers are elastomers. This can be better viewed from Figure 1 which shows a graph of the moduli of the various compounds versus pounds per square inch. The steeper slope of the curve indicates an incompatibility of the polymers. This is quite apparent with the polyurethane indicating that a compatibilizing agent (polymeric plasticizer) should be used for better flexibility. On the other hand, the nitrile rubber would probably not be made any more compatible than it is nor would the ethylene interpolymer. The CPE has the best compatibility of the polymers tried.

## Processing

To carry this comparison further, an analysis of the Brabender viscosities show that the CPE, DOP and polymeric plasticizers have reached an equilibrium in their viscosity, while the polyurethane is still dropping in viscosity indicating that it is still moving into the interstices of the PVC. On the other hand, the increase in viscosities of the nitrile and modified EVA show that they are cross-linking. This implies that CPE and the polyurethane are more compatible as plasticizers with PVC than the other two materials. It is not meant that the ethylene interpolymer and nitrile rubber cannot be used to form an alloy with PVC; they certainly can but they do have limitations compared with the other two. However, this does indicate that CPE and polyurethane are acting as true thermoplastics and thus are probably more compatible with PVC than nitrile or ethylene interpolymer. In other words, they can be more adapted to uses that are in harmony with the type of plasticization accomplished by monomer and polymeric plasticizers.

## Low Temperature

Low temperature properties as expressed by stiffness (modulus of rigidity or  $T_g$ ) conform to a pattern set by CPE, ethylene interpolymer and polyurethane blends. The  $T_g$  of the nitrile rubber blend responds more readily to the presence of polymeric plasticizer than CPE which is relatively unaffected by its presence as observed by its higher hardness and modulus readings. Impact brittleness temperatures are extremely good and only the PVC/nitrile rubber blend fails to measure up to the other three alloys but still excels in impact brittleness resistance when compared with the DOP or the polymeric plasticizer.

It therefore can be seen that some properties are obtainable or unique to certain polymers and the judicious selection of combinations of these polymers with PVC may result in a compound having good plasticizing efficiency coupled with the low temperature properties necessary for a utilitarian compound.

## Permanence

The ability of a plastic to retain as much as possible of its original properties is a measure of its resistance to attack by extractive media such as solvents or other polymers. Extraction tests in oil show the affinity of CPE and the ethylene terpolymer for aromatic oils; the liquid plasticizers, however, are more attracted by the oil than by PVC thus extracting into that medium. Analysis of the tensile retention data reveals that the plasticizing efficiency of CPE and the monomeric plasticizer are more adversely affected by oil than the other systems.

Water extraction is merely a reflection of the residual ionic impurities in the alloys. This can be corrected in the case of CPE by using improved grades developed specifically for wire and cable. Nitrile rubber, on the

other hand, has a serious water growth/absorption problem and little can be done to correct it.

Migration properties are excellent for the PVC alloys; the trace migrations of the CPE and nitrile compounds are probably caused by the polymeric plasticizer but it is a marginal effect. The polymeric plasticizer also performs quite well in this area.

The volatility characteristics of the compounds are all quite good and indicate that a PVC/polymer combination would perform well under conditions requiring resistance to high temperatures (90° and 105°C wire insulation).

## Summary

This work reveals that PVC may be plasticized by means other than standard monomeric and polymeric plasticizers. Coupled with other polymers (or solid plasticizers) and, in some cases, conventional polymeric plasticizers, it offers nonmigrating compounds with outstanding low temperature and volatility characteristics. These are two usually diverse characteristics; one usually being sacrificed at the cost of the other. The use for compounds with these characteristics is endless but it certainly can be concluded that they can broaden the application of PVC in the wire and cable field.

## References

1. W. D. Young, "Formulation and Behavior of Non-Plasticized Flexible Compounds Based on Chlorinated Polyethylene," presented at the 30th SPE Antec (1972).
2. J. P. Tordella, "New Permanent Plasticizer Resins for Polyvinyl Chloride," presented at the 33rd SPE Antec (1975).
3. M. E. Woods, D. G. Frazer, "The Modification of PVC with Powdered Nitrile Elastomers," presented at the 32nd SPE Antec (1974).
4. Hooker Chemicals' Laboratory Report 69-9, "Blends of Polyurethane with Polyvinyl Chloride Resins," 8/15/69.



TABLE I  
PVC ALLOY FORMULATIONS

	<u>A</u>	<u>B</u>	<u>C</u>	<u>D</u>	<u>E</u>	<u>F</u>
PVC (Rel. Visc. 2.30) <sup>1</sup>	50	50	50	50	100	100
Chlor. Polyethylene (CPE) <sup>2</sup>	50	--	--	--	--	--
Nitrile Rubber <sup>3</sup>	--	50	--	--	--	--
Ethylene Interpolymer <sup>4</sup>	--	--	50	--	--	--
Polyurethane <sup>5</sup>	--	--	--	50	--	--
DOP	--	--	--	--	50	--
Polymeric Plasticizer <sup>6</sup>	20	20	--	--	--	60
Epoxidized Soybean Oil <sup>7</sup>	5	5	--	5	--	--
CaCO <sub>3</sub> Filler <sup>8</sup>	--	15	--	--	--	--
Lead Stabilizer <sup>9</sup>	6	6	6	6	6	6
Lubricant <sup>10</sup>	1.5	1.5	1.5	1.5	0.25	0.5

- |   |  |
|---|--|
| 1. PVC 225 (Rel. Visc. 2.30)                  | Tenneco Chemicals, Inc.                    |
| 2. Chlorinated Polyethylene - CPE 4213        | Dow Chemicals, Inc.                        |
| 3. Nitrile Rubber - Hycar 1042                | B. F. Goodrich Chemical Co.                |
| 4. Ethylene Interpolymer - PB 3042            | E. I. du Pont de Nemours Co.               |
| 5. Polyurethane - Rucothane P-53              | Hooker Chemical Co.                        |
| 6. Nuoplaz 6187 - Polymeric Plasticizer       | Tenneco Chemicals, Inc.                    |
| 7. Epoxidized Soybean Oil - Nuoplaz 849       | Tenneco Chemicals, Inc.                    |
| 8. Calcium Carbonate Filler - Atomite         | Thompson, Weinman & Co.                    |
| 9. Dythal -XL (Coated Dibasic Lead Phthalate) | NL Industries                              |
| 10. Lubricants                                | Glyco Chemicals Co. (Acrawax C)            |
|   | Tenneco Chemicals, Inc. (Calcium Stearate) |

TABLE II  
TEST METHODS

Ultimate Tensile Strength ) 100, 200, 300% Modulus ) Ultimate Elongation )	ASTM D-412
Hardness, 10 second delay	ASTM D-2240
Specific Gravity	ASTM D-792
Stiffness (Clash-Berg) T <sub>f</sub>	ASTM D-1043
Impact Brittleness, T <sub>b</sub>	ASTM D-746
Oil Agings (7 days at 70°C in ASTM Oil No. 2)	U.L. 62, Standard for Flexible Cords and Fixture Wires
Water Absorption, Mechanical (7 days at 70°C in distilled water)	U.L. 82, Standard for Thermoplastic Insulated Wires
Volatiles, percent weight loss (7 days in forced air oven at 113°C)	Tenneco Procedure
Brabender Viscosity	Tenneco Procedure

TABLE III  
PERFORMANCE OF VINYL ALLOY COMPOUNDS

	Solid Polymer Plasticizers					
	CPE	Nitrile Rubber	Eth. Int.	P. Urethane	DOP	Polymeric Plasticizer
<u>Physical Properties:</u>						
Tensile Properties:						
100% Modulus, psi	1205	665	880	1435	1300	1300
200% Modulus, psi	1500	980	1405	2255	1450	1550
300% Modulus, psi	1760	1230	1795	2765	1500	1700
Ultimate Tensile Strength, psi	2060	2265	1920	3350	2600	3150
Elongation, %	395	525	340	445	330	350
<u>Hardness, 10 Sec.</u>						
Shore A <sub>2</sub>	85	69	71	86	81	84
<u>Low Temperature Properties:</u>						
Clash Berg - T <sub>f</sub> , °C	-6.5	-16	-11	-5.5	-24	-18
Brittleness, T <sub>b</sub> , °C	<-70	-35	<-70	<-70	-27	-18
<u>Melt Viscosities:</u>						
Brabender Viscosity @ 190°C						
5 Min., M-Gms.	900	1100	1090	910	660	760
10 Min., M-Gms.	860	1400	1060	710	590	690
15 Min., M-Gms.	850	1400	1160	630	540	670
20 Min., M-Gms.	830	1460	1180	600	540	665
<u>Oil Aging, 7 Days @ 70°C</u>						
% Retained Tensile Strength	89.4	110.0	104.6	108.2	100.0	100.0
% Retained Elongation	82.9	101.0	108.1	97.6	75.0	92.8
% Weight Change	4.0	1.6	5.5	-0.4	-8.8	-4.9
<u>Mechanical Water Absorption:</u>						
7 Days @ 70°C						
Weight Gain, mg./inches <sup>2</sup>	4.6	23.3	1.9	2.1	0.35	-0.50
Weight Gain, % by Weight	7.8	46.2	3.7	4.0	0.6	-1.0
Volatiles, % Weight Loss	-0.63	-1.0	-1.89	-2.1	-7.4	-1.5
7 Days @ 113°C						
<u>Migration:</u>						
Polystyrene - 24 hours @ 40C and 1 psi	None	None	None	None	Mars	None
Nitrocellulose - 24 hours @ 40C and 1 psi	Tr	Tr	None	None	Mars	Sl. Mar

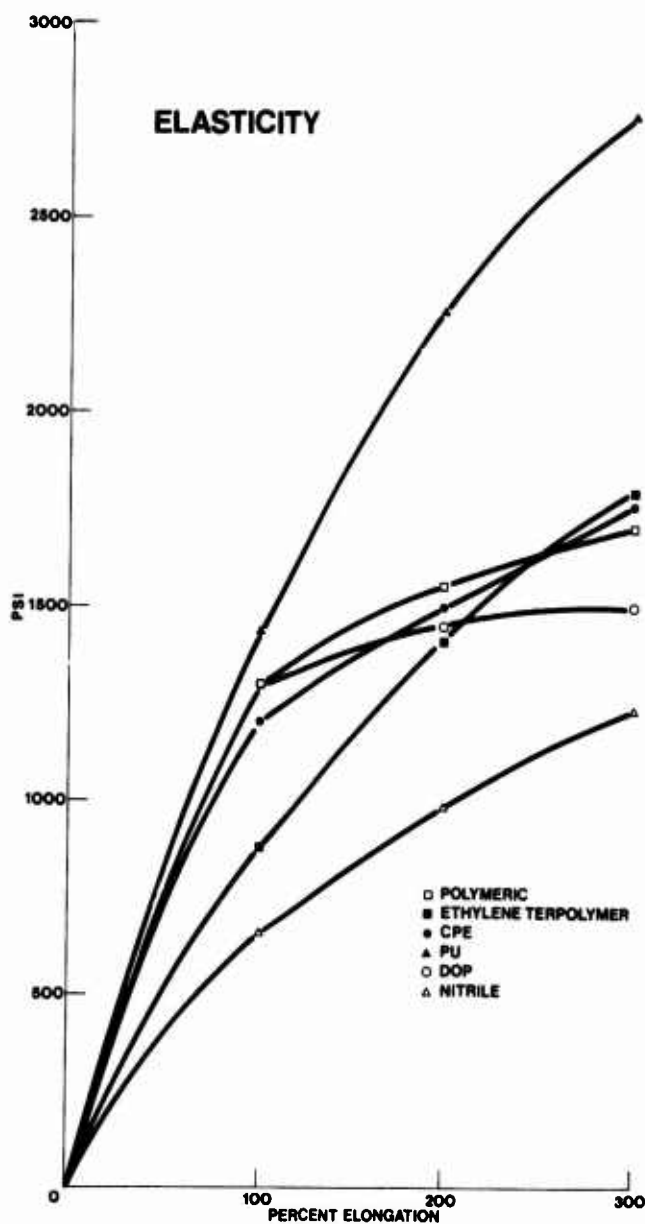


Fig. 1



Fred Roesler  
Tenneco Chemicals, Inc.  
Flemington, New Jersey

Mr. Roesler attended City College of New York where he received a B.S. degree in Chemistry in 1953. He has been associated with the wire and cable industry most of his professional career. His career encompasses direct manufacture of wire and cable plus the development of new compounds. Currently, he is senior chemist for the Flexible Compound Group in Tenneco's Polymer Applications and Development Laboratory. He is a member of the Society of Plastics Engineers.



John McBroom  
Tenneco Chemicals, Inc.  
Flemington, New Jersey

John McBroom is Supervisor of Compound Development for Tenneco Chemicals Organics and Polymers Division. He is responsible for all aspects of compound development and has been with Tenneco for five years. Prior to this he was a principal in a chemical company and group leader of Plastics Intermediates for CONOCO. He holds a B.S. in Chemistry from Oklahoma Central State University and an MBA from Fairleigh Dickinson University. Mr. McBroom holds several patents and has written many papers on PVC formulating. He is a member of the Society of Plastics Engineers.

RHEOLOGICAL AND MECHANICAL PROPERTIES OF A NEW POLYVINYLIDENE FLUORIDE RESIN  
SUITABLE FOR HIGH SPEED WIRE COATING

By J. E. Dohany, K. N. Davis, H. Stefanou

Pennwalt Corporation  
900 First Avenue  
King of Prussia, Pennsylvania 19406

Rheological, viscoelastic and mechanical properties are given for a new grade of polyvinylidene fluoride. The effect of temperature, induced crystallization and electron beam radiation on the physical properties is shown. High speed extrusions on 30 gauge wire without detrimental melt flow effects are demonstrated.

### I. Introduction

Polyvinylidene fluoride under the registered trademark KYNAR® is an electrical insulating material which serves in a variety of applications, including primary insulation on wire used in computers, and as jacketing on aircraft wire and geophysical cable. Polyvinylidene fluoride is used as primary insulation on hook-up wire used in computer back panels because they require not only satisfactory electrical properties, but also exceptional physical toughness of a wire insulation.<sup>1</sup>

In other insulation applications, use of polyvinylidene fluoride heat shrinkable tubing is at present growing rapidly. This non-burning semi-rigid insulation offers superior resistance to most industrial fuels, solvents, and chemicals and is designed for applications requiring high mechanical strength up to temperatures of 175°C. Shrinkable tubing is used for so-called "solder sleeves" since it will not split when shrunk over sharp or irregular shapes. This device is extensively used in the electronic, aircraft, and aerospace industries.

Polyvinylidene fluoride resins presently on the market are being extruded at modest speeds, up to 550 feet per minute. The natural desire of wire and cable manufacturers is to process resins at highest possible speeds in order to achieve an optimum productivity. The purpose of this paper is to present an improved KYNAR® polyvinylidene fluoride grade which will have the added benefit of higher extrusion rates and improved extrudate quality, both of which would greatly increase productivity in polyvinylidene fluoride extrusion.

### II. Experimental

In this study two commercial KYNAR® polyvinylidene fluoride grades (PVDF or PVF<sub>2</sub>), e.g. grades 301 and 881, were compared to a new improved KYNAR® 451. While KYNAR® 881 is polymerized in suspension recipes, grades 301 and 451 are polymerized in emulsion recipes.

Molecular weight determinations were made on a Water Associates Gel Permeation Chromatograph (GPC) Model 200 equipped with Porasil columns operated at 80°C. The solvent was N,N'-dimethylacetamide (DMAC). The GPC column was calibrated with NBS polysty-

rene standards. Each count was the average of three observations and each sample was run in duplicate. The Angstrom number average ( $\lambda_n$ ) and the Angstrom weight average ( $\lambda_w$ ) was computed in standard fashion.

Crystallization kinetics measurements were carried out with a Perkin Elmer Differential Scanning Calorimeter Model 1B. A scan rate of 10°C/min. was used for melting point determinations. The crystallization rate data were obtained by first removing the samples crystalline memory with a heat treatment at 200°C for 10 minutes and then allowing it to cool to the desired crystallization temperature where the sample was thereafter isothermally crystallized. The fraction crystallized, obtained from the cumulative area under the DSC exotherm curve, was plotted versus time. The linear portions of these sigmoidal curves were used to calculate crystallization rate.

Melt flow measurements were made on a Sieglaff-McKelvey Capillary Rheometer using the constant velocity mode of operation at temperatures from 400 to 550°F. A capillary length to diameter ratio of 25 with flat entry was used for flow measurements. Apparent shear rate,  $\dot{\gamma}$ , was calculated as:

$$\dot{\gamma} = \frac{4Q}{\pi R^3} \quad (1)$$

where Q is the melt flux rate and R is the radius of capillary. Shear stress,  $\tau$ , was calculated from:

$$\tau = \frac{PR}{2L} \quad (2)$$

where P is the pressure applied at top of rheometer barrel. The apparent viscosity,  $\eta_a$ , was then obtained from Newton's equation for flow:

$$\eta_a = \frac{\tau}{\dot{\gamma}} \quad (3)$$

Using a computer program the flow data were fitted to the equation of the form of:

$$\log \eta_a = A + B \log \dot{\gamma} + C \log^2 \dot{\gamma} \quad (4)$$

where A, B, C are coefficients of the parabolic function.<sup>2</sup>

Melt fracture determination was made by examining the surface of the extrudate for roughness. The shear stress at which surface roughness occurred on the extrudate is taken as the critical shear stress.

Die swell of the extrudates was measured with a micrometer after they cooled to room temperature. Post extrusion swell, S, was

then calculated from:

$$S = \frac{D}{D_0} \quad (5)$$

where D is diameter of extrudate and  $D_0$  is diameter of capillary.

Melt working experiments were conducted using a C. W. Brabender Plasticorder. A constant charge of 70 g of resin was used and a temperature of 225°C was maintained while roller speeds were varied.

Irradiation of melt pressed samples was carried out by passing them through an electron beam source of  $\beta$  radiation. Dose levels of 5 through 60 megarads (Mrads) were evaluated. The higher dosages were obtained by subjecting the sample to successive 5 Mrad increments until the desired dose levels were obtained. Gel fraction data was obtained by successive extractions of the irradiated samples in refluxing DMAC. The residue was dried at 80°C to constant weight.

Demonstrations of wire coating and wire jacketing were made using processing conditions and equipment normal for polyvinylidene fluoride. For these trials pelletized KYNAR® 301, 451, and 881 were used, i.e. KYNAR® 300, 450, and 880 respectively.

### III. Results

#### 1. General Properties

From the gel permeation chromatograms shown in Figures 1 and 2, it is evident that polyvinylidene fluoride can have a unimodal or bimodal distribution of the molecular weight. KYNAR® 301 and 451 have a bimodal distribution while KYNAR® 881 has a unimodal distribution. The net effect of the significant differences in molecular size distributions is that it greatly controls crystallization, melt flow and crosslinking characteristics of the resin.

Comparison of physical properties is shown in Figure 3. Grade KYNAR® 881 with its unimodal GPC curve is slightly higher in melting point, density and thermal conductivity. Although grade KYNAR® 451 and 301 have a bimodal molecular weight distribution, KYNAR® 451 is higher in Angstrom weight average but lower in melt viscosity and has the highest Angstrom number average. The mechanical and electrical properties are equivalent for all these grades.

The thermomechanical (TMA) properties of polyvinylidene fluoride are reflected in its resistance to penetration. A graph obtained from a Perkin Elmer Thermomechanical Analyzer Model TMS-1 shown in Figure 4 shows a 1 mil penetration temperature of 137°C at a load of 200 g, e.g. 284.4 psig, for KYNAR® 451. The higher 1 mil penetration temperature of 141°C shown for KYNAR® 881 is accounted for by the higher melting point and degree of crystallinity possessed by this grade. This test is supporting evidence for the known excellent cut-through resistance of PVDF coated wires.

#### 2. Crystallization Kinetics

In Figure 5 is shown the Arrhenius plot<sup>3</sup> of crystallization rate versus temperature for the samples.

$$r_{CR} = Ae^{-E/RT} \quad (6)$$

where  $r_{CR}$  is crystallization rate, E is activation energy of crystallization, R is gas constant, and T is temperature. KYNAR® 451 shows slowest rate of crystallization compared to the other samples. The crystallization of polyvinylidene fluoride is obviously very much temperature dependent. Since the total crystallization rates are determined by both nucleation and growth rate then either or both have to be lower for KYNAR® 451 to give the effect shown in the Arrhenius plot. Slower crystal growth and slower nucleation will contribute to less internal stresses in the polymer. The practical implications of this phenomenon should be obvious to the user.

#### 3. Radiation Crosslinking

In 1962 Timmerman<sup>4</sup> has shown that polyvinylidene fluoride can be radiation crosslinked without detrimental effects on physical properties. In Figure 6 are plotted the gel fractions remaining after DMAC extraction as a function of radiation dosage. The data were fitted to the Arrhenius plot:

$$G = Ae^{-B/d} \quad (7)$$

where G is gel fraction, d the radiation dose and A and B are empirical constants. From Figure 6 it is obvious that polyvinylidene fluoride shows a very rapid change in network structure<sup>5</sup> and KYNAR® 451 crosslinks more efficiently than the other two samples. It is known from crosslinking studies on polyethylene that crosslinking efficiency is dependent upon crystallinity and chain length.<sup>5</sup> Therefore our crystallization studies and GPC data suggest that grades 451, 301, and 881 behave in predictable way. That is, the more crystalline and shorter the chain the smaller will be the resulting crosslinking density and vice versa. KYNAR® 451 has the largest Angstrom number average and lowest crystallinity. Hence its highest crosslinking efficiency for non activated systems, e.g. compounds not containing radiation sensitizers.

#### 4. Melt Rheology

In Figure 7 are shown plots of shear rate versus apparent viscosity. As expected the polyvinylidene fluoride melts are non-Newtonian. Two interesting phenomena are observed: (a) the unimodal material, i.e. KYNAR® 881, exhibits very low shear sensitivity up to a moderate shear rate but in general the apparent viscosity shows much larger curvature than the bimodal material; (b) the apparent viscosity of the KYNAR® 451 is lower at any shear rate than grade 301 yet it has bigger Angstrom weight and number averages. The lower melt viscosity is probably

a result of the lower frequency of entanglements. Grade 451 has much higher weight fraction of the high molecular weight spike than grade 301. It therefore has not only a much larger proportion of large molecules but even larger portion of short molecules. Rudd suggested that the function of these latter would presumably be to facilitate molecular disentanglements by separating the larger polymer molecules acting as high molecular weight plasticizers.<sup>6</sup>

The temperature dependence of the apparent viscosity,  $\eta_a$ , follows a simple Arrhenius type equation:

$$\eta_a = A e^{\Delta E/RT} \quad (8)$$

where R is the gas constant, T is the absolute temperature and  $\Delta E$  is the activation energy. The coefficient A depends upon the reference temperature and  $\Delta E$  depends upon structural and composition variables of the polymer.<sup>7</sup> In Figure 8 are shown these Arrhenius plots for all three samples. KYNAR® 451 has the lowest activation energy for flow and is least sensitive to temperature change. We interpret these results with the presence of large number of molecules below the critical molecular weight of entanglement. Therefore KYNAR® 451 has an elastic entanglement network that is more easily deformed than that of the other samples.

#### 5. Quality of Extrudates

The presence of hydrodynamic instability in the extrusion of polymer melts is a problem in the processing of polymers.<sup>8</sup>

At lower shear rates polyvinylidene fluoride extrudates are smooth. At moderately high rates of shear irregular elastic recovery results in surface roughness. Often the term "rippling" is applied to this sort of roughness. In extreme it may amount to a very "knotty" appearance.

At high shear rates the extrudates are characterized by an appearance of surface tearing. Variations in the shape, regularity and depth of the tearing lead to a range of melt fracture. Terms used for this type of roughness are: "shark skin" or "scale" or "screw". We found that the surface tearing (Figure 9) occurs at characteristic critical shear stresses during the extrusion of various polyvinylidene fluoride grades. KYNAR® 451 has the highest critical shear stress of all polyvinylidene fluoride samples.

Tearing on fracture results from the large amount of deformation imposed in the approach to the capillary. As a result of the slow relaxation times relative to the deformation rates, the stress exceeds the strength of the polymer and a fracture results.<sup>9</sup>

#### 6. Post Extrusion Swell

Further evidence for improved melt flow of KYNAR® 451 is shown in Figure 10. The plot of shear stress versus die swell show that as expected the die swell increases with

shear stress at the die wall. Graessley et al. using rubber elasticity theory showed that die swell is due to elastic recovery of the material.<sup>10</sup>

Qualitatively we propose that lower die swell of grade 451 is related to the presence of relatively large amount of shorter molecules which facilitate molecular disentanglements and thus act as high molecular weight plasticizers. The net result is that the normal stresses in the melt may be smaller than those observed for the other two grades. The die swell ratio for grade 881 is intermediate because unlike grade 451 it has a unimodal distribution and is less resistant to viscoelastic strain which upon die exit is manifested in greater swell ratio. On the other extreme is grade 301 which has a bimodal distribution like grade 451 but does not have enough short chain molecules to "lubricate" the flow. The result is high elastic deformation with less relaxation manifested in the higher die swell.

#### 7. Extrusion Simulation

The Brabender Plasticorder was used to simulate extrusion at varying levels of shear. From the decay in the torque-residence time curves, the effect of melt working on KYNAR® 451 and KYNAR® 301 could be seen.

Figure 11 shows that KYNAR® 451 is only slightly affected by varying levels of shear, while KYNAR® 301 shows a greater change. The absolute values of the torque readings along with the change in torque as a result of increased roller speeds are direct indications that KYNAR® 451 experiences less shear degradation. A significant consequence of this phenomena is the fact that screw designs and processing condition currently suitable for grade KYNAR® 301 are more than adequate for KYNAR® 451.

Melt working of the samples in the Brabender Plasticorder correlates with observations made with the capillary rheometer. KYNAR® 451 is much more easily disentangled than KYNAR® 301, hence, reaches an "equilibrium" torque much faster to achieve a state of uniform melt. The practical implication from these observations should be obvious, e.g. KYNAR® 451 should require less shear history by the extruder screw than KYNAR® 301. We believe, therefore, a gradual transition screw usually used for extrusion of polyvinylidene fluoride resins should be even more efficient with KYNAR® 451 and the torque, i.e. horsepower requirement would be lower. Therefore a saving in operating cost or increased output is potentially possible.

#### 8. Extrusion of Wire Coating and Wire Jackets

"Proof of Performance" trials in the field demonstrated that the improved vinylidene fluoride polymer has potential for extrusions at higher rates than common for polyvinylidene fluoride resins.

Polyvinylidene fluoride grades KYNAR® 450 and 300 were blended with a color concentrate in 20:1 let down ratio and pressure extruded in two different 30 AWG computer



wire setups. The first setup (Section A on Figure 12) involved a short crosshead die used with other thermoplastic resins. The second setup (Section B on Figure 12) involved a long crosshead die normally used with KYNAR® polyvinylidene fluoride.

With the short crosshead die extrusion rates of 600-1100 feet per minute were achieved with KYNAR® 450 (Section A on Figure 12). The insulation was smooth at 600-650 feet per minute extrusion rate, however, at the 1100 feet per minute rate it became as rough as KYNAR® 300 did at 400-450 feet per minute.

On the crosshead die for polyvinylidene fluoride (Section B on Figure 12) KYNAR® 450 was run at maximum line speed (550 fpm). From processing standpoint KYNAR® 450 was equivalent to KYNAR® 300 but showed superior insulation resistance.

The MIL W 22759/13-15 FEP coated 22 AWG stranded wire was jacketed with KYNAR® polyvinylidene fluoride (see Figure 13). Signs of melt fracture appeared even at low throughput (200 fpm) with KYNAR® 800. KYNAR® 450 extruded at the maximum (550 fpm) that the take-up would allow. No melt fracture appeared. With KYNAR® 300 the highest line speed attainable without fissures in the jacket was 500 fpm. Insulation resistance of the wire jacketed with KYNAR® 450 was superior to the control, i.e. KYNAR® 300.

An insulation consisting of a .003 inch extrusion coated jacket of KYNAR® 450 over .032 inch crosslinked polyethylene on 16 AWG passed the UL 83 vertical flame test (Figure 14). Thus coating polyethylene with polyvinylidene fluoride brought the flame resistance of the insulation above the threshold of acceptability for the above test. Abrasion resistance of the construction was also greatly improved by the application of a KYNAR® 450 jacket.

In test extrusions for thin wall tubing (Figure 15), which is akin to the jacket extrusion KYNAR® 450 exhibited the smallest axial shrinkage.

The excellent performance of KYNAR® 450 in jacket and thin wall tubing extrusion is related to the excellent viscoelastic properties of its melt.

#### IV. Conclusions

By careful control of the molecular weight and molecular weight distribution an improved polyvinylidene fluoride grade KYNAR® 451 results, which as we have shown, is a superior material for extrusion applications. It has excellent physical characteristics and melt flow characteristics and can be efficiently crosslinked to enhance its physical properties.

The user should have the added benefit of higher extrusion rates and improved quality of the extrudate which greatly would increase productivity of the operation.

#### V. Acknowledgements

The authors wish to thank Messrs. O. Odhner and E. Derowski of the Plastics Technical Service Laboratory of the Pennwalt Corporation for the extrusion of wire coatings and jackets in the field and for the data on these experiments.

#### References

1. J. E. Dohany, A. A. Dukert, S. S. Preston, Enc. Polym. Sci. and Tech., John Wiley & Sons, Inc., 14, 600 (1971).
2. D. Grant, S. Dieckmann, J. Appl. Polymer Sci., 9, 3231 (1965).
3. L. Mandelkern, "Crystallization of Polymers", McGraw-Hill Book Company, New York, 1964.
4. R. Timmerman, W. Greyson, J. Appl. Polymer Sci., 6 (22), 456 (1962).
5. A. Charlesby, "Atomic Radiation and Polymers", Pergamon Press, 1960.
6. J. F. Rudd, J. Polymer Sci., 44, 459 (1960).
7. R. A. Mendelson, in "Computer Programs for Plastics Engineers", Ed. I. Klein and D. I. Marshall, Reinhold Book Corp., p. 117, 1968.
8. L. V. McIntire, J. Appl. Polymer Sci., 16, 2901 (1971).
9. J. P. Tordella, J. Appl. Phys., 27, 454 (1956).
10. W. Graessley, S. Glasscock, R. Crawley, Trans. Soc. Rheo., 14, 519 (1970).



Dr. Julius E. Dohany

Group Leader, Research and Development, Technical Division, Pennwalt Corporation. He has the Masters degree in Chemical Engineering from the Budapest Technical University in Budapest, Hungary and the Doctor of Technical Sciences degree from the Swiss Federal Institute of Technology in Zurich, Switzerland. In 1964 he joined Pennwalt and since then is involved in polymer research and development activities.



Kenneth N. Davis

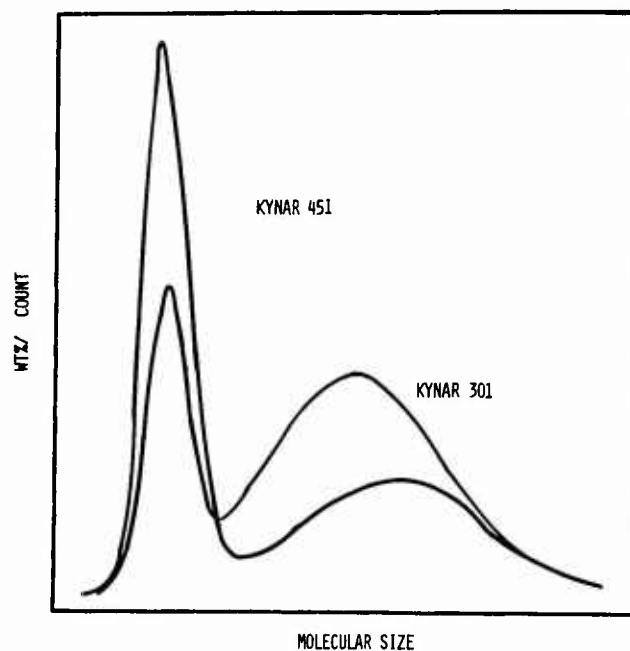
Research Chemist, Research and Development, Technical Division, Pennwalt Corporation. He has a B.Sc. degree in chemistry from Lincoln University in Oxford, Pa. Prior to joining Pennwalt, he worked at the Edgewood Arsenal in Maryland as a chemist. He joined Pennwalt in 1968 and since then he is involved in polymer research and development projects.



Dr. Harry Stefanou

Senior Research Chemist, Research and Development, Technical Division, Pennwalt Corporation. He has a B.Sc. degree in chemistry from City College of New York, N. Y. and a Ph.D. degree from City University of New York, N. Y. Prior to joining Pennwalt, he was a postdoctoral research associate with the Princeton University. In 1973 he joined Pennwalt and is involved in polymer research and development projects.

FIGURE 2. GPC CURVES FOR KYNAR 301 & 451



PHYSICAL PROPERTY DATA  
POLYVINYLIDENE FLUORIDE RESINS  
Figure 3

PROPERTY	UNIT	GRADE 451	GRADE 301	GRADE 881	METHOD
<b>PHYSICAL PROPERTIES</b>					
Melting Point	°C	156	156	166	DEC
Density	g/cc	1.757	1.759	1.783	ASTM D-792
Refractive Index	25°C, 589 mμ	1.41	1.41	1.41	
Melt Viscosity	Poise, 100 sec-1	2.8x10 <sup>4</sup>	3.5x10 <sup>4</sup>	2.8x10 <sup>4</sup>	Seiglaiff McKelvey
<b>MECHANICAL PROPERTIES</b>					
Tensile Yield	psi	6200	6400	6400	ASTM 1708u
Tensile Break	psi	4900	9000	9000	ASTM 1708
Elongation at Break	%	250	260	250	ASTM 1708
<b>THERMAL PROPERTIES</b>					
Conductivity	g cal cm / cm <sup>2</sup> sec °C	0.24x10 <sup>-3</sup>	0.25x10 <sup>-3</sup>	0.27x10 <sup>-3</sup>	DuPont Tester M-12
Coefficient of Expansion	in/in/°C	1.8x10 <sup>-4</sup>	1.37x10 <sup>-4</sup>	1.37x10 <sup>-4</sup>	
Specific Heat	cal/g °C	0.293	0.285	0.301	TMA DEC
<b>ELECTRICAL PROPERTIES</b>					
Volume Resistivity	ohm-cm, 73°C	2x10 <sup>14</sup>	2x10 <sup>14</sup>	2x10 <sup>14</sup>	Keithly Electrometer
Dielectric Strength	V/mil, 125 mil	260	260	260	ASTM D-149

FIGURE 1. GPC CURVE FOR KYNAR 881

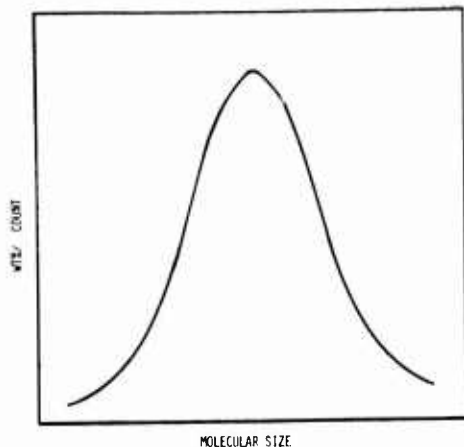


FIGURE 4. THERMOMECHANICAL ANALYSIS

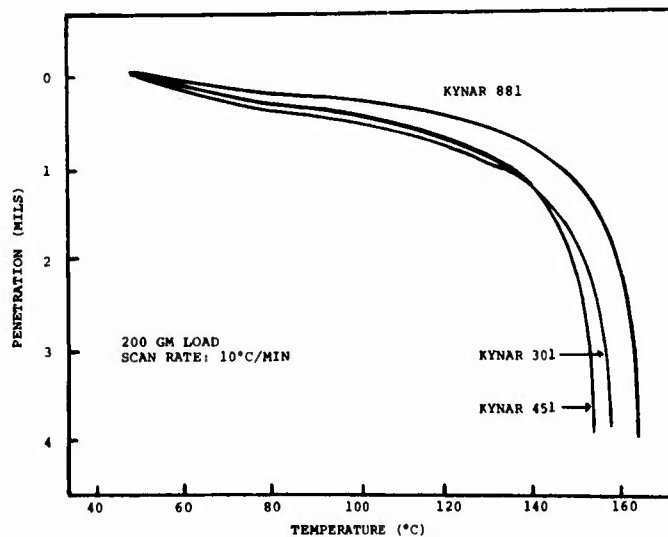


FIGURE 5. ARRHENIUS PLOTS OF THE CRYSTALLIZATION KINETICS

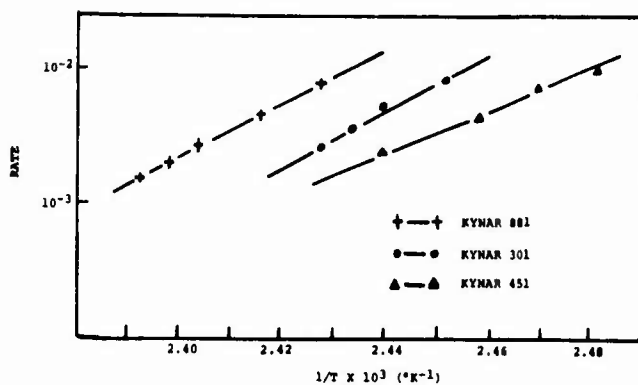


FIGURE 8. ARRHENIUS PLOT OF MELT VISCOSITY<sup>1</sup> VS. TEMPERATURE

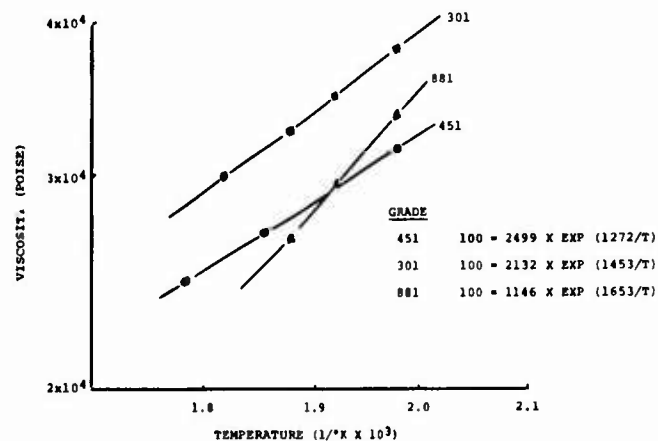


FIGURE 6. RADIATION OF POLYVINYLIDENE FLUORIDE

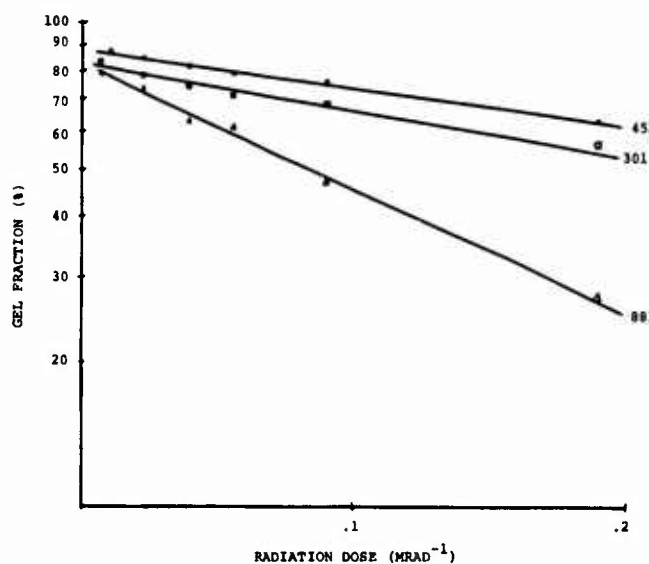


FIGURE 9. STRESS-SHEAR RATE PROFILE

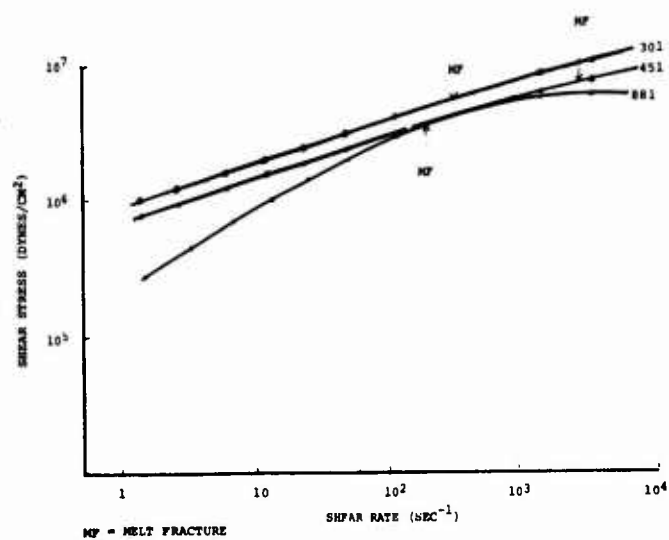


FIGURE 10. CAPILLARY RHEOMETRY - DIE SWELL VS. SHEAR STRESS

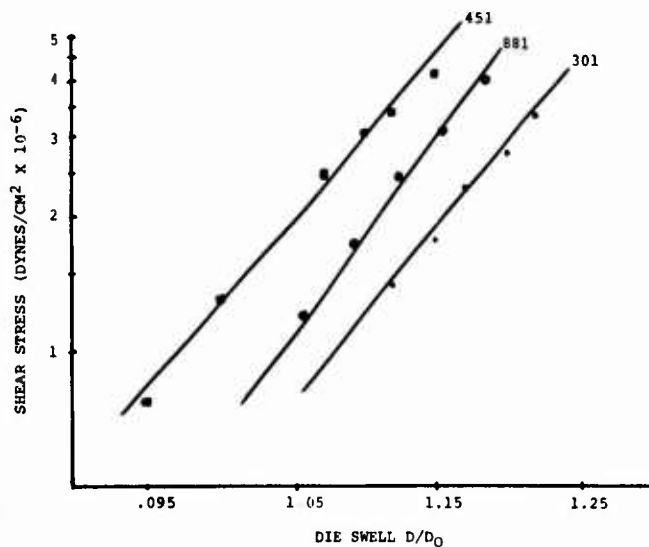
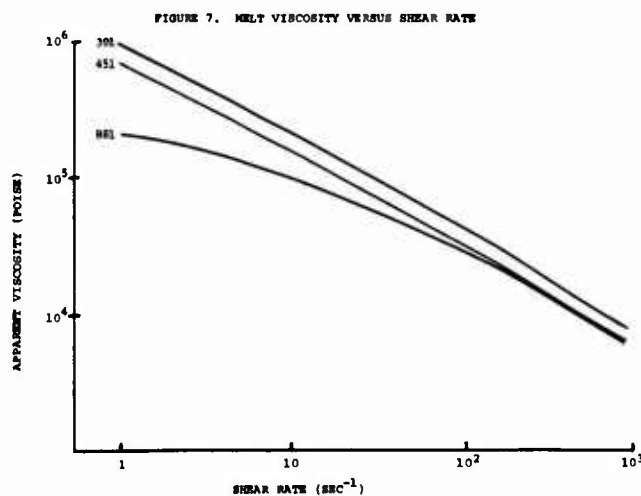


FIGURE 11. EFFECT OF MELT WORKING PVDF IN THE BRABENDER

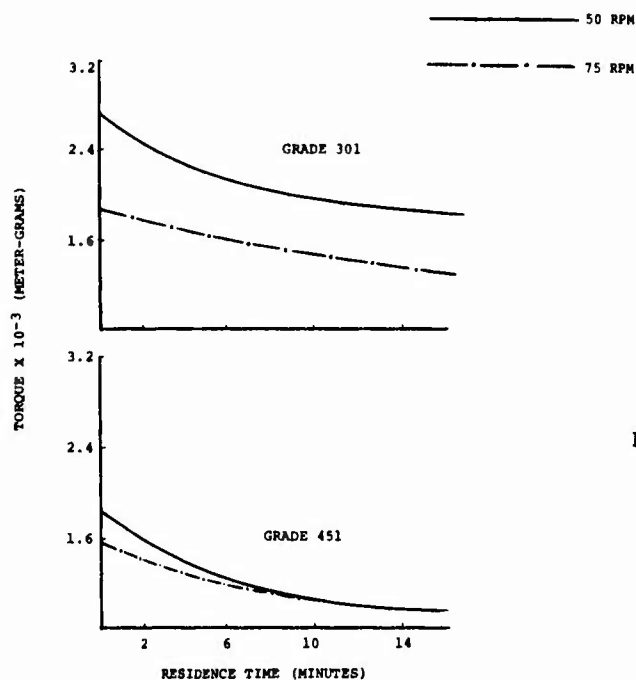


FIGURE 12. INSULATION RESISTANCE ON 30 AWG WIRE INSULATED WITH PVDF (UL1422-23)

A. SHORT CROSSHEAD DIE USED WITH OTHER THERMOPLASTICS				
GRADE	EXTRUDATE RATE (FT/MIN)	INSULATION RESISTANCE (MOHM/1000 FT)	PIGMENT COLOR	COATING SURFACE
KYNAR 300	200	~50	YELLOW	SMOOTH
KYNAR 450	600	1725	GREEN	SMOOTH
KYNAR 450	650	1725	GREEN	SMOOTH
KYNAR 450	1100	1350	GREEN	ROUGH

B. NORMAL CROSSHEAD DIE FOR KYNAR PVDF				
GRADE	EXTRUDATE RATE (FT/MIN)	INSULATION RESISTANCE (MOHM/1000 FT)	PIGMENT COLOR	COATING SURFACE
KYNAR 300	550	893	GREEN	SMOOTH
KYNAR 450	550	1260	GREEN	SMOOTH

FIGURE 13. KYNAR JACKETING ON FEP 22 AWG STRANDED WIRE (MIL SPECIFICATION W-22759/1-15)

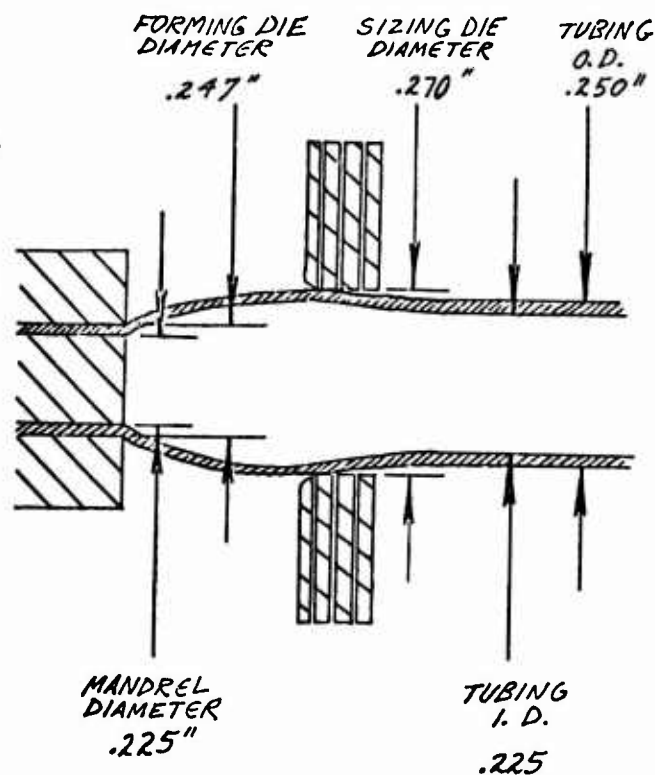
GRADE	<sup>1</sup> EXTRUDER SCREW (RPM)	OUTPUT RATE (FT/MIN)	CONE LENGTH (INCH)	CONDITION OF JACKET
450	13.5	200	1.75	SMOOTH
450	14.0	300	3.50	SMOOTH
450	40.0	550	6.00	SMOOTH
300	41.5	500	1.00	SMOOTH
300	43.5	550	3.50	FISSURES
880	14.0	200	1.00	MELT FRACTURE

<sup>1</sup>DIE TIP TEMPERATURE = 700-800°F  
EXTRUDER MOTOR POWER = 6.5-9.5 AMPS

FIGURE 14. FLAMMABILITY TEST ON CROSSLINKED POLYETHYLENE 16 AWG WIRE (UL STYLE 3272) JACKETED WITH KYNAR GRADE 450

	NOT JACKETED	JACKETED GRADE 451
FLAME TEST UL 83	FAILED INDICATOR BURNED 25%	PASSED
ABRASION TEST	0.41% WT. LOSS (30 MINUTES)	0.12% WT. LOSS (30 MINUTES)
OXYGEN INDEX ON PRIMARY INSULATION	26.9	N/A

FIGURE 15. EXTRUSION OF PVDF FOR THIN WALL TUBING



SHRINKAGE DATA (290°F, 16 HRS)

GRADE	SHRINK RATIO
450	1.0
300	5.8
880	6.8

# FULLY-FILLED TELEPHONE CABLE WITH CELLULAR POLYETHYLENE

## INSULATION AFTER 10 YEARS SERVICE

by

J. Pritchett

British Post Office

Wembley, Middlesex, U.K.

E.L. Mather

S. Verne

BICC Telecommunication Cables Limited  
Prescot, Merseyside, U.K.

BICC Research & Engineering Limited,  
London, U.K.

### Abstract

The experience of the British Post Office with fully-filled telephone cables, since their introduction ten years ago, is reviewed. The original technical and service objectives are re-examined and the extent to which they have been realised is considered. A cable examined after ten years in service shows transmission characteristics well within the current specification. The cellular insulation has substantially unchanged permittivity, excellent mechanical properties and very good resistance to ageing.

### 1 Introduction

#### 1.1 General

Since 1968 the British Post Office (BPO) demands for the supply of new local distribution cables have been met exclusively by the purchase of the fully-filled type. This Paper traces the course of the development which led to the adoption of fully-filled cables as a standard provision and reports on the present condition of one of the very first of these cables which was manufactured in 1964. This cable was recovered for examination and assessment in 1975 after having given some 10 years of satisfactory service in Plymouth, England.

#### 1.2 British Post Office Local Networks

In the United Kingdom there are over 6000 local exchanges (central offices), each with its own cable network. In order to allow for proper provision of service with the minimum of capital outlay, flexibility cabinets are installed at various points. These form the interface between the main network\* which radiates from the exchange and the distribution network\*\* which connects the cabinets to the various subscribers.<sup>1</sup> The cables of the main network range in size from 4800 to 100 pairs, while those of the distribution network range from 100 to 2 pairs.

For many years all local network cables used copper conductors insulated with lapped paper and were sheathed in lead. Mostly, these were laid in ducts to enable additions to be made from time to time to allow for growth, but some, particularly those in rural areas, were attached to poles as aerial cables.

\*Sometimes known as the primary network

\*\*Sometimes known as the secondary network

#### 1.3 Introduction of Plastics

With the introduction of plastics in commercial quantities in the late 1950's it became possible to adopt extruded polyethylene in place of lead as the sheathing material and solid polyethylene instead of paper for the conductor insulation. The first all-polyethylene cables were introduced into the distribution networks in 1948 on a trial basis.

Later on, the use of polyethylene was extended to the cables of the local main network and for these a sheath of natural polyethylene bonded to a thin aluminium foil to act both as a moisture barrier<sup>2</sup> and an electrical screen was adopted in place of lead. Solid polyethylene was introduced for conductor insulation but its use was originally confined to terminating lengths because it was more expensive than the paper equivalent. The development of cellular extrusion techniques overcame this difficulty and allowed cellular polyethylene to compete directly with paper for intermediate lengths of cable as well.

Subsequently pressurisation systems were installed in the local main networks to give these cables a measure of protection against the ingress of moisture in the event of sheath damage. However, it was not practicable to pressurise the cables beyond the flexibility cabinets and thus this form of protection was not extended to the cables of the distribution network.

#### 1.4 Experience with All-Polyethylene Cables

When the all-polyethylene cables were first installed in the distribution networks the field reaction was extremely favourable. Apart from the obvious saving in weight which eased the handling problem, it was apparent that terminations were simpler to make and that wires would be more easily manipulated at jointing points. It was realised that the polyethylene sheath would be free from the corrosion hazard and it was expected that, in contrast to paper, the polyethylene insulation would give immunity from low insulation troubles in the event of ingress of water.

The obvious toughness of the polyethylene sheath suggested that direct burial by trenching or mole-ploughing would be practicable and this policy was adopted in situations where further growth was unlikely—for example, for the small cables on

housing estates. The installation of new ducts thus became unnecessary and the consequent savings on capital outlay more than offset the extra cost of the all-polyethylene cables which were at that time more expensive than their paper/lead equivalents. Production was increased progressively until they entirely superseded the paper/lead cables for the local distribution network in 1960.

As field experience with these cables grew, it soon became apparent that the handling, terminating and manipulating advantages were outweighed by increased maintenance problems caused by sheath damage in a wet situation. In these circumstances water entered the cable and travelled towards the lowest point in the route to cause a fault wherever it encountered exposed conductors. Fault location by conventional electrical means — a simple operation with a paper/lead cable — thus became impossible because the position of the sheath damage was remote from the site of the fault as determined electrically.

Exposure of the conductors was attributable partly to imperfections or pinholes in the polyethylene insulation and partly to the method of jointing. The situation was eased by improving the quality of the polyethylene extrusion over the conductors during manufacture and by modifying the joints. A sealing arrangement using a wax or resin compound was developed for installation at the extremity of each joint and adopted as standard in 1955. These in situ seals were successful in isolating the joints from the cable and although they were costly to install the fault rate dropped significantly. However, the provision of these seals did nothing to prevent the ingress of water at points of sheath damage and many cables remained partly or wholly waterlogged but serviceable. In due course a proposal to incorporate water blocks into the cables themselves at regular intervals of 20 metres during manufacture was adopted and again some improvement resulted. These discrete blocks caused manufacturing difficulties and occasional jointing problems but nevertheless they eased the fault location problem.

A special survey made over the period June 1957 to July 1959 showed conclusively that the main source of trouble on these new distribution cables was sheath damage caused by digging or the pressure of sharp stones — troubles brought about directly by the abandonment of ducts and the use of direct burial techniques. Furthermore, it was realised that improvement in extrusion quality of polyethylene and the provision of water blocks were doing nothing to prevent the ingress of water to the cables but were merely ways of restricting its flow after entry. The concept of a waterlogged cable system was clearly unacceptable and various solutions were investigated. Among these were: a reversion to the use of ducts, the adoption of armouring, and extension of the air pressurisation system then being installed in the local main network cables.

### 1.5 The Advent of Fully-Filling

The novel but subsequently widely accepted solution to this problem was in retrospect remarkably simple, ingenious in concept and effective. It provided for a continuous and complete filling of the cable core with petroleum jelly thus rendering it completely waterproof and unaffected by sheath damage in a wet situation. The use of cellular polyethylene instead of solid polyethylene for the conductor

insulation allowed the original wire-to-wire capacitance to be retained, without increasing the overall diameter of the cable<sup>4</sup>.

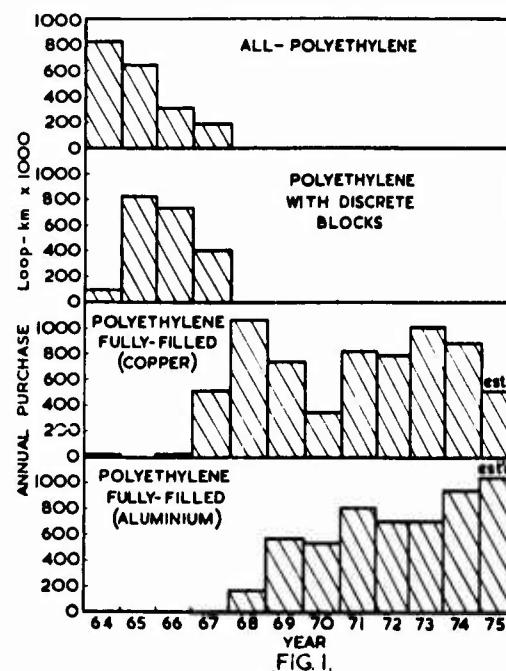


FIG. 1  
THE CHANGING PATTERN OF PURCHASE  
ANNUAL POST OFFICE PURCHASE OF  
DISTRIBUTION NETWORK CABLES

So came the fully-filled cable of the kind made in 1964 and installed at Plymouth. These cables were rapidly accepted by the field force despite the presence of the petroleum jelly and the consequent slight inconvenience in handling the wires for jointing and terminating. Maintenance problems were at once lessened and the incidence of imperfections in the cellular polyethylene insulation became a comparatively unimportant matter. During the course of the progressive development which followed various detailed changes were made in the manufacturing techniques but the basic design concept remained unaltered. General adoption of the fully-filled technique involved the modification of many factory plants and by 1967 the U.K. manufacturers were in a position to supply substantial quantities to the BPO. Since that time the entire annual demand for distribution cables has been met by the supply of fully-filled cables. In 1968 EC grade aluminium began to replace copper as the conductor<sup>5,6,7,8</sup> and in 1973 this was itself superseded by aluminium alloy<sup>9</sup>. Fig. 1 shows how the purchasing pattern has changed over the last 10 years.

## 2 Original Design Considerations

### 2.1 Environmental Conditions

The 1964 cable was designed for direct burial. The temperature conditions in soil in N.W. Europe had been known from a recent study by Schulze<sup>10</sup>. This made clear that at the depth of about 0.6 m the



daily temperature cycle was already completely attenuated (daily amplitude less than 2% of that on the surface). The annual cycle, (i.e. the cycle of daily or monthly averages) attenuated more slowly with phase delay, at this depth, of about a fortnight. It was inferred that in the United Kingdom, the temperature of a buried cable would never exceed 20°C or fall below 3°C. This was subsequently confirmed by Mochlinski's comprehensive study<sup>11</sup> of soil conditions in the U.K.

Only the short cable lengths in terminations above ground would be exposed to higher temperatures and the original requirement was that the resistance to ageing of the insulation of the fully-filled cable should be at least as good as that of the all-polyethylene cables in use at that time.

## 2.2 Waterproofness

By the time the 1964 fully-filled cable was designed, the BPO had carried out extensive moisture permeation tests on all-polyethylene cables. The amount of moisture which would diffuse through a polyethylene sheath, throughout the service life, was quite small and formation of saturated atmosphere inside the cable was prevented by the desiccant properties of a paper wrapping over the core. For the local main cables, the aluminium foil barrier bonded to the sheath virtually eliminated moisture permeation. For local distribution cables, which had no such barrier, the already reduced danger of condensation from moisture-containing air was eliminated by replacing the air between various cable components with a filling compound. Moreover, while condensing moisture in the all-polyethylene cables could produce short circuit paths between pinholes in the insulation of neighbouring conductors, this could not occur at all when the interstitial spaces were filled. It was further intended that in case of water entering through a faulty joint or sheath damage, the effect on the transmission characteristics should be minimal. The filling compound was intended to provide two mechanisms of protection: one, of preventing water from propagating along the cable through spaces between the core bundle and the sheath and the other, of preventing water from penetrating radially into the core bundle, and into interstitial spaces between insulated conductors, where its effect would be to change the mutual capacitance and other transmission characteristics. Of these two objectives, the latter has been found to be the more important: that a fully-filled cable should continue to function with substantially unchanged characteristics even if water gained access to the core bundle through multiple damage to the sheath. A theoretical possibility of moisture condensing in the gas cells of the insulation was also considered. A summary of these early considerations is included in Table 1.<sup>12</sup>

## 2.3 Filling Compound

The original design considerations required that the filling compound should have a low permittivity (its lowest achievable for a liquid or solid being a little in excess of 2), and a low loss tangent, below 0.001 if possible, at audio frequencies. It was essential that the compound should have sufficiently low surface tension to wet the surface of polyethylene, but that it should not cause cracking or other damage to the polyethylene insulation. There were also mechanical requirements that the compound should not become excessively hard at

the minimum temperature or excessively fluid at the maximum temperature of the range within which the cable was to be used. The compound had to be hydrophobic, and its dielectric and other physical properties had to remain unchanged on contact with water. Finally, there was one other basic requirement. The compound had to be very safe in handling, which meant freedom from toxic and dermatological hazards. These design requirements appeared to be met by commercially available grades of pharmaceutical petroleum jelly. The British Pharmacopoeia identified two grades: White Soft Paraffin and Yellow Soft Paraffin. The two grades had the same melting range, 38° to 56°C, which was considered lower than technically desirable but acceptable, and were very similar in most properties. The white petroleum jelly (or White Soft Paraffin) was more highly refined and because of this, more susceptible to oxidation. The yellow petroleum jelly (or Yellow Soft Paraffin), which was selected for use in cables, had the valuable property of high resistance to ageing and was cheaper.

## 2.4 Insulation

The polyethylene compound for cellular insulation had to comply with various extrusion processing requirements. In addition, importance was attached to insulation toughness; resistance to cracking and high elongation at break. The latter characteristic, which arises from a combination of material properties and extrusion conditions has proved to be important because it has been observed that insulation with highest initial extensibility showed least change on ageing. The medium density polyethylene compound selected, met the original requirements and showed relatively little swelling with good retention of properties on prolonged contact with the filling compound. The polyethylene contained a nominal 0.1% of a phenolic stabiliser, but its resistance to oxidative ageing was greatly increased by contact with the filling compound<sup>13</sup>. In the concept of the cellular structure it was recognised at the time, though not achieved in the 1964 cable, that it was preferable to have many small cells rather than fewer large ones. A fine cellular structure was thought to give a better chance of being free from pinholes, it was less prone to the propagation of cracks, offered the best balance of low permittivity and good mechanical properties and, theoretically, the smaller the cells the less likely it was that moisture condensation could cause problems.

## 2.5 Compatibility of Insulation and Filling Compound

At the time when the first fully-filled cable was being manufactured in 1964, it was a novel idea to design a high-reliability, long-life engineering product from two components, polyethylene and petroleum jelly, which were known to interact. It was known that above 90°C the polyethylene insulation would dissolve in the filling compound and that at lower temperatures the polyethylene would absorb the filling compound and gradually swell to an equilibrium value dependent on the temperature. The two materials were described as compatible in the classical meaning of the word; capable of co-existing, although each was affected by being in contact with the other. It was ascertained that, at cable service temperatures, the insulation would swell to an acceptable equilibrium value, its mechanical properties of hardness, tensile strength and extensibility would change to a very small extent only and there would

Table I

Possible Modes of Failure of Fully-Filled Cables for the Local  
Distribution Network as Considered by the British Post Office in 1964

Mechanism	Effect	Prevention	Remarks	BPO Experience and Subsequent Experimental Results
SHORT TERM				
Interaction between filling compound and polyethylene insulation and/or sheath	(a) Excessive swelling of insulation leading to dimensional instability (b) Cracking of insulation (c) Softening of sheath (d) Cracking of sheath	(a), (b), (c) and (d) prevented by selection of materials and introduction of compatibility tests into the specification	(c) & (d) preventable by using a bonded foil or any other suitable barrier	No record of field failures due to these causes. Changes in dimensions and mutual capacitance negligible even after 16 months at 55°C <sup>14</sup>
Water ingress into poorly filled cable.	Increase in attenuation	Safeguard QA test for percentage fill and resistance to water penetration	For similarities and differences with unfilled cables cf. Section 2.2	No record of failures
MEDIUM TERM				
Diffusion of oil fraction of petroleum jelly through sheath into surrounding soil, leaving incompletely filled cable	Moisture gradually entering unfilled spaces with slow increase in inter-wire capacitance. Partial loss of fully-filled protection against water.	If necessary, use of bonded metal foil sheath or any other suitable barrier	In U.K. conditions (wet soil, normal temperature span 5-15°C) not thought to be a problem within 40 years. BPO advise overseas administrations with hot, dry, dusty soil to use bonded foil moisture barrier	Extent of diffusion into a dry, highly absorbent Arizona dust, in 16 months at 55°C reported <sup>14</sup>
LONG TERM				
Saturation of gas cells in insulation with water vapour followed by temperature cycling leading to accumulation of liquid water in cells	Increase in mutual capacitance	In the unlikely case of this mechanism taking place under extreme conditions of humidity and temperature cycling use bonded metal foil barrier	BPO does not use moisture barriers in local distribution cables	No record of failures due to this cause
Migration of oil fraction of petroleum jelly into gas cells of insulation	Gradual increase in mutual capacitance and removal of compound from inter-wire spaces leaving incompletely filled cable	Not known whether 100% preventive measure possible. Avoid high-oil content petroleum jellies		No sign of this effect at 55°C over a period of 16 months <sup>14</sup>

\* The consequences of this mechanism, if it occurred, would be minimal. In the United Kingdom a buried cable experiences one annual temperature cycle of range 5 - 15°C and not exceeding 3 - 20°C. The maximum weight of water precipitated in the cells of cellular insulant depends on the volume of the cells per length of cable and the difference between the saturation of air at 20° and 30°C. For a 100 pair cable with 0.5 mm diameter conductors, made to BPO specification CW 1128, the total volume of insulation per 1000 m is about 0.09 m<sup>3</sup>. With the partial volume of gas cells of 0.3 saturated with moisture at 20°C, the amount of moisture precipitated on cooling to 3°C would be 0.3 cm<sup>3</sup> or 3.3 ppm of insulation. This is much less than the likely variations in the moisture content of polyethylene itself. Even if each temperature cycle could add a further 0.3 cm<sup>3</sup> of water, the total, after 40 cycles, of 132 ppm of insulant would be too small to produce cable changes at audio frequencies. In fact, however, a structure of small non-intercommunicating cells precludes a cumulative mechanism. The moisture may not even condense on cooling in a small cell for lack of nucleation. If it does condense, it will remain as a thin film or a tiny water meniscus and will re-evaporate when the temperature increases. The increase of water content in the cell on successive cycling should be nil.

be no tendency for the insulation to crack. Moreover, swelling of the insulation would have little effect on either the mutual capacitance or the degree of interstitial filling, because both the permittivity and the specific volume of the petroleum jelly filling compound were similar to those of polyethylene. The manufacturing process was scrutinised to confirm that there was no risk of overheating the polyethylene insulation/petroleum jelly system. The compatibility was checked over a temperature range which was far wider than that to be expected for a buried cable in service.

## 2.6 Consideration of Possible Modes of Failure

In 1964 the BPO considered various possible modes of failure of the fully-filled cable. Table I lists these considerations, indicating in each case the possible mechanism of failure, the effect on the cable, and the means of prevention. An outline of subsequent experience is also included.

## 3. Developments and Experience in use in Local

### Distribution Networks

### 3.1 Cables

The early fully-filled cables were designed to cater for the whole range of pair sizes and wire gauges then in use in local distribution networks. However, since that time the requirements of the system have been reviewed and steps have been taken to rationalise the range of cables procured in order to simplify manufacturing and purchasing procedures. The current range of local distribution cables is shown in Table II. All have wrappings of paper over the core bundle and each has a black polyethylene sheath to avoid deterioration when exposed to sunlight.

Table II

Range of Local-Distribution Cables in Current Use

Conductor Pairs	Aluminium Alloy		Copper		
	24 AWG 0.5 mm	21 AWG 0.7 mm	24 AWG 0.5 mm	22 AWG 0.63 mm	19 AWG 0.9 mm
2	-	-	x	-	x
5	x	x	x	x	x
10	x	x	x	x	x
20	x	x	x	x	x
50	x	x	x	x	x
100	x	x	x	x	x

\*Only for Aerial Cables

The basic range of cables is suitable for installation in ducts, attachment to the walls of buildings, direct burial in suitable soils or cleating to distribution poles. Where direct burial in stony ground is planned the cables are protected by conventional steel wire armouring laid over the black polyethylene sheath and covered overall with an extrusion of natural polyethylene. For the small sizes of cable used on housing estates an alternative construction in the form of a loose natural polyethylene over-sheath has been developed recently. This appears to give satisfactory protection against the effect of sharp stones and domestic digging implements and when in full production it is likely to be cheaper to manufacture than steel wire armouring.

For aerial use a steel strand is incorporated into the black polyethylene sheath during manufacture to provide a combined cable and suspension wire of figure-of-eight section.

### 3.2 Conductor Jointing

For the first all-polyethylene cables the standard crank-handle twist-joint, already well established for paper/lead cables, was adopted. Later on a polyethylene sleeve filled with silicone grease was introduced instead of an open paper one to insulate the twisted wires. Provision of grease reduced the problem of exposed conductors at joints but it by no means gave a permanent seal. Experiments with crimping methods followed and trials were made with various devices which penetrated the polyethylene insulation to make contact with the conductor without the need for stripping. Successful results with the American B-wire connector in these experiments led to introduction of the Connector, Wire, Insulation (CWI) and an appropriate hand-crimping tool. Early versions of the CWI were dry but following the introduction of fully-filled cables a version packed with petroleum jelly was introduced.

### 3.3 Sheath Closures

In the early days of the all-polyethylene cable many proposals were made for an inexpensive but effective sheath closure suitable for field use. These included bakelite half-shells filled with wax, polyethylene sleeves with shaped ends sealed to the cable sheaths with tape, and polyethylene sleeves sealed to the sheaths by the pressure of an expanding rubber plug.

Tape joints of various kinds were put into service. Tapered nozzles moulded from polyethylene allow various sizes of cable to be accommodated. A small version was also produced having the tapered cable entries as part of the sleeve. In this case the sleeve was split longitudinally and it was necessary to apply sealing tape overall. Provision was made for a tee connection.

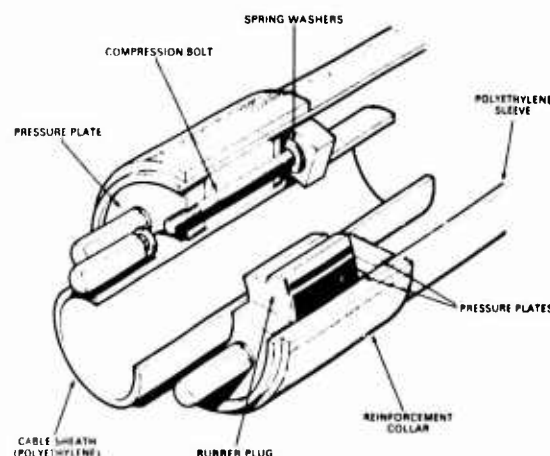


FIG. 2.  
EXPANDING - PLUG JOINT

The expanding-plug joint became accepted as a standard form of construction for in-line joint and cap-ended (slack splice) joints. It consisted of a rubber plug which was fitted over the cable (or cables) and placed into the end of the jointing sleeve as shown in Fig. 2. Bolts which passed through the rubber plug were then tightened to compress the plug between two pressure plates thus causing the rubber to form a mechanical seal between the outside surface of the cable sheath and the inside surface of the jointing sleeve. It was necessary to reinforce the ends of the sleeves. This kind of closure was used for the 1964 Plymouth cable.

Both tape joints and expanding plug joints can be made simply and reliably but they tend to give trouble if dismantled when access is required for re-arrangement of existing pairs or for making tests during the course of fault location. The fundamental need for some kind of ready-access jointing point had been recognised for many years and the cap-ended expanding plug joint was a close approach to the concept of a sheath closure which could be dismantled but the consequent hazard of exposing wire joints remained. However, the introduction of fully-filled cables with wires jointed by means of the jelly-filled CWI lessened the risk of trouble of this kind and a truly re-enterable sheath closure has now been developed and put into service. This closure is shown in Fig. 3.

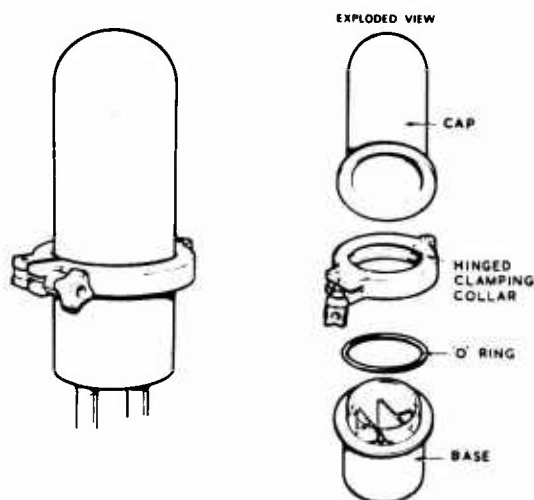


FIG. 3  
READY-ACCESS SHEATH CLOSURE

The cables enter the base of the device through holes made as required and are then sealed with resin; several separate compartments are provided so that other cables can be added later. A moulded cap fits over the base and is secured by a hinged clamping collar. A sound seal between the tapered castings on both cap and base is provided by a rubber O-ring. The cables are flexible enough to allow this kind of joint to be made conveniently above the surface of the ground and then to be coiled down into the joint box.

A jointing jig has been developed for use with this ready-access sheath closure. During the jointing operation the cables are clamped to the jig while the jointer is comfortably positioned on a seat with his feet on a footrest. A supply of connectors is conveniently placed in a tray for insertion into the lever-operated crimping device attached to the jig framework.

This kind of ready-access closure has been adopted as standard for new work. It is particularly suited to radial distribution layouts on housing estates.

Existing tape joints are being improved by filling them with petroleum jelly which seals them completely.

### 3.4 Maintenance Aspects

Field trials of the early fully-filled cables were closely monitored and the performance of these was undoubtedly very satisfactory. The subsequent adoption of cables of this kind as standard led to a gradual change in the composition of local distribution networks in general. Fig. 4 shows how this has changed over the last 20 years with the fully-filled cables gradually assuming a dominant position at the expense of the original paper/lead cables and the earlier all-polyethylene cables. During this period of time there has been a general improvement in the fault rate attributable partly to the introduction of the fully-filled cable and partly to the development of new jointing techniques.

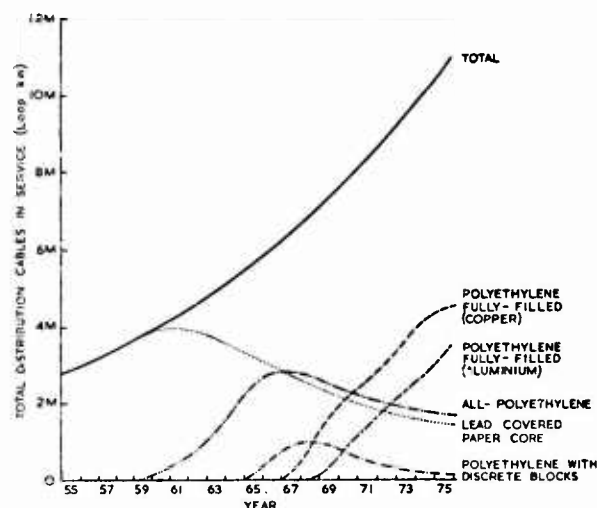


FIG. 4.  
THE DEVELOPING NETWORK  
THE COMPOSITION OF POST OFFICE  
LOCAL DISTRIBUTION NETWORKS

## 4 Examination of Ten Year Old Cable and Comparison With the Currently Made Cables

### 4.1 Recovery of the Plymouth Cable

The Plymouth cable, containing 100 pairs of 0.5 mm (24 AWG) copper wires, was manufactured in 1964 and installed as part of a housing estate development in 1965. In accordance with usual practice for the distribution network it was drawn into existing ducts where these were available but otherwise was buried directly in the ground.

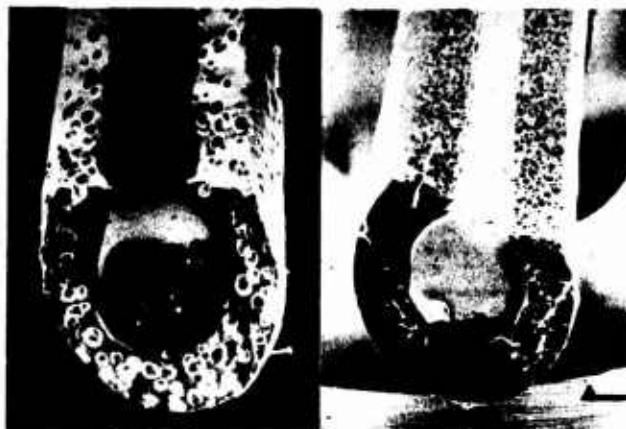
The Appendix describes the recent recovery of a 25 m section of this cable and records the site condition in which it was found. It would have been prohibitively expensive to remove a directly-buried section because since the original installation was made the surface paving had been laid. For this reason a short ducted section of the cable was chosen for removal and examination. Although this section had not been in contact with soil and stones it had evidently been immersed in surface water at various times.

Details of the subsequent laboratory examination of the 25 m length of cable are given in the following paragraphs.

### 4.2 Insulation

The polyethylene used in the 1964 cable was of a similar medium density type to that currently used by BICC but the cellular structure was very coarse. The gas cells in the 1964 cable range from 50 to 150  $\mu$ m diameter and distribution was non-uniform. By 1966 the production techniques were improved and new standards for cellular structure were established. This was recognised by the BPO<sup>15</sup>.

Plate 1 compares the cellular structure of the 1964 cable with that of the current production. The cells in the latter are 15 - 30  $\mu\text{m}$  diameter and uniformly distributed; a dense layer or "skin" near the outer surface can also be seen.



After 10 years in service, the average density of the insulation was found to be  $0.65 \text{ g/cm}^3$ , as compared with  $0.63 \text{ g/cm}^3$  for a cable of recent manufacture and the average permittivity at 1 kHz was 1.73, the same as in the recent cable. There was no evidence that either of these two properties had changed since the cable was installed in 1965 and, in particular, there was no sign of the filling compound replacing gas in the cells.

The measured permittivity of the 1964 insulation varied by up to  $\pm 12\%$  from the value predicted by the Lichtenecker expression for the two component (polyethylene/air) dielectric

$$\log E_i = V_p \log E_p$$

where  $E_i$  and  $E_p$  are the permittivities of insulation and solid polyethylene respectively and  $V_p$  is the volume fraction of solid polyethylene. This was presumably because of the size and distribution of the gas bubbles; the permittivity of the current insulation, with fine cellular structure, is very near to the predicted value.

An experiment was carried out in order to answer an interesting question as to whether the coarse cellular structure in the 1964 insulation was more or less resistant to cell filling by petroleum jelly than the fine cellular structure of the current insulation. Insulated conductors from the 1964 cable and from one made in 1975 were extracted with n-hexane at  $40^\circ\text{C}$ , dried and their weight measured in air and water. Similar measurements were made on duplicate samples of the 1975 cable not subjected to extraction by n-hexane.

All three types of samples were then immersed at  $70^\circ\text{C}$  in the petroleum jelly of the 1975 cable (known to produce cell filling at this temperature). The samples were re-weighed in air and water after 2 and 4 weeks immersion. The changes in density of the insulation and the proportion of the gas space replaced by petroleum jelly in the cellular insulation are shown in Table III.

Table III

Comparison of Rates of Cell Filling at  $70^\circ\text{C}$  in Coarse

Cellular Structure of 1964 Insulation and Fine

Cellular Structure of Current Insulation

	1964 Cable Insulation Extracted	1975 Cable Insulation Extracted	1975 Cable Insulation Un- Extracted
2 weeks immersion at $70^\circ\text{C}$			
Initial density, $\text{g/cm}^3$	0.649	0.711	0.668
Final density, $\text{g/cm}^3$	0.888	0.777	0.755
Density increase, %	37	9	13
% Gas space filled	84	30	33
4 weeks immersion at $70^\circ\text{C}$			
Initial density, $\text{g/cm}^3$	0.630	0.676	0.661
Final density, $\text{g/cm}^3$	0.919	0.779	0.788
Density increase, %	46	15	19
% Gas space filled	95	40	46

The results show that the cellular structure of the currently made insulation, with fine non-intercommunicating cells 15 - 30  $\mu\text{m}$  in diameter and a smooth skin on the outer surface is more resistant to cell filling than the coarse cell insulation of 1964. A small difference between the apparent rates of cell filling of the hexane extracted and unextracted samples of the 1975 insulation was expected. Before the process of cell filling can commence the petroleum jelly must dissolve in the polyethylene in the case of the extracted samples, while in the unextracted specimens the polyethylene already contains petroleum jelly at the beginning of the immersion period.

The mechanical properties (average tensile strength of 5.8N and average elongation of 490%) of the insulation of the 1964 cable did not show any significant difference from those recorded for the present day cable. Also no stress crack failures were recorded in the BTL wrap test<sup>16</sup> at  $60^\circ\text{C}$  and  $70^\circ\text{C}$ . Therefore it was concluded that the insulation had suffered no serious deterioration during the 10 year period.

As was the current practice at the time, the insulation used in the 1964 cable contained a nominal 0.1% of a phenolic antioxidant and no copper inhibitor. This level of stabilisation would have given it a life of about 200 hours in an accelerated ageing test in air at  $105^\circ\text{C}$ <sup>13</sup> if tested immediately after manufacture. The results of tests on insulation from the recovered cable show the life-times at  $105^\circ\text{C}$  of 1200-2400 hours, again illustrating the previously reported<sup>13</sup> improvement due to absorption of filling compound. This insulation would now pass the current BICC requirement (of not less than 1000 hours at  $105^\circ\text{C}$ ) as having adequate resistance to ageing in surface cabinets or pedestals. The currently made insulation has a higher level of initial stabilisation, which gives, for insulation from a freshly made cable, a life time of



1500 - 3500 hours at 105°C. This improvement has been introduced because cables may be jointed soon after manufacture and before the insulation has derived the benefit of prolonged contact with the petroleum jelly.

#### 4.3 Filling Compound

The filling compound in the recovered cable did not comply with the subsequently introduced requirements. The drop point (IP-31) was only 38°C as compared with 55°C minimum specified by the BPO<sup>17</sup> (i.e. for cables used in the UK).

An infra-red spectroscopy examination of the filling compound from the 10 year old cable showed general chemical similarities to the currently used material and there was no evidence of oxidative ageing. The viscosity of the 1964 compound was very low as compared with that of the currently used material as would be expected from the difference in their drop points. A comparison was also carried out of the dielectric properties of the filling compound from the recovered 1964 cable with those from a recently made cable. Table VI shows that at 1 kHz the properties are similar. The volume resistivity of the 1964 compound is lower and the loss tangent generally higher; this would be an expected consequence of low viscosity although higher moisture content could be a contributing factor.

The degree of filling under the core wrapping remained substantial, 90% as measured by the direct air displacement method, which generally gives lower results than other methods. As the degree of filling at manufacture cannot now be established, it is not known whether the 1964 cable was less completely filled than those of current manufacture or whether this value reflects a subsequent change.

The recovered length of the 1964 cable did not pass the BPO test for resistance to water penetration (which was not formulated until two years later in 1966). The currently made cables which meet the requirements of this test all contain higher viscosity, higher softening point filling compounds. The lower viscosity of the filling compound used in 1964 may account for the poorer performance but incomplete filling, particularly between the core bundle and the sheath, may have been a contributory factor.

Table VI

Properties of Filling Compounds in the 1964 and 1975 Cables

Property	1964 Cable	1975 Cable
Drop Point (IP-31)°C	38	73
Permittivity at 23°C 1 kHz - 1 MHz	2.3	2.3
Loss Tangent at 1 kHz		
24°C	0.0003	0.0001
30°C	0.0003	0.0001
39°C	0.0003	0.0001
46°C	0.0003	0.0001
52°C	0.0003	0.0001
61°C	0.0007	0.0001
Loss Tangent at 1 MHz, 23°C	0.0081	0.0050
Volume Resistivity at 23°C (ohm.cm)	$6.4 \times 10^{13}$	$2 \times 10^{15}$

#### 4.4 Paper Wrapping

Since there were indications of presence of moisture in the original underground joint, tests were carried out on the paper wrap. Its moisture content and dielectric properties were compared with those of a similar paper wrap of a recently made cable. On drying for 7 days, at room temperature, over phosphorus pentoxide, the 1964 cable paper lost 8% of its original weight and its loss tangent (at 1 kHz) decreased from 0.048 to 0.005. Under similar conditions, the paper from a recently made cable showed a 2.3% loss in weight, with loss tangent decreasing from 0.030 to 0.005. There was little further change, after 14 days drying.

#### 4.5 Transmission Characteristics

It was felt that an examination of transmission characteristics above the audio band would be of interest in view of the probable future need for wide-band transmission facilities in the existing local networks.

Fig. 5 shows the attenuation and phase shift up to 1 MHz for both old and new cables. Similarly Fig. 6 shows a comparison of the corresponding impedance characteristics. The similarity between the two cables is obvious. For completeness the corresponding primary line coefficients are compared in Figs. 7 and 8. These characteristics were derived by measurement of open circuit and short circuit impedances followed by calculations in the usual way. The only parameter to show a significant difference is the shunt leakance which is much higher for the old cable and may be related to the differences in the loss tangents and resistivities of the two filling compounds (Section 4.3). However, this parameter does not affect the transmission characteristics in the measured range of frequencies.

#### 4.6 Jointing

On recovery of the 25 m length, the remainder was jointed to a replacement length of cable using the CWI mentioned in Section 3.2. The jelly filled version was used and no difficulties arose.

A complete joint of the kind described in Section 3.3 and illustrated in Fig. 3 was made at the BPO External Plant Development Laboratories, using part of the 25 m recovered length. The joint was made without difficulty and there was no sign of permeated petroleum jelly interfering with the resin seal between the cable sheath and the base of the closure.

Although it is not the current BPO practice to use injection welding techniques for the sheath closure of local distribution cables, several such closures were made successfully on part of the 25 m recovered length which had been returned to the manufacturer's laboratory.<sup>18</sup> In all cases the welds were satisfactory and peeling tests caused the sheath to break before the weld. There was no sign of damage to the wire insulation as a result of the welding operation.

#### 4.7 Summary of Main Findings in Relation to the 10 Year Old Cable

The above findings may be summarised as follows:



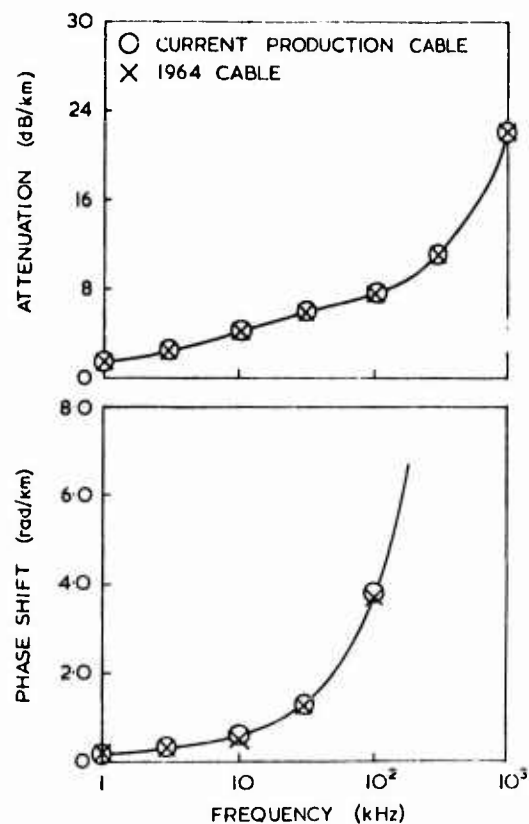


FIG. 5  
TRANSMISSION CHARACTERISTICS

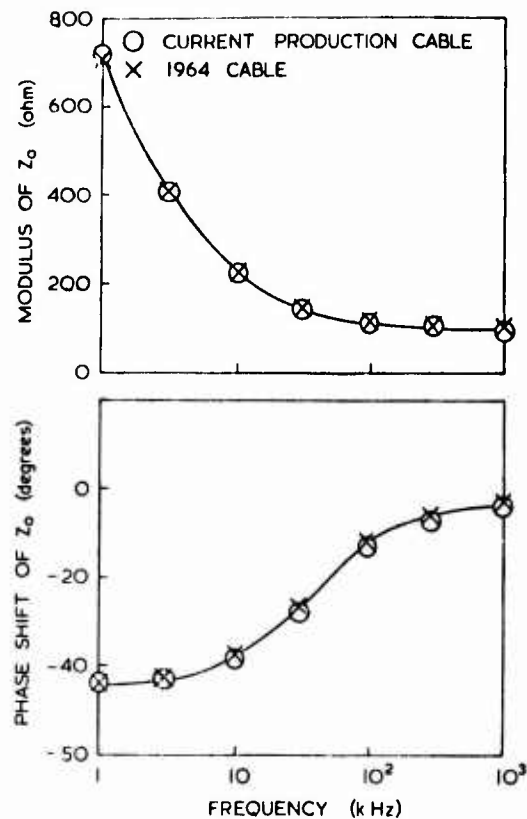


FIG. 6  
CHARACTERISTIC IMPEDANCE

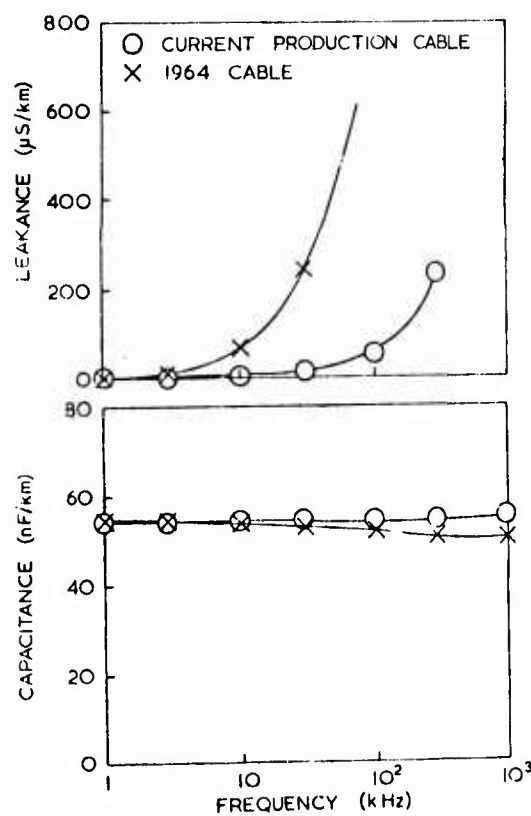


FIG. 7  
PRIMARY COEFFICIENTS (SHUNT)

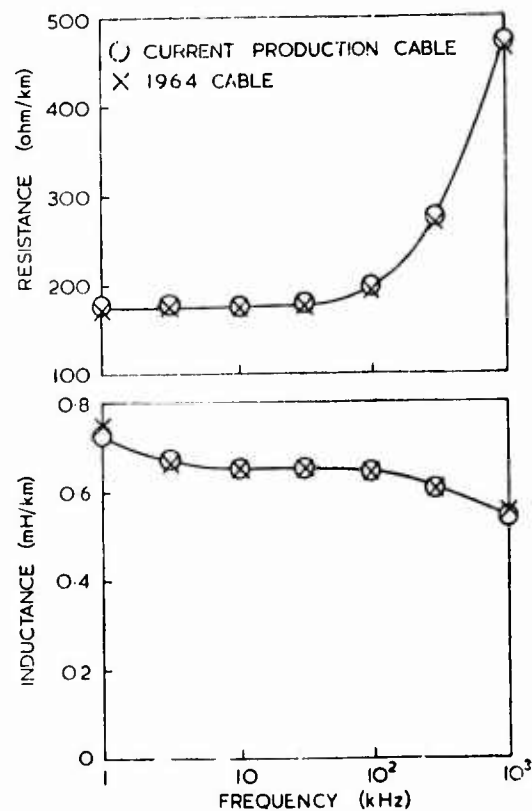


FIG. 8  
PRIMARY COEFFICIENTS (SERIES)

- (a) Transmission characteristics are substantially unaltered, not only at audio frequencies, but also at frequencies up to 1 MHz.
- (b) Mechanical condition and properties of insulation and sheath remained excellent and readily permitted rejoining of the cable using modern methods.
- (c) Permeation of filling compound into the air cells had not taken place despite the coarse cell structure.
- (d) There was some evidence of moisture permeation, particularly in the outer paper wrap. This had not affected the electrical parameters of practical importance. The degree of filling remained substantial.
- (e) The general condition of the cable leads to an expectation of continuing satisfactory performance.

#### 5. Further Developments Since 1964

Since 1964 the use of the cellular insulated, petroleum jelly filled cable has been extended to cover many areas outside the U.K. Also the design of the present day cable has been changed in a number of details, generally with a view to extending the operating conditions. It is necessary and relevant therefore before concluding the paper to discuss the extended environment likely to be encountered and the effect of the changes in design.

##### 5.1 Environmental Factors

This subject has been introduced briefly in Section 2.1. The earth's surface temperature being largely dependent on solar radiation will clearly reach much higher levels in tropical climates, but otherwise, as regards soil burial conditions, the remarks in Section 2.1 apply. A search of the literature suggests that at a depth of 0.6 m the temperature of a buried cable is unlikely to exceed 35°C anywhere in the world.<sup>10</sup> The temperature of aerial cables depends on a more complex mechanism of energy exchange with the ambient environment. The literature indicates that the temperature of these cables is likely to reach 50-55°C for an air temperature of 40°C.

For cable laid on the surface of the ground or stored on unlagged drums temperatures as high as 60 - 65°C may be encountered in extreme conditions.

These conclusions are supported by recent measurements made on our behalf by East Africa Posts and Telegraphs.

##### 5.2 Cable Design Improvements

The first step was to raise the drop point of the filling compound to 55°C thereby permitting a continuous cable service temperature of up to 35°C, but still allowing cold pumping of the filling compound into the cable during manufacture. This remains the current BPO Specification requirement<sup>17</sup> for drop point. Later, a further enhancement of drop point to about 70°C permitting continuous operation of the cable up to 50°C was adopted by some manufacturers, so that filled cables would be suitable

for direct burial anywhere in the world. This filling compound was too stiff to be pumped in the solid state and a hot liquid filling technique was adopted.

This remains the situation for UK manufacture up to the present. Since a maximum aerial cable temperature of 50° to 55°C was expected (Section 5.1), and as laboratory work indicated that permeation of the filling compound into the air cells of the insulation did not occur below 55°C<sup>14</sup>, the change in filling compound permitted use of this design of cable to be extended for aerial application even in hot climates.

It was realised that the small portion of buried cable which entered a flexibility cabinet would experience wider extremes of temperature than the buried portion and could be at risk because of the higher temperature involved when these above-ground structures are exposed to sunlight. Therefore, stabilised insulating and sheathing materials were used from the outset and the selection of filling compound which would not detract from the stability of the plastic materials was carefully studied. However, these laboratory studies together with reports regarding the high rate of insulation failures of dry solid polyethylene insulation in terminal cabinets in the southern part of the USA led to the conclusion that for the widest application (i.e. tropical and sub-tropical areas) a substantial improvement in the oxidation stability of the dry insulation was needed. Standards for laboratory testing (1000 hours at 105°C under specified conditions) were established and cellular polyethylene formulations were developed in collaboration with materials suppliers to achieve this performance.

Improved protection of the cellular insulation on copper conductor against thermal oxidation has been achieved by the use of a more powerful stabiliser system comprising an efficient phenolic antioxidant and a copper inhibitor. The increased stability of the insulation is not adversely affected by prolonged contact with the selected grades of petroleum jelly filling compounds in current use. The latter contain natural constituents which act as effective oxidation inhibitors, and absorption of these filling compounds enhances the resistance to oxidation of the insulation and compensates for any loss of antioxidant from the insulation by diffusion into the filling compound.<sup>13</sup>

The preferred antioxidant is 2:2'-methylenebis-[6-( $\alpha$ -methylcyclohexyl)-4-methylphenol] which combines desirable characteristics of high effectiveness in solid polyethylene as well as in complex cellular polyethylene compositions, low volatility and excellent compatibility with low and medium density polyethylene. It is now well recognised that the performance of many commercial antioxidants in the critical temperature range 50° to 70°C is seriously impaired by their poor solubility in the polymer which leads to partial migration of the antioxidant to the surface of the insulation and its subsequent loss.<sup>19</sup> The outstanding solubility characteristics of the antioxidant used in the current product are illustrated in Fig. 9, showing the results of accelerated oxidation tests carried out on polyethylene sheet (0.6 mm thick) containing initially 0.2% antioxidant, after periods of exposure to air at 50°C. The test specimens were washed with acetone to remove any antioxidant present at the polyethylene surface, and the oxidation induction period at 180°C was determined using a conventional oxygen absorption test method.

Copper inhibitor N:N' - dibenzal (oxalyl dihydrazide) has been found satisfactory for

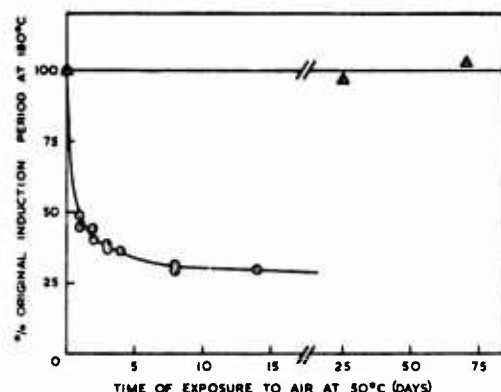


FIG. 9  
EFFECT OF LOSS OF ANTIOXIDANT FROM POLYETHYLENE  
BY DIFFUSION TO THE SURFACE AT 50°C ON  
RESISTANCE TO OXIDATION

- △ 2,2'-METHYLENE BIS [5-(4-METHYLCYCLOHEXYL)-4-METHYLPHENOL]  
○ 4,4'-THIO BIS (3-METHYL-6-TERT-BUTYLPHENOL)

Copper inhibitor N:N' - dibenzal (oxalyl dihydrazide) has been found satisfactory for use in combination with the above antioxidant in both solid and cellular polyethylene insulation.

Laboratory ageing tests<sup>13</sup> at temperatures between 70° and 105°C indicate that the insulation on copper conductor meeting the BICC test performance requirement (not less than 1000 hours life-time at 105°C) would be expected to have a life of 15 years at a constant temperature of 50°C. This level of resistance to oxidation of the current product is considered adequate to ensure 25 - 30 years service life in practically all climatic regions.

The problem of rapid ageing of insulation does not arise with the current use of aluminium alloys in the BPO for local network cables.

Since manufacture of the Plymouth cable, the development of both raw materials and the processes for the production of cellular insulation have made considerable progress. Space precludes discussion of the details, but the aims have been a progressively finer cellular structure of non-communicating cells, smooth surface finish both internally, (i.e. on the surface adjacent the wire) and most important - externally, the absence of plate-out; and of course a high process speed. The main motivation in the pursuit of a finer cellular structure was the attainment of the best mechanical properties at low permittivities and thicknesses. A fine structure, by allowing lower insulation densities (higher blow rates), also permits a saving in materials. Today, cellular structures range from 10 to 30 µm in cell diameter, i.e. 1/3rd to 1/5th of the cell sizes in the Plymouth cable. This improvement in cellular structure has by no means been fully exploited by cable manufacturers and further substantial economies in cable size and materials usage are in principle possible. However,

it is the view of the authors, that because of other considerations, this potential should be pursued with some caution.

6.

#### The Future

The use of cellular polyethylene insulated, fully-filled cable is already firmly established as standard BPO practice for the local distribution network. It seems clear that, both on operating and economic grounds, the use of such cables will gain increasingly wide acceptance throughout the world.

A number of fully-filled cables (some with copper and some with aluminium as a conductor) in sizes up to 1600 pairs have been manufactured for and installed by the BPO in selected local main networks, on an experimental basis.

However, BPO local main networks are, in general, pressurised and an economic study has shown that given an existing pressurisation system it is cheaper to retain it and improve if necessary, rather than to abandon it in favour of fully-filling. Although the manufacturers had difficulty at first in completely filling cables with bonded aluminium moisture barrier the cables have given a good service. Further development in this field is not envisaged by the BPO in the near future because the adoption of fully-filling in this part of the network cannot be justified.

However, for some countries which do not have an already existing capital investment in pressurisation equipment, and for whom development of their network is at an early stage, the fully-filled concept is likely to prove attractive, and this is leading increasingly to inquiries and orders for such cables. Methods for filling such large sizes are being progressively developed, and cables up to 2400 pairs have been made in U.K. and supplied to export customers.

As already explained, BPO practice is to protect local main cables by a polyethylene sheath and bonded aluminium foil barrier. This has imposed a problem for the filled version, because it is exceedingly difficult to block completely the water path between the moderately stiff and circular screen, and the softer and more misshapen core bundle. The problem has been mitigated to some extent by coating the core bundle with a filling material modified for maximum immobility and good wetting characteristics, as well as development of tight screen application techniques. However, this problem has not yet been fully solved and the work is continuing. A complete solution may involve quite specialised materials and techniques.

The bonded foil was originally incorporated in the unfilled cable of the local main network as a moisture barrier although it provided also an electrical screen. For filled cables, in cases where the electrical screening is not necessary, (and this may apply to the majority of applications), it may be possible to omit the screen altogether or replace it by a suitable flexible wrapping material which will serve as a barrier against petroleum jelly permeation.

The present design of filled cable using cellular insulation and an economically attractive type of filling compound with a good overall balance of properties, is suitable for prolonged operation up to 50°C. There are few situations in which the operational requirements of telephone cables involve high temperatures. Nevertheless, with the rapidly expanding usage of fully-filled cables, the requirements are kept under review. Should a need for a higher than 50°C service

temperature become recognised, cellular polyethylene insulation will be used but with a re-formulated petroleum jelly compound. The development work on filling compounds is generally towards a further improvement in the balance of low and high temperature properties with a close watch on the economic factor.

Cable development is a continuing process and close technical collaboration between the user, who has the field experience, and the suppliers, who have the manufacturing expertise, is essential if the best use is to be made of new materials as they appear and new production techniques which evolve in consequence. The fully-filled cable is but one example of this development process.

#### Acknowledgements

The authors wish to express their thanks to the Senior Director of Planning and Purchasing of the BPO and to the Directors of BICC Cables Limited for permission to make use of the information contained in this paper.

The Authors gratefully acknowledge the help of many of their colleagues in preparing this paper and in particular of Dr. J.C. Hartison in providing information on the original design considerations.

#### References

1. N.S. Dean, 17th International Wire and Cable Symposium, 1968
2. British Patent No. 886417, also D.W. Glover and E.J. Hooker, Post Off. Elect. Engrs' J., 53, January 1961, p.253
3. British Patent No. 987508
4. G.A. Dodd, The Trends in Telephone Subscriber Cable, Transmission Aspects of Communications Network, IEE Conference 1964
5. H.J.C. Spencer, Proc. I.E.E., 116, No. 4, April 1969, p.481
6. E.E.L. Winterborn, Post Off. Elect. Engrs' J., 64, October 1971, p.146
7. K.I. Kincaid and D.K. Smith, Electrical Communication, 46, No. 1, 1971, p.72
8. J. Pritchett, Post Off. Elect. Engrs' J., 64, Part 4, January 1972, p.208.
9. J. Pritchett and D.W. Stenson, Post Off. Elect. Engrs' J., 68, October 1975, pp.132-143
10. W.M.H. Schultze, Telefunken-Zeitung, 35, June 1962, p.143
11. K. Mochlinski, E.R.A. Report No. 5289 (1969)
12. J.C. Harrison, Private Communication
13. S. Verne, R.T. Puckowski and A.A. Pinching, Proc. 20th International Wire and Cable Symposium 1971, p.218

14. S. Verne, A.A. Pinching and J.M.R. Hagger, Proc. 22nd International Wire and Cable Symposium 1973, p.244
15. British Post Office Specification CW-128P (June 1966)
16. M.C. Biskeborn and D.P. Dobbin, 17th International Wire and Cable Symposium, 1968
17. British Post Office Specification CW-142B (October 1972)
18. J.G. Nevison and D.T. Parr, Proc. 23rd International Wire and Cable Symposium, 1974, p.375
19. J.B. Howard, Proc. 21st International Wire and Cable Symposium, 1972, p.329

#### Appendix

##### Report on Recovery of 1964 Fully-Filled

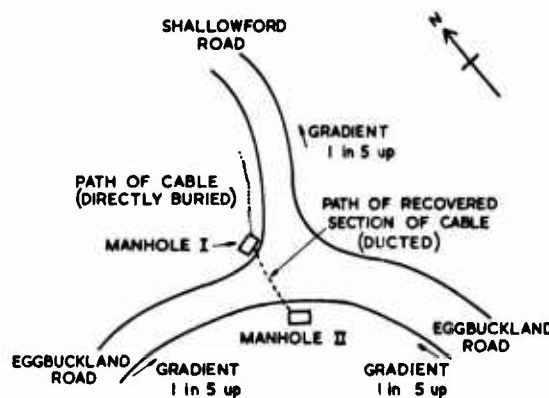
#### Cable

##### 1. Introduction

In co-operation with the BPO, a short length (about 25 m) of early CW128 fully-filled local distribution cable was recovered on Tuesday 8th April, 1975.

##### 2. Location

The cable was situated on the Frogmore Farm Estate, Eggbuckland, Plymouth, Devon. The section removed was a ducted section between two manholes - the precise location is shown on the sketch map below.



LOCATION OF FULLY - FILLED CABLE  
RECOVERED IN PLYMOUTH ON 8.4.1975

### 3. Observations

#### 3.1 Manholes

Both manholes were about 0.9 x 0.6 m and about 1.2 m deep. They had concrete bottoms and brick walls.

Manhole I had a thin layer of mud covering the bottom.

Manhole II had water to a depth of about 150 mm, i.e. to the level of the lowest exit duct.

Manhole II was slightly below the level of Manhole I.

#### 3.2 Duct

The duct carrying the cable across the road was a single bore earthenware type of about 150 mm diameter.

As well as the recovered cable there were six other cables in the duct, all with black polyethylene sheaths.

There were no lead sheathed cables in the duct in either of the manholes.

#### 3.3 Cable

The cable was a 100 pair, 0.5 mm (24 AWG) CW128 cable. In Manhole II it had been jointed to an unfilled (all-polyethylene) cable. In Manhole I the cable ran straight through and into the ground below the pavement in Shallowford Road. It was therefore necessary to cut the cable in Manhole I.

#### 3.4 Closure

The closure in Manhole II was of the expanded plug type which appeared undamaged, and was well above the level of the water. There was no water inside the closure.

#### 3.5 Joint

The jointing of individual conductors had been the standard crank-handle twisting method and then covered with a silicone-grease filled polyethylene sleeve. The majority of the bared copper conductors showed some slight tarnishing, and in one case definite greening.

The insulation which had been exposed in the joint appeared to be basically sound. There was no evidence of stress-cracking of twisted portions. There was however, considerable evidence of colour fading, particularly on the orange which had become almost white.

### 4. Removal of Cable

The cable was sealed at each end using self amalgamating tape. The end which had been cut in Manhole I was covered with a yellow tape.

The cable was pulled out from Manhole I. It was noted that it was thinly coated with wet silt. There was no evidence of sheath puncture.

### 5. Samples

The following samples were recovered for possible examination:

- A. Water from bottom of Manhole II
- B. Silt attached to cable when pulled from duct
- C. Mud from bottom of Manhole I
- D. Various pieces of insulation from joint
- E. Silicone grease filled polyethylene sleeves from joint

### 6. Miscellaneous Information

During the removal operation the jointers carrying out the work volunteered observations and opinions based on their local experience.

6.1 Cable damage due to puncture of the polyethylene sheath was frequent but always due to digging accidents. There were no known instances of failure due to environmental factors.

6.2 The system of ducts and manholes gets very wet. Some ducts seem to act as land drains, it being stated that water flows continuously through some ducts, even in the absence of rainfall. Many manholes become completely filled with water.

6.3 Where possible all joints are left above the water level in a manhole. Where this does not happen, or is not possible, jointers have reported heavy greening of copper inside closures.

6.4 Jointers considered that the expanding plug type of closure (which is now obsolete) was less reliable than the current types.

6.5 Jointers commented that colour fading in filled cables, especially with orange, had sometimes given problems in identification.



JACK PRITCHETT  
British Post Office,  
External Plant Development Division,  
Carlton House,  
Carlton Avenue East,  
Wembley, Middlesex HA9 8QH

Mr. Pritchett joined the BPO in 1935. After service in Royal Signals during the war he graduated at London University and is now employed on cable development at the Telecommunication Headquarters of the BPO. He is a Member of the I. Mech.E and the I.E.E.



EDWARD L. MATHER  
BICC Telecommunication Cables Limited,  
Prescot,  
Merseyside L34 5UQ

Mr. Mather graduated in Electrical Engineering with a speciality in Electronics, at Liverpool University, England, in 1944. After 3 years service in the army he joined BICC early in 1948 as a Research Engineer and worked in the Telephone Cable measurement and instrumentation field until early 1959. He then joined Automatic Telephone and Electric Co. Ltd. (now the Plessey Co. Ltd.) and spent the next ten years in development work in the data processing field. He rejoined BICC Telephone Cables Division in 1970 as Technical Manager. He is a Fellow of the Institution of Electrical Engineers.



STEFAN VERNE  
BICC Research and Engineering Limited,  
38 Wood Lane,  
London W12 7DZ

Mr. Verne has been studying polymeric materials and dielectric properties since 1950. First qualified in Rubber Technology. Graduated in chemistry in 1951 and his first post-graduate work was on dielectric properties of liquids. Joined BICC in 1954 to work on utilisation of polymeric materials in power and communication cables. Head of Polymers Department of BICC Research and Engineering Limited.



## A NEW TYPE OF LONGITUDINALLY WATERPROOF TELEPHONE CABLE

Dr. F.H. Kreuger  
NKF GROEP B.V.  
Rijswijk Holland

Ir. H.L. Gorissen and Ing. J.F. Kooy  
NKF KABEL B.V.  
Delft Holland

### Summary

Up till now the method generally used for making telephone cables waterproof is to fill the complete cable core with petroleum jelly. An important disadvantage of this method is the high increase of the mutual capacitance of the cable (about 15%). By applying blocks of self vulcanizing rubber NKF has succeeded in combining the excellent waterblocking properties of petroleum jelly with a low dielectric constant.

### The drawbacks of plastic insulation

When changing over from paper to plastic insulation for telephone cables two inherent problems arise that have to be solved. The first and most widely recognized problem is the fact that the dielectric constant of polyethylene-air insulation is up to 25% higher than that of paper-air insulation. A common solution to this problem is the choice of cellular polyethylene. This choice in its turn raises some difficulties, but these facts do not form a subject of this paper.

A further problem, that is recognized after introducing plastic insulation, is water penetration along the core of the cable. In paper cable water entry into the core can easily be recognized by the fast deterioration of the transmission performance. On the other hand the paper swells and blocks the water more or less. Repairing the cable within a short time after damage is possible and a comparative short length of cable has to be replaced. This problem has also a rather classical answer: the filling of the polyethylene insulated cable core with a petroleum-jelly compound. This filling however, leads to a further increase of the dielectric constant by 15 to 20%.

### Water blocks

In order to minimize the  $\epsilon_r$ -increase we developed cables with blocks, which cover only 5 to 10% of the cable length. The degree of filling depends mainly on the blocking-compound, the injection technique, the maximum acceptable increase of  $\epsilon_r$  and the maximum allowable amount of water in the cable core in case of a sheath damage. For a 10% filled cable an  $\epsilon_r$  increase of about 3% is achieved. At this low value the diameter of a filled cable needs hardly to be larger than that of an unfilled cable with the same capacitance.

### Blocking compound

The blocking compound has to meet the following requirements.

- low viscosity during filling operation to enable the filling of all interstices of the cable core and especially the hearts of the quads.
- viscosity directly after injection such that the compound does not drip from the cable core.
- compatible with other materials used in the cable core.
- no noticeable effect on the electrical and mechanical properties of the cable.
- acceptable handling properties for manufacturing and installation personnel.
- no significant influence on normal jointing techniques and compatible with jointing materials.

The blocks should meet the following requirements.

- excellent waterproof properties.
- blocklength as short as possible in order to reach the lowest possible  $\epsilon_r$  increase.
- flexible so that there is no significant difference in bending behaviour between a filled and an unfilled cable.
- stable even after thermal or mechanical action over long periods.

For these blocks no petroleum-jelly compounds or even petroleum-jelly/polyethylene compounds can be used as these compounds melt at higher temperatures and water blocking would be impaired.

NKF has developed a blocking compound that meets all the requirements mentioned above. The compound is slightly foamed in order to reach a lower capacitance; hence the name Aquafoam. The compound is based on a selfvulcanizing silicone rubber. After vulcanization the block is mechanically stable even at temperatures, which amount at least 100°C.

### Production technique

A production technique has been developed for a cable with quads in concentric layers, which is the normal type of cable in Holland. The main difficulty encountered with cables of this type is to reach the heart of the quads with the blocking compound. This could not be done by filling the complete core of the cable in one shot. The best results were obtained by filling each individual layer during the stranding operation.

In order to reach this result the following major items had to be developed to generate a full proof production technique :

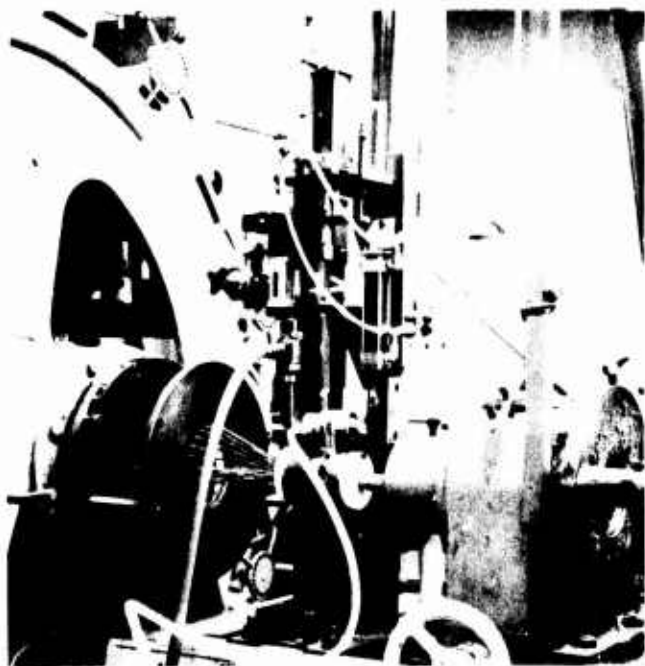


Fig. 1 : An injection system

1. An injector in which the layer is formed and the blocking compound is injected. The major aspect in the development was to reach sufficient pressure of the compound directly after the injector in order to reach the heart of the quads.
2. A system for feeding the injectors. The main problem was to obtain an injection time of 0.1 sec. or less in order to reach a sufficiently short block. Figure 1 shows a complete injection system.
3. An electronic system for the synchronization and the control of the injection units. Synchronization is needed for situating the block in each layer on top of each other. This system is controlled by the speed of the stranding machine, therefore synchronization is not affected by variations in stranding speed. In figure 2 this system is shown.

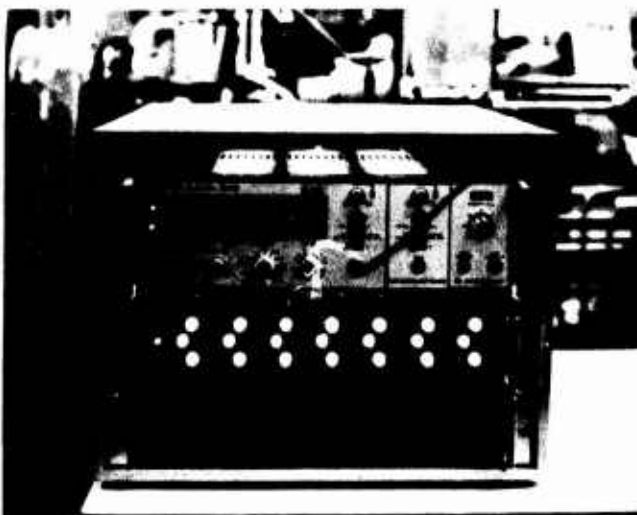


fig. 2 : The electronic control system.

The length of the blocks is about 15 cm and the block distance can be varied from 0.5 m up to several meters. With this production technique concentric cables up to 150 quads have been manufactured, without any reduction in stranding speed as compared to usual.

#### Actual cables and results

To investigate the long term stability and the effects of the blocks on the electrical properties of the cable an aging test is performed. For this purpose the following cables have been studied :

- \* Two cables with 0.5 mm conductors and solid polyethylene insulation (a normal distribution cable).
- \* Two cables with 0.8 mm conductors and foam polyethylene insulation (a cable with extremely low capacitance unbalance).

Both types consist of 27 quads in 3 layers. One cable of each type has Aquafoam blocks with a length of 15 cm and a distance between the blocks of 1.5 m. The other cables are unfilled and are used as a reference. After manufacturing a number of electrical properties have been measured, of which the most important are :

- mutual capacitance
- capacitance unbalance within the quad and between pairs of different quads
- far-end crosstalk at 1 MHz
- insulation resistance

No difference was found between filled and unfilled cables for all electrical properties; only the mutual capacitance differed as was to be expected (table 1).

	solid PE	foam PE
unfilled	36.8 nF/km	31.9 nF/km
with blocks	37.7 nF/km	32.7 nF/km
increase in cap.	2.4%	2.5%

Table 1 : Mutual capacitance of the cables under test.

These cables were aged at a temperature of 50°C during 65 days. After this period all electrical properties were measured again and no change in electrical properties was found.

#### Field trial

In the telephone network in the Netherlands distribution cables up to 50 quads are plastic or paper insulated, larger cables are paper insulated. NKF has developed a new type of waterproof plastic insulated distribution cable with 150 quads and filled with Aquafoam blocks. 10 km of this cable has recently been manufactured and will be used by the Dutch PTT for a field trial. The conductors of this cable have a diameter of 0.5 mm and are insulated with solid polyethylene. The core has a centre of 3 quads surrounded by 6 concentric layers with respectively 9-15-21-27-34 and 41 quads. The core is closely wrapped with plastic tape. The cable has a PE-AL-PE sheath and armouring of plastic insulated steelwires.

A cross section of this cable is shown in fig. 3, in fig. 4 a cable core with Aquafoam blocks is shown.

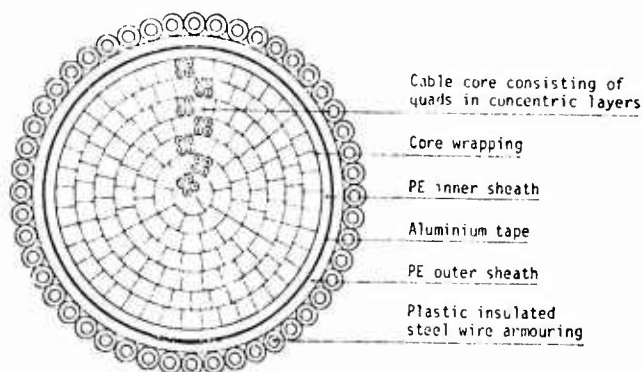


fig. 3 : Cross section of a 150x4x0,5 mm cable.



fig. 4 : The core of a cable with Aquafoam blocks.

The main electrical characteristics are indicated in table 2. These results are almost identical with those of an unfilled cable.

Table 2 Electrical characteristics of a cable type 150x4x0,5 mm with Aquafoam blocks.

mutual capacitance - 800 Hz	$\bar{x}$	37	nF/km
capacitance unbalance - 800 Hz	$\bar{x}$	20	pF/500 m
within the quad	max.	98	"
between pairs of different quads	max.	68	"
insulation resistance - 500 V	min.	$23 \cdot 10^3$	Mohm km

During the waterpenetration test - 1 m watercolumn during 7 days - the tested cable samples remained waterproof. In fig. 5 this test is shown.

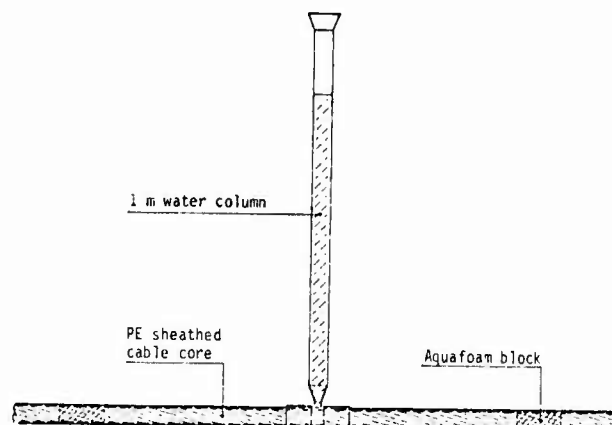


fig. 5 : Water penetration test.

#### Material savings

Important material savings can be achieved by the application of Aquafoam blocks instead of petroleum jelly. For quad cables the decrease of the core diameter by using blocks instead of petroleum jelly is about 15%. This reduction in diameter results in less insulation material and with armoured cables in less materials for sheathing and armouring.

Figure 6 gives the relative material costs for cables with 150 quads and with the construction mentioned above. Material costs are based on July 1975 prices. The total savings are 12% of which 6% is caused by reduction in insulation material and filling compound and 6% by reduction of the sheathing and armouring materials.

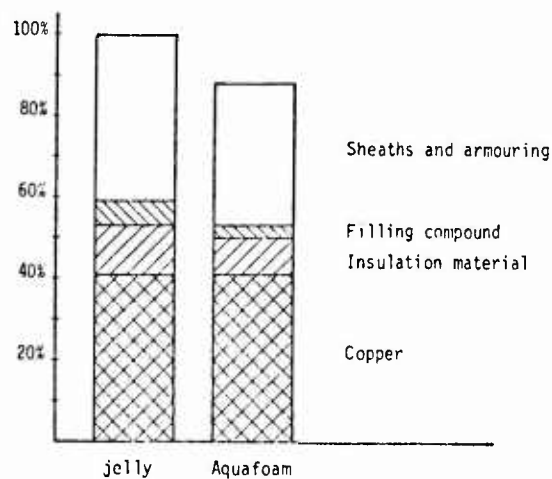


fig. 6 : Relative material costs for a 150x4x0,5 mm cable with Aquafoam blocks.

### Future aspects

Other cable constructions with Aquafoam blocks such as paired- or unit type cable are under development. Paired cables can far easier be injected so that the present technique can easily be used for these cables. Unit type cables can also be processed in this way, but further development work is needed to cover this field. NKF believes that this new technique is an encouraging method for making longitudinally water tight cables without the drawbacks as experienced with the usual water blocking methods.



Dr. F.H. Kreuger received his electrical engineering degree in 1954 and his Doctor's degree in technical science in 1961 from Delft University. He worked as a high voltage research engineer in Sweden and England before joining NKF, Delft in 1956. He successively became Head of the High Voltage Research Department and Research manager of NKF KABEL and is at present Director Research & Development of NKF GROEP, Rijswijk.



Ir. H.L. Gorissen received his electrical engineering degree in 1971 from Delft Technical University. He joined NKF, Delft in 1960 and worked in the Telecommunication Cable Development. In 1971 he became head of the Telecommunication Cable Laboratory and is at present R & D manager Telecommunication cables.



Ing. J.F. Kooy joined NKF, Delft in 1966 and has been active in the development of telecommunication cables, accessories and measuring techniques. As senior development engineer of the Telecommunication Cable Laboratory he is now responsible for the development of symmetrical telecommunication cables. He is a graduate of the Higher Technical school in The Hague since 1964.

# CHANGE OF CROSSTALK PROPERTIES IN CORRELATION TO THE INTERACTION OF POLYETHYLENE/PETROLEUM-JELLY

H.J. Anderka, H.G. Dageförde, H.A. Mayer

AEG-TELEFUNKEN KABELWERKE AG  
Development Center

Mülheim-Ruhr  
West-Germany

## SUMMARY

It is a well-known fact that the transmission characteristics of PE-insulated telephone wires are modified when petro-jelly fillings are used. These changes were measured with particular reference to the crosstalk characteristics on solid PE foamed PE and dual insulation after storage at temperatures up to 70 °C. The wires were ring-marked and stranded to form star-quads.

In order to describe the experimental conditions more closely, it is necessary to discuss the properties of the polymer insulating materials, and those of the six different European petro-jelly types used in the tests and to specify the design of the cables under investigation.

Single wires insulated with PE, were first stored in an excess of PJ under laboratory conditions at temperatures of up to 70 °C, and the variations in diameter, weight, and capacity were measured, the latter in a water bath.

1000 m lengths of cable on drums were then stored in a high-capacity thermal chamber at 70 °C. The cable lengths filled with PJ and reference cables of the same length but without PJ fillings were treated simultaneously in the same thermal chamber.

The variations in the mechanical and chemical properties, and particularly in the electrical properties such as mutual capacitance, capacitance unbalances, and side capacities were determined.

These electrical properties change in filled cables with ringmarked PE conductors in a manner, which has an adverse effect on crosstalk properties, which means that repeated balancings in the field would be necessary.

The rate of diffusion and the concentration of the PJ in the PE are governed by temperature.

Conditioning of the PE insulated conductors at 70 °C in PJ accelerates diffusion and provides trend data suitable as a starting point for planning the investigations on cables.

The measurements and recordings of the above mentioned variations indicate that the properties affecting crosstalk, are stabilized within a few days at a temperature of 70 °C.

The possibility for the application of PJ-filled cables with ringmarking are discussed with reference to current and future applications.

## INTRODUCTION

Efficient communication by wire calls for a constant transmission quality within a defined scope over long periods. When assessing transmission quality, the subscriber tends to stress volume and range. This conviction stems from a period when engineers were not yet able to compensate line losses by means of amplifier equipment.

The same user, however, will scarcely express gratitude if his call is disturbed by eavesdroppers and crosstalk.

In view of the large number of transmission channels in modern telephone cables, adequate crosstalk attenuation values are imperative today. These can be obtained by stable characteristics of the components in the telephone cable and have to be guaranteed over long periods. It is not possible to make adjustments by instrument matching, such as is possible in the case of line attenuation by adjustment of the amplifier.

Following a development process occupying the space of several years, it is now possible to stabilize the mechanical and chemical properties of the PE/PJ system. A variation in the mutual capacitance due to aging, which is mentioned in several reports 3, 4, 7, 8 can be accepted within certain limits.

However, crosstalk attenuation values are a direct function of the capacitance unbalances. If capacitance unbalances occur due to aging, the function

$$FEX = \ln \frac{8}{\omega ZK}$$

results in a modification of the crosstalk attenuation values, i.e. the incidence of listening-in increases.

The investigations discussed in this report concern the stability of mutual capacitance unbalances in PJ-filled cable with star-quads configuration and ringmarking of the wires, such as are being used in increasing degree in Germany and some other European countries.

The following discussion of the results obtained from these investigations starts with comments on the cable material and the mutual interactions, both in an excess of petroleum jelly and in cables with various constructions and different petroleum-jelly types. The values of the capacitance unbalances which occurred are stated so that the effects on current installations and future systems can be assessed.

#### MATERIALS AND CABLE TYPES USED IN THE EXPERIMENTS

##### Petroleum jellies as filling compounds

To date, two systems have been used successfully for longitudinal sealing of plastic-insulated telephone cables:

- polyurethane foam<sup>1</sup> and petrolatum<sup>2</sup>.
- Petrolatum, also called petroleum jelly (PJ), as used in these experiments, is a compound of components (with boiling points  $\geq 280^\circ\text{C}$ ) obtained during the distillation of crude oil:
  - microcrystalline waxes
  - paraffins
  - oils (naphthenic, with paraffinic and aromatic components)

The petroleum jellies contained the same phenolic antioxidant as the PE as an additive in equilibrium concentration.

The petro-jellies used did not contain any polyethylene additives.

In order to examine whether various types of PJ have different effects on the electrical properties of the insulation, six common petrolatum types from three different European countries were used. All six types conform with the requirements of the Federal German Postal Authorities<sup>6</sup> (FTZ, 72 TV1, Sheet 3) and of the British Post Office (M 142).

Table 1 shows a selection of the main properties of the petro-jellies used.

Table 1

Type	Limit according to FTZ 72 TV1	less shrinking			more shrinking		
		softer			harder		
		P	Q (RGA)	R	S	T	U
Shrinking $\frac{\Delta L}{L_0} \cdot 100$ Vol	-	55	6	7	85	85	95
Penetration at 25°C 1 mm	30	95	2	60	58	53	38
Drop point °C	70	73	0	74	78.5	74	74
Viscosity cP at 100°C	10	25	16	17	17.5	18.5	18
Flash point	230	290	260	300	300	305	300
Adhesion at 10°C	passed	passed	passed	passed	passed	passed	passed
Oil separation	passed	passed	passed	passed	passed	passed	passed
Dielectric constant at RT	23	217	218	215	228	228	230
Weight increase of PE Type 2YJ2 (d 0.928-0.933) at 70°C 10 d average %	10	7-8	8-9	7-8	~7	~7	~7

Table 1 European petrolatum types used in the experiments

The designations are not related to the symbols used in earlier symposia. Shrinkage is an important criterion for the minimisation of void formation during cooling.

With the fillers used in our experiments, it became apparent that shrinkage of softer petroleum jellies with higher penetration

factors is less than with the harder compounds having low penetration factors. Although shrinkages of up to 10 % on cooling from 90 to 20 °C appear acceptable, jellies with shrinkage rates of up to 7 % are advantageous for filling the cable spaces in the molten state.

#### Properties of the PE insulating materials used

The following polyolefin types are generally used as wire insulation in telephone cables:

- polyethylene (LD-PE and HD-PE)
- polypropylene (PP)
- ethylene-propylene copolymers

The state in which these insulating materials are used for insulation permits a subdivision into:

- solid polyolefin
- cellular polyolefin
- cellular/solid polyolefin (foam skin)<sup>9</sup>

All three forms of polyolefin were used in these experiments. LD-PE and MD-PE with a density  $\leq 0.936$  was used as a basis of comparison for all three forms of insulation. In the case of cellular/solid PE (also called "foam skin" or "dual insulation") the outer layer can consist of a different polymer as the basic polymer of the cellular layer. It is thus, for example, possible to reduce the permeability of the outer layer with respect to  $\text{P}_0$ .

Table 2 shows a restricted selection of the properties of the insulation materials used, which are all common in various countries.

Table 2

Properties at RT	PE-Type				
	Solid	Cellular	Cellular + Solid	Obs.	
Density g/cm <sup>3</sup>	0.925-0.935	0.46-0.58 *	0.46-0.48	0.925-0.935	*different foaming degrees
Melt-index g/10 min. at 190°C of basic PE or 140°C (cellular)	0.3	0.6-0.9 *	0.6-0.9 *	0.3	*in some cable types: 0.3
Foaming degree of cellular layer	0	33 to 50 *	50-58	0	*usually 38 to 43 %

Table 2 Properties of the PE materials used for the insulation

Solid and cellular PE contained commercially available phenolic antioxidants and some had synergistic additives or copper deactivators.

The corresponding antioxidants were also contained in the PJ.

Before and after aging for 10 days at 70 °C, elongation at rupture of the solid PE was  $\geq 300$  % (cellular PE  $\geq 125$  %), as specified<sup>5</sup>, and the wrap test was passed, regardless of whether conditioning for 7 days at 70 °C in PJ had been carried out or not. The weight increase after 10 days at 70 °C in PJ was  $< 10$  %.

In this respect attention must be drawn to a particular feature of the German cable design: the star-quads with solid PE and cellular PE insulation were ringmarked as required



with a black ringmarking paint (free from carbon black), which cannot be wiped off even after prolonged contact with PJ and which is used by various firms for virtually all PJ filled cables with ringmarking. Several cables without ringmarking conductors were produced for cross-checking purposes.

#### Design data of the cables examined

Wall thicknesses of the insulation of the examined cables:

Table 3

Type	Cable-Number of	Insulation Type	Wall-Thickness mm	Conductor Diameter mm	Number of Pairs	Obs
A2YF (L) 2Y 100 · 2 · 0.6	6*	Solid-PE	0.4	0.6	100	6 cables with 6 different PJ according to table 1
AQ2Y F (L) 2Y 100 · 2 · 0.6	1	Cellular-PE	0.25	0.6	100	Foaming degree ~ 40%
AQ2Y 2Y F (L) 2Y 10 · 2 · 0.6	1	(Cellular + Solid)-PE	0.3 · 0.1	0.6	10	Degree of blowing (cellular layer) ~ 50-58%

Table 3 Construction data of the measured PJ filled cables

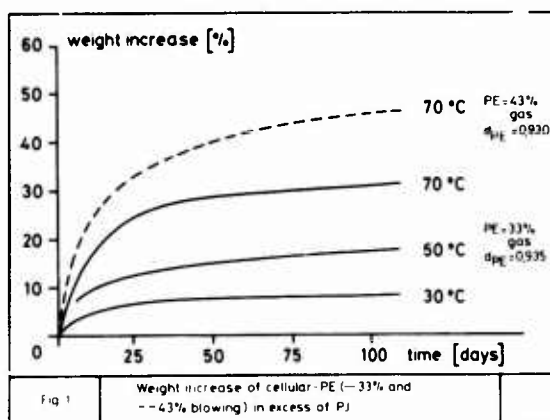
All cables featured a layer sheat of co-polymer-coated aluminium tape. The spaces in the cable were filled with various types of PJ and the spaces in one length of each cable type were left empty to provide comparison samples; these were also subjected to the same thermal cycle as the filled cables.

1000-m lengths of each cable (the foam-skin type was only 300 m long) were treated in a thermal chamber at increased temperature.

#### INVESTIGATIONS AND RESULTS

##### MEASUREMENTS ON SINGLE CONDUCTORS IN AN EXCESS OF PETROLATUM

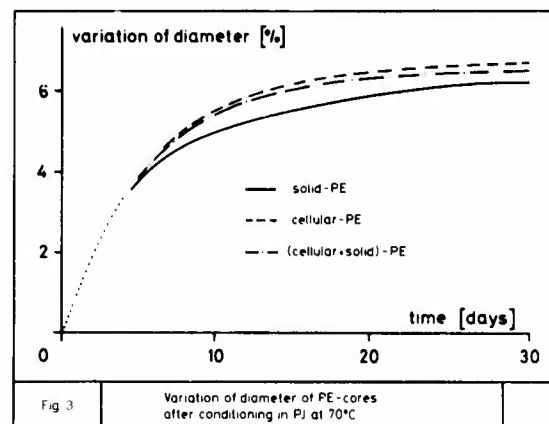
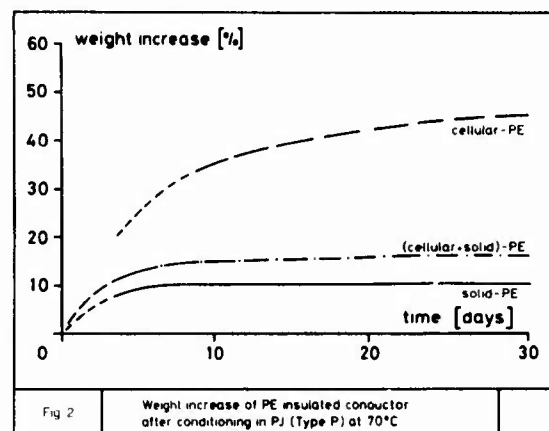
Such investigations have only a restricted practical value, of course. However, we undertook them to determine the tendency of the variations caused by the interaction of PE/PJ on the components used in the cable, and in order to keep the number of investigation on cables within reasonable limits. As to be expected, cellular PE absorbs increasing quantities of petrolatum when stored for long periods in a surplus of petrolatum, the cells becoming partially filled during the process.



The diagram shows the known behaviour of cellular PE.

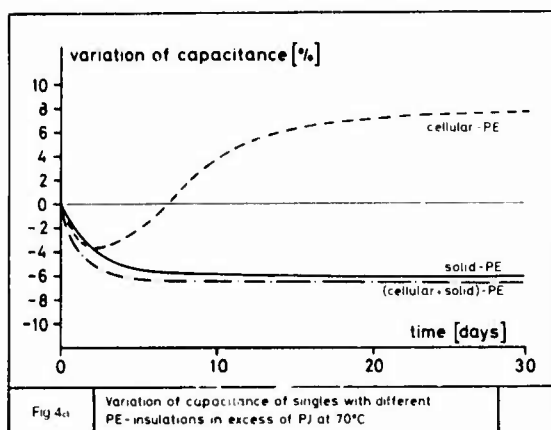
The increase in weight, exceeding the proportion of PE (approx. 8 %) indicates partial filling of the cells. A more highly foamed PE absorbs correspondingly more PJ.

The types of PE used for insulation in our cable investigations, namely solid PE, cellular PE and cellular/solid PE, were also checked for weight increase in a surplus of PJ (type P, drop point 73 °C) before the investigations were made using full cable lengths:



Due to swelling, the diameter of the insulated conductors stored in a surplus of PJ at 70 °C, increased by approx. 5 - 6 % for all the discussed insulation types within the first 10 days and thereafter only slightly. Measurement or calculation of the wall thickness reveals a variation of between 8 and 14 %.

Fig. 4a shows the variation in the capacity of the insulated conductors as measured in a water bath after storage for approx. 30 days in a surplus of petrolatum (type P) at 70 °C.



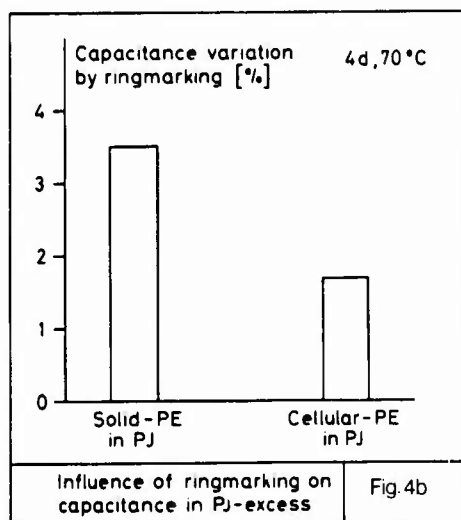
The capacity as measured in a water bath after storage in PJ

- first drops, then increases in the case of cellular PE due to partial filling of the cells with PJ and the resulting rise in the dielectric constant, which outweighs the increase in diameter;
- decreases in the case of solid PE due to the increase in diameter;
- decreases in the case of cellular/solid PE due to the increase in diameter, accompanied by a relatively slight change in the dielectric constant.

Under these conditions, the behaviour of cellular/solid PE insulation is similar to that of solid PE.

The ringmarking was found to have a considerable effect.

In order to determine this effect on the change in capacity in a water bath after storage in PJ type P at 70 °C, single conductors insulated with solid PE and conductors insulated with cellular PE were stored in PJ at 70 °C, some without ringmarking and others with ringmarking covering 24 % of the surface. The PJ was then removed from the conductors and the change in capacity and weight of insulation was determined.



Whereas the weight increase remained approximately the same (13 % in the case of cellular PE and 8 % in the case of solid PE), the capacity of the ringmarked conductors changed in higher degree than was true of the unmarked wires.

#### MEASUREMENTS ON CABLES FILLED WITH PETROLATUM

##### Comparative investigations on star-quads in cables filled with PJ and cables with empty spaces between the conductors

The design of the cables, their wall thicknesses, and types of insulation are specified in Table 3.

It should be mentioned here that only cables with solid PE insulation are filled with petrolatum within the area of the Bundespost. Cables with cellular PE and cellular/solid PE insulation were filled with PJ especially for the experiments.

For the measurements on the cable the 3 insulation types:

- solid PE (100 pair, ringmarked and unmarked)
- cellular PE (100 pair, ringmarked)
- cellular/solid PE (10 pair, unmarked)

and also the petrolatum types were varied (for solid PE, 6 different petrolatum fillers were tested). For comparison purposes, the unfilled cables were also thermally treated. Cable drums with 1000 m of each type of cable stored in a thermal chamber at 70 °C.

It was found that the capacitance unbalances changed greatly within the first week, and then only slightly; for this reason, the storage conditions were initially fixed at 7 days and a temperature of 70 °C, and conditioning was carried out in two or more periods of 7 days or longer.

The mutual capacitances were measured and recorded before and during this thermal treatment. Most cables were cooled after the thermal treatment and measured again at RT. After 7 days at 70 °C and an appropriate cooling period of 2 days, the changes in the insulated conductors diameter and the weight increase of the insulation were as follows:

Table 4

Type of insulation	Density of basic PE g/cm <sup>3</sup>	Degree of blowing %	Wall-thickness mm	Variation after 7 or 14 days at 70°C compared to the original PE %				
				Weight increase after conditioning at 70°C			Diameter	
				before	7 days	14 days	7 d	14 d
Solid-PE	0.928	-	0.25	~ 4	7-8	8-9	2-4	~ 5
Cellular-PE	0.935	38-43	0.3		10-11	16-18	2-3	3-4
(Cell + Solid)-PE	0.928	50-58	0.3/0.1	~ 5	~ 8	~ 9	~ 2-3	3-4

The influence of storage for 7 days at 70 °C on the mechanical and chemical properties was measured to determine whether the insulation still complied with the regulations of VDE 0209 and of the Bundespost 6.

The minimum values for tensile strength, elongation at rupture, resistance to aging after 10 days at 100 °C, wrap-test, etc. were met both before storage of the PJ

filled cables and after storage for 7 days at 70 °C in the thermal chamber. Elongation at rupture of the wire insulation was still better than 400 % for solid PE even after the petrolatum-filled cable had been conditioned for 2 weeks at 70 °C. Accordingly, these cables still comply with the regulations regarding mechanical and chemical properties.

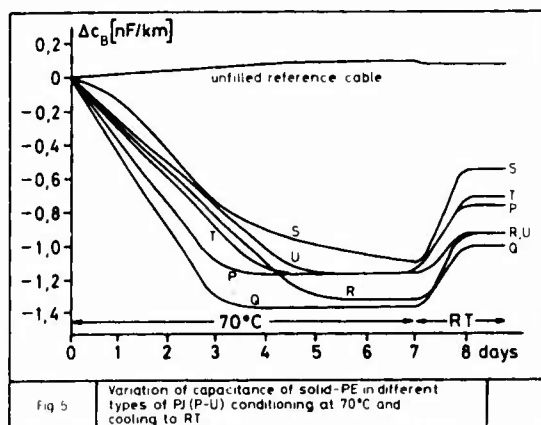
3 m long sections were cut from various filled cable lengths with solid PE insulation for testing of longitudinal water tightness (1 m water column over 7 days) following conditioning over 7 days at 70 °C. The samples checked were waterproof.

#### Modification of mutual capacitance in the cable

(during and after one week storage of the filled cable at 70 °C).

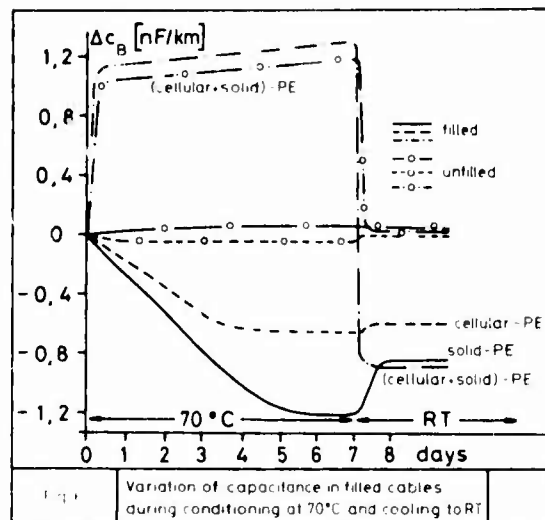
The processes which take place during the first week of storage of the filled cables at 70 °C appeared interesting with respect to the variation of mutual capacitance, which was recorded during the heating period and measured at 70 °C and then after 7 days when cooled to room temperature.

The following table shows the variation in the mutual capacitance of 6 cables (all 100 x 2 x 0,6) which were filled with various PJ types, P to U. An unfilled cable of the same design was measured for comparison purposes.



The initial value for mutual capacitance of the PJ filled solid PE cables was approx. 43 nF/km, that of the unfilled cables approx. 36 nF/km. Whereas the mutual capacitance of the reference cable remained practically unchanged at 70 °C, it decreased in the case of the filled cables. In general mutual capacitance exhibited its greatest difference of - 1.1 to - 1.4 nF/km after approx. 3 - 5 days at 70 °C, and then remained constant up to the 7th day. After cooling to room temperature, the capacity increased again, and the final overall deviations were in the range of - 0.6 to - 1.0 nF/km as compared with the initial values.

The next diagram shows the comparison between the insulation types solid PE, cellular PE, and solid/cellular PE.



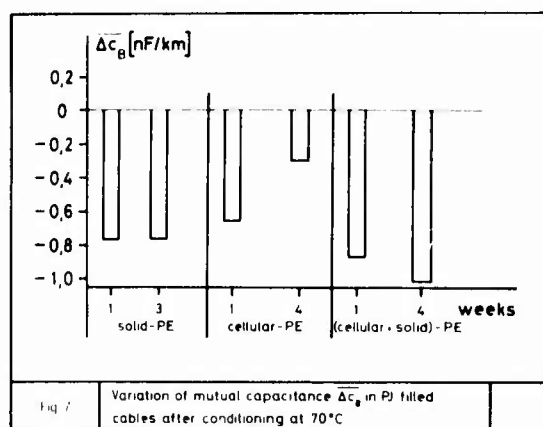
The initial values for mutual capacitance of the filled cable were approx. 43 nF/km for solid PE and for cellular PE, 40 nF/km for cellular/solid PE, and about 36 nF/km for the unfilled reference cables and 34 nF/km for solid/cellular PE.

During the thermal treatment period of 7 days at 70 °C the mutual capacitance of the PJ filled cables fell by approx. - 0.6 nF/km for cellular PE (in approx. 3 days), and by about - 1.2 nF/km for the solid PE (in approx. 4 - 5 days), while the reference cables remained virtually unchanged. In contrast, the difference in the mutual capacitance of the cables insulated with cellular/solid PE increased to + 1.1 nF/km at 70 °C within one day, due to the low thermal inertia of the 10-pairs cable; this applies to both the filled and unfilled cable.

After cooling to room temperature, the mutual capacitance of the unfilled cables with all three types of insulation is virtually unchanged as compared with the initial value.

In the case of filled cables the difference is - 0.6 nF/km for cellular PE and - 0.8 nF/km for cellular/solid PE. This is approximately the same value as for the solid PE insulation used as a comparison (- 0.8 nF/km). The reduction in mutual capacitance is thus approx. 1.5 to 2.5 %.

The following diagram shows the variation of difference in mutual capacitance after 7 and 21 or 28 days of thermal treatment, after cooling to room temperature.

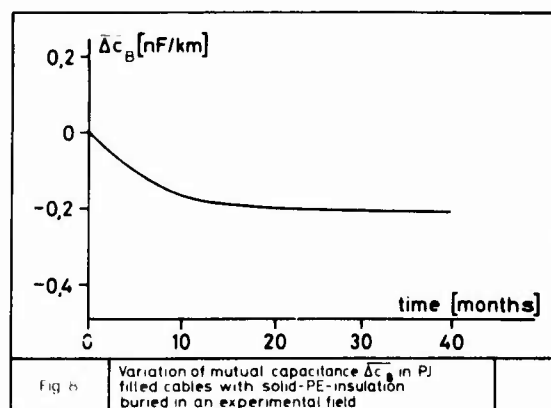


At 70 °C, the curve of mutual capacitance for cellular PE increased again in the second and following weeks, but was still in the minus range after 4 weeks. The process has not yet terminated, however, and storage at 70 °C is being continued. After 4 weeks the reduction in the mutual capacitance for cellular PE (measured at room temperature) was - 0.3 nF/km (i.e. an increase of 0.3 nF/km compared with the end of the first week). In the case of "foam skin", mutual capacitance fell between the first and fourth week from - 0.8 to - 1.0 nF/km. The trend is still under observation. Solid PE shows virtually no change. The long-term trends for the 3 types of insulation in filled cables are still under examination.

If the results of capacitance measurements on single PE insulated conductors which were stored in a surplus of PJ are compared with the changes in mutual capacitance in the cable, the different definitions and methods in measuring the capacity in a water bath and the mutual capacity between two conductors of a cable have to be taken into account. In addition, the limited amount of PJ in the cable and the relatively unlimited amount of PJ when storing single wires in a surplus of PJ must also be taken into account. By and large, these investigations confirm the previously recorded results (on single wires) but were necessary in order to provide a basis for studying the processes which can lead to a change in capacity unbalances.

#### Correlation of the measured results of the mutual capacitance with practical results

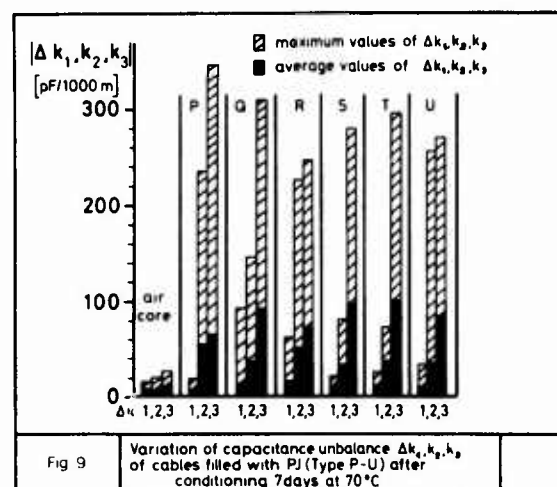
Cables with solid PE insulation and PJ fillings have been buried for 3 1/2 years in an experimental field in Germany (average ground temperature + 12 °C). The mutual capacitances have been measured at regular intervals. The following diagram shows the mean values (obtained from widely scattered results from different cables) and indicates this trend:



If the results of laboratory conditioning in the thermal chamber are compared with the practical results, it is obvious that burial with a mean change of 0.25 nF/km in 3 1/2 years has resulted in approx. one third of the equilibrium value in the thermal chamber.

#### Variation in capacitance unbalances

This can be measured only on the cable. The capacitance unbalances change in filled cables after a storage of 7 days at 70 °C as compared to the initial values, as shown in the following diagrams (the cumulative frequencies of the differences, compared with the starting values, are shown without taking the sign into account, i.e. whether it was an increase or decrease).



The diagram shows the mean (black) and maximum (shaded) variations in capacitance unbalances  $\Delta K_1$ ,  $\Delta K_2$ , and  $\Delta K_3$  of cables with solid PE insulation (all conductors ringmarked) (100 x 2 x 0.6) which were filled with 6 different types of petrolatum (P, Q, R, S, T, U). These variations are taken from cumulative frequency curves. Whereas  $\Delta K_1$  changes on an average by less than 20 pF/1000 m, the average  $\Delta K_2$  and  $\Delta K_3$  vary by up to 50 or 100 pF/1000 m, and the maxima up to 350 pF/1000 m.

In the case of an unfilled cable which was also conditioned for 7 days at 70 °C for reference purposes K1, K2, and K3 show scarcely any change, i.e. an average by 5 - 10 pF/1000 m with a maximum of 30 pF/1000 m. The influence of the PJ filling on the changes in capacity unbalances  $\Delta K1$ , and particularly  $\Delta K2$  and  $\Delta K3$ , is not inconsiderable. No basic differences result from the 6 PJ types employed.

A typical cumulative frequency curve concerning the change  $\Delta K2$  and  $\Delta K3$  of capacity unbalances due to storage at 70 °C is shown in Fig. 10.

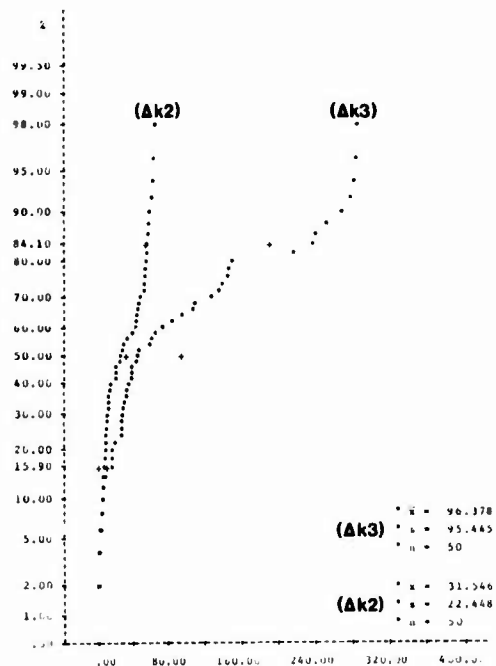


Fig 10	Cumulative Frequencies of differences in capacitance unbalance, caused by conditioning	5039E
--------	--	-------

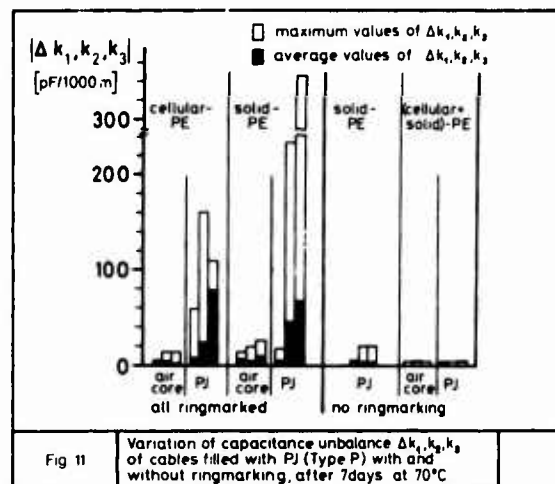
In Fig 9 and 10, it will be noted that  $\Delta K2$  and  $\Delta K3$  are larger than  $\Delta K1$ , and that K3 capacitance unbalances change more than the K2 capacitance unbalances.

It thus seemed logical to examine more closely the differences in the cable which cause these results, in which connection ringmarking is particularly interesting.

In order to determine the effect of the insulation structure, the capacitance unbalances K1, K2, and K3 of cables with solid, cellular, and cellular/solid PE insulation, both with and without PJ filling and with (solid, cellular PE) and without (solid PE and cellular/solid PE) ringmarking were measured before and after storage for one week at 70°C.

The results are shown in the next diagram; a solid PE cable is included for comparison

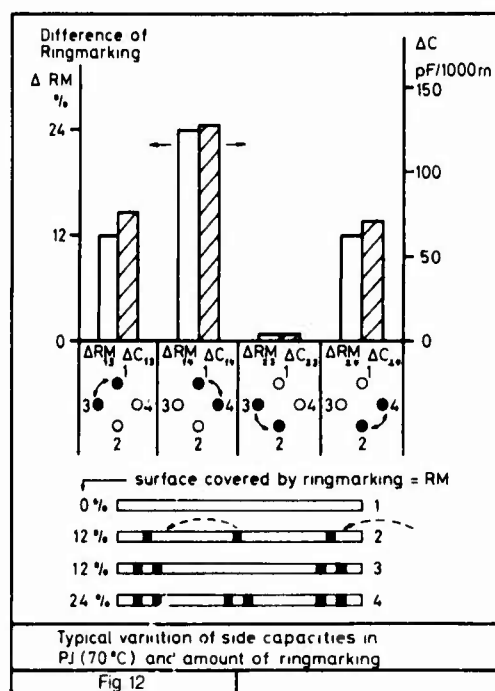
All insulations with one PJ type. In this case the maximum values of  $\Delta K1$ ,  $\Delta K2$ , and  $\Delta K3$  are not shaded.



The capacitance unbalances of solid PE and cellular PE conductors (both with ringmarking) change in the unfilled state by an average of less than 10 pF/1000 m and a maximum of 30 pF/1000 m, i.e. within acceptable limits. In the case of cellular PE with filling, the capacitance unbalances change on an average in a similar way to solid PE, and maximum values are slightly lower. But as can be assumed from the values in Fig. 9, no effect is apparent without ringmarking: The cable with solid/cellular PE (unmarked) shows virtually no change in the filled or unfilled state;  $\Delta K1$ ,  $\Delta K2$ ,  $\Delta K3$  have a maximum of 5 pF/1000 m.

In a solid PE cable which was deliberately produced without ringmarking of the wires very low changes were measured, namely  $\Delta K1=2$ ,  $\Delta K1 \text{ max.} = 4$  pF/1000 m, and average values of  $\Delta K2$  and  $\Delta K3$  about 4 pF/1000 m with maximum values of 20 pF/1000 m, i.e. practically no change (cable filled with PJ).

This means that the different variations in the capacitance unbalances of PJ filled cables are less connected with the structure of the insulation itself than with the ringmarking. This effect calls for an explanation: the desing of a star-quad and the side capacities must be examined. Ringmarking paint covers 0 (unmarked), 12, 12 and 24% of the surface of the 4 conductors of a star-quad. The changes affecting cross-talk have to be governed by this.



The side capacities were numbered C 1/3, C 1/4, C 2/3, C 2/4, and the change shown in a bar chart.

The diagram shows a typical example of the changes in a star-quad (basic colour white). As indicated by the diagram this situation shows that changes in the side capacities are correlated with the differences of the conductor surface covered by ringmarking (0-24%).

The largest variation in the side capacities always occurs between the unmarked wires and the wires with the largest amount of marking (24% coverage), and the lowest change (practically 0) between the two wires, which are marked with 12% coverage (these wires differ only in the spacing of the rings). The absolute values of the side capacity changes are higher in the case of certain insulation colours, demonstrating that the colour of the insulation exerts an influence. However, the tendency is the same. The influence of the colour of the bundle is still being examined.

With unfilled cables, practically no differences were measured in the side capacities. These measurements also indicate the pronounced influence of the ringmarking on side capacities (see also Fig. 4b).

As already indicated, the ringmarking paint used is a "PJ resistant" type used by several cable manufacturers because of its resistance to wiping. Its use is limited by specification.

The strong influence of the ringmarking paint can be traced to mutual interaction with the petrolatum. Components with higher dielectric constants (e.g. plasticizing components, solvent residues, and other extractable substances) are extracted by PJ, or migrate into the PJ, and are partially replaced by components of the PJ (dielectric

constant  $\approx 2.3$ ).

The resulting changes in the dielectric constant of the ringmarking paint can lead to unbalance of the capacitances due to varying quantity of paint on the conductors of a star-quad.

Two effects should be distinguished in the variations of the capacities, capacitance unbalances and side capacities:

- surface effects, which particularly concern the ringmarking and take place relatively quickly, and
- volume effects, which concern the insulation and require longer diffusion times due to the larger layer thickness.

## CONCLUSIONS

The average service life of telephone cables is 30 - 40 years, and their mechanical and electrical properties must be sufficiently stable over this period. This is the only way to meet the requirements for such cables.

While the mechanical and capacitive changes in PE cables with PJ fillings have been dealt with in other publications, this report discusses details of the crosstalk instability of PJ filled plastic insulated cables. The reason is the interaction of the petrolatum with the insulation and the ringmarking, which causes side capacity unbalance. The resulting changes in capacitance unbalance during the service life of the cable remain within acceptable limits if the cable is used for house connections at the end of networks for voice frequency operation. However, if PJ cable is to be used for higher levels on the network, where the stability of the capacitance unbalances is important, then conventional PJ cables should not be used. Other methods should be given preference.

For such applications, the following measures should be taken:

- the colour-coding system should be modified by:
  - o quantitative matching of the paint marking of the conductors
  - o selection of dielectrically more neutral ringmarking points which are less sensitive to PJ but are still resistant to wiping, and easily to identify.
- improved selection of the material components and the technological parameters to obtain better stability of the capacitance unbalances
- replacement of ringmarking by other marking systems
- other technological methods

All in all, unlimited employment of longitudinally sealed PE cables with PJ filling for general purposes, i.e. for all distances and frequencies, would at present appear only to be a possibility for coming years.



## Bibliography

1. "Modern Plastic Cable Constructions with Moisture Barrier"  
H. Falke; 17th International Wire & Cable Symposium 1968
2. "Shear and Flow Characteristics of Waterproof Petrolatum-based Cable Filler Compounds",  
J.J. Kaufmann, T.E. Luisi, 23rd International Wire & Cable Symposium
3. "Compatibility Problems in Filled Cellular Polyolefin Insulated Telephone Cables";  
S.G. Foord, 22nd International Wire and Cable Symposium 1973
4. "Long-Term Stability of Fully-Filled Cables",  
S. Verne, A.A. Pirching, I.M.R. Hagger, 22nd International Wire & Cable Symposium 1973
5. VDE-Vorschrift 0209/DIN 57 209
6. FTZ-Norm 72 TV1, Teil 3 (1972)
7. "Cellular Insulation as an Answer to Material Conservation",  
E.D. Metcalf, 23rd International Wire & Cable Symposium 1974
8. "Effect of Water and Petroleum Jelly Migration on Capacitance of Plastic Insulated Cables",  
C.J. Aloisio, E.D. Nelson 22nd International Wire & Cable Symposium 1973
9. "Recent Developments in the High Speed Insulation of Quality Telephone Cables",  
E. Kertscher, 22nd International Wire and Cable Symposium 1973



Hans A. Mayer

(Speaker)

AEG-TELEFUNKEN KABELWERKE  
Aktiengesellschaft  
Development Center  
W. Germany

22-28 Sommerfeld  
433 Mülheim/Ruhr-Saarn

1951 - 1956 he studied industrial chemistry and obtained his degree as a Dipl.-Ing. Then he was 5 years in the plastics & rubber industry and 3 years in the organic chemical industry as Head of quality control and central laboratories. In 1965 he joined AEG-TELEFUNKEN KABELWERKE. Presently he is Head of the Materials Development Department.



H.G. Dageförde is Head of the Development Department for symmetrical communication cables of the AEG-TELEFUNKEN KABELWERKE. As a Dipl.-Ing. of the Technische Hochschule Aachen, he joined Kabelwerk Duisburg (now a subsidiary company of AEG-TELEFUNKEN) in 1952. Since then he is engaged in testing, quality control, installation and development of communication cables.



Hans-J. Anderka studied 1971 - 1974 electro-technics and telecommunications at Fachhochschule Duisburg and obtained his degree as Ing.(grad). Since 1974 he is engaged with AEG-TELEFUNKEN KABELWERKE as a development engineer in the Department of Symmetrical Cables Development.

EVALUATION OF ADHESIVE AND COHESIVE CHARACTERISTICS  
OF PETROLATUM BASED FLOODING COMPOUNDS

J. J. Kaufman, T. E. Luisi

Witco Chemical Corporation

New York, New York

Summary

Laboratory procedures are used to evaluate flooding compounds that have recently come into use in filled telephone cable. Properties including adhesion and cohesion and corrosion resistance are examined.

Introduction

For the purpose of this discussion, we differentiate, on an application basis, what we mean between a flooding compound and a filling compound. The filling compound is the material used to fill the core of the cable. The flooding compound is applied at all interfaces beyond the core wrap, for example: between the core wrap and the shield, shield and jacket. A flooding compound might also be used between the core and the core wrap. The principal function of the flooding compound is to provide a watertight flexible seal between the interfaces. A secondary function of the flooding compound is as an adhesive between shield and jacket to inhibit slippage of the jacket over the shield when the cable is being pulled. Desirably, it should also provide corrosion protection to the shield.

Asphaltic type flooding compounds have been used for flooding between the shield and jacket and, initially, these compounds have excellent adhesive properties. They soon become brittle and are subject to "crazing" or cracking, resulting in moisture penetration between the shield and jacket and corrosion of the shield material. With the advent of the waterproof filled cable, the PE/PJ filling compound was often used both as a filling compound and flooding compound. While the PE/PJ compound performed reasonably well as a flooding compound, it was observed that in the Moisture Penetration Test (1) failure occurred most often at one of the interfaces. Also, there is some opinion that the PE/PJ compound could act more as a lubricant than as an adhesive between the jacket and shield during a difficult cable pull. To improve on flooding compound performance, several new flooding compounds have been introduced which are based on a cable filler type petrolatum and an amorphous polymer.

The amorphous polymers increase the cohesive character and viscosity of the flooding compounds. To be effective a flooding compound should retain these characteristics, as well as the characteristic of adhesion, over the entire temperature range the cable may experience during installation (-40°F [-40°C] to +120°F [49°C]). The characteristics of adhesion and cohesion must also be balanced since a failure in either mode can result in the development of water paths or sheath slippage.

Let us now define adhesion and cohesion.

Cohesion is the molecular force exerted across a liquid or a solid that resists internal rupture (2).

Adhesion is the molecular force exerted across a surface of contact between unlike liquids or solids that

resists interfacial separation.

With these definitions it will be easy to determine if the bonding failure of a flooding compound is cohesive or adhesive. In the case of the former, flooding compound will remain on both the shield and jacket surfaces. In the latter case, one of the surfaces will be free of flooding compound with all of the compound on the second surface or possibly the compound will delaminate from both surfaces.

In our evaluations, the stress on the test specimens is the same kind of stress imposed on the flooding compound between the shield and jacket as in the case of the REA Sheath Slip Strength Test (3).

Testing Procedure

In order to arrive at data which would give a relative ranking to the samples tested, it was necessary to keep the sample preparation and testing as simple and uniform as possible. In the cable itself, probably the most significant factor in controlling sheath slip is the degree of fill of the shield corrugations by the jacketing compound. This variable had to be ignored for the purposes of our testing. We used samples of low density 75 mil (1.91 mm) polyethylene (4) jacketing material and uncoated 10 mil (0.254 mm) aluminum shielding which were cut into 2.54 x 6.35 cm (1 x 2.5 inch) rectangular tabs, and coated by dipping into the molten test compound at 121°C (250°F) except for Compound II which, due to its high viscosity, was coated at 150°C (302°F). The tabs, on removal from the compound, were immediately placed together to form a 6.45 cm<sup>2</sup> (1 inch<sup>2</sup>) overlap. A 120 gm weight was placed on the seal which was then cooled to ambient temperature. The specimens were then placed in a Sentinel heat sealer (5) which is a test device used primarily for laminating substrates. With it, bonding time, temperature and pressure can be accurately controlled. A pressure of 4.54 kilograms (10 lbs.) was applied for a period of three seconds at a temperature of 25°C (77°F) and 50% R.H. These conditions were established as optimum.

The yield point of the bond between the two tabs was determined by the use of a KVP (6) tensile tester utilizing a Chatillon (7) strain gauge. The KVP tester utilizes a constant speed motor driving a chain belt, via a gear box, at a speed of 12.5 cm/min (5 inches/min). One tab of the test specimen was fastened to the chain belt and the other to the Chatillon strain gauge which registers the maximum force being applied. The force was applied parallel to the plane of the contact surface of the tabs.

During the course of testing, it was determined that bond strength is not only affected by initial bonding pressure, but also by subsequent aging of the bond. This is illustrated in Table 1. Accordingly, all specimens were conditioned for 18 hours, and tested, in an environment maintained at 25°C (77°F) and 50% R.H.

As a matter of practicality, it was decided that a shear force of 400 grams per square centimeter (equivalent to a pulling force of 17 lbs. per inch of cable on one-inch diameter cable) would constitute an upper limit for testing.

#### Compound Selection

Table 2 illustrates the effect of increasing the level of atactic polypropylene on the physical properties. Because of the almost completely amorphous nature of this particular polypropylene there is little effect on the congealing point of the compound. On the other hand, the drop point, hardness (lower consistency), viscosity and yield point show a progressive increase with maximum change occurring at the 15-20% level. A flooding compound containing 20% APP is currently being used in telephone cable. Since this concentration of APP coincides with what appears, from the data in Table 2, to be an optimum level, it was decided to evaluate all of the petrolatum-APP blends at the same APP concentration.

For our evaluation we selected eight compounds which are identified as follows:

- I. A typical PE/PJ compound, that has been used for both filling and flooding, selected as the control.
- II. 100% APP.
- III-VI. Flooding compounds consisting of petrolatum plus different grades of APP at the same concentration.
- VII. A flooding compound consisting of petrolatum plus an elastomer.
- VIII. A new experimental filling compound which has promise of also functioning satisfactorily as a flooding compound.

The physical properties of these compounds are listed in Table 3.

#### Evaluation Results

Examination of the specimens after testing, at 25°C (77°F), indicated that all of the failures were due to cohesive failure and not adhesive failure. This was to be expected, at ambient temperature, based on prior experience. The data are presented in Table 4.

If adhesive failure were to occur, it would occur at temperatures considerably below ambient. Accordingly, the KVP tester was placed in a cold box and the testing was repeated at -29°C (-20°F). With the exception of Compound II all of the samples exceeded the limits of the strain gauge, indicating excellent adhesive and cohesive properties at low temperature. In the case of Compound II (the 100% APP) we experienced an adhesive failure when the sample was being prepared for testing. The specimen had delaminated at the aluminum surface.

In view of the REA "Cable Bend Test" (1) at -40°C (-40°F) we subjected the test tabs to a temperature of -44.5°C (-50°F). Due to equipment limitations, the specimens were evaluated more subjectively. Again, the only tabs to show adhesive failure were those prepared with Compound II. Additionally, all specimens were flexed to form an angle of approximately 135°. No sign of bond weakening was observed with the exception of Compound II. In the case of Compound II there was adhesive failure at the aluminum surface without

any stress being applied. With all of the APP on the polyethylene surface, the polyethylene tab was flexed and the APP, which was below its glass transition temperature, shattered.

As might be expected, Compound II, the 100% APP, exhibited adhesive and cohesive properties superior to the 20% APP compounds (III-VI) at 77°F. Poor adhesion and hardness approaching embrittlement at lower temperatures, raise questions regarding its suitability as a flooding compound.

Compound VI was evaluated since it had been under consideration as a commercial flooding compound and appeared superior to the other 20% APP compounds. The atactic polypropylene in this compound, however, is apparently contaminated by crystalline polypropylene which is indicated by its high congealing point (Table 3). Due to this contamination, it has a tendency to develop a gel structure even at elevated temperature (138°C [280°F]). We would expect that a flooding compound based on this material would be much more difficult to handle in plant production than the other compounds tested.

Compound VII, containing an elastomer at a much lower additive level, outperforms Compounds III-VI on a cost/performance basis in terms of cohesiveness. Because of its high viscosity, however, it may have to be handled at a somewhat higher temperature than the APP compounds.

Compound VIII is an exceptionally promising experimental filling compound whose properties as a flooding compound place it in the mid-range of the 20% APP compounds, making it a potential flooding compound as well. This material would have the advantage of offering the cable manufacturer one product for both applications, obviating the necessity of dual systems and dual inventories.

Based upon the yield point data, all of the specimens evaluated will exceed the requirements of the REA "Sheath Slip Strength Test" (3).

#### Corrosion Inhibition

It was not our original intention to include in this paper the performance of flooding compounds as corrosion inhibitors. However, since corrosion inhibition would be an obvious asset to any flooding compound, it was decided to evaluate their performance in this regard. Buried cable is subjected to ground water which usually contains dissolved salts and is further subjected to electro-magnetic fields. Thus the mode of corrosion is essentially galvanic. Accordingly, for our corrosion evaluations, we used a salt fog chamber in which minute droplets of water containing 5% sodium chloride are maintained in suspension in the fog chamber. Cold rolled steel Q panels (8) were coated with the test compounds to a thickness of 0.5 mil (0.0125 millimeters) and 1.0 mil (0.025 millimeters) and placed in the salt fog chamber. Compound A was a petrolatum containing amorphous polypropylene. We believe its resistance to corrosion would be representative of the flooding compounds I through VIII. Compounds B and C are modifications of Compound A, containing an oil soluble, barrier-type corrosion inhibitor at additive levels of 5% and 10% respectively. Each compound was run in triplicate. The criteria for minimum failure is the development of three rust spots of any size or one spot of more than one millimeter in diameter.

The data developed to date appears in Table 5.

The salt fog test is a particularly severe corrosion test and we cannot at this time draw any conclusions as to the extrapolation of this data to the field. Undoubtedly, Compounds B and C represent a distinct improvement compared to Compound A, but further cost/effectiveness evaluations of the use of corrosion inhibitors in flooding compounds will have to be conducted before drawing any conclusions concerning the practicality of adding corrosion inhibitors to the flooding compounds.

#### Conclusion

The flooding compounds evaluated appear to have all of the requisite properties to satisfy the current requirements of REA with regard to jacket slip and water blockage, with the exception of Compound II, the 100% APP. We can conclude that petrolatum performs a critical role in the flooding compounds as an active vehicle, particularly at lower temperatures.

The selection of a specific compound by the cable manufacturer would be based on cost/performance and plant processing considerations.

Further work needs to be done concerning the economic practicality of improving the corrosion inhibition properties of flooding compounds.

#### Acknowledgement

The authors are grateful for the assistance of their colleagues, Messrs. J. D. Burkhard, D. G. Palmgren, T. J. Roessing, in developing the data for this paper.

#### References

1. REA Specification P. E. 39, eff. 5/1/73.
2. "Physical Chemistry of Adhesion," D. H. Kaelble, J. Wiley & Sons, N. Y., 1971.
3. REA Specification P. E. 39, draft of Appendix B, "Simulated Environmental Tests for Filled Telephone Wires and Cables."
4. Union Carbide, DFDA 0588 Black 9865.
5. Sentinel Heat Sealer, Model 12AS, Packaging Industries Inc., Montclair, N. J.
6. KVP Tensile Tester, Model K-70-1, KVP Div., Brown Paper Co., Kalamazoo, Mich.
7. Chatillon Strain Gauge, Model DPP 2.5 Kg, John Chatillon & Sons Inc., Kew Gardens, N. Y.
8. Stock # R36, Q Panel Corp., Cleveland, Ohio.

(Speaker)  
Thomas E. Luisi  
Witco Chemical Corporation  
277 Park Avenue  
New York, New York 10017



Tom Luisi is Product Manager for Telephone Cable Products and Market Development Manager for the Sonneborn Division of Witco Chemical Corp. A graduate of the City College of New York, with a B.S. Degree, he has been with Witco for 19 years in various technical marketing functions.

(Co-author)  
J. J. Kaufman  
Witco Chemical Corporation  
Petrolia, Pa. 16050



John Kaufman is Director of R&D for Wax and Related Products for the Sonneborn Division of Witco Chemical. He graduated from the University of Pittsburgh with a B.S. in chemistry. John is a member of the Joint Committee on Wax Testing sponsored by ASTM and TAPPI.

TABLE 1

Effect of Aging Upon Yield Point\*

Conditioning Time, Hrs.: (77°F.; 50% R.H.)	18	90	186
Bond Strength, g/cm <sup>2</sup>	242	293	334
Strength Range, g/cm <sup>2</sup>	228-260	268-320	313-360

\* Data obtained with a commercial flooding compound of petrolatum and A.P.P.

TABLE 2

Effect of Atactic Polypropylene Upon Physical Properties

<u>Composition, Wt. %</u>						
Base Petrolatum	100	95	90	85	80	75
Atactic Polypropylene	0	5	10	15	20	25
<u>Melting Point</u>						
Congeaing, ASTM L-938, °F.	119	130	126	130	134	126
Drop Point, IP 31/66, °F.	126	126	133	145	165	172
<u>Cone Penetration</u>						
Petrolatum, ASTM D-937 77°F. (25°C), 0.1 mm	128	126	125	126	111	110
<u>Viscosity</u>						
Kinematic, ASTM D-445						
SUS @ 210°F. (99°C)	82	154	287	511	1213	1429
SUS @ 266°F. (130°C)	53	82	136	226	371	574
SUS @ 302°F. (150°C)	46	65	77	156	246	386
<u>Average Yield Point</u> g/cm <sup>2</sup>	35	76	86	112	150	166
<u>Yield Point Range</u> g/cm <sup>2</sup>	34-37	67-82	78-91	114-133	138-155	158-171

TABLE 3

## Physical Properties of Flooding Compounds

	<u>I</u>	<u>II</u>	<u>III</u>	<u>IV</u>	<u>V</u>	<u>VI</u>	<u>VII</u>	<u>VIII</u>
<u>Melting Point</u>								
Congealing, ASTM D-938, °F.	183	NA	119	125	134	192	140	128
Drop Point, IP 31/66, °F.	207	>250	142	129	165	219	131	192
<u>Cone Penetration</u>								
Petrolatum, ASTM D-937								
77°F. (25°C.), 0.1 mm	60	29	109	103	111	93	66	106
<u>Viscosity</u>								
Kinematic, ASTM D-445								
SUS @ 210°F. (99°C.)	154*	NA	256*	857*	1213	NA	NA	910
SUS @ 266°F. (130°C.)	76	1929	113	562	371	348	4116	417
SUS @ 302°F. (150°C.)	-	1187	82	237	246	247	2496	286
<u>Density</u>								
Viscous Liquids, ASTM D-1480 mod.**								
@ 77°F. (25°C.)	.8728	.8630***	.8667	.8729	.8708	.8933	.8741	.9044
@ 122°F. (50°C.)	.8479	.8383	.8409	.8448	.8436	.8647	.8451	.8738
@ 158°F. (70°C.)	.8350	.8276	.8280	.8301	.8306	.8506	.8325	.8605
<u>Coefficient of Expansion</u>								
Thermal Exp. ASTM D-1903								
Solid/Solid Transition								
N x 10 <sup>-3</sup> cc/g/°C.								
25 - 50°C.	78	71	84	92	86	92	98	100
50 - 70°C.	21	12	25	35	26	30	22	24
<u>Volume Change (70°C - 25°C)</u>								
Volume %	4.33	4.10	4.46	4.85	4.61	4.78	4.76	4.85

## Note:

\*Cloudy

\*\*Convection Oven; aluminum, 11 ml Pycnometer

\*\*\*@ 73.4°F. (23°C.)

TABLE 4

## Comparative Yield Points of Flooding Compounds at 77°F.

	<u>I</u>	<u>II</u>	<u>III</u>	<u>IV</u>	<u>V</u>	<u>VI</u>	<u>VII</u>	<u>VIII</u>
Average Yield Point g/cm <sup>2</sup>	154	>400	85	127	143	177	265	117
Yield Point Range g/cm <sup>2</sup>	140-167	>400	77-90	118-134	136-152	160-188	256-272	108-128

TABLE 5

## Salt Fog Evaluation of Flooding Compounds

<u>Compound</u>	<u>A</u> (no corrosion inhibitor)	<u>B</u> (5% corrosion inhibitor)	<u>C</u> (10% corrosion inhibitor)
0.5 mil panels	24 hrs*	72 hrs	72 hrs
1.0 mil panels	120 hrs	264 hrs**	456 + hrs***

\* severe failure

\*\* 2 of 3 panels failed

\*\*\* 2 of 3 panels still running



# THE PROPERTIES OF CELLULAR POLYETHYLENE INSULATED FILLED COMMUNICATION CABLE AND ITS INCREASING USE

S. M. Beach, K. R. Bullock, D. F. Cretney

Phillips Cables Limited

Brockville, Canada

## Summary

Temperature conditions prevailing in Canada have been considered in detail and their effect on the performance of cellular insulated fully-filled cables discussed. A quantitative assessment of changes likely to occur in the lifetime of these cables has been made on the basis of long term laboratory tests. The satisfactory field experience to date has been reviewed.

## Introduction

In Canada, telephone cable development in the late sixties resulted in a trend away from air core polyethylene insulated cables to the use of filled cables first with solid polyethylene, and then cellular polyethylene insulation applied by single extrusion or by dual extrusion with a separately extruded solid layer.

The introduction of solid filled polyethylene insulated cables was instigated by Canadian telephone operating companies looking for more reliability due to experience of water ingress problems. In 1968 no suitable cellular polyethylene or propylene materials or appropriate extrusion technology existed in Canada or the U.S.A., so filled cable production began in both countries with solid materials. However, a few trial lengths were produced in Canada using British-made cellular polyethylenes<sup>1</sup> and this led to increasing pressure from the operating companies for this more economical cable.

It must be remembered that most direct buried cable being used in this period was of the PAP (double sheathed air core) type. Thus the step from double jacketed air core to single jacketed solid filled was an economic trade-off, while the next step to single jacketed cellular filled cable was an economic advantage for the user.

The concept of filled telephone cable was proposed by G. A. Dodd in the U.K. in 1963 and the first installations were made in 1964 at Stevenage and 1965 at Plymouth, England, by the British Post Office. By 1966 it had been accepted as a regular product in the British Post Office network. It should be noted that the development of suitable cellular polyethylenes for extrusion in thin walls and the adoption of petroleum jelly compound as the filling material occurred parallel with the developing design.

So, in 1968 when Alberta Government Telephones first proposed the use of filled cable in Canada, there was some background experience to draw on which influenced the initial stages of Canadian production quite noticeably.

While the first solid polyethylene insulated cables were being installed and used in Alberta and B.C., the eventual trend to cellular insulated was recognized. For a year or two United Kingdom-manufactured cellular materials were used, but Union

Carbide Canada produced the first Canadian-made compound successfully in 1971 and it quickly superseded imported materials.

The filling compounds used are produced in Canada and were selected with regard to Canadian operating conditions.

## Construction and Manufacturing

The construction and manufacturing of the cellular insulated fully-filled cable (Celseal<sup>®</sup>) produced by Phillips Cables Limited is similar to that of solid filled cable. The principal area of difference lies in the control required over the insulation extrusion line. Key features of the extrusion equipment have been described previously<sup>2</sup>. The practice described therein has proven to be reliable and remains in current use although important detail improvements have been made. The equipment produces medium density polyethylene insulation with a fine, uniform and non-interconnecting cell structure and a dense layer at the outer surface. The structure of insulation is critical to cable performance. Cables with insulation not having the most significant of these features would not achieve the satisfactory standards of performance described in this paper.

This equipment also produces excellent solid insulation and no special training is required for its operation. In fact, since 1973, Phillips Cables Limited has commissioned two new plants where the personnel have had no previous experience of cable manufacture.

Pairing is accomplished by means of conventional equipment. Standard North American colour coding and pair twists are employed. For assembling the pairs into a cable an arrangement employing driven let-off stands with associated unit forming and identification devices, unit oscillating and filling equipment, core wrap, overfill, shield application and jacket extrusion all in a tandem configuration, has proven successful for up to 50 pair cables. For assemblies up to 200 pairs a somewhat similar arrangement is used, with the exception of the tandem sheathing unit. Cables larger than 200 pairs are treated as special cases with the manufacturing technique dependent upon the plant involved.

The core wrap is a flat, longitudinally applied, polyester tape having assured adequate overlap. The cable shield is a flat, double-coated aluminum tape formed longitudinally. Applied overall is a black low density polyethylene or medium density polyethylene jacket chosen for good stress crack resistance, mechanical toughness and compatibility with the filling compound.

<sup>®</sup> Registered Trade Mark

## Materials

### Insulation

The cellular insulation is produced from a medium density, fully compounded polyethylene specially designed for the application and having a nominal resin density of 0.935 g/cm<sup>3</sup>. This material is capable of producing a fine, uniform cell structure. The blowing agent is included in sufficient quantity to produce the degree of expansion required to meet the design criteria for the range of products produced. The partial volume of air is generally 25-35% in non-interconnecting cells of 20 µm and less.

Pigments are selected with regard to colour intensity, non-interference with the blowing agent and final electrical properties. An antioxidant and copper inhibitor are also incorporated into the insulant.

Further details may be found in references 2 and 3.

### Filling Compound

The filling compound used has been an electrical grade petroleum jelly incorporating antioxidant and intended for application by a high temperature filling technique. The principal selection criteria applied when choosing the filling compound were:

- a) Retention of adequate physical properties over the required temperature range.
- b) Suitable dielectric properties, substantially unaffected by water.
- c) Compatibility with primary insulant and jacket.
- d) Ease of manufacturing application.
- e) Acceptability to telephone company craftsmen.
- f) Cost and availability.

Development filling compounds are becoming available, still based on petroleum jelly, but containing thixotropic additives. These compounds display certain advantages at both low and elevated temperatures. We are conducting an extensive, continuing investigation into this type of material and some of the relevant findings are reported in this paper.

### Temperature Requirements

#### Definition of Circumstances

In any discussion of the long-term testing of cables the question of temperature invariably arises. The interaction between filling compound and insulation is a temperature dependent function of time. Moreover, as the temperature increases a change in the mechanism of interaction occurs and it is inappropriate to carry out accelerated life tests above this temperature. Life tests at an excessive temperature can be shown to put materials in a wrong order of merit; adequate material can be rejected with consequent economic penalties, or even an inferior material may be selected with significant technical deficiencies. An example of this is referred to in Appendix 3.

It is obviously important to identify and define the various environmental conditions to which cable is exposed, both before and after installation. These are:

- a) Storage on reels
- b) Aerial cable
- c) Buried cable
- d) Pedestals

Investigations of long-term cable stability must be based on tests incorporating times and temperatures relevant to the above situations.

### Field Measurements

In order to ascertain the maximum temperatures reached in cable cores a series of tests were carried out in Western Canada. In these tests maximum indicating thermometers (0° - 100°C) were embedded in the centre of the cable cores. The cable sheath was then replaced and black tape used to restore the integrity of the specimen. In this way maximum temperatures were then measured on cables,

- (i) Buried 3 feet underground
- (ii) Lying on the ground
- (iii) Suspended in air at a height of 4 feet above ground level
- (iv) A full length on an unlagged reel.

All locations were chosen to ensure maximum exposure to direct sunlight.

The results recorded during the hottest part of summer 1975 (July - August) in a selected high temperature location are shown in Table 1.

TABLE 1

Maximum Cable Core Temperatures Recorded in Western Canada (Kamloops, B.C.) During a Period when Maximum Air Temperature Reached 42°C

Location	Maximum Core Temperature °C
Buried (36")	19
On Ground	62
In Air	56
* On Reel 1st Layer at a Vertical Position	59
On Reel 1st Layer 30° from Vertical to West	63
On Reel 2nd Layer at Vertical Position	48

\* Axis of reel was N-S.

For comparison Table 2 presents the results obtained during January and February (hottest season) in Equatorial East Africa by an associated company.

TABLE 2

Maximum Cable Core Temperatures Recorded in Equatorial East Africa (Kampala, Uganda) During a Period when Maximum Air Temperature Reached 43°C

Location	Maximum Core Temperature °C
Buried (18")	27
On Ground	60
In Air	47
On Reel	62

Although the maximum temperatures recorded in Western Canada and Africa were similar it is recognised that the extremes encountered in Africa may persist for longer durations.

It is clear from the results in Tables 1 and 2 that:

- (i) Buried cable remains cool.
- (ii) A cable on the ground exposed to sun may reach a temperature some 20°C above air temperature (but this situation is not of practical interest).
- (iii) Maximum temperature of an aerial cable may reach up to 15°C above air temperature.
- (iv) Parts of the outermost layer of a cable on an unlagged reel may reach a temperature 20°C above the air temperature.

The above data has been used in assessing the long term performance of cellular insulated filled cables in the following sections.

#### Long Term Laboratory Tests

Long-term aging tests at 60°C have been carried out on cables of current design and others incorporating an experimental filling compound. The descriptions of the two cables of current design are given in Table 3.

The cables were in the form of coils and were approximately 30 feet in length. The coils were placed in a walk-in environmental cabinet<sup>2</sup> at 60°C. The plane of the coil was vertical and the ends of the cables, in addition to having a neoprene cap placed over them, were pointing up to minimize compound leakage.

TABLE 3

#### Description of Cables Tested

Cable	AWG	Pairs	Details of Cellular Insulation		Aging Temp./Time
			Partial Volume of Cells	Wall Thickness (Mils)	
1	19	25	0.31	12.9	60°C/28 Months
1c	19	25	0.31	12.9	Room Temp.
2	24	25	0.32	8.1	60°C/12 Months
2c	24	25	0.32	8.1	Room Temp.

#### Notes:

- (1) "c" denotes the control sample kept at room temperature for the same time period.
- (2) Both cables were of concentric construction with a 5 mil polyester wrap and a double coated aluminum shield applied over the core. A medium density polyethylene jacket was applied overall.
- (3) Both cables were filled with the currently used electrical grade of petroleum jelly compound with a drop melting point (ASTM-D127) of 90°C minimum.

These cables were periodically removed from the cabinet, allowed to cool to room temperature and their transmission properties measured. Finally a part of each cable was subjected to a waterproofness test, and another part was dissected for examination of insulated singles. Results from each of the cables were compared with the corresponding results obtained on a control specimen which in each case was the consecutive length of the same cable kept at room temperature.

The properties investigated were:

- a) Stability of transmission properties
- b) Structural stability of cellular polyethylene
- c) Waterproofness.

#### Transmission Stability

The results of measurements of transmission properties on cables are summarized in Table 4, and detailed results are given in Appendix 1. Measurements were accomplished by means of an impedance bridge, null detector and oscillator.

TABLE 4

Comparison of Transmission Properties of Cables  
Kept at 60°C and at Room Temperature

(average from measurements on 25 pairs)

Property	Cable 1	Cable 1c	Cable 2	Cable 2c
<u>Measurements at 1 kHz</u>	<u>60°C</u>	<u>R.T.</u>	<u>60°C</u>	<u>R.T.</u>
Impedance $Z_0$ (ohm)	410	403	725	717
Angle of Impedance (rad x 10)	- 7.50	- 7.50	- 7.70	- 7.70
Phase Shift $\beta$ (radians/mile)	0.16	0.16	0.27	0.27
Attenuation $\alpha$ (dB/mile)	1.3	1.3	2.3	2.3
Inductance L (mH/mile)	1.02	1.03	1.01	1.01
Capacitance C (nF/mile)	83.6	83.7	81.4	82.7
Resistance R (ohm/mile)	88	85	269	267
Loss Tangent x $10^4$	4	3	4	4
<u>Measurements at 1 MHz</u>	<u>60°C</u>	<u>R.T.</u>	<u>60°C</u>	<u>R.T.</u>
Impedance $Z_0$ (ohm)	98	98	102	101
Angle of Impedance (rad x $10^3$ )	- 3.7	- 3.8	- 6.6	- 6.7
Phase Shift $\beta$ (radians/mile)	51.3	51.4	51.6	51.9
Attenuation $\alpha$ (dB/mile)	17.5	17.5	30.2	30.9
Inductance L (mH/mile)	0.802	0.798	0.833	0.828
Capacitance C (nF/mile)	83.0	83.8	80.7	82.0
Resistance R (ohm/mile)	386	385	700	706
Loss Tangent x $10^4$	18	16	15	17

It will be noticed from Table 4 that none of the properties listed shows any difference of practical importance between the lengths of the cable kept at room temperature and 60°C.

Only in the case of Cable 2 has the average mutual capacitance shown any significant change, and this is a decrease of 1.5% instead of the increase that might have been expected from theoretical considerations of the consequences of cell filling.

#### Structural Stability of Cellular Insulation

The cellular structure of the insulation remains stable unless air in the cells becomes displaced by the filling compound. Filling compound, or some of its components may diffuse through the solid portion of cellular insulation and above a certain critical temperature enter and gradually fill the cells. The rate of cell filling increases with temperature but it has been observed that the process does not occur below a temperature which is characteristic of each filling compound<sup>4</sup>.

The effects of cell filling are twofold:

- (a) Filling compound increases the permittivity of cellular insulation and may thus effect a change in transmission properties.
- (b) Some filling compound is lost from the interstitial regions thus possibly making the cable less waterproof.

Because density is an easily measured property which is sensitive to cell filling effects long term immersion tests in an excess petroleum jelly were carried out on insulated singles at several temperatures and their densities were determined periodically.

In order to interpret these density changes in terms of percentage cell filling, two factors must be considered; (a) the initial degree of expansion of the cellular insulation, and (b) the density change of the solid component of the insulation.

With reference to (b) it has been found that the density of solid medium density polyethylene of the type under consideration, increases on exposure to filling compound at the test temperatures used. Accordingly percentage cell filling, expressed as percentage displacement of the partial volume of air present in the insulation, was calculated using the following formula, which is derived in Appendix 4.

$$\text{Percentage Cell Filling} = \frac{d_p}{d_f} \left( \frac{1}{B} - 1 \right) (r - R) \times 100$$

where  $d_p$  = density of solid polymer

$d_f$  = density of filling compound

$B$  = initial partial volume of gas

$r$  = ratio of final to initial density of the cellular insulation

$R$  = ratio of final to initial density of the solid polymer

Results derived from measurements of insulation density after immersion at 50°, 55° and 60°C are presented in Figure 1.

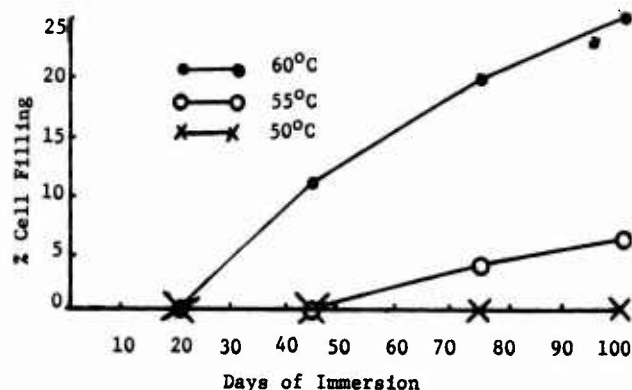


Figure 1 - Effect of Temperature and Time on Cell Filling Produced in Insulated Singles Immersed in an Excess of Filling Compound.

These results were obtained on insulated singles in an excess of filling compound and consequently it was important to determine to what extent cell filling had occurred in the insulation of cables aged at 60°C.

To this end, at the conclusion of the transmission tests described in the previous section, all of the cables had 6 inches of each end cut and discarded (since it was possible that a small amount of compound may have been lost from the end) and then a further 6 foot length cut for insulation tests. In the measurements the following were recorded:

1. Diameter (d) of conductor and insulation (D)
2. Coaxial capacitance (C) of insulated single
3. Density ( $\rho$ ) of insulation
4. Tensile strength and elongation of insulation.

The detailed results of measurements are contained in Appendix 2 and a summary is presented in Table 5. Calculations of percentage cell filling were done as previously described.

TABLE 5

Changes of Properties of Singles from Cables Kept at 60°C and Room Temperature

Cable	25 Pair/ 19 AWG	25 Pair/ 24 AWG
Insulation thickness (mils)	12.9	8.1
Degree of expansion, %	31	32
Duration of aging (days)	840	365
Diameter increase, %	3.4	3.3
Coaxial capacitance change, %	-1.0	-1.3
Permittivity increase, %	6	4
Density increase, %	12	13
Cell filling, %	22	24
Mutual capacitance change, %	-0.1	-1.6
Elongation, % reduction	11.6	24
Breaking strength, % reduction	6.8	7.1

N.B. Permittivity ( $\epsilon$ ) was calculated from measured diameters and trough capacitance of insulated singles by use of the formula

$$C = 16.9 \epsilon / \ln (D/d) \text{ pf/ft.}$$

Table 5 shows that

- (i) the degree of cell filling was 22-24%. This is considerably less than expected considering the results on insulated singles in a large excess of filling compound at 60°C. (25% at 100 days, Figure 1)
- (ii) an increase in permittivity, of the order of 5% has occurred.
- (iii) swelling of the insulation wall of about 15% has occurred.

It has been shown that the degree of cell filling found in these cables has not resulted in any significant changes in the transmission properties. This can be attributed to swelling counteracting the effect of cell filling as far as mutual capacitance is concerned.

#### Waterproofness

The following test was carried out to investigate the resistance of the cables to longitudinal water penetration. This was done in order to find out if any significant difference in waterproofness of the cables occurred as a result of high temperature aging and the accompanying partial cell filling.

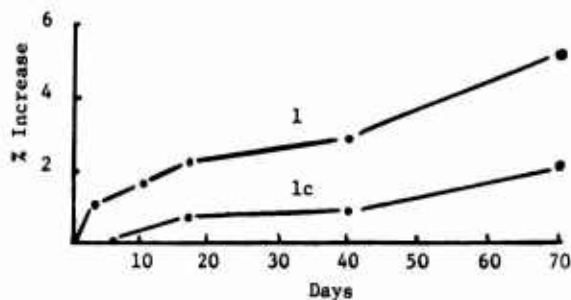
- 1) The cables were straightened out while at room temperature.
- 2) Approximately 20 feet of each cable had three holes drilled carefully into the core at the centre. These holes were equally spaced around the circumference and penetrated the core wrap.
- 3) A 3 foot head of water was applied to the centre of the cables taking care not to restrict possible longitudinal water flow in the cable core.
- 4) Mutual capacitance of 15 pairs in each cable was monitored over a period of 70 days.

The results, displayed in Figure 2, show that for both cables the difference between the 60°C sample and the room temperature sample is no greater than the expected variations between samples cut from the same cable.

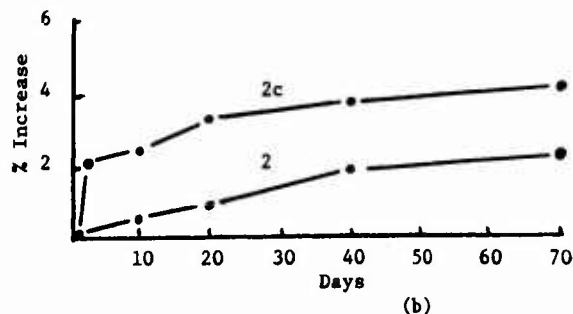
#### Time/Temperature Considerations

It is now useful to discuss the two conditions of exposure involving high temperatures, namely, storage on reels and aerial installations, since underground cables remain permanently at a low temperature (below 30°C).

Cables stored on unlagged reels exposed to direct sunlight encounter the highest temperature conditions. In the most severe case that can be envisaged in Canada, stored reels may be exposed to 60°C for 8 hours/day for 4 months of the year and it follows that 1 year of continuous exposure to 60°C would represent 9 years of storage under such circumstances. It has been demonstrated that 1 year continuous exposure to 60°C has caused negligible changes in the cable performance characteristics. Moreover, laboratory tests have shown that periodic exposure to high temperature, (e.g. daily cycling) does not result in a greater degree of cell filling than that occurring on continuous exposure over an equivalent period of time. It is also noteworthy in this context that the outer layer of a reel suffers the greatest temperature increase and that this layer usually accounts for only 5-10% of total length. Cable reels for export to hot climates are lagged which prevents a temperature rise above 50°C.



(a)



(b)

Figure 2 - Increase of mutual capacitance (average of 15 pairs tested) over a period of 70 days due to waterproofness test, for heat-aged and room temperature cables. (a) Cable 1/lc; (b) Cables 2/2c.

Aerial cable experiences service temperature conditions intermediate between those of buried cable and stored cable. Our tests indicated that the maximum cable core temperature reached in Western Canada in the summer of 1975 was 56°C. This occurred on a day when a record air temperature of 41.7°C was reached at the location. This figure is in agreement with findings of other investigations which show that the maximum temperature in an aerial cable does not exceed the maximum air temperature by more than 10° - 15°C.

Maximum daily air temperatures recorded for the Kamloops Airport show that, in the 5 year period between 1970 and 1974, a temperature of 35°C was reached or exceeded on 37 days. Taking this as typical there may be 150 such days in 20 years. Even if the cable core temperature on each such day reached 55°C for 12 hours, this would be only equivalent to a continuous exposure of 75 days at 55°C. Figure 1 shows that this has resulted in only 3.5% cell filling.

#### Aging Resistance of Insulation

Aging resistance is the ability of the insulation to resist deterioration due to thermal oxidation. The most critical consequence of oxidation is the loss of mechanical toughness and embrittlement which can lead to spontaneous cracking of the insulation and circuit failure, as sometimes experienced in pedestals in the U.S.A.

In the buried cables and aerial cables there is no risk of oxidative aging because (a) the aluminum shield and the filling compound effectively restrict access of oxygen to the insulation and (b) the service temperatures are relatively low. In pedestals, however, insulation on the copper conductors, exposed to air at temperatures which, for periods of time, may exceed the ambient air temperature by 20°C - 25°C and, under Canadian conditions, may occasionally reach 65°C - 70°C. The insulation must therefore be adequately stabilized against copper-catalysed oxidation to survive exposure under these conditions for 25 - 35 years.



In the case of fully-filled cables it is essential to check the resistance to oxidation of the insulation before and after exposure to filling compound since contact with the latter may improve or degrade this property<sup>5</sup>. It is considered important that the insulation from the freshly-made cable should have adequate resistance to aging in the "as extruded" condition even when using filling compounds which confer enhanced oxidation stability on the insulation. This approach has been adopted because occasionally cables could be installed, spliced and terminated soon after manufacture and before sufficient absorption of the filling compound has taken place for the full beneficial effect to occur. For the above reasons, oxidation resistance tests were carried out on insulated conductors before and after conditioning in excess filling compound at 70°C for 14 days, as well as on singles removed from cables which had been similarly conditioned.

Aspects of the aging resistance testing of cellular insulation are considered in Appendix 3 in which the accelerated aging test method employed is also discussed. This gravimetric test provides a simple and convenient means of determining the oxidation induction period, i.e. the time to the commencement of autocatalytic oxidation, as indicated by the onset of increase in weight of the insulation.

The aging test involves exposure of a coiled length of insulated conductor to air maintained at 105°C in a continuously-ventilated glass cell. An air flow is maintained at a controlled rate corresponding to six complete cell atmosphere changes per hour. The weight of the specimen is checked periodically, and the induction period (or lifetime), defined as the time for the weight of the insulation to increase by 0.5%, is determined.

The results obtained for our presently-used cellular insulation taken from cables, both before and after conditioning, show that the lifetime was generally in excess of 1000 hours in all cases including the case of the thinnest insulation wall on 26 AWG conductors, although the minimum value of 700 hours was recorded for this latter case.

It is considered that this level of resistance to aging will ensure an adequate service life for the insulation in Canadian locations. For further discussion of the significance of these test results, Appendix 3 should be consulted.

#### Development Work on Filling Compounds

Work on further optimisation of filling compound has been in progress and experimental cables have been evaluated in long term tests similar to those described earlier. The results have shown that the extent of cell filling at 60°C can be substantially reduced by using modified petroleum jelly compounds.

Table 6 shows the test results for three representative cables made with filling compound "B". It can be seen that after 35 months at 60°C there was less than 4% cell filling for 19 to 26 AWG insulated conductors, even for a degree of expansion as high as 40%.

It has been concluded from this work that, should the requirement ever arise, a compound based on petroleum jelly can be developed with markedly reduced propensity to cell filling at 60°C which will also meet other necessary requirements described earlier.

#### Dielectric Strength

Conductor-to-conductor factory test values have been established as follows:

19 AWG - 5000 volts - dc - 3 seconds  
22 AWG - 4000 volts - dc - 3 seconds  
24 AWG - 3000 volts - dc - 3 seconds  
26 AWG - 2500 volts - dc - 3 seconds

These values are identical to, or fractionally higher than those test values that have been used for many years in the U.S.A. and Canada for air core PIC cables 6,7.

Concern about the withstand capability of cellular insulation compared to solid insulation has been shown to be unfounded.

Conductor-to-shield test values of 15 kv were established for filled cables with solid insulation and some Canadian telephone specifications retained this value for cellular insulated filled cables.

However a 10 kv value, which has been used for many years for air core PIC cables, is a more realistic figure for cellular insulated filled cables considering the reduced insulation wall thickness.

Obviously in an area of heavy lightning incidence it may be desirable to have a higher conductor-to-shield withstand protection and this can be provided by design modifications to the core wrap.

However, this company has supplied more than 9000 miles of Calseal<sup>®</sup> cable since 1972, primarily for direct burial without any adverse field experience.

#### Field Experience

The data provided were obtained from two of the earliest orders for cellular insulated filled cable in 1972 and 1973. The specific orders were traced to two sites in Western Canada in Fort Saskatchewan, Alberta and Lamburg, Saskatchewan, where tests were conducted in August 1974 and again in July and August 1975. Cables in both areas are direct buried and operating in normal telephone systems, Fort Saskatchewan being in Alberta Government Telephones territory and Lamburg is in Lamburg Rural Telephone Company territory. Operating experience to date is 26 months at Fort Saskatchewan and 36 months at Lamburg.

The value of these data lies in the fact that no special precautions were taken at time of manufacture or installation. However, because these are operating cables, some pairs are not available for testing. The real benefits from the data relate to the fact that the cables are subject to normal operating conditions and not to the artificial constraints met in the laboratory such as short lengths, temperature conditions, etc.

TABLE 6

Effect of Aging for 35 Months at 60° C on Insulation  
of Cables with Experimental Filling Compound 'B'

Cable	25 pair/19 AWG	25 pair/24 AWG	25 pair/26 AWG
Insulation thickness (mil)	13.2	8.3	7.1
Degree of expansion, %	40	34	25
Diameter increase, %	1.1	1.7	1.3
Coaxial capacitance change, %	1.0	0.4	2.2
Permittivity increase, %	3	2	4
Density increase, %	5	2	5
Cell filling, %	3.6	Nil	3.2
Mutual capacitance change, %	0.10	-1.4	-3.8
Elongation, % reduction	33	14	8.5
Breaking Strength, % reduction	13	7	12

It is planned to continue testing at the sites for at least three more years.

A few words on the areas involved:

#### Fort Saskatchewan, Alberta

Fort Saskatchewan, Alberta is a town of approximately 8000 people located 15 miles north-east of Edmonton, the provincial capital of Alberta. The cable area is in the vicinity of several petrochemical plants and this area may grow in the future with the development of the tar-sands.

#### Lemberg, Saskatchewan

Lemberg, Saskatchewan a rural community of 400 people, is located approximately 100 miles east of Regina, the provincial capital, in the heart of prairie country in Western Canada. Cables are plowed in this area between the months of May and October when the air temperature will be anywhere from 5°C to 35°C. After October the ground becomes frozen until March and April when it thaws and becomes muddy. Thus for seven months of the year little direct plowing can be carried out.

While air temperatures in winter will frequently drop to -30°C which will be experienced in pedestals, ground temperatures will only reach -1°C.

#### Comments on the Results

Fort Saskatchewan, Alberta - 50 pair #24. Field tests consisted of:

Mutual capacitance at 1 kHz  
d.c. conductor resistance  
Capacitance unbalance  
Insulation resistance at 500 volts.

Test results are shown in Table 7.

Mutual capacitance increases were less than 0.1 nF/mile over a period of one year.

It will be noticed that conductor resistance is lower and insulation resistance higher in 1975. The explanation accepted is that ground temperatures were 4°C lower in 1975 than in 1974.

Lemberg, Saskatchewan. Test results are shown in Table 8.

Mutual capacitance changes on five different sizes of cable were:

25 pair 24	+ 0.2 nF/mile
16 pair 24	+ 0.1 nF/mile
11 pair 24	+ 0.1 nF/mile
6 pair 24	nil
4 pair 22	+ 0.1 nF/mile.

This amounts to 0.2% increase in the worst case.

#### Conclusions

The work reported in this paper clearly demonstrates that products currently manufactured using commercially available Canadian material meet satisfactorily all known Canadian service conditions and provide very significant safety margins over normal life expectancy for the product.

These same products can also be expected, on the basis of reported results, to have an adequate life under more arduous climatic conditions. Should special circumstances arise requiring cables capable of operating for prolonged periods in a high temperature environment, materials could be made available to meet this requirement without any need for changing present construction.

TABLE 7  
FORT SASKATCHEWAN, ALBERTA  
ALBERTA GOVERNMENT TELEPHONES  
 Individual Pair Readings of Mutual Capacitance (nF/mile)  
 3924' - 50 Pair #24 Celseal

	Pair	Aug. '74	July '75		Pair	*Mar. '73	Aug. '74	July '75
Blue/White	12	80.7	80.8	Orange/White	31		82.6	82.6
Binder	14	81.9	81.9	Binder	32		81.3	81.3
	15	82.8	82.8		33		82.2	82.3
	16	82.0	82.1		34		81.8	81.8
	17	82.9	83.0		35		81.9	82.0
	18	83.1	83.1		36		81.9	82.0
	19	82.5	82.6		37		81.9	81.9
	20	82.5	82.6		38		80.5	80.6
	21	81.4	81.4		39		82.2	82.3
	22	83.5	83.6		40		82.3	82.3
	23	82.6	82.7		42		81.3	81.4
	24	81.7	81.8		43		82.6	82.7
	25	82.1	82.1		44		81.7	81.8
Orange/White	26	82.5	82.5		45		81.7	81.7
Binder	27	82.1	82.2		46		81.6	81.6
	28	83.2	83.2		47		82.9	83.0
	29	80.7	80.7		48		82.2	82.3
	30	83.0	83.0		49		81.8	81.8
					50		81.6	81.8
				Average		*81.3	82.1	82.1
				σ %			0.69	0.69

\* Test value based on a 5 pair average from the original factory length of 6565'

OTHER ELECTRICAL PROPERTIES

		Aug. '74	Aug. '75
Conductor Resistance ohms/loop mile	Average (ten readings)	268.3	264.3
Capacitance Unbalance pair-pair pF/1000'	Average (nine readings)	3.1	2.6
Insulation Resistance megohm/miles	Average (six readings)	37,000	50,000

**TABLE 8**  
**LEMBURG, SASKATCHEWAN**  
**LEMBURG, RURAL TELEPHONE COMPANY**

Individual Pair Readings of Mutual Capacitance (nF/mile)

CELSEAL

2534' - 25 Pair #24				3594' - 16 Pair #24				3594' - 11 Pair #24			
Pair	*July '72	Aug '74	Aug '75	Pair	*July '72	Aug '74	Aug '75	Pair	*July '72	Aug '74	Aug '75
1		82.0	83.0	1		80.1	80.1	1		78.2	78.3
15		81.7	81.8	8		79.3	79.2	2		78.2	78.3
16		81.9	81.9	16		78.4	78.5	3		79.8	79.9
18		81.9	81.9	Average *79.0			79.3	Average *78.0			78.8
19		82.9	83.0	$\sigma$ %			.84 .82	$\sigma$ %			.92 .96
20		82.0	82.2								
21		80.9	81.0								
22		81.6	81.7								
23		81.7	81.8								
24		82.3	82.4								
25		82.0	82.1								
Average *80.0			81.9 82.1								
$\sigma$ %			.58 .58								

4500' - 6 Pair #24				4500' - 4 Pair #22			
Pair	*July '72	Aug '74	Aug '75	Pair	*July '72	Aug '74	Aug '75
1		78.4	78.4	1		81.2	81.3
2		77.4	77.4	2		81.1	81.2
3		77.4	77.4	3		79.4	79.4
5		77.6	77.6	4		79.9	80.0
6		77.6	77.6	Average *80.4			80.5
Average *79.0			77.7 77.7	$\sigma$ %			.89 .90
$\sigma$ %			.40 .43				

\*Original test values for July 1972 are group averages and were not measured on the same cable lengths as were measured in the field. However, it is possible to relate the field length tested to the factory length, or part of it, in all cases.

OTHER ELECTRICAL PROPERTIES

		Pair Count	Aug. '74	Aug. '75
Conductor Resistance ohms/loop mile - Average	(11)	25/24	274.1	271.5
	(3)	16/24	265.9	263.8
	(3)	11/24	263.7	260.9
	(5)	6/24	267.7	265.7
	(4)	4/22	165.4	163.5
Capacitance Unbalance pair-pair pF/1000'	(Group)	25/24	1.26	2.51
	(3)	16/24	3.90	3.70
	(3)	11/24	7.38	2.81
	(4)	6/24	8.40	7.07
	(3)	4/22	1.70	9.11

### Acknowledgments

The authors wish to express their appreciation for the guidance and encouragement provided by Mr. Stefan Verne and Mr. Noel Dean of BICC Limited. In addition we acknowledge the cooperation of the following persons who made the field testing possible.

Mr. Walter Konhauser, Alberta Government Telephones  
Mr. Robert Beveridge and Mr. Walter Harder of Saskatchewan Telephone  
Mr. G. Robinson, Dept. of Telephones, Saskatchewan Government and Mr. Peter Miller, Contractor.

### References

1. Twenty-First IWCS - 1972, *Extrusion of Telephone Cable Insulation Using Expandable Medium Density Polyethylene Compounds*, J.K. Normanton.
2. Twenty-Second IWCS - 1973, *Cellular Insulated Fully-Filled Cable with High Dielectric Strength*, S.M. Beach, J. Ruskin and D.F. Cretney.
3. Society of the Plastics Industry Conference, October 1973, Vancouver, Canada, *Cellular Polyethylene for Telephone Cables*, J.J. Helbling and R.A. Houben.
4. Twenty-Second IWCS - 1973, *Long Term Stability of Fully-Filled Cables*, S. Verne, A.A. Pinching and J.M.R. Hagger.
5. Twentieth IWCS - 1971, *Long Term Stability of Polyethylene Insulated Fully-Filled Telephone Distribution Cables*, S. Verne, R.T. Puckowski and A.A. Pinching.
6. Twenty-Third IWCS - 1974, *Cellular Insulation as an Answer to Material Conservation*, E.D. Metcalf.
7. USITA Convention, October 1974, *Lower Cost Water Tight Telephone Cable*, J.S. Tyler.
8. J.B. Howard, *Polymer Engineering and Science*, November 1973, Vol. 13, No. 6, P. 429.
9. Proposed Test Requirements for Inclusion in the REA Specification PE-39.
10. Twenty-Third IWCS - 1974, *Raw Material Inspection for Expandable Polyolefin Insulations*, D.J. Marshall, J.M. Turnipseed and F.R. Wight.
11. J.B. Howard and H.M. Gilroy, *Polymer Engineering and Science*, April 1975, Vol. 15, No. 4, P. 268.
12. Twenty-Third IWCS - 1974, *System Evaluation and Protection of Conductor Insulation in Outside Plant*, L. Ance and J.P. McCann.
13. Twentieth IWCS - 1971, *Evaluation of Thermal Degradation in Polyethylene Telephone Cable Insulation*, B.B. Pusey, M.T. Chen and W.L. Roberts.
14. Twenty-Second IWCS - 1973, *Methods of Life Prediction of Insulations of Air Core Cables and Filled Cables*, G.A. Schmidt.
15. Nineteenth IWCS - 1970, *Compatibility of Polyolefin Insulation and Hydrocarbon Fillers in Telephone Cables*, S. Verne, R.T. Puckowski and J.M.R. Hagger.

APPENDIX 1

TABLE A

TRANSMISSION MEASUREMENTS (1 KHZ) CABLES 1/1C

PAIR	IMPEDANCE ( $Z_0$ ) Ohms		(-) ANGLE OF IMPEDANCE Radians x 10		PHASE SHIFT ( $\beta$ ) Radians/mile		ATTENUATION ( $\alpha$ ) dB/mile		INDUCTANCE (L) mH/mile		CAPACITANCE (C) nF/mile		RESISTANCE (R) Ohms/mile		LOSS TANGENT $\tan \delta \times 10^4$	
	1	1C	1	1C	1	1C	1	1C	1	1C	1	1C	1	1C	1	1C
1	412	410	7.49	7.46	.16	.15	1.3	1.2	1.02	1.07	82.0	82.0	87	86	3.4	3.4
2	426	407	7.53	7.47	.17	.15	1.4	1.2	1.00	1.06	85.2	82.5	87	86	3.2	3.4
3	409	400	7.49	7.48	.16	.16	1.3	1.3	1.02	1.02	84.1	84.8	88	85	3.3	3.3
4	415	404	7.48	7.48	.16	.16	1.3	1.3	1.06	1.02	82.0	84.3	89	86	3.4	3.3
5	411	404	7.46	7.48	.16	.15	1.2	1.3	1.07	1.02	82.0	83.6	87	86	3.4	3.4
6	409	409	7.49	7.46	.16	.16	1.3	1.2	1.02	1.06	83.6	80.3	88	85	3.4	3.5
7	405	404	7.48	7.46	.16	.16	1.3	1.3	1.02	1.06	84.1	83.6	86	85	3.2	3.4
8	418	402	7.47	7.47	.15	.16	1.2	1.3	1.06	1.04	78.7	83.8	86	85	3.6	3.3
9	412	408	7.47	7.46	.16	.16	1.3	1.2	1.04	1.07	81.8	82.7	87	86	3.5	3.4
10	407	402	7.49	7.47	.16	.16	1.3	1.3	1.00	1.04	84.1	84.3	87	85	3.5	3.3
11	411	403	7.50	7.49	.16	.15	1.3	1.3	.986	.986	85.0	83.6	90	85	3.5	3.4
12	402	403	7.49	7.49	.16	.15	1.3	1.3	1.00	.986	85.2	83.6	86	85	3.3	3.4
13	407	408	7.49	7.47	.16	.16	1.3	1.2	1.02	1.06	84.1	81.8	87	86	3.3	3.4
14	420	403	7.50	7.48	.16	.16	1.3	1.3	1.04	1.02	82.7	84.3	91	86	3.4	3.3
15	404	401	7.48	7.49	.16	.16	1.3	1.3	1.02	.986	84.8	84.3	87	85	3.3	3.3
16	412	403	7.48	7.48	.15	.15	1.2	1.3	1.02	1.02	81.1	83.6	86	85	3.5	3.4
17	416	409	7.46	7.46	.15	.16	1.2	1.2	1.07	1.07	79.6	81.3	86	85	3.5	3.4
18	409	399	7.50	7.48	.16	.16	1.3	1.3	1.00	1.02	84.8	85.4	89	85	3.3	3.3
19	406	400	7.50	7.48	.16	.16	1.3	1.3	1.00	1.00	85.9	84.8	89	85	3.3	3.3
20	409	398	7.49	7.49	.16	.16	1.3	1.3	1.00	.986	84.0	85.7	88	85	3.3	3.3
21	403	406	7.50	7.47	.16	.16	1.3	1.3	1.00	1.04	86.8	83.2	88	86	3.2	3.4
22	401	402	7.49	7.48	.16	.16	1.3	1.3	1.00	1.02	85.9	84.1	87	85	3.3	3.3
23	405	397	7.50	7.48	.16	.16	1.3	1.3	.986	1.00	84.5	86.1	87	85	3.3	3.3
24	406	403	7.49	7.48	.16	.16	1.3	1.3	1.02	1.00	84.5	84.1	87	86	3.3	3.3
25	407	401	7.48	7.48	.16	.16	1.3	1.3	1.02	1.00	84.1	84.7	87	85	3.3	3.3
AVG.	410	403	7.49	7.48	.16	.16	1.3	1.3	1.02	1.03	83.6	83.7	88	85	3.4	3.3



## APPENDIX 1

TABLE B  
TRANSMISSION MEASUREMENTS (1 MHZ) CABLES 1/1C

PAIR	IMPEDANCE ( $Z_0$ ) Ohms		(-) ANGLE OF IMPEDANCE $\angle$ Radians $\times 10^2$		PHASE SHIFT ( $\beta$ ) Radians/mile		ATTENUATION ( $\alpha$ ) dB/mile		INDUCTANCE (L) mH/mile		CAPACITANCE (C) nF/mile		RESISTANCE (R) Ohms/mile		LOSS TANGENT $\tan \delta \times 10^3$	
	1	1C	1	1C	1	1C	1	1C	1	1C	1	1C	1	1C	1	1C
1	101	103	3.7	3.5	51.4	53.0	17.3	16.8	.821	.870	81.4	81.7	392	389	1.64	1.60
2	97	101	3.9	3.6	51.3	52.2	18.0	17.1	.787	.837	84.6	82.2	392	389	1.48	1.59
3	99	96	3.7	3.9	52.0	51.4	17.4	17.8	.820	.787	83.4	84.8	390	388	1.58	1.38
4	102	97	3.5	3.8	51.7	51.2	16.8	17.6	.838	.787	80.8	84.1	384	383	1.94	1.67
5	102	98	3.6	3.8	51.7	51.4	16.8	17.8	.838	.804	80.7	83.3	386	396	1.80	1.53
6	100	103	3.7	3.5	51.8	52.1	17.5	16.6	.820	.854	82.7	80.5	392	385	1.61	1.64
7	99	99	3.7	3.7	52.0	52.1	17.3	17.3	.820	.820	83.2	83.5	387	386	1.75	1.52
8	103	97	3.6	3.8	50.5	51.0	16.5	17.4	.822	.787	78.4	83.5	379	380	1.92	1.66
9	100	101	3.6	3.6	51.5	52.2	17.0	17.0	.821	.837	81.7	82.2	384	386	1.88	1.68
10	96	97	3.9	3.8	50.6	51.2	17.9	17.4	.770	.787	84.0	84.1	387	380	1.65	1.62
11	95	93	3.9	4.0	50.9	50.9	18.0	18.4	.770	.753	85.0	86.9	386	384	1.72	1.94
12	96	92	3.9	4.0	50.8	50.3	17.9	18.4	.770	.736	84.7	87.0	385	380	1.72	2.03
13	99	103	3.7	3.5	52.0	52.4	17.4	16.8	.820	.854	83.2	81.5	391	389	1.58	1.61
14	99	97	3.7	3.7	51.0	51.2	17.3	17.4	.804	.787	81.9	84.1	385	379	1.88	1.66
15	97	95	3.9	3.9	51.1	51.1	17.8	18.2	.787	.770	83.8	85.9	390	388	1.61	1.86
16	99	96	3.7	3.8	50.1	50.4	17.1	17.4	.788	.770	80.6	83.4	381	376	1.97	1.68
17	103	101	3.5	3.6	51.2	51.2	16.3	16.7	.838	.821	79.2	80.9	376	377	2.05	1.82
18	97	97	3.8	3.0	51.2	52.0	17.8	17.7	.787	.803	84.3	85.1	388	389	1.63	1.40
19	96	96	3.8	3.9	51.5	50.8	17.9	17.8	.787	.770	85.1	84.7	389	385	1.59	1.45
20	97	94	3.8	3.9	51.0	50.4	17.6	17.9	.787	.753	83.5	85.4	385	379	1.81	1.53
21	96	100	3.8	3.7	51.9	51.9	18.3	17.7	.786	.820	86.5	83.0	391	390	2.08	1.52
22	97	98	3.8	3.7	51.9	51.6	17.7	17.4	.803	.804	84.8	83.9	389	386	1.60	1.46
23	96	94	3.9	3.9	50.6	50.5	17.8	17.9	.770	.753	84.2	85.7	385	380	1.62	1.53
24	98	97	3.7	3.7	51.4	51.1	17.5	17.4	.804	.787	83.3	84.0	386	379	1.79	1.70
25	97	97	3.8	3.8	50.9	51.3	17.5	17.8	.787	.787	83.1	84.5	383	388	1.82	1.40
AVG.	98	98	3.7	3.8	51.3	51.4	17.5	17.5	.802	.798	83.0	83.8	386	385	1.75	1.62

APPENDIX 1

TABLE C  
TRANSMISSION MEASUREMENTS (1 KHZ) CABLES 2/2C

PAIR	IMPEDANCE (Z <sub>0</sub> ) Ohms		(-) ANGLE OF IMPEDANCE Radians x 10		PHASE SHIFT (β) Radians/mile		ATTENUATION (α) dB/mile		INDUCTANCE (L) mH/mile		CAPACITANCE (C) nF/mile		RESISTANCE (R) Ohms/mile		LOSS TANGENT Tan δ x 10 <sup>4</sup>	
	2	2C	2	2C	2	2C	2	2C	2	2C	2	2C	2	2C	2	2C
1	726	708	7.73	7.73	.27	.27	2.3	2.3	1.02	1.00	81.5	84.0	270	265	3.4	3.4
2	727	719	7.74	7.73	.27	.27	2.3	2.3	1.00	1.02	82.0	82.9	272	269	3.4	3.4
3	722	711	7.74	7.73	.27	.27	2.3	2.3	1.00	1.00	82.0	83.8	269	266	3.4	3.3
4	734	718	7.73	7.73	.26	.27	2.2	2.3	1.02	1.00	80.3	82.7	272	268	3.5	3.4
5	738	720	7.74	7.73	.27	.26	2.3	2.2	1.00	1.00	80.1	81.7	274	266	3.5	3.4
6	721	712	7.73	7.73	.27	.27	2.3	2.3	1.00	1.00	81.8	83.2	268	265	3.4	3.4
7	722	713	7.73	7.73	.27	.27	2.3	2.3	1.02	1.02	81.8	83.2	268	266	3.4	3.4
8	725	722	7.73	7.73	.27	.26	2.3	2.2	1.04	1.00	81.8	81.1	270	265	3.4	3.4
9	720	737	7.74	7.73	.27	.26	2.3	2.2	1.00	1.04	83.1	78.1	271	267	3.4	3.6
10	738	731	7.74	7.73	.27	.27	2.3	2.3	1.00	1.02	80.4	81.1	275	272	3.5	3.4
11	717	705	7.73	7.73	.27	.27	2.2	2.3	1.00	1.00	82.2	84.3	266	263	3.4	3.3
12	725	712	7.73	7.73	.26	.27	2.2	2.3	1.00	1.00	81.0	84.1	268	268	3.5	3.3
13	736	714	7.73	7.73	.26	.27	2.2	2.3	1.02	1.00	78.5	83.4	267	267	3.6	3.3
14	729	716	7.73	7.73	.26	.27	2.2	2.3	1.00	1.00	79.7	82.9	266	267	3.5	3.4
15	722	712	7.73	7.74	.27	.27	2.3	2.3	1.00	.986	82.0	84.1	268	268	3.4	3.3
16	718	707	7.73	7.73	.27	.27	2.3	2.3	1.00	1.00	82.5	83.6	263	263	3.4	3.3
17	725	729	7.73	7.73	.26	.26	2.2	2.3	1.02	1.00	81.1	80.4	268	268	3.4	3.5
18	725	720	7.74	7.73	.27	.27	2.2	2.3	1.00	1.00	81.3	82.0	269	267	3.4	3.4
19	743	713	7.73	7.73	.26	.26	2.2	2.3	1.00	1.02	81.5	84.0	268	268	3.4	3.3
20	725	727	7.73	7.74	.26	.27	2.2	2.3	1.02	1.00	80.4	81.1	266	269	3.5	3.4
21	725	728	7.73	7.73	.27	.27	2.3	2.3	1.02	1.04	82.2	81.7	271	272	3.4	3.4
22	726	718	7.73	7.73	.26	.27	2.2	2.3	1.04	1.04	81.0	83.2	268	270	3.5	3.4
23	713	712	7.73	7.73	.26	.26	2.2	2.2	1.02	1.02	82.2	82.4	262	262	3.4	3.4
24	729	720	7.73	7.73	.26	.27	2.2	2.3	1.04	1.04	80.8	82.5	270	269	3.5	3.4
25	716	712	7.73	7.74	.27	.27	2.3	2.3	.986	.968	84.7	85.5	273	272	3.5	3.3
AVG.	725	717	7.73	7.73	.27	.27	2.3	2.3	1.01	1.01	81.4	82.7	269	267	4.0	3.4

## APPENDIX 1

TABLE D

## TRANSMISSION MEASUREMENTS (1 MHZ)

CABLES 2/2C

PAIR	IMPEDANCE (Z <sub>0</sub> ) Ohms		(-) ANGLE OF IMPEDANCE Radians x 10 <sup>2</sup>		PHASE SHIFT (°) Radians/mile		ATTENUATION (α) dB/mile		INDUCTANCE (L) mH/mile		CAPACITANCE (C) nF/mile		RESISTANCE (R) Ohms/mile		LOSS TAN δ x 10 <sup>3</sup>	
	2	2C	2	2C	2	2C	2	2C	2	2C	2	2C	2	2C	2	2C
1	103	101	6.5	6.7	52.3	52.5	30.0	31.0	.855	.837	80.8	83.0	706	712	1.25	1.44
2	102	102	6.6	6.6	52.1	52.8	30.5	30.7	.838	.854	81.7	82.5	707	715	1.22	1.27
3	102	100	6.6	6.8	52.1	52.0	30.5	31.4	.838	.821	81.7	83.2	706	714	1.23	1.16
4	104	102	6.4	6.7	51.9	52.1	29.7	30.9	.855	.838	79.5	81.8	703	714	1.29	1.29
5	101	101	6.6	6.6	51.4	51.4	30.1	30.5	.821	.821	81.2	81.1	691	699	1.52	1.82
6	100	99	6.7	6.8	50.9	51.3	30.5	31.0	.805	.804	81.3	82.6	693	697	1.51	1.81
7	104	102	6.4	6.6	52.8	52.9	29.7	30.9	.871	.854	80.7	82.6	706	716	1.16	1.53
8	101	102	6.6	6.6	51.4	51.2	30.1	30.3	.821	.821	81.1	80.4	691	698	1.62	1.87
9	100	105	6.6	6.4	51.8	51.4	30.4	29.3	.821	.855	82.4	77.8	693	698	1.67	1.91
10	102	101	6.7	6.7	51.1	51.3	30.3	30.9	.822	.821	80.1	80.9	701	707	1.45	1.95
11	100	98	6.7	6.9	51.0	51.1	30.7	31.7	.804	.787	81.6	83.6	694	700	1.81	1.94
12	102	99	6.6	6.8	51.2	51.4	30.2	31.2	.821	.804	80.4	82.9	694	700	1.89	1.92
13	104	100	6.4	6.6	50.9	51.9	29.3	30.9	.839	.821	78.0	82.9	691	699	1.67	1.84
14	103	99	6.6	6.8	50.7	51.2	29.7	31.0	.822	.804	78.9	82.3	691	698	1.58	1.86
15	102	100	6.6	6.8	52.1	52.1	30.7	31.7	.838	.821	81.7	83.2	710	718	1.27	1.45
16	102	101	6.7	6.7	52.1	52.3	30.8	31.2	.838	.837	81.8	82.5	712	717	1.25	1.51
17	101	99	6.6	6.8	51.4	51.5	30.3	31.4	.821	.804	81.1	83.1	695	703	1.74	1.94
18	102	101	6.6	6.6	51.2	51.4	30.2	30.5	.821	.821	80.4	81.2	696	699	1.52	1.86
19	101	102	6.6	6.6	51.4	51.0	30.4	30.4	.821	.822	81.1	79.9	697	701	1.73	2.00
20	103	103	6.7	6.7	51.5	51.7	30.5	31.0	.838	.838	79.8	80.3	714	722	1.40	1.53
21	102	102	6.5	6.5	52.0	51.9	30.0	30.2	.838	.838	81.5	81.2	692	698	1.65	1.91
22	105	102	6.4	6.4	52.6	52.9	29.7	30.1	.871	.854	80.3	82.6	706	696	1.25	1.64
23	102	103	6.6	6.5	52.0	52.5	30.5	30.5	.838	.854	81.5	81.5	709	712	1.13	1.62
24	105	104	6.3	6.4	52.6	53.2	29.6	30.4	.871	.871	80.1	81.9	704	714	1.28	1.51
25	101	97	6.8	7.1	50.6	51.5	30.8	32.4	.805	.787	80.1	85.0	704	711	1.64	1.67
AVG.	102	101	6.6	6.7	51.6	51.9	30.2	30.9	.833	.828	80.7	82.0	700	706	1.47	1.69

# APPENDIX 2

## TABLE E

MEASUREMENTS ON SINGLES REMOVED FROM CABLES 1/1C

Pair and Colour	Cond. Dia. (d) Mils	D.O.D. (D) Mils		Trough Capacitance (c) pF/ft.		Permittivity ( $\epsilon$ )		Density ( $\rho$ ) gms/cm <sup>3</sup>		Elong. (%)		U.T.S. psi	
		<u>1</u>	<u>1C</u>	<u>1</u>	<u>1C</u>	<u>1</u>	<u>1C</u>	<u>1</u>	<u>1C</u>	<u>1</u>	<u>1C</u>	<u>1</u>	<u>1C</u>
1 -W	35.7	63.9	61.8	54.2	57.0	1.81	1.85	0.711	.656	420	493	2422	2590
-B	35.7	63.3	61.7	53.8	56.8	1.82	1.84	0.688	.632	398	460	2243	2381
2 -W	35.7	64.1	61.8	58.1	56.4	2.01	1.83	0.758	.656	407	475	2407	2574
-O	35.8	64.3	62.2	59.1	56.8	2.05	1.86	0.757	.649	403	475	2373	2571
3 -W													
-G													
4 -W	35.8	64.2	62.5	57.8	56.6	2.00	1.87	0.770	.667	425	485	2370	2586
-BR	35.8	63.7	61.2	58.0	57.2	1.98	1.81	0.755	.637	413	443	1959	2278
5 -W													
-S													
6 -R													
-B													
7 -R	36.0	64.0	61.8	56.5	57.0	1.92	1.82	0.736	.652	400	470	2344	2528
-O	35.9	64.2	61.8	57.6	56.4	1.98	1.81	0.763	.652	405	478	2330	2533
8 -R	36.0	63.6	62.0	55.0	56.4	1.85	1.81	0.709	.640	393	465	2361	2516
-G	36.0	63.6	61.9	55.2	56.4	1.86	1.81	0.707	.638	390	470	2239	2422
9 -R													
-BR													
10 -R	35.9	63.6	61.2	55.0	58.1	1.86	1.83	0.705	.656	380	430	2179	2269
-S	35.8	63.3	61.2	55.2	57.6	1.86	1.83	0.702	.646	375	455	2082	2259
11 -BK	35.8	63.2	61.2	56.3	56.8	1.89	1.80	0.708	.637	403	463	2205	2313
-B	35.9	63.4	61.4	56.2	56.4	1.89	1.79	0.719	.637	403	463	2207	2351
12 -BK													
-O													
13 -BK	35.8	63.7	61.2	55.2	57.4	1.88	1.82	0.706	.635	398	455	2182	2296
-G	36.0	64.1	61.6	57.7	56.7	1.97	1.80	0.729	.688	398	465	2226	2430
14 -BK	35.9	63.4	61.3	56.4	56.9	1.90	1.80	0.715	.677	398	460	2131	2350
-BR	35.7	63.3	61.0	56.6	57.3	1.93	1.82	0.722	.595	355	430	2090	2216
15 -BK													
-S													
16 -Y	35.9	64.4	62.2	57.3	57.1	1.98	1.86	0.747	.655	385	470	2265	2427
-B	35.8	63.9	61.7	55.8	56.8	1.91	1.83	0.723	.640	353	460	2125	2298
17 -Y													
-O													
18 -Y													
-G													
19 -Y													
-BR													
20 -Y	36.1	64.2	62.0	53.1	56.6	1.98	1.81	0.758	.657	398	475	2380	2541
-S	35.8	63.5	61.8	55.6	56.6	1.89	1.83	0.712	.645	408	465	2222	2344
21 -P													
-B													
22 -P	35.9	63.6	61.5	57.7	56.8	1.95	1.81	0.730	.637	380	445	2182	2329
-O	36.0	64.5	62.0	57.7	56.8	1.99	1.83	0.741	.655	403	475	2325	2508
23 -P	35.8	63.2	61.4	54.5	56.6	1.83	1.81	0.689	.635	378	453	2169	2307
-G	35.9	63.7	61.5	54.3	57.0	1.84	1.82	0.694	.649	410	463	2289	2370
24 -P													
-BR													
25 -P													
-S													
AVG	35.9	63.8	61.7	56.3	56.9	1.92	1.82	0.725	.647	395	447	2243	2407

# APPENDIX 2

## TABLE F

MEASUREMENTS ON SINGLES REMOVED FROM CABLES 2/2C

Pair and Colour	Cond. Dia. (d) Mils	D.O.D. (D) Mils		Trough Capacitance (c) pF/ft.		Permittivity ( $\epsilon$ )		Density ( $\rho$ ) gms/cm <sup>3</sup>		Elong. (%)		U.T.S. psi	
		2	2C	2	2C	2	2C	2	2C	2	2C	2	2C
1 -W	20.0	37.3	36.1	51.5	52.3	1.90	1.83	.738	.655	308	388	2547	2822
-B	20.3	37.7	36.7	51.3	51.8	1.88	1.82	.714	.632	338	398	2390	2624
2 -W	20.2	36.6	35.8	52.4	53.1	1.84	1.80	.705	.623	295	378	2157	2362
-O	19.9	37.7	36.1	50.6	52.1	1.91	1.84	.721	.644	323	390	2575	2777
3 -W													
-G													
4 -W	20.1	37.4	36.1	51.5	52.3	1.89	1.81	.729	.649	318	390	2550	2812
-BR	20.3	37.6	36.0	51.1	51.2	1.86	1.74	.699	.617	285	365	2317	2513
5 -W	20.1	37.9	36.3	50.8	51.4	1.91	1.78	.701	.622	145	378	1603	1767
-S	20.1	37.3	36.1	50.0	50.6	1.83	1.75	.701	.599	168	370	1481	1644
6 -R													
-B													
7 -R	20.2	37.0	35.8	53.2	52.7	1.91	1.78	.726	.640	325	400	2359	2603
-O	20.1	37.3	36.2	50.6	51.9	1.85	1.81	.725	.646	320	395	2508	2741
8 -R	20.1	37.5	36.5	50.6	52.1	1.87	1.84	.702	.634	338	393	2376	2585
-G	20.2	37.3	36.4	53.6	52.7	1.95	1.84	.740	.643	308	375	2422	2599
9 -R													
-BR													
10-R	19.9	37.2	36.0	50.0	51.6	1.85	1.81	.702	.644	390	270	1865	2132
-S	19.9	37.0	35.7	49.5	51.0	1.82	1.76	.682	.618	190	368	1505	1693
11-BK	20.2	37.5	36.2	50.4	52.7	1.84	1.82	.714	.655	358	435	2467	2745
-B	20.1	37.1	35.8	51.5	52.3	1.87	1.79	.709	.627	300	388	2209	2506
12-BK													
-O													
13-BK	20.2	37.6	36.3	50.6	51.9	1.86	1.80	.716	.650	360	433	2627	2773
-G	20.3	37.2	36.3	51.7	52.1	1.85	1.79	.725	.635	318	393	2403	2543
14-BK	20.2	37.5	36.3	51.0	53.1	1.87	1.84	.722	.655	385	425	2701	2759
-BR	20.0	37.0	36.2	52.1	51.9	1.90	1.82	.728	.630	290	383	2345	2526
15-BK													
-S													
16-Y	20.2	36.9	35.7	53.0	53.2	1.89	1.79	.735	.639	290	358	2422	2478
-B	20.1	37.1	35.8	51.5	52.3	1.87	1.79	.710	.625	303	390	2341	2498
17-Y													
-O													
18-Y													
-G													
19-Y													
-BR													
20-Y	20.0	37.4	35.9	50.1	50.8	1.86	1.76	.708	.628	250	380	1753	1867
-S	19.9	36.9	35.8	54.4	51.4	1.99	1.79	.744	.619	203	368	1575	1679
21-P													
-B													
22-P	20.2	38.9	37.2	50.8	52.2	1.97	1.89	.776	.692	395	475	2582	2478
-O	20.0	38.1	36.6	50.1	52.1	1.91	1.86	.754	.687	338	425	2533	2687
23-P	20.3	37.5	36.3	51.4	52.1	1.87	1.79	.709	.633	343	418	2589	2682
-G	20.3	37.4	36.3	51.4	52.1	1.86	1.79	.726	.644	330	405	2585	2749
24-P													
-BR													
25-P													
-S													
AVG.	20.1	37.4	36.2	51.3	52.0	1.88	1.81	.720	.639	300	395	2279	2453

### APPENDIX 3

#### Testing of Polyethylene Insulation For Resistance to Aging

Recent field experience with the polyethylene insulation on copper conductors in the above ground pedestals of telephone distribution networks in the U.S.A. has emphasized the need for adequate protection of the insulation against oxidative degradation, and for reliable methods of assessment of the resistance to aging. Insulation stabilized in a way known to be adequate for other cable applications, was found to fail after only a few years service under adverse climatic conditions by copper-catalysed thermal oxidation of polyethylene. This leads to severe embrittlement and eventual cracking of the insulation. It is now generally recognized that substantial increases in stabilization levels are essential, to ensure that the insulation meets the requirements for exposure in pedestals in which maximum internal temperatures can exceed the ambient air temperature by 20° - 25°C.

When considering the question of tests for resistance to aging several factors which determine the life of the insulation must be borne in mind. The main of these are listed below:

##### Copper Conductor

Contact with copper accelerates drastically the rate of thermal oxidation of polyethylene both at processing temperatures and in service, and is a dominant factor affecting the resistance to aging of the insulation. The adverse effect increases with increasing ratio of surface area in contact with copper to volume. It also depends on the state of oxidation of the conductor surface, the presence of atmospheric corrosion products, contamination with lubricants, etc.

It is important to note that similar grades of low and medium density polyethylene, produced in different polymerization plants, and containing the same type and quantity of antioxidant, can show widely different resistance to aging in the presence of copper.

##### Thickness

The life of the insulation decreases rapidly with decreasing thickness.

##### Stabilizers

The effectiveness of the oxidation inhibitors and copper deactivators in providing long-term protection against oxidative degradation is determined by their chemical activity as well as physical characteristics, namely volatility, stability and compatibility with polyethylene, and also the state of dispersion in the polymer. In service, loss of antioxidant from the insulation by evaporation or extraction by condensing moisture or the cable filling compound, can be an important life reducing factor.

### Pigments and Other Additives

Some commercial pigments when used in polyethylene insulation in the presence of certain stabilizers are known, from field and laboratory experience, to produce a substantial lowering of resistance to ageing. The latter may also be impaired by chemical interaction between stabilizers and other additives present in the insulation.

##### Effect of Processing

The life of the insulation can be adversely affected by the conditions of extrusion processing which may lead to excessive consumption of stabilizers, loss of stabilizers by volatilization, excessive degradation of the polymer, contamination with pro-oxidants, etc.

Consideration of this list dictates that to obtain a meaningful assessment of any insulation's resistance to aging it is essential (a) to test the final product, i.e. the extruded pigmented insulation on the copper conductor, and (b) to ensure that the test method takes into account, as far as practicable, the above life-determining factors.

Specific analytical methods for the determination of many commercial antioxidants and copper inhibitors in polyethylene are now available and provide a useful quality control procedure for monitoring the compositional consistency of the polyethylene compound. Chemical analysis methods alone, however, are inadequate for quality assurance testing of insulation since they only yield, in principle, information about the residual stabilizer content without reference to any of the other factors affecting the resistance to aging. Moreover, as a result of oxidation reactions and interactions between additives during processing the insulation may contain a complex mixture of unchanged stabilizers and their reaction products some of which may still be active as antioxidants or copper inhibitors, and the analytical methods which determine the unchanged stabilizers only, would thus underestimate the total active stabilizer present.

The analysis can be particularly complicated in the case of cellular insulation of complex composition. It has been found, for example, that a partial loss of copper inhibitor N: N-dibenzal (oxalyl dihydrazide) can occur by reaction with the decomposition products of blowing agent azodicarbonamide at processing temperatures.

Accelerated tests on insulated conductor at high temperatures (above the melting range of the insulation material) based on DSC or DTA techniques, have been proposed (8,9). These rapid test methods appear suitable for monitoring the level of stabilization of polyethylene compound but not for testing its stability in the presence of copper (10). Further, the applicability of DSC and DTA to testing of insulation on copper conductors is in doubt as it is recognized that the performance in these tests at 200°C does not provide a reliable indication of the level of resistance to aging of different types of insulation under service conditions. A criticism of these accelerated test methods has recently been published (11).



The limitations of the high temperature test methods are particularly apparent in the case of cellular insulation in fully-filled cables. Above the melting range of the insulation not only is the cellular structure destroyed but the integrity of the insulation is lost as the molten polymer tends to flow off the conductor and spread on the metal dish surface, and the critical factors of thickness and area of contact with copper are thus disturbed. This effect is especially evident when the insulation contains some absorbed filling compound. Currently-used cellular insulation may contain several complex constituents which can chemically interact at high temperatures, particularly in the presence of copper, and these changes can adversely affect the performance in the DSC/DTA test. Moreover, this test may discriminate against stabilizers which provide satisfactory long-term protection under normal service conditions but possess relatively high vapour pressure at 200°C and hence are readily lost by evaporation during the test.

A test method avoiding these shortcomings was communicated to the International Wire & Cable Symposium in 1971<sup>(5)</sup>. In this test the resistance to thermal oxidation of the insulation on copper conductor is determined at a temperature below the melting range of the insulation. A temperature of 105°C is normally selected, being regarded as the highest test temperature at which reliable accelerated aging tests can be carried out on low density polyethylene insulation. The test is carried out in air under conditions of continuous moderate ventilation at a controlled rate as it is considered that such conditions correspond more closely to the actual service environment<sup>(12)</sup>. At intervals the test sample is examined for evidence of the onset of oxidative degradation of the insulation as manifested by (a) gain in weight and (b) deterioration of mechanical toughness, i.e. embrittlement.

In this test, polyethylene insulation on copper conductors similar to that which had failed prematurely in service in the U.S.A. (stabilized with Santonox R antioxidant at nominally 0.1% concentration) was found to give a lifetime of 120 to 200 hours. Analogous results for 0.2G - 0.33 mm thick PIC insulation manufactured until recently in North America, have been obtained in other laboratories under similar test conditions in air at 100° - 110°C (13,14). It is known that, in a number of cases, the service life of the insulation of this type in pedestals in the Southern States of the U.S.A. was about 3 years. Based on these data, a test lifetime of at least 1000 hours at 105°C is necessary to ensure service life of 25 years under the more severe climatic conditions.

When tested by this method at temperatures in the range 70° to 105°C, both solid and cellular polyethylene insulations have been shown to follow the relationship

$$\log L = a + \frac{b}{T}$$

where L is lifetime, T is absolute temperature (°K) and a and b are constants. Test data indicate that the insulation satisfying the above test requirement (1000 hours minimum lifetime at 105°C) would be expected to have a life of 15 years on continuous exposure to a constant temperature of 50°C.

In evaluating insulation of fully-filled cables it is essential to test the insulation which has been exposed to the cable filling compound since contact with certain types of filling compounds can adversely affect the resistance to oxidation of polyethylene insulation while with selected types of petroleum jelly compounds a beneficial effect is obtained<sup>(15,5)</sup>. Many stabilizers in current use diffuse from the insulation into the filling compound and cease to be available for protection of the insulation when the filling compound is subsequently removed in the cable termination procedure. If the filling compound itself is highly susceptible to oxidation, the absorption of such material by the insulation may also impair the aging performance. On the other hand, absorption of petroleum jelly compound containing natural oxidation inhibitors can substantially enhance the resistance to aging of the insulation<sup>(5)</sup>.

#### APPENDIX 4

In order to develop a simple formula for the purpose of calculating percent cell filling it is convenient to define the following set of symbols:

- $\Delta W$  - Total weight of filling compound absorbed by cellular insulation.
- $\Delta W_s$  - Weight of filling compound absorbed by solid component of insulation.
- $\Delta W_c$  - Weight of filling compound residing in cellular portion of insulation.

$$\Delta W = \Delta W_s + \Delta W_c \quad (1)$$

- $d_f$  - Density of filling compound (0.89 g/cm<sup>3</sup>)
- $d_p$  - Density of unexpanded (solid) polymer prior to filling compound absorption (0.935 g/cm<sup>3</sup>).
- $d'_p$  - Density of solid polymer after absorption of filling compound.
- R - Ratio of density of solid polymer after filling compound absorption to density before absorption. That is

$$R = \frac{d'_p}{d_p} \quad (2)$$

Note: It has been experimentally determined that R is approximately equal to 1.025 for the temperatures and combinations of materials under consideration at present.

- B - Volume fraction of air present in cellular insulation prior to absorption of filling compound.
- V - Total volume of cellular insulation before absorption of filling compound.
- V' - Total volume of cellular insulation after absorption of filling compound.
- $\rho$  - Density of cellular insulation prior to absorption of filling compound.
- $\rho'$  - Density of cellular insulation after absorption of filling compound.

$$\Delta W = \rho' V' - \rho V \text{ (gms)} \quad (3)$$

$V_s$  - Volume of solid component of cellular insulation prior to absorption of filling compound.

$V'_s$  - Volume of solid component of cellular insulation after absorption of filling compound.

$$\Delta W_s = V'_s d_p' - V_s d_p \quad (4)$$

$$= V' (1 - B) d_p' - V(1-B) d_p \quad (4A)$$

The above equation employs the fact that the volume fractions of cells present in the original and swollen insulation are equal.

$$\Delta W_s = V' R d_p (1 - B) - V (1 - B) d_p \quad (5)$$

$$= V' R \rho - V \rho \quad (6)$$

therefore;

$$\Delta W_c = V' \rho (r - R) \quad (7)$$

$$r = \frac{\rho'}{\rho} \quad (8)$$

$V_c$  = Volume of air cells present in cellular insulation prior to filling compound absorption.

$V'_c$  = Volume of cells present in cellular insulation after filling compound absorption.

The percent cell filling is defined as:

$$\frac{\text{Volume of Filling Compound in Cells}}{\text{Volume of Cells}} \times 100 \quad (9)$$

therefore;

$$\% \text{ Cell Filling} = \frac{d_p}{d_f} (1/B - 1) (r - R) \times 100 \quad (10)$$



Don Cretney was born in Vancouver, B.C. and graduated from the University of British Columbia in Electrical Engineering in 1964. He joined the Communication Cables Engineering Department of Phillips Cables in 1970, having previously worked for the B.C. Telephone Co., The Boeing Co., Seattle Wash., and International Power & Engineering Consultants in Vancouver.

Mr. Cretney is a member of the British Columbia Association of Professional Engineers.



K. R. Bullock  
Commercial Manager  
Communication Products Div.  
Phillips Cables Limited  
Brockville, Ontario, Canada

Kenneth R. Bullock was born in Portsmouth, England in 1927. He graduated from McGill University in Montreal in 1952 with a B. Eng. degree in Electrical Engineering.

He has been employed in the Wire and Cable Industry for twenty-two years. From 1953-1959 he was with Phillips Cables as a design engineer, from 1959-1965 with Anaconda Wire and Cable Company latterly as Senior Communication Cable Engineer, and from 1965-1974 with Canada Wire and Cable Company in various positions in Manufacturing and Engineering management. In 1974 he rejoined Phillips Cables and has been in his present position since January 1975.

He is a Senior Member of IEEE, a Fellow of IEE (U.K.) and a Member of the Association of Professional Engineers of Ontario.



Shirley (Mike) Beach was educated in Brockville, Ontario and has been employed by Phillips Cables Limited principally since 1936. He has been employed in both administrative and technical capacity relating to rubber and plastics technology and processing. During this period he has attended a number of courses provided

by the industry related to the rubber and plastics industry.

# CAPACITANCE RELATIONSHIPS IN FILLED TELEPHONE CABLES AND EQUILIBRIUM PREDICTION FROM WATER IMMERSION TESTS

J. A. Olszewski  
Research Center, General Cable Corporation  
Union, New Jersey

## Abstract

Solution of problems in filled telephone cables requires intimate knowledge of cable parameters. Of these, capacitance relationships are of the utmost importance. Capacitance relationships have been extensively studied on air core cables and are familiar to cable designers and transmission engineers, but comparatively little was published on capacitance relationships in filled cables. This subject is investigated and derived capacitance relationships are used to study two current areas of concern, that is, that of high capacitance unbalance to ground in filled cables and prediction of mutual capacitance equilibrium in industry standardized water immersion tests.

It is shown mathematically that filled cables have inherently higher capacitance unbalance to ground than air core cables. The ratio appears to be close to 1.65.

Also, it is shown that increase in wire-to-wire, as well as wire-to-ground, capacitances in water immersion tests is due to diffusion of moisture into the petrolatum based filling compounds and that the rate of change of capacitance associated with cable core filled space in wire-to-ground series capacitances is governed approximately by a function  $e^{-at}$  while that due to filled space in wire-to-wire capacitances chain by  $e^{-bt}$  function, where  $t$  is the time of immersion while  $a$  and  $b$  are numerical constants determined by the efficiency of filling operation and the type of filling compound. The study shows that with time the aforementioned core space capacitances, due to a continuous process of moisture ingress, effectively tend to infinity and zero respectively and consequently the equilibrium is reached with mutual capacitance being equal to half value of insulated wire self-capacitance. The time to equilibrium is a function of the filling compound design.

In light of these findings, specific cable performance specification changes are recommended.

For clarity, the study is limited to 22 gauge cables.

## Introduction

Capacitance relationships in multipair telephone cables are of primary interest since they affect transmission properties and influence cable construction and manufacturing processes. The capacitance values for air core cables are well known and documented, but comparatively little was published on capacitances in filled cables.

The purpose of this paper is to analyze the capacitance relationships in filled cables and to use the results for evaluation of capacitance unbalance to ground, and mutual capacitance changes during water immersion tests on filled cables. Capacitance unbalance to ground determines the noise susceptibility of cables, while the change in capacitance during water immersion test of filled

cables is an indication of a degree of waterproofness under service conditions.

The capacitances of telephone cables employing petrolatum based filling compounds, which were not exposed to moisture, are known to be practically constant over voice and carrier frequencies<sup>1</sup>, while the capacitances of filled cables subjected to moisture ingress vary with frequency and the amount of moisture in the core. The study presented in this paper is limited to 22 gauge cables and the capacitance data was taken at 1000 Hz only.

## Capacitance Relationships

The unbalance to ground and changes in mutual capacitance, due to moisture ingress into filled cable cores, can be explained on the basis of individual values of partial capacitance rather than total capacitance between wires of a pair or capacitances from wires to ground.

The capacitance model of a pair in a multipair telephone cable is shown in Figure 1, but its values are not known quantitatively. In order to

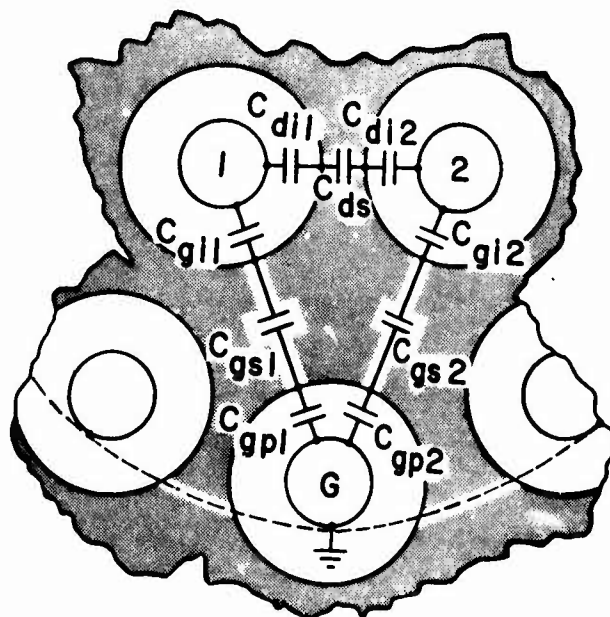


FIGURE 1: Capacitance Diagram of a Pair in a Multipair Telephone Cable

determine all the individual components of wire-to-wire capacitance  $C_d$  and wire-to-ground capacitance  $C_g$ , special cables were manufactured from the same run of singles and cable core. Two 50 pair cables were produced which employed propylene-ethylene insulated singles of filled cable dimensions (DOD=.0525"),

one filled and one unfilled, as well as two 50 pair cables employing LDPE insulated singles of air core cable dimensions (DOD = .044"), again one filled and one unfilled. Measured average 1000 Hz capacitance results per 1000 feet length of cables, at room temperature, are given in Table 1 below:

Table 1

Average 1000 Hz Capacitance of Four  
Experimental 22 AWG Cables in nF/1000 Ft.

	Filled Dimensions		Air Core Dimensions	
	Filled	Unfilled	Filled	Unfilled
Measured wire to grounded core capacitance $C_A = C_d + C_g$	24.232	20.181	28.283	23.356
Measured pair to grounded core capacitance $C_B = 2C_g$	35.474	28.498	40.114	32.304
Wire-to-wire capacitance, $C_d$	6.495	5.932	8.226	7.204
Wire-to-ground capacitance, $C_g$	17.737	14.249	20.057	16.152
Mutual capacitance, $C_m$	15.363	13.056	18.254	15.280

Denoting capacitance in an unfilled cable by primes, the following equations can be set-up using the capacitance model in Figure 1, and measured values of capacitances shown in Table 1:

(a) Filled dimensions cables:

$$\frac{2}{C_{di}} + \frac{1}{C_{ds}} = \frac{1}{C_d} \quad (1)$$

$$= \frac{1}{6.495}$$

$$\frac{1}{C_{gi}} + \frac{1}{C_{gs}} + \frac{1}{C_{gp}} = \frac{1}{C_g} \quad (2)$$

$$= \frac{1}{17.737}$$

$$\frac{2}{C'_{di}} + \frac{1}{C'_{ds}} = \frac{1}{C'_d} \quad (3)$$

$$= \frac{1}{5.932}$$

$$\frac{1}{C'_{gi}} + \frac{1}{C'_{gs}} + \frac{1}{C'_{gp}} = \frac{1}{C'_g} \quad (4)$$

$$= \frac{1}{14.249}$$

It is assumed in the above equations that the capacitances of the insulation of each wire are equal

as shown below and are not dependent on presence or absence of the filling compound, i.e.

$$C_{di1} = C_{di2} = C_{di} = C'_{di1} = C'_{di2} = C'_{di} \quad (5)$$

$$C_{gi1} = C_{gi2} = C_{gi} = C'_{gi1} = C'_{gi2} = C'_{gi} \quad (6)$$

$$C_{gp1} = C_{gp2} = C_{gp} = C'_{gp1} = C'_{gp2} = C'_{gp} \quad (7)$$

Also, since the dielectric constant of the filling compound is 2.2 while that of air space is 1.0, then

$$C_{ds} \approx 2.2 C'_{ds} \quad (8)$$

$$C_{gs} \approx 2.2 C'_{gs} \quad (9)$$

Finally, it can be assumed that

$$C_s \approx C_{gi} + C_{di} \approx \frac{7.36 E}{\log \frac{DOD}{d}} \text{ nF/1000 ft.} \quad (10)$$

(b) Air Core dimensions cables:

The same equations as (1) through (10) can be set-up to solve for partial capacitance in air core dimensions cables.

The equations (5) through (9) are approximate because they do not take into account the differences in the electrical field distribution in air and filled cable cores. In addition, equations (8) and (9) assume that the filling operation does not change the distances between singles in the cable core; and small degree of core spreading was observed in experimental filled cables. The assumptions made in equation (10) are self-evident. The errors resulting from these assumptions will not affect qualitative results obtained in the subject studies.

Using the above equations, the partial capacitances were calculated for filled and air core (Alpeth) cables, described in Table 1. The resultant average partial capacitances are given in Table 2 in nF per 1000 feet of cable.

Table 2

Estimated Partial Capacitances of Experimental 22 AWG Cables  
nF/1000 Ft.

	Filled Cable	Air Core Cable
(A) Wire-to-Wire Capacitances, nF		
$C_{di}$	14.106	18.658
$C_{ds}$	82.124	31.628
(B) Wire-to-Ground Capacitances, nF		
$C_s$	51.144	69.211
$C_{gi}$	37.038	50.533
$C_{gs}$	86.950	45.251
$C_{gp}$	55.931	49.921

The above data are used for studies of capacitance unbalance to ground in filled and air core cables and for analysis of moisture ingress into filled cables.

### Capacitance Unbalance to Ground

For some time now, there is a considerable effort in the industry, to reduce capacitance unbalances to ground in filled cables which tend to run considerably higher than in air core cables. The industry specifications, however, call for the same control of capacitance unbalance to ground in both types of cables, or 150-200 pF maximum average per 1000 feet of cable. There is a good reason for concern and tight control since this characteristic determines noise pick-up on paired circuits.

The capacitance unbalance to ground in filled cables,  $CU_g$ , was analyzed by comparison with that in air core cables,  $CU'_g$ . This was done by using basic definition of unbalance, i.e.

$$\frac{CU_g}{CU'_g} = \frac{C_{g1} - C_{g2}}{C'_{g1} - C'_{g2}} \quad (11)$$

where  $CU_g$  = capacitance unbalance to ground in filled cable.

$CU'_g$  = capacitance unbalance to ground in air core cable.

and by reference to Figure 1

$$C_{g1} = \frac{C_{g11} C_{gs1} C_{gp1}}{C_{gs1} C_{gp1} + C_{g11} C_{gp1} + C_{g11} C_{gs1}}$$

Subscript 1 refers to wire 1 and subscript 2 refers to wire 2 of a pair as shown in Figure 1. Substituting partial capacitances into equation (11) yields:

$$\frac{CU_g}{CU'_g} = A B \quad (12)$$

$$\text{where } A = \frac{C_{g1} C_{g2}}{C'_{g1} C'_{g2}} \approx \frac{C_g^2}{C'_g{}^2} \quad (12a)$$

$$\text{and } B = \frac{\frac{\Delta_{g1}}{C_{g11}} + \frac{\Delta_{gs}}{C_{gs1}} + \frac{\Delta_{gp}}{C_{gp1}}}{\frac{\Delta'_{g1}}{C'_{g11}} + \frac{\Delta'_{gs}}{C'_{gs1}} + \frac{\Delta'_{gp}}{C'_{gp1}}} \quad (12b)$$

$\Delta_x$  in equation (12b) represents fractional unbalance of partial capacitance (x) and is defined as:

$$\Delta_x = \frac{C_{x1} - C_{x2}}{C_{x2}}$$

Assuming that capacitance unbalance to ground is caused by an inequality  $\Delta$  of one cable component only and that this inequality is the same in filled as in air core cables - an assumption representing practical conditions since typically the same manufacturing equipment and its controls are used for production of both types of cables - then the following capacitance unbalance to ground ratios for filled to air core cables are calculated from equations (12), (12a) and (12b) and Tables 1 and 2:

- i. Inequality in insulation of a pair,  
 $CU_g/CU'_g \approx 1.65$ .
- ii. Inequality in interstices,  
 $CU_g/CU'_g \approx 0.52$
- iii. Inequality in insulations of wires surrounding a pair,  
 $CU_g/CU'_g \approx 0.89$

It is unlikely that the capacitance unbalance to ground, due to inequality of insulations of wires surrounding the pair, can appear in actual paired cables. Also, although fractional interstitial capacitance unbalances  $\Delta_{gs}$  and  $\Delta'_{gs}$  for filled and air core cables were assumed to be the same in the above calculations, in actual filled cables  $\Delta_{gs}$  may be higher than  $\Delta'_{gs}$  in air core cables. Ununiformity of surface conditions on singles of a pair can cause different per cent fill around these singles and hence some differences in dielectric constant of filled core space. This can increase  $CU_g/CU'_g$  ratio, due to interstitial inequality, to above unity, but the unbalances to ground due to such conditions in practice cannot be of controlling magnitude. The main cause for higher unbalance to ground in filled cables than in air core cables is the unbalance in the insulation of pair singles.

The ratio of capacitance unbalance to ground of filled to air core cables, measured in one of our manufacturing facilities over a six months period, revealed an average value of 1.79. This value is somewhat higher than that calculated for unbalance in insulations of singles only and consequently indicates the the unbalances in the interstices of cable cores may play some part in the unbalance to ground of filled cables.

In summary, it can be stated that higher unbalances to ground in filled cables are due to the nature of these cables since the unbalances are determined by insulation and filled core interstitial capacitance relationships. The specifications limits for capacitance unbalance to ground in filled cables should be increased by at least 65 per cent from their present air cable levels until better controls of cable manufacturing processes can be developed and introduced in production.

### Capacitance Equilibrium in Water Immersion Tests

Industry specifications require determination of 1000 Hz mutual capacitance increase in 30 days of immersion in water. The maximum increase is limited to 1.5 per cent. From the point of view of the user, it is essential to predict the increase in capacitance over the service life of the filled cables. It was established herein that such a prediction can be made on the basis of analysis of partial capacitance changes. Other performance characteristics of filled cables, or other parameters of filling compounds are not discussed.

The study of mutual capacitance increase in water immersion tests was performed utilizing No. 22 AWG cables with solid propylene-ethylene copolymer insulation, covered with our standard FPA sheath and filled with:

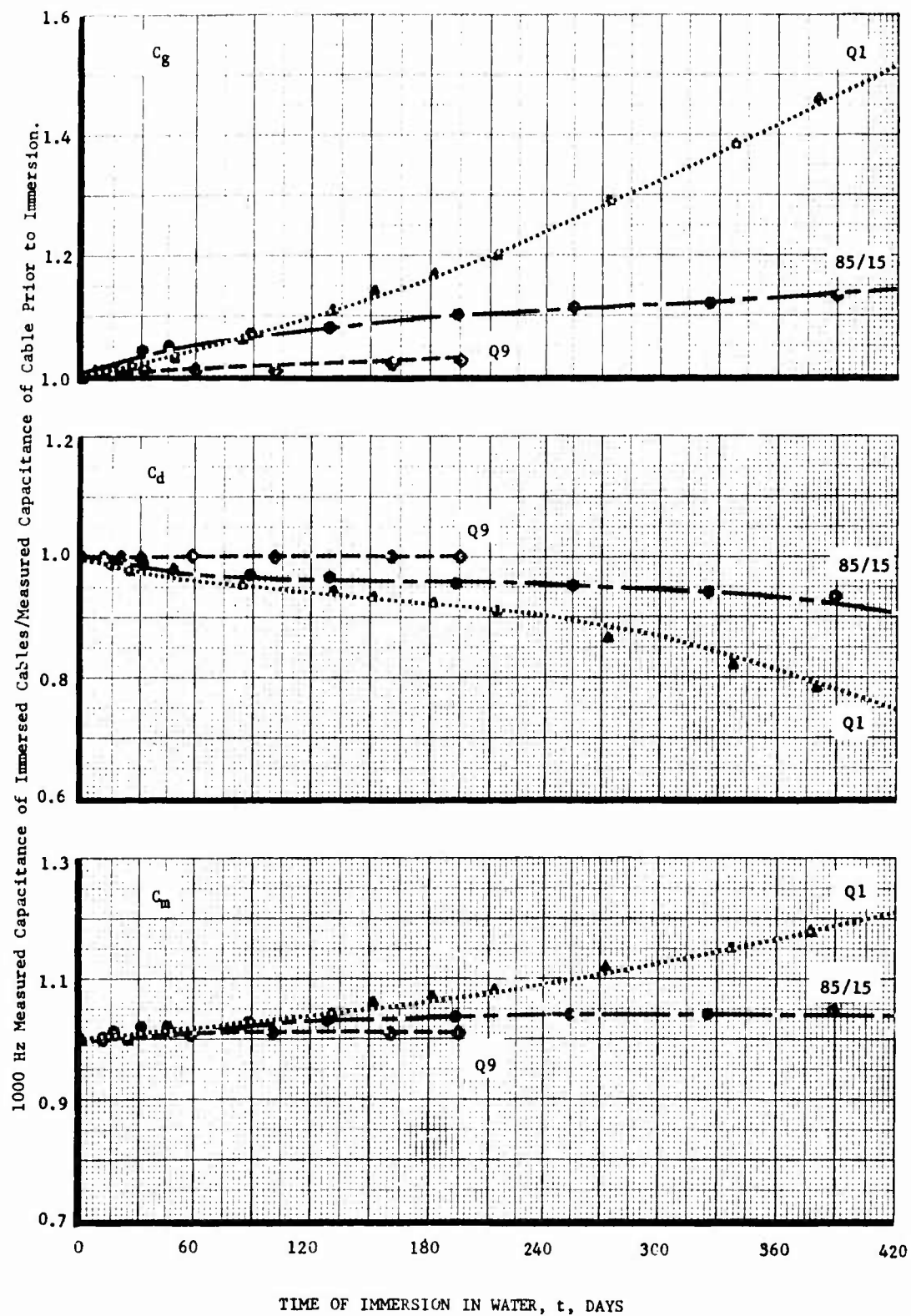


FIGURE 2: Linear Plots of Measured Capacitance Stability in Water Immersion Tests  
Wire-to-Ground, Wire-to-Wire and Mutual Capacitances of Selected Cables.



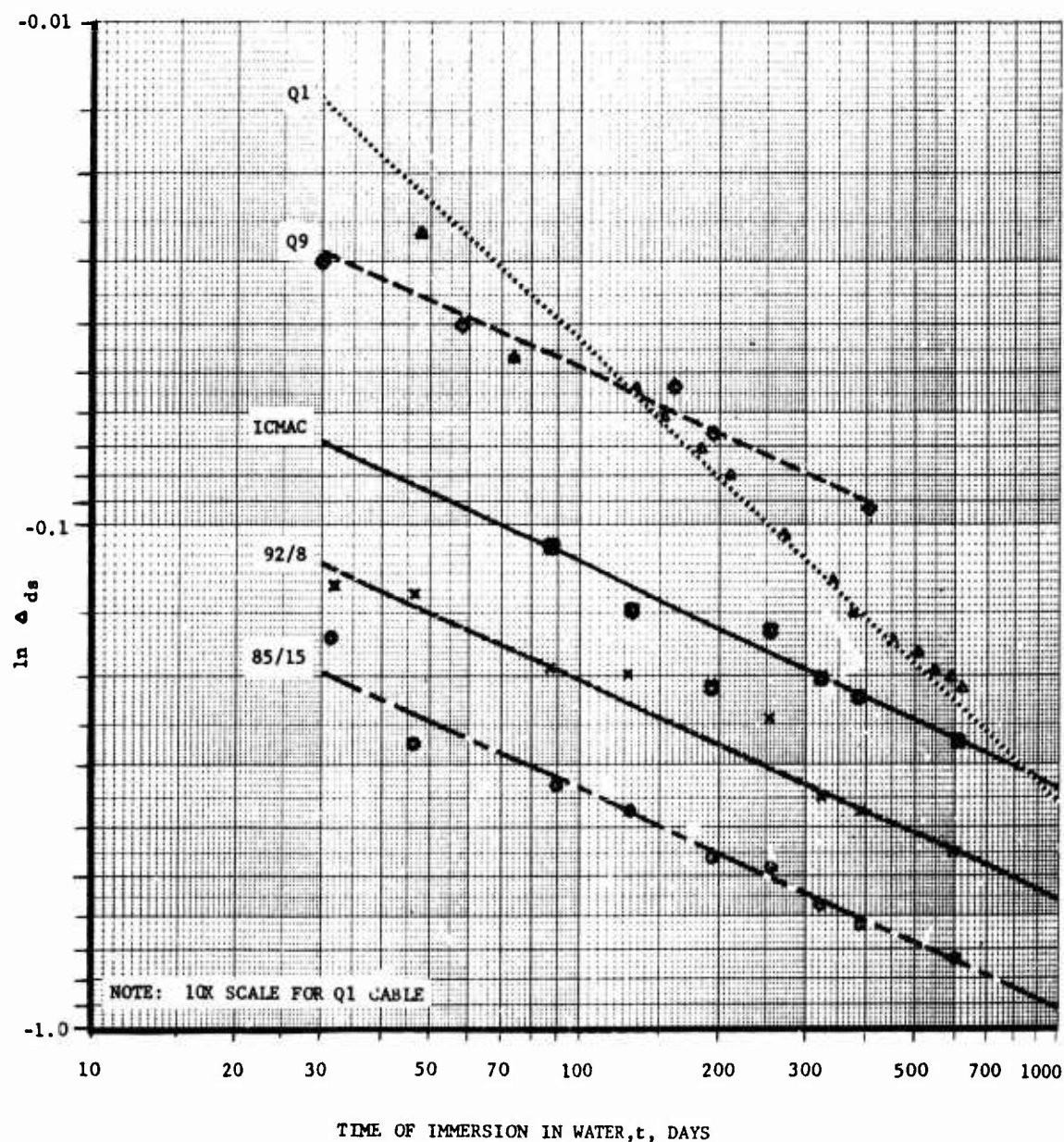


FIGURE 3A: Natural Logarithm of Immersed to Dry Wire-to-Wire Interstitial Space Capacitance Ratio Versus Time of Immersion in Water.

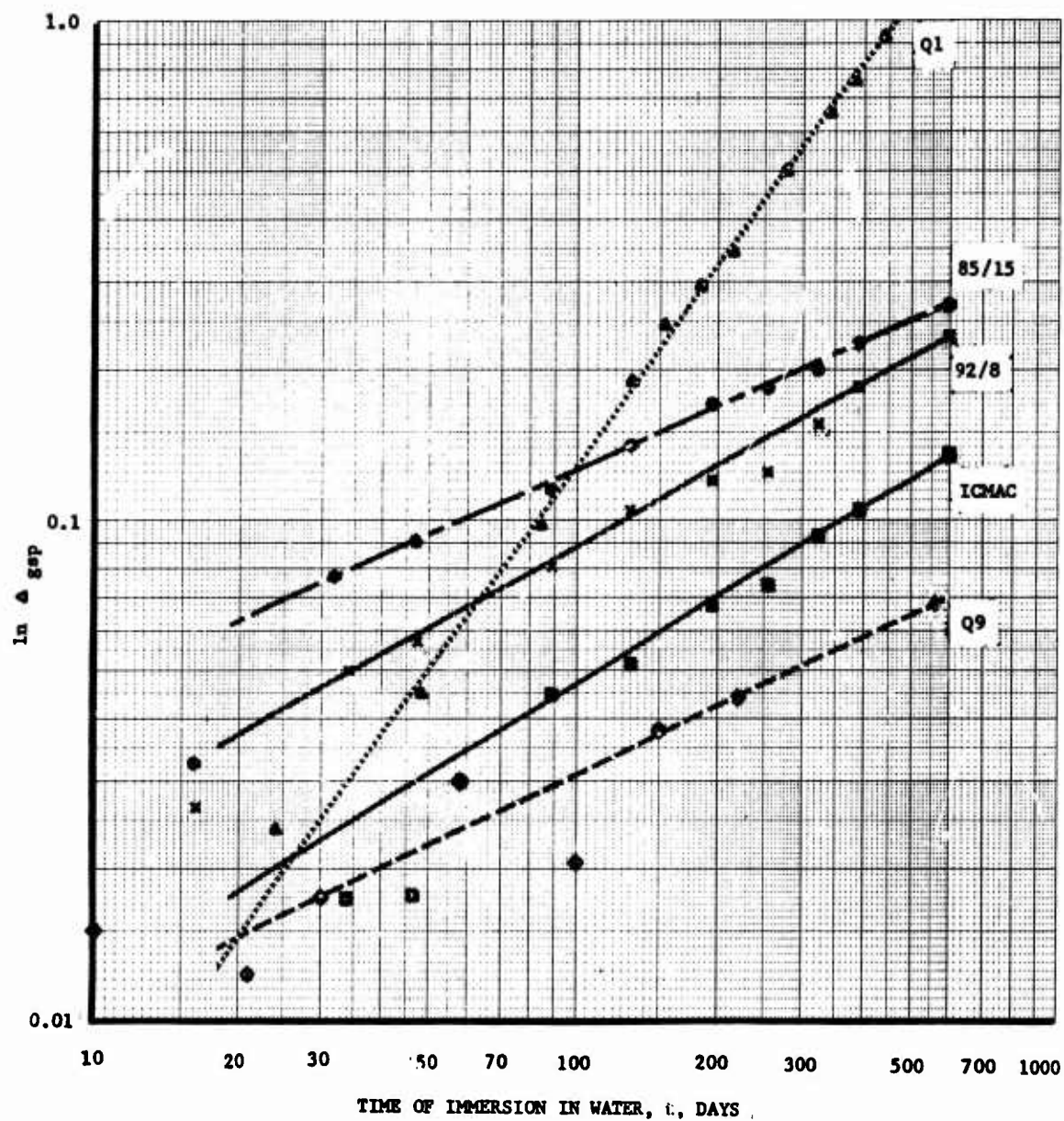


FIGURE 3B: Natural Logarithm of Immersed to Dry Wire-to-Ground Interstitial Space and Surrounding Wires Capacitance Ratio Versus Time of Immersion in Water.

- i. 85/15 compound - 85% PJ + 15% PE + stabilizers.
- ii. 92/8 compound - 92% PJ + 8% PE + stabilizers.
- iii. ICMAC compound - 100% PJ blend + stabilizers.
- iv. GCC production compound Q9 - composition proprietary.
- v. GCC experimental compound Q1 - 96% PJ + 4% SiO<sub>2</sub> + stabilizers.

All samples used in the water immersion tests were 30 ft. long with 26 ft. length immersed under a 3 ft. head of water at room temperature. Holes 3/8" in diameter were cut through cable sheaths, including core tape. The holes were 1 ft. apart and rotated 90° from each other in a fixed direction. Wire-to-wire and wire-to-ground capacitances were measured periodically at 1000 Hz, using 0.1% accuracy capacitance bridge. The changes in capacitances of pairs in outer sub-units were determined over a 2 year period of immersion and the average values for different cable types are shown in Figure 2.

The initial, or prior to water immersion, partial capacitances were estimated under an assumption that their division is the same as for cables specified and analyzed in Tables 1 and 2. Specifically,

- (a) Wire-to-wire capacitances:  
 $1/C_{d0} = 100.00\%$   
 $1/C_{dio} = 46.04\%$  each  
 $1/C_{dso} = 7.91\%$
- (b) Wire-to-ground capacitances:  
 $1/C_{g0} = 100.00\%$   
 $1/C_{gio} = 47.89\%$   
 $1/C_{gso} = 20.40\%$   
 $1/C_{gpo} = 31.71\%$

where a subscript "0" denotes capacitances prior to immersion of cables in water.

First, wire-to-wire capacitance change with time of immersion in water was studied. Assuming that partial capacitances due to insulation are not affected by water entry into the cable core, i.e.  $C_{di} = C_{dio}$  = constant, the values of natural logarithms of partial capacitance changes  $\Delta_{ds} = C_{ds}/C_{dso}$  versus time of immersion  $t$  in days were plotted on log-log coordinates and are shown in Figure 3A.

It appears from this graph that the change of partial capacitance due to space between wires of a pair fits the following equation

$$C_{ds} = C_{dso} e^{-at^b} \quad (13)$$

Next, wire-to-ground capacitance change with time of immersion in water, was considered.  $C_{gs}$  and  $C_{gp}$  partial capacitances were combined, i.e.

$$\frac{1}{C_{gs}} + \frac{1}{C_{gp}} = \frac{1}{C_{gsp}} \quad (14)$$

since water entry into the filled cable core in effect changes both these partial capacitances simultaneously.

Also,  $C_{gi}$  and its changes with time of immersion were assumed to be a function of changes in  $C_d$ , specifically with aid of equation (10):

$$C_{gi} = C_{gio} + C_{dio} \left( 1 - \frac{C_d}{C_{d0}} \right) \quad (15)$$

Values of  $C_{gsp}$  were isolated from measured  $C_g$  values, that is

$$\frac{1}{C_{gsp}} = \frac{1}{C_g} - \frac{1}{C_{gi}}$$

and natural logarithms of its changes  $\Delta_{gsp} = C_{gsp}/C_{gspo}$  versus time of immersion  $t$  in days were plotted on log-log coordinates in Figure 3B. This graph shows that the change of partial capacitance  $C_{gsp}$ , in the wire to ground series capacitances chain, fits equation

$$C_{gsp} = C_{gspo} e^{ct^d} \quad (16)$$

The correlation coefficients between data points and straight lines drawn in Figures 3A and 3B were calculated to be as high as 0.99 for immersion periods from 30 days up.

The calculated values of  $a$ ,  $b$ ,  $c$  and  $d$ , used in equations (13) and (16) for cables studied are given in Table 3 below.

Table 3  
Calculated Values of  $a$ ,  $b$ ,  $c$  and  $d$  for  
Cables in Water Immersion Tests

Cable Type (Filling compound type)	a	b	c	d
85/15	.0437	.442	.0175	.427
92/8	.0261	.445	.00754	.535
ICMAC	.0140	.461	.00314	.585
GCC - Q9	.00654	.444	.00373	.458
Experimental Q1	.00622	.916	.000265	1.34

Using the above, anticipated changes in mutual capacitance  $C_m$ , with time of immersion in water, were calculated for each cable under study, using the following relationship:

$$C_m \approx C_d + \frac{C_g}{2} \quad (17)$$

$$\text{where } C_d = \frac{C_{dio} C_{dso} e^{-at^b}}{C_{dio} + 2C_{dso} e^{-at^b}} \quad (17a)$$

$$C_g = \frac{C_{gspo} e^{ct^d}}{1 + \frac{C_{gspo} e^{ct^d}}{C_{gio} + C_{dio} \left[ 1 - \frac{C_{dio} C_{dso} e^{-at^b}}{C_{d0} (C_{dio} + 2C_{dso} e^{-at^b})} \right]}} \quad (17b)$$

The resultant mutual capacitance plots shown in Figure 4, indicate that all studied filled cables in water immersion tests, similarly as air core cables, tend to equilibrium represented by self capacitance of the singles, or  $C_g/2$ . The time to equilibrium can be short,

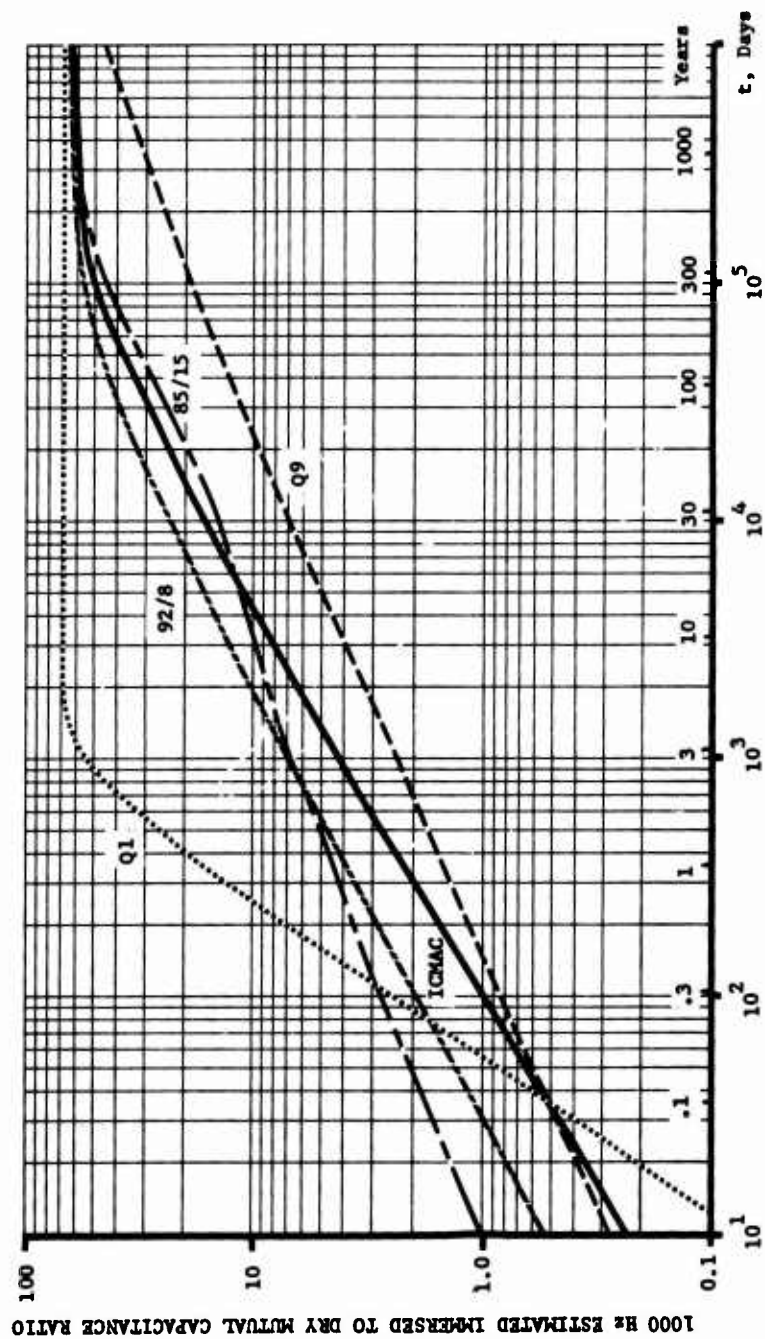


FIGURE 4: Estimated Change in 1000 Hz Mutual Capacitance of Cables Immersed in Water Versus Time of Immersion.

however, for good filling compounds can also be millenniums. Judging by a 30 year required service life, commercially used compounds can be classified from best to worst as: (1) GCC production compound Q9, (2) ICMAC, (3) 85/15 compound, (4) 92/8 compound. The GCC production compound Q9 appears to be about 3 to 4 times better than other commercial compounds studied.

Of some interest is a cable with GCC experimental filling compound Q1 which employed a small amount of fumed silica. Its rate of change of core space capacitance is substantially higher. Absorption of water by fumed silica and entrapment of air bubbles appears to be a main problem. This cable in a 30 day test looked good but in two years of immersion in water exhibited close to 30% increase in mutual capacitance and is predicted to reach equilibrium with 70% capacitance increase (self-capacitance of filled cable pair) in about 5 years. This analysis indicated early the deficiency of Q1 compound and removed it from further consideration.

Test data for two years of immersion are in good agreement with theoretical plots from about 50 days up. Test points below 30 to 50 days of immersion show rather large scatter because:

- (a) Filling compound cracks or channels in cable core from time to time continue to be abruptly penetrated by water.
- (b) Less than 1% capacitance changes are more subject to experimental errors due to small temperature changes, rearrangement of conductors at ends of short cable samples, etc.

Once the cracks or channels are filled with water, however, then the moisture begins to penetrate the core in a predictable manner, or the capacitance changes become predictable for given type of filling compound. The importance of tight limits of mutual capacitance in the 30 day water immersion test is very apparent and can readily be seen from predicted mutual capacitance plots for cables under study shown in the attached Figure 4. High initial increases can very markedly shorten time to saturation. Short lengths of water saturated core at the point of sheath damage can give rise to transmission problems due to reflections. In addition, the control of water flow is very important since this determines changes in capacitance, impedance, attenuation, etc., in long lengths of installed cable.

The above study points to the necessity for revision of water immersion test requirements as follows:

- i. Specify measurement of wire-to-wire and wire-to-ground capacitances.
- ii. Introduce capacitance rate of change limits.
- iii. Base capacitance changes determination on measurements before immersion.
- iv. Introduce long term capacitance stability test.

## Conclusions

1. High capacitance unbalances to ground of filled cables and increases of mutual capacitance in water immersion tests can be explained by partial capacitance relationships and their changes.
2. Higher capacitance unbalances to ground in filled cables compared to air core cables are mainly caused by use of the filling compound with the dielectric constant of 2.2 as opposed to 1.0 for the interstices of air core cables. The capacitance unbalances to ground for both types of cables are primarily caused by non-uniformity of insulations.
3. Experimental functions have been established for changes in wire-to-wire and wire-to-ground capacitances of filled cables in water immersion tests. The increase in mutual capacitance during service life of filled cables, with water having access to their cores, has been determined for a number of filling compounds based on established experimental functions. It has been also demonstrated that a proper formulation of the filling compound can limit mutual capacitance increases to 10% within a 30 year service life of the cables.
4. Recommendations were made for revisions of specifications concerning limits of capacitance unbalance to ground and procedures for water immersion tests on filled cables.

## Acknowledgments

The author wishes to express thanks to Dr. G. Bahder for his guidance and to Messrs. J. Peveler and R. Neher for performing measurements and calculations for this study.

## References

1. L. Jachimowicz, J. A. Olszewski and I. Kolodny, "Transmission Properties of Filled Thermoplastic Insulated and Jacketed Telephone Cables at Voice and Carrier Frequencies", International Conference on Communications, June 19-21, 1972, Philadelphia.
2. Hewlett-Packard "9810A Stat Pac", Volume 1.
3. J. A. Olszewski, V. W. Pehrson and H. Simon, "The Effects of Water in Plastic Insulated Telephone Cable", 21st International Wire and Cable Symposium, Atlantic City, N.J., 1972.



J.A. Olszewski, Assistant Director of Research in charge of research and development of communication wires and cables, General Cable Corporation, Research Center, 800 Rahway Avenue, Union, New Jersey 07083



# AUTHOR INDEX

Aida, K.	83	Lupton, E. C., Jr.	1
Andjerka, H. J.	365	Manfre, Dr. G.	67
Asada, K.	168	Matsubara, H.	15
Beach, S. M.	62, 379	Matsunaga, C.	15
Bernstein, B. S.	202	Matsuoka, S.	75
Billigmer, J. E.	112	Mather, E. L.	347
Blee, J. J.	276	Mayer, H. A.	365
Brauer, M.	104	McAda, R. B.	225
Brokke, B. M.	37	McBroom, J. W.	335
Brown, M.	292	Monte, S. J.	300
Bullock, K. R.	379	Murayama, Y.	4
Cannon, T. C., Jr.	143	Nantz, T. D.	175
Checkland, J. A.	26	Naruse, T.	168
Chen, A.	325	Negishi, Y.	83
Choo, T. S.	190	Obsasnick, J.	1
Clatterbuck, C. H.	92	Oguchi, M.	168
Cretney, D. F.	379	Okada, M.	53
Daane, J. H.	75	Olszewski, J. A.	399
Dageforde, H. G.	136, 365	O'Rell, D. D.	231
D'Annessa, A. T.	276	Otomo, S.	213
Davis, K. N.	340	Park, J. J.	92
Dohany, J. E.	340	Patel, A.	231
Doty, D.	255	Pehrson, V. W.	260
Fairfield, J.	158	Pritchett, J.	347
Fialcowitz, R. P.	164	Rall, D. L.	62
Fleischhacker, J.	270	Remley, J. C.	37
Friesen, H. W.	150	Riekkinen, A.	43
Fulenwider, J. E.	282	Roesler, F.	335
Gill, D.	99	Rokunohe, M.	53
Gorissen, H. L.	361	Sabia, R.	104
Goto, Y.	180	Santana, M. R.	143
Gouldson, E. J.	26	Sharpe, P. D.	300
Gregor, P.	136	Smith, D. T.	276
Hendricks, W. R.	329	Snyder, J. L.	329
Inoue, A.	15	Stefanou, H.	340
Kaufman, J. J.	374	Sugerman, G.	300
Kaufman, S.	9	Tahlmore, D. C.	1
Killinger, G. B.	282	Takashima, H.	213
Kincaid, J.	126	Thonnessen, Dr. G.	136
Kishi, H.	213	Ueno, Y.	53
Kokta, E. T.	220	van Kesteren, J. P. I.	361
Konishi, J.	53	Verne, S.	347
Kooy, J. F.	361	Wimsey, J. E.	237
Kottle, S.	225	Woollerton, G. R.	26
Kreuger, F. H.	361	Yamaguchi, K.	213
Kreutzberg, J.	175	Yashiro, T.	83
Kusunoki, M.	180	Yasuda, N.	15
Landreth, C. A.	9	Yasuhara, H.	168
Lee, P. N.	202	Yoshizawa, A.	4
Luisi, T. E.	374		





# INTERNATIONAL WIRE & CABLE SYMPOSIUM

CO-SPONSORED BY INDUSTRY AND U.S. ARMY ELECTRONICS COMMAND

16, 17 & 18 November 1976

Cherry Hill Hyatt House, Cherry Hill, N. J.

Please provide in the space below a 100-500 word abstract of a proposed technical paper on such subjects as design, application, materials, and manufacturing of Communications and Electronics Wire & Cable of interest to the commercial and military-aerospace industries. Such offers should be submitted no later than 5 April 1976 to the Commanding General, U. S. Army Electronics Command, Att: AMSEL-TL-ME, Fort Monmouth, N.J. 07703.

Title: \_\_\_\_\_

Authors: \_\_\_\_\_

Company: \_\_\_\_\_

Address: \_\_\_\_\_

For additional information, call E. F. Godwin 201-535-2770

Staple

Fold here

Stamp

Commanding General  
U.S. Army Electronics Command  
Att: AMSEL-TL-ME  
Fort Monmouth, N.J. 07703

Fold here